

# INTRODUCTION TO FOURIER ANALYSIS

Norman Morrison



Includes disks







---

**Introduction to  
Fourier Analysis**

---



---

# **Introduction to Fourier Analysis**

---

**Norman Morrison**

*University of Cape Town  
Rondebosch, South Africa*



A Wiley-Interscience Publication  
**JOHN WILEY & SONS, INC.**

New York • Chichester • Brisbane • Toronto • Singapore

The programs on the accompanying disks were written in True BASIC.<sup>®</sup>  
All graphic printouts were done on HP LaserJet IIP using a software package called PIZAZZ.  
True BASIC<sup>®</sup> is a registered trademark of True BASIC, Inc.  
HP LaserJet IIP is a product of the Hewlett-Packard Company.  
PIZAZZ is a registered trademark of Application Techniques, Inc.  
MACINTOSH is a registered trademark of Apple Computer Inc.

This text is printed on acid-free paper.

Copyright © 1994 by John Wiley & Sons, Inc.

All rights reserved. Published simultaneously in Canada.

Reproduction or translation of any part of this work beyond  
that permitted by Section 107 or 108 of the 1976 United  
States Copyright Act without the permission of the copyright  
owner is unlawful. Requests for permission or further  
information should be addressed to the Permissions Department,  
John Wiley & Sons, Inc., 605 Third Avenue, New York, NY  
10158-0012.

*Library of Congress Cataloging in Publication Data:*

Morrison, Norman.

Introduction to Fourier analysis

Norman Morrison.

p. cm.

Includes bibliographical references (p. — ).

ISBN 0-471-01737-X (acid-free)

1. Fourier analysis. I. Title.

QA403.5.M67 1994

93-44636

515'.2433--dc20

CIP

Printed in the United States of America

10 9 8 7 6 5 4 3 2

**To Ariel and Shira**



---

# Contents

Preface	xiii
Acknowledgments	xviii
Nomenclature and Abbreviations	xix

---

## PART 1 CONTINUOUS FOURIER ANALYSIS

---

<b>1 Background</b>	<b>3</b>
1.1 Types of Problems / 3	
1.2 Historical Background / 4	
<b>2 Fourier Series for Periodic Functions</b>	<b>9</b>
2.1 Orthogonality of Vectors and Functions / 9	
2.2 The Complex Exponentials / 10	
2.3 Properties of the Complex Fourier Coefficients / 21	
2.4 Parseval's Theorem for Periodic Waveforms / 32	
2.5 Convergence of Fourier Series / 37	
Notes and Comments / 44	
Exercises / 45	
<b>3 The Fourier Integral</b>	<b>62</b>
3.1 Introduction / 62	
3.2 The Fourier Integral / 62	
3.3 What Does the Fourier Integral Mean? / 68	
3.4 Two Basic Theorems / 73	
3.5 Parseval's Theorem for Pulses / 78	
3.6 Existence of the Fourier Integral / 83	
3.7 Asymptotic Bounds for $F(\omega)$ / 86	
Exercises / 88	

<b>4 Fourier Transforms of Some Important Functions</b>	<b>97</b>
4.1 Introduction / 97	
4.2 The Rectangular Pulse / 98	
4.3 The Single-Sided Decaying Exponential / 99	
4.4 The Double-Sided Decaying Exponential / 104	
4.5 The Signum Function / 105	
4.6 The Dirac Delta or Unit Impulse / 109	
4.7 The Unit Step / 123	
4.8 The Eternal Complex Exponential / 127	
4.9 The Eternal Cosine and Sine Functions / 129	
4.10 Periodic Functions / 130	
4.11 The Periodic Impulse Train / 133	
Exercises / 135	
<b>5 The Method of Successive Differentiation</b>	<b>145</b>
5.1 The Differentiation Property / 145	
5.2 Differentiating Functions with Discontinuities / 147	
5.3 The Method of Successive Differentiation / 154	
5.4 One Small Complication and How to Resolve It / 160	
5.5 Nonpolynomial Sections / 163	
Exercises / 164	
<b>6 Frequency-Domain Analysis</b>	<b>172</b>
6.1 Introduction / 172	
6.2 Response of a Linear Time-Invariant System to a Pulse Function / 173	
6.3 AC Circuit Analysis Using the Fourier Transform / 187	
6.4 Response of a Network to a Periodic Function / 195	
6.5 Finding the Transfer Function for Pulses / 197	
Exercises / 203	
<b>7 Time-Domain Analysis</b>	<b>212</b>
7.1 Introduction / 212	
7.2 The Impulse Response / 213	
7.3 Convolution / 217	
7.4 What Does the Convolution Product Mean? / 220	
7.5 Convolution the Graphical Way / 227	
7.6 Evaluating the Convolution Integral Analytically / 233	
7.7 Convolution in the Frequency Domain / 238	
Exercises / 245	

<b>8 The Properties</b>	<b>257</b>
8.1 The Linearity Property / 257	
8.2 The Realness Property / 258	
8.3 The Symmetry Properties / 258	
8.4 The Area Property / 261	
8.5 The Duality Property / 262	
8.6 The Reciprocal-scaling Property / 264	
8.7 The Time-shift Property / 266	
8.8 The Frequency-shift Property / 267	
8.9 Time-domain Differentiation / 268	
8.10 Frequency-domain Differentiation / 268	
8.11 Time-domain Convolution / 269	
8.12 Frequency-domain Convolution / 270	
8.13 Two Properties of the Dirac Delta / 270	
8.14 The Integration Property / 271	
Exercises / 271	
<b>9 The Sampling Theorems</b>	<b>284</b>
9.1 Introduction / 284	
9.2 Time-domain Impulse Sampling / 284	
9.3 Time-domain Analysis of the Recovery Process / 297	
9.4 Sampling with Pulses Other than Dirac Deltas / 299	
9.5 Sampling in the Frequency Domain / 302	
Exercises / 311	

---

## PART 2 DISCRETE FOURIER ANALYSIS

---

<b>10 The Discrete Fourier Transform</b>	<b>323</b>
10.1 Introduction / 323	
10.2 The Discrete Complex Exponentials / 323	
10.3 The Discrete Fourier Transform / 330	
10.4 Properties of the DFT / 338	
Notes and Comments / 341	
Exercises / 343	
<b>11 Inside The Fast Fourier Transform</b>	<b>348</b>
11.1 Introduction / 348	
11.2 The FFT for Small Values of $N$ / 348	
11.3 The General Radix-2 FFT Algorithm / 354	
11.4 Setting Up the Rules / 358	
11.5 The Complete FFT Flowchart / 363	

11.6	The Cooley–Tukey Derivation of the Radix-2 Algorithm / 365	
11.7	Final Comments / 368	
<b>12</b>	<b>The Discrete Fourier Transform as an Estimator</b>	<b>372</b>
12.1	Introduction / 372	
12.2	Relationships Based on the Rectangular Rule / 373	
12.3	Aliasing / 378	
12.4	The FFT as an Estimator for the CFTs / 383	
12.5	Inverting CFT Spectra Using the FFT / 390	
	Exercises / 395	
<b>13</b>	<b>The Errors in Fast Fourier Transform Estimation</b>	<b>399</b>
13.1	Introduction / 399	
13.2	The Errors in the Estimates / 400	
13.3	Canonical Pulses and Order of Continuity / 401	
13.4	The Error Expressions / 403	
13.5	Some Properties of $E_N(n)$ / 404	
13.6	The Log-Linear Z-curves / 406	
13.7	Asymptotic Behavior of Noncanonical Functions / 409	
13.8	Break Points not at a Sampling Instant / 415	
13.9	Error Correction of FFT Estimates / 418	
13.10	Confirmation of Theoretical Results / 419	
13.11	Zero Padding Increases the Estimation Errors / 419	
	Exercises / 420	
<b>14</b>	<b>The Four Kinds of Convolution</b>	<b>432</b>
14.1	Introduction / 432	
14.2	The Four Kinds of Convolution / 435	
14.3	The Span Restriction / 442	
14.4	Discrete Circular Convolution on the FFT / 447	
14.5	Discrete Linear Convolution Using the FFT / 451	
14.6	Continuous Linear Convolution Using the FFT / 451	
14.7	Continuous Circular Convolution Using the FFT / 453	
14.8	Operation Count to Perform Convolution / 454	
	Exercises / 457	
<b>15</b>	<b>Emulating Dirac Deltas and Differentiation on the Fast Fourier Transform</b>	<b>463</b>
15.1	Time-domain Dirac Deltas on the FFT / 463	
15.2	Frequency-domain Dirac Deltas on the FFT / 466	
15.3	Differentiation on the FFT / 467	
	Exercises / 474	

---

**PART 3 THE USER'S MANUAL FOR THE ACCOMPANYING DISKS**

---

**Chapters 16, 17, and 18 (Located in README files on the disks)**

(A) Macintosh Disk	481
(B) DOS Disk	482
Appendix 1 References and Further Reading	485
Appendix 2 A. Three Short Tables of Fourier Transforms	488
B. The Properties	491
Answers to the Exercises	493
Index	555



---

# Preface

**FOR THE EDUCATOR, THE STUDENT,  
OR THE PRACTICING PROFESSIONAL**

Fourier analysis is now central to electrical engineering, yet in many universities throughout the world it is only taught briefly before students are expected to begin applying it.

A partial list of subjects requiring Fourier analysis as a background might read as follows:

- |   |   |
|---|---|
| <ul style="list-style-type: none"><li>• Electronic Circuits</li><li>• Electronic Measurements</li><li>• Circuits and Signals</li><li>• Electrical Networks</li><li>• Telecommunication Engineering</li><li>• Biomedical Engineering</li><li>• Communication Theory</li><li>• Signal Processing and<br/>Telecommunications</li></ul> | <ul style="list-style-type: none"><li>• Underwater Acoustics</li><li>• Radar Systems Engineering</li><li>• Image Processing</li><li>• Optical Electronics</li><li>• Communication Networks</li><li>• Radar Signal Processing</li><li>• Digital Communication</li><li>• Multidimensional Digital<br/>Signal Processing</li></ul> |
|---|---|

As this list suggests, Fourier analysis contains in it all of the central ideas of electrical engineering, among them:

- The time and frequency domains,
- Representation of waveforms in terms of complex exponentials and sinusoids,
- Complex exponentials and sinusoids as the eigenfunctions of linear systems,
- Convolution,
- Impulse response and the frequency transfer function,
- Magnitude and phase spectra, and
- Modulation and demodulation.

This book is intended to serve as an introduction to all of these concepts. It also introduces the reader to the fast Fourier transform (FFT). When we set out to write this book, we did so in the belief that Fourier analysis and the FFT should be introduced in the second half of the second year, rather than in the beginning of the third, as is typically done in many universities in courses known loosely as Signals and Systems. As such it should be considered as a book that precedes typical books on signals and systems rather than being a replacement for them.

By introducing students to Fourier analysis as early as the second half of their second year, *sufficient time is allowed for this wide range of new ideas to take root*. Thus when these topics are encountered in the third year the student already has some familiarity with them, rather than having to learn them on the fly while simultaneously also having to apply them.

For many years the University of Cape Town followed the procedure of teaching Fourier analysis as part of signals and systems in the third year, similar to what is done today in many universities. Then a new idea was tried... why not give the students a formal one-semester course either in the second half of their second year or, at the latest, in the first half of their third? (At our university the course has been taught in the second year for the past five years.) The results were startling, and the subsequent levels of achievement exceeded even the most optimistic expectations. A number of questions might naturally be asked:

- *Are second-year students ready for the material?* The answer, based on five years of teaching experience, is definitely yes.
- *What of the Laplace and the Z-transform?* The answer is that they will have to be taught in another course. The one envisaged here covers 36 lectures solely on Fourier analysis and the FFT.

The text has been written with engineering students expressly in mind, and so there are a number of features that will be found in it:

- Wherever possible *mathematical digression was omitted*, and so only such mathematics as was deemed to be essential was included. The reader will note the frequent inclusion of theorems. However, these are seldom proved formally and are merely a summary of the latest critical developments that have just been covered in an informal manner.
- *Intermediate steps* in the proofs and developments are often provided rather than omitted. It is possible that some students might, on occasion, find this a trifle less challenging. However, we had in mind the needs of the other 90 percent when we wrote this text.
- The text is carefully linked to a *complete FFT system* on the disks that accompany it, on which almost all of the exercises can be either carried out or verified.

The FFT system makes what are otherwise abstract ideas visible and concrete. However, it can only be effective to the extent that the reader makes use of it.

- The *exercises* at the end of each chapter have been carefully constructed to serve as a development and consolidation of the ideas discussed in the text. If possible they should all be attempted. Answers are given at the end of the text, and an instructor's manual with complete solutions is available from the publisher.

We had our best success when we structured the course as follows:

- *Three classroom lectures per week* covering Chapters 1 through 10 and Chapter 12 over a total of 36 lectures. The remaining four chapters, namely 11, and 13 through 15, can easily be read by the students themselves at a later stage. Chapters 16 and 17 are the user's manual for the disks (they have been included as README files on the disks) and will have to be read in order to take full advantage of it. However, they are filled with a large amount of practical material regarding the FFT, and so the students will naturally want to read them anyway.
- *A two-hour problem session per week* in which the students, either in groups or alone, were expected to work problems in the text using pencil and paper, with the instructor thereafter working them on the black-board.
- *A weekly 90-minute computer lab* in which the students were expected to work problems assigned by the lecturer, with help provided by third-year teaching assistants. The lab sessions consisted of the students using the FFT system on the disk to solve assigned problems, examples of which are included in the instructor's manual.
- *A three-hour open-book final exam* on the course material and a *one-hour exam* on the use of the disk.

NORMAN MORRISON

Cape Town, South Africa



---

# Acknowledgments

I am particularly indebted to *Dr. Erwin Brüning*, from whom I learned an immense amount. Dr. Brüning is a fine mathematician with a deep understanding of Fourier analysis and a remarkable sense of what goes on in the physical world. He read the entire manuscript and made many invaluable suggestions, virtually all of which were adopted without question.

I also wish to express my gratitude to *Professor Brian Hahn* for constant encouragement and help regarding the preparation of the disk that accompanies this text. I am also indebted to *Professors R. Becker, R. Braun, C. Brink, G. Brümmer, G. de Jager, B. Downing, J. Greene, M. Inggs, and D. Reddy*, as well as *Dr. D. Martin*, for their encouragement and support.

I am grateful to four of my students, *Sean Borman, David Garvin, Susan Kritzinger, and George Tattersfield*, who read the many drafts of the manuscript and made numerous comments and suggestions on how it could be made more easily understood, and to the large number of excellent students that attended my lectures and who made the writing of this book such a pleasure.

Special thanks to *Lynn Waldron, Dan Franco, Lenny Lotz, and Fuad Tape*. Lynn was always happy to respond to requests for assistance. Dan and Lenny were always there when the technology issues became really complex. Fuad and his staff of maintenance engineers never once kept me waiting longer than was absolutely necessary when my machine needed servicing.

Without the cooperation of the *True BASIC Corporation* it would not have been possible to make available the disks that accompany this text. I thank *John Lutz*, the president of True BASIC, and *Mike Gildersleave* for their assistance in this regard. I am also deeply indebted to the *Chairman's Fund of the Anglo American Corporation*, whose financial support made the writing of this book possible.

Finally, I wish to thank my editor, *George Telecki*, for his excellent suggestions and constant encouragement, and I am also grateful to *Lisa Van Horn and Perry King*, and all other Wiley staff who assisted in the production of this book. Ultimately it is an author's own responsibility to ensure that his work is error free, and so I take full responsibility for any errors and omissions that may still exist in the published form of this book.

N.M.



---

# Nomenclature and Abbreviations

There do not appear to be any established nomenclature standards in Fourier analysis, and so we have elected instead to strive for consistency. Our notation will be as follows:

- $f_p(t) \Leftrightarrow F(n)$  will represent the transformation of a periodic function to its Fourier coefficients, and vice versa.
- $f(t) \Leftrightarrow F(\omega)$  will represent the transformation of a one-time pulse to its Fourier transform, and vice versa.
- $f_k \Leftrightarrow F_n$  will represent the transformation of a discrete sequence to its discrete Fourier spectrum, and vice versa.

When the possibility of confusion arises between  $F(n)$  and  $F(\omega)$ , we shall append a subscript  $p$  to  $F(n)$ . Then

- $F_p(n)$  will be the Fourier spectrum of a periodic function.
- $F(\omega)$  will be the Fourier transform of a pulse.
- $F(n\omega_0)$  will be  $F(\omega)$  that has been sampled at  $\omega = n\omega_0$ .

Other notation that we shall use is as follows:

$\omega$	The continuous frequency variable
$k$	An integer, usually the discrete time variable
$n$	An integer, usually the discrete frequency variable
$\mathbb{R}$	The set of all real numbers
$I$	The set of all integers ( $-\infty$ to $\infty$ )
$\mathbb{C}$	The set of all complex numbers
$\forall n$	For all $n$
$n \in I$	For any integer $n$
■	The end of a proof
□	The end of an example
LHS	Left-hand side
RHS	Right-hand side

iff If and only if  
 wrt With respect to

### The Greek Alphabet

A	$\alpha$	alpha	N	$\nu$	nu
B	$\beta$	beta	$\Xi$	$\xi$	xi
$\Gamma$	$\gamma$	gamma	O	$\circ$	omicron
$\Delta$	$\delta$	delta	$\Pi$	$\pi$	pi
E	$\epsilon$	epsilon	P	$\rho$	rho
Z	$\zeta$	zeta	$\Sigma$	$\sigma$	sigma
H	$\eta$	eta	T	$\tau$	tau
$\Theta$	$\theta$	theta	$\Upsilon$	$\upsilon$	upsilon
I	$\iota$	iota	$\Phi$	$\phi$	phi
K	$\kappa$	kappa	X	$\chi$	chi
$\Lambda$	$\lambda$	lambda	$\Psi$	$\psi$	psi
M	$\mu$	mu	$\Omega$	$\omega$	omega

---

**Introduction to  
Fourier Analysis**

---



---

**PART 1**

---

# Continuous Fourier Analysis



# Background

This book is primarily for electrical engineers, although people from other fields wishing to learn about Fourier analysis will readily find in it the starting point that they are seeking.

---

## 1.1 TYPES OF PROBLEMS

---

Fourier analysis is now central to electrical engineering, and there is scarcely a course in a modern curriculum for which at least some knowledge of the subject is not required. A few simple examples of the types of problems that it will enable us to solve are as follows:

### Network Analysis

Given the mathematical statement for the input and the details of the electrical network shown in Figure 1.1, find an expression for the response. The input may be a one-time pulse of current or voltage, or it may be a periodic function that repeats itself endlessly.

### Modulation

Given a waveform, which we shall call the signal, we desire to modulate it onto a carrier. (See Fig. 1.2.) One method is to form the product of the signal and the carrier, which is typically a sine wave. Given the mathematical definition of the signal, Fourier analysis enables us to specify precisely the mathematical representation and properties of the modulated output.

### Sampling

Signals are often sampled and digitized prior to transmitting them. (See Figure 1.3.) Given the necessary details of such a signal we would like to know how fast we must sample it in order to be sure that we will be able to reconstruct it from those samples.

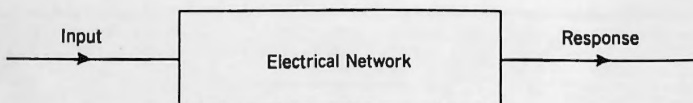


Figure 1.1.

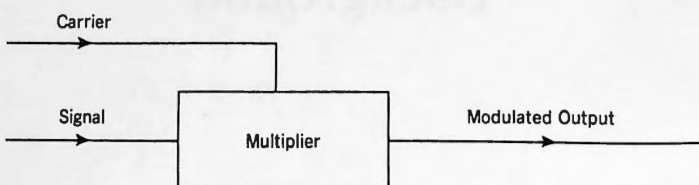


Figure 1.2.

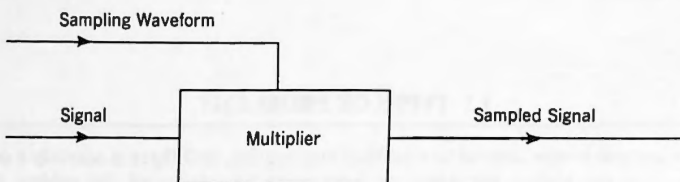


Figure 1.3.

## 1.2 HISTORICAL BACKGROUND

---

Electrical engineering did not yet exist when Fourier submitted his celebrated treatise "The Analytical Theory of Heat" to the Paris Academy of Science in 1807 (it would not be published until 1822). It is thus almost certain that neither he nor any of the three referees, Lagrange, Laplace, and Legendre, could have conceived that his (and their) discoveries would some day become the very foundation on which the entire field of what is known today as electrical engineering would stand.

Yet it was only a few years after his death in 1830 that people who were already being called "electricians" were beginning to make use of his discoveries regarding heat, and of the Laplace transform (discovered by Lagrange<sup>†</sup>), and of the Fourier transform (discovered by Laplace<sup>†</sup>), but now applying them instead to problems involving electricity—first to telegraphy, later to telephony, and eventually to radio communication and power systems engineering.

Today the discoveries of Fourier and Laplace form the basis of what we call **Fourier analysis**, and the methods initiated by them underlie much of the mathematics that we now apply to a huge variety of technical problems that have been spawned by the information age in which we live.

<sup>†</sup>See Stigler (1986). (References will always be quoted in this way, with their full details being listed in Appendix 1.)

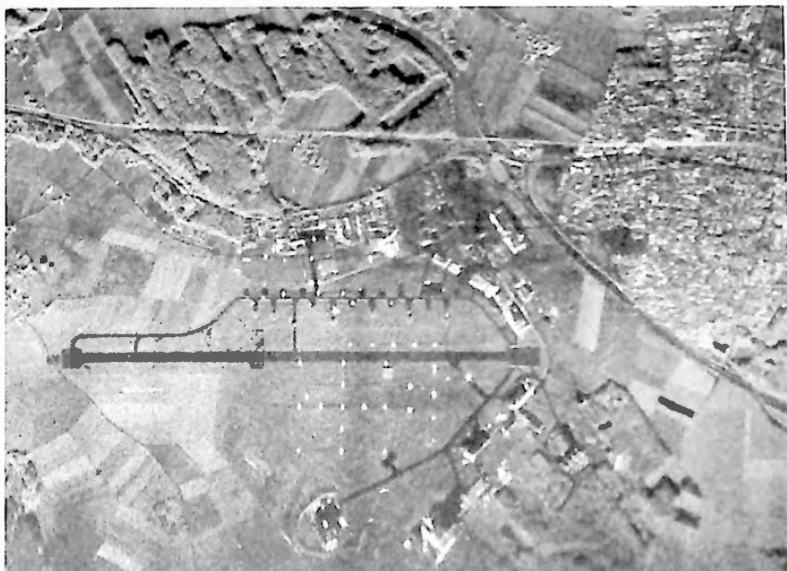


**Figure 1.4.** An aerial photograph of the Oberpfaffenhofen airport produced by airborne synthetic aperture radar (SAR) with signal processing using the fast Fourier transform (FFT). (Reproduced courtesy of the German Aerospace Research Establishment (DLR), Institute for Radiofrequency Technology, Oberpfaffenhofen, Germany. Image obtained with the DLR's multifrequency airborne synthetic aperture system E-SAR during overflights of the DLR Oberpfaffenhofen research center.)

This book tells that story, mostly from a mathematical standpoint, but occasionally from an historical one, the story of a body of mathematical theory and an applied discipline between which there is a fit so remarkable and so beautiful that one is often hard-pressed to remember that Fourier was concerned only with the flow of heat and Laplace (when he did the work to which we refer) only with mathematical probability, and in all likelihood both knew very little whatsoever about electricity.

Prior to 1830 electricity was in the hands of men who today would be described as physicists, investigating its properties simply because they existed, men like Franklin, Faraday, Oersted, and Volta, but then came the telegraph, and with it the birth of electrical engineering.

As with many explosive discoveries that are destined to alter the course of history, the telegraph originated spontaneously in a number of places—with Gauss and Weber in Göttingen, Germany, in 1833, and with Henry in the United States at about the same time, all of whom sent messages over some distance by electricity through wires. Made possible by Oersted's discovery in 1820 of the magnetic effect of a current, which was made possible by Volta's discovery of the chemical battery in 1800, telegraphy soon passed into the hands of men more interested in practice and profit, "electrical engineers" like Morse in America and Cooke in England, the last of whom constructed the first commercially successful telegraph links in 1835 and 1836.

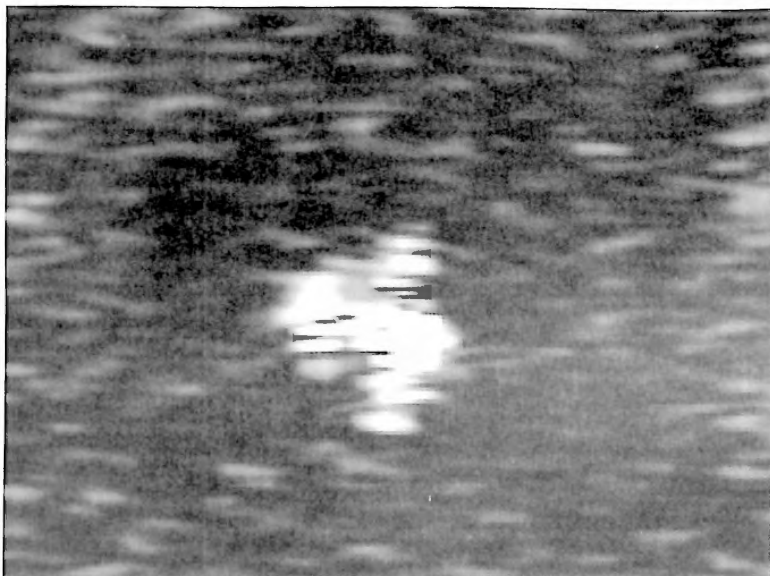


**Figure 1.5.** An aircraft on the Oberpfaffenhofen airport.

(Reproduced courtesy of the German Aerospace Research Establishment (DLR), Institute for Radiofrequency Technology, Oberpfaffenhofen, Germany. Image obtained with the DLR's multifrequency airborne synthetic aperture system E-SAR during overflights of the DLR Oberpfaffenhofen research center.)

Each generation of discoveries formed a springboard for the next. In 1840 Wheatstone and Cooke in England began to introduce a series of instruments (some of them even driven by punched paper tape) that were so effective and well conceived that they were still being used in the British Post Office as recently as 1926. Morse's recording telegraph, first deployed in 1835 in America, was, with only minor modifications, widely used in the United States and many other countries well into the 1920s.

Each level of technology also made possible a new level of business achievement. At first the telegraph was used only between nearby towns. Then lines began to spring up all over England, Europe, and the United States, and soon undersea lines began to link England to the continent in a number of places. The railroads, spawned by the dual inventions of steam and steel, were now also beginning to crisscross those same regions, and it was soon obvious that the telegraph and the railroads were natural allies—alongside every railway line the poles and wires of the newly discovered information-carrying miracle of telegraphy.

Almost everywhere that the telegraph ran newspapers began to spring up, and thus were sown the seeds of the information age in which we live today.

The early electricians, as electrical engineers were then known, mainly improvised, guided only by a practical sense of what will and will not work. Mathematics had yet to come to electrical engineering.

At first they tried iron wire and then discovered the advantages of copper. They experimented with various types of insulation, and England, which controlled Malaya, became the sole supplier of gutta-percha, a rubberlike compound grown in the faraway eastern jungles and found to be an ideal insulator for the coaxial cables that were being laid under the English Channel and the Irish Sea. Because of this, and because of their natural inventiveness, British engineers and entrepreneurs were soon at the peak of the pyramid of worldwide telegraph activity.

In 1854 the time had come to take on the greatest challenge of them all, the 2000 mile trans-Atlantic link that would join London to New York. A group of British promoters, the directors of the Atlantic Telegraph Company, wise enough to know that this was an entirely new kettle of fish, asked a 30-year-old professor of natural philosophy of the University of Glasgow named **William Thomson** to undertake a mathematical study of the problems that they were likely to encounter. Today best remembered as Lord Kelvin, Thomson quickly set to work, and thus was born the idea that electrical engineering should be founded on a solid bedrock of mathematics.

He already knew of Fourier's seminal work, which had finally been published in 1822, fifteen years after it was first submitted to the Academy, and as a student at Cambridge he had completely mastered it in two weeks, thereafter often referring to it as a "mathematical poem." He had also formed there what was to be a lifelong friendship with George Gabriel Stokes, of Stokes-theorem fame, then a Cambridge mathematics professor, and had studied other areas that were soon to be of inestimable help to him, such as the potential theory of Gauss and Green.

After graduation he spent a year in the Paris laboratory of Regnault working on the thermal properties of steam, and in 1848, at the ripe old age of 24, he conceived of the idea of absolute zero and of the temperature scale that now bears his name. In 1851, aged 27, he delivered a paper to the Royal Society that was to be the foundation of what has today become the field of thermodynamics, including its second law, probably the most profound theoretical contribution of his long and prolific life.

Shortly after starting work on the Atlantic cable project he was able to show that the 2000-mile coaxial cable being envisaged would be governed by the same partial differential equation (PDE) as the one that Fourier had derived regarding the flow of heat, some 50 years earlier. (Fourier's PDE is known as the "heat equation" and Thomson's as the "telegraph equation," but mathematically they are identical.) This immediately told him that all of the work that Fourier had done on the heat equation would then also be applicable to the task that now lay before him.

Having established the PDE that governed the problem, he then set about solving it. The solutions that he developed were based partly on Fourier's infinite series methods and partly on the independent mathematical discoveries being made by Stokes, with whom he was in constant contact.

Stokes had taken another tack, different from the infinite-series approach of Fourier, and had derived a closed-form integral solution of Thomson's telegraph equation, based on what is today called the Green's function for the PDE. (Its mathematical structure is very similar to what we call convolution, which we consider in Chapter 7.)

All of this mathematics in Thomson's remarkably able hands soon culminated in what was perhaps the greatest engineering achievement of the nineteenth century, the first trans-Atlantic cable of 1858, through which passed for a short while intelligence between London and New York.

Alas, history records that the chief engineer of the cable company, a certain (medical) Dr. Whitehouse, was a staunch antitheorist who derided mathematical theory as being dangerous and irrelevant despite Thomson's manifest successes. Whitehouse determined that very high voltages would be the answer to the intersymbol interference that they were soon experiencing, and that Thomson had predicted if messages were sent beyond a certain baud rate, and so he ordered that a series of huge induction coils be constructed with which he began to drive the line with no less than 2000 volts. Of course this soon broke down the cable's insulation and it ceased to work after only a few weeks of history-making achievement.

Whitehouse was dismissed and Thomson immediately began preparations for the next attempt by exploring even wider aspects of the problem, such as the manufacture of purer copper that would have less resistance per mile and the development of ultrasensitive measuring devices so that extremely small signals could be detected. He also took a strong and creative interest in the shipboard mechanical-engineering aspects of cable-laying technology and in problems relating to a cable's strength and to the manufacture of cables. **In short, he was a total engineer.**

After a brief delay caused by the American Civil War, a new and better cable was successfully laid in 1866, and then another and another, so that soon England was linked to almost every corner of the globe. One might imagine that by then the need for mathematical theory in electrical engineering would have become firmly accepted, but that was not to be the case for many more decades.

Before commencing our study of Fourier analysis we pause briefly to tell of some of Thomson's other remarkable achievements. In later life he developed a complete range of measuring instruments for physics and electricity, many of them still in use today, and even perfected the mariner's compass. He also established standards for all of the quantities in use in physics, an achievement that ranks with his undersea cable engineering and contributions in thermodynamics. In all he published over 300 major technical papers during the 53 years that he held the chair of Natural Philosophy at the University of Glasgow. Had he been Japanese he would almost certainly have been declared a living national treasure.

William Thomson, Lord Kelvin, died in 1907 at the age of 83. He was buried in Westminster Abbey in London where he lies today, adjacent to Isaac Newton.<sup>†</sup>

<sup>†</sup>Information for Lord Kelvin's story and on Oliver Heaviside, whom we shall encounter frequently, came from two sources: An article in *The Encyclopedia Britannica* (1926) and Nahin (1987).

---

## CHAPTER 2

---

# Fourier Series for Periodic Functions

### 2.1 ORTHOGONALITY OF VECTORS AND FUNCTIONS

---

Two vectors are said to be orthogonal if their inner product is equal to zero. Letting  $\mathbf{u}$  and  $\mathbf{v}$  be two such  $n$ -vectors, both assumed to be real, we write this as

$$(\mathbf{u}, \mathbf{v}) = 0 \quad (2.1)$$

by which we mean

$$\sum_{i=1}^n u_i v_i = 0 \quad (2.2)$$

As an example, the three vectors

$$\mathbf{u} = \begin{bmatrix} 1 \\ 4 \\ 1 \end{bmatrix} \quad \mathbf{v} = \begin{bmatrix} 1 \\ 0 \\ -1 \end{bmatrix} \quad \mathbf{w} = \begin{bmatrix} -2 \\ 1 \\ -2 \end{bmatrix}$$

are all orthogonal to each other, as is easily verified by the fact that the inner product of any two of them is zero. Thus

$$(\mathbf{u}, \mathbf{v}) = 1 \times 1 + 4 \times 0 + 1 \times (-1) = 0 \quad (2.3)$$

with a similar result for  $(\mathbf{u}, \mathbf{w})$  and  $(\mathbf{v}, \mathbf{w})$ .

When a set of such vectors

$$S = \{\mathbf{u}_1, \mathbf{u}_2, \mathbf{u}_3, \dots\} \quad (2.4)$$

satisfies the condition

$$(\mathbf{u}_n, \mathbf{u}_m) = 0 \quad \text{when } n \neq m \quad (2.5)$$

then we say that the elements of  $S$  are **mutually orthogonal** and that they form an **orthogonal basis** for the space spanned by  $S$ . Then any vector lying in that space can be expressed as a linear combination of those basis vectors.

The concept of orthogonality and basis can be extended to **sets of functions**, and in what follows we shall make repeated use of this property. Thus, consider the set of functions

$$S = \{f_1(t), f_2(t), f_3(t), \dots, f_n(t), \dots\} \quad (2.6)$$

We say that the members of  $S$  form an orthogonal set over the interval  $a < t < b$  if

$$\int_a^b f_n(t) f_m(t) dt = 0 \quad \text{when } n \neq m \quad (2.7)$$

where the integral represents the inner product of the pair of functions being considered. In the next section we shall show that the set

$$S = \{\dots e^{-j3\omega_0 t}, e^{-j2\omega_0 t}, e^{-j\omega_0 t}, 1, e^{j\omega_0 t}, e^{j2\omega_0 t}, \dots, e^{j\pi\omega_0 t}, \dots\} \quad (2.8)$$

forms such an orthogonal set, and hence forms a basis for functions lying in the space spanned by  $S$ . This will then lead to the ability to express periodic current or voltage waveforms as linear combinations of these functions.

We begin with **periodic** functions but later on we shall show that these techniques can be extended to **nonperiodic** waveforms as well, that is, to one-time pulses.

## 2.2 THE COMPLEX EXPONENTIALS

---

We now state a few elementary facts from complex algebra that we shall be using frequently throughout the text. Let  $z = x + jy$  be any point in the complex plane where  $j = \sqrt{-1}$ . Then

$$z^* = x - jy \quad (2.9)$$

$$\text{mod}(z) = |z| = (x^2 + y^2)^{1/2} = (zz^*)^{1/2} \quad (2.10)$$

$$\arg(z) = \arctan(y/x) \quad (2.11)$$

$$z + z^* = 2\text{Re}(z) = 2x \quad (2.12)$$

$$z - z^* = 2j\text{Im}(z) = 2jy \quad (2.13)$$

$$e^{\pm j\Theta} = \cos(\Theta) \pm j \sin(\Theta) \quad (2.14)$$

$$\cos(\Theta) = [e^{j\Theta} + e^{-j\Theta}]/2 \quad (2.15)$$

$$\sin(\Theta) = [e^{j\Theta} - e^{-j\Theta}]/2j \quad (2.16)$$

### Accompanying Disk

Readers will find that they can read this entire book without ever making use of the accompanying disk, and that all of it is still completely intelligible. However, far more will be obtained if use is continually made of the disk, since then what are abstract concepts will be made visible and concrete.

There are two modules on the disk,

- The fast Fourier transform (FFT) system
- A module called PLOTS

We shall soon begin to make extensive use of the FFT system.

PLOTS consists of a number of subprograms, each of which is a demonstration of something important in the development that we are undertaking.

The demonstration called ORTHOGONALITY(G) illustrates very effectively what we are discussing here regarding **orthogonality**. By running it you will soon see how the orthogonality property of the set of **sines** and **cosines** operates. These functions are closely related to the complex exponentials that we are now beginning to investigate and we shall soon see that the orthogonality of the sines and cosines is directly linked to the orthogonality of the complex exponentials.

Orthogonality is the mathematical foundation on which Fourier analysis is based. Once fully understood, all of the results that are derived from it in the rest of this text will appear to be almost trivial.

In this chapter we are concerned with the complex exponentials  $e^{jn\omega_0 t}$ , where  $n$  is every integer, positive or negative. Taken together they form the following set:

$$S = \{ \dots e^{-j3\omega_0 t}, e^{-j2\omega_0 t}, e^{-j\omega_0 t}, 1, e^{j\omega_0 t}, e^{j2\omega_0 t}, \dots, e^{jn\omega_0 t}, \dots \} \quad (2.17)$$

The set of complex exponentials so defined possesses an orthogonality property that will form the basis on which all the work of this chapter, and indeed all of the rest of this text, depends. This is stated in the following theorem.

#### ■ THEOREM 2.1: Orthogonality of the Complex Exponentials

The complex exponentials  $e^{jn\omega_0 t}$  satisfy the orthogonality condition

$$\frac{1}{T_0} \int_{-T_0/2}^{T_0/2} e^{jn\omega_0 t} e^{jm\omega_0 t^*} dt = \begin{cases} 0 & \text{if } n \neq m \\ 1 & \text{if } n = m \end{cases} \quad (2.18)$$

where  $T_0 = 2\pi/\omega_0$ .

*Proof:*

$$\frac{1}{T_0} \int_{-T_0/2}^{T_0/2} e^{jn\omega_0 t} e^{jm\omega_0 t^*} dt = \frac{1}{T_0} \int_{-T_0/2}^{T_0/2} e^{j(n-m)\omega_0 t} dt \quad (2.19)$$

When  $n \neq m$ , then  $n - m$  is a nonzero integer, which we shall call  $p$ , and so (2.19) continues as

$$\begin{aligned} \dots &= \frac{1}{T_0} \int_{-T_0/2}^{T_0/2} e^{jp\omega_0 t} dt = \frac{e^{jp\omega_0 t}}{T_0 jp\omega_0} \Big|_{-T_0/2}^{T_0/2} \\ &= \frac{e^{jp\pi} - e^{-jp\pi}}{T_0 jp\omega_0} = 0 \end{aligned} \quad (2.20)$$

On the other hand, when  $n = m$  then (2.19) continues as

$$\dots = \frac{1}{T_0} \int_{-T_0/2}^{T_0/2} dt = 1 \quad (2.21)$$

and the proof is complete. ■

*Note:* In all of the preceding we have used the symmetric interval

$$-\frac{T_0}{2} \quad \text{to} \quad \frac{T_0}{2}$$

over which we carried out our integration, but the reader should be aware that there is nothing special about that interval and that the preceding is true as long as integration takes place over **any complete interval** of length  $T_0$ . (Go back and verify this.) It will be seen later that there are many practical situations where it is preferable to integrate from say 0 to  $T_0$  rather than from  $-T_0/2$  to  $T_0/2$ .

We now make use of this orthogonality property as follows. Let  $f_p(t)$  be a periodic waveform with period  $T_0$ , and assume that it can be expressed as an infinite sum of complex exponentials, that is, that

$$f_p(t) = \sum_{n=-\infty}^{\infty} F(n) e^{jn\omega_0 t} \quad (2.22)$$

where values for the constants  $F(n)$  are yet to be determined. Note that this is not an unreasonable assumption since the complex exponentials on the right-hand side (RHS) all repeat at least once whenever  $t$  is increased by  $T_0$ , and so both sides of (2.22) are periodic with period  $T_0$ . We must now show that we can in fact find a

formula for generating the constants  $F(n)$ , and to do that we multiply both sides by  $e^{-jm\omega_0 t}$  and integrate, obtaining

$$\begin{aligned} & \frac{1}{T_0} \int_{-T_0/2}^{T_0/2} f_p(t) e^{-jm\omega_0 t} dt \\ &= \frac{1}{T_0} \int_{-T_0/2}^{T_0/2} \sum_{n=-\infty}^{\infty} F(n) e^{jn\omega_0 t} e^{-jm\omega_0 t} dt \end{aligned} \quad (2.23)$$

We now interchange the order of summation and integration on the right (we return to that later), and so (2.23) continues as

$$\dots = \sum_{n=-\infty}^{\infty} F(n) \left[ \frac{1}{T_0} \int_{-T_0/2}^{T_0/2} e^{jn\omega_0 t} e^{-jm\omega_0 t} dt \right] \quad (2.24)$$

Then, by Theorem 2.1, the quantity in square brackets is equal to zero as long as  $n \neq m$ . However, for the single case when  $n = m$  it is equal to 1, and so (2.24) collapses down to the single term  $F(m)$ . We have thus shown that

$$\frac{1}{T_0} \int_{-T_0/2}^{T_0/2} f_p(t) e^{-jm\omega_0 t} dt = F(m) \quad (2.25)$$

We now replace  $m$  by  $n$ , obtaining

$$F(n) = \frac{1}{T_0} \int_{-T_0/2}^{T_0/2} f_p(t) e^{-jn\omega_0 t} dt \quad (2.26)$$

which is the required formula for finding the constants  $F(n)$  in (2.22). We summarize all of this as Theorem 2.2. (See important note on p. 61.)

### ■ THEOREM 2.2: Complex Fourier Series for Periodic Functions

Let  $f_p(t)$  be periodic with period  $T_0$ , defined analytically. Then it can also be represented by the infinite series of complex exponentials

$$f_p(t) = \sum_{n=-\infty}^{\infty} F(n) e^{jn\omega_0 t} \quad (2.27)$$

where the coefficients  $F(n)$  can be found from the analytical definition of  $f_p(t)$  as follows:

$$F(n) = \frac{1}{T_0} \int_{-T_0/2}^{T_0/2} f_p(t) e^{-jn\omega_0 t} dt \quad (\forall n) \quad (2.28)$$

Later in this chapter we shall examine the question of what sorts of functions can be represented by a Fourier series of the kind appearing in (2.27) and we shall find that **any physically realizable** periodic waveform can be restated in that form. Thus what Theorem 2.2 means is that

**Any physically realizable periodic waveform can be expressed as a sum of complex exponentials.**

This and the corresponding statement for one-time pulses that we examine in Chapter 3 constitute the central results of Fourier analysis and form the basis for all the work that we do in the rest of this book.

The various parts of the last theorem have the following names:

- Equation (2.27) is called the **synthesis equation**.
- Equation (2.28) forms what is called the **analysis equation**.
- The constants  $F(n)$  are called the **complex Fourier coefficients**.
- The term  $F(0)$  is called the **average value** or **dc value** of the waveform. It is sometimes also called the **zeroth harmonic**.
- The pair of terms

$$h(1) \equiv F(1)e^{j1\omega_0 t} + F(-1)e^{-j1\omega_0 t} \quad (2.29)$$

is called the **fundamental** or sometimes the **first harmonic**.

- The next pair

$$h(2) \equiv F(2)e^{j2\omega_0 t} + F(-2)e^{-j2\omega_0 t} \quad (2.30)$$

forms what is called the **second harmonic**, and so on, the  **$n$ th harmonic** being the pair

$$h(n) \equiv F(n)e^{jn\omega_0 t} + F(-n)e^{-jn\omega_0 t} \quad (2.31)$$

In order to conserve energy we use the following notation to represent Theorem 2.2.

**Definition:** The expression

$$f_p(t) \Leftrightarrow F(n)$$

means that the periodic waveform  $f_p(t)$  has  $F(n)$  as its Fourier coefficients per (2.28). Moreover  $F(n)$  can be used to synthesize  $f_p(t)$  per (2.27).

Theorem 2.2 has the structure shown in Figure 2.1.

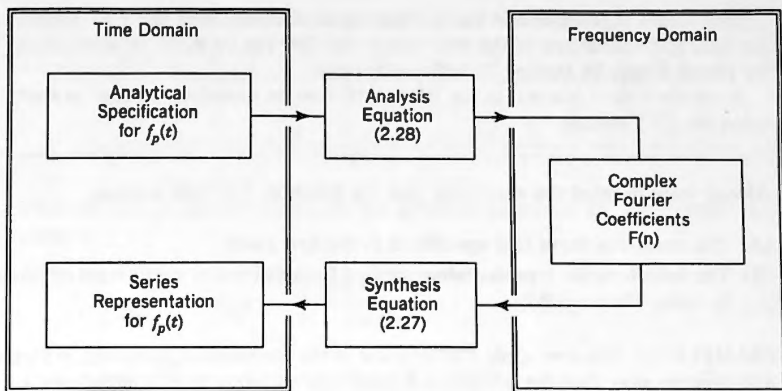


Figure 2.1. Theorem 2.2 for periodic waveforms.

Starting with a periodic waveform  $f_p(t)$  specified analytically in the **time domain** on the left of the figure, we can send its details to the analysis equation, thereby producing the complex Fourier coefficients  $F(n)$  in the **frequency domain**.

Those coefficients can then be examined and conclusions can be drawn regarding  $f_p(t)$ . They can also be sent to the synthesis equation, producing once again the periodic function in the time domain, but this time as an infinite series of complex exponentials.

Think of this as sending the waveform to a frequency analyzer, a system that analyzes the input and then calculates the values of the coefficients  $F(n)$ . As we shall soon see, the FFT system on your disk is **precisely** such an analyzer, and very much more.

#### Accompanying Disk

The FFT system on the accompanying disk performs all of the operations shown in Figure 2.1.

The system allows you to enter the analytical definition of a periodic waveform, from which it produces a vector of samples for use by the FFT.

The values so created are then operated on by the Analysis procedure, and numerical values of the Fourier coefficients are produced in the frequency domain. These can be plotted by the system and they can also be displayed numerically.

Starting from the Fourier coefficients we can then carry out the Synthesis procedure. The result is a numerical version of the original periodic waveform, now back in the time domain.

If we so desire, we can also use the system to operate on the Fourier coefficients in the frequency domain, performing a variety of signal-processing operations prior to inverting the result back to the time domain.

The values that we obtain for the Fourier coefficients from the FFT system are only approximations of the true values, but they can be made as accurate as we please simply by making  $N$  sufficiently large.

Read the User's Manual in the README files on your disk in order to start using the FFT system.

Always keep in mind the two forms that the function  $f_p(t)$  can assume:

- (A) The analytical form that specifies it in the first place
- (B) The infinite series representation created from its Fourier coefficients obtained by using Theorem 2.2.

**EXAMPLE 2.1:** We now apply Theorem 2.2 to the waveform  $f_p(t)$  shown in Figure 2.2. First we note that the analytical definition of the waveform is as follows:

$$f_p(t) = \begin{cases} 0 & (-2 < t < -1) \\ 1 & (-1 < t < 1) \\ 0 & (1 < t < 2) \end{cases} \quad f_p(t+4) = f_p(t)$$

Observe how the definition is made up of three parts over the period that we have considered. Observe also how we show that the period  $T_0$  is equal to 4.

In order to restate  $f_p(t)$  as an infinite series of complex exponentials we must first find the Fourier coefficients  $F(n)$ . We use the analysis equation, and for that purpose we note that  $\omega_0 = 2\pi/T_0 = \pi/2$ . Then

$$\begin{aligned} F(n) &= \frac{1}{T_0} \int_{-T_0/2}^{T_0/2} f_p(t) e^{-jn\omega_0 t} dt = \frac{1}{4} \int_{-1}^1 1 e^{-jn\pi t/2} dt \\ &= \frac{1}{4} \left. \frac{e^{-jn\pi t/2}}{-jn\pi/2} \right|_{-1}^1 = \frac{1}{2} \frac{e^{jn\pi/2} - e^{-jn\pi/2}}{2j(n\pi/2)} \\ &= \frac{1}{2} \frac{\sin(n\pi/2)}{n\pi/2} \end{aligned}$$

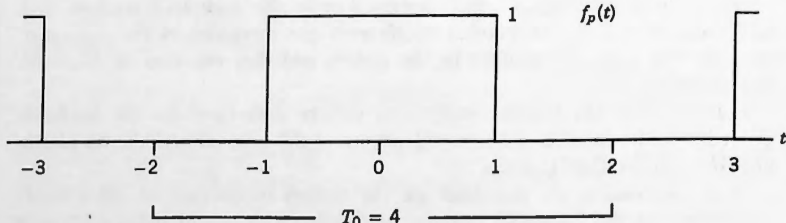


Figure 2.2.

TABLE 2.1 Fourier Coefficients of Example 2.1

$n$	0	$\pm 1$	$\pm 2$	$\pm 3$	$\pm 4$	$\pm 5$
$F(n)$	$\frac{1}{2}$	$\frac{1}{\pi}$	0	$-\frac{1}{3\pi}$	0	$\frac{1}{5\pi}$

Thus for this particular waveform the general expression for the Fourier coefficients is

$$F(n) = \frac{1}{2} \frac{\sin(n\pi/2)}{n\pi/2} \quad (n \text{ an integer}) \quad (2.32)$$

This completes the analysis portion. We display some of the coefficients in Table 2.1. Using these values for  $F(n)$ , the synthesis equation (2.27) now gives us the following series representation for  $f_p(t)$ :

$$\begin{aligned} f_p(t) &= \sum_{n=-\infty}^{\infty} F(n) e^{jn\pi t/2} \\ &= \frac{1}{\pi} \left[ \dots + \frac{1}{5} e^{-j5\pi t/2} - \frac{1}{3} e^{-j3\pi t/2} + \frac{1}{1} e^{-j\pi t/2} + \frac{\pi}{2} \right. \\ &\quad \left. + \frac{1}{1} e^{j\pi t/2} - \frac{1}{3} e^{j3\pi t/2} + \frac{1}{5} e^{j5\pi t/2} + \dots \right] \end{aligned} \quad (2.33)$$

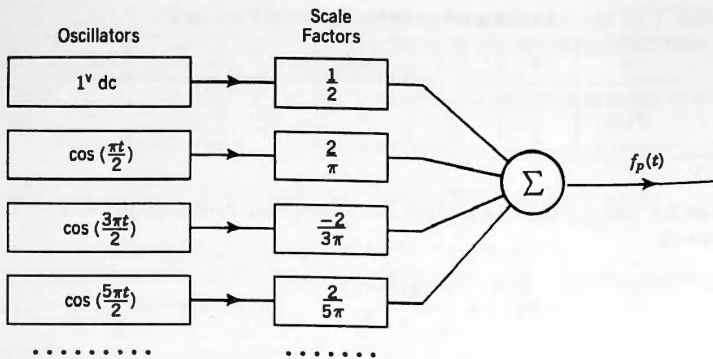
In this series form we can see precisely what our waveform is comprised of. The average value is  $F(0) = \frac{1}{2}$ , which is in agreement with what we see from Figure 2.2. The first few nonzero harmonics are

$$\begin{aligned} h(1) &= F(1)e^{j\omega_0 t} + F(-1)e^{-j\omega_0 t} \\ &= \frac{1}{\pi} e^{j\pi t/2} + \frac{1}{\pi} e^{-j\pi t/2} = \frac{2}{\pi} \cos \frac{\pi t}{2} \\ h(3) &= \frac{-1}{3\pi} e^{j3\pi t/2} + \frac{-1}{3\pi} e^{-j3\pi t/2} = \frac{-2}{3\pi} \cos(3\pi t/2) \end{aligned}$$

and so on. What all of this means is that we could synthesize our waveform by combining the outputs of an array of cosine oscillators, using the amplitudes shown earlier. Thus our waveform could be generated as follows:

$$f_p(t) = \frac{1}{2} + \frac{2}{\pi} \cos \frac{\pi t}{2} - \frac{2}{3\pi} \cos \frac{3\pi t}{2} + \frac{2}{5\pi} \cos \frac{5\pi t}{2} - \dots$$

This is depicted in Figure 2.3.

Figure 2.3. Synthesis of  $f_p(t)$ .

The function appearing in (2.32) occurs so often that it has been given a special name.

### Definition

$$\text{Sa}(x) \equiv \frac{\sin(x)}{x} \quad (2.34)$$

"Sa" stands for "sine over argument" and is often pronounced as "sah." (See Notes and Comments at the end of the chapter regarding a related function called  $\text{sinc}(x)$ , which is used by many authors.)  $\text{Sa}(x)$  is depicted in Figure 2.4a and is seen to have a maximum value of unity at  $x = 0$  and approaches zero in an oscillatory manner as  $x$  goes to  $\pm\infty$ . Because  $\sin(n\pi) = 0$  it follows that  $\text{Sa}(x)$  crosses the  $x$ -axis whenever  $x$  is an integral multiple of  $\pi$ .

Using (2.34) we can now restate (2.32) as

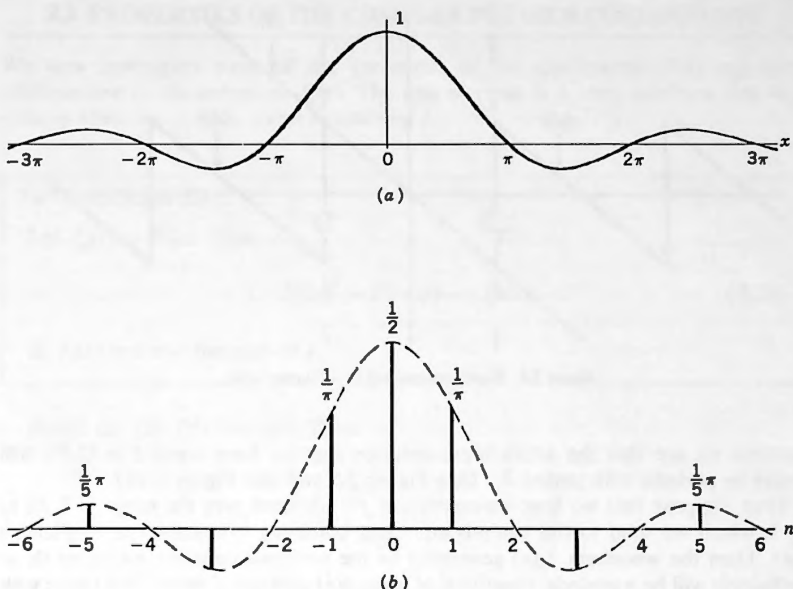
$$F(n) = \frac{1}{2}\text{Sa}\frac{n\pi}{2} \quad (n \text{ an integer}) \quad (2.35)$$

which is shown in Figure 2.4b. Observe that we now have a set of lines, each of which represents a coefficient in (2.33) with their lengths given by (2.35) whenever  $n$  is an integer. However, if we let  $n$  take on all real values, then we get the dashed line shown in Figure 2.4b, which is the **envelope** of the ends of the lines.

The infinite series representation of  $f_p(t)$  shown in (2.33) can now be written as

$$f_p(t) = \frac{1}{2} \sum_{n=-\infty}^{\infty} \text{Sa} \frac{n\pi}{2} e^{jn\pi t/2} \quad (2.36)$$

This then is the **complex Fourier series** representation of the periodic waveform that

Figure 2.4. (a).  $\text{Sa}(x)$ . (b).  $\frac{1}{2} \text{Sa}(n\pi/2)$ .

we have been considering. It is a remarkably compact expression, and the surprising thing is that it retains the extremely simple structure

$$f_p(t) = \sum_{n=-\infty}^{\infty} F(n) e^{jn\omega_0 t} \quad (2.37)$$

no matter how complicated the waveform that it represents.  $\square$

The procedure that we have just followed in this simple case is actually of great mathematical and engineering importance. It represents a distinct break with the earlier **power series** expansions of functions, a format that is completely unable to handle periodic waveforms of the kind just considered.

In the preceding example we saw that the analytical statement for  $f_p(t)$  was made up of various expressions that applied over only parts of the  $t$ -axis, and it was not necessary that we have a single unified analytical expression for it. If the analytical statement does consist of multiple expressions, then we simply break up the integral (2.28) and evaluate it piece by piece over the ranges in which the respective statements apply.

Note also that (2.28) only requires that our waveform be specified over one complete period with no concern being given to its definition outside of that range. However, because of the periodicity of the complex exponentials used in the synthesis

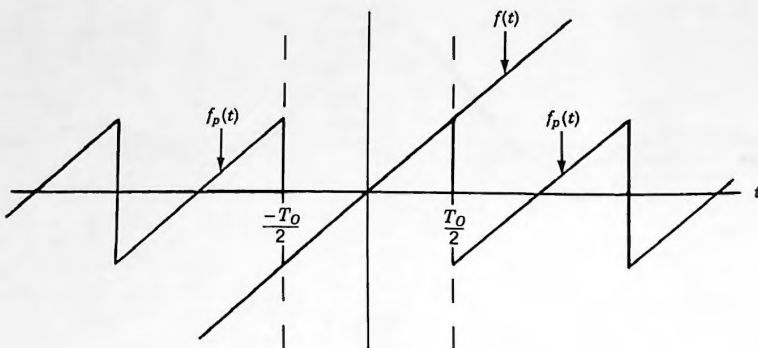


Figure 2.5. Waveform created by a Fourier series.

equation we see that the series representation that we have created in (2.27) will always be periodic with period  $T_0$ . (See Figure 2.5 and also Figure 2.10.)

Thus, suppose that we have an expression  $f(t)$  defined over the range  $-T_0/2$  to  $T_0/2$ , which we send to the analysis equation, obtaining values for the coefficients  $F(n)$ . Then the waveform  $f_p(t)$  generated by the synthesis equation based on those coefficients will be a periodic repetition of what  $f(t)$  consists of inside that range with no regard to what it was outside of it. The resulting waveform  $f_p(t)$  created by the synthesis equation is called the **periodic extension** of  $f(t)$ .

**Fourier series are the only series that inherently repeat a function in a periodic manner. In engineering, waveforms that repeat periodically are extremely common.**

#### Accompanying Disk

The programs A through F in PLOTS are all demonstrations of how Fourier series work.

Each program has a short introduction explaining what it is meant to show. By running them you will soon get a feel for what can be done with Fourier series and how they can be used to express various waveforms as sums of complex exponentials.

From those programs you will see how Fourier series are used to find solutions for the **telegraph equation** that William Thomson (Lord Kelvin) derived in 1854 when he began the mathematical studies that led to the first trans-Atlantic telegraph cable of 1858.

You will also see how they can be used to model the response of a resistance-inductance-capacitance (**RLC**) electrical network to a periodic waveform as the input. (You will be able to select values for  $R$ ,  $L$ , and  $C$ , and to observe the results on the waveform emerging from the network.)

### 2.3 PROPERTIES OF THE COMPLEX FOURIER COEFFICIENTS

We now investigate some of the properties of the coefficients  $F(n)$  and their relationships to the nature of  $f_p(t)$ . The first of these is a basic attribute that they possess whenever  $f_p(t)$  is a real function of  $t$ .

#### ■ THEOREM 2.3

Let  $f_p(t) \Leftrightarrow F(n)$ . Then

$$F(n)^* = F(-n) \quad (\forall n) \quad (2.38)$$

iff  $f_p(t)$  is a real function of  $t$ .

*Proof:* (a) Let  $f_p(t)$  be real. Then

$$\begin{aligned} F(n)^* &= \left[ \frac{1}{T_0} \int_{-T_0/2}^{T_0/2} f_p(t) e^{-jn\omega_0 t} dt \right]^* \\ &= \frac{1}{T_0} \int_{-T_0/2}^{T_0/2} f_p(t)^* e^{jn\omega_0 t} dt \\ &= \frac{1}{T_0} \int_{-T_0/2}^{T_0/2} f_p(t) e^{jn\omega_0 t} dt = F(-n) \end{aligned} \quad (2.39)$$

(b) On the other hand, let  $F(n) = F(-n)^*$ . Then

$$\begin{aligned} \frac{1}{T_0} \int_{-T_0/2}^{T_0/2} f_p(t) e^{-jn\omega_0 t} dt &= \left[ \frac{1}{T_0} \int_{-T_0/2}^{T_0/2} f_p(t) e^{jn\omega_0 t} dt \right]^* \\ &= \frac{1}{T_0} \int_{-T_0/2}^{T_0/2} f_p(t)^* e^{-jn\omega_0 t} dt \end{aligned} \quad (2.40)$$

from which

$$\frac{1}{T_0} \int_{-T_0/2}^{T_0/2} [f_p(t) - f_p(t)^*] e^{-jn\omega_0 t} dt = 0 \quad (\forall n) \quad (2.41)$$

This states that the function in square brackets has all of its Fourier coefficients equal to zero, and that can only mean that the function in square brackets is itself zero.

Thus we continue:

$$f_p(t) - f_p(t)^* = 0 \quad (2.42)$$

from which  $f_p(t) = f_p(t)^*$ , which means that  $f_p(t)$  is real. ■

In general the Fourier coefficients  $F(n)$  will be complex, and we can write them in terms of their real and imaginary parts as

$$F(n) = A(n) + jB(n) \quad (2.43)$$

which is known as the **Cartesian** representation of  $F(n)$ . We can also write them in terms of their magnitudes and arguments as

$$F(n) = |F(n)|e^{j\Theta(n)} \quad (2.44)$$

which is known as the **polar** representation of  $F(n)$ . The quantities  $|F(n)|$  and  $\Theta(n)$  can be derived from  $A(n)$  and  $B(n)$  by

$$|F(n)| = [A(n)^2 + B(n)^2]^{1/2} \quad (2.45)$$

and

$$\Theta(n) = \arctan \frac{B(n)}{A(n)} \quad (2.46)$$

*Note:* Great care must be taken when computing the arctangent shown in (2.46) since the final angle that is derived can lie in any of the **four** quadrants, whereas hand calculators and programming languages often assume that an arctangent lies only in one of **two** quadrants (first or fourth). This problem and its solution are explored in detail in the exercises.

The inverse relationships of (2.45) and (2.46) are

$$A(n) = |F(n)|\cos[\Theta(n)] \quad (2.47)$$

and

$$B(n) = |F(n)|\sin[\Theta(n)] \quad (2.48)$$

Starting from these we can quickly obtain (2.45) and (2.46) and vice versa.

When  $F(n)$  is real we can plot it as a function of  $n$ , giving us what is called the **amplitude spectrum** of  $f_p(t)$ . When complex we need two plots to display it, the first being  $|F(n)|$  versus  $n$ , giving us what is called the **magnitude spectrum**, and the second  $\Theta(n)$  versus  $n$ , which is called the **phase spectrum**.

It is important to note that for periodic functions all of these plots will be sets of lines, since the spectra are functions of the variable  $n$ , which is discrete. We call such plots **line spectra** to distinguish them from the types of spectra that we shall

encounter in Chapter 3, where the independent variable is  $\omega$  and is continuous rather than discrete, resulting in **continuous spectra** or what we call **spectral densities**.

### Accompanying Disk

The FFT system on your disk enables you to obtain estimates of the coefficients of a Fourier series, and to generate plots of magnitude and phase.

Figure 2.6 shows a small section of the FFT's magnitude line-spectrum for the waveform that we have been considering, and in Figure 2.7 we show the corresponding portion of the phase spectrum.

In order to see how the system obtained the values for the phase spectrum note the following: By the **phase** of  $F(n)$  we mean its argument, that is, the angle that it makes with the positive real axis in the complex plane.

Real numbers lie on the real axis, and so every positive real number has argument zero. Thus, referring to Table 2.1, the phases of  $F(0)$  and  $F(1)$  are zero. Negative real numbers have arguments of either  $\pi$  or  $-\pi$ , and we must select from these in such a way that the overall phase plot is what we call **odd**. (We discuss this again later in this chapter.) Thus we have selected the phase of  $F(3)$  as  $\pi$  and that of  $F(-3)$  as  $-\pi$ . Finally, a spectral element such as  $F(2)$ , which is zero, is said to have zero argument, and so its phase is zero.

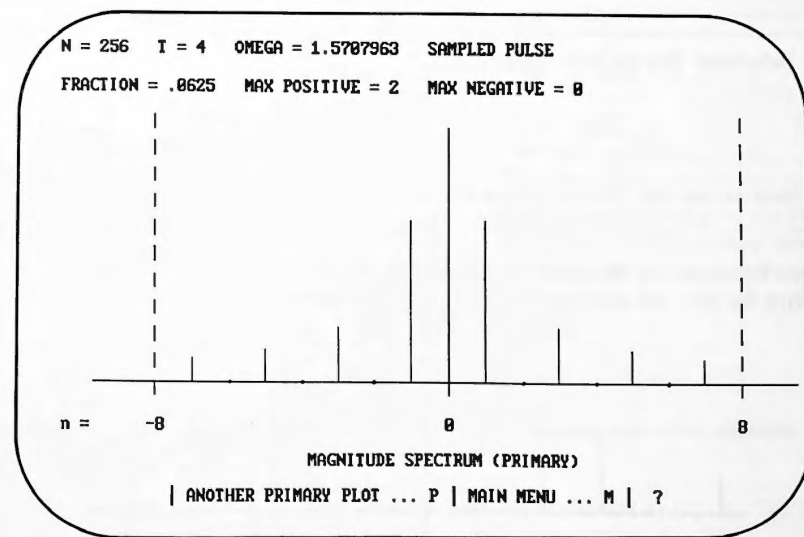


Figure 2.6. A section of the magnitude spectrum.

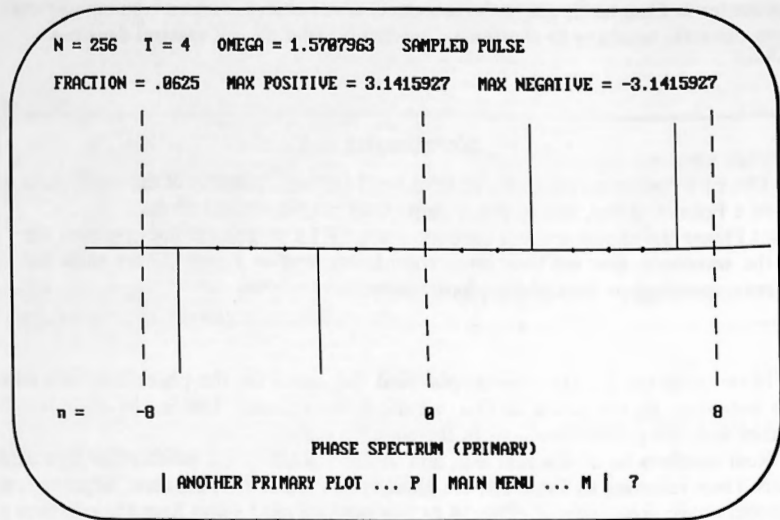


Figure 2.7. A section of the phase spectrum.

Consider now the following two classes of functions:

### Even Functions

**Definition:** If a function satisfies

$$f(n) = f(-n) \quad (2.49)$$

then we say that  $f(n)$  is an **even** function of  $n$ .

Even functions can be easily identified by the fact that the vertical axis serves as a mirror for their left and right halves. (See Figure 2.8.)

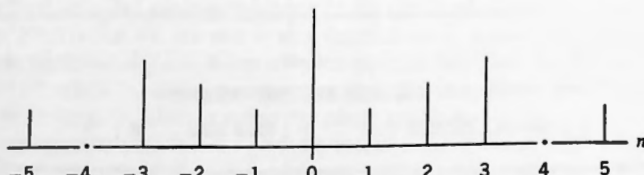


Figure 2.8. Example of an even function.

Examples of even functions are:

$$f(n) = 3, \quad n^2, \quad \cos(n), \quad n^4 \cos(n), \quad n \sin(n), \quad \frac{1}{2}(e^n + e^{-n})$$

for which it is readily apparent that (2.49) holds in each case. For example, if  $f(n) = n \sin(n)$ , then

$$f(-n) = -n \sin(-n) = f(n) \quad (2.50)$$

and so we can conclude that  $n \sin(n)$  is an even function.

We have been considering functions of the discrete variable  $n$ , but the same definition applies to functions of the continuous variable  $t$ . Thus

$$f(t) = 3, \quad t^2, \quad \cos(t), \quad t^4 \cos(t), \quad t \sin(t), \quad \frac{1}{2}(e^t + e^{-t})$$

are all even functions of  $t$ .

Even functions of  $t$  have the following important property that we shall soon be making frequent use of

$$\int_{-a}^a f(t) dt = 2 \int_0^a f(t) dt \quad (f(t) \text{ even}) \quad (2.51)$$

that is, if an integrand is even and the range of integration is symmetric, we need only integrate over half the range and then double the result to obtain the correct answer.

### Odd Functions

**Definition:** If a function satisfies

$$f(-n) = -f(n) \quad (2.52)$$

then we say that  $f(n)$  is an **odd** function of  $n$ .

Referring to Figure 2.9 we see that odd functions can be easily identified by the fact that if the right half of the function is reflected in the vertical axis and **then again reflected** in the negative horizontal axis, we obtain the left half of the function. Notice that every odd function must be zero at the origin.

Examples of odd functions are

$$f(n) = n, \quad \sin(n), \quad n^2 \sin(n), \quad n \cos(n), \quad \frac{1}{2}(e^n - e^{-n})$$

for which it is readily apparent that (2.52) holds in each case. For example, if  $f(n) = \frac{1}{2}(e^n - e^{-n})$ , then

$$f(-n) = \frac{1}{2}(e^{-n} - e^n) = -\frac{1}{2}(e^n - e^{-n}) = -f(n) \quad (2.53)$$

and so we can conclude that  $\frac{1}{2}(e^n - e^{-n})$  is an odd function.

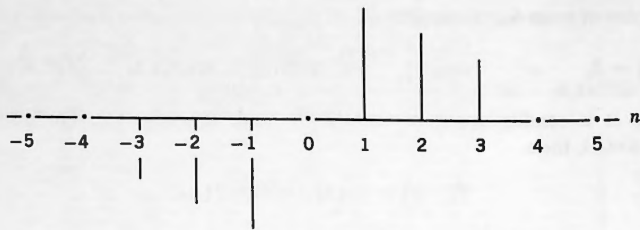


Figure 2.9. Example of an odd function.

Again, the same definition applies to functions of the continuous variable  $t$ . Thus

$$f(t) = t, \quad \sin(t), \quad t^2 \sin(t), \quad t \cos(t), \quad \frac{1}{2}(e^t - e^{-t})$$

are all odd functions of  $t$ . Odd functions of  $t$  also have an important property that we shall soon be making frequent use of, namely

$$\int_{-a}^a f(t) dt = 0 \quad (f(t) \text{ odd}) \quad (2.54)$$

that is, if an integrand is odd and the range of integration is symmetric, then the result is zero by inspection.

Finally, note the following facts regarding products comprised of even and odd functions:

#### ■ Products of Even and Odd Functions

Even  $\times$  even = even

Odd  $\times$  odd = even

Even  $\times$  odd = odd

Consider now the following theorem regarding some of the properties of  $A(n)$ ,  $B(n)$ ,  $|F(n)|$ , and  $\Theta(n)$  that we defined in (2.43) and (2.44).

#### ■ THEOREM 2.4

Let  $f_p(t)$  be a real function with Fourier coefficients  $F(n)$ . Then

$A(n)$  and  $|F(n)|$  are even

$B(n)$  and  $\Theta(n)$  are odd

*Proof:* From (2.38)

$$|F(n)^*| = |F(-n)| \quad (2.55)$$

However, for any complex quantity

$$|F(n)^*| = |F(n)| \quad (2.56)$$

and so

$$|F(-n)| = |F(n)| \quad (2.57)$$

which means that  $|F(n)|$  is even. Moreover  $F(n) = A(n) + jB(n)$ , and so

$$F(n)^* = A(n) - jB(n) \quad \text{and} \quad F(-n) = A(-n) + jB(-n) \quad (2.58)$$

By (2.38) these two expressions are equal, and so we can equate their real and imaginary parts, obtaining

$$A(n) = A(-n) \quad \text{and} \quad B(n) = -B(-n) \quad (2.59)$$

which shows that  $A(n)$  is even and  $B(n)$  is odd. Finally, using (2.59),

$$\begin{aligned} \Theta(n) &= \tan^{-1} \frac{B(n)}{A(n)} = \tan^{-1} \frac{-B(-n)}{A(-n)} \\ &= -\tan^{-1} \frac{B(-n)}{A(-n)} = -\Theta(-n) \end{aligned} \quad (2.60)$$

which means that  $\Theta(n)$  is odd. This completes the proof. ■

We now investigate how the real and imaginary parts of  $F(n)$  are related to the time-domain function  $f_p(t)$  from which they came, but first we note the following: When a function  $f(t)$  is neither odd nor even, it can always be split into its even and odd parts by the following simple algorithm.

$$f_{ev}(t) = \frac{1}{2}[f(t) + f(-t)] \quad (2.61a)$$

$$f_{od}(t) = \frac{1}{2}[f(t) - f(-t)] \quad (2.61b)$$

If we apply our tests,  $f_{ev}$  is seen to be an even function and  $f_{od}$  is seen to be odd. Moreover, if we add them together, we obtain the original function  $f(t)$ . Thus it is clear that (2.61a) and (2.61b) will correctly resolve any function  $f(t)$  into its even and odd parts.

The analysis equation (2.28) automatically does the same thing to any real function that is presented to it, transforming the even part of the function into  $\text{Re}[F(n)]$  and the odd part into  $j \text{Im}[F(n)]$ . This is proved in the following theorem.

**■ THEOREM 2.5**

For  $f_p(t)$  a real function with even part  $f_{ev}(t)$  and odd part  $f_{od}(t)$

$$f_{ev}(t) \Leftrightarrow A(n) \quad \text{and} \quad f_{od}(t) \Leftrightarrow jB(n) \quad (2.62)$$

*Proof:*

$$f_{ev}(t) = \frac{1}{2}[f_p(t) + f_p(-t)] \quad (2.63)$$

to which we now apply the synthesis equation, continuing as

$$\begin{aligned} \dots &= \frac{1}{2} \sum_{n=-\infty}^{\infty} F(n)e^{jn\omega_0 t} + \frac{1}{2} \sum_{n=-\infty}^{\infty} F(n)e^{-jn\omega_0 t} \\ &= \sum_{n=-\infty}^{\infty} F(n) \frac{1}{2}(e^{jn\omega_0 t} + e^{-jn\omega_0 t}) \\ &= \sum_{n=-\infty}^{\infty} F(n)\cos(n\omega_0 t) \\ &= \sum_{n=-\infty}^{\infty} A(n)\cos(n\omega_0 t) + j \sum_{n=-\infty}^{\infty} B(n)\cos(n\omega_0 t) \end{aligned} \quad (2.64)$$

However,  $B(n)$  has been shown to be an odd function of  $n$ , whereas  $\cos(n\omega_0 t)$  is an even one. Thus their product is odd, and so the final infinite sum in (2.64) must be zero. We therefore continue

$$\dots = \sum_{n=-\infty}^{\infty} A(n)\cos(n\omega_0 t) = \sum_{n=-\infty}^{\infty} A(n)[\cos(n\omega_0 t) + j\sin(n\omega_0 t)] \quad (2.65)$$

in which we have added nothing, since the product of  $A(n)$  (which is even) with  $\sin(n\omega_0 t)$  (which is odd) must be odd, and so it sums to zero. We therefore continue further as

$$\dots = \sum_{n=-\infty}^{\infty} A(n)e^{jn\omega_0 t} \quad (2.66)$$

We have thus shown that, for  $f_p(t)$  real,

$$f_{ev}(t) = \sum_{n=-\infty}^{\infty} A(n)e^{jn\omega_0 t} \quad (2.67)$$

that is,  $f_{ev}(t) \Leftrightarrow A(n)$ . A similar argument shows that  $f_{od}(t) \Leftrightarrow jB(n)$ , and so the proof is complete. ■

**■ COROLLARY**

- (a)  $F(n)$  is real and even iff  $f_p(t)$  is even.
- (b)  $F(n)$  is purely imaginary and odd iff  $f_p(t)$  is odd.

*Proof:*

$$F(n) = A(n) \quad \text{iff} \quad jB(n) = 0 \quad \text{iff} \quad f_p(t) \text{ is even} \quad (2.68)$$

But  $A(n)$  is real, and by Theorem 2.4 it is also even. Hence  $F(n)$  is real and even iff  $f_p(t)$  is even, and so (a) is proved. The proof for (b) follows similarly. ■

The preceding theorems are summarized in the following box for ease of reference.

**■ Summary of Theorems 2.3, 2.4, and 2.5: Properties of  $F(n)$  for  $f_p(t)$  Real**

$$F(n)^* = F(-n)$$

$$f_{ev}(t) \Leftrightarrow A(n) \quad \text{and} \quad f_{od}(t) \Leftrightarrow jB(n)$$

- (a)  $A(n)$  is even,  $B(n)$  is odd
- (b)  $|F(n)|$  is even,  $\Theta(n)$  is odd
- (c)  $F(n)$  is real and even iff  $f_p(t)$  is even
- (d)  $F(n)$  is imaginary and odd iff  $f_p(t)$  is odd

**□ EXAMPLE 2.2**

- (a) Find the complex coefficients for the function  $f_p(t)$  shown in Figure 2.10.
- (b) Compare the results that you obtain for  $A(n)$ ,  $B(n)$ ,  $|F(n)|$ , and  $\Theta(n)$  with those predicted by Theorems 2.3, 2.4, and 2.5.

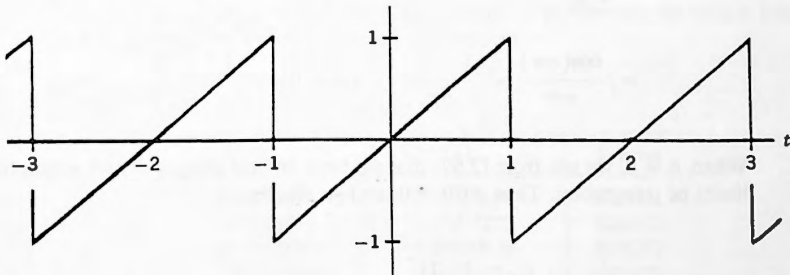


Figure 2.10.

- (c) Run this problem using the FFT system on the disk and compare the values of  $F(n)$  for  $n = 1$  to 5 so obtained to their exact values. Use  $N = 1024$  for the computer run.

**Solution:** First let's make some predictions about the coefficients based on the three theorems that we have just proved:

- The waveform  $f_p(t)$  is real, and so we expect that  $F(n)*$  will be equal to  $F(-n)$ .
- The waveform is odd, which means that  $F(n)$  will be purely imaginary and odd, that is,  $A(n) = 0$  and  $F(n) = jB(n)$ .
- We expect that  $A(n)$  will be even,  $B(n)$  odd,  $|F(n)|$  even, and  $\Theta(n)$  odd.

- (a) Let's now find the complex coefficients and see if we are correct. The function shown in the figure has the following analytical definition:

$$f_p(t) = t \quad (-1 < t < 1) \quad f_p(t+2) = f_p(t)$$

Since  $T_0 = 2$  we have  $\omega_0 = 2\pi/T_0 = \pi$ . Then, from (2.28)

$$\begin{aligned} F(n) &= \frac{1}{T_0} \int_{-T_0/2}^{T_0/2} f_p(t) e^{-j n \omega_0 t} dt \quad (n \neq 0) \\ &= \frac{1}{2} \int_{-1}^1 t [\cos(n\pi t) - j \sin(n\pi t)] dt \end{aligned} \quad (2.69)$$

However,  $t \cos(n\pi t)$  is odd,  $t \sin(n\pi t)$  is even, and the limits of integration are symmetric, and so we continue as

$$\begin{aligned} \dots &= \frac{2}{2} \int_0^1 -jt \sin(n\pi t) dt = -j \left[ -t \frac{\cos(n\pi t)}{n\pi} + \frac{\sin(n\pi t)}{n^2\pi^2} \right]_0^1 \\ &= j \frac{\cos(n\pi)}{n\pi} = j \frac{(-1)^n}{n\pi} \quad (n \neq 0) \end{aligned}$$

When  $n = 0$ , we see from (2.69) that we have an odd integrand and symmetric limits of integration. Thus  $F(0) = 0$ , and so, finally,

$$F(n) = j \frac{(-1)^n}{n\pi} \quad (n \neq 0), \quad F(0) = 0 \quad (2.70)$$

TABLE 2.2

$n$	$F(n)$	$\Theta(n)$
-2	$j \frac{(-1)^{-2}}{(-2)\pi} = -\frac{j}{2\pi}$	$-\frac{\pi}{2}$
-1	$j \frac{(-1)^{-1}}{(-1)\pi} = \frac{j}{\pi}$	$\frac{\pi}{2}$
0	0	0
1	$j \frac{(-1)^1}{(1)\pi} = -\frac{j}{\pi}$	$-\frac{\pi}{2}$
2	$j \frac{(-1)^2}{(2)\pi} = \frac{j}{2\pi}$	$\frac{\pi}{2}$

This then is the required formula for  $F(n)$ , from which we see the following, all of which are fully as expected:

- (b) •  $F(n)^* = -j(-1)^n/n\pi = F(-n)$
  - $F(n)$  is purely imaginary and odd
  - $A(n) = 0$  and hence even
  - $B(n) = (-1)^n/n\pi$  and hence odd
  - $|F(n)| = 1/|n|\pi$  and hence even
  - $\Theta(n)$  is evaluated in Table 2.2 where we see that it is odd. Note that the number  $j$  or any positive multiple thereof has an argument equal to  $\pi/2$ , and so that is its phase.
- (c) In order to run this problem on the FFT system we must first create sampled values of one complete period of the waveform of Figure 2.10. The sequence of steps to accomplish that is given in Example 16.1 at the end of the file README16 on the disk. The exact values computed for  $F(n)$  using the formula (2.70) and those obtained from the FFT (using  $N = 1024$ , SAMPLED, and  $T = 2$ , PERIODIC) are shown in Table 2.3. Since  $A(n) = 0$ , we only show values for  $B(n)$ . Observe how close the agreement is between the values from the formula and the values from the FFT system.

TABLE 2.3

$n$	$B(n)_{\text{formula}}$	$B(n)_{\text{FFT}}$	% error
1	-0.31830989	-0.31830889	0.00031
2	0.15915494	0.15915295	0.00125
3	-0.10610330	-0.10610030	0.00282
4	$7.9577472e-2$	$7.9573477e-2$	0.00502
5	$-6.3661977e-2$	$-6.3656984e-2$	0.00784

*Note:* By "error" we always mean "relative error" defined by

$$\text{Error} = \frac{\text{estimate} - \text{exact}}{\text{exact}} \quad (2.71)$$

□

## 2.4 PARSEVAL'S THEOREM FOR PERIODIC WAVEFORMS

We now examine the energy and power relationships for periodic waveforms. Suppose that a periodic waveform  $f_p(t)$  were in fact a voltage that is being applied across an  $R$ -ohm resistor. Then it is well known that the instantaneous power being dissipated would be

$$P(t) = \frac{[f_p(t)]^2}{R} \quad \text{watts} \quad (2.72)$$

It is customary to write this as

$$P(t) = \frac{|f_p(t)|^2}{R} \quad (2.73)$$

in which we show the **modulus** of  $f_p(t)$  being squared rather than just  $f_p(t)$  being squared. Clearly (2.72) and (2.73) are consistent when talking about a real  $f_p(t)$ , but (2.73) has the added advantage of being able to handle theoretical situations where  $f_p(t)$  is complex.

Likewise if the waveform were a current flowing through the resistor, the power would be

$$P(t) = |f_p(t)|^2 R \quad \text{watts} \quad (2.74)$$

For  $R$  equal to 1 ohm (2.73) and (2.74) both become

$$P(t) = |f_p(t)|^2 \quad (2.75)$$

and so this is the statement that is usually used when talking about power in a waveform, whether a current or a voltage. The  $P(t)$  in (2.75) is referred to as the **1-ohm power** in the signal.

From (2.75) it now follows that the total 1-ohm energy in any one period is

$$E = \int_{-T_0/2}^{T_0/2} |f_p(t)|^2 dt \quad \text{joules} \quad (2.76)$$

and so the average 1-ohm power in the waveform considered over one complete

period must be

$$P_{\text{ave}} = \frac{1}{T_0} \int_{-T_0/2}^{T_0/2} |f_p(t)|^2 dt \quad \text{watts} \quad (2.77)$$

This must then also be the average power over the entire waveform and it is a simple fact that:

**Every physically realizable periodic waveform has finite average power.**

However, there can be mathematically defined periodic functions for which this is not the case, and to distinguish between them we introduce the following:

**Definition:** If  $P_{\text{ave}}$  defined in (2.77) is finite, that is, if

$$P_{\text{ave}} < \infty \quad (2.78)$$

then we say that  $f_p(t)$  is a **power signal**.

From here on we shall drop the “ave” subscript in  $P_{\text{ave}}$ , and simply refer to the average power in the waveform as  $P$ . We shall also drop the “1-ohm” statement, but we must always bear it in mind.

There is a fundamental relationship between  $P$  and the complex coefficients  $F(n)$ , known as Parseval’s theorem for periodic waveforms. (See the following box.)

### ■ THEOREM 2.6: Parseval’s Theorem for Periodic Waveforms

Let  $f_p(t)$  be a power signal with Fourier coefficients  $F(n)$ . Then the average power in the waveform satisfies

$$P = \frac{1}{T_0} \int_{-T_0/2}^{T_0/2} |f_p(t)|^2 dt = \sum_{n=-\infty}^{\infty} |F(n)|^2 \quad (2.79)$$

What this theorem tells us is that there are two ways in which the average power in a periodic waveform can be computed:

- (A) From the analytical definition of  $f_p(t)$  using the integral formulation shown in (2.79).
- (B) From the series representation for  $f_p(t)$  by summing the squared moduli of the coefficients as shown in the infinite sum in (2.79).

Note how (2.79) connects the time-domain representation of the power (the integral) with the frequency-domain representation (the infinite sum).

*Proof of Theorem 2.6:* Although we have been assuming throughout that  $f_p(t)$  is a real function of  $t$ , nothing is lost if we momentarily generalize and assume that it is a complex function. Then  $|f_p(t)|^2 = f_p(t)f_p^*(t)$ . (Certainly this is true also for  $f_p(t)$  real.) That being the case

$$\begin{aligned} P &= \frac{1}{T_0} \int_{-T_0/2}^{T_0/2} |f_p(t)|^2 dt = \frac{1}{T_0} \int_{-T_0/2}^{T_0/2} f_p(t)f_p(t)^* dt \\ &= \frac{1}{T_0} \int_{-T_0/2}^{T_0/2} \left[ \sum_{n=-\infty}^{\infty} F(n)e^{jn\omega_0 t} \right] \left[ \sum_{m=-\infty}^{\infty} F(m)^* e^{jm\omega_0 t^*} \right] dt \\ &\quad (\text{Note the use of different arguments } n \text{ and } m.) \\ &= \sum_{n=-\infty}^{\infty} \sum_{m=-\infty}^{\infty} F(n)F(m)^* \left[ \frac{1}{T_0} \int_{-T_0/2}^{T_0/2} e^{jn\omega_0 t} e^{jm\omega_0 t^*} dt \right] \end{aligned} \quad (2.80)$$

By Theorem 2.1 the quantity in square brackets in (2.80) is equal to zero when  $n \neq m$ , and so all products in the double sum for which  $n \neq m$  will be multiplied by zero. Likewise, when  $n = m$  the quantity in square brackets equals 1, and so the products in the double sum for which  $n = m$  will survive. Hence (2.80) continues as

$$\cdots = \sum_{n=-\infty}^{\infty} F(n)F(n)^* = \sum_{n=-\infty}^{\infty} |F(n)|^2 \quad (2.81)$$

and the proof is complete. ■

We now note the following: Parseval's theorem is actually a statement that can be considered **term by term**, for if the average power in the entire waveform is given by (2.79), then the power in, say, the third term in the complex Fourier series must be

$$P(3) = |F(3)|^2 \quad (2.82)$$

and so we are able to see precisely how much power any term or group of terms in the series contributes to the total average power. Thus if we were to plot the values of  $|F(n)|^2$  versus  $n$ , we would obtain a **line-spectrum of the power** in the waveform.

**Definition:** The **power spectrum** of a periodic function  $f_p(t)$  whose  $n$ th complex coefficient is  $F(n)$ , is

$$P(n) \equiv |F(n)|^2 \quad (n \text{ any integer}) \quad (2.83)$$

**EXAMPLE 2.3**

- (a) Find the total average power and then the power contributed by each term in the waveform

$$f_p(t) = 4 + 2 \cos(3t) + 3 \sin(4t) \quad (2.84)$$

- (b) Sketch the power spectrum of  $f_p(t)$ .

**Solution:** The total average power can be evaluated using the integral definition for power given in (2.79). Observe from (2.84) that the value of  $\omega_0$  for this periodic waveform must be 1 since that is the only integer that will divide into 3 and 4 without a remainder. Thus the period must be  $T_0 = 2\pi$ , and (2.79) then gives

$$\begin{aligned} P &= \frac{1}{T_0} \int_{-T_0/2}^{T_0/2} |f_p(t)|^2 dt \quad (T_0 = 2\pi) \\ &= \frac{1}{2\pi} \int_{-\pi}^{\pi} [4 + 2 \cos(3t) + 3 \sin(4t)]^2 dt \\ &= \frac{1}{2\pi} \left[ \int_{-\pi}^{\pi} 4^2 dt + \int_{-\pi}^{\pi} [2 \cos(3t)]^2 dt + \int_{-\pi}^{\pi} [3 \sin(4t)]^2 dt \right] \end{aligned}$$

in which all of the remaining products can be ignored since the sines and cosines form an orthogonal set. (See Exercise 2.13.) The results are as follows:

- For the first term we obtain  $P[4^V \text{ dc}] = 16$  watts.
- For the next term we have

$$P[2 \cos(3t)] = \frac{1}{2\pi} \int_{-\pi}^{\pi} [2 \cos(3t)]^2 dt = \frac{4}{2\pi} \int_{-\pi}^{\pi} \frac{1}{2} [\cos(6t) + 1] dt = 2 \text{ watts} \quad (2.85)$$

- In the same way the final term gives  $P[3 \sin(4t)] = \frac{9}{2}$  watts. The total is  $\frac{45}{2}$  watts from the complete series.

To find the power contributions using Parseval's theorem we must first find the coefficients of the complex Fourier series. This is easily done by inspection as follows:

$$\begin{aligned} f_p(t) &= 4 + 2 \cos(3t) + 3 \sin(4t) \\ &= 4 + 2 \frac{e^{j3t} + e^{-j3t}}{2} + 3 \frac{e^{j4t} - e^{-j4t}}{2j} \end{aligned}$$

and so the complex Fourier series is

$$f_p(t) = \frac{3j}{2}e^{-j4\omega_0 t} + 1e^{-j3\omega_0 t} + 4$$

$$+ 1e^{j3\omega_0 t} - \frac{3j}{2}e^{j4\omega_0 t}$$

in which the fundamental frequency is  $\omega_0 = 1$ . From this we have

$$F(-4) = \frac{3j}{2}, \quad F(-3) = 1, \quad F(0) = 4, \quad F(3) = 1, \quad F(4) = -\frac{3j}{2}$$

and by Parseval's theorem the power contributed by each of the terms in the series is

$$P(-4) = \left| \frac{3j}{2} \right|^2 = \frac{9}{4}, \quad P(-3) = |1|^2 = 1, \quad P(0) = |4|^2 = 16,$$

$$P(3) = 1, \quad \text{and} \quad P(4) = \frac{9}{4}$$

for a total of  $\frac{45}{2}$  watts in all. This is the same result that we obtained by direct integration, but notice how the theorem breaks out the power for us **term by term**.

If we were asked to find the power contributed by the complete third harmonic in this waveform, then since a harmonic is made up of a pair of terms in the complex series, we must combine the contributions  $P(3)$  and  $P(-3)$ , giving a total of 2 watts, which agrees with (2.85).

Always keep in mind the assumption of a 1-ohm resistor. If this should change, then so would the power. The 1-ohm power spectrum for the preceding waveform is shown as the line spectrum of Figure 2.11. □

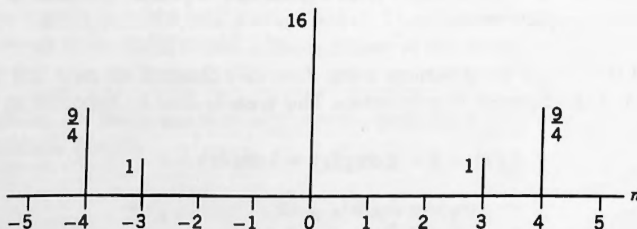


Figure 2.11. Power spectrum.

TABLE 2.4

$n$	0	$\pm 1$	$\pm 2$	$\pm 3$	$\pm 4$	$\pm 5$
$P(n)$	0	0.101321	0.025330	0.011258	0.006333	0.004053

**EXAMPLE 2.4**

- (a) Compute and display the power spectrum for the function of Example 2.2, for  $-5 \leq n \leq 5$ .  
 (b) Find the total average power and calculate what percentage of this total the set of values in (a) represents.

**Solution:** (a) From the formula derived for  $F(n)$  in (2.70), we have

$$F(n) = j \frac{(-1)^n}{n\pi} \quad (n \neq 0), \quad F(0) = 0$$

Hence the power from the  $n$ th term in the series will be

$$P(n) = |F(n)|^2 = \frac{1}{n^2\pi^2} \quad (n \neq 0)$$

We display the required values of  $P(n)$  in Table 2.4.

(b) The total average power in the waveform can be obtained using (2.79) as follows:

$$P = \frac{1}{T_0} \int_{-T_0/2}^{T_0/2} |f_p(t)|^2 dt = \frac{1}{2} \int_{-1}^1 t^2 dt = 0.33333 \text{ watt}$$

Adding the terms in the table (and doubling the result because of the  $\pm$ ) gives 0.29659 watt, which is thus 88.98% of the total average power.  $\square$

## 2.5 CONVERGENCE OF FOURIER SERIES

Recall that in going from (2.23) to (2.24) we quietly interchanged the order of summation and integration. This is procedurally a simple thing to do but it gives rise to a large number of mathematical complications regarding the convergence of the series that are so derived. The committee at the Paris Academy that was judging Fourier's paper was thus deeply concerned with this question, causing them to delay their evaluation for a number of years. However, in their concerns they were not alone. It is such a complex and important question that generations of mathematicians have been studying it ever since, and still are.

In other words, given the analytical definition of the function  $f_p(t)$  we can readily obtain its Fourier coefficients  $F(n)$  using the integration formula (2.28). We can then assemble the infinite series shown on the RHS of (2.27).

**Question:** Does the series that we have assembled converge to the analytical  $f_p(t)$  from which the coefficients were derived?

The necessary and sufficient conditions under which the Fourier series for a given function converges correctly to that function are still not known. There are known **sufficient** conditions, however, and fortunately they cover all physically realizable cases. We shall present two of the most important ones later.

### Convergence at a Discontinuity

Wherever a periodic waveform has a jump discontinuity, that is, a finite step, it will be found that its Fourier series representation converges to the **average of the values on each side of the step**. Thus, for the periodic waveform that we considered earlier in Figure 2.2, the series converges as follows:

At  $t = -1$ : The series converges to  $(0 + 1)/2 = \frac{1}{2}$

At  $t = 1$ : The series converges to  $(1 + 0)/2 = \frac{1}{2}$

with similar values at all of the other discontinuities. For the waveform shown in Figure 2.10 the Fourier series converges to zero at each of the discontinuities, that is, at  $t$  any odd integer. (See also Notes and Comments regarding the Gibbs phenomenon.)

### Rates of Convergence

We now address the following topic:

Assuming that a Fourier series does converge correctly, we would like to have some idea of how quickly convergence takes place.

This knowledge is of importance to us, for example, when we desire to compute a numerical answer from a Fourier series, since the rate of convergence will determine how many terms we have to include for a required degree of accuracy. The rate of convergence is also an indicator of how much bandwidth we require in order to transmit a good representation of a periodic waveform over a communication channel (e.g., the transmission of an electrocardiogram from a point in the field to a hospital).

The Fourier series of (2.27) can be reorganized as follows:

$$\begin{aligned}
 f_p(t) &= \sum_{n=-\infty}^{\infty} F(n) e^{jn\omega_0 t} = \sum_{n=-\infty}^{\infty} [A(n) + jB(n)] e^{jn\omega_0 t} \\
 &= \sum_{n=-\infty}^{\infty} A(n) [\cos(n\omega_0 t) + j \sin(n\omega_0 t)] \\
 &\quad + \sum_{n=-\infty}^{\infty} jB(n) [\cos(n\omega_0 t) + j \sin(n\omega_0 t)]
 \end{aligned} \tag{2.86}$$

in which  $A(n)$  is even and  $jB(n)$  is odd, since we are assuming that  $f_p(t)$  is real, and so (2.86) continues as

$$\dots = \sum_{n=-\infty}^{\infty} A(n) \cos(n\omega_0 t) - \sum_{n=-\infty}^{\infty} B(n) \sin(n\omega_0 t)$$

in which both summands are even, and so

$$\dots = F(0) + \sum_{n=1}^{\infty} 2A(n) \cos(n\omega_0 t) - \sum_{n=1}^{\infty} 2B(n) \sin(n\omega_0 t) \quad (2.87)$$

(Note that  $F(0) = A(0) + jB(0) = A(0)$  since  $B(0) = 0$ , a consequence of the fact that  $B(n)$  is odd.) We now define the following:

$$\begin{aligned} a(n) &= 2A(n) = 2 \operatorname{Re}(F(n)) \\ a(0) &= 2F(0) \\ b(n) &= -2B(n) = -2 \operatorname{Im}(F(n)) \end{aligned} \quad (2.88)$$

Using these equations (2.87) becomes

$$f_p(t) = \frac{a(0)}{2} + \sum_{n=1}^{\infty} a(n) \cos(n\omega_0 t) + \sum_{n=1}^{\infty} b(n) \sin(n\omega_0 t) \quad (2.89)$$

Observe that the coefficients here are lowercase  $a(n)$  and  $b(n)$ , whereas uppercase  $A(n)$  and  $B(n)$  are the real and imaginary parts of  $F(n)$  that we have been working with so far in this chapter.

**Definition:** The Fourier coefficients that we have been working with up to now,  $F(n) = A(n) + jB(n)$ , are called the **complex Fourier coefficients**, whereas  $a(n)$  and  $b(n)$  defined in (2.88) are called the **real coefficients**.

*Historical Note:* Fourier used the real form of the Fourier series (2.89) in his paper in 1807. It was also used by both Euler and d'Alembert as early as 1747, some 60 years before him (Carslaw, 1930). The complex form, which Fourier never used, was first discovered by Laplace in 1782, about 25 years before Fourier submitted his paper (Burkhardt, 1904). Fourier's name has become attached to both forms, however, not because he discovered them, but because he was the first to use one of them for solving partial differential equations.

Returning to (2.89), we see that the Fourier coefficients  $a(n)$  and  $b(n)$  multiply their respective cosine and sine terms in the synthesis equation. Since in magnitude the sines and cosines are all less than or equal to unity, the rate of convergence of a Fourier series will be determined solely by how quickly the **coefficients converge** (die out).

The following is fairly easy to prove for a waveform that meets the sufficiency conditions for convergence to be discussed below (see, e.g., Carslaw, 1930):

■ Rate of Convergence of the Coefficients

If  $f_p(t)$  has discontinuities, then its real Fourier coefficients satisfy

$$|a(n)| < K/n \quad (\text{for large } n) \quad (2.90)$$

where  $K$  is some positive constant, with a similar statement for  $b(n)$ .

What is true for  $a(n)$  and  $b(n)$  must also be true for  $A(n)$  and  $B(n)$ , by virtue of (2.88). If you return to (2.32) where we derived the expression for  $F(n)$  for the periodic waveform of Example 2.1, you will see that it does in fact die out like  $K/n$ . The same is also true for the waveform of Example 2.2.

Things get better as  $f_p(t)$  becomes more and more continuous as the following shows:

■ If  $f_p(t)$  is everywhere continuous but  $f'_p(t)$  is discontinuous, then for large  $n$ ,

$$|a(n)| < K_1/n^2 \quad \text{and} \quad |b(n)| < K_2/n^2 \quad (2.91)$$

For the general case one can prove the following by induction.

■ If  $f_p(t)$  and its first  $m$  derivatives are continuous but its  $(m + 1)$ -th is not, then for large  $n$ ,

$$|a(n)| < K_1/n^{m+2} \quad \text{and} \quad |b(n)| < K_2/n^{m+2} \quad (2.92)$$

In Examples 2.1 and 2.2,  $f_p(t)$  had discontinuities, and so the coefficients died out only like  $K/n$ . In the exercises at the end of this chapter we examine periodic waveforms that are everywhere continuous but their first derivatives are not. You will find that the coefficients die out like  $K/n^2$ . In two of the exercises we also consider cases where the waveform has continuity up to and including its first derivative ( $m = 1$ ), and you will find that convergence will be like  $K/n^3$ . For ease of reference we summarize all of these results in Table 2.5.

TABLE 2.5 Rates of Convergence

Zeroth derivative not continuous:	$K/n$
Zeroth derivative continuous, first not:	$K/n^2$
First derivative continuous, second not:	$K/n^3$
Second derivative continuous, third not:	$K/n^4$

*Note:* It is not guaranteed that both  $a(n)$  and  $b(n)$  will satisfy the condition shown in Table 2.5, but that at least one of them will. In Exercise 2.17 we consider the periodic function

$$f_p(t) = \begin{cases} e^t & (0 < t < 1) \\ 0 & (1 < t < 2) \end{cases} \quad f_p(t+2) = f_p(t)$$

which is discontinuous at  $t$  any integer. It will be seen there that  $b(n)$  converges like  $K/n$ , but that  $a(n)$  converges like  $K/n^2$ . This means, however, that the Fourier series as a whole converges like  $K/n$ , and so the condition just mentioned regarding rates of convergence still holds correctly.

Note also that if the terms in the Fourier series were converging like  $K/n$ , say, then the terms in the power spectrum would be converging like  $K/n^2$ . Thus the dc term and the first few harmonics invariably contain the bulk of the power contributed by the terms of a Fourier series.

In Example 2.4 we saw that the central 11 terms of the complex Fourier series contained 88.98 percent of the total power in the waveform.

### Sufficient Conditions for Convergence

Even today, the necessary and sufficient conditions for the convergence of Fourier series to the functions from which they are derived are still not known. There are a number of known **sufficient** conditions, however, although none of these is necessary. We now present two of the most important ones, and fortunately they include all physically realizable cases.

(a) **The Square Integrability Criterion.** Let  $\Phi(t)$  be the function that we obtain from the RHS of the synthesis equation (2.27), whatever it may be, that is,

$$\Phi(t) \equiv \sum_{n=-\infty}^{\infty} F(n) e^{jn\omega_0 t} \quad (2.93)$$

where  $F(n)$  is formally defined by

$$F(n) = \frac{1}{T_0} \int_{-T_0/2}^{T_0/2} f_p(t) e^{-jn\omega_0 t} dt \quad (2.94)$$

Then the Square Integrability Criterion for the existence of  $F(n)$  and for  $\Phi(t)$  converging to  $f_p(t)$ , can be shown to hold. (See box.)

### Accompanying Disk

In B of PLOTS you will notice that only about seven or eight terms are required for a good representation of the original waveform and that many more are required in A (perhaps 80 or 90). The reason for this should now be completely clear.

In B we are expanding a triangular waveform that is everywhere continuous, but its first derivative is not, and so the coefficients die out like  $K/n^2$ . Hence not many terms are required in the series representation.

In A, on the other hand, we are expanding a square wave that has discontinuities, and so the coefficients only die out like  $K/n$ . Hence many more terms must be included in the series before the effects of truncation become unimportant.

### ■ The Square Integrability Criterion

Let  $f_p(t)$  be square integrable, that is, let

$$\int_{-T_0/2}^{T_0/2} |f_p(t)|^2 dt < \infty \quad (2.95)$$

Then

- (a) The integral (2.94) exists, that is, we can obtain the coefficients  $F(n)$  as finite numbers from it.
- (b) If we form the difference between the series (2.93) and the original function  $f_p(t)$ , that is, if we form

$$e(t) = \Phi(t) - f_p(t) \quad (2.96)$$

then  $e(t)$  may be nonzero on a discrete set of values of  $t$ , but

$$\int_{T_0/2}^{T_0/2} |e(t)|^2 dt = 0 \quad (2.97)$$

Observe that (2.95) in the box applies to any periodic waveform that has finite energy in one period, which means that it applies to all realizable waveforms. Thus,

what this criterion tells us is that

**Every physically realizable periodic waveform has a correctly convergent Fourier series.**

While there may be differences between  $\Phi(t)$  and the analytical definition of  $f_p(t)$  at discrete values of  $t$ , what (2.96) and (2.97) imply is that the error function will contain zero energy, which is all that we care about.

Keep in mind that while the preceding condition is sufficient, it is by no means necessary, and in Chapter 4 we shall see that there are mathematical functions that have infinite average power, but that nevertheless have well-behaved Fourier series that converge correctly.

(b) **The Dirichlet Criterion.** A second sufficient condition, perhaps the most famous regarding Fourier series, was proved in two memoirs published in 1829 and 1837 by a German mathematician named Dirichlet<sup>†</sup>. First we require the following:

**Definition:** A periodic function  $f_p(t)$  is said to satisfy the **Dirichlet conditions** if

- (a)  $f_p(t)$  is bounded.
- (b) In any one period  $f_p(t)$  has at most a finite number of discontinuities and a finite number of local maxima and minima.

*Note:* There are a number of ways of stating these conditions. We have selected what we believe to be the simplest.

Periodic functions that satisfy these conditions are a subset of the periodic functions that are square integrable. Thus we have the following Venn diagram:

Periodic functions that are square integrable

Periodic functions that satisfy  
the Dirichlet conditions

It is a simple fact that

All physically realizable periodic functions also satisfy the Dirichlet conditions.

<sup>†</sup>Peter Gustave Lejeune-Dirichlet (1805–1859), a friend and disciple of Gauss, was the first mathematician who set out to put the discoveries that Fourier had made onto a mathematically rigorous basis.

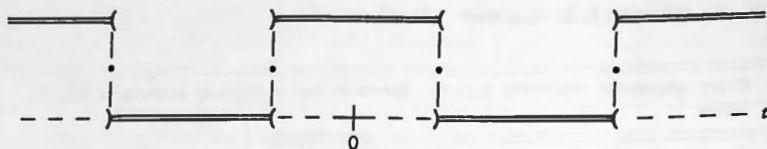


Figure 2.12. Convergence of Fourier series of Example 2.1.

The following celebrated result was first proved by Dirichlet but it nevertheless goes by the name of "Fourier's theorem".

### ■ Fourier's Theorem

If a periodic function  $f_p(t)$  satisfies the Dirichlet conditions, then its Fourier coefficients can be found from its analytical definition by (2.28).

The associated Fourier series (2.27) converges to  $f_p(t)$  at any point where  $f_p(t)$  is continuous, and converges to

$$\frac{1}{2}[f_p(t^+) + f_p(t^-)]$$

wherever  $f_p(t)$  is discontinuous.

Interpreted for the waveform  $f_p(t)$  that we considered in Example 2.1, this theorem tells us that the Fourier series shown in (2.36) converges as shown in Figure 2.12.

In the figure the double lines show where the waveform  $f_p(t)$  is continuous and the half cups signify the ends of open intervals. All along the double lines the Fourier series converges to the waveform as defined, but precisely at the discontinuities the series converges to the average of the values on each side of the discontinuity, as shown by the dots.

**Definition:** Throughout the rest of this text we shall refer to these average values at a discontinuity as the **half-values**.

---

### NOTES AND COMMENTS

---

(A) **The Sinc function** is defined as follows:

$$\text{Sinc}(x) \equiv \frac{\sin(\pi x)}{\pi x}$$

Thus  $\text{Sinc}(x) = \text{Sa}(\pi x)$  and  $\text{Sa}(x) = \text{Sinc}(x/\pi)$ .

**(B) The Gibbs Phenomenon** Immediately on each side of a discontinuity a Fourier series exhibits certain behavior known as the Gibbs phenomenon.

If we calculate values using a **truncated version** of the series (which we must always do in practice), we find that the results exhibit an oscillatory behavior immediately on each side of a discontinuity. (This is evident if you examine the waveforms generated by PLOTS on your disk, using more and more terms in the series.)

However, as we extend the truncation point of the series and take more and more terms into account the oscillations move closer and closer to the discontinuity, and we can always find a truncation point for which they are insignificant no matter how closely we position ourselves to it. (The overshoot peaks out at about 9 percent of the value of the waveform and becomes narrower and narrower as we increase the number of terms that are summed.)

This was first observed in 1898 by the American physicist Albert Michalson (of Michalson–Morley fame, whose well-known experiment stimulated Albert Einstein to create the theory of relativity). Michalson reported it to Josiah Gibbs, an American mathematical physicist, who examined the phenomenon in detail and accounted for its behavior completely, hence the name.

Gibbs and Oliver Heaviside were the coinventors of the vector calculus that is so widely used today by electrical engineers in electromagnetic field theory (including the div and curl operations), and it was they who first stated Maxwell's equations in the form in which we now use them (Nahin, 1987).

## EXERCISES

---

**2.1** Here are four trigonometric identities that we shall need frequently:

$$\sin(A)\cos(B) = \frac{1}{2}[\sin(A+B) + \sin(A-B)] \quad (1)$$

$$\cos(A)\sin(B) = \frac{1}{2}[\sin(A+B) - \sin(A-B)] \quad (2)$$

$$\cos(A)\cos(B) = \frac{1}{2}[\cos(A+B) + \cos(A-B)] \quad (3)$$

$$\sin(A)\sin(B) = \frac{1}{2}[\cos(A-B) - \cos(A+B)] \quad (4)$$

Prove each of these results, and learn how to write them quickly because they will prove to be invaluable.

**2.2** Find the values of the following integrals. (Try one of them as an integration-by-parts problem, and you will quickly become addicted to the identities derived in the previous exercise.)

$$(a) \int_{-1}^1 \cos(t)\cos(2\omega_0 t) dt \quad (b) \int_0^2 \sin(\pi t)\cos(n\pi t) dt$$

$$(c) \int_0^1 \cos(\pi t)\sin(n\pi t) dt \quad (d) \int_{-2}^2 \sin(t)\sin(n\pi t) dt$$

**2.3** For each of the periodic waveforms shown in the following figures, write the complete analytical definition, using as the period the range  $0 < t < T_0$ . Where the waveform is either even or odd give the analytical definition over the first half of this range and then state "even" or "odd."

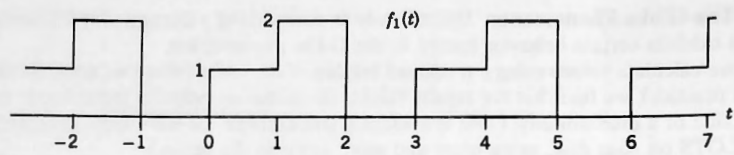


Figure 2.13.

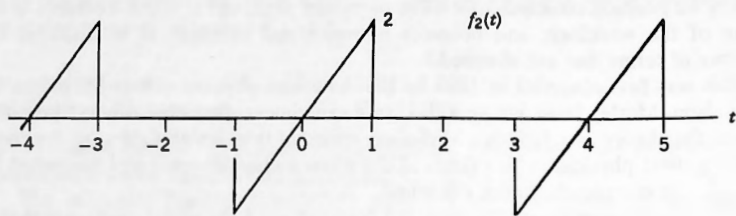


Figure 2.14.

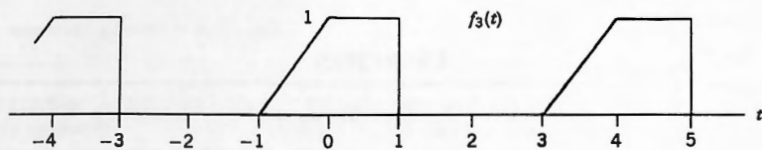


Figure 2.15.

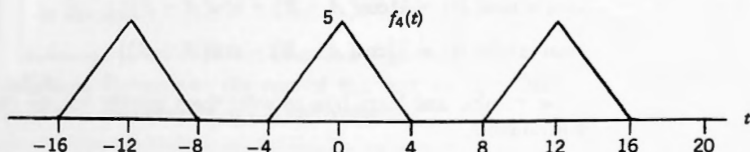


Figure 2.16.

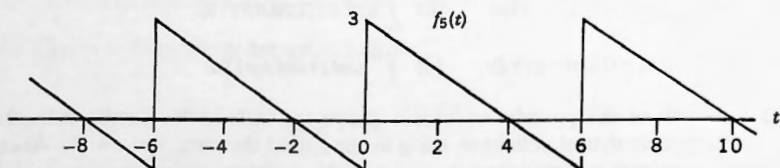


Figure 2.17.

**2.4** Sketch the following waveforms, showing two complete periods.

$$(a) f(t) = \begin{cases} 3 & (0 < t < 2) \\ -2 & (2 < t < 3) \end{cases} \quad f(t+3) = f(t)$$

$$(b) f(t) = \begin{cases} t & (0 < t < 1) \\ 2-t & (1 < t < 2) \end{cases} \quad f(t+2) = f(t)$$

$$(c) f(t) = \begin{cases} 1-t & (0 < t < 2) \\ t-3 & (2 < t < 4) \\ 0 & (4 < t < 6) \end{cases} \quad f(t+6) = f(t)$$

$$(d) f(t) = \begin{cases} \sin(\pi t) & (0 < t < 1) \\ 2-t & (1 < t < 3) \end{cases} \quad f(t+3) = f(t)$$

$$(e) f(t) = e^t \quad (0 < t < 2) \\ f(t) \text{ is even} \quad f(t+4) = f(t)$$

$$(f) f(t) = e^t \quad (0 < t < 2) \\ f(t) \text{ is odd} \quad f(t+4) = f(t)$$

**2.5** Find the value of  $\omega_0$  for each of the following waveforms, and hence find  $T_0$ , the smallest period of each. Find the complex Fourier coefficients for each by inspection.

$$(a) \cos(2\pi t) \quad (b) 1 + \sin(t) + \sin(2t)$$

$$(c) 3 + 4 \cos(\pi t) - 2 \cos(2\pi t) + 6 \cos(5\pi t)$$

$$(d) 5 - 3 \sin(2t) + 2 \sin(8t) + 5 \sin(10t)$$

$$(e) 4 - 2 \sin(3t) + 3 \cos(2t) + 4 \sin(5t)$$

$$(f) 3 \cos(100\pi t) + 5 \sin(70\pi t)$$

$$(g) \cos(2\pi t/3) + 2 \cos(5\pi t/3)$$

$$(h) \cos(t/2) - 2 \sin(t/3)$$

$$(i) \cos(2t) + \sin(\pi t)$$

$$(j) f_p(t) = \frac{1}{4} + \sum_{n=1}^4 \left[ \frac{1}{n^2} \cos \frac{nt}{5} + \frac{(-1)^n}{(2n+1)^2} \sin \frac{nt}{5} \right]$$

$$(k) f_p(t) = \frac{1}{2} + \frac{2}{\pi} \sum_{k=1}^3 \frac{1}{2k-1} \sin[(2k-1)2\pi t]$$

**2.6** Find  $\omega_0$ ,  $T_0$ , the complex Fourier coefficients, the power spectrum, and the total power for the following:

$$(a) f(t) = 2 \sin(3t) \quad (b) f(t) = 3 \cos(2t)$$

If (b) was a voltage across 100 ohms, what would the total power be? If a current through 100 ohms?

$$(c) f(t) = 5 \sin(5t) + 7 \cos(6t) + 3$$

If this were a voltage across 10,000 ohms, what would the total power be? If a current through 0.01 ohm?

- 2.7 What are the expressions for the complex Fourier coefficients of the following functions? In each case, also give the period  $T_0$ , and state if the function in the time domain is real or complex. If real, then state:

- If it is even or odd or neither
- If it has discontinuities in its zeroth, first, or second derivative
- What its average value is

$$(a) f_p(t) = \sum_{n=-\infty}^{\infty} \text{Sa} \frac{n\pi}{2} e^{jn\pi t/2}$$

$$(b) f_p(t) = \frac{1}{2} + \frac{j}{2\pi} \sum_{\substack{n=-\infty \\ n \neq 0}}^{\infty} \frac{(-1)^n - 1}{n} e^{jn2\pi t}$$

$$(c) f_p(t) = \sum_{\substack{n=-\infty \\ n \neq 0}}^{\infty} \frac{\cos(n\pi/2) - j \sin(n\pi/2)}{n(n^2 - 4)} e^{j4nt}$$

$$(d) f_p(t) = \frac{2j}{\pi} \sum_{\substack{n=-\infty \\ n \neq 0}}^{\infty} \frac{1 - (-1)^n}{n(n^2 - 4)} e^{jnt}$$

$$(e) f_p(t) = \frac{1}{2} \sum_{n=-\infty}^{\infty} \frac{(-1)^n e^{-1}}{1 - jn\pi} e^{(jn\pi)t}$$

- 2.8 What is the time-domain representation for the periodic functions  $f_p(t)$  that have the following coefficients? State in each case if  $f_p(t)$  is real or not and give its average value.

$$(a) F(n) = \begin{cases} \frac{1}{2} & (n = 0) \\ \frac{\cos(n\pi) - 1}{n^2\pi^2} & (n \neq 0) \end{cases} \quad T_0 = 2$$

$$(b) F(n) = j \frac{n \cos(n\pi/2) - \sin(n\pi/2)}{n^2} \quad (n \neq 0) \quad T_0 = \pi$$

$$(c) F(n) = \frac{1}{2} \frac{\sin(n\pi/2) - jn \cos(n\pi/2)}{n\pi/2} \quad (\forall n) \quad T_0 = 4$$

- 2.9 (a) Prove that if  $z$  and  $w$  are two complex quantities then

$$(1) |zw| = |z||w| \quad \text{and} \quad \arg(zw) = \arg(z) + \arg(w)$$

$$(2) |z/w| = |z|/|w| \quad \text{and} \quad \arg(z/w) = \arg(z) - \arg(w)$$

Thus the magnitude of a product is the product of the magnitudes, and the argument of a product is the sum of the arguments.

- (b) What are the expressions for the magnitudes and phases of the following?

$$(1) F(n) = \frac{je^{-jn\pi/2}}{n\pi/2} \quad (n \neq 0)$$

$$(2) F(n) = \frac{1 - e^{-jn} - jne^{-jn}}{(jn)^2} e^{jn} \quad (n \neq 0)$$

$$(3) F(n) = \frac{(1+jn)(2-j3n)(4+j5n)}{(6+j7n)(8+j9n)(10+j11n)}$$

### ■ Warning Regarding Arctangents

It is extremely easy to use a hand calculator to derive arctangents, but if not properly done you will be wrong half the time as the following shows.

$$(1) \arg(1+j) = \tan^{-1}(1/1) = \tan^{-1}(1) = 0.7854 \text{ Right.}$$

$$(2) \arg(-1-j) = \tan^{-1}(-1/-1) = \tan^{-1}(1) = 0.7854 \text{ WRONG!}$$

$\arg(-1-j)$  is in the **third quadrant**, and so after finding  $\tan^{-1}(1) = 0.7854$ , we must then subtract  $\pi$  to give the correct answer as  $-2.3562$

$$(3) \arg(1-j) = \tan^{-1}(-1/1) = \tan^{-1}(-1) = -0.7854 \text{ Right.}$$

$$(4) \arg(-1+j) = \tan^{-1}(1/-1) = \tan^{-1}(-1) = -0.7854 \text{ WRONG!}$$

$\arg(-1+j)$  is in the **second quadrant**, and so after finding  $\tan^{-1}(-1) = -0.7854$ , we must then add  $\pi$  to give the correct answer as  $2.3562$

Simply sending a single number  $x$  to an **arctangent** function, whether on a hand calculator or in a computer language, will result in an answer that was based on the assumption that the angle  $\arctan(x)$  lies in the **first quadrant** if  $x > 0$  and in the **fourth quadrant** if  $x < 0$ .

It is up to you to capture the correct quadrant information from the two components of the complex number and then to take the appropriate steps to obtain the correct answer.

*Note 1:* Whenever we find that a phase angle has a value exceeding  $\pi$  or less than  $-\pi$ , then we must restate it as an angle lying in the range  $-\pi < \Theta \leq \pi$  by subtracting or adding appropriate multiples of  $2\pi$ .

(c) Find the magnitude and argument of the following quantities:

$$(1) 3+j \quad (2) 1-3j \quad (3) -1-2j$$

$$(4) -3+4j \quad (5) -1 \quad (6) \pi$$

$$(7) j\pi \quad (8) -j\pi/5 \quad (9) 1/j\pi$$

$$(10) -2/j\pi \quad (11) e^{j\pi} \quad (12) e^{-j\pi/2}$$

$$(13) -e^{j\pi/2} \quad (14) (1-2j)e^{j\pi/2}$$

$$(15) -(1-j)/j\pi \quad (16) -(1-j)j\pi$$

$$(17) (1+j)/(1-2j) \quad (18) (-3+4j)/(-4j\pi - 2)j\pi/3$$

$$(19) -j(1-3j)/(-2+j)e^{2j} \quad (20) j[(-1)^3e^{-1}-j]/[1+j3\pi]$$

### Accompanying Disk

One of the many things for which the system can be used is to obtain estimates for the Fourier coefficients that we have been discussing in this chapter.

After you have carried out the analytical work in the following exercises, run the problem on the system. You will then be able to check what you have obtained (using pencil and paper) by comparing the values of your coefficients with the values obtained from the system.

Read Chapter 16, The User's Manual, Part I, in the file README16 on your disk in order to learn enough about the use of the system and how to get started quickly. (Also read README1.) Pay particular attention to Section 16.9 in Chapter 16 where we state the following:

When using the FFT to approximate Fourier series coefficients or Fourier transforms, if a sampling instant falls on a discontinuity, then always use the half-value, that is, the average of the values on each side of the discontinuity, as the value that is loaded at that point.

Whenever there is a discontinuity in the analytical expression for your waveform, the system will use the half-value at that point. You will be able to see this by carefully inspecting a plot of any functions that you have entered.

- 2.10** (a) Write the analytical definition of the periodic function shown in Figure 2.18. What is the value of  $T_0$  and of  $\omega_0$ ?
- (b) Find the general expression for the complex Fourier coefficients. What are the values of  $A(n)$  and  $B(n)$  for  $0 \leq n \leq 5$ ?
- (c) Write out the Fourier series for the waveform showing the central five nonzero terms explicitly.
- (d) To what values does your series converge at the points where there are discontinuities, that is, wherever  $t$  is an integer? What does the theory in Section 2.5 predict?
- (e) At what rate do the coefficients converge to zero?
- (f) Use the FFT system to obtain estimates for the coefficients of the Fourier series for  $f_p(t)$ , and verify the results shown in Table 2.6, observing that  $A(n)$  is even and  $B(n)$  is odd. (Use  $N = 256$ .)
- (g) Do the values in the table confirm the ones that you obtained in (b)?

*Note:* The FFT does not give exact values for the Fourier series coefficients, but gives approximations that become more and more accurate as the value of  $N$  is increased. This is discussed in full detail in Part II of the text.

- (h) From the final column of the table infer that the FFT's estimates of the coefficients die out approximately like  $1/n$ .

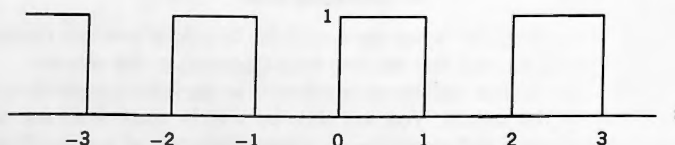


Figure 2.18.

TABLE 2.6 FFT Estimates of  $F(n)$ 

$n$	$A(n)$	$B(n)$	$ B_1/B(n) $
-7	0	$4.5360933e-2$	7.0169171
-5	0	$6.3582062e-2$	5.0060331
-3	0	0.10605535	3.0012056
-1	0	0.31829391	1
0	$\frac{1}{2}$	0	—
1	0	-0.31829391	1
3	0	-0.10605535	3.0012056
5	0	-6.3582062e-2	5.0060331
7	0	-4.5360933e-2	7.0169171

- 2.11 (a) Write the analytical definition for the periodic waveform shown in Figure 2.19.
- (b) Find the complex Fourier series for this waveform, showing explicitly the central four nonzero terms.
- (c) To what value should your series converge at  $t = 1, 3, 5, \dots$ ? What value does it in fact converge to at those points?
- (d) At what rate do your coefficients converge to zero?
- (e) Run this problem using the FFT system to confirm your results. Use  $N = 256$  and verify that the coefficients obtained are as follows:

$$F(1) = 0.31829391 \quad F(3) = -0.10605536 \quad F(5) = 6.358206e-2$$

$$F(7) = -4.53609330e-2 \quad F(9) = 3.5223837e-2$$

- (f) Why is  $F(n)$  real for all values of  $n$ ?

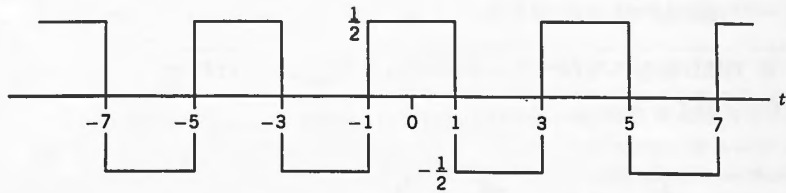


Figure 2.19.

- 2.12 (a) Write the analytical definition and then find the complex Fourier coefficients for the periodic waveform  $f_p(t)$  shown in Figure 2.20.
- (b) Now convert your coefficients to their real form (see (2.88)) and then write out the real series explicitly, showing the first five nonzero terms.
- (c) To what values does your series converge at  $t = 1$  and at all of the other points of discontinuity?
- (d) At what rate do the coefficients converge to zero?

- (e) Run this problem on the FFT system with  $N = 256$  to confirm your results in (b). (See Table 2.7.)
- (f) Repeat the FFT run using  $N = 1024$ . For each run calculate the relative error in the first 5 FFT coefficients. Observe how much smaller the relative errors are for  $N = 1024$  compared to  $N = 256$ .

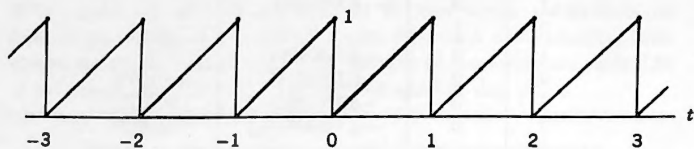


Figure 2.20.

TABLE 2.7 FFT Estimates of  $a(n)$  and  $b(n)$ 

$n$	$a(n)$	$b(n)$
0	1	0
1	0	-0.31829391
2	0	-0.15912298
3	0	-0.10605535
4	0	-7.9513545e-2
5	0	-6.3582062e-2

2.13 Use the identities

$$\cos(A)\cos(B) = \frac{1}{2}[\cos(A+B) + \cos(A-B)] \quad (2.98)$$

$$\sin(A)\sin(B) = \frac{1}{2}[\cos(A-B) - \cos(A+B)] \quad (2.99)$$

to prove that the set of sines and cosines forms an orthogonal set as stated in Theorem 2.7.

*Hint for the proof of (2.101):* Is the integrand even, odd or neither?

■ THEOREM 2.7: Orthogonality of the Set of Sines and Cosines

For  $n$  and  $m$  nonnegative integers and  $\omega_0 = 2\pi/T_0$ ,

$$\int_{-T_0/2}^{T_0/2} \cos(n\omega_0 t) \cos(m\omega_0 t) dt = \begin{cases} 0 & (n \neq m) \\ T_0/2 & (n = m \neq 0) \\ T_0 & (n = m = 0) \end{cases} \quad (2.100)$$

$$\int_{-T_0/2}^{T_0/2} \cos(n\omega_0 t) \sin(m\omega_0 t) dt = 0 \quad (\forall n \text{ and } m) \quad (2.101)$$

$$\int_{-T_0/2}^{T_0/2} \sin(n\omega_0 t) \sin(m\omega_0 t) dt = \begin{cases} 0 & (n \neq m) \\ T_0/2 & (n = m \neq 0) \\ 0 & (n = m = 0) \end{cases} \quad (2.102)$$

**2.14** For the periodic waveform

$$f_p(t) = 3 - \cos(4t) + 2\sin(5t) - 7\cos(9t)$$

- (a) What is the value of  $T_0$ ?
- (b) What is the total average power?
- (c) Find the complex Fourier coefficients.
- (d) Using Parseval's theorem, find the power spectrum.
- (e) Show that the total average power from (d) agrees with what you obtained in (b).

*Hint:* Make use of Theorem 2.7.

**2.15** Prove that

$$(a) \sum_{n=-\infty}^{\infty} F(n) = f_p(0) \quad (b) \int_{-T_0/2}^{T_0/2} f_p(t) dt = T_0 F(0)$$

From (a) we can obtain the sum of the coefficients by reading off the value of  $f_p(t)$  at  $t = 0$ , and from (b) we can obtain the area under  $f_p(t)$  over one period as  $T_0 F(0)$ .

- 2.16** (a) Find the complex Fourier series for the periodic function  $f_p(t)$  shown in Figure 2.21.
- (b) To what values does the series converge at  $t = 0$  and  $t = \frac{1}{2}$ ? Establish this by examining your Fourier series.
- (c) For large  $n$  the Fourier coefficients converge like  $K/n^p$ . What is the value of  $p$ ?
- (d) Find the expression for the power spectrum.
- (e) Compute magnitude, phase, and power for this waveform for  $-5 \leq n \leq 5$  and the sum of the power in these terms.
- (f) What percentage of the total average power in the waveform is contained in the terms in (e)?
- (g) Verify your results in (e) using the FFT system. You can find the FFT's value for the power in all of the terms in (e) as follows: After you have obtained the spectrum for the waveform take main menu G, then F, POWER. This is an item in the F postprocessor that computes energy or power in a waveform. You will be prompted for M, which is the highest harmonic number to be included. In this case it is 5. The result should be very close to your value in (e).

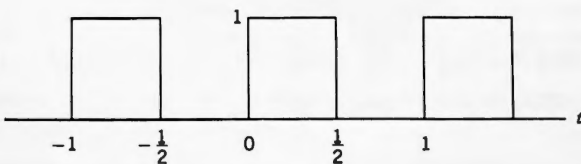


Figure 2.21.

**2.17** (a) Sketch the following function and find its complex Fourier coefficients:

$$f_p(t) = \begin{cases} 0, & (-1 < t < 0) \\ e^t, & (0 < t < 1) \end{cases} \quad f_p(t+2) = f_p(t)$$

- (b) According to Fourier's theorem, to what value does the Fourier series converge at  $t = -1$ ,  $t = 0$ , and  $t = 1$ ? Is this obvious from the series?
- (c) Sketch the function to which the Fourier series converges in the range  $-2.5 \leq t \leq 2.5$ .
- (d) For large  $n$  the Fourier coefficients converge like  $K/n^p$ . What is the value of  $p$ ?
- (e) Compute magnitude and phase for  $-5 \leq n \leq 5$ .
- (f) Find the expression for the power spectrum. Compute total average power, and the values of the power spectrum up to  $n = \pm 5$ . What percentage of total power is included in these terms?
- (g) Verify your results in (e) and (f) using the FFT system.

**2.18** Use Theorem 2.7, which appeared earlier in this section to prove Theorem 2.8, which is a statement of the analysis and synthesis equations for the real form of the Fourier series.

*Hint:* Follow the method used to derive (2.27) and (2.28).

### ■ THEOREM 2.8: Real Fourier Series for Periodic Waveforms

Let  $f_p(t)$  be periodic with period  $T_0$ , defined analytically. Then it can be synthesized from the infinite series of sines and cosines

$$f_p(t) = a(0)/2 + \sum_{n=1}^{\infty} a(n) \cos(n\omega_0 t) + \sum_{n=1}^{\infty} b(n) \sin(n\omega_0 t) \quad (2.103)$$

where the Fourier coefficients  $a(n)$  and  $b(n)$  can be found from the analytical definition of  $f_p(t)$  by

$$a(n) = 2/T_0 \int_{-T_0/2}^{T_0/2} f_p(t) \cos(n\omega_0 t) dt \quad (n = 0, 1, 2, \dots) \quad (2.104)$$

and

$$b(n) = 2/T_0 \int_{-T_0/2}^{T_0/2} f_p(t) \sin(n\omega_0 t) dt \quad (n = 1, 2, 3, \dots) \quad (2.105)$$

- 2.19** (a) Using Theorem 2.8, find the real Fourier series for the periodic waveform shown in Figure 2.22.
- (b) At what rate do the coefficients converge to zero?
- (c) What should the series converge to at  $t = 1$ ? Is this result immediately obvious from the series that you have obtained?
- (d) Convert your series to the complex form.  
*Hint:* Solve for  $A(n)$  and  $B(n)$  from (2.88).
- (e) What is the sum of all of the elements of the power spectrum?
- (f) Run this problem using the FFT system to confirm all of your results.

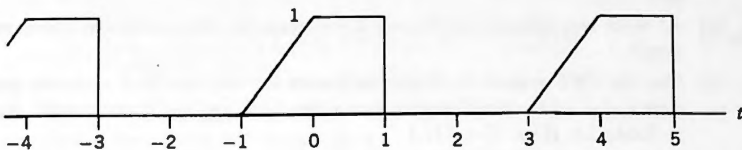


Figure 2.22.

- 2.20** (a) Show that if  $f_p(t)$  is real and even, then its real Fourier series consists only of cosines.
- (b) Show that if  $f_p(t)$  is real and odd, then its real Fourier series consists only of sines.
- 2.21** Using the results of Exercise 2.20, find a series of cosines that converges to the following, showing the first four nonzero terms explicitly. In each case sketch the waveform that the series converges to over two of the intervals shown.
- (a)  $f(t) = \cos^2(t)$       ( $0 < t < \pi$ )
- (b)  $f(t) = \sin(\pi t/2)$       ( $0 < t < 2$ )  
 Observe that we are using an infinite series of cosines to express a sine.
- (c) At what rate do the coefficients die out in (b)? Explain.
- (d) Find the average power for the waveform in (b).
- (e) Run this problem using the FFT system to confirm your results. Verify the average power in (d).
- 2.22** Using the results of Exercise 2.20, find a series of sines that converges to the following, showing the first four nonzero terms explicitly. In each case sketch the waveform that the series converges to over two of the intervals shown.
- (a)  $f(t) = \cos(\pi t/2)$       ( $0 < t < 2$ )  
 Observe that we are using an infinite series of sines to express a cosine.
- (b)  $f(t) = \sin^2(t)$       ( $0 < t < \pi$ )
- (c) At what rate do the coefficients die out in (b)? Explain.

- (d) Run (b) on the FFT, using  $N = 1024$  to confirm your results. You will observe almost perfect agreement between the FFT values of the coefficients and the exact values, a direct consequence of the fact that the coefficients are dying out like  $1/n^3$ . This is examined in detail in Chapters 12 and 13.

**2.23** (a) Sketch  $f_p(t)$  defined analytically as follows:

$$f_p(t) = \begin{cases} 1 - t^2 & (0 < t < 1) \\ t^2 - 4t + 3 & (1 < t < 2) \end{cases} \quad f_p(t+4) = f_p(t) \quad f_p(t) \text{ is even}$$

- (b) Verify that the zeroth and first derivatives of  $f_p(t)$  are everywhere continuous.
- (c) At what rate should the Fourier coefficients for this waveform converge to zero?
- (d) Use the FFT system to obtain estimates for the first four nonzero coefficients  $a(n)$  of the real Fourier series for  $f_p(t)$  and verify the results shown in Table 2.8. (Use  $N = 512$ .)  
Infer from the final column that the FFT's estimates of the coefficients shown in the table are dying out approximately like  $1/n^3$ .

TABLE 2.8 FFT Estimates of  $a(n)$

$n$	$a(n)$	$ a_1/a(n) $	$n^3$
1	1.03204910	1	1
3	-3.8224041e-2	26.9999998	27
5	8.2563923e-3	125.000008	125
7	-3.0088888e-3	343.000083	343

#### 2.24 Elapsed Time to Run the FFT

The FFT system tells you what the elapsed time was to run either ANALYSIS, SYNTHESIS, or CONVOLUTION. Note the times to find approximations for the Fourier coefficients for the waveform shown in Figure 2.13, using the following values:

$$N = 256 \quad (2 \times 2 \times 2 \times 2 \times 2 \times 2 \times 2 \times 2)$$

$$N = 252 \quad (2 \times 2 \times 3 \times 3 \times 7)$$

$$N = 255 \quad (3 \times 5 \times 17)$$

$$N = 257 \quad (\text{prime})$$

Even though these values of  $N$  are all close to one another, you will find that the elapsed time to run the FFT increases rapidly as we depart from a power-of-2 value and approach a prime.

- 2.25 (a) Prove **Bessel's theorem** for the average power in a real periodic waveform:

$$P = \frac{1}{T_0} \int_{-T_0/2}^{T_0/2} |f_p(t)|^2 dt = \frac{a(0)^2}{4} + \frac{1}{2} \sum_{n=1}^{\infty} [a(n)^2 + b(n)^2] \quad (2.106)$$

This is a restatement of Parseval's theorem, but here we use the real coefficients rather than the complex ones.

*Hint:* Start from Parseval's theorem and then use (2.88).

- (b) Use Bessel's theorem to prove that, for a real periodic function, the total power is equal to the sum of the power in the even and the odd parts, that is,

$$P[f_p(t)] = P[f_{\text{ev}}(t)] + P[f_{\text{od}}(t)] \quad (2.107)$$

- 2.26 (a) Show that the expression for the complex Fourier coefficients of the waveform shown in Figure 2.23 is

$$F(n) = \begin{cases} \frac{j}{4n\pi} [2(-1)^n - 1 - e^{-j\pi n/2}] & (n \neq 0) \\ \frac{3}{8} & (n = 0) \end{cases}$$

- (b) Sketch the even and odd parts of this waveform and state the expressions for their Fourier coefficients.  
(c) Load the waveform into the **X** vector of the FFT system and then create plots of its even and odd parts, thus verifying your sketches in (b).  
(d) Using  $N = 256$ , load the expression for  $F(n)$  from (a) into the **F** vector and run SYNTHESIS. Then plot the result.

*Hint:* You will have to split it into  $A(n)$  and  $B(n)$ .

When prompted, use level-0 aliasing. Then repeat with level-5. Also use a higher aliasing level if you have the patience. (See Section 17.3 in README17 for an explanation of how aliasing works.)

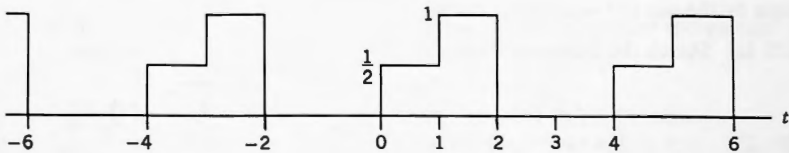


Figure 2.23.

- 2.27 (a) Find the complex Fourier series for the periodic function  $f_p(t)$  shown in Figure 2.24.
- (b) Is it true that for  $n$  large,  $|F(n)|$  converges like  $K/n^2$ ? Can you see why?
- (c) Compute magnitude, phase, and power for  $-5 \leq n \leq 5$ .
- (d) Compute total average power and find how large  $N$  must be in order to contain 99 percent of total power in the range  $-N \leq n \leq N$ .
- (e) Verify your results in (c) using the FFT system.
- (f) Using  $N = 256$ , load the expression for  $F(n)$  that you obtained in (a) into F and run SYNTHESIS. Then plot the result.

*Hint:* You will have to split it into  $A(n)$  and  $B(n)$ .

Because the waveform has no discontinuities, the spectrum dies out like  $1/n^2$ , that is, quite quickly. Thus to produce a good version of the FFT spectrum from the one that you obtained in (a) you will only have to alias a small amount.

Use level-0 and level-5 aliasing as discussed in Section 17.3 and observe that in fact no aliasing at all is required because of the rapid convergence of the spectrum.

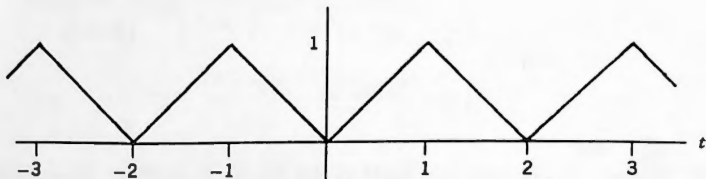


Figure 2.24.

- 2.28 Provide proofs showing which of the following are true and which are false.

- (a)  $f_p(t)$  even implies  $F(n) = 2/T_0 \int_0^{T_0/2} f_p(t) e^{-jn\omega_0 t} dt$
- (b)  $f_p(t)$  even implies  $F(n) = 2/T_0 \int_0^{T_0/2} f_p(t) \cos(n\omega_0 t) dt$
- (c)  $f_p(t)$  odd implies  $F(n) = -2j/T_0 \int_0^{T_0/2} f_p(t) \sin(n\omega_0 t) dt$

Later in the text we shall see how the Fourier coefficients of the waveforms in this set of exercises can all be found without integration. However, for now we must find them by the use of the analysis equation.

- 2.29 (a) Sketch the following waveform:

$$f_p(t) = \begin{cases} t & (0 < t < 1) \\ 0 & (1 < t < 4) \end{cases} \quad f_p(t+4) = f_p(t)$$

and find its complex Fourier coefficients.

- (b) Sketch its even and odd parts and state the expressions for their Fourier coefficients.
- (c) Load  $f_p(t)$  into the  $\mathbf{X}$  vector of the FFT system and then create plots of its even and odd parts. See the hint in Exercise 2.26(c).
- (d) Using  $N = 256$ , load the expression for  $F(n)$  that you obtained in (a) into the  $\mathbf{F}$  vector and run SYNTHESIS. Then plot the result. When prompted, use level-0 aliasing. Then repeat with level-5. Also use a higher aliasing level if you have the patience. (See Section 17.3 in README17 for an explanation of how aliasing works.)

**2.30** (a) Sketch and find the Fourier coefficients of

$$f_p(t) = \begin{cases} 0 & (-2 < t < -1) \\ t + 1 & (-1 < t < 0) \\ 1 & (0 < t < 1) \\ 0 & (1 < t < 2) \end{cases} \quad f_p(t+4) = f_p(t)$$

- (b) Sketch its even and odd parts and state the expressions for their Fourier coefficients.
- (c) Load  $f_p(t)$  into  $\mathbf{X}$  and then create plots of its even and odd parts. See the hint in Exercise 2.26(c).
- (d) Load the expression for  $F(n)$  that you obtained in (a) into  $\mathbf{F}$  and run SYNTHESIS. Then plot the result. Use  $N = 256$  with level-0 and level-5 aliasing.

**2.31** Prove that for  $f_p(t)$  real,  $f_{od}(t) \Leftrightarrow jB(n)$ .

**2.32** Prove that for  $f_p(t)$  real,  $F(n)$  is purely imaginary and odd iff  $f_p(t)$  is odd.

### 2.33 The Various Forms of the Coefficients

Note carefully, once again, the difference between  $a(n)$  and  $b(n)$  on the one hand and  $A(n)$  and  $B(n)$  on the other.

$A(n)$  and  $B(n)$  are the real and imaginary parts of the complex coefficients  $F(n)$  that were derived in Theorem 2.2;  $a(n)$  and  $b(n)$  are the real coefficients that were derived from  $A(n)$  and  $B(n)$  in (2.88).

- (a) Show that the real form of the Fourier series can be further reorganized as follows:

$$f_p(t) = \sum_{n=0}^{\infty} H(n) \cos[n\omega_0 t - \Phi(n)] \quad (2.108)$$

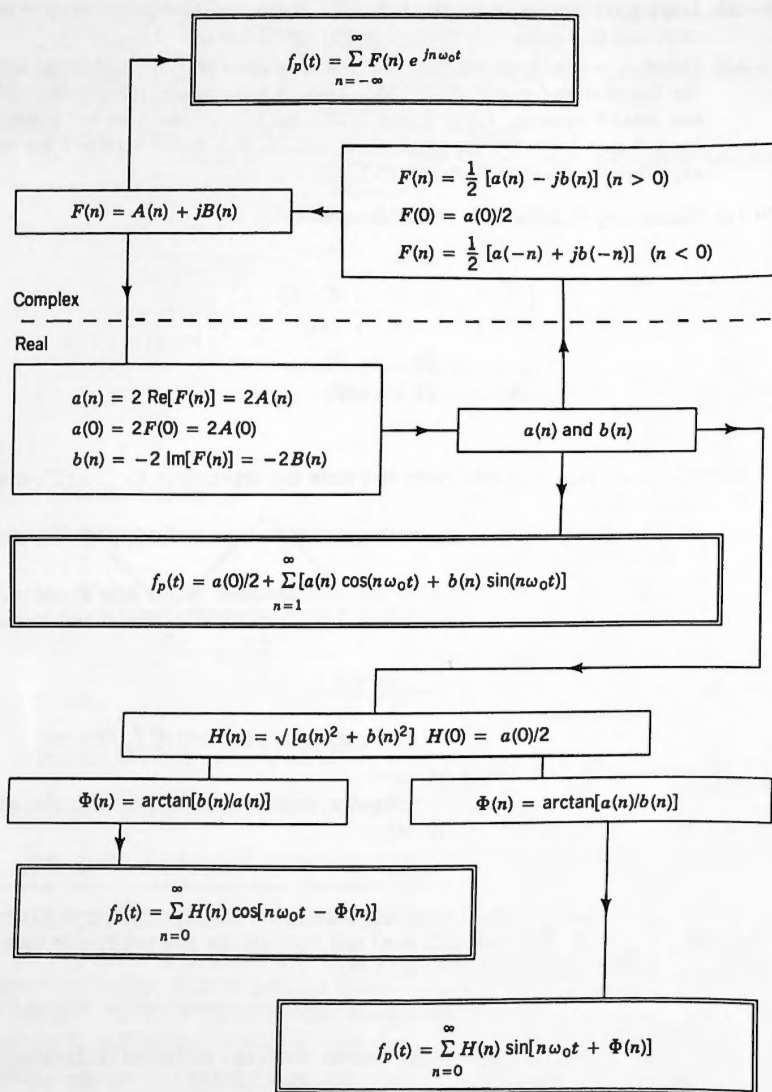


Figure 2.25. Real and complex Fourier series.

where

$$\left. \begin{aligned} H(n) &= [a(n)^2 + b(n)^2]^{1/2}, H(0) = a(0)/2, \\ \Phi(n) &= \arctan[b(n)/a(n)] \end{aligned} \right\} \quad (2.109)$$

(b) Also show that the real form can be written as

$$f_p(t) = \sum_{n=0}^{\infty} H(n) \sin(n\omega_0 t + \Phi(n)) \quad (2.110)$$

where

$$\left. \begin{aligned} H(n) &= [a(n)^2 + b(n)^2]^{1/2}, H(0) = a(0)/2, \\ \Phi(n) &= \arctan[a(n)/b(n)] \end{aligned} \right\} \quad (2.111)$$

All of these relationships are shown in Figure 2.25.

*Note:* In the statement of Theorem 2.2 we show the limits of integration in (2.28) as the period from  $-T_0/2$  to  $T_0/2$ . However (2.28) is still valid when any other complete period is used (e.g. 0 to  $T_0/2$ ). It is often more convenient to use the latter, as would be the case with the waveform in Figure 2.20.

Accordingly, (2.28) would best be written as follows

$$F(n) = \int_{\text{any one period}} f_p(t) e^{-jna_0 t} dt$$

All of this is true because the orthogonality of the complex exponentials (Theorem 2.1) applies over any one complete period.

---

## CHAPTER 3

---

# The Fourier Integral

---

### 3.1 INTRODUCTION

---

Up to now the waveforms that we have considered have all been periodic, for each of which there has always been a Fourier series representation. However it is not always the case that the waveforms that we wish to analyze are periodic. Far more often they are single pulses that occur just once and do not repeat themselves. Fourier analysis covers single pulses as well, and for that reason we now commence the study of what is known as the **Fourier integral**.

We shall also see that the periodic waveforms that we have been examining can sometimes best be thought of as single, infinitely long pulses that occur just once, and that the Fourier integral for one-time pulses that we are about to explore also applies to them. It will thus be seen to be a unifying tool that covers both classes of waveform, pulse and periodic.

---

### 3.2 THE FOURIER INTEGRAL

---

We are interested in applying Fourier analysis to the single pulse  $f(t)$ . From the preceding chapter we know how to do this for periodic signals, and so the following idea comes to us: Let's think of our pulse as being embedded in a single period of a periodic waveform and then let  $T_0$  tend to infinity. Perhaps this will result in a pair of Fourier "analysis" and "synthesis" equations for  $f(t)$ .

Referring to Figure 3.1, we accordingly create the periodic function  $f_p(t)$  as follows: In Figure 3.1a we show the single pulse  $f(t)$ . Then in Figure 3.1b we show that same pulse embedded in the periodic waveform  $f_p(t)$ , which is constantly repeating  $f(t)$  every  $T_0$  seconds. Thus the waveform in Figure 3.1b has the analytical definition

$$\left. \begin{aligned} f_p(t) &= f(t) & (-T_0/2 < t < T_0/2) \\ f_p(t + T_0) &= f_p(t) \end{aligned} \right\} \quad (3.1)$$

Note how  $f(t)$  constitutes the single-period definition of  $f_p(t)$  in (3.1), and with  $T_0$  still finite we clearly are able to find the complex Fourier series for  $f_p(t)$  based on this definition. Then we let  $T_0$  tend to infinity and we have only the single pulse

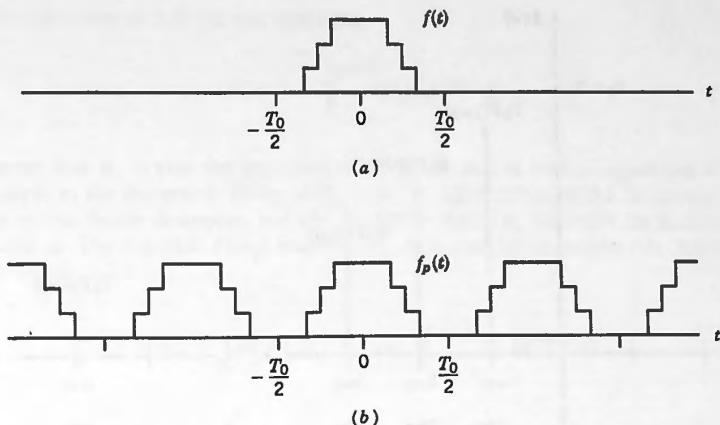


Figure 3.1.  $f(t)$  embedded in a periodic waveform.

remaining. Hopefully our complex Fourier series representation will have metamorphosed into some form of Fourier-type representation for  $f(t)$ .

Starting with the analysis equation applied to  $f_p(t)$  we have

$$F(n) = \frac{1}{T_0} \int_{-T_0/2}^{T_0/2} f_p(t) e^{-j n \omega_0 t} dt \quad (3.2)$$

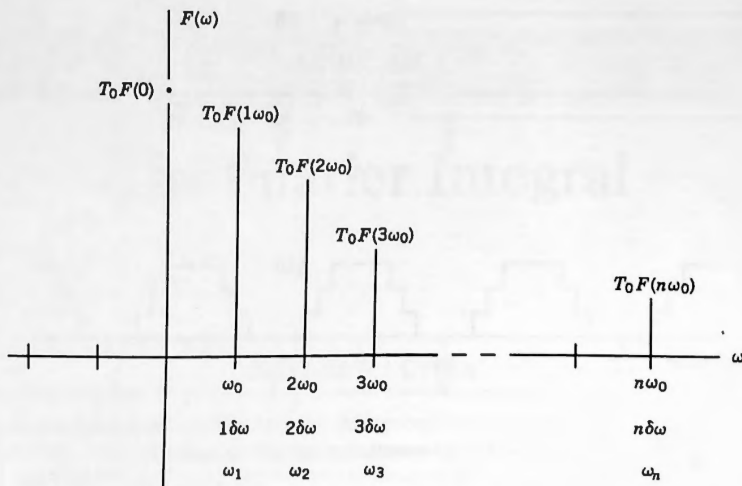
First we note that  $n$  and  $\omega_0$  are being multiplied together in the integrand. That being the case they should still be multiplied together after the integration is completed, and so we could just as well have called the result  $F(n\omega_0)$  rather than  $F(n)$ . Knowing what lies ahead we accordingly begin doing that, and so we rewrite (3.2) as

$$F(n\omega_0) = \frac{1}{T_0} \int_{-T_0/2}^{T_0/2} f(t) e^{-j n \omega_0 t} dt \quad (3.3)$$

Observe also that we have now written  $f(t)$  into the integrand, because that is the expression for  $f_p(t)$  in the period being considered within the limits of the integral.

We are planning to let  $T_0 \rightarrow \infty$  while keeping  $f(t)$  unchanged, and what we see on the RHS of (3.3) is the average value of the expression  $f(t)e^{-j n \omega_0 t}$  computed over the range of integration. Clearly as  $T_0 \rightarrow \infty$ , that average will go to zero, which would be an undesirable result. Thus our next step is to rearrange (3.3) so as to avoid this problem, and so we rewrite it as

$$T_0 F(n\omega_0) = \int_{-T_0/2}^{T_0/2} f(t) e^{-j n \omega_0 t} dt \quad (3.4)$$

Figure 3.2. Plot of coefficients on the  $\omega$ -axis.

Carrying out the integration appearing here we obtain the line spectrum  $T_0 F(n\omega_0)$  ( $-\infty < n\omega_0 < \infty$ ), part of which is shown in Figure 3.2.

In the figure we show the horizontal axis being called the  $\omega$ -axis, and at the points  $\omega = n\omega_0$  we see a few of the spectral lines for our endless periodic waveform. These are identical to what we became familiar with in Chapter 2, except that now we have multiplied them by  $T_0$  according to the LHS of (3.4).

Recalling that  $\omega_0 = 2\pi/T_0$ , we know that as  $T_0 \rightarrow \infty$ ,  $\omega_0$  will diminish to zero, and so the spectral lines will become infinitely dense. The plot will probably cease to be a line spectrum and we begin to suspect that it will become a continuous curve.

While  $T_0$  is still finite our discrete spectral lines occur at values of  $\omega$  equal to  $n\omega_0$ . The vertical axis has been called  $F(\omega)$ , which is the name that our emerging function will be given. We now define the following three quantities that are also needed when we let  $T_0 \rightarrow \infty$ :

$$\delta\omega \equiv \omega_0 \quad (3.5)$$

$$\omega_n \equiv n\delta\omega \quad (3.6)$$

$$F(\omega_n) \equiv T_0 F(n\omega_0) \quad (3.7)$$

- Observe first in (3.5) that  $\delta\omega$  is the name that we give to the interval  $\omega_0$ . In the preceding figure we show a second labeling of the horizontal axis using  $\delta\omega$  as the unit of distance.
- In (3.6) we show the point  $n\delta\omega$  on the  $\omega$ -axis being called  $\omega_n$ . In the figure we show the horizontal axis labeled a third time in this way.
- Finally, in (3.7) we show the quantity  $T_0 F(n\omega_0)$  being called  $F(\omega_n)$ , which is certainly the case by virtue of the third labeling of the horizontal axis.

Then, returning to (3.4), we can now write

$$F(\omega_n) = \int_{-T_0/2}^{T_0/2} f(t) e^{-j\omega_n t} dt \quad (3.8)$$

Observe how  $\omega_n$  is now the argument of  $F$  on the left as well as appearing in the exponent in the integrand. Then, as  $T_0 \rightarrow \infty$ , the subdivisions of the horizontal axis close in and finally disappear, and the discrete variable  $\omega_n$  becomes the continuous variable  $\omega$ . The function  $F(\omega_n)$  becomes  $F(\omega)$ . It thus seems reasonable that from (3.8) we can write

$$\begin{aligned} F(\omega) &= \lim_{T_0 \rightarrow \infty} F(\omega_n) = \lim_{T_0 \rightarrow \infty} \int_{-T_0/2}^{T_0/2} f(t) e^{-j\omega_n t} dt \\ &= \int_{-\infty}^{\infty} f(t) e^{-j\omega t} dt \end{aligned} \quad (3.9)$$

This (much simplified) argument thus gives us the required **analysis equation** for our single pulse, which we now write as

$$F(\omega) = \int_{-\infty}^{\infty} f(t) e^{-j\omega t} dt \quad (3.10)$$

Consider now the synthesis equation. Starting once more with  $T_0$  finite, the synthesis equation for our periodic waveform is

$$f(t) = \sum_{n=-\infty}^{\infty} F(n\omega_0) e^{jn\omega_0 t} \quad (-T_0/2 < t < T_0) \quad (3.11)$$

Observe that we are writing  $f(t)$  on the left rather than  $f_p(t)$ . We know, however, that the synthesis equation for a periodic function will generate every one of the repetitions of the waveform  $f_p(t)$ , depending on the range of values that we use for  $t$  in the RHS. Thus using  $f(t)$  on the LHS of (3.11) is perfectly justified over the time range that we have shown there. We now replace  $F(n\omega_0)$  by  $F(\omega_n)/T_0$  according to (3.7), and so (3.11) becomes

$$f(t) = \sum_{n=-\infty}^{\infty} \frac{F(\omega_n) e^{jn\omega_0 t}}{T_0} \quad (3.12)$$

However,  $1/T_0 = \omega_0/2\pi = \delta\omega/2\pi$ , and so (3.12) can be written as

$$f(t) = \frac{1}{2\pi} \sum_{n=-\infty}^{\infty} F(\omega_n) e^{j\omega_n t} \delta\omega \quad (3.13)$$

If we now let  $T_0 \rightarrow \infty$ , then  $\delta\omega \rightarrow 0$  and  $\omega_n \rightarrow \omega$ . Once more it seems reasonable to

believe that the infinite sum in (3.13) becomes an integral, and indeed, under very general conditions it can be shown that it converges to

$$f(t) = \frac{1}{2\pi} \int_{-\infty}^{\infty} F(\omega) e^{j\omega t} d\omega \quad (3.14)$$

This then is the required **synthesis equation** for our single pulse. We summarize all of this as Theorem 3.1.<sup>†</sup>

■ **THEOREM 3.1: Fourier Transform for a Single Pulse**

(Provided that the integrals exist)

**Synthesis:**

$$f(t) = \frac{1}{2\pi} \int_{-\infty}^{\infty} F(\omega) e^{j\omega t} d\omega \quad (3.15)$$

**Analysis:**

$$F(\omega) = \int_{-\infty}^{\infty} f(t) e^{-j\omega t} dt \quad (3.16)$$

Equation (3.16) shows that a time function  $f(t)$  can be **analyzed** to give an associated frequency function  $F(\omega)$  that contains all of the information in  $f(t)$ . We call  $F(\omega)$  in (3.16) the **Fourier transform** of  $f(t)$  or the **Fourier spectral density** of  $f(t)$ . Sometimes, by analogy with the Fourier series case where we had coefficients  $F(n)$ , the function  $F(\omega)$  is also referred to as the **coefficient function**.

In (3.15), on the other hand, we see how we can **synthesize** a pulse, given its spectral density function. It is called the **inverse Fourier transform** of  $F(\omega)$ , or the **Fourier integral representation** of  $f(t)$ .

Theorem 3.1 displays a pair of equations that are so far-reaching that there is scarcely a field of applied mathematics, engineering, or physics for which they do not have some relevance.

Observe that the limits of integration in (3.16) are  $\pm\infty$ , which means that the “one-time pulses” that we can transform and reassemble with the preceding pair of equations can have unrestricted time durations. Thus, in addition to finite-time-duration pulses, such as the one appearing in Figure 3.1(a), we will also soon be able to

<sup>†</sup>The complete justification of the process whereby equations (3.9) and (3.14) emerge as  $T_0 \rightarrow \infty$  is far from as simple as we have presented it, and indeed extremely complicated. For a more complete discussion see first Wylie and Barrett, then Carslaw or Churchill and Brown.

transform infinite-length pulses such as

$$f(t) = e^{-\beta|t|} \quad (t \in \mathbb{R}) \quad (3.17)$$

and

$$g(t) = \begin{cases} 1 & (t > 0) \\ 0 & (t < 0) \end{cases} \quad (3.18)$$

Moreover, as we shall soon see, periodic waveforms can also be regarded as infinitely long “one-time pulses,” and so the analysis and synthesis equations that appear in Theorem 3.1 apply to them as well. Thus the Fourier pair (3.15) and (3.16) becomes a unifying tool, able to operate on all possible cases, namely

- One-time pulses of finite duration
- One-time pulses of infinite duration
- Periodic waveforms that inherently have infinite duration

We now introduce the following notation:

**Definition:** The expression

$$f(t) \Leftrightarrow F(\omega)$$

will be used to represent Theorem 3.1, stating that the Fourier transform of  $f(t)$  is  $F(\omega)$  per (3.16) and the inverse Fourier transform of  $F(\omega)$  is  $f(t)$  per (3.15).

All of this gives rise to the structure shown in Figure 3.3.

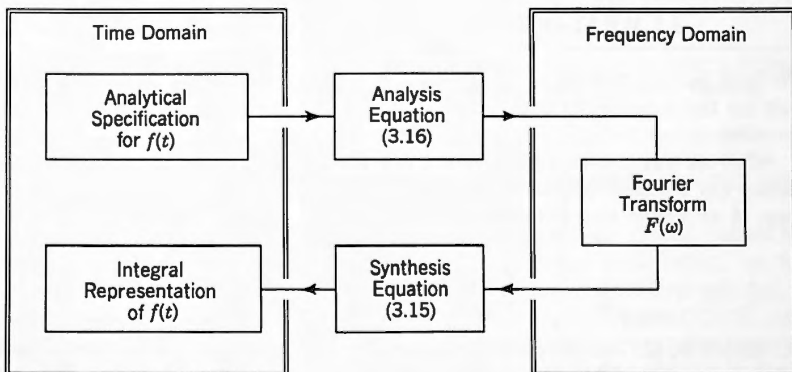


Figure 3.3. Fourier integral for one-time pulses.

In the figure we start with an analytical specification for  $f(t)$  in the time domain. Carrying out the analysis transformation (3.16), we obtain the Fourier transform  $F(\omega)$  in the frequency domain. We can then examine  $F(\omega)$  and draw certain conclusions from it regarding  $f(t)$ .

We can also send  $F(\omega)$  to the synthesis equation (3.15), thereby obtaining the integral representation for  $f(t)$  in the time domain as an alternative to the analytical specification that we started out with.

### Accompanying Disk

The FFT system on the accompanying disk performs all of the operations shown in Figure 3.3.

We can enter the time-domain analytical definition of a pulse from which the system then creates the  $\mathbf{X}$  vector of sampled values. Alternatively we can create an external disk file of such sampled values that can then be read into the system and placed in  $\mathbf{X}$ . That vector of samples is then operated on by the ANALYSIS procedure, and numerical values of the Fourier transform are produced in the frequency domain. Starting from those numerical values of the Fourier transform we can carry out the SYNTHESIS procedure. The result is a numerical version of the original one-time pulse, now back in the time domain.

If we so elect, we can also operate on the numerical values of the Fourier transform in the frequency domain, performing a variety of signal processing operations prior to inverting the result back to the time domain.

The values that we obtain for the Fourier transform from the fast Fourier transform (FFT) system represent samplings taken from the continuous spectrum  $F(\omega)$ , separated by the step size  $\omega_0 = 2\pi/T$ , where  $T$  for a pulse is discussed later (see Section 17.2). These sampled values are only approximations of the true values that would be found at those points, but they can be made as accurate as we please simply by making  $N$  sufficiently large.

### 3.3 WHAT DOES THE FOURIER INTEGRAL MEAN?

We have derived the pair of equations (3.15) and (3.16), which are called the **Fourier pair** for the function  $f(t)$ . But what exactly do they mean? Let's try to answer that question.

When we investigated Fourier series in Chapter 2 we saw that they enabled us to restate any periodic function as a linear combination of complex exponentials in the form of an infinite sum as follows:

$$f_p(t) = \sum_{n=-\infty}^{\infty} F(n) e^{jn\omega_0 t} \quad (3.19)$$

On the left we see the analytical definition of the waveform, and on the right its series representation. All frequencies occurring in the series are multiples of the base frequency  $\omega_0$ .

The other part of that derivation was a statement of the rule whereby we must select the constants  $F(n)$  for the infinite series so that it converges point by point to the desired function. In the case of (3.19) the rule for the selection of the  $F(n)$ 's was

$$F(n) = \frac{1}{T_0} \int_{-T_0/2}^{T_0/2} f_p(t) e^{-jn\omega_0 t} dt \quad (3.20)$$

However, the essential idea that emerged was the fact that:

**Every periodic function can be expressed as a linear combination of complex exponentials.**

In this chapter we started from a periodic function, and by letting  $T_0 \rightarrow \infty$ , we obtained a single pulse. The Fourier series for the periodic function led to the Fourier integral representation for the single pulse, namely

$$f(t) = \frac{1}{2\pi} \int_{-\infty}^{\infty} F(\omega) e^{j\omega t} d\omega \quad (3.21)$$

However, (3.21) is once again only a “linear combination” of complex exponentials  $e^{j\omega t}$  with coefficient function  $F(\omega)$ . To see this we need only go back to (3.13), where  $f(t)$  is being clearly expressed in that form.

On the RHS of (3.13) we see a discrete sum of complex exponentials, each of frequency  $\omega_n$ , each being multiplied by a coefficient  $F(\omega_n)$ . As  $\delta\omega \rightarrow 0$ , those frequencies pull closer and closer together. Ultimately, we replaced the  $\Sigma$  with an integral, but that was only a shorthand statement for the fact that the limit of a series has been involved. When that limit is taken, the coefficients  $F(\omega_n)$  merge together to form the coefficient function  $F(\omega)$ .

What is essential to recognize is the fact that, once again,  $f(t)$  has been expressed as a “linear combination” of complex exponentials. Thus the Fourier integral (3.15) is simply a restatement of what we learned about periodic functions, but now in much more general form, namely:

**Any physically realizable waveform can be expressed as a sum of complex exponentials**

Notice, however, that here we no longer have to use the word “periodic” when talking about our waveforms.

Equation (3.16) is the second half of the process. It gives us the precise method for choosing the “multipliers” that are to be used in that “linear combination” so that the integral (3.15) correctly sums to the required function  $f(t)$ . Notice now that in dealing with one-time pulses, the frequencies in the linear combination (3.15) cease to be integral multiples of a base frequency, but instead become **every possible frequency** from  $\omega = -\infty$  to  $\omega = \infty$ . Associated with this is the fact that the multipliers are no longer a discrete set specified for each of the integers  $n$ , but are instead

specified as a continuous function of  $\omega$  called  $F(\omega)$ . However, the central fact still remains:

The Fourier integral is simply a representation of  $f(t)$  as a linear combination of complex exponentials.

□EXAMPLE 3.1: (a) Find the Fourier transform and (b) write the Fourier integral representation for the pulse  $f(t)$  shown in Figure 3.4.

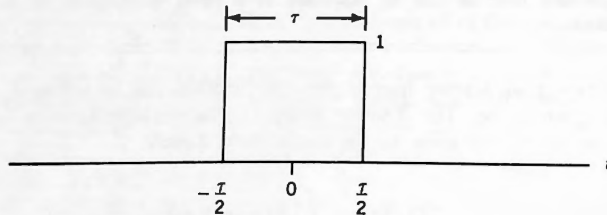


Figure 3.4.

The pulse shown in the figure occurs so often that it is given a special name. We call it the **rectangular pulse** (width  $\tau$ ), for which we have the following definition:

**Definition:** The rectangular pulse, width  $\tau$  and height 1, is called  $\text{Rect}(t/\tau)$ , where

$$\text{Rect}(t/\tau) \equiv \begin{cases} 1 & |t| < \tau/2 \\ 0 & |t| > \tau/2 \end{cases} \quad (3.22)$$

Continuing with the problem: Using the analysis equation (3.16) and the analytical definition given in (3.22), it follows that

$$\begin{aligned} F(\omega) &= \int_{-\infty}^{\infty} f(t) e^{-j\omega t} dt = \int_{-\tau/2}^{\tau/2} e^{-j\omega t} dt \\ &= \int_{-\tau/2}^{\tau/2} [\cos(\omega t) - j \sin(\omega t)] dt \end{aligned}$$

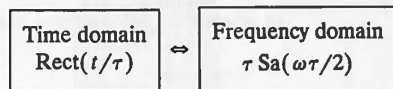
The sine term is odd, however, and so we can drop it. We thus continue as

$$\cdots = 2 \int_0^{\tau/2} \cos(\omega t) dt = 2 \frac{\sin(\omega t)}{\omega} \Big|_0^{\tau/2} = \tau \frac{\sin(\omega \tau/2)}{\omega \tau/2} = \tau \text{Sa} \frac{\omega \tau}{2} \quad (3.23)$$

where  $\text{Sa}$  was defined in (2.34). This gives us our first Fourier transform pair

$$\text{Rect} \frac{t}{\tau} \Leftrightarrow \tau \text{Sa} \frac{\omega \tau}{2} \quad (3.24)$$

which says



In Appendix 2 we show a list of such pairs that we derive in these pages, and in Figure 3.5 we show a plot of  $\tau \text{Sa}(\omega \tau/2)$  for  $\tau = 1$ .

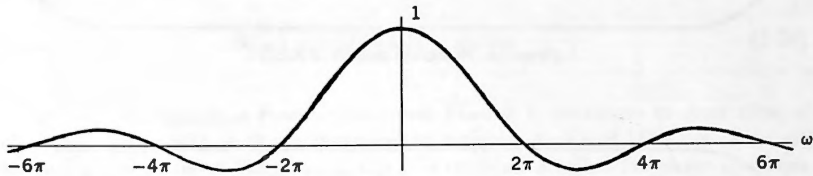


Figure 3.5.  $\text{Sa}(\omega/2)$ .

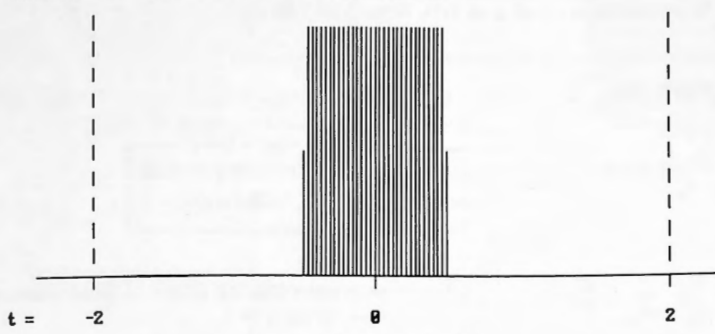
We were also asked, as part (b) of the problem, to write the Fourier integral representation of the pulse  $\text{Rect}(t/\tau)$ . From the synthesis equation (3.15) plus (3.24) the required expression is

$$f(t) = \frac{1}{2\pi} \int_{-\infty}^{\infty} \tau \text{Sa} \frac{\omega \tau}{2} e^{j\omega t} d\omega \quad (3.25)$$

This then is the way Fourier analysis represents the pulse  $\text{Rect}(t/\tau)$ , whose analytical definition we were given in (3.22). If properly evaluated, the integral on the RHS of (3.25) is guaranteed to lead to (3.22), that is, to the pulse shown in Figure 3.4.  $\square$

In Figure 3.6 we show a plot of the pulse  $\text{Rect}(t)$  as it was submitted to the FFT, and in Figure 3.7 we show a plot of its Fourier transform. Note how these two plots compare to Figures 3.4 and 3.5.

N = 256 I = 8 Ts = .03125 SAMPLED PULSE  
 FRACTION = .5 MAX POSITIVE = 1 MAX NEGATIVE = 0

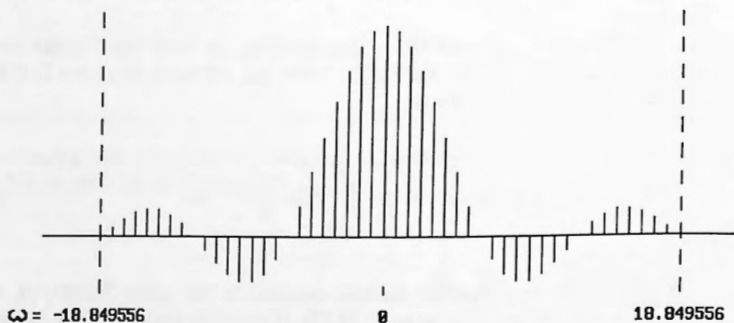


REAL PART OF X VECTOR

| ANOTHER PRIMARY PLOT ... P | MAIN MENU ... M | ?

Figure 3.6. Numerical samples of  $\text{Rect}(t)$ .

N = 256 I = 8 OMEGA = .78539816 SAMPLED PULSE  
 FRACTION = .1875 MAX POSITIVE = 1 MAX NEGATIVE = -.21257566



REAL PART OF F VECTOR

| ANOTHER PRIMARY PLOT ... P | MAIN MENU ... M | ?

Figure 3.7. Samples of Fourier transform of  $\text{Rect}(t)$ .

### 3.4 TWO BASIC THEOREMS

There are many properties of the Fourier transform that we shall examine in later chapters. We consider here two of the more basic ones.

In general a Fourier transform  $F(\omega)$  is a complex function of the variable  $\omega$ . That being the case, we can either show its real and imaginary parts in **Cartesian form** as

$$F(\omega) = A(\omega) + jB(\omega) \quad (3.26)$$

or else its magnitude and argument in **polar form** as

$$F(\omega) = |F(\omega)|e^{j\Theta(\omega)} \quad (3.27)$$

where

$$|F(\omega)| = [A(\omega)^2 + B(\omega)^2]^{1/2} \quad (3.28)$$

and

$$\Theta(\omega) = \arg[F(\omega)] = \arctan \frac{B(\omega)}{A(\omega)} \quad (3.29)$$

In order to visualize a Fourier transform  $F(\omega)$  it is customary to draw plots of  $|F(\omega)|$  and  $\Theta(\omega)$  with  $\omega$  as the independent variable. A plot of  $|F(\omega)|$  is called the **magnitude spectrum** of the pulse, and a plot of  $\Theta(\omega)$  is called the **phase spectrum**. Note that since the independent variable in these plots is now the continuous variable  $\omega$  rather than the discrete variable  $n$ , as in Chapter 2, they are no longer simply line spectra but instead are continuous spectra.

We shall only be interested in **real** pulses  $f(t)$ . This has an immediate effect on the nature of  $F(\omega)$ , as the following two theorems show. (Because they are the counterparts to corresponding results in the preceding chapter we have omitted the proofs. However, the reader is urged to carry them out.)

#### ■ THEOREM 3.2

Let  $f(t) \leftrightarrow F(\omega)$ . Then

$$F^*(\omega) = F(-\omega) \quad (\forall \omega) \quad (3.30)$$

iff  $f(t)$  is a real function of  $t$ .

#### ■ COROLLARY

For  $f(t)$  real,  $A(\omega)$  and  $|F(\omega)|$  are even,  $B(\omega)$  and  $\Theta(\omega)$  are odd.

**■ THEOREM 3.3**

If  $f(t)$  is real with even part  $f_{ev}(t)$  and odd part  $f_{od}(t)$ , then

$$f_{ev}(t) \Leftrightarrow A(\omega) \quad (3.31)$$

and

$$f_{od}(t) \Leftrightarrow jB(\omega) \quad (3.32)$$

**■ COROLLARY**

For  $f(t)$  real:

- (a)  $F(\omega)$  is real and even iff  $f(t)$  is even.
- (b)  $F(\omega)$  is imaginary and odd iff  $f(t)$  is odd.

We summarize these results in the following box.

**■ THEOREMS 3.2 and 3.3: Properties of  $F(\omega)$  for  $f(t)$  Real**

$$F^*(\omega) = F(-\omega)$$

$$f_{ev}(t) \Leftrightarrow A(\omega) \quad f_{od}(t) \Leftrightarrow jB(\omega)$$

- (a)  $A(\omega)$  is even,  $B(\omega)$  is odd,  $|F(\omega)|$  is even,  $\Theta(\omega)$  is odd.
- (b)  $F(\omega)$  is real and even iff  $f(t)$  is even.
- (c)  $F(\omega)$  is imaginary and odd iff  $f(t)$  is odd.

**EXAMPLE 3.2:** Find the magnitude and phase spectra for the pulse considered earlier in Example 3.1.

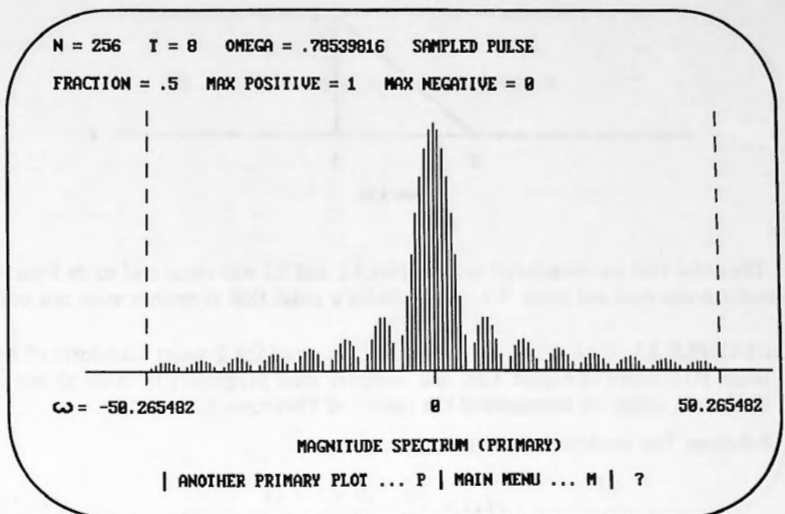
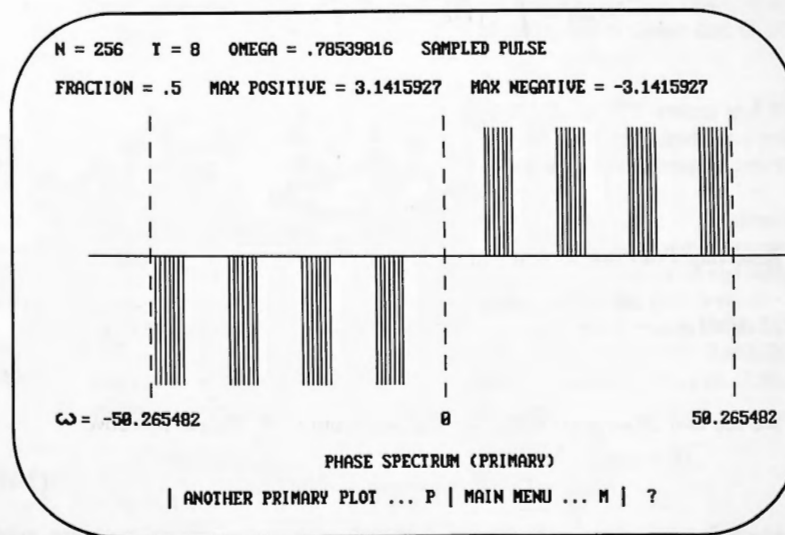
**Solution:** For the magnitude spectrum (3.24) gives us

$$|F(\omega)| = \left| \tau \text{Sa} \frac{\omega\tau}{2} \right| = \tau \left| \frac{\sin(\omega\tau/2)}{\omega\tau/2} \right| \quad (3.33)$$

and for the phase spectrum we note that the pulse has a real Fourier transform (to be expected from the fact that  $f(t)$  is even), and so

$$\Theta(\omega) = \begin{cases} 0 & \text{when } F(\omega) \text{ is positive} \\ \pm\pi & \text{when } F(\omega) \text{ is negative} \end{cases} \quad (3.34)$$

The choice of  $+\pi$  or  $-\pi$ , while arbitrary, must nevertheless be made so that  $\Theta(\omega)$  is an odd function.  $|F(\omega)|$  and  $\Theta(\omega)$ , as obtained from the FFT, are shown in Figures 3.8 and 3.9 below. □

Figure 3.8. Magnitude spectrum of  $\text{Rect}(t)$ .Figure 3.9. Phase spectrum of  $\text{Rect}(t)$ .

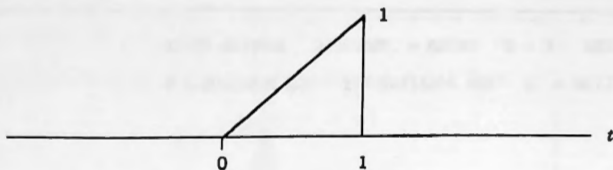


Figure 3.10.

The pulse that we considered in Examples 3.1 and 3.2 was even, and so its Fourier transform was real and even. We now consider a pulse that is neither even nor odd.

**EXAMPLE 3.3:** Find the real and imaginary parts of the Fourier transform of the pulse  $f(t)$  shown in Figure 3.10, and compare their properties to those shown in the box in which we summarized the results of Theorems 3.2 and 3.3.

**Solution:** The analytical definition of the pulse is

$$f(t) = \begin{cases} t & (0 < t < 1) \\ 0 & \text{otherwise} \end{cases} \quad (3.35)$$

and so the analysis equation gives

$$\begin{aligned} F(\omega) &= \int_{-\infty}^{\infty} f(t) e^{-j\omega t} dt = \int_0^1 t e^{-j\omega t} dt \\ &= \left[ \frac{te^{-j\omega t}}{-j\omega} - \frac{e^{-j\omega t}}{(-j\omega)^2} \right]_0^1 \\ &= \frac{e^{-j\omega}}{-j\omega} - \frac{e^{-j\omega} - 1}{(-j\omega)^2} = \frac{1 - e^{-j\omega} - j\omega e^{-j\omega}}{(j\omega)^2} \end{aligned}$$

Resolving  $F(\omega)$  into its real and imaginary parts, we obtain

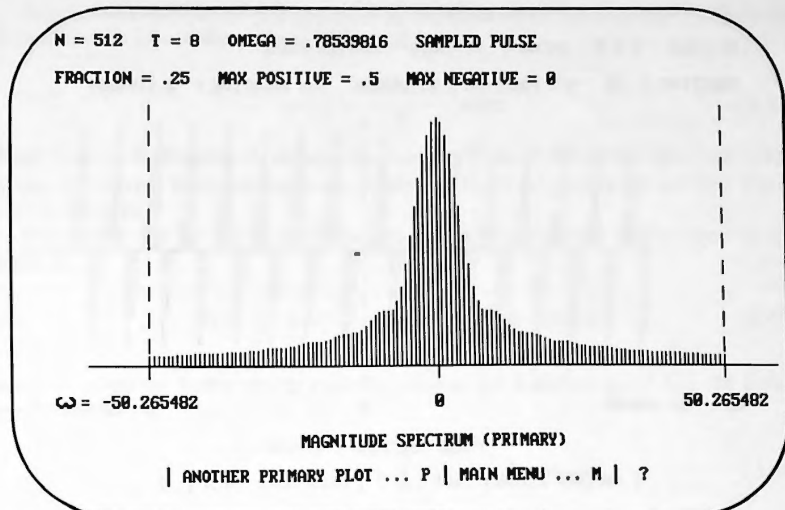
$$A(\omega) = \frac{\omega \sin(\omega) + \cos(\omega) - 1}{\omega^2} \quad \text{and} \quad B(\omega) = \frac{\omega \cos(\omega) - \sin(\omega)}{\omega^2} \quad (3.36)$$

We see that  $A(\omega)$  is even and  $B(\omega)$  is odd, both as predicted. Moreover

$$|F(\omega)| = [A(\omega)^2 + B(\omega)^2]^{1/2} \quad (3.37)$$

which is even since both of the quantities inside the square root are even. Similarly,

$$\Theta(\omega) = \tan^{-1} \frac{B(\omega)}{A(\omega)} \quad (3.38)$$

Figure 3.11.  $|F(\omega)|$ .

and since  $B(\omega)$  is odd and  $A(\omega)$  is even, it follows immediately that  $B(\omega)/A(\omega)$  is odd, and hence so is the arctangent of such a quantity, which shows that  $\Theta(\omega)$  is odd.  $\square$

We loaded the pulse from the preceding example into the FFT system and then ran ANALYSIS. In Figures 3.11 and 3.12 we show a plot of its magnitude and phase spectra,  $|F(\omega)|$  and  $\Theta(\omega)$ , using  $N = 512$  and  $T = 8$ . Observe from those figures that  $|F(\omega)|$  is even and  $\Theta(\omega)$  is odd.

In Table 3.1 we show a small section of the numerical values for  $F(\omega)$  obtained from the FFT system, using  $N = 1024$  and  $T = 16$ . We see again the evenness of  $A(\omega)$  and  $|F(\omega)|$ , and the oddness of  $B(\omega)$  and  $\Theta(\omega)$ . The final column of the table is part of the energy spectrum of the pulse, which we examine in the next section.

In order to compare the values in the table with the exact values from (3.36) through (3.38) we proceed as follows. Since  $T = 16$  we have  $\omega_0 = 2\pi/T = 0.39269908$ . (This is shown as OMEGA in the system displays.) Evaluating  $A(\omega)$  in (3.36) at  $\omega = n\omega_0$  gives us

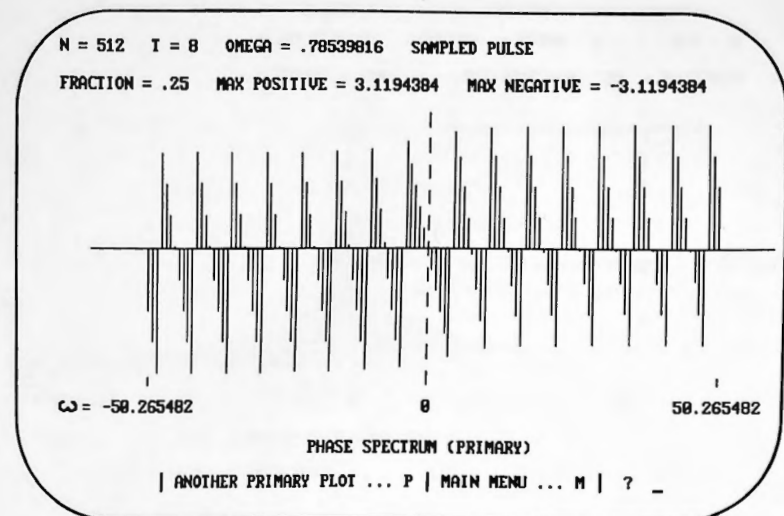
$$n = 0: \quad A(0\omega_0) = 0.5 \quad (\text{analysis equation with } \omega = 0)$$

$$n = 1: \quad A(1\omega_0) = 0.4808879$$

$$n = 2: \quad A(2\omega_0) = 0.4254957$$

$$n = 3: \quad A(3\omega_0) = 0.3394329$$

and so on, with similar results for  $B(\omega)$ ,  $F(\omega)$ , and  $\Theta(\omega)$ . The FFT values in the first

Figure 3.12.  $\Theta(\omega)$ .TABLE 3.1 FFT Values of  $F(\omega)$ 

$n$	$FRE(n)$	$FIM(n)$	$ F(n) $	$THETA(n)$	$ENERGY(n)$
-4	0.2312827	0.4053050	0.4666518	1.052245	$3.465820e-2$
-3	0.3393981	0.3408571	0.4810142	0.7875428	$3.682442e-2$
-2	0.4254784	0.2460277	0.4914891	0.5242641	$3.844571e-2$
-1	0.4808833	0.1289073	0.4978613	0.2619061	0.0394490
0	0.5	0.	0.5	0.	$3.978873e-2$
1	0.4808833	-0.1289073	0.4978613	-0.2619061	0.0394490
2	0.4254784	-0.2460277	0.4914891	-0.5242641	$3.844571e-2$
3	0.3393981	-0.3408571	0.4810142	-0.7875428	$3.682442e-2$
4	0.2312827	-0.4053050	0.4666518	-1.052245	$3.465820e-2$

Note:  $N = 1024$ ,  $T = 16$ .

column of the table compare very well with these numbers. Had we used a larger value for  $N$ , the comparison would have been even better. (See Chapter 13 and Section 17.2.)

### 3.5 PARSEVAL'S THEOREM FOR PULSES

In Chapter 2 we showed how the power spectrum of a periodic waveform can be obtained from its complex Fourier spectrum. We now show how a similar relationship can be derived for one-time pulses, but this time involving energy rather than average power.

Suppose that we have a voltage pulse  $v(t)$  applied to an  $R$ -ohm resistor. Then the instantaneous power that is being delivered is

$$p(t) = \frac{|v(t)|^2}{R} \text{ watts} \quad (3.39)$$

Note that, as in Chapter 2, we are showing  $|v(t)|^2$  in (3.39) rather than just  $v(t)^2$ . When  $v(t)$  is real then this makes no difference, but it does allow for the case where  $v(t)$  is complex.

When  $R = 1$  it follows from (3.39) that the total energy that is dissipated by the pulse is

$$E = \int_{-\infty}^{\infty} p(t) dt = \int_{-\infty}^{\infty} |v(t)|^2 dt \text{ joules} \quad (3.40)$$

which is called the **1-ohm energy content**. Likewise for a current pulse  $i(t)$ , the 1-ohm energy content is

$$E = \int_{-\infty}^{\infty} p(t) dt = \int_{-\infty}^{\infty} |i(t)|^2 dt \text{ joules} \quad (3.41)$$

It is a simple fact that

**Every physically realizable pulse has finite energy content.**

There are mathematically defined pulses for which this is not the case, however, and to distinguish between them we have the following:

**Definition:** If a pulse carries a finite amount of energy, then we call it an **energy pulse**.

Thus, by (3.40) or (3.41), every energy pulse  $f(t)$  satisfies

$$\int_{-\infty}^{\infty} |f(t)|^2 dt < \infty \quad (3.42)$$

We now prove the following counterpart to Parseval's theorem for periodic waveforms:

#### ■ THEOREM 3.4: Parseval's Theorem for Pulses

Let  $f(t)$  be an energy pulse with Fourier transform  $F(\omega)$ . Then the total (1-ohm) energy in  $f(t)$  is given by

$$E = \int_{-\infty}^{\infty} |f(t)|^2 dt = \frac{1}{2\pi} \int_{-\infty}^{\infty} |F(\omega)|^2 d\omega \quad (3.43)$$

What the theorem states is that the total energy in the pulse can be evaluated in either one of two ways:

- (1) From the time-domain analytical definition of the pulse  $f(t)$ , using the first integral in (3.43).
- (2) From the frequency-domain spectrum of the pulse, as shown in the second integral in (3.43).

To prove this theorem we first need Parseval's lemma.

■ Parseval's Lemma

Let  $f(t)$  and  $g(t)$  be energy pulses. Then

$$\int_{-\infty}^{\infty} f(t)g(t)^* dt = \frac{1}{2\pi} \int_{-\infty}^{\infty} F(\omega)G(\omega)^* d\omega \quad (3.44)$$

*Proof of Parseval's Lemma:* Restating  $g(t)$  using the synthesis equation we obtain

$$\int_{-\infty}^{\infty} f(t)g(t)^* dt = \int_{-\infty}^{\infty} f(t) \left[ \frac{1}{2\pi} \int_{-\infty}^{\infty} G(\omega)^* e^{-j\omega t} d\omega \right] dt$$

Interchanging the order of integration this now continues as

$$\dots = \frac{1}{2\pi} \int_{-\infty}^{\infty} G(\omega)^* \left[ \int_{-\infty}^{\infty} f(t) e^{-j\omega t} dt \right] d\omega$$

the analysis equation, however, the quantity in square brackets is simply  $F(\omega)$ , and so we continue further as

$$\dots = \frac{1}{2\pi} \int_{-\infty}^{\infty} G(\omega)^* F(\omega) d\omega \quad (3.45)$$

which proves the lemma. ■

*Proof of Theorem 3.4:* If we now let  $g(t) = f(t)$  in (3.44), we obtain Parseval's theorem immediately, namely:

$$E = \int_{-\infty}^{\infty} |f(t)|^2 dt = \frac{1}{2\pi} \int_{-\infty}^{\infty} |F(\omega)|^2 d\omega \text{ joules} \quad (3.46)$$

This completes the proof. ■

As it stands, (3.46) gives us the total energy contained in a pulse. As with Parseval's theorem for periodic waveforms, however, (3.46) is also a statement regarding the **energy spectrum** because it tells us the following:

- The energy contained in a pulse in the frequency range  $\omega_1 < \omega < \omega_2$  is

$$\Delta E = \frac{1}{2\pi} \int_{\omega_1}^{\omega_2} |F(\omega)|^2 d\omega \text{ joules} \quad (3.47)$$

From this we can compute the amount of energy contained in a pulse over any desired range of frequencies.

**Definition:** The **energy spectrum** of a pulse whose Fourier transform is  $F(\omega)$ , is

$$E(\omega) \equiv \frac{1}{2\pi} |F(\omega)|^2 \text{ joules/radian} \quad (3.48)$$

For example, if  $f(t)$  is applied to the input of an ideal filter whose passband is  $10 < \omega < 20$ , then the total energy in the pulse that emerges will be

$$\Delta E = \int_{10}^{20} E(\omega) d\omega = \frac{1}{2\pi} \int_{10}^{20} |F(\omega)|^2 d\omega \text{ joules} \quad (3.49)$$

■ **EXAMPLE 3.4:** Find the expression for the energy spectrum of the pulse

$$f(t) = \begin{cases} t & (-1 < t < 1) \\ 0 & \text{otherwise} \end{cases}$$

**Solution:** The pulse is as shown in Figure 3.13, from which we note that it is an odd function of  $t$ . Thus we expect that its Fourier transform will be a purely

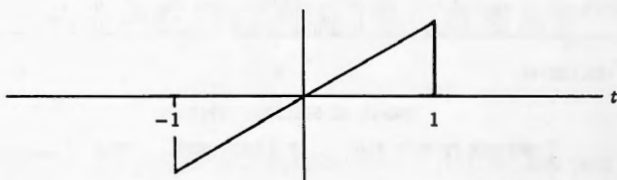


Figure 3.13.

imaginary and odd function of  $\omega$ . From the analysis equation

$$F(\omega) = \int_{-\infty}^{\infty} f(t) e^{-j\omega t} dt = \int_{-1}^1 t [\cos(\omega t) - j \sin(\omega t)] dt$$

However,  $t \cos(\omega t)$  is odd and so it can be dropped. Moreover,  $t \sin(\omega t)$  is even, and so we continue as

$$\dots = -2j \int_0^1 t \sin(\omega t) dt = -2j \left[ -t \frac{\cos(\omega t)}{\omega} + \frac{\sin(\omega t)}{\omega^2} \right]_0^1$$

giving us, finally,

$$F(\omega) = 2j \frac{\omega \cos(\omega) - \sin(\omega)}{\omega^2}$$

We see that  $F(\omega)$  is purely imaginary and odd, as expected. We also see that it goes to zero like  $1/\omega$ , as would be the case for the Fourier series coefficients of a periodic train of such pulses, a consequence of the fact that  $f(t)$  has discontinuities. This rate of convergence is discussed later.

Finally, to find the energy spectrum of the pulse, we have

$$E(\omega) = \frac{1}{2\pi} |F(\omega)|^2 = \frac{2}{\pi} \left| \frac{\omega \cos(\omega) - \sin(\omega)}{\omega^2} \right|^2$$

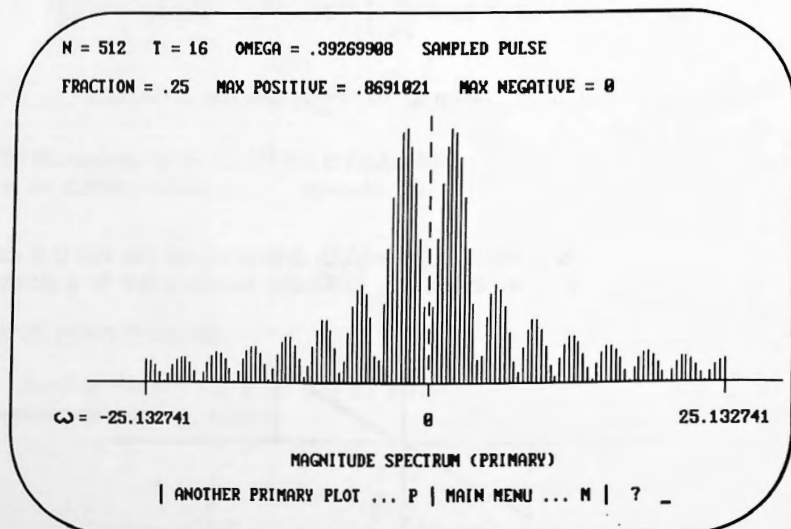
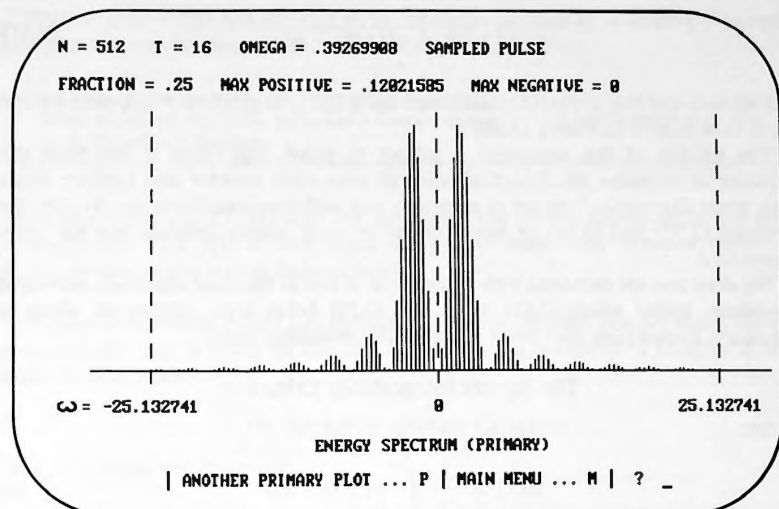


Figure 3.14.  $|F(\omega)|$ .

Figure 3.15.  $E(\omega)$ .

Note how the energy spectrum goes to zero like  $1/\omega^2$  for large  $\omega$ , which means that the bulk of the energy in the pulse is contained in a relatively small band of central frequencies. □

For the preceding pulse, Figures 3.14 and 3.15 show FFT plots of

- The magnitude spectrum  $|F(\omega)|$ .
- The energy spectrum  $E(\omega)$ .

Observe how rapidly the energy spectrum goes to zero compared to the magnitude spectrum.

### 3.6 EXISTENCE OF THE FOURIER INTEGRAL

In going from (3.13) to (3.14) we made the statement “under very general conditions it can be shown that . . .”. Our simplified approach then led us to the expression

$$f(t) = \frac{1}{2\pi} \int_{-\infty}^{\infty} F(\omega) e^{j\omega t} d\omega \quad (3.50)$$

which we called the Fourier integral representation of  $f(t)$ . We also used a considerably simplified argument to derive an expression that we called the Fourier transform, namely

$$F(\omega) = \int_{-\infty}^{\infty} f(t) e^{-j\omega t} dt \quad (3.51)$$

and we asserted that if  $f(t)$  is transformed using (3.51) to produce  $F(\omega)$ , then we can get it back from  $F(\omega)$  using (3.50).

The validity of this statement is subject to proof, and while it has been the objective of intensive mathematical research ever since Fourier and Laplace made their great discoveries,<sup>†</sup> no set of necessary and sufficient conditions on  $f(t)$  for the integrals (3.50) and (3.51) to exist and to be each other's inverses has yet been formulated.

We shall content ourselves with a brief look at two of the most important **sufficient conditions** under which (3.51) exists and (3.50) holds true, neither of which is necessary. Fortunately they cover all physically realizable cases.

### The Square Integrability Criterion

Define

$$\Phi(t) \equiv \frac{1}{2\pi} \int_{-\infty}^{\infty} F(\omega) e^{j\omega t} d\omega \quad (3.52)$$

#### ■ The Square Integrability Criterion

Assume that  $f(t)$  is square integrable, that is, that

$$\int_{-\infty}^{\infty} |f(t)|^2 dt < \infty \quad (3.53)$$

Then the following can be proved to hold.

- (a) The integral (3.51) exists, that is, we can find an expression from it that we call  $F(\omega)$ .
- (b) If we form the difference between the function  $\Phi(t)$  that we obtain from integrating  $F(\omega)$  in (3.52) and the original function  $f(t)$ , that is, if we form

$$e(t) \equiv \Phi(t) - f(t) \quad (3.54)$$

then  $e(t)$  may differ significantly from zero at a discrete set of values of  $t$ , but

$$\int_{-\infty}^{\infty} |e(t)|^2 dt = 0 \quad (3.55)$$

<sup>†</sup>Laplace discovered the complex form of the Fourier integral that we have been discussing in this chapter in 1785 (in connection with his work on mathematical probability) (Stigler, 1986) some 22 years before Fourier submitted his paper in 1807, in which he was the first to use the sine-cosine formulation (Burkhardt, 1904).

We see that (3.53) defines  $f(t)$  as an energy pulse, and so it follows that every energy pulse satisfies the square integrability criterion. Hence:

**Every physically realizable pulse has a Fourier transform that can be inverted to give back the original function.**

Note that (3.54) and (3.55) mean the following: The energy contained in the error between  $\Phi(t)$  and  $f(t)$  is zero, even though the error itself between these two functions may be nonzero at isolated points. ■

Square integrability is only one sufficient condition. As with Fourier series there is a second one that is based on the Dirichlet conditions discussed in Chapter 2, with slight modifications.

### The Dirichlet–Jordan Criterion

First we require the following:

**Definition:** A pulse function  $f(t)$  will be said to satisfy the **Dirichlet conditions for pulses** if

- (a) It is bounded
- (b) It has at most a finite number of discontinuities and a finite number of maxima and minima in any finite time interval
- (c) It is absolutely integrable in the sense

$$\int_{-\infty}^{\infty} |f(t)| dt < \infty \quad (3.56)$$

Pulse functions that satisfy these conditions are a subset of the pulse functions that are square integrable, that is, we have the following Venn diagram:

Pulse functions that are square integrable

Pulse functions that satisfy the Dirichlet conditions

It is a simple fact that

All physically realizable pulse functions satisfy the Dirichlet conditions.

The following result was proved to hold by C. Jordan, a nineteenth-century French mathematician (see, e.g., Titchmarsh, 1937):

### ■ The Dirichlet–Jordan Criterion

If a pulse function  $f(t)$  satisfies the Dirichlet conditions for pulses, then its Fourier transform can be found from the analytical definition of  $f(t)$  by the analysis equation (3.16).

The associated Fourier integral (3.15) converges to  $f(t)$  at any point where  $f(t)$  is continuous, and converges to

$$\frac{1}{2}[f(t^+) + f(t^-)]$$

when there is a discontinuity at the point  $t$ .

Bear in mind that the square integrability criterion is by no means necessary (and hence neither is the Dirichlet–Jordan criterion), and we'll soon see that there are mathematically defined pulses for which neither of the preceding two conditions holds, and yet they have perfectly well-behaved Fourier transform representations.

## 3.7 ASYMPTOTIC BOUNDS FOR $F(\omega)$

Equation (2.92) in Chapter 2 gave us an indication of how quickly the coefficients in a Fourier series die out. An analogous result holds for the Fourier transform of a pulse function, as shown in the following box. For ease of reference we summarize this result in Table 3.2.

### ■ Asymptotic Bounds for $F(\omega)$

Let  $f(t)$  be a pulse that meets appropriate conditions. Then if  $f(t)$  and its first  $m$  derivatives are continuous but its  $(m+1)$ -th is not, its Fourier transform  $F(\omega)$  will satisfy

$$|F(\omega)| < K/|\omega|^{m+2} \quad (\text{for large } \omega) \quad (3.57)$$

where  $K$  is some positive constant.

TABLE 3.2 Rates of Convergence

Zeroth derivative not continuous:	$K/ \omega $
Zeroth derivative continuous, first not:	$K/ \omega ^2$
First derivative continuous, second not:	$K/ \omega ^3$
Second derivative continuous, third not:	$K/ \omega ^4$

□ **EXAMPLE 3.5:** For the pulse  $\text{Rect}(t)$  the zeroth derivative is not continuous ( $m = -1$ ), and so by the preceding statement on the asymptotic bounds, we would expect its Fourier transform to die out like  $K/|\omega|$ . In fact, from (3.24), we have

$$F(\omega) = \text{Sa} \frac{\omega}{2} = \frac{\sin(\omega/2)}{\omega/2} \quad (3.58)$$

from which

$$|F(\omega)| = \left| \frac{\sin(\omega/2)}{\omega/2} \right| \leq \frac{2}{|\omega|} \quad (\text{for large } \omega) \quad (3.59)$$

Thus  $F(\omega)$  does in fact die out like  $K/\omega$  as predicted. □

Since the energy spectrum of a pulse is proportional to  $|F(\omega)|^2$  it follows that if a pulse has a Fourier transform that dies out like  $K/|\omega|^{m+2}$ , then its energy spectrum will die out like  $M/|\omega|^{2m+4}$ .

□ **EXAMPLE 3.6:** Let  $f(t) = \Lambda(t)$  (where  $\Lambda$  is a capital lambda) be the triangular pulse shown in Figure 3.16. Then  $f(t)$  is everywhere continuous, but its first derivative is not. This means that in (3.57)  $m = 0$ , and so  $|F(\omega)|$  should die out like  $K/\omega^2$  and its energy spectrum like  $M/\omega^4$ .

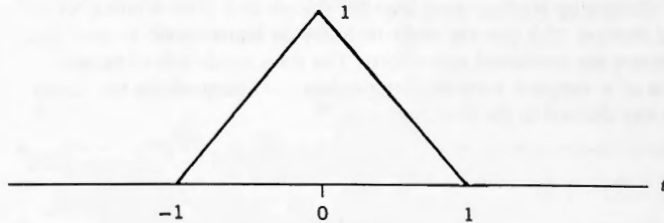


Figure 3.16. Triangular pulse.

For this pulse it is easy to show (see Exercise 3.10) that  $F(\omega) = \text{Sa}^2(\omega/2)$ , and so, for large  $\omega$ ,

$$|F(\omega)| = \left[ \frac{\sin(\omega/2)}{(\omega/2)} \right]^2 \leq \frac{4}{\omega^2} \quad (3.60)$$

Thus  $|F(\omega)|$  dies out like  $K/\omega^2$ , as predicted. The energy spectrum of the pulse is

$$E(\omega) = \frac{1}{2\pi} \left[ \frac{\sin(\omega/2)}{(\omega/2)} \right]^4 \leq 8/\pi\omega^4 \quad (\text{for large } \omega) \quad (3.61)$$

that is, it dies out like  $M/\omega^4$ . □

**Accompanying Disk**

Use the FFT system to check your results in the following exercises, where you are asked to find expressions for the Fourier transforms of pulses. After you have carried out the analytical work in the exercises using pencil and paper, you will be able to check your formulas by inserting specific values for  $\omega$  and comparing your theoretical results to the numbers obtained from the FFT. (See the demonstration at the end of Example 3.3 where we compared exact values from the formulas against those obtained from the FFT.)

You will also be able to see plots on your screen of what the Fourier spectra look like. Read Chapters 16 and 17 in the README files on your disk in order to learn enough about how to use the system for this purpose, and remember:

When using the FFT to approximate Fourier series coefficients or Fourier transforms, if any of the sampling instants falls on a discontinuity, then we always use the half-value as the value that is loaded at that point.

Eventually you will have to read all of Chapters 10 through 17 in order to understand fully how the FFT works and how its results are related to those that we obtained in this and the preceding chapter.

You will also be able to invert your formulas for  $F(\omega)$  back to  $f(t)$  in the time domain by loading them into the system and then running SYNTHESIS. Read Section 17.3 (on the disk) in order to learn about aliasing and why it eliminates the unwanted side-effects. The final result should be a plot on your screen of a sampled version of the pulse  $f(t)$ , from which the expression for  $F(\omega)$  was derived in the first place.

---

**EXERCISES**

---

3.1 (a) Prove that

$$\int_{-\infty}^{\infty} f(t) dt = F(0)$$

where  $F(0)$  means  $F(\omega)$  at  $\omega = 0$ . Thus we can quickly find the area under  $f(t)$  by setting  $\omega = 0$  in its Fourier transform. This can be used as a sanity test that can be applied to the expression for  $F(\omega)$ .

(b) Prove that

$$\int_{-\infty}^{\infty} F(\omega) d\omega = 2\pi f(0)$$

Thus the area under  $F(\omega)$  is equal to  $2\pi f(0)$ . Since  $f(0)$  is usually easy to read from a sketch of a pulse, this equation often gives important information regarding  $F(\omega)$ .

- (c) Compare these results for pulses to those of Exercise 2.15 for periodic functions.

*Hint:* For (a), start from the definition for  $F(\omega)$ . For (b), start from the Fourier integral representation of  $f(t)$ .

### 3.2 Show that

$$F(\omega) = 2 \int_0^\infty f(t) \cos(\omega t) dt \quad \text{if } f(t) \text{ is even}$$

and

$$F(\omega) = -2j \int_0^\infty f(t) \sin(\omega t) dt \quad \text{if } f(t) \text{ is odd}$$

### 3.3 For each of the pulses whose integral representations follow, state

- The Fourier transform of  $f(t)$
- If the pulse is a real function of  $t$

For those which are real, state

- The Fourier transforms of  $f_{cv}(t)$  and  $f_{od}(t)$
- If the pulse is even or odd or neither
- The total area under the pulse
- Whether or not the pulse has discontinuities

$$(a) f(t) = \frac{1}{2\pi} \int_{-\infty}^{\infty} \frac{1}{\beta + j\omega} e^{j\omega t} d\omega \quad (\beta > 0)$$

$$(b) f(t) = j \int_{-\infty}^{\infty} \frac{\omega \cos(\omega) - \sin(\omega)}{\omega^2} e^{j\omega t} d\omega$$

$$(c) f(t) = \int_{-\infty}^{\infty} \frac{\omega \sin^2(\omega) - 2\cos(\omega)}{\omega^2} e^{j\omega t} d\omega$$

$$(d) f(t) = \frac{1}{2\pi} \int_{-\infty}^{\infty} e^{j\omega t} d\omega$$

$$(e) f(t) = \frac{1}{2\pi} \int_{-\infty}^{\infty} e^{-\beta|\omega|} e^{j\omega t} d\omega \quad (\beta > 0)$$

$$(f) f(t) = \frac{1}{2\pi} \int_{-\infty}^{\infty} \frac{j\omega + 2}{(j\omega)^2 + \omega + 1} e^{j\omega t} d\omega$$

**3.4** For each of the pulses whose Fourier transforms are given below, state if the pulse is a real function of  $t$ . For those that are, state:

- The integral representation of the pulse
- The integral representations of the even and the odd parts of the pulse
- Whether the pulse is even or odd or neither
- Whether or not the pulse has discontinuities
- The total area under the pulse

$$(a) F(\omega) = \text{Sa} \frac{\omega}{4}$$

$$(b) F(\omega) = e^{-j\omega/2} \text{Sa}(\omega/4)$$

$$(c) F(\omega) = 2j \left[ \frac{\omega \cos(\omega) - \sin(\omega)}{\omega^2} \right]$$

$$(d) F(\omega) = \frac{1 - e^{-j\omega} - j\omega e^{-j\omega}}{(j\omega)^2}$$

$$(e) F(\omega) = \frac{1 + j\omega}{1 + j\omega + (j\omega)^2}$$

$$(f) F(\omega) = \cos(\omega) - j \sin \frac{\omega}{4}$$

**3.5** State which of the following Fourier transforms came from a pulse that is a real function of  $t$ .

$$(a) F(\omega) = \frac{1 + 3j\omega}{1 + 5j\omega + (j\omega)^2}$$

$$(b) F(\omega) = \frac{\sin(\omega) + j \cos(\omega)}{j\omega}$$

$$(c) F(\omega) = \frac{1}{1 + j\omega}$$

$$(d) F(\omega) = je^{-\beta|\omega|} \quad (\beta > 0)$$

**3.6 (a)** Prove the following:

- (1) When two complex expressions are multiplied, their magnitudes multiply and their phases add.
- (2) When two complex expressions are divided, their magnitudes divide and their phases subtract.

**(b)** What are the expressions for the magnitudes and phases of the following?

$$(1) F(\omega) = \frac{e^{j\omega} - 1 - j\omega e^{-j\omega}}{(j\omega)^2} e^{-j\omega}$$

$$(2) F(\omega) = \frac{j\omega - 1 + e^{-j\omega}}{(j\omega)^2} e^{-j3\omega}$$

$$(3) F(\omega) = \frac{(2 - j3\omega)(4 + j5\omega)(6 + j7\omega)}{(8 + j9\omega)(10 + j11\omega)(12 + j13\omega)}$$

- 3.7 For each of the given pulses determine whether the square integrability criterion guarantees the existence of its Fourier transform or not.

- (a)  $f(t) = e^{-\beta t}$  ( $t \geq 0$ ) ( $\beta > 0$ )
- (b)  $f(t) = e^{\beta t}$  ( $t \geq 0$ ) ( $\beta > 0$ )
- (c)  $f(t) = te^{-\beta t}$  ( $t \geq 0$ ) ( $\beta > 0$ )
- (d)  $f(t) = e^{-\beta|t|}$  ( $\forall t$ ) ( $\beta > 0$ )
- (e)  $f(t) = 1$  ( $t \geq 0$ )
- (f)  $f(t) = \cos(t)$  ( $\forall t$ )
- (g)  $f(t) = \sin(t)$  ( $\forall t$ )

*Note:* The square integrability criterion is only one sufficient condition. If it is satisfied, then the existence of the Fourier transform is guaranteed. If not, then we cannot say. In fact, Fourier transforms exist for all of the preceding except (b). We shall be deriving them all later.

- (h) Find the Fourier transform of the pulse in (a).

- 3.8 (a) Find the Fourier transform for the pulse  $f(t)$  shown in Figure 3.17 and then see if your result is consistent with (3.24).  
 (b) Is it true that the area under  $f(t)$  equals  $F(0)$ ?  
 (c) What is the value of

$$\int_{-\infty}^{\infty} F(\omega) d\omega$$

- (d) At what rate should  $F(\omega)$  decay to zero? Does it?  
 (e) To what values does the Fourier transform invert for  $t = -\frac{1}{4}$ ,  $t = -\frac{1}{8}$ , and  $t = \frac{1}{4}$ ?  
 (f) Find the expression for the energy spectrum  $E(\omega)$  and find the total area under  $E(\omega)$ .  
 (g) Sketch the magnitude, phase, and energy spectra for this pulse for  $-12\pi \leq \omega \leq 12\pi$ .  
 (h) Use the FFT system to verify the result that you obtained in (a). Use  $N = 1024$  and  $T = 2$ .

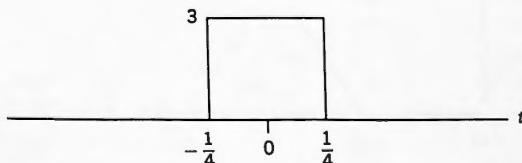


Figure 3.17.

- 3.9 (a) In Figure 3.18 we show the pulse of Figure 3.17 delayed by  $\frac{1}{4}$  time unit. Show that its Fourier transform becomes  $e^{-j\omega/4}$  times the transform of the undelayed pulse.
- (b) Find the expression for the magnitude spectrum.
- (c) Find the expression for the energy spectrum.
- (d) Sketch the magnitude and energy spectra of this pulse for  $-12\pi \leq \omega \leq 12\pi$ . Are they the same as for Exercise 3.8? If not, how do they differ?
- (e) Sketch the phase spectrum for  $-12\pi \leq \omega \leq 12\pi$ . Is it the same as for Exercise 3.8? If not, how do they differ?
- (f) Use the FFT system to verify the result that you obtained in (a), (c), and (e). Use  $N = 1024$  and  $T = 2$ .

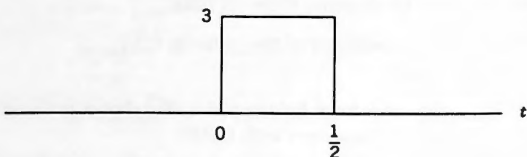


Figure 3.18.

- 3.10 The pulse shown in Figure 3.19 is known as a **triangular pulse** and is written as  $\Lambda(t/\tau)$ . Observe that it has width  $2\tau$  and height 1, whereas  $\text{Rect}(t/\tau)$  has width  $\tau$  and height 1.

- (a) Prove that its Fourier transform is

$$\Lambda(t/\tau) \Leftrightarrow F(\omega) = \tau \text{Sa}^2(\omega\tau/2)$$

- (b) Is it true that the area under  $f(t)$  is equal to  $F(0)$ ?
- (c) At what rate does the Fourier transform go to zero? Is it consistent with what you would expect from (3.57) and Table 3.2?

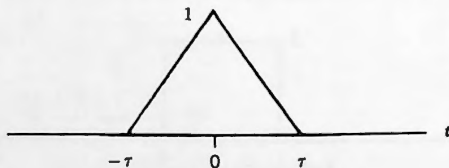


Figure 3.19. Triangular pulse.

- (d) At what rate does the energy spectrum of this pulse go to zero?  
 (e) Prove that  $\int_{-\infty}^{\infty} \text{Sa}^2(x) dx = \pi$ .  
 (f) For  $\tau = 1$ , sketch the magnitude, phase, and energy spectra for  $-6\pi \leq \omega \leq 6\pi$ .  
 (g) What is the value of  $1/2\pi \int_{-\infty}^{\infty} \text{Sa}^2(\omega/2)e^{j\omega t} d\omega$  for  $t = -2, -1, -\frac{1}{2}, 0, \frac{1}{2}, 1$ , and  $2?$   
 (h) Use the FFT system to verify the result you obtained in (a) and the sketches that you obtained in (f). Use  $\tau = 1$ ,  $N = 1024$ , and  $T = 16$ .

3.11 (a) Find  $F(\omega)$  for the pulse  $f(t) = e^t$  ( $0 < t < 1$ ).

- (b) What is the value of  $1/2\pi \int_{-\infty}^{\infty} F(\omega)e^{j\omega t} d\omega$  for  $t = 0$ ,  $t = \frac{1}{2}$ , and  $t = 1$ ?  
 (c) What should the value of  $F(0)$  be? Is that in fact the case?  
 (d) Sketch  $f_{ev}(t)$  and  $f_{od}(t)$ , and state their Fourier transforms.  
 (e) At what rates do the transforms of  $f_{ev}(t)$  and  $f_{od}(t)$  decay to zero?  
 (f) Load the pulse  $f(t)$  into the FFT system using  $N = 1024$  and  $T = 16$ , and display plots of  $f_{ev}(t)$  and  $f_{od}(t)$ .

*Hint:* Use the F postprocessor.

- (g) Use the FFT system to verify the results that you obtained in (a), (d), and (e).

3.12 The pulse shown in Figure 3.20a is

$$f(t) = e^{-\beta|t|} \quad (\forall t) \quad (\beta > 0)$$

It is called the **double-sided decaying exponential** and is examined further in Chapter 4. In Figure 3.20b we show its first derivative.

- (a) Prove the correctness of the following Fourier pair:

$$e^{-\beta|t|} \Leftrightarrow \frac{2\beta}{\beta^2 + \omega^2}$$

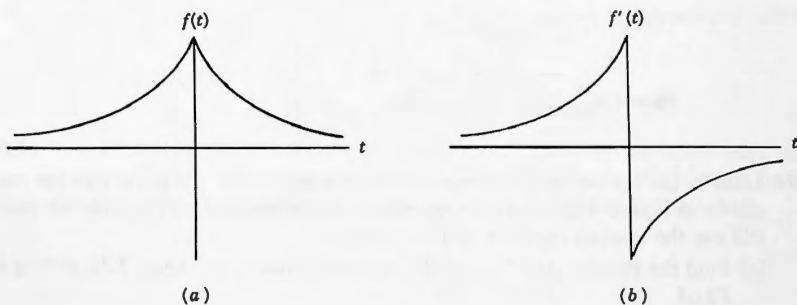


Figure 3.20.

- (b) Observe that  $f(t)$  is everywhere continuous but  $f'(t)$  has a discontinuity at  $t = 0$ , and so the value of  $m$  in (3.57) for this pulse is zero. We would thus expect  $F(\omega)$  to decay like  $K/\omega^2$ . Is that the case?
- (c) What do

$$\int_{-\infty}^{\infty} A(\omega) e^{j\omega t} d\omega \quad \text{and} \quad \int_{-\infty}^{\infty} B(\omega) e^{j\omega t} d\omega$$

evaluate to, where  $A(\omega)$  and  $B(\omega)$  were defined in (3.26)?

- (d) What is the expression for  $E(\omega)$ , the energy spectrum for this pulse, and what is the value of

$$\int_{-\infty}^{\infty} E(\omega) d\omega$$

- (e) Use the FFT system to verify  $F(\omega)$  as stated in (a), as well as the expression for  $E(\omega)$ . Use  $\beta = 2$ ,  $N = 1024$ , and  $T = 10$ .

### 3.13 When $f(t)$ is a real function of $t$ , then

$$E[f(t)] = E[f_{ev}(t)] + E[f_{od}(t)] \quad (3.62)$$

that is, the energy in  $f(t)$  is equal to the energy in its even part plus the energy in its odd part.

(a) Prove this in two ways:

- In the time domain, using  $f(t) = f_{ev}(t) + f_{od}(t)$
- Using Parseval's theorem.

- (b) Sketch the even and odd parts of the pulse shown in Figure 3.21, and verify that (3.62) holds true.

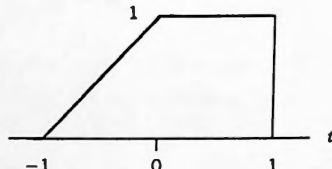


Figure 3.21.

- 3.14 Later in the text we shall see how the Fourier transform of a pulse like the one shown in Figure 3.22 can be found essentially by inspection. For now we must still use the analysis equation and integration.

- (a) Find the Fourier transform of the pulse  $f(t)$  shown in Figure 3.22, calling it  $F_1(\omega)$ .
- (b) Is it true that the area under  $f(t)$  equals  $F_1(0)$ ?

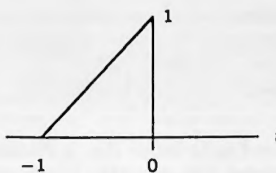


Figure 3.22.

- (c) Sketch the even and odd parts of this pulse, calling them  $f_{ev}(t)$  and  $f_{od}(t)$ , respectively.
- (d) State the Fourier transforms of  $f_{ev}(t)$  and  $f_{od}(t)$ , calling them  $F_2(\omega)$  and  $F_3(\omega)$ , respectively.
- (e) State how the transforms of all three pulses decay with increasing  $\omega$ . Is what you find consistent with (3.57)?
- (f) Compute the total energy in each of the three pulses  $f(t)$ ,  $f_{ev}(t)$ , and  $f_{od}(t)$ . Does the energy in  $f(t)$  equal the energy in  $f_{ev}(t)$  plus the energy in  $f_{od}(t)$ ? (See Exercise 3.13.)
- (g) Write the expressions for the energy that each of the three pulses contains in the range  $1 < \omega < 2$ .
- (h) For each pulse find the total area under its Fourier transform.
- (i) Use the FFT system to verify your results in (a) and (d). Use  $N = 1024$ ,  $T = 4$ .
- (j) Use the FFT system to synthesize the three pulses  $f(t)$ ,  $f_{ev}(t)$ , and  $f_{od}(t)$  starting from their Fourier transforms. Use  $N = 256$ ,  $T = 4$ . (Refer to Section 17.3.) Since two of the pulses have spectra that converge only like  $1/\omega$ , you will have to use aliasing when forming the FFT spectrum from the continuous spectrum. Try level-0 and level-5 aliasing for all three cases and note the improvement in the case of  $f(t)$  and  $f_{od}(t)$ , and that  $f_{ev}(t)$  does not require aliasing because its spectrum converges like  $1/\omega^2$ .

**3.15** Prove that for any real pulse  $f(t) \leftrightarrow F(\omega)$ ,

$$\begin{aligned} (a) \quad f_{ev}(t) &\leftrightarrow A(\omega) \\ f_{od}(t) &\leftrightarrow jB(\omega) \end{aligned}$$

(b)  $F(\omega)$  is real and even iff  $f(t)$  is even,  $F(\omega)$  is purely imaginary and odd iff  $f(t)$  is odd.

### A Project Involving the FFT System

**3.16** The F postprocessor can operate on the FFT spectrum in many ways, and among its other functions we can also use it to perform numerical integration on the **energy spectrum**. This is done as follows. Starting from the fact that

$$E(\omega) = \frac{A(\omega)^2 + B(\omega)^2}{2\pi}$$

for the FFT this becomes

$$E(n\omega_0) = \frac{1}{2\pi} \left( \frac{T}{N} \right)^2 [\text{FRE}(n)^2 + \text{FIM}(n)^2] \quad (3.63)$$

where  $T/N$  is a required scale factor that is discussed in Chapter 12.

The simplest algorithm for numerical integration is the **rectangular rule**, namely

$$\int_{-X}^X g(x) dx \approx \sum_{n=-M/2}^{M/2-1} g_n \Delta x \quad (3.64)$$

in which the range of integration  $-X$  to  $X$  has been divided into  $M$  equal intervals, each of length  $\Delta x$ , with sampling at the left endpoint of each interval. Applying (3.64) to (3.63), we obtain the following algorithm for integrating the energy spectrum:

$$\int_{-(M/2)\omega_0}^{(M/2-1)\omega_0} E(\omega) d\omega \approx \sum_{n=-M/2}^{M/2-1} \frac{1}{2\pi} \left( \frac{T}{N} \right)^2 [\text{FRE}(n)^2 + \text{FFIM}(n)^2] \omega_0 \quad (3.65)$$

Note that

$$\frac{1}{2\pi} \omega_0 = \frac{1}{2\pi} \frac{2\pi}{T} = \frac{1}{T} \quad (3.66)$$

We can now easily write the code for the RHS of (3.65) and place it in the F postprocessor. We would want to include a prompt for the value of  $M$ , as well as a print statement to display the result on the screen. Also we must keep in mind that values for  $n$  in the FFT spectrum run from 0 to  $N - 1$ , and that negative values will not be accepted.

On your disk you will find that the code for this routine has been included in the F postprocessor. (See Section 17.1 in the manual on your disk.) You can now use it to find the amount of energy contained in parts of an energy spectrum. We have also included the capability to find the amount of power in a periodic waveform from its power spectrum. (See Exercise 2.16(g).)

Even with its primitive rectangular-rule integration, the code gives results with errors less than 1 percent for  $N = 256$ . Using a better numerical integration method, for example, Simpson's rule, does not give more accurate results. The only way to improve the accuracy of the results is to

- Use a larger value for  $N$
- When in PULSE mode, use a smaller value for  $T$ .

# Fourier Transforms of Some Important Functions

### 4.1 INTRODUCTION

---

The nineteenth century saw many of its renowned mathematicians working to place Fourier's and Laplace's discoveries on a more rigorous basis, but despite the fact that a large amount of theoretical ground was covered the central question of necessity and sufficiency for the convergence of Fourier series and integrals remained (and still remains) unsolved.

Much of the effort was of an analytical nature, with people seeking to introduce rigor into what had been discovered and not fully proved. For example, Fourier made the statement: "There is no function  $f(x)$  or part of a function, which cannot be expressed by a trigonometric series." It was Dirichlet who first gave a working set of sufficient conditions under which the statement was true, and others were able to demonstrate functions for which it was false (Coppel, 1969).

In the 1920s a major extension to Fourier analysis came from an unexpected quarter that was soon to be of great value to engineers. A 25-year-old British mathematical physicist named Paul Adrien Maurice Dirac (1902–1984) presented a paper on quantum mechanics to the Royal Society of London in 1927, in which he introduced his **delta function**, now known as the "Dirac delta" and symbolized as  $\delta(t - \tau)$ .<sup>†</sup>

Although Dirac had created the delta function primarily for use in quantum mechanics, it was soon found to be extremely useful in many other fields, especially electrical engineering where its role is now central. We shall begin to explore some of the properties of the Dirac delta later in this chapter, and we shall find that it is one of the most valuable of all the tools in Fourier analysis, despite the fact that it

- Has infinite energy and cannot be realized in the laboratory
- Does not satisfy the requirements of either the square integrability or the Dirichlet criterion discussed in Chapter 3

In fact, by all accounts it violates everything that we know about the sufficiency conditions for the existence of a Fourier transform. Yet it has such a transform, and a

<sup>†</sup>Dirac shared a Nobel prize in 1933 with the Austrian physicist Erwin Schrödinger (1887–1961) for work that they had done, independently of each other, in quantum mechanics.

very nice one at that. As we shall soon be able to show,

$$\delta(t - \tau) \Leftrightarrow e^{-j\omega\tau} \quad (4.1)$$

from which the Dirac delta is seen to be intricately bound up with the complex exponentials that we have been working with so extensively.

Dirac's discovery stimulated mathematicians to investigate what exactly such an expression, which in theory contains infinite energy, really means. It was quickly noted that there were many others, such as the **signum function**, Heaviside's **step function**,  $\sin(\omega t)$  and  $\cos(\omega t)$ , all containing infinite energy, and so all of them violating the square integrability criterion, yet all of them having well-behaved Fourier transforms if appropriately handled.

This led to the opening up of the mathematical field known as **distribution theory**, or **generalized function theory**, and while many people made major contributions to it, and others still are doing so, perhaps the one most highly regarded was the French mathematician **Laurent Schwartz** (1913– ). Schwartz was particularly interested in the application of distribution theory to engineering and physics, and coincidentally, for much of his career he occupied the chair of analysis at the École Polytechnique in France, a position once held by Fourier.

We shall touch only lightly on distribution theory in this chapter. Our approach will be extremely superficial, just enough to enable us to find the Fourier transforms of a number of essential pulses, such as

- The Dirac delta
- The step function
- The signum function
- The eternal complex exponential
- The eternal constant (a dc voltage or current)
- The eternal sine or cosine (an ac voltage or current)
- Any periodic waveform that has a Fourier series

But as the reader can quickly see from the entries in this list, there are indeed a number of waveforms here that are of significant interest to us as electrical engineers.

Perhaps the biggest surprise of all must be the fact that prior to the 1930s such pulses were not properly available to users of Fourier analysis when seeking to solve problems related to electrical engineering. William Thomson (Lord Kelvin) made use of an ingenious approximation of the Dirac delta in his investigations for the trans-Atlantic cable, and also used the Heaviside step function (Nahin), but neither was done in a setting that required Fourier transformation, perhaps because the mathematics had not yet advanced to where it is today.

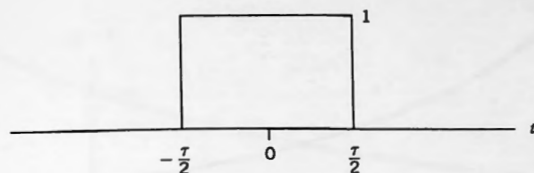
Heaviside also made frequent use of the step function, and although his “mathematics” has raised a great deal of controversy, it is clear that he came very close to the discovery of the Dirac delta. We shall return to this briefly at a later stage.

## 4.2 THE RECTANGULAR PULSE

---

$$f(t) = \text{Rect}(t/\tau)$$

This waveform (shown in Fig. 4.1) is also known as the **gate pulse**, and so some

Figure 4.1.  $\text{Rect}(t/\tau)$ .

authors write it as  $\text{Ga}(t/\tau)$  or simply  $G(t/\tau)$ . We have already encountered  $\text{Rect}(t/\tau)$  in Chapter 3. Its Fourier transform was shown in (3.24) to be

$$F(\omega) = \tau \text{Sa} \frac{\omega\tau}{2} = \tau \frac{\sin(\omega\tau/2)}{\omega\tau/2} \quad (4.2)$$

At a later stage we shall need to know the total area under  $\text{Sa}(x)$ , which we can now find from (4.2) as follows. By the synthesis equation:

$$\text{Rect} \frac{t}{\tau} = \frac{1}{2\pi} \int_{-\infty}^{\infty} \tau \text{Sa} \frac{\omega\tau}{2} e^{j\omega t} d\omega \quad (4.3)$$

For  $t = 0$  the LHS equals 1. Setting  $t = 0$  in the RHS, we obtain

$$\frac{1}{2\pi} \int_{-\infty}^{\infty} \tau \text{Sa} \frac{\omega\tau}{2} d\omega = \frac{1}{\pi} \int_{-\infty}^{\infty} \text{Sa} \frac{\omega\tau}{2} d \frac{\omega\tau}{2} = \frac{1}{\pi} \int_{-\infty}^{\infty} \text{Sa}(x) dx \quad (4.4)$$

Combining this with the fact that the LHS equals 1 then gives the desired result as

$$\int_{-\infty}^{\infty} \text{Sa}(x) dx = \pi \quad (4.5)$$

Compare this result to Exercise 3.10(e) where you were asked to prove that

$$\int_{-\infty}^{\infty} \text{Sa}^2(x) dx = \pi \quad (4.6)$$

### 4.3 THE SINGLE-SIDED DECAYING EXPONENTIAL

---

This pulse is defined as follows:

$$f(t) = \begin{cases} 0 & (t < 0) \\ \frac{1}{2} & (t = 0) \\ e^{-\beta t} & (t > 0) \quad (\beta > 0) \end{cases} \quad (4.7)$$

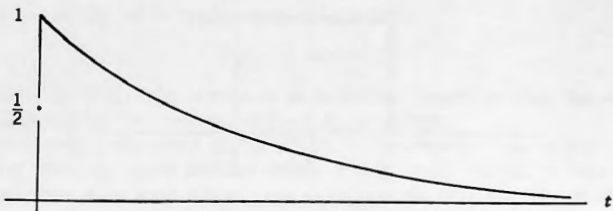


Figure 4.2. Single-sided decaying exponential.

Note that  $\beta$  is always taken to be positive, which is what makes the exponential decay as  $t$  increases. In Figure 4.2 we show a plot of  $f(t)$ . The preceding definition can be written more succinctly as

$$f(t) = e^{-\beta t} U(t) \quad (\forall t) \quad (4.8)$$

where  $U(t)$  is called the unit step.

**Definition:** The unit step  $U(t)$  is defined by

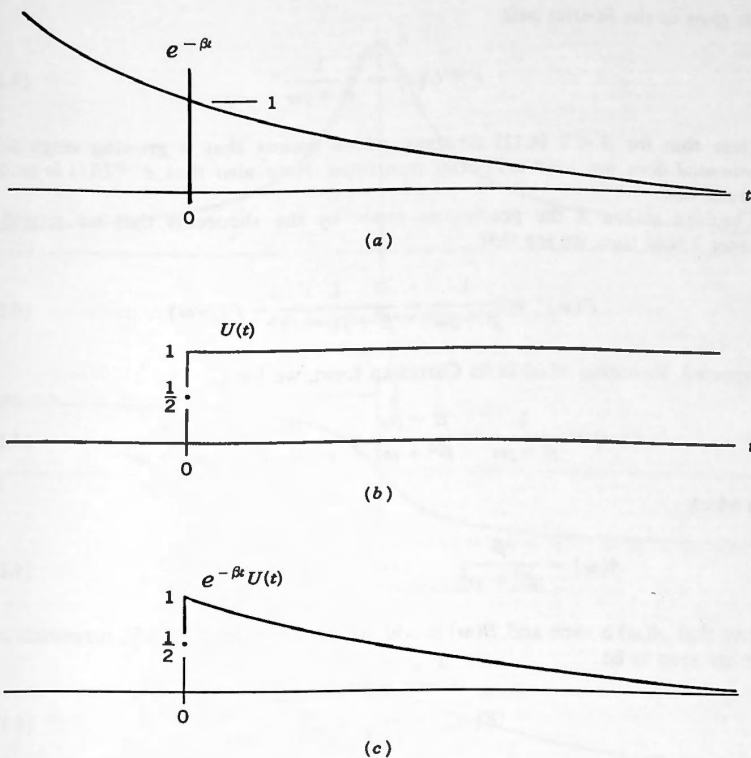
$$U(t) \equiv \begin{cases} 0 & (t < 0) \\ \frac{1}{2} & (t = 0) \\ 1 & (t > 0) \end{cases} \quad (4.9)$$

The unit step will be used very often, and in Figure 4.3b we show what it looks like. Note the step-increase from zero on the left of the origin to one on the right. For exactly  $t = 0$  the function is defined as having a value of  $\frac{1}{2}$ . In Figure 4.3c we depict the product  $e^{-\beta t} U(t)$ . Observe how the unit step zeros out a function where  $t$  is negative, and retains, without change, the portion where  $t$  is positive. At  $t = 0$  the function's value is multiplied by  $\frac{1}{2}$ .

Testing to see if  $e^{-\beta t} U(t)$  is an energy pulse, we find its energy content to be

$$\begin{aligned} E[f(t)] &= \int_{-\infty}^{\infty} [e^{-\beta t} U(t)]^2 dt = \int_0^{\infty} e^{-2\beta t} dt \\ &= \left. \frac{e^{-2\beta t}}{-2\beta} \right|_0^{\infty} = \frac{1}{2\beta} < \infty \end{aligned} \quad (4.10)$$

Thus  $f(t)$  has finite energy, and so it is an energy pulse. By the square integrability criterion of Chapter 3 we are therefore guaranteed that its Fourier transform exists

Figure 4.3.  $e^{-\beta t}U(t)$ .

and also that the latter inverts to the original function. Deriving its Fourier transform we have

$$\begin{aligned}
 F(\omega) &= \int_{-\infty}^{\infty} f(t) e^{-j\omega t} dt = \int_0^{\infty} e^{-\beta t} e^{-j\omega t} dt \\
 &= \int_0^{\infty} e^{-(\beta + j\omega)t} dt = \frac{e^{-(\beta + j\omega)t}}{-(\beta + j\omega)} \Big|_0^{\infty} \\
 &= \frac{e^{-\beta t} e^{-j\omega t}}{-(\beta + j\omega)} \Big|_0^{\infty} = \frac{1}{\beta + j\omega}
 \end{aligned} \tag{4.11}$$

This gives us the Fourier pair

$$e^{-\beta t}U(t) \Leftrightarrow \frac{1}{\beta + j\omega} \quad (4.12)$$

Note that for  $\beta < 0$  (4.11) diverges, which means that a **growing** single-sided exponential does not have a Fourier transform. Note also that  $e^{-\beta t}U(t)$  is neither even nor odd.

Checking to see if the predictions made by the theorems that we proved in Chapter 3 hold true, we see that

$$F(\omega)^* = \frac{1}{\beta - j\omega} = \frac{1}{\beta + j(-\omega)} = F(-\omega) \quad (4.13)$$

as expected. Restating  $F(\omega)$  in its Cartesian form, we have

$$F(\omega) = \frac{1}{\beta + j\omega} = \frac{\beta - j\omega}{\beta^2 + \omega^2} = \frac{\beta}{\beta^2 + \omega^2} - j \cdot \frac{\omega}{\beta^2 + \omega^2} \quad (4.14)$$

from which

$$A(\omega) = \frac{\beta}{\beta^2 + \omega^2} \quad \text{and} \quad B(\omega) = \frac{-\omega}{\beta^2 + \omega^2} \quad (4.15)$$

Observe that  $A(\omega)$  is even and  $B(\omega)$  is odd, as expected. From (4.15), magnitude and phase are seen to be

$$|F(\omega)| = \frac{1}{\sqrt{(\beta^2 + \omega^2)}} \quad (4.16)$$

and

$$\Theta(\omega) = \arctan \frac{-\omega}{\beta} \quad (4.17)$$

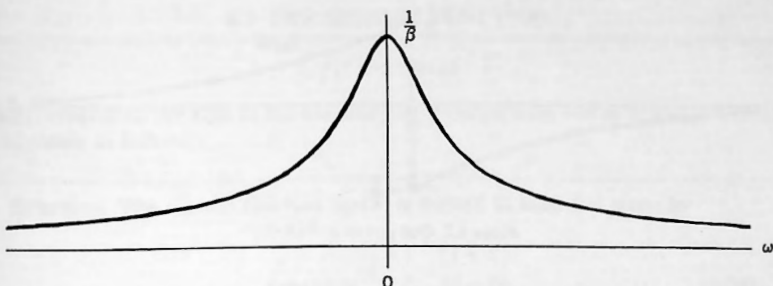
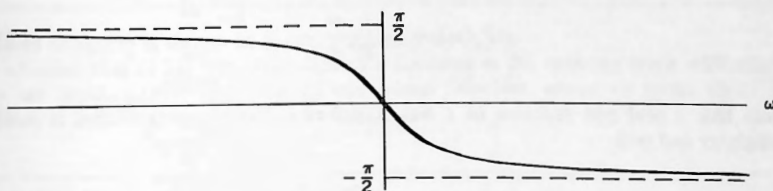
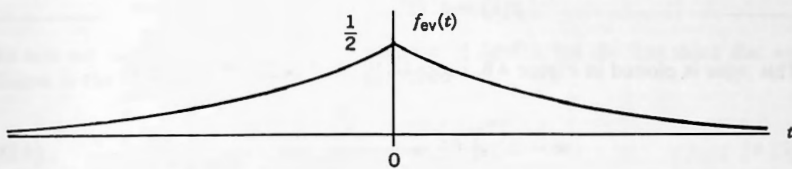
These are plotted in Figures 4.4 and 4.5. We note that  $|F(\omega)|$  is even and  $\Theta(\omega)$  is odd, both also as expected.

We can obtain two further Fourier transforms from (4.12), both of which will be needed, as follows: The even part of  $e^{-\beta t}U(t)$  is

$$\begin{aligned} f_{ev}(t) &= \frac{1}{2}[f(t) + f(-t)] \\ &= \frac{1}{2}[e^{-\beta t}U(t) + e^{\beta t}U(-t)] \end{aligned} \quad (4.18)$$

which is plotted in Figure 4.6. From the figure we see that

$$f_{ev}(t) = \frac{1}{2}e^{-|\beta|t} \quad (4.19)$$

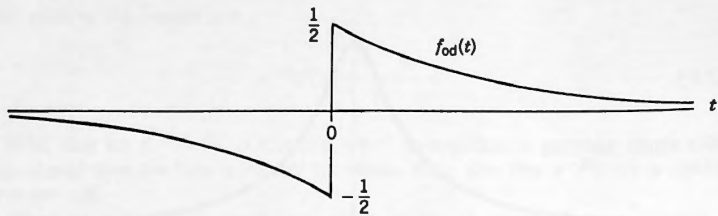
Figure 4.4. Magnitude spectrum of  $e^{-\beta t}U(t)$ .Figure 4.5. Phase spectrum of  $e^{-\beta t}U(t)$ .Figure 4.6. Even part of  $e^{-\beta t}U(t)$ .

and since  $f_{ev}(t) \Leftrightarrow A(\omega)$ , from (4.15) we see that its Fourier transform must be

$$F_1(\omega) = \frac{\beta}{\beta^2 + \omega^2} \quad (4.20)$$

Note how a real even function of  $t$  has transformed to a real even function of  $\omega$ . Similarly, the odd part of  $e^{-\beta t}U(t)$  is

$$\begin{aligned} f_{od}(t) &= \frac{1}{2}[f(t) - f(-t)] \\ &= \frac{1}{2}[e^{-\beta t}U(t) - e^{\beta t}U(-t)] \end{aligned} \quad (4.21)$$

Figure 4.7. Odd part of  $e^{-\beta|t|}U(t)$ .

which is plotted in Figure 4.7. Since  $f_{od}(t) \Leftrightarrow j\beta(\omega)$ , we see from (4.15) that its Fourier transform must be

$$F_2(\omega) = -j \frac{\omega}{\beta^2 + \omega^2} \quad (4.22)$$

Note how a real odd function of  $t$  has transformed to a function that is purely imaginary and odd.

#### 4.4 THE DOUBLE-SIDED DECAYING EXPONENTIAL

---

$$f(t) = e^{-\beta|t|} \quad (\beta > 0)$$

This pulse is plotted in Figure 4.8. From (4.19) and (4.20) we see that

$$e^{-\beta|t|} \Leftrightarrow \frac{2\beta}{\beta^2 + \omega^2} \quad (4.23)$$

Observe that the pulse is real and even, and so is its Fourier transform, as expected. Moreover we also see that the pulse is everywhere continuous, which is consistent with the fact that for large  $\omega$  its Fourier transform dies out like  $1/\omega^2$ .

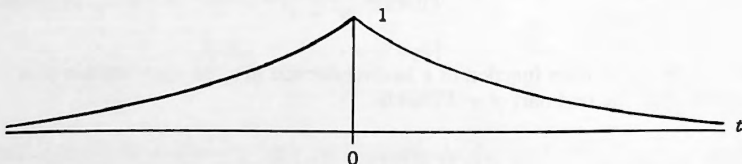


Figure 4.8. Double-sided decaying exponential.

## 4.5 THE SIGNUM FUNCTION

$$f(t) = \text{Sgn}(t)$$

$\text{Sgn}(t)$  represents the **sign** of the variable  $t$  as it ranges from  $-\infty$  to  $\infty$ , and is defined analytically as follows:

**Definition:** The signum function  $\text{Sgn}(t)$  is defined in analytical terms by

$$\text{Sgn}(t) = \begin{cases} -1 & (t < 0) \\ 0 & (t = 0) \\ +1 & (t > 0) \end{cases} \quad (4.24)$$

A plot of  $\text{Sgn}(t)$  is shown in Figure 4.9 based on (4.24).

Observe that (4.24) is a definition of a function in the ordinary sense with which we are familiar (first proposed by our friend Dirichlet, whom we spoke about in Chapters 2 and 3), namely:

### ■ Dirichlet's Definition of a Function

A function  $f$  is given if we have any rule that assigns a definite value  $f(t)$  to every  $t$  in a certain set of points.

We now set out to find the Fourier transform of  $\text{Sgn}(t)$ , but the first thing that we observe is that it is not an energy pulse. Indeed

$$E = \int_{-\infty}^{\infty} |\text{Sgn}(t)|^2 dt = \int_{-\infty}^{\infty} dt = \infty \quad (4.25)$$

and so  $\text{Sgn}(t)$  is seen to have infinite energy. Thus the square integrability criterion is not applicable and we are not guaranteed that it has a Fourier transform. Indeed,

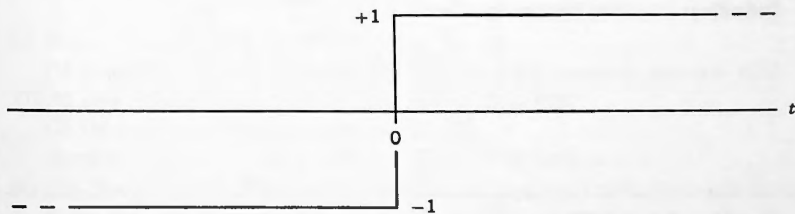


Figure 4.9.  $\text{Sgn}(t)$ .

attempting to find its Fourier transform using the analysis equation we quickly run into trouble as the following shows:

$$\begin{aligned}
 F(\omega) &= \int_{-\infty}^{\infty} \text{Sgn}(t) e^{-j\omega t} dt \\
 &= \int_{-\infty}^0 (-1) e^{-j\omega t} dt + \int_0^{\infty} (+1) e^{-j\omega t} dt \\
 &= \frac{-e^{-j\omega t}}{-j\omega} \Big|_{-\infty}^0 + \frac{e^{-j\omega t}}{-j\omega} \Big|_0^{\infty} \tag{4.26}
 \end{aligned}$$

after which we are unable to assign values to  $e^{-j\omega t}$  at  $-\infty$  and  $\infty$ , and so further progress is blocked. Does  $\text{Sgn}(t)$  then have a Fourier transform at all? The answer is as follows:

If  $\text{Sgn}(t)$  is viewed as a function in the ordinary (Dirichlet) sense with its analytical definition as given in (4.24), then we shall not be able to find a Fourier transform for it. There is, however, a totally different way of viewing  $\text{Sgn}(t)$ , as what is called a **generalized function** or a **distribution**, which, happily, enables us to get around the preceding impasse.

There are two ways in which generalized functions or distributions can be defined, but in this text we concern ourselves with only the one that we believe is the more easily understood by nonmathematicians. The other is based on what are called **testing functions**, an indispensable concept for a more serious investigation of distribution theory. The reader who is interested in taking the next step beyond what we present in this chapter is referred to the discussion in the excellent and reader-friendly monograph by Hwei P. Hsu. (See Hsu, 1984.)

**Definition:** A **generalized function** or **distribution** is defined as the limit of a sequence of appropriately chosen ordinary functions, each of which has a Fourier transform in the usual sense.

In the case of  $\text{Sgn}(t)$  we redefine it as a distribution in the following way:

**Definition:** The **distribution**  $\text{Sgn}(t)$  is defined by

$$\text{Sgn}(t) \equiv \lim_{k \rightarrow 0^+} \begin{cases} e^{-kt} & (t > 0) \\ 0 & (t = 0) \\ -e^{+kt} & (t < 0) \end{cases} \tag{4.27}$$

(Note that  $k$  is always positive while approaching zero.) Let's take a careful look at what (4.27) says. In it  $\text{Sgn}(t)$  is defined as the **limit of a sequence of functions** and not

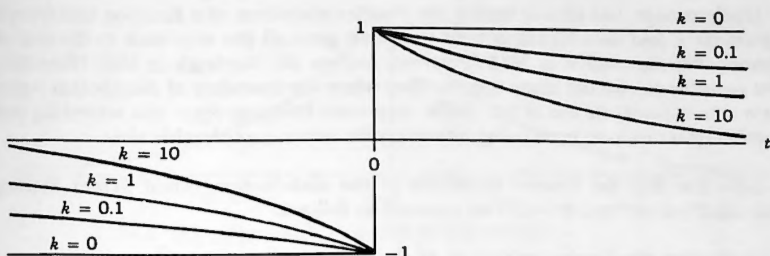


Figure 4.10.  $\text{Sgn}(t)$  as the limit of a sequence of exponentials.

as a function. The expression on the RHS of (4.27), namely

$$f_k(t) \equiv \begin{cases} e^{-kt} & (t > 0) \\ 0 & (t = 0) \\ -e^{+kt} & (t < 0) \end{cases} \quad (4.28)$$

is plotted in Figure 4.10 for various values of  $k$ . As  $k \rightarrow 0$  a sequence of functions results, and we see in the figure how that sequence tends to the same  $\text{Sgn}(t)$  that we defined analytically in (4.24).

The function  $f_k(t)$  of (4.28) is called a **sequence function** for  $\text{Sgn}(t)$ . It is not the only possible choice, but it was selected because it gives us the results that we need with little or no effort. Observe the following:

- (1)  $f_k(t)$  has  $k$  as a second variable, in addition to  $t$ . When we take its Fourier transform,  $t$  will disappear but  $k$  will survive. Later we will let  $k$  go to zero.
- (2) In (4.27) the limit to which  $k$  tends is zero, but this is not necessarily the case for all distributions. For other distributions the sequence-variable  $k$  could tend to some other limit, for example, infinity.

### ■ Fundamental Properties of Distributions

- (a) It can be shown that if we
  - (1) take the Fourier transform of a distribution's sequence function  $f_k(t)$  holding  $k$  constant
  - (2) then let  $k$  tend to its limit
 the result will be a valid Fourier transform of the distribution.
- (b) The Fourier transform so obtained can be combined with Fourier transforms that have been obtained for ordinary (finite-energy) pulses by the use of the analysis equation.

Oddly enough, this idea of finding the Fourier transform of a function containing a parameter  $k$  and then letting  $k$  tend to a limit goes all the way back to the time of Fourier. Poisson used it in 1818 (Poisson), and so did Rayleigh in 1889 (Rayleigh), and probably so also did many others. Thus when the founders of distribution theory were able to justify its use in the 1930s, they were bringing rigor into something that people appear to have been using intuitively for some considerable time.

Let's now find the Fourier transform of the **distribution** called  $\text{Sgn}(t)$ . Starting from  $\text{Sgn}(t)$  as defined in (4.27) we proceed as follows:

(1) **Finding the Fourier transform of the sequence function, holding  $k$  constant:**

The sequence function  $f_k(t)$  in (4.28) is the same as twice the odd part of the single-sided decaying exponential considered earlier, with  $\beta$  replaced by  $k$ . Hence from (4.22) its Fourier transform is

$$F_k(\omega) = -j \frac{2\omega}{k^2 + \omega^2} \quad (4.29)$$

(2) **Letting  $k$  tend to its limit:**

$$\lim_{k \rightarrow 0} \left[ -j \frac{2\omega}{k^2 + \omega^2} \right] = \frac{2}{j\omega} \quad (4.30)$$

which gives us the required Fourier transform. Expressed as a Fourier pair, we have

$$\text{Sgn}(t) \Leftrightarrow \frac{2}{j\omega} \quad (4.31)$$

■

The impasse that we encountered earlier has thus been completely circumvented, and in the process we have found our first Fourier transform of a pulse that does not have finite energy. We note from (4.31) that  $F(\omega) = 2/j\omega$  is purely imaginary and odd, which is consistent with the fact that  $\text{Sgn}(t)$  is real and odd.

In order to plot the magnitude and phase spectra of  $\text{Sgn}(t)$  we must first express  $F(\omega)$  in polar form. To accomplish this we write it as

$$F(\omega) = \frac{-2j}{\omega} \quad (4.32)$$

from which

$$|F(\omega)| = \frac{2}{|\omega|} \quad \text{and} \quad \Theta(\omega) = \begin{cases} \frac{\pi}{2} & \omega < 0 \\ -\frac{\pi}{2} & \omega > 0 \end{cases} \quad (4.33)$$

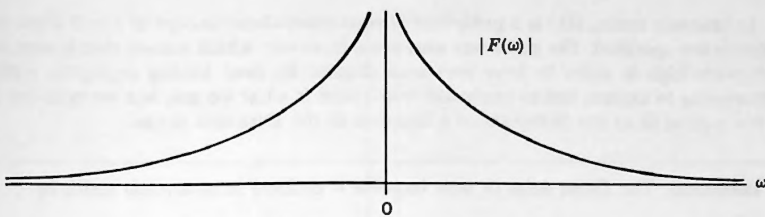


Figure 4.11. Magnitude spectrum of  $\text{Sgn}(t)$ .

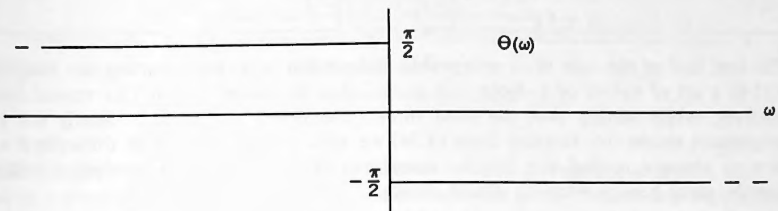


Figure 4.12. Phase spectrum of  $\text{Sgn}(t)$ .

These are plotted in Figures 4.11 and 4.12. Note that  $|F(\omega)|$  is even and  $\Theta(\omega)$  is odd, as expected from Chapter 3.

## 4.6 THE DIRAC DELTA OR UNIT IMPULSE

---

$$f(t) = \delta(t)$$

The **Dirac delta or unit impulse**  $\delta(t)$  is our second example of a distribution or generalized function and, as we shall soon discover, it is one of the most valuable tools in the entire field of Fourier analysis. We shall use the terms “Dirac delta” and “unit impulse” interchangeably.

The Dirac delta came to Fourier analysis only as recently as the 1930s, after Paul Dirac introduced it in 1927, and he and mathematicians like Laurent Schwartz created a rigorous basis called distribution theory to explain its properties.<sup>†</sup>

<sup>†</sup>The newness of pulses of this kind is underscored by the fact that in a monograph published as recently as 1949, a prominent applied mathematician of that time named J. C. Jaeger could make the following statement: “Examples of functions for which the Fourier transform does not exist are 1,  $e^t$  or  $\sin(t)$ ” (Jaeger, 1949).

From the context of the quotation, by “1” Jaeger was referring to the unit step  $U(t)$ , and by “ $\sin(t)$ ” he meant  $\sin(t)U(t)$ . As we shall soon see, both of these have well-defined Fourier transforms involving the Dirac delta, something that Jaeger was evidently still not aware of 22 years after Dirac first used it in quantum mechanics. (The third function to which Jaeger was referring, namely  $e^tU(t)$ , did not have a Fourier transform in 1949 and never will have.)

In heuristic terms,  $\delta(t)$  is a pulse that is zero everywhere except at  $t = 0$  where its value is not specified. The pulse has unit area, however, which means that it must be extremely high in order to have unit area despite its base having negligible width. Attempting to express this in analytical terms here is what we get, but we note that it is not a good fit to the definition of a function in the Dirichlet sense:

**Definition:** The Dirac delta or unit impulse is defined in analytical terms by

$$\delta(t) = 0 \quad \text{for } t \neq 0, \quad \text{and} \quad \int_{-\infty}^{\infty} \delta(t) dt = 1 \quad (4.34)$$

The first half of the rule is an acceptable assignment of values relating the function  $\delta(t)$  to a set of values of  $t$ . Note that it excludes the point  $t = 0$ . The second half, however, while stating that the area under the pulse is unity, is clearly not an assignment statement. Starting from (4.34) we would thus have great difficulty if we were to attempt to find the Fourier transform of  $\delta(t)$  using the analysis equation directly, since here is what we would obtain:

$$F(\omega) = \int_{-\infty}^{\infty} [?] e^{-j\omega t} dt \quad (4.35)$$

And now we would be unable to decide what to put inside the square brackets as the required analytical statement.

As with  $\text{Sgn}(t)$  we can circumvent this impasse if we redefine  $\delta(t)$  as a distribution, whereupon everything starts to work properly. In order to specify  $\delta(t)$  as a distribution we shall state it as the limit of a sequence of functions, each of which has a Fourier transform in the usual sense. We start with the pulse shown in Figure 4.13, which is a specially selected Rect function whose width is  $k$  and whose height is  $1/k$ . We call this the **box function**  $B_k(t)$ , where

$$B_k(t) \equiv \frac{1}{k} \text{Rect} \frac{t}{k} \quad (4.36)$$

Then  $B_k(t)$  is seen to have area equal to unity, regardless of the value of  $k$ . If we now

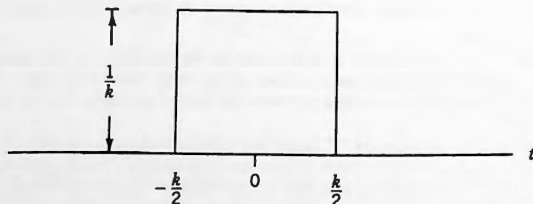
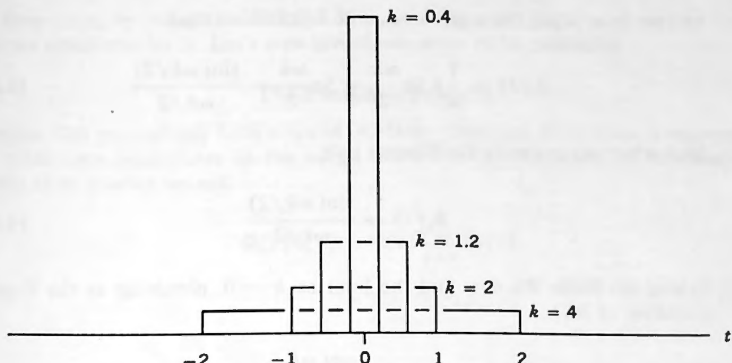


Figure 4.13. Box function  $B_k(t)$ .

Figure 4.14. Sequence of box functions  $B_k(t)$ .

take successively smaller values of  $k$ , then we obtain a sequence of pulses each of which is occupying less and less of the  $t$ -axis and each getting higher and higher, and yet all of whose areas are unity. (See Fig. 4.14.) Moreover, all of them have Fourier transforms.

Stated as the limit of a sequence of functions we now have:

**Definition:** The Dirac delta or unit impulse is the distribution defined by

$$\delta(t) \equiv \lim_{k \rightarrow 0} B_k(t) \quad (4.37)$$

This definition and the one given in (4.34) are clearly consistent, since as  $k \rightarrow 0$  we see that  $B_k(t) = 0$  for  $t \neq 0$ , and the following integral is always true:

$$\int_{-\infty}^{\infty} B_k(t) dt = 1 \quad (\forall k > 0) \quad (4.38)$$

Thus  $B_k(t)$  as selected constitutes an acceptable sequence function for  $\delta(t)$ . We now set out to find the Fourier transform of the distribution  $\delta(t)$ , and, as we did with  $\text{Sgn}(t)$ ,

- (1) First we find the transform of the sequence function  $B_k(t)$  treating  $k$  as a constant.
- (2) Then we let  $k$  tend to its limit.

**(1) Finding the Fourier transform of the sequence function:** Recall from (4.2) that

$$\text{Rect} \frac{t}{k} \Leftrightarrow k \text{ Sa} \frac{\omega k}{2} \quad (4.39)$$

and so, from (4.36), for a given value of  $k$  it follows that

$$B_k(t) \Leftrightarrow \frac{1}{k} k \operatorname{Sa} \frac{\omega k}{2} = \operatorname{Sa} \frac{\omega k}{2} = \frac{\sin(\omega k/2)}{\omega k/2} \quad (4.40)$$

from which we can write the Fourier pair

$$B_k(t) \Leftrightarrow \frac{\sin(\omega k/2)}{\omega k/2} \quad (4.41)$$

(2) **Taking the limit:** We now find the limit as  $k \rightarrow 0$ , obtaining as the Fourier transform of  $\delta(t)$

$$F(\omega) = \lim_{k \rightarrow 0} \frac{\sin(\omega k/2)}{\omega k/2} = 1 \quad (4.42)$$

which finally gives us the Fourier pair

$$\delta(t) \Leftrightarrow 1 \quad (4.43)$$

The Dirac delta thus has as its Fourier transform,  $F(\omega) = 1$  (see Fig. 4.15). This remarkable result shows the following:

- The magnitude spectrum of  $\delta(t)$  is everywhere unity (even) and its phase spectrum is everywhere zero (odd).
- The Dirac delta is even, as evidenced by the fact that its Fourier transform is real and even.

Using Parseval's theorem to find the amount of energy in  $\delta(t)$ , we obtain

$$E = \frac{1}{2\pi} \int_{-\infty}^{\infty} |F(\omega)|^2 d\omega = \frac{1}{2\pi} \int_{-\infty}^{\infty} d\omega = \infty \quad (4.44)$$

Thus  $\delta(t)$  contains infinite energy, and so it obviously is not an energy pulse. Yet, as

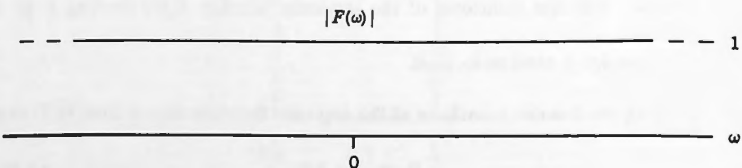


Figure 4.15. Magnitude spectrum of  $\delta(t)$ .

we have seen, by using the concept of a distribution we have been able to find a Fourier transform for it. Let's now investigate some of its properties.

### The Sampling Property

Suppose that we multiply both sides of (4.37) by a function  $\Phi(t)$ , which is assumed to be continuous everywhere in the range over which the sequence of box functions exists. Here is what we get:

$$\begin{aligned}\Phi(t)\delta(t) &= \Phi(t) \lim_{k \rightarrow 0} B_k(t) \\ &= \lim_{k \rightarrow 0} \Phi(t) B_k(t)\end{aligned}\quad (4.45)$$

In Figure 4.16 we show  $\Phi(t)$  being multiplied by a single box function, namely

$$\Phi(t)B_k(t) = \Phi(t) \frac{1}{k} \text{Rect} \frac{t}{k} \quad (4.46)$$

Observe how the formerly flat top of the Rect function in  $B_k(t)$  whose height was  $1/k$  has now become a section of the function  $\Phi(t)$  multiplied by  $1/k$ , and how outside the range of  $B_k(t)$  the function  $\Phi(t)$  is nulled out.

We now take the limit shown in (4.45). Then  $B_k(t)$  becomes narrower and higher, zeroing out more and more of  $\Phi(t)$  with its top tending toward the constant value  $\Phi(0)/k$ . The LHS of (4.46) becomes  $\Phi(t)\delta(t)$ , and so we have

$$\begin{aligned}\Phi(t)\delta(t) &= \lim_{k \rightarrow 0} \Phi(t) B_k(t) \\ &= \lim_{k \rightarrow 0} \Phi(t) \frac{1}{k} \text{Rect} \frac{t}{k} \\ &= \Phi(0)\delta(t)\end{aligned}\quad (4.47)$$

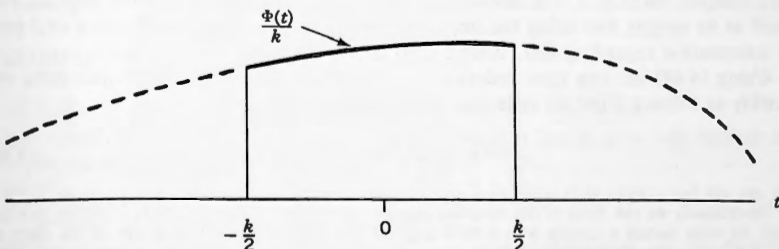


Figure 4.16.  $\Phi(t)B_k(t)$ .

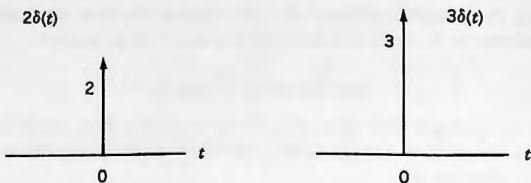


Figure 4.17. Two weighted impulses.

We state this as follows:

■ **The Sampling Property of the Unit Impulse**

$$\Phi(t)\delta(t) = \Phi(0)\delta(t) \quad (4.48)$$

*Note:* Many authors refer to (4.48) as the sifting property.

**The Area or Weight of an Impulse**

Up to now we have talked only about a unit impulse. However,

$$\int_{-\infty}^{\infty} \Phi(0)\delta(t) dt = \Phi(0) \int_{-\infty}^{\infty} \delta(t) dt = \Phi(0) \quad (4.49)$$

from which we see that the impulse  $\Phi(0)\delta(t)$  has an area equal to  $\Phi(0)$ . Thus impulses can have areas under them other than unity. We call the area under a Dirac delta its weight and we use the symbolization shown in Figure 4.17, where the arrowheads signify that we are talking about impulses, and the numbers 2 and 3 adjacent to the arrowheads are their weights. We often use the heights of adjacent impulses to display their relative weights, although we know that their heights are really undefined.

Returning to (4.48) we now see why it is called the sampling property. The impulse  $\delta(t)$  samples  $\Phi(t)$  at  $t = 0$ , obtaining the value  $\Phi(0)$ , which it then imprints onto itself as its weight, becoming the impulse  $\Phi(0)\delta(t)$ . Thereafter it carries a vital piece of information regarding  $\Phi(t)$  bound onto itself.<sup>†</sup>

Using (4.48) we can now rederive the Fourier transform of a Dirac delta very quickly as follows. First we note that (4.48) means

$$e^{-j\omega t}\delta(t) = e^0\delta(t) = \delta(t) \quad (4.50)$$

<sup>†</sup>Heuristically we can think of the sampling property as follows: An object  $\Phi(t)$  is moving in a dark room. At some instant a camera with a flash goes off (the Dirac delta). The details of the object are captured or sampled by the flash as  $\Phi(0)$ , and are recorded on the film as the weight or area of the impulse.

and so, by direct application of the analysis equation,

$$F(\omega) = \int_{-\infty}^{\infty} \delta(t) e^{-j\omega t} dt = \int_{-\infty}^{\infty} \delta(t) dt = 1 \quad (4.51)$$

giving us the same result as (4.43). However, notice how our heightened understanding of the Dirac delta has enabled us to proceed around the impasse appearing in (4.35).

### Further Properties

We can now extend the concept of the Dirac delta further in a number of ways as follows. All of the box functions in the definition of  $\delta(t)$  in (4.37) were positioned symmetrically about the origin. Suppose that we now shift them all to the right by an amount  $\tau$ . Then they would all have been written as  $B_k(t - \tau)$ .

However, now the same limiting process of letting  $k \rightarrow 0$  would have resulted in a Dirac delta located at  $t = \tau$ , which we would have to have written as  $\delta(t - \tau)$ . This then means that we can have unit impulses located anywhere on the  $t$ -axis.

**Rule:** To establish where the impulse  $\delta(t - \tau)$  is located, find out what value of  $t$  makes its argument equal to zero.

#### EXAMPLE 4.1

- (a)  $3\delta(t - 6)$  lies at  $t = 6$  and has weight 3.
- (b)  $-4\delta(t + 2)$  lies at  $t = -2$  and has weight -4.
- (c)  $(2 + j5)\delta(t + \tau)$  lies at  $t = -\tau$  and has weight  $2 + j5$ . □

Note that we do not restrict ourselves to positive weights as (b) shows, nor to real weights as (c) shows. Nor do we restrict ourselves only to the  $t$ -axis as the following shows.

**Definition:** The Dirac delta  $\delta(z - \zeta)$  is a unit impulse on the  $z$ -axis located at  $z = \zeta$ .

#### EXAMPLE 4.2

- (a)  $T_0\delta(\omega - \omega_0)$  on the  $\omega$ -axis lies at  $\omega = \omega_0$  and has weight  $T_0$ .
- (b)  $-j\pi\delta(\omega + \Theta)$  has weight  $-j\pi$ . On the  $\omega$ -axis it lies at  $\omega = -\Theta$ , but on the  $\Theta$ -axis it would lie at  $\Theta = -\omega$ .
- (c)  $T_0\delta(\omega_0 - \omega)$  is the same as the impulse in (a) since it is even, and so, on the  $\omega$ -axis, it lies at  $\omega = \omega_0$  and has weight  $T_0$ .
- (d)  $\delta(\omega - \omega_0 - \Theta)$  on the  $\omega$ -axis lies at  $\omega = \omega_0 + \Theta$ . However, on the  $\Theta$ -axis it would lie at  $\Theta = \omega - \omega_0$ . □

The fact that impulses can be located anywhere means that the sampling property can also be extended. Thus we can state (4.48) in more general form as:

■ The Sampling Property of the Unit Impulse

Time domain

$$\Phi(t)\delta(t-\tau) = \Phi(\tau)\delta(t-\tau) \quad (4.52)$$

Frequency domain

$$G(\omega)\delta(\omega-\alpha) = G(\alpha)\delta(\omega-\alpha) \quad (4.53)$$

Using (4.52) we can now find the Fourier transform of the delayed Dirac delta  $\delta(t-\tau)$  as follows:

$$\begin{aligned} \int_{-\infty}^{\infty} \delta(t-\tau) e^{-j\omega t} dt &= \int_{-\infty}^{\infty} \delta(t-\tau) e^{-j\omega\tau} dt \\ &= e^{-j\omega\tau} \int_{-\infty}^{\infty} \delta(t-\tau) dt = e^{-j\omega\tau} \end{aligned} \quad (4.54)$$

from which we can write the Fourier pair

$$\delta(t-\tau) \Leftrightarrow e^{-j\omega\tau} \quad (4.55)$$

When  $\tau = 0$  the LHS of this equation becomes simply  $\delta(t)$  and the RHS becomes 1, which takes us back to (4.43). Thus (4.55) is the general statement for the Fourier transform of a Dirac delta in which  $\tau$  can be any real number, positive or negative.

■ **EXAMPLE 4.3:** In Figure 4.18 we show three impulses,  $-\delta(t+\tau)$ ,  $2\delta(t)$ , and  $-\delta(t-\tau)$ . Find the Fourier transform of this group.

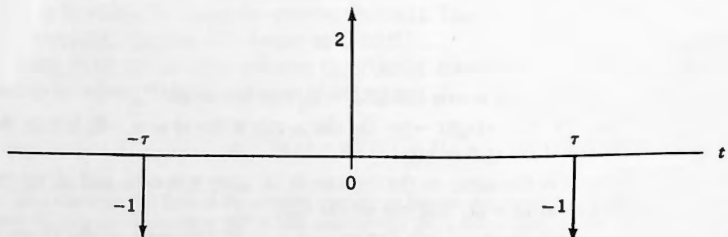


Figure 4.18. Three Dirac deltas.

**Solution:** Transforming the three impulses using (4.55) we obtain

$$\begin{aligned}-\delta(t+\tau) + 2\delta(t) - \delta(t-\tau) &\Leftrightarrow -e^{j\omega\tau} + 2 - e^{-j\omega\tau} \\&= -[e^{j\omega\tau} - 2 + e^{-j\omega\tau}] = -[e^{j\omega\tau/2} - e^{-j\omega\tau/2}]^2 \\&= -\left[\frac{e^{j\omega\tau/2} - e^{-j\omega\tau/2}}{2j}\right]^2 (2j)^2 = 4 \sin^2 \frac{\omega\tau}{2}\end{aligned}$$

We note that the group of impulses in Figure 4.18 is even and that its Fourier transform is real and even, as expected.  $\square$

Observe from (4.55) that the magnitude spectrum of  $\delta(t-\tau)$  is

$$|F(\omega)| = |e^{-j\omega\tau}| = 1 \quad (4.56)$$

and that the phase spectrum is

$$\Theta(\omega) = -\tau\omega \quad (4.57)$$

Thus the magnitude spectrum of  $\delta(t-\tau)$  is always 1 regardless of whether or not it is located at the origin, but its phase is a straight-line function of  $\omega$  whose slope is equal to  $-\tau$ , the amount of the delay of the impulse.

In Figure 4.19 we have plotted the phase spectrum of  $\delta(t-\tau)$ . Observe that whenever the phase angle goes out of bounds we move it back into the allowable range of  $\pm\pi$ . Observe also that the phase of  $\delta(t-\tau)$  will always be an odd function, regardless of the value of  $\tau$ .  $\blacksquare$

Consider now the following integral:

$$\begin{aligned}\int_{-k/2}^{k/2} e^{j\omega t} d\omega &= \frac{e^{j\omega t}}{jt} \Big|_{-k/2}^{k/2} = k \frac{e^{jkt/2} - e^{-jkt/2}}{2j(kt/2)} \\&= k \frac{\sin(kt/2)}{kt/2} = k \operatorname{Sa} \frac{kt}{2}\end{aligned} \quad (4.58)$$

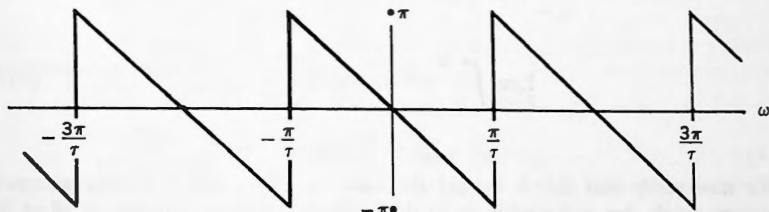
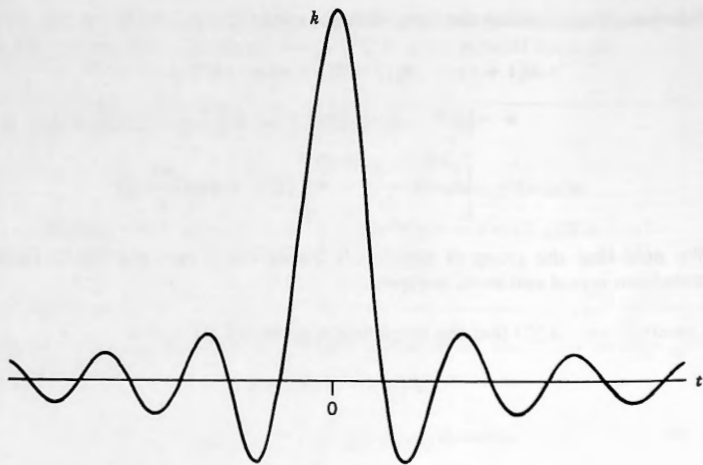


Figure 4.19. Phase spectrum of  $\delta(t-\tau)$ .

Figure 4.20.  $k \text{Sa}(kt/2)$  for small  $k$ .

The function  $k \text{Sa}(kt/2)$  is plotted in Figure 4.20. The first  $t$ -axis crossing takes place where  $kt/2 = \pi$ , that is, at  $t = 2\pi/k$ , and the central node has height  $k$ . From (4.5) we know that the total area under  $\text{Sa}(x)$  is  $\pi$ , and so the area under  $k \text{Sa}(kt/2)$  must be

$$\int_{-\infty}^{\infty} k \text{Sa} \frac{kt}{2} dt = 2 \int_{-\infty}^{\infty} \text{Sa} \frac{kt}{2} d \frac{kt}{2} = 2 \int_{-\infty}^{\infty} \text{Sa}(x) dx = 2\pi \quad (4.59)$$

Note that its area does not depend on the value of  $k$ . If we now let  $k \rightarrow \infty$ , then (see Fig. 4.21) the Sa function in the figure becomes higher and higher at its center and the  $t$ -axis crossings all tend to zero, but its area always remains equal to  $2\pi$ .

We thus suspect that it is tending toward a Dirac delta with weight  $2\pi$ , and that the function  $k \text{Sa}(kt/2)$  is simply another sequence function for the generalized function  $2\pi\delta(t)$ , that is, that

$$\lim_{k \rightarrow \infty} \int_{-k/2}^{k/2} e^{j\omega t} d\omega = 2\pi\delta(t) \quad (4.60)$$

We now verify that this is in fact the case, obtaining the following extremely important result that will enable us to derive the Fourier transforms of all of the remaining generalized functions that we shall require.



Figure 4.21.  $k \text{Sa}(kt/2)$  for large  $k$ .

■ THEOREM 4.1

$$\lim_{k \rightarrow \infty} \int_{-k/2}^{k/2} e^{j\omega t} d\omega = 2\pi \delta(t) \quad (4.61)$$

(Heuristically, what this theorem is telling us is that if we add together (integrate) all possible complex exponentials in equal amounts the result will be a Dirac delta.)

*Proof:* We have shown that  $\delta(t) \Leftrightarrow 1$ , and so it follows from the Fourier inversion integral that

$$\delta(t) = \frac{1}{2\pi} \int_{-\infty}^{\infty} 1 e^{j\omega t} d\omega = \frac{1}{2\pi} \lim_{k \rightarrow \infty} \int_{-k/2}^{k/2} e^{j\omega t} d\omega \quad (4.62)$$

Multiplying through by  $2\pi$  we obtain

$$\lim_{k \rightarrow \infty} \int_{-k/2}^{k/2} e^{j\omega t} d\omega = 2\pi \delta(t) \quad (4.63)$$

which completes the proof. ■

In the statement of the theorem we see that the exponent in the integrand has a positive sign. The theorem also holds if the sign is negative, as the following generalization shows:

■ COROLLARY

$$\lim_{k \rightarrow \infty} \int_{-k/2}^{k/2} e^{\pm jzy} dz = 2\pi\delta(y) \quad (4.64)$$

*Proof:* Consider first the plus sign in the exponent. Then (4.64) follows immediately from (4.61) simply by replacing  $\omega$  with  $z$  and  $t$  with  $y$ .

Now consider the minus sign in the integrand. Replacing  $\omega$  with  $z$  and  $t$  with  $-y$  in (4.61) gives

$$\lim_{k \rightarrow \infty} \int_{-k/2}^{k/2} e^{-jzy} dz = 2\pi\delta(-y) = 2\pi\delta(y) \quad (4.65)$$

(because  $\delta(y)$  is even). This completes the proof. ■

Using Theorem 4.1 we can now find the Fourier transform of the eternal constant

$$f(t) = v_0 \quad (t \in \mathbb{R}) \quad (4.66)$$

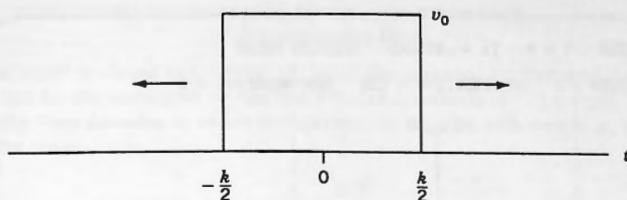
This function can be thought of as an **eternal dc voltage** whose value is  $v_0$  volts. Clearly  $f(t)$  is not an energy pulse because it contains infinite energy and so, once again, the square integrability criterion does not hold. Attempting to find its Fourier transform by a direct application of the analysis equation will fail. However, if we redefine  $f(t)$  as the following generalized function

$$f(t) \equiv \lim_{k \rightarrow \infty} v_0 \operatorname{Rect} \frac{t}{k} \quad (4.67)$$

in which  $v_0 \operatorname{Rect}(t/k)$  is the sequence function shown in Figure 4.22, then here is what happens when we set out to find its Fourier transform.

Being a generalized function we must follow the two-step procedure that we have used previously. Thus, first we find the transform of the sequence function shown in the figure for a fixed value of  $k$ , obtaining

$$F_k(\omega) = \int_{-\infty}^{\infty} v_0 \operatorname{Rect} \frac{t}{k} e^{-j\omega t} dt = v_0 \int_{-k/2}^{k/2} e^{-j\omega t} dt \quad (4.68)$$

Figure 4.22.  $v_0 \text{Rect}(t/k)$ .

Then we let  $k$  tend to its limit, in this case  $\infty$ , obtaining

$$F(\omega) = v_0 \lim_{k \rightarrow \infty} \int_{-k/2}^{k/2} e^{-j\omega t} dt = 2\pi v_0 \delta(\omega) \quad (\text{by Theorem 4.1}) \quad (4.69)$$

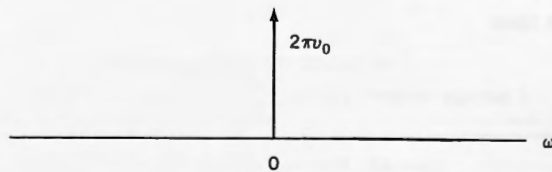
This gives us the Fourier pair

$$v_0 \Leftrightarrow 2\pi v_0 \delta(\omega) \quad (4.70)$$

The Fourier transform of an eternal constant whose value is  $v_0$  is thus a Dirac delta in the frequency domain located at  $\omega = 0$ , of weight  $2\pi v_0$ . (See Fig. 4.23.)

Since  $F(\omega)$  is zero everywhere except at  $\omega = 0$ , we conclude that an eternal dc voltage has all of its infinite amount of energy concentrated at  $\omega = 0$ . (Where else?) ■

Before concluding our brief discussion on the Dirac delta we note the following: The box function used earlier is not the only sequence function that leads to  $\delta(t)$ . As we have seen, the Sa function can also serve as one. There are infinitely many others, one more of which we consider in the exercises at the end of this chapter.

Figure 4.23. Spectrum of  $f(t) = v_0$ .

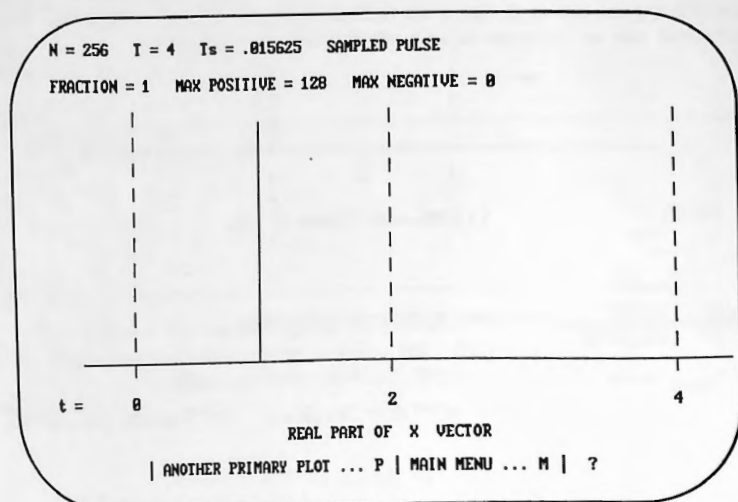
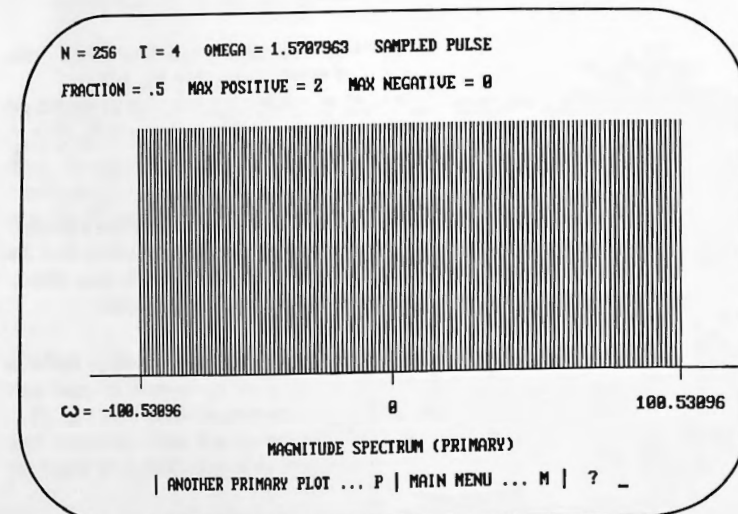


Figure 4.24. The Dirac delta on the FFT.

Figure 4.25. Magnitude spectrum of  $\delta(t)$ .

### Accompanying Disk

As discussed in detail in Chapter 15, all of the essential attributes of the Dirac delta can be implemented on the fast Fourier transform (FFT) system.

**In the time domain**, in order to represent an impulse with weight  $\mu$ , we must load the single value

$$V = \frac{\mu N}{T} \quad (4.71)$$

(This statement applies whether we are using either PERIODIC or PULSE.) For example, if we wish to load into X the impulse  $2\delta(t - 1)$  using  $N = 256$  and  $T = 4$ , then  $256/4 = 64$ , and so from (4.71) we must place in XRE(64) the value

$$V = \frac{\mu N}{T} = \frac{2 \times 256}{4} = 128$$

Once loaded, the Dirac delta can be used as one does any other function. For example, it can be transformed to the frequency domain to examine its spectrum as was done in the two plots in Figures 4.24 and 4.25.

**In the frequency domain**, in order to represent an impulse with weight  $\mu$ , we must load the single value

$$V = \frac{\mu T}{2\pi} \quad (4.72)$$

(This holds only for PULSE, since there are no Dirac deltas in the frequency domain for PERIODIC.)

Thus to load F with  $4\pi\delta(\omega - 20\pi)$  using  $T = 5$ , we would proceed as follows: Since  $\omega_0 = 2\pi/5$ , we see that  $20\pi = 50\omega_0$ , from which the spectral element-number is  $n = 50$ .

The required weight is  $4\pi$ , and so from (4.72) we see that we must place in FRE(50) the value

$$V = \frac{\mu T}{2\pi} = 4\pi \times \frac{5}{2\pi} = 10$$

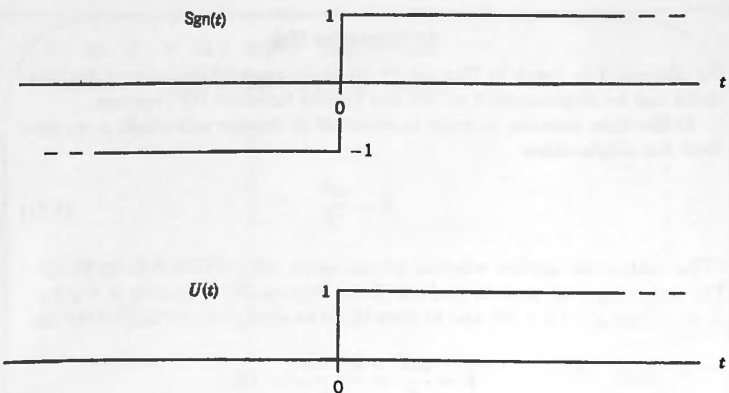
All of this is discussed in greater detail in the first two sections of Chapter 15.

## 4.7 THE UNIT STEP

---


$$f(t) = U(t)$$

This pulse was used extensively by Oliver Heaviside in the circuit-analysis investigations that he carried out, and for that reason it is often still called the Heaviside

Figure 4.26. Sgn( $t$ ) and  $U(t)$ .

function. He symbolized it simply as 1. His followers often used  $H(t)$ . We shall call it the step function, and when the step is of height 1, the unit step function, symbolizing it as  $U(t)$ . Note that by showing it as a function of  $t$  we can also create steps at points other than the origin. Thus  $3U(t - \tau)$  would be a delayed step of height 3 at  $t = \tau$ .

The unit step  $U(t)$  that we defined in (4.9) is clearly not an energy pulse, since it has infinite energy. Any attempt to find its Fourier transform by a direct application of the analysis equation will fail. We shall thus have to think of it as a generalized function, which we can do as follows.

The unit step function  $U(t)$  can be viewed as the generalized function  $\text{Sgn}(t)$  shifted up by 1 and the result then divided by 2. (See Fig. 4.26.) Thus

$$U(t) = \frac{1}{2}\text{Sgn}(t) + \frac{1}{2} \quad (4.73)$$

in which we see how  $U(t)$  has now been stated as the sum of two generalized functions. Observe that its odd part is  $\frac{1}{2}\text{Sgn}(t)$  and its even part is the eternal constant  $\frac{1}{2}$ . By (4.31) and (4.70) these two transform as follows,

$$\frac{1}{2}\text{Sgn}(t) \Leftrightarrow \frac{1}{j\omega} \quad \text{and} \quad \frac{1}{2} \Leftrightarrow \pi\delta(\omega) \quad (4.74)$$

and so (4.74) gives us the Fourier pair

$$U(t) \Leftrightarrow \frac{1}{j\omega} + \pi\delta(\omega) \quad (4.75)$$

Since  $U(t)$  is neither odd nor even we would expect it to have a complex Fourier transform. From (4.75) we see that to be the case. Its odd part has transformed into the purely imaginary and odd function  $1/j\omega$ , and its even part into the real and even function  $\pi\delta(\omega)$ . This is consistent with what we would expect from the theorems of Chapter 3.

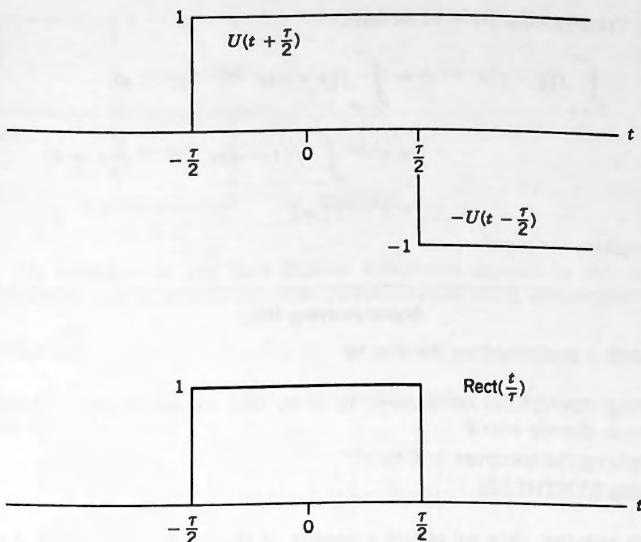


Figure 4.27. Two unit steps make a Rect pulse.

**EXAMPLE 4.4:** Using two shifted unit steps we can assemble a Rect function as shown in Figure 4.27. Thus

$$\text{Rect}\frac{t}{\tau} = U\left(t + \frac{\tau}{2}\right) - U\left(t - \frac{\tau}{2}\right) \quad (4.76)$$

Show that the Fourier transforms of the LHS and RHS of this statement are equal.

**Solution:** In order to find the Fourier transform of the RHS of (4.76) we require the following theorem, which we shall be using over and over again throughout the remainder of the text.

■ THEOREM 4.2: Time Shift

Let  $f(t) \Leftrightarrow F(\omega)$ . Then

$$f(t - \tau) \Leftrightarrow e^{-j\omega\tau}F(\omega) \quad (4.77)$$

As the name of the theorem suggests, it tells us what happens when a function  $f(t)$  undergoes a delay (time shift) and becomes  $f(t - \tau)$ —its Fourier transform becomes multiplied by  $e^{-j\omega\tau}$ .

*Proof:* Transforming  $f(t - \tau)$  we have

$$\begin{aligned} \int_{-\infty}^{\infty} f(t - \tau) e^{-j\omega t} dt &= \int_{-\infty}^{\infty} f(t - \tau) e^{-j\omega(t-\tau)} e^{-j\omega\tau} dt \\ &= e^{-j\omega\tau} \int_{-\infty}^{\infty} f(t - \tau) e^{-j\omega(t-\tau)} d(t - \tau) \\ &= e^{-j\omega\tau} F(\omega) \end{aligned}$$

which completes the proof. ■

### Accompanying Disc

Time shift is performed on the disc by

- Running ANALYSIS on a pulse in X to find its spectrum, or loading a spectrum directly into F
- Multiplying the spectrum in F by  $e^{j\omega\tau}$
- Running SYNTHESIS

If  $\tau$  was negative, then we obtain a version of the pulse that is shifted to the right, and if positive, then the shift is to the left.

To use time shift, go into the F postprocessor, where you will find the option

MULTIPLY F by  $e^{j\omega\tau}$

After that just respond to the prompts. Then exit from the postprocessor and run SYNTHESIS.

Returning to Example 4.4: Fourier transforming the LHS of (4.76) gives

$$\text{Rect} \frac{t}{\tau} \Leftrightarrow \tau \text{Sa} \frac{\omega\tau}{2}$$

and transforming the RHS using (4.75) and Theorem 4.2, gives

$$\begin{aligned} U\left(t + \frac{\tau}{2}\right) - U\left(t - \frac{\tau}{2}\right) &\Leftrightarrow \left[ \frac{1}{j\omega} + \pi\delta(\omega) \right] e^{j\omega\tau/2} - \left[ \frac{1}{j\omega} + \pi\delta(\omega) \right] e^{-j\omega\tau/2} \\ &= \frac{1}{j\omega} [e^{j\omega\tau/2} - e^{-j\omega\tau/2}] \\ &\quad + \pi\delta(\omega) [e^{j\omega\tau/2} - e^{-j\omega\tau/2}] \\ &= \tau \frac{e^{j\omega\tau/2} - e^{-j\omega\tau/2}}{2j\omega\tau/2} + \pi\delta(\omega)(1 - 1) \\ &= \tau \text{Sa}(\omega\tau/2) \end{aligned}$$

which is the same as the LHS. ■

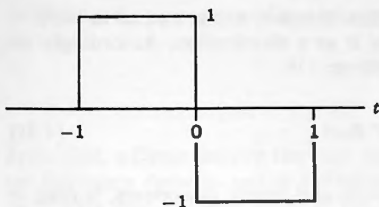


Figure 4.28.

From this example we see how Fourier transforms derived by the use of the analysis equation can be mixed with transforms obtained using distribution theory.

#### EXAMPLE 4.5:

The pulse shown in Figure 4.28 can be written either as the sum of two shifted Rect pulses as follows

$$f_1(t) = \text{Rect}\left(t + \frac{1}{2}\right) - \text{Rect}\left(t - \frac{1}{2}\right) \quad (4.78)$$

or else as the sum of three step functions as

$$f_2(t) = U(t+1) - 2U(t) + U(t-1) \quad (4.79)$$

We leave it as an exercise to show that  $f_1(t)$  and  $f_2(t)$  both transform to the same result.  $\square$

---

## 4.8 THE ETERNAL COMPLEX EXPONENTIAL

---

$$f(t) = e^{j\omega_0 t}$$

Together with the Dirac delta, the eternal complex exponential is one of the most important pulses in Fourier analysis, and we shall soon find that they both lie at the very heart of the subject. In Chapter 6 we shall see how the eternal complex exponential plays a key role in the frequency-domain analysis of linear systems such as electric circuits, and in Chapter 7 how the Dirac delta does the same thing in the time domain.

The eternal complex exponential  $e^{j\omega_0 t}$  is the only complex time-domain pulse that we consider in this text. Being complex, we would not expect the results of the theorems in Chapter 3 to hold. First we note that  $e^{j\omega_0 t}$  is not an energy pulse since its energy is infinite. Thus

$$\int_{-\infty}^{\infty} |e^{j\omega_0 t}|^2 dt = \int_{-\infty}^{\infty} 1 dt = \infty \quad (4.80)$$

This means that the square integrability criterion does not apply, and so in order to find its Fourier transform we have to think of it as a distribution. Accordingly, we redefine it by gating it with a Rect pulse as follows:

$$f(t) = \lim_{k \rightarrow \infty} e^{j\omega_0 t} \operatorname{Rect} \frac{t}{k} \quad (4.81)$$

As  $k \rightarrow \infty$  the gate pulse becomes infinitely wide and finally disappears, leaving us with  $e^{j\omega_0 t}$ . In (4.81) the sequence function is seen to be

$$f_k(t) = e^{j\omega_0 t} \operatorname{Rect} \frac{t}{k} \quad (4.82)$$

Thus, in order to find the Fourier transform of  $f(t)$  we first find the Fourier transform of  $f_k(t)$ , obtaining

$$\begin{aligned} F_k(\omega) &= \int_{-\infty}^{\infty} e^{j\omega_0 t} \operatorname{Rect} \frac{t}{k} e^{-j\omega t} dt \\ &= \int_{-k/2}^{k/2} e^{-j(\omega - \omega_0)t} dt \end{aligned} \quad (4.83)$$

Then we let  $k \rightarrow \infty$ , obtaining the transform of  $f(t)$  as

$$F(\omega) = \lim_{k \rightarrow \infty} \int_{-k/2}^{k/2} e^{-j(\omega - \omega_0)t} dt = 2\pi\delta(\omega - \omega_0) \quad (\text{by Theorem 4.1}) \quad (4.84)$$

This gives us the extremely important Fourier pair

$$e^{j\omega_0 t} \Leftrightarrow 2\pi\delta(\omega - \omega_0) \quad (4.85)$$

The Fourier transform of an eternal complex exponential whose frequency is  $\omega = \omega_0$  is thus a Dirac delta in the frequency domain of weight  $2\pi$  lying at  $\omega = \omega_0$  (see Fig. 4.29). We see that all of the energy of  $e^{j\omega_0 t}$  is thus concentrated at  $\omega = \omega_0$ . (Where else?) ■

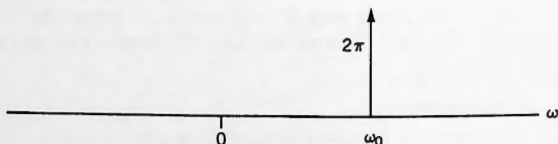


Figure 4.29. Spectrum of  $e^{j\omega_0 t}$ .

Observe the symmetry of the two statements that we have derived:

$$\delta(t - \tau) \Leftrightarrow e^{-j\omega\tau} \quad (4.86)$$

$$e^{j\omega_0 t} \Leftrightarrow 2\pi\delta(\omega - \omega_0) \quad (4.87)$$

In the first, a Dirac delta in the time domain transforms into a complex exponential in the frequency domain, and in the second a complex exponential in the time domain transforms into a Dirac delta in the frequency domain. The Dirac delta and the complex exponential are indeed closely related.

## 4.9 THE ETERNAL COSINE AND SINE FUNCTIONS

---

$$f_1(t) = \cos(\omega_0 t) \quad \text{and} \quad f_2(t) = \sin(\omega_0 t)$$

These are not energy pulses because they each contain infinite energy, and so the square integrability criterion is again not applicable. Thus to find their Fourier transforms we must treat them as generalized functions. We do this by redefining them as linear combinations of the complex exponential  $e^{j\omega_0 t}$  that we considered in the previous section. Thus

$$\cos(\omega_0 t) = \frac{1}{2}(e^{j\omega_0 t} + e^{-j\omega_0 t}) \quad (4.88)$$

Then from (4.85) we obtain the Fourier pair

$$\cos(\omega_0 t) \Leftrightarrow \pi[\delta(\omega - \omega_0) + \delta(\omega + \omega_0)] \quad (4.89)$$

This tells us that the Fourier transform of  $\cos(\omega_0 t)$  consists of two impulses on the  $\omega$ -axis (see Fig. 4.30), one at  $\omega = \omega_0$  and the second at  $\omega = -\omega_0$ , both of weight  $\pi$ . Thus half the energy of  $\cos(\omega_0 t)$  is concentrated at  $\omega = \omega_0$  and the other half at  $\omega = -\omega_0$ . Note that  $\cos(\omega_0 t)$  is real and even and we have obtained its Fourier transform as a function that is real and even.

Similarly, we redefine  $\sin(\omega_0 t)$  as a generalized function by also stating it as a linear combination of complex exponentials, obtaining

$$\sin(\omega_0 t) = \frac{e^{j\omega_0 t} - e^{-j\omega_0 t}}{2j} \quad (4.90)$$

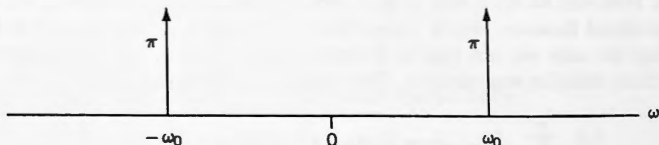
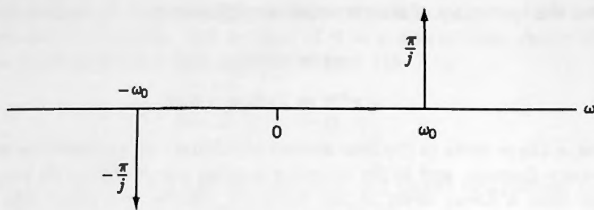


Figure 4.30. Spectrum of  $\cos(\omega_0 t)$ .

Figure 4.31. Spectrum of  $\sin(\omega_0 t)$ .

from which, again by (4.85), we obtain the Fourier pair

$$\sin(\omega_0 t) \leftrightarrow \frac{\pi}{j} [\delta(\omega - \omega_0) - \delta(\omega + \omega_0)] \quad (4.91)$$

Referring to Figure 4.31, this tells us that the Fourier transform of  $\sin(\omega_0 t)$  consists of two impulses on the  $\omega$ -axis, one at  $\omega = \omega_0$  of weight  $\pi/j$  and the second at  $\omega = -\omega_0$  of weight  $-\pi/j$ .

As with the cosine, we see that  $\sin(\omega_0 t)$  has its energy equally divided between  $\omega = \omega_0$  and  $\omega = -\omega_0$ . Note that  $\sin(\omega_0 t)$  is real and odd and we have obtained its Fourier transform as being purely imaginary and odd, as expected.

## 4.10 PERIODIC FUNCTIONS

---

$$f(t) = f_p(t)$$

Periodic functions are eternal, and so they have infinite energy when viewed as single pulses. Thus the square integrability criterion will not be applicable. To obtain their Fourier transforms we have to think of them in terms of generalized functions.

Let  $f_p(t)$  be a periodic function with period  $T_0 = 2\pi/\omega_0$  that has finite energy in any one period. Then, as we saw in Chapter 2, we are guaranteed that it can be restated as the Fourier series

$$f_p(t) = \sum_{n=-\infty}^{\infty} F_p(n) e^{jn\omega_0 t} \quad (4.92)$$

where the complex coefficients  $F_p(n)$  can be obtained from the Fourier-series analysis equation. However, (4.92) is seen to be a sum of complex exponentials, each of which is a generalized function, which means that  $f_p(t)$  is in fact a generalized function. That being the case we can find its Fourier transform by using (4.85) to transform each of those complex exponentials. The result is the Fourier pair

$$\sum_{n=-\infty}^{\infty} F_p(n) e^{jn\omega_0 t} \leftrightarrow 2\pi \sum_{n=-\infty}^{\infty} F_p(n) \delta(\omega - n\omega_0) \quad (4.93)$$

which shows that the transform of a periodic function  $f_p(t)$  with complex coefficients  $F_p(n)$  is

$$F(\omega) = 2\pi \sum_{n=-\infty}^{\infty} F_p(n) \delta(\omega - n\omega_0) \quad (4.94)$$

This is seen to be an infinite train of frequency-domain impulses separated by equal spacing  $\omega_0$ , where the weight of the impulse at  $n\omega_0$  is equal to  $2\pi F_p(n)$ .

We know that a periodic function is made up of a sum of the harmonics of the function, each of frequency  $n\omega_0$ , and in (4.94) we see that each of the impulses constitutes an energy concentration on the  $\omega$ -axis at  $\omega = n\omega_0$ . Thus a periodic function is seen to have its energy concentrated at the discrete values of  $\omega$  that correspond to the frequencies of each of the harmonics in its Fourier series.

We summarize the preceding as follows:

**Rule:** To find the Fourier transform of a periodic function:

- (a) First find its complex Fourier series
- (b) Then transform each of the complex exponentials in that series using (4.85)

□**EXAMPLE 4.7:** Find the Fourier transform of the periodic function  $f_p(t)$  of Example 2.1.

**Solution:** We follow the rule just given.

- (a) Starting from the given analytical specification for  $f_p(t)$ , we obtain the coefficients for its Fourier series as [see (2.35)]

$$F_p(n) = \frac{1}{2} \text{Sa} \frac{n\pi}{2} \quad (4.95)$$

We display numerical values of these coefficients in Table 4.1. Using (4.95) we can now assemble the Fourier series for  $f_p(t)$ :

$$f_p(t) = \frac{1}{2} \sum_{n=-\infty}^{\infty} \text{Sa} \frac{n\pi}{2} e^{jn\omega_0 t} \quad (4.96)$$

TABLE 4.1 Coefficients of Fourier Series

$n$	0	$\pm 1$	$\pm 2$	$\pm 3$	$\pm 4$	$\pm 5$	...
$F_p(n)$	$\frac{1}{2}$	$1/\pi$	0	$-1/3\pi$	0	$1/5\pi$	...

TABLE 4.2 Weights of Impulses in Fourier Transform

$\omega$	0	$\pm\omega_0$	$\pm 2\omega_0$	$\pm 3\omega_0$	$\pm 4\omega_0$	$\pm 5\omega_0$	...
$W(n)$	$\pi$	2	0	$-\frac{2}{3}$	0	$\frac{2}{5}$	...

(b) We now find the Fourier transform of this Fourier series as follows: Equation (4.96) is a sum of complex exponentials, and so its Fourier transform can be found simply by transforming each of those complex exponentials. Equation (4.85) enables us to do that, giving us the Fourier transform of  $f_p(t)$  as

$$F(\omega) = \frac{1}{2} \sum_{n=-\infty}^{\infty} \text{Sa} \frac{n\pi}{2} 2\pi \delta(\omega - n\omega_0) \quad (4.97)$$

□

Let's take a closer look at what we obtained in the example. From (4.97) we see that  $F(\omega)$  is a train of Dirac deltas on the  $\omega$ -axis with spacing  $\omega_0 = 2\pi/T_0$ . The weight of the  $n$ th impulse is  $2\pi F_p(n)$ , and so the weights and their locations on the  $\omega$ -axis are as shown in Table 4.2.

In Figure 4.32 we show a plot of  $F(\omega)$ . Observe that we have used arrows on the lines because they are all Dirac deltas. The plot shows us that a periodic function has its energy concentrated at discrete points on the  $\omega$ -axis located at integral multiples of the fundamental frequency  $\omega_0$ . These are the energy concentrations associated with its dc term and each of its harmonics, with the relative amount of energy in each concentration being proportional to the magnitude of the respective harmonic, or, equivalently, to the weight of the respective Dirac delta.

The two representations of a periodic function discussed in this section, its Fourier series and its Fourier transform, are fully equivalent, but there are occasions when the one format is to be preferred over the other.

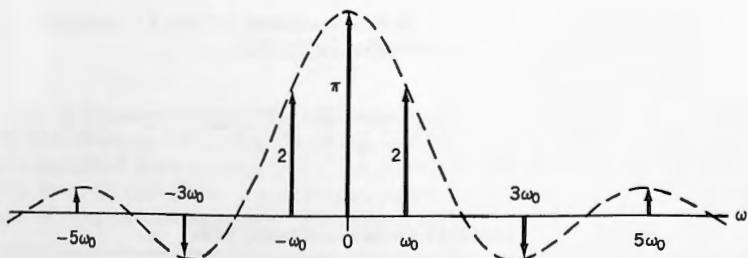


Figure 4.32. Fourier transform of a periodic waveform.

### Accompanying Disk

The FFT system on the disk displays Fourier spectra in six different ways:

- (1) **Complex Fourier series coefficients** for periodic functions as discussed in Chapter 2
- (2) **Real Fourier series coefficients** for periodic functions as discussed in Chapter 2
- (3) **Fourier transforms of single pulses** as discussed in Chapter 3
- (4) **Fourier transforms of periodic functions** as discussed in the present section<sup>†</sup>
- (5) Fourier series coefficients derived from discrete periodic functions
- (6) Fourier transforms derived from discrete pulse functions

Item (4): The system displays the **weights** of the Dirac deltas in the plots as well as in the numerical displays.

Items (5) and (6) are discussed further in Parts 2 and 3 of the text.

---

## 4.11 THE PERIODIC IMPULSE TRAIN

---

$$f(t) = \delta_T(t)$$

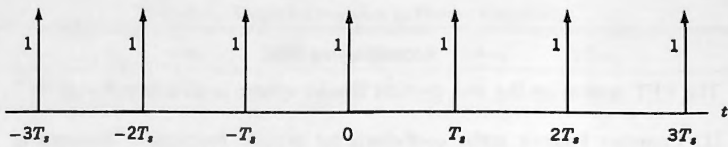
One extremely important periodic function is the infinite train of unit impulses spaced  $T_s$  seconds apart, shown in Figure 4.33. We call this a **periodic impulse train** and use the symbol  $\delta_T(t)$ . We also refer to it as a **Dirac comb**. Clearly,  $\delta_T(t)$  is a periodic function that has infinite energy in any one period, and so we are not guaranteed that it even has a Fourier series representation, let alone a Fourier transform. As we now show, however, in the sense of distributions it has both.

Since none of the impulses overlaps any other,  $\delta_T(t)$  is simply the union of the individual impulses. The  $k$ th one is  $\delta(t - kT_s)$ , and so the entire train can be written as

$$\delta_T(t) = \sum_{k=-\infty}^{\infty} \delta(t - kT_s) \quad (4.98)$$

We observe that  $\delta_T(t)$  is a periodic function with period  $T_s$ . To find its Fourier transform we must first find its Fourier series. Applying the Fourier series analysis

<sup>†</sup>To get the FFT system to display in this mode see Chapter 16.

Figure 4.33.  $\delta_T(t)$ .

equation gives us

$$\begin{aligned} F_p(n) &= \frac{1}{T_0} \int_{-T_0/2}^{T_0/2} \delta_T(t) e^{-jn\omega_0 t} dt \quad (\omega_0 = 2\pi/T_0) \\ &= \frac{1}{T_s} \int_{-T_s/2}^{T_s/2} \delta(t) e^{-jn\omega_s t} dt \end{aligned} \quad (4.99)$$

Observe that we have replaced  $T_0$  by  $T_s$ , because the latter is the period of our function. We have also replaced  $\omega_0$  by  $\omega_s$  defined by  $\omega_s \equiv 2\pi/T_s$ . By the sampling property the integrand becomes  $\delta(t)e^{jn\omega_s t}$ , and so (4.99) continues as

$$\dots = \frac{1}{T_s} \int_{-T_s/2}^{T_s/2} \delta(t) dt = \frac{1}{T_s} \quad (4.100)$$

Thus the coefficients for the series exist. We note that they are all equal, namely

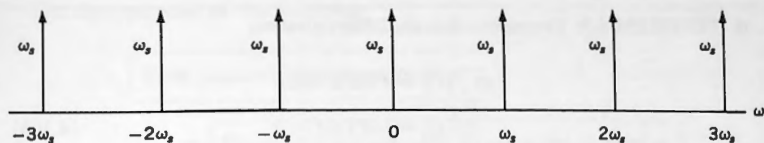
$$F_p(n) = \frac{1}{T_s} \quad (\forall n) \quad (4.101)$$

We now assemble the Fourier series using the synthesis equation, obtaining

$$\begin{aligned} \delta_T(t) &= \sum_{n=-\infty}^{\infty} F_p(n) e^{jn\omega_0 t} \\ &= \frac{1}{T_s} \sum_{n=-\infty}^{\infty} e^{jn\omega_s t} \end{aligned} \quad (4.102)$$

and it can be shown that the series in (4.102) converges correctly to  $\delta_T(t)$  (in the sense of distributions). Since our objective was to find the Fourier transform of  $\delta_T(t)$ , we must now make use of (4.85) to transform (4.102). We obtain

$$\begin{aligned} F(\omega) &= \frac{2\pi}{T_s} \sum_{n=-\infty}^{\infty} \delta(\omega - n\omega_s) \\ &= \omega_s \sum_{n=-\infty}^{\infty} \delta(\omega - n\omega_s) \end{aligned} \quad (4.103)$$

Figure 4.34. Fourier transform of  $\delta_T(t)$ .

This is seen to be the train of equally spaced impulses shown in Figure 4.34. Here the impulses are on the  $\omega$ -axis spaced  $\omega_s$  apart, all with weights  $\omega_s$ . Thus  $\delta_T(t)$  and its Fourier transform are both Dirac combs, one in the time domain and the other in the frequency domain. By analogy with (4.98) we now give the impulse train shown in (4.103) the following name:

$$\delta_\Omega(\omega) \equiv \omega_s \sum_{n=-\infty}^{\infty} \delta(\omega - n\omega_s) \quad (4.104)$$

and so we have obtained the Fourier pair

$$\delta_T(t) \leftrightarrow \delta_\Omega(\omega) \quad (4.105)$$

The impulse train  $\delta_T(t)$  and its Fourier transform  $\delta_\Omega(\omega)$  play a key role in the mathematical analysis of systems in which signals are transmitted and received in sampled form. We make extensive use of them in Chapter 9, where we discuss what are known as the sampling theorems. We also use them in Part II, where we examine the discrete Fourier transform (which leads to the FFT) and its relationships to the Fourier transforms and Fourier series that we are now familiar with.

## EXERCISES

---

**4.1** (a) Find the total energy in

$$f_1(t) = te^{-\beta t}U(t) \quad (\beta > 0) \quad (4.106)$$

What can you say about its transform?

- (b) Find the Fourier transform of  $f_1(t)$  using the analysis equation.
- (c) Now start from the analysis equation

$$F(\omega) = \int_{-\infty}^{\infty} f(t)e^{-j\omega t} dt \quad (4.107)$$

and prove the result shown as Theorem 4.3 below.

**■ THEOREM 4.3: Frequency-domain Differentiation**

Let  $f(t) \Leftrightarrow F(\omega)$ . Then

$$if(t) \Leftrightarrow j\omega F(\omega) \quad (4.108)$$

*Hint:* Differentiate both sides of (4.107).

The theorem tells us the following:

Time domain: multiplication by $t$	$\Leftrightarrow$	Frequency domain: $j \times$ differentiation wrt $\omega$
------------------------------------	-------------------	---

- (d) Use Theorem 4.3 to find the Fourier transform of the function  $f_1(t)$  in (4.106).
- (e) Generalize (4.108) to obtain the following corollary.

**■ COROLLARY to Theorem 4.3**

$$t^n f(t) \Leftrightarrow (j)^n \frac{d^n}{d\omega^n} F(\omega) \quad (4.109)$$

- (f) Use the corollary to find the transform of

$$f_2(t) = t^2 e^{-\beta t} U(t)$$

- (g) Verify that for the transforms of  $f_1(t)$  and  $f_2(t)$ , just given,  $A(\omega)$  and  $|F(\omega)|$  are even and  $B(\omega)$  and  $\Theta(\omega)$  are odd.
- (h) Find the expressions for the energy spectra of  $f_1(t)$  and  $f_2(t)$ .

**4.2** Sketch  $f_1(t)$  of Exercise 4.1 and then sketch its even and odd parts, stating their Fourier transforms.

**4.3** (a) Using the analysis equation, prove the result shown as Theorem 4.4.

**■ THEOREM 4.4: Frequency Shift**

Let  $f(t) \Leftrightarrow F(\omega)$ . Then

$$e^{j\omega_0 t} f(t) \Leftrightarrow F(\omega - \omega_0) \quad (4.110)$$

The theorem tells us the following:

Time domain: multiplication by  $e^{j\omega_0 t}$

$\Leftrightarrow$  Frequency domain: shift  $F(\omega)$  to the right by  $\omega_0$

This result is also called the **modulation property** (we shall see why in Chapter 7) and sometimes **Heaviside's shifting theorem**. Note that it is the dual to Theorem 4.2 (called the time-shift property), in which

$$f(t - \tau) \Leftrightarrow e^{-j\omega\tau}F(\omega) \quad (4.111)$$

In (4.111) the sign of  $\tau$  is the same on both sides, whereas in (4.110) the sign of  $\omega_0$  is reversed from one side to the other.

#### Accompanying Disc

Frequency shift is performed on the system by

- Loading a pulse into **X**
- Multiplying it by  $e^{j\omega_0 t}$
- Running ANALYSIS

If  $\omega_0$  was positive, then we obtain a spectrum that is shifted to the right, and if negative, then the shift is to the left.

To use frequency shift, go into the **X** postprocessor where you will find the option

MULTIPLY X by  $e^{j\omega_0 t}$

After that just respond to the prompts. Then exit from the postprocessor and run ANALYSIS.

In Figure 4.35 we show a shifted Sa function produced on the system as follows:  $\text{Rect}(2t)$  was loaded into **X**. Using the **X** postprocessor, this was then multiplied by  $e^{j\omega_0 t}$ , with  $\omega_0 = 32\pi$ . Then we ran ANALYSIS. Observe that the Sa has been moved to the right by precisely  $32\pi$  radians.

(b) For each of the functions

$$f_1(t) = e^{-\beta t} \cos(\omega_0 t)U(t) \quad (\beta > 0)$$

and

$$f_2(t) = e^{-\beta t} \sin(\omega_0 t)U(t) \quad (\beta > 0)$$

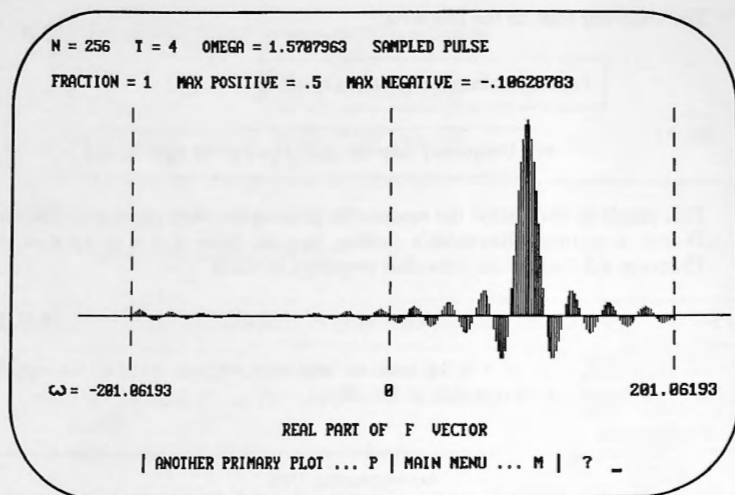


Figure 4.35. Shifted Sa produced by frequency shift.

show that their energy content satisfies  $E < 1/2\beta$ , and hence infer that they are both energy pulses. We can therefore expect them to have Fourier transforms.

(c) Starting from

$$e^{-\beta t} U(t) \Leftrightarrow \frac{1}{\beta + j\omega} \quad (\beta > 0)$$

plus Theorem 4.4, verify the following two results:

$$e^{-\beta t} \cos(\omega_0 t) U(t) \Leftrightarrow \frac{j\omega + \beta}{(j\omega + \beta)^2 + \omega_0^2} \quad (4.112)$$

$$e^{-\beta t} \sin(\omega_0 t) U(t) \Leftrightarrow \frac{\omega_0}{(j\omega + \beta)^2 + \omega_0^2} \quad (4.113)$$

*Hint:* Express  $\cos(\omega_0 t)$  and  $\sin(\omega_0 t)$  as complex exponentials.

(d) Using the results of part (c), find the inverse of

$$F(\omega) = \frac{8j\omega + 4}{(j\omega)^2 + 4j\omega + 20} \quad (4.114)$$

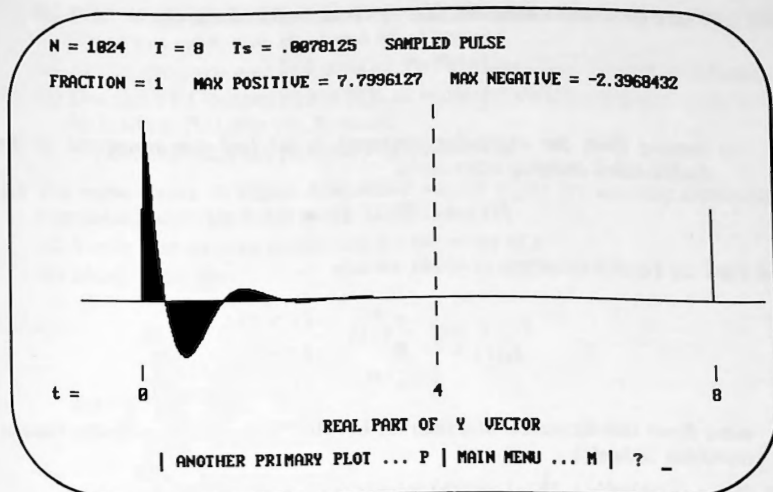


Figure 4.36. Inverse of (4.114).

(e) Show that for (d), the real and imaginary parts are

$$A(\omega) = \frac{28\omega^2 + 80}{\omega^4 - 24\omega^2 + 400} \quad \text{and} \quad B(\omega) = \frac{-8\omega^3 + 144\omega}{\omega^4 - 24\omega^2 + 400}$$

- (f) Invert the expression in (d) using the FFT system as follows: Start from main menu A. Use  $N = 1024$ , SAMPLED,  $T = 8$ , PULSE, Continue, CREATE  $H(j\omega)$ , 1, 2, 4, 8, 20, 4, 1. Then LOAD using an alias level of 20. Then use the swopping package in the F postprocessor (main menu G, then F) to move the spectrum that you have created from the F2 vector to the F vector. Then invert using SYNTHESIS. Then plot the Y vector. What you see is the inverse of (4.114). (See Fig. 4.36.)
- (g) Take numerical samples from your result in (d) and compare them to the values for Y obtained in (f) in order to verify the result that you obtained in (d).

- 4.4 The pulse shown in Figure 4.28 can be written either as the sum of two shifted Rect pulses as follows

$$f_1(t) = \text{Rect}(t + \frac{1}{2}) - \text{Rect}(t - \frac{1}{2})$$

or else as the sum of three step functions as

$$f_2(t) = U(t + 1) - 2U(t) + U(t - 1)$$

Show that  $f_1(t)$  and  $f_2(t)$  both transform to the same result.

4.5 (a) Using the analysis equation, find the Fourier transform of

$$f_k(t) = \begin{cases} e^{-\beta|t|} & (|t| < k/2) \\ 0 & (|t| > k/2) \end{cases} \quad (\beta > 0)$$

(b) Starting from the expression obtained in (a) find the transform of the double-sided decaying exponential

$$f(t) = e^{-\beta|t|} \quad (-\infty < t < \infty)$$

4.6 Find the Fourier transform of (4.28), namely

$$f_k(t) = \begin{cases} e^{-kt} & (t > 0) \\ 0 & (t = 0) \\ -e^{+kt} & (t < 0) \end{cases}$$

using direct transformation and then let  $k \rightarrow 0^+$ , thereby obtaining the Fourier transform of  $\text{Sgn}(t)$ .

4.7 Sketch (a)  $\text{Rect}[(t - k)/\tau]$  and (b)  $\text{Rect}[(t/\tau) - k]$ .

*Hint:* Sketch  $\text{Rect}(t/\tau)$  for  $\tau = 2$ . Then sketch (a) and (b) for  $\tau = 2$  and  $k = 3$ .

(c) Now use the time-shift property of Theorem 4.2 to verify the following two results:

$$\text{Rect}[(t - k)/\tau] \Leftrightarrow \tau \text{Sa}(\omega\tau/2)e^{-j\omega k}$$

$$\text{Rect}[(t/\tau) - k] \Leftrightarrow \tau \text{Sa}(\omega\tau/2)e^{-j\omega k\tau}$$

4.8 (a) Make use of the time-shift property (Theorem 4.2) to find the Fourier transform of  $f(t)$  in Figure 4.37.

*Hint:*

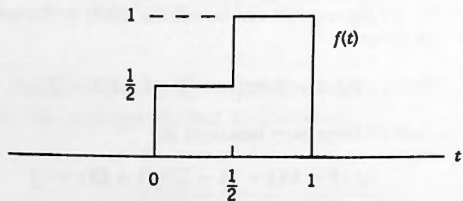


Figure 4.37.

- (b) Find  $A(\omega)$ ,  $B(\omega)$ ,  $|F(\omega)|$ , and  $\Theta(\omega)$  for this pulse, and verify that  $A(\omega)$  and  $|F(\omega)|$  are even, and  $B(\omega)$  and  $\Theta(\omega)$  are odd.  
 (c) Sketch the even and odd parts of  $f(t)$  and state their Fourier transforms.  
 (d) Use the FFT system on the disk to verify the sketches that you made in (c) by loading  $f(t)$  into the X vector.

*Hint:* ANALYSIS plus the F postprocessor.

- 4.9 The pulse shown in Figure 4.38, which we call  $\Lambda_k(t)$ , is a specially constructed triangular pulse that leads to the Dirac delta.

- (a) Verify that its area equals one for all values of  $k$ .  
 (b) Hence infer that

$$f(t) = \lim_{k \rightarrow 0^+} \Lambda_k(t)$$

satisfies

$$f(t) = 0 \quad (t \neq 0), \quad \text{and} \quad \int_{-\infty}^{\infty} f(t) dt = 1$$

Since this is the definition of  $\delta(t)$ , we can conclude that  $\Lambda_k(t)$  is a sequence function for  $\delta(t)$ .

- (c) Find the Fourier transform of  $\Lambda_k(t)$  for  $k$  constant, and then show that as  $k \rightarrow 0^+$  it tends to 1. Thus in the limit, this pulse has the same form as  $\delta(t)$  in both the time and frequency domains.

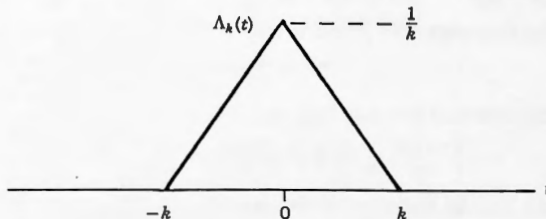


Figure 4.38.

- 4.10 Use the sampling property of the Dirac delta to simplify the following expressions:

- (a)  $e^{-2t}\delta(t)$       (b)  $\frac{1}{2}e^{-3t}[\delta(t+1) + \delta(t-1)]$   
 (c)  $\sin(t)\delta(t - \pi/2)$     (d)  $\cos(\omega/2)\delta(\omega - \pi)$   
 (e)  $e^{j\omega}\delta(\omega - n\pi)$    (f)  $j\omega[\delta(\omega - 1) - \delta(\omega + 1)]$

**4.11** Evaluate the following integrals:

- (a)  $\int_{-\infty}^{\infty} \sin(\pi t) \delta(t - 1/2) dt$       (b)  $\int_{-\infty}^{\infty} \cos(\pi t) \delta(t - 1/2) dt$   
 (c)  $\int_{-\infty}^{\infty} \cos(\omega/2) \delta(\omega - \pi/2) d\omega$       (d)  $\int_{-\infty}^{\infty} \omega \cos(\omega/2) \delta(\omega - \pi/2) d\omega$   
 (e)  $\int_{-\infty}^{\infty} \cos(2\omega) \delta(\omega - n\pi/2) e^{j\omega t} d\omega$

**4.12** Find the Fourier transforms of:

- (a)  $\delta(t - 1)$       (b)  $3\delta(t + 2)$   
 (c)  $\delta(t + 1) + 2\delta(t) + \delta(t - 1)$       (d)  $e^{j\omega_0 t} - 2 + e^{-j\omega_0 t}$   
 (e)  $\cos^2(\omega_0 t)$       (f)  $\sin^2(\omega_0 t)$

(g) Use the results of (e) and (f) to find the Fourier transform of the eternal constant 1.

**4.13** Use the frequency-shift property (Theorem 4.4) to find the transforms of:

- (a)  $\cos^2(\omega_0 t)$       (b)  $\sin^2(\omega_0 t)$       (c)  $\sin(\omega_0 t)\cos(\omega_0 t)$   
 (d) Show that your result for (c) is consistent with (4.91).

**4.14** Find the inverse of each of the following by direct use of the synthesis equation. Then transform your result using either frequency shift or time shift to obtain the original expression.

- (a)  $\delta(\omega + 2)$       (b)  $\delta(\omega - 3)$   
 (c)  $\delta(\omega + 1) - 2\delta(\omega) + \delta(\omega - 1)$   
 (d)  $\sin(\omega)$       (e)  $\cos(2\omega)$   
 (f)  $\sin^2(3\omega)$       (g)  $\cos^3(4\omega)$

**4.15** Use the synthesis equation to find the inverse Fourier transform of:

- (a)  $2\pi\delta(\omega)$       (c)  $\pi[\delta(\omega - \omega_0) + \delta(\omega + \omega_0)]$   
 (b)  $2\pi\delta(\omega - \omega_0)$       (d)  $\frac{\pi}{j}[\delta(\omega - \omega_0) - \delta(\omega + \omega_0)]$

**4.16** (a) Use the frequency-shift property plus  $1 \Leftrightarrow 2\pi\delta(\omega)$  to prove that

$$e^{j\omega_0 t} \Leftrightarrow 2\pi\delta(\omega - \omega_0)$$

(b) Use the time-shift property plus  $\delta(t) \Leftrightarrow 1$  to prove that

$$\delta(t - \tau) \Leftrightarrow e^{-j\omega\tau}$$

**4.17** (a) Find the Fourier transform of the periodic function shown in Figure 4.39.  
 (b) Use the FFT system on the disk to verify the result that you obtained in (a).

*Hint:* Main-menu I, then F, ETERNAL.

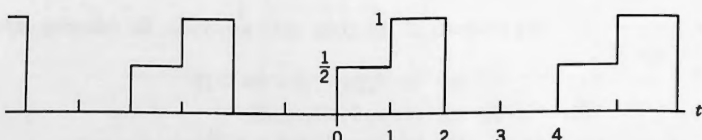


Figure 4.39.

4.18 (a) Sketch the following waveform and find its Fourier transform.

$$f_p(t) = \begin{cases} t & (0 < t < 1) \\ 0 & (1 < t < 4) \end{cases} \quad f_p(t+4) = f_p(t)$$

(b) What are the energies in the spectrum for  $-5 \leq n \leq 5$  as a fraction of the energy at  $n = 0$ ?

(c) Use the FFT system to verify your results. ( $N = 1024$ ,  $T = 4$ , PERIODIC)

4.19 Find the total area under the function  $\text{Sa}^2(x)$  using Parseval's theorem and compare your result to Exercise 3.10(e).

*Hint:* Start from  $\text{Rect}(t/\tau)$ .

4.20 (a) Verify that the definition of the shifted Dirac comb shown in Figure 4.40 is

$$f_{TS}(t) = \sum_{n=-\infty}^{\infty} \delta(t - nT_s - T_s/2)$$

(b) Using the method for finding the Fourier transform of  $\delta_T(t)$  in Section 4.11, verify that for this train of impulses the transform pair is as follows:

$$\delta_{TS}(t) \Leftrightarrow \delta_{NS}(\omega) = \omega_s \sum_{n=-\infty}^{\infty} (-1)^n \delta(\omega - n\omega_s)$$

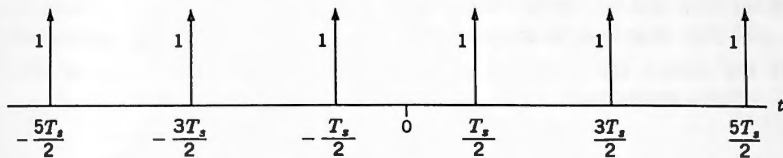


Figure 4.40. Shifted Dirac comb  $\delta_{TS}(t)$ .

4.21 Prove that

$$\delta_T(t) = \frac{1}{T_s} \left[ 1 + 2 \sum_{n=1}^{\infty} \cos \frac{n2\pi t}{T_s} \right]$$

where  $\delta_T(t)$  is defined in (4.98), and where  $T_s$  is the spacing between the impulses.

4.22 How would the following time-domain Dirac deltas be represented on the FFT system? (See (4.71).)

- (a)  $2\delta(t)$ , using  $N = 100$  and  $T = 5$ .
- (b)  $3\delta(t - 2)$ , using  $N = 256$  and  $T = 4$ .
- (c)  $5\delta(t + 1)$ , using  $N = 240$  and  $T = 12$ .

In each case load the impulse and then plot its magnitude and phase spectrum, first by hand and then by using the ANALYSIS transformation of the system, and reconcile them. (Start from main-menu A.)

- 4.23** How would the following frequency-domain Dirac deltas be represented on the system? (See (4.72).)

- $6\pi\delta(\omega)$ , using  $N = 100$  and  $T = 5$ .
- $4\pi\delta(\omega - 12\pi)$ , using  $N = 256$  and  $T = 4$ .
- $(1 + 2j)\delta(\omega + 4\pi)$ , using  $N = 250$  and  $T = 12$ .

In each case state what the inverse Fourier transform should be. Then load the impulse and use SYNTHESIS to verify what you stated. (Start from main-menu A.)

- 4.24** Use the FFT system to obtain the Fourier transforms of:

- The eternal constant: 4.
- The eternal cosine:  $\cos(\omega_0 t)$ , where  $\omega_0 = 2\pi \times 4$ .
- The eternal sine:  $\sin(\omega_0 t)$ , where  $\omega_0 = 2\pi \times 3$ .

For all three problems, use  $N = 240$  and  $T = 5$ . Prove that the frequency-domain Dirac deltas in the plots have the correct heights and are in the correct locations. (See (4.72).)

- 4.25** Use the FFT system to find the Fourier coefficients for the following two periodic impulse trains

$$(a) \delta_T(t) = \sum_{n=-\infty}^{\infty} \delta(t - nT_s) \quad (b) \delta_{TS}(t) = \sum_{n=-\infty}^{\infty} \delta(t - nT_s - T_s/2)$$

Use  $N = 256$  and  $T = 2$ , and verify the correctness of the FFT coefficients.

- 4.26** (a) Show that the energy contained in a Dirac delta of weight  $c$  is infinite.

(b) Now show that the energy per unit bandwidth is equal to  $c^2$  joules/hertz.

- 4.27** The analysis and synthesis equations of Chapter 2 are based on the set of complex exponentials

$$S_1 = \{e^{jn\omega_0 t} | n \in I\}$$

which was shown to satisfy the orthogonality property

$$\frac{1}{T_0} \int_{-T_0/2}^{T_0/2} e^{jn\omega_0 t} e^{jm\omega_0 t^*} dt = \begin{cases} 0 & \text{if } n \neq m \\ 1 & \text{if } n = m \end{cases} \quad (4.115)$$

Prove the following result for the set of complex exponentials that forms the basis for the Fourier integral of Chapter 3.

■ **THEOREM 4.5** The set of complex exponentials

$$S_2 = \{e^{j\omega t} | \omega \in \mathbb{R}\} \quad (4.116)$$

satisfies the orthogonality property

$$\int_{-\infty}^{\infty} e^{j\omega_1 t} e^{j\omega_2 t^*} dt = 2\pi\delta(\omega_2 - \omega_1) \quad (4.117)$$

*Hint:* Let  $\omega_2$  be the general frequency variable  $\omega$ .

# The Method of Successive Differentiation

## 5.1 THE DIFFERENTIATION PROPERTY

---

The Fourier transform is of such great value in engineering largely because of Theorem 5.1 below, and we shall soon see some of the remarkable places to which it leads us. We now examine one of its consequences—the fact that it enables us to find most Fourier transforms **without the use of the analysis equation**. In Chapter 9 we shall extend that capability to Fourier series as well.

Before examining Theorem 5.1 we must first define what is called the  $D$  operator, a form of mathematical shorthand.

**Definition:** The  $D$  operator means differentiation with respect to (wrt) time, that is

$$D \equiv \frac{d}{dt} \quad (5.1)$$

Using the  $D$  operator we can make the following statements:

$$Dx(t) = \frac{d}{dt}x(t) = x'(t) \quad (5.2)$$

$$D^2x(t) = \frac{d}{dt} \frac{d}{dt}x(t) = x''(t) \quad (5.3)$$

and so on. Now let's take a look at the theorem itself.

---

**■ THEOREM 5.1: Time-domain differentiation**

If  $f(t) \Leftrightarrow F(\omega)$ , then

$$Df(t) \Leftrightarrow j\omega F(\omega) \quad (5.4)$$

The theorem tells us the following:

Time domain: differentiation wrt $t$	↔ Frequency domain: multiplication by $j\omega$
--------------------------------------	---

Compare this to Theorem 4.3, which is its dual.

*Proof:* By the synthesis equation,

$$f(t) = \frac{1}{2\pi} \int_{-\infty}^{\infty} F(\omega) e^{j\omega t} d\omega \quad (5.5)$$

Differentiating both sides wrt  $t$  gives

$$\begin{aligned} Df(t) &= \frac{1}{2\pi} \int_{-\infty}^{\infty} F(\omega) [j\omega e^{j\omega t}] d\omega \\ &= \frac{1}{2\pi} \int_{-\infty}^{\infty} [j\omega F(\omega)] e^{j\omega t} d\omega \end{aligned} \quad (5.6)$$

which means that

$$Df(t) \Leftrightarrow j\omega F(\omega) \quad (5.7)$$

and so the proof is complete. ■

The theorem also works for repeated differentiation, as the following corollary shows.

### ■ COROLLARY 1

$$D^n f(t) \Leftrightarrow (j\omega)^n F(\omega) \quad (5.8)$$

*Proof:* Differentiating both sides of (5.5)  $n$  times, we obtain

$$D^n f(t) = \frac{1}{2\pi} \int_{-\infty}^{\infty} (j\omega)^n F(\omega) e^{j\omega t} d\omega \quad (5.9)$$

which is the same as

$$D^n f(t) \Leftrightarrow (j\omega)^n F(\omega) \quad (5.10)$$

■

■ EXAMPLE 5.1: Use Theorem 5.1 to find the Fourier transform of

$$f(t) = ax''(t) + bx'(t) + cx(t) \quad (5.11)$$

**Solution:** The expression on the RHS of (5.11) can be written more compactly using the  $D$ -operator as

$$f(t) = aD^2x(t) + bDx(t) + cx(t) \quad (5.12)$$

which we then rearrange as follows:

$$f(t) = [aD^2 + bD + c]x(t) \quad (5.13)$$

The operator is now seen to be formally a second-degree polynomial in  $D$ , which we shall call  $P(D)$ , that is,

$$P(D) = aD^2 + bD + c \quad (5.14)$$

Then (5.13) becomes

$$f(t) = P(D)x(t) \quad (5.15)$$

Fourier transforming (5.13) by making use of Theorem 5.1 gives

$$F(\omega) = [a(j\omega)^2 + bj\omega + c]X(\omega) = P(j\omega)X(\omega) \quad (5.16)$$

in which the quantity that we have called  $P(j\omega)$  is simply the polynomial  $P(D)$ , with  $D$  now replaced by  $j\omega$ . □

We summarize this result as a second corollary to Theorem 5.1.

### ■ COROLLARY 2

Let  $P(D)$  be any polynomial in  $D$ . Then

$$P(D)x(t) \Leftrightarrow P(j\omega)X(\omega) \quad (5.17)$$

## 5.2 DIFFERENTIATING FUNCTIONS WITH DISCONTINUITIES

In first-year calculus we learn how to differentiate simple functions, but it is always stressed that they should be what is called “sufficiently smooth” for successful differentiation to take place at a given point. If the function has a step discontinuity at a point, we are invariably told that differentiation there is impossible. As we shall now see, that is not entirely correct.

The problem arises simply because we have no way to represent the derivative of a step if we restrict ourselves to ordinary functions. If we permit the use of generalized functions, however, then the problem disappears. We now show that differentiation precisely at a step discontinuity is not only possible but also often highly desirable.

The following sequence of examples demonstrates much of this process. Please follow it patiently until its conclusion because it contains a great deal of very useful material.

**□EXAMPLE 5.2:** Find the derivative of the unit step  $U(t)$ .

**Solution:** We start by examining the integral of the unit impulse, and we find that

$$\int_{-\infty}^t \delta(\tau) d\tau = \begin{cases} 0 & (t < 0) \\ 1 & (t > 0) \end{cases} \quad (5.18)$$

Referring to Figure 5.1, what (5.18) tells us is that if we are trying to find the area under a unit impulse from  $-\infty$  to  $t$ , then

- If  $t$  lies to the left of the impulse, the area is zero (true)
- If  $t$  lies to the right of the impulse, then the area is 1 (also true)

The RHS of (5.18), however, is precisely the definition of  $U(t)$  and so we can restate it as

$$\int_{-\infty}^t \delta(\tau) d\tau = U(t) \quad (\forall t) \quad (5.19)$$

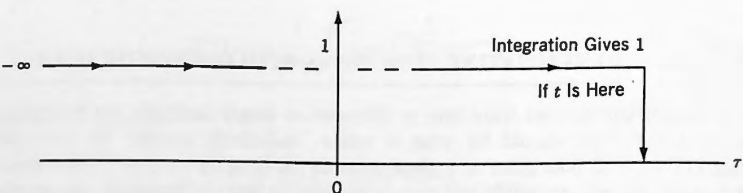
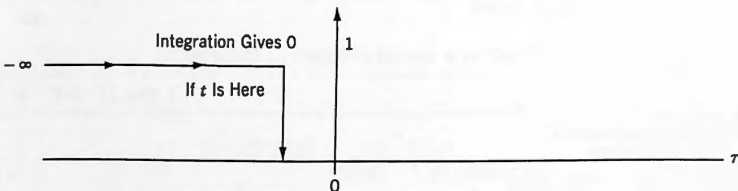
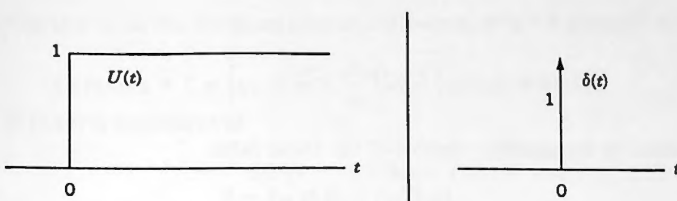


Figure 5.1. Integration of  $\delta(t)$ .

Figure 5.2.  $U(t)$  and its derivative  $\delta(t)$ .

That being the case, by differentiating both sides of (5.19) we see that the following must also be true:

$$DU(t) = \delta(t) \quad (\forall t) \quad (5.20)$$

□

Thus the derivative of  $U(t)$  that we were asked to find is a Dirac delta. Observe that (5.20) includes all values of  $t$ .

Equations (5.19) and (5.20) are thus two further important properties of the Dirac delta, and they show its relationship to the unit step. They are depicted graphically in Figure 5.2.

*Historical Note:* Oliver Heaviside came within a micron of deriving (5.20) and with it the unit impulse, as we see from the following (Nahin, 1987):

But the outstanding feature of Heaviside's creative imagination was the calm assurance with which he differentiated the step function to give the impulse function which is zero if  $t > 0$  or  $t < 0$ , and infinite if  $t = 0$ .

Heaviside himself wrote:

$DU(t)$  means a function of  $t$  which is wholly concentrated at the moment  $t = 0$ , of total amount 1. It is an impulsive function, so to speak.... The function  $DU(t)$  involves only ordinary ideas of differentiation and integration pushed to their limit.

It is also worth noting that Paul Dirac, who in fact did derive (5.20), did his undergraduate work in electrical engineering and was both familiar with all of Heaviside's work and a great admirer of his.

Now let's examine how (5.20) can also be obtained by the use of Theorem 5.1.

■ EXAMPLE 5.3: Differentiate  $U(t)$  using Theorem 5.1.

**Solution:** By (4.75)

$$U(t) \Leftrightarrow \frac{1}{j\omega} + \pi \delta(\omega) \quad (5.21)$$

and so Theorem 5.1 gives

$$DU(t) \Leftrightarrow j\omega F(\omega) = j\omega \left[ \frac{1}{j\omega} + \pi \delta(\omega) \right] = 1 + \pi j\omega \delta(\omega) \quad (5.22)$$

However, by the sampling property of the Dirac delta

$$j\omega \delta(\omega) = j0 \delta(\omega) = 0 \quad (5.23)$$

and so (5.22) ends up as

$$DU(t) \Leftrightarrow 1 \quad (5.24)$$

which is equivalent to

$$DU(t) = \delta(t) \quad (5.25)$$

□

Thus Theorem 5.1 has differentiated the unit step for all values of  $t$  and in so doing it has verified that the result is a unit impulse.

We now extend all of the preceding to step discontinuities that are not at the origin.

□**EXAMPLE 5.4:** Use the time-shift property plus Theorem 5.1 to show that

$$DU(t - \tau) = \delta(t - \tau) \quad (5.26)$$

**Solution:** By the time-shift property, the delayed unit step  $U(t - \tau)$  transforms as follows:

$$\begin{aligned} U(t - \tau) &\Leftrightarrow e^{-j\omega\tau} F(\omega) = e^{-j\omega\tau} \left[ \frac{1}{j\omega} + \pi \delta(\omega) \right] \\ &= \frac{e^{-j\omega\tau}}{j\omega} + \pi e^{-j\omega\tau} \delta(\omega) \end{aligned} \quad (5.27)$$

in which sampling takes place, and so we continue as

$$\dots = \frac{e^{-j\omega\tau}}{j\omega} + \pi \delta(\omega) \quad (5.28)$$

Then by Theorem 5.1,

$$\begin{aligned} DU(t - \tau) &\Leftrightarrow j\omega F(\omega) = j\omega \left[ \frac{e^{-j\omega\tau}}{j\omega} + \pi \delta(\omega) \right] \\ &= e^{-j\omega\tau} + \pi j\omega \delta(\omega) = e^{-j\omega\tau} \end{aligned} \quad (5.29)$$

(the final step from the sampling property). However,

$$e^{-j\omega\tau} \Leftrightarrow \delta(t - \tau) \quad (5.30)$$

and so (5.29) is equivalent to

$$DU(t - \tau) = \delta(t - \tau) \quad (5.31)$$

□

We see that wherever a function has a step of height  $h$  its derivative will have a Dirac delta of weight  $h$ .

Theorem 5.1 is thus seen to be a powerful tool for finding the derivatives of functions and their associated Fourier transforms, and as we have seen, it does its differentiating for all values of  $t$ , including points where discontinuities might be present.

Now that we have seen what Theorem 5.1 can do for us we can even manage without it at times, relying instead directly on (5.20).

□**EXAMPLE 5.5:** Without using Theorem 5.1, find the derivatives of

- (1)  $\cos(t)U(t)$
- (2)  $\sin(t)U(t)$

**Solution:** The first expression has a discontinuity at  $t = 0$ , and the second is everywhere continuous. Thus we can expect to obtain a derivative with a Dirac delta at the origin for the first and no Dirac delta anywhere for the second.

(1)  $\cos(t)U(t)$  is shown in Figure 5.3a. Using the product rule for differentiation,

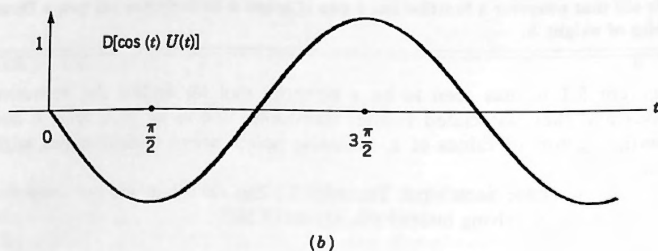
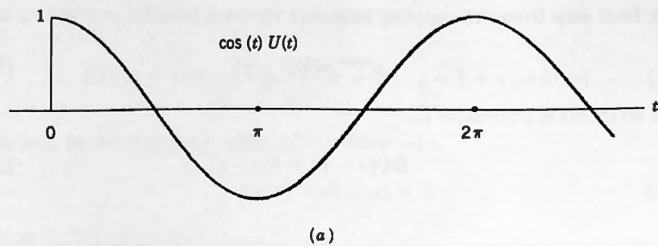
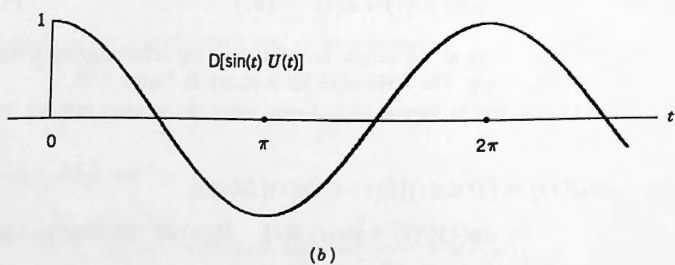
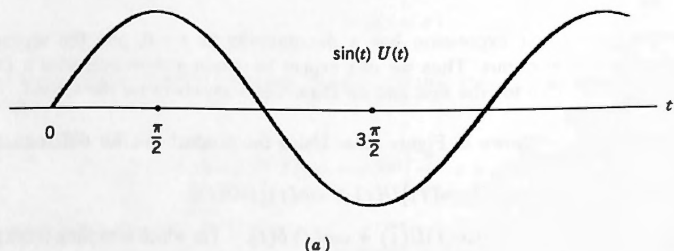
$$\begin{aligned} D[\cos(t)U(t)] &= [D\cos(t)]U(t) + \cos(t)[DU(t)] \\ &= -\sin(t)U(t) + \cos(t)\delta(t) \quad (\text{in which sampling takes place}) \\ &= -\sin(t)U(t) + \delta(t) \quad (\forall t) \end{aligned} \quad (5.32)$$

Note the Dirac delta at the origin, brought about by differentiating a step of height 1 at the origin. The RHS of (5.32) is shown in Figure 5.3b.

(2)  $\sin(t)U(t)$  is plotted in Figure 5.4a. Again, using the product rule for differentiation,

$$\begin{aligned} D[\sin(t)U(t)] &= [D\sin(t)]U(t) + \sin(t)[DU(t)] \\ &= \cos(t)U(t) + \sin(t)\delta(t) \quad (\text{in which sampling takes place}) \\ &= \cos(t)U(t) \quad (\forall t) \end{aligned} \quad (5.33)$$

Observe that this time there is no Dirac delta since there was no discontinuity. □

Figure 5.3.  $\cos(t)U(t)$  and its derivative.Figure 5.4.  $\sin(t)U(t)$  and its derivative.

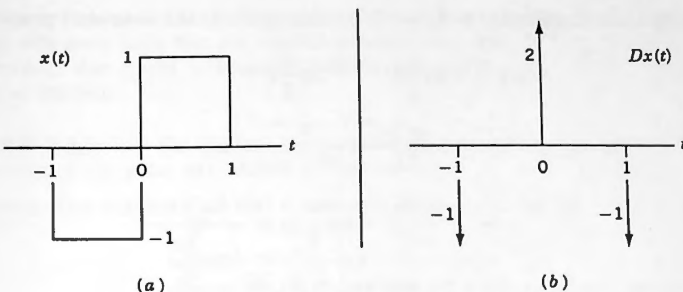


Figure 5.5. A discontinuous function and its derivative.

Henceforth, whenever we differentiate a function in which step discontinuities are present, we shall always go about it in the manner demonstrated in the preceding example. In Figure 5.5 we show a pulse  $x(t)$  with three step discontinuities and we also show its derivative. Because  $x(t)$  has a negative-going unit step at  $t = -1$  we see that the derivative has a Dirac delta of weight  $-1$  at that location. Similarly, the other two discontinuities in  $x(t)$  will produce their Dirac deltas in the derivative as shown.

Since Figure 5.5b is the derivative of Figure 5.5a, it follows by Theorem 5.1 that the Fourier transform of Figure 5.5b must be equal to  $j\omega$  times the Fourier transform of Figure 5.5a. We now verify that.

#### EXAMPLE 5.6

- (1) Find the Fourier transform of the pulse shown in Figure 5.5b.
- (2) Derive the Fourier transform of the pulse shown in Figure 5.5a, multiply it by  $j\omega$ , and verify that the result is the same as that obtained in (1).

**Solution:** For (1) we start from Figure 5.5b, which we call  $g(t)$ . Thus

$$g(t) = -\delta(t + 1) + 2\delta(t) - \delta(t - 1) \quad (5.34)$$

Then, by the time-shift property,

$$G(\omega) = -e^{j\omega} + 2 - e^{-j\omega} \quad (5.35)$$

For (2) we could obtain  $X(\omega)$  by direct application of the analysis equation. As we see from Figure 5.5a, however,  $x(t)$  is made up of two shifted Rect pulses. Thus,

$$x(t) = -\text{Rect}\left(t + \frac{1}{2}\right) + \text{Rect}\left(t - \frac{1}{2}\right) \quad (5.36)$$

and we know that  $\text{Rect}(t) \Leftrightarrow \text{Sa}(\omega/2)$ . Hence, again by the time-shift property

$$\begin{aligned} X(\omega) &= -\text{Sa}\frac{\omega}{2}e^{j\omega/2} + \text{Sa}\frac{\omega}{2}e^{-j\omega/2} \\ &= -\text{Sa}\frac{\omega}{2}\left[\frac{e^{j\omega/2} - e^{-j\omega/2}}{2j}\right]2j \\ &= \frac{-\sin(\omega/2)}{\omega/2}\sin\frac{\omega}{2}2j = \frac{4\sin^2(\omega/2)}{j\omega} \end{aligned} \quad (5.37)$$

Multiplying this by  $j\omega$  as we are required to do, we obtain

$$j\omega X(\omega) = 4\sin^2\frac{\omega}{2} \quad (5.38)$$

We leave it to the reader to verify that this is the same result as (5.35).  $\square$

The derivation of the Fourier transforms of Figure 5.5a and b has provided us with a demonstration of the validity of Theorem 5.1. We now show how we can use the theorem to find the Fourier transforms of many pulses without ever using integration. (In Chapter 9 we extend it to finding the Fourier coefficients of periodic functions as well.)

### 5.3 THE METHOD OF SUCCESSIVE DIFFERENTIATION

---

Returning to Figure 5.5a, we now Fourier transform the pulse  $x(t)$  by starting from its derivative in Figure 5.5b. The latter was

$$Dx(t) = -\delta(t+1) + 2\delta(t) - \delta(t-1) \quad (5.39)$$

from which, using Theorem 5.1 on the left and time shift on the right:

$$j\omega X(\omega) = -e^{j\omega t} + 2 - e^{-j\omega t} \quad (5.40)$$

Division by  $j\omega$  then gives

$$X(\omega) = \frac{-e^{j\omega t} + 2 - e^{-j\omega t}}{j\omega} \quad (5.41)$$

and so we have obtained the Fourier transform of the original pulse essentially by inspection, and completely without the use of integration.  $\blacksquare$

We call this procedure the **method of successive differentiation**. It will always work when the pulse whose Fourier transform we are seeking is made up of sections that are polynomials in  $t$ , like constants, straight lines, and quadratics. It will also work for many others that are not of this form, and we examine a few such cases later in the chapter.

We now present three worked examples of the method of successive differentiation together with some rules that are needed to carry it out. After that we draw attention to a problem that could arise under certain circumstances and show how it can quickly be resolved.

**EXAMPLE 5.7:** Use the method of successive differentiation to derive the Fourier transform of the pulse  $x(t)$  shown in Figure 5.6a.

**Solution:** The derivative of  $x(t)$  is shown in Figure 5.6b, where we see that

$$Dx(t) = \delta(t) + \delta(t - 1) - 2\delta(t - 2) \quad (5.42)$$

Using Theorem 5.1 on the left and time shift on the right we obtain

$$j\omega X(\omega) = 1 + e^{-j\omega} - 2e^{-j2\omega} \quad (5.43)$$

and so

$$X(\omega) = \frac{1}{j\omega} [1 + e^{-j\omega} - 2e^{-j2\omega}] \quad (5.44)$$

□

Compare the amount of work done here to what you would have had to do if you derived the transform of  $x(t)$  using the analysis equation.

**EXAMPLE 5.8:** We may have to differentiate twice in order to apply the method of successive differentiation, as happens when we try to find the Fourier transform of the triangular pulse  $x(t)$  shown in Figure 5.7a. Differentiating once gives us the pulse shown in Figure 5.7b, which we cannot use yet, so we differentiate a second time, obtaining the three Dirac deltas shown in Figure 5.8. From this figure we see

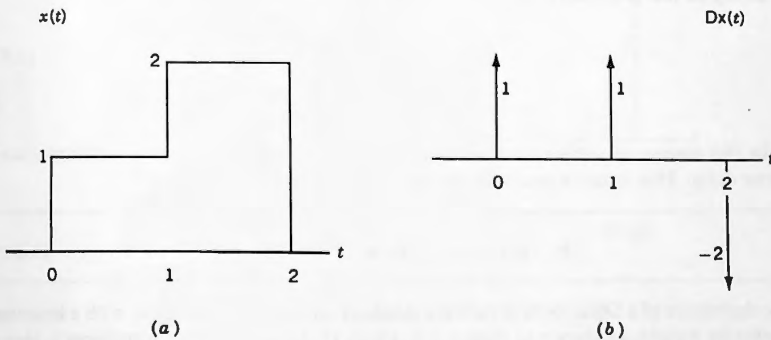
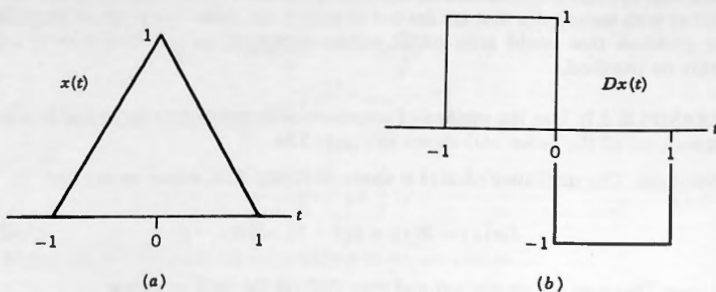
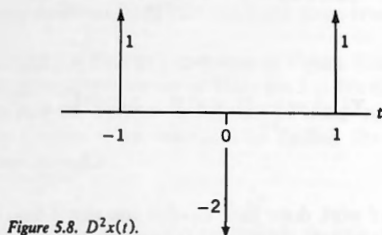


Figure 5.6.  $x(t)$  and its derivative.

Figure 5.7.  $x(t)$  and its derivative.Figure 5.8.  $D^2x(t)$ .

that

$$D^2x(t) = \delta(t+1) - 2\delta(t) + \delta(t-1) \quad (5.45)$$

and so (Theorem 5.1 on the left and time shift on the right)

$$(j\omega)^2 X(\omega) = e^{j\omega} - 2 + e^{-j\omega} \quad (5.46)$$

giving us the required Fourier transform as

$$X(\omega) = \frac{e^{j\omega} - 2 + e^{-j\omega}}{(j\omega)^2} \quad (5.47)$$

□

In the course of differentiating more than once we may have to differentiate a Dirac delta. This is not a problem because, by Theorem 5.1:

If $\delta(t) \Leftrightarrow 1$ then $D\delta(t) \Leftrightarrow j\omega$	(5.48)
--	--------

The derivative of a Dirac delta is called a **doublet**, and we symbolize it with a lowercase  $d$ , plus its weight, as shown in Figure 5.9. From (5.48) its Fourier transform is seen to be  $j\omega$ . (For further discussion regarding the doublet, see Exercises 5.3 and 5.5.)

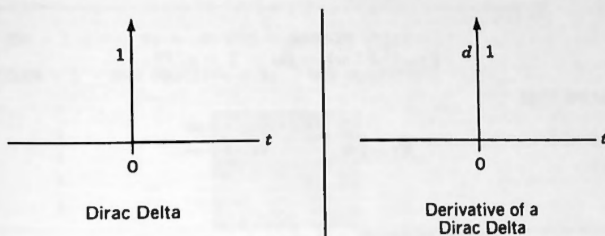
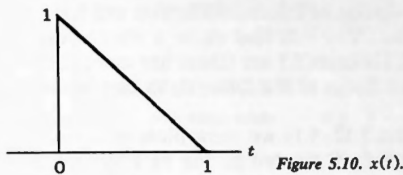


Figure 5.9.

Figure 5.10.  $x(t)$ .

**EXAMPLE 5.9:** Find the Fourier transform of the pulse in Figure 5.10.

**Solution:** Differentiating once we obtain the pulse shown in Figure 5.11a, where we see a Dirac delta and a Rect pulse. We then differentiate a second time, obtaining a doublet and two Dirac deltas as shown in Figure 5.11b. From that figure:

$$D^2x(t) = D\delta(t) - \delta(t) + \delta(t - 1) \quad (5.49)$$

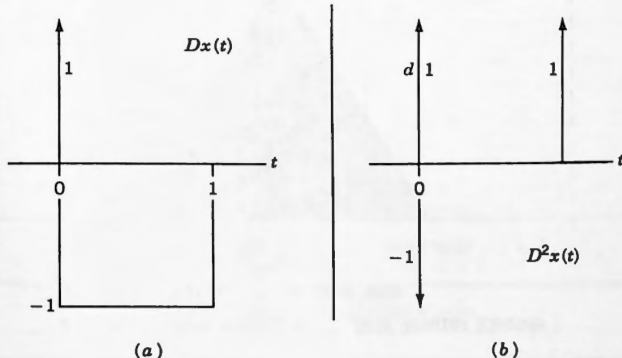


Figure 5.11.

and so

$$(j\omega)^2 X(\omega) = j\omega - 1 + e^{-j\omega} \quad (5.50)$$

which means that

$$X(\omega) = \frac{j\omega - 1 + e^{-j\omega}}{(j\omega)^2} \quad (5.51)$$

□

### Accompanying Disk

The fast Fourier transform (FFT) system on the accompanying disk implements a discrete version of Theorem 5.1. You will have to read Chapter 15 to see how that is done. You will find there a simple explanation of what the discrete versions of Theorem 5.1 are (there are more than one), as well as how all of the essential attributes of the Dirac delta can be implemented for use on the FFT system.

In Figures 5.12–5.14 we show plots of a triangular pulse, its first derivative, and its second, all created by the FFT system using the methods discussed in Chapter 15. Observe that the first and third Dirac deltas in Figure 5.14 have values of  $V = 64$ . Since  $T = 4$  and  $N = 256$ , that means [see (4.71)] that their weights are  $\mu = V \times T/N = 1$ . The middle Dirac delta has value  $V = -128$ , and so its weight is  $\mu = -128 \times T/N = -2$ , all exactly as required.

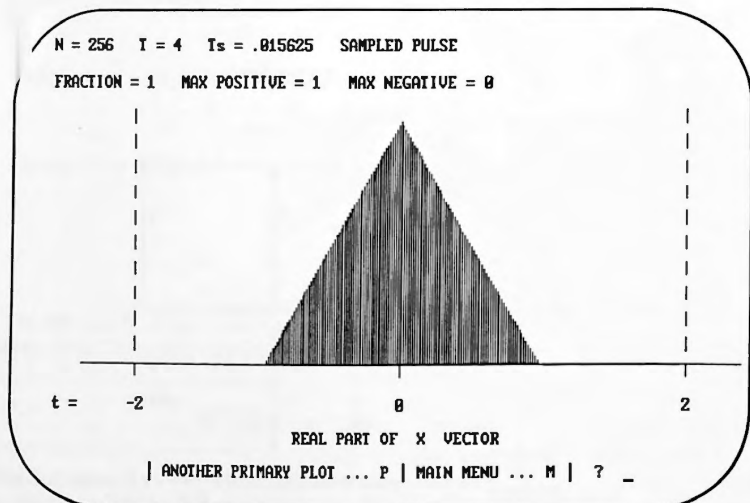


Figure 5.12. Triangular pulse.

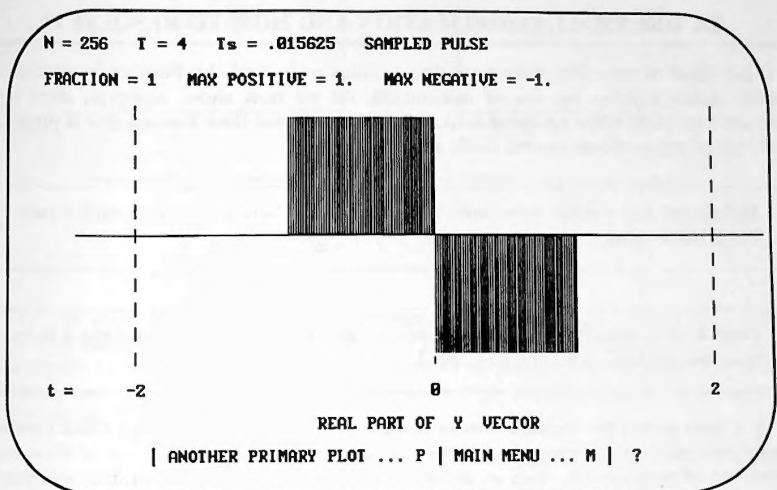


Figure 5.13. First derivative of pulse.

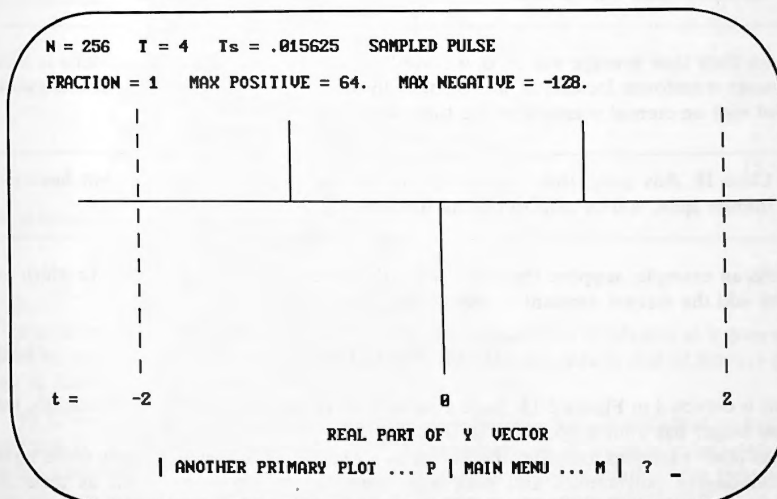


Figure 5.14. Second derivative of pulse.

## 5.4 ONE SMALL COMPLICATION AND HOW TO RESOLVE IT

The method of successive differentiation enables us to find the Fourier transforms of many pulses without the use of integration. As we now show, however, there is a possible problem when applying it to pulses that are **not time limited**, but if properly addressed the problem can be easily resolved.

**Definition:** Let a pulse have finite time duration. Then we say that such a pulse has a **finite span**.

**Class I:** Any pulse that is made up only of polynomial sections and has a **finite span** will be said to belong to Class I.

For such pulses the method always works successfully. Examples of Class I pulses were presented in the preceding section where we saw that every one of them was made up of polynomials, such as constants, straight lines and quadratics, and every one of them had finite time duration, that is, they all had finite spans.

**It thus follows that the average value of all of those pulses is zero, when considered over the entire  $t$ -axis,  $-\infty < t < \infty$ .**

Since their time average was zero, we would not expect to find a Dirac delta in their Fourier transforms located at  $\omega = 0$ , namely  $\delta(\omega)$ , since such an impulse is associated with an eternal constant in the time domain.

**Class II:** Any pulse that is made up only of polynomial sections, but has an **infinite span**, will be said to belong to Class II.

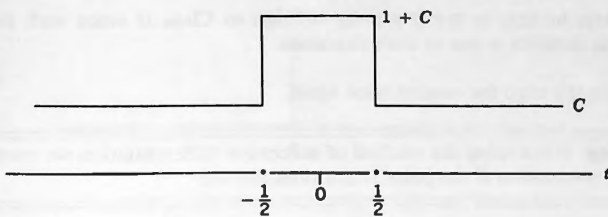
As an example, suppose that we start with the Class I pulse  $\text{Rect}(t)$ , to which we then add the eternal constant  $C$ . We obtain the pulse

$$f(t) = \text{Rect}(t) + C \quad (5.52)$$

This is depicted in Figure 5.15. Such a pulse is also made up only of polynomials, but it no longer has a finite span and so it is now in Class II.

As other examples, consider the pulses  $\text{Sgn}(t)$  and  $U(t)$ . Both are only made up of zeroth-degree polynomials and both have infinite spans. Pulses such as these all belong to Class II.

**The average of a Class II pulse over the entire real line may be nonzero.**

Figure 5.15.  $\text{Rect}(t) + C$ .

For the pulse in Figure 5.15 the average is equal to  $C$  and so the Dirac delta  $2\pi C\delta(\omega)$  must be present in its Fourier transform, because that is the transform of the eternal constant  $C$ . If we apply the method of successive differentiation to this pulse, however, then the constant  $C$  becomes nulled out after the first time that we differentiate. Thus

$$Df(t) = D[\text{Rect}(t) + C] = D \text{Rect}(t) \quad (5.53)$$

in which we note that  $C$  has now disappeared. We then continue as follows:

$$\cdots = \delta(t + \frac{1}{2}) - \delta(t - \frac{1}{2}) \quad (5.54)$$

Transforming we obtain

$$\begin{aligned} j\omega F(\omega) &= e^{j\omega/2} - e^{-j\omega/2} \\ &= \frac{e^{j\omega/2} - e^{-j\omega/2}}{2j(\omega/2)} j\omega \\ &= j\omega \text{Sa} \frac{\omega}{2} \end{aligned} \quad (5.55)$$

from which we conclude that

$$F(\omega) = \text{Sa} \frac{\omega}{2} \quad (5.56)$$

The constant  $C$  in the analytical definition was annihilated in (5.53) and so it does not show up in (5.56). The Fourier transform that we have obtained is that of  $\text{Rect}(t)$  and not of  $\text{Rect}(t) + C$ .

*To fix the problem:* When a pulse is seen from its time-domain definition to belong to Class II, we must add back the Fourier transform of its **average value over the entire  $t$ -axis** after completing the method of successive differentiation. For this pulse the average value over  $-\infty < t < \infty$  was  $C$ , and so we must add  $2\pi C\delta(\omega)$  to the result obtained in (5.56), giving us the correct answer

$$F(\omega) = \text{Sa} \frac{\omega}{2} + 2\pi C\delta(\omega) \quad (5.57)$$

It will always be easy to see if a pulse belongs to Class II since such pulses have infinite time duration in one or both directions. ■

We stress the need for caution once again.

**Warning:** When using the method of successive differentiation we must take special precautions if the pulse is not time limited.

□**EXAMPLE 5.10:** Use the method of successive differentiation to find the Fourier transforms of

$$(a) \quad f(t) = \text{Sgn}(t) \quad (5.58)$$

$$(b) \quad f(t) = U(t) \quad (5.59)$$

Neither of these pulses has finite time duration, and so they are both Class II pulses.

(a) From Figure 5.16 we see that

$$D \text{Sgn}(t) = 2\delta(t) \quad (5.60)$$

and so

$$j\omega F(\omega) = 2 \quad (5.61)$$

from which

$$F(\omega) = \frac{2}{j\omega} \quad (5.62)$$

From the figure we also see that the average value of  $\text{Sgn}(t)$  over the entire  $t$ -axis is zero, and so we do not need to add a Dirac delta at  $\omega = 0$  to (5.62). It is in fact the correct answer.

(b) We have seen earlier that

$$DU(t) = \delta(t) \quad (5.63)$$

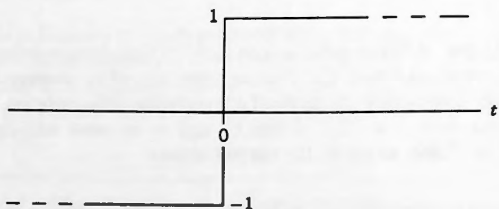
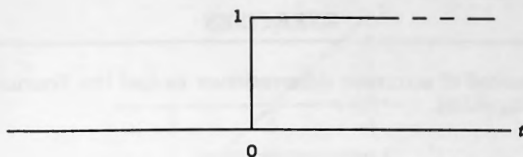


Figure 5.16.  $\text{Sgn}(t)$ .

Figure 5.17.  $U(t)$ .

and so

$$j\omega F(\omega) = 1 \quad (5.64)$$

from which

$$F(\omega) = \frac{1}{j\omega} \quad (5.65)$$

We now note from Figure 5.17, however, that the average value of  $U(t)$  over the entire  $t$ -axis is  $\frac{1}{2}$ , and so we must add the Fourier transform of such an eternal constant to (5.65). Since  $\frac{1}{2} \Leftrightarrow \pi\delta(\omega)$  the final answer becomes

$$U(t) \Leftrightarrow \frac{1}{j\omega} + \pi\delta(\omega) \quad (5.66)$$

which we know to be correct. □

## 5.5 NONPOLYNOMIAL SECTIONS

There are many pulses that are made up of sections that are not polynomials. Examples are the decaying exponential

$$f(t) = e^{-\beta t}U(t) \quad (5.67)$$

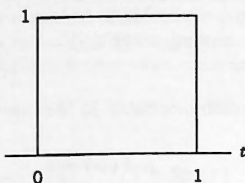
and the gated cosine pulse

$$f(t) = \cos(\pi t) \operatorname{Rect}(t) \quad (5.68)$$

The method of successive differentiation will work successfully even for these and for many other such pulses. Of course, the same precautions must be taken if the pulse is not time limited, in which case we must add a frequency-domain Dirac delta to the result of successive differentiation, whose weight is equal to  $2\pi$  times the average of the pulse over the entire  $t$ -axis. Pulses such as these are considered in Exercises 5.7 through 5.10.

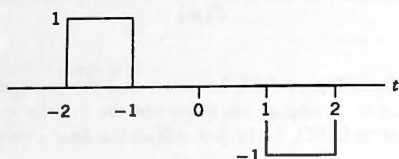
**EXERCISES**

- 5.1 Use the method of successive differentiation to find the Fourier transforms of the following pulses.



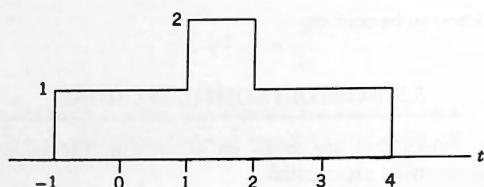
(a)

Figure 5.18.



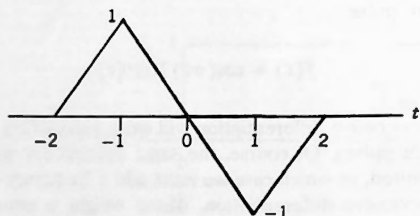
(b)

Figure 5.19.



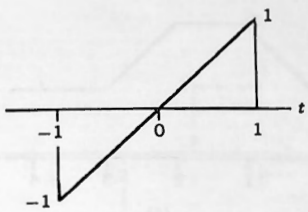
(c)

Figure 5.20.



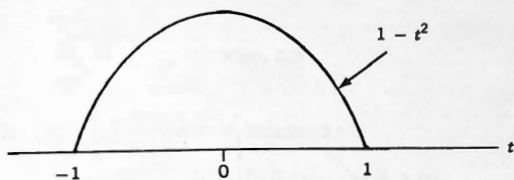
(d)

Figure 5.21.



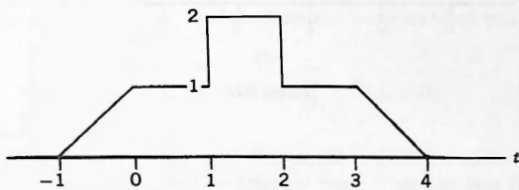
(e)

Figure 5.22.



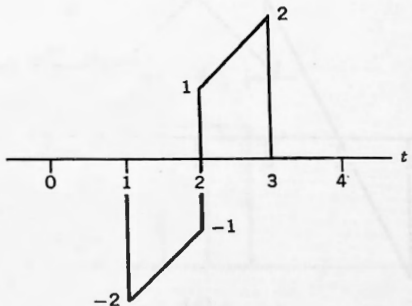
(f)

Figure 5.23.



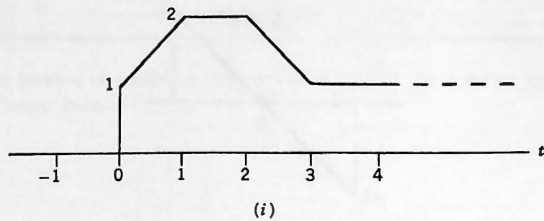
(g)

Figure 5.24.



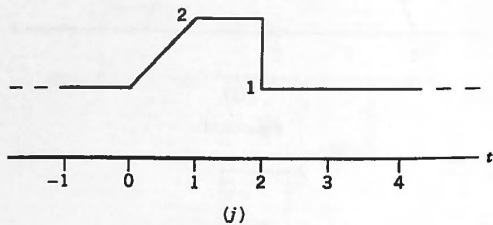
(h)

Figure 5.25.



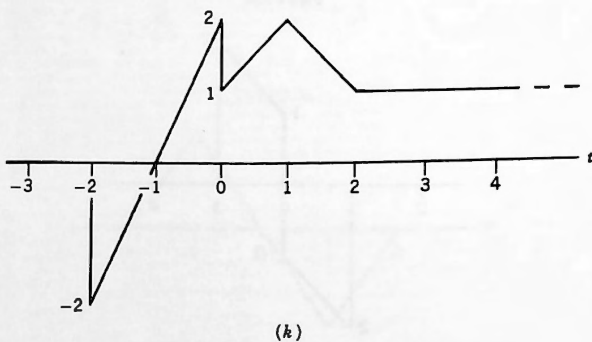
(i)

Figure 5.26.



(j)

Figure 5.27.



(k)

Figure 5.28.

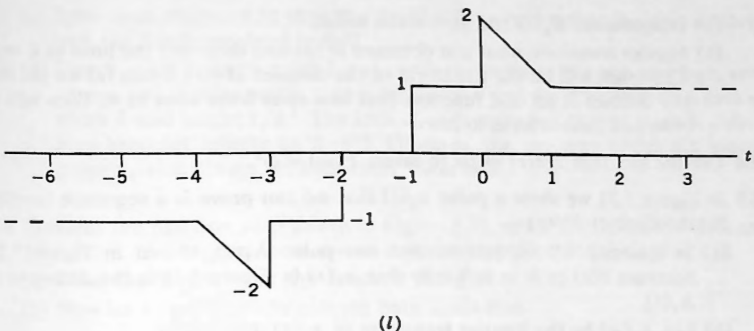


Figure 5.29.

5.2 (a) Find the Fourier transform in two ways of

$$D[e^{-\beta t}U(t)] \quad (\beta > 0)$$

(1) By direct transformation plus Theorem 5.1.

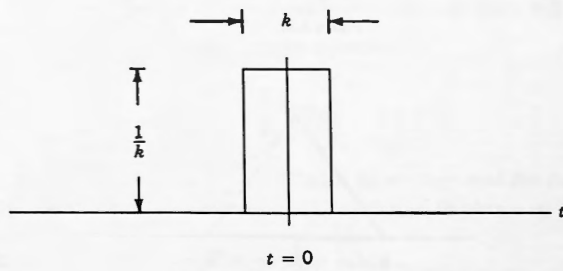
(2) By first differentiating  $e^{-\beta t}U(t)$  and then Fourier transforming the resulting expression. It should be the same as what you obtained in (1).

(b) Repeat for

$$D[te^{-\beta t}U(t)] \quad (\beta > 0)$$

5.3 To find the Fourier transform of the doublet  $D\delta(t)$ , which we introduced in Example 5.9, we can proceed as follows: Start from the Box function  $B_k(t)$  in Figure 5.30, which we know satisfies

$$\lim_{k \rightarrow 0} B_k(t) = \delta(t)$$

Figure 5.30. Box function  $B_k(t)$ .

- (a) Differentiate  $B_k(t)$  and sketch the result.  
 (b) Fourier transform what you obtained in (a) and then find the limit as  $k \rightarrow 0$ .  
 The result will be the transform of the doublet  $D\delta(t)$ . From (a) we see that the doublet is an odd function that first rises from zero to  $\infty$ , then falls to  $-\infty$ , and then returns to zero.

**5.4** Use the fact that  $D\delta(t) \leftrightarrow j\omega$  to invert  $F(\omega) = \omega^2$ .

**5.5** In Figure 5.31 we show a pulse  $x_k(t)$  that we can prove is a sequence function for the doublet  $D\delta(t)$

- (a) In Exercise 4.9 we proved that the pulse  $\Lambda_k(t)$ , shown in Figure 5.32, becomes  $\delta(t)$  as  $k \rightarrow 0$ . Verify that  $x_k(t)$  in Figure 5.31 is the derivative of  $\Lambda_k(t)$ .  
 (b) Let  $X_k(\omega)$  be the Fourier transform of  $x_k(t)$ . Prove that

$$\lim_{k \rightarrow 0} X_k(\omega) = j\omega$$

Since  $j\omega$  is the Fourier transform of the doublet, we have proved that  $x_k(t)$  in Figure 5.31 satisfies

$$\lim_{k \rightarrow 0} x_k(t) = D\delta(t)$$

and so  $x_k(t)$  is a sequence function for the doublet. This tells us that the doublet first rises to  $\infty$ , then falls to  $-\infty$ , and then returns to zero. Its net area is zero.

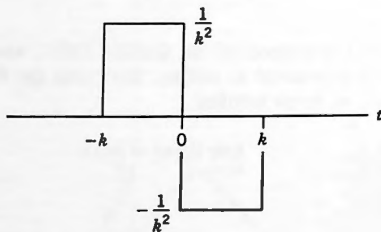


Figure 5.31.  $x_k(t)$ .

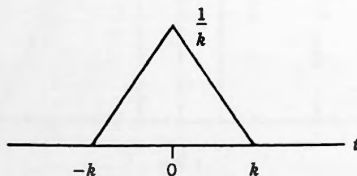


Figure 5.32.  $\Lambda_k(t)$ .

- (c) Infer from Figure 5.31 that the doublet is an odd pulse. Is this consistent with the result obtained in (b)?
- (d) Sketch  $x_k(t)$  for very small  $k$  and verify that it looks like two very high, very narrow rectangular pulses, one going positive and the other negative, each of width  $k$  and height  $1/k^2$ . The area of each pulse is  $1/k$ , and so each pulse's area becomes infinite as  $k \rightarrow 0$ . However, the net area under the overall pulse  $x_k(t)$  is always zero for every value of  $k$ .
- 5.6** Consider the function  $\mu(t)$  shown in Figure 5.33, which is zero for  $t < -k/2$  and 1 for  $t > k/2$ . Between those points it is a straight line whose slope is  $1/k$ .
- Form the derivative of this function and plot it.
  - Now let  $k \rightarrow 0$ , thereby proving once again that

$$DU(t) = \delta(t)$$

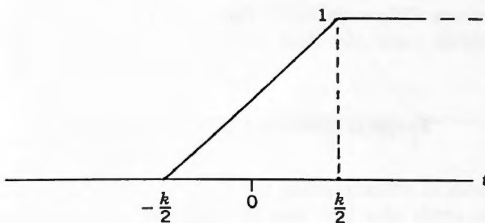


Figure 5.33.  $\mu(t)$ .

### Successive Differentiation Applied to Pulses Containing Nonpolynomial Sections

The method of successive differentiation will work on many pulses whose sections are not polynomials. As the following shows, if we obtain the original pulse back after differentiating it one or more times, then successive differentiation will work.

- 5.7** The following pulse has a nonpolynomial section.

$$f(t) = e^{-\beta t} U(t) \quad (\beta > 0)$$

- The pulse has an infinite span. What is its average over the entire  $t$ -axis?
  - Apply the method of successive differentiation to obtain its Fourier transform.
- Hint:* Differentiate using the product rule.
- Do we need to add a frequency-domain Dirac delta to the final result?

- 5.8 (a)** Sketch and then find the Fourier transform of the following pulse using the analysis equation:

$$f(t) = \cos(\pi t) \operatorname{Rect}(t)$$

- (b) Now use successive differentiation to find its transform.

*Hint:* Differentiate twice using the product rule.

- 5.9 (a)** Sketch the following pulse.

- (b) Use successive differentiation to find its Fourier transform

$$f(t) = e^t \operatorname{Rect}\left(t - \frac{1}{2}\right)$$

- 5.10 (a)** Sketch the following pulse

$$f(t) = e^{\beta t} U(-t) + e^{-\beta t} U(t) + 1 \quad (\beta > 0)$$

- (b) Use successive differentiation to find its Fourier transform. *Hint:* Split  $f(t)$  into its three parts and deal with each one individually. Then add the results.

### Projects Involving the FFT System

- 5.11** Sketch the result of differentiating the pulse shown in Figure 5.24. Now use the FFT system to verify what you have sketched as follows:

- (a) Load the pulse shown in the figure into the FFT system. Use  $N = 512$ , SAMPLED,  $T = 4 * \text{PI}$ , PULSE.
- (b) Run ANALYSIS and obtain the spectrum of the pulse.
- (c) From the main menu

take option G: RUN POSTPROCESSORS

followed by

option F: RUN F POSTPROCESSOR

You should now have a menu on your screen offering you a selection of packages. Run the differentiation package

BACKWARD DIFF 1st DERIVATIVE

followed by SYNTHESIS. Now inspect the result by viewing a plot of Y. You should have obtained a plot similar to what you sketched.

Verify that the heights of the lines are consistent with Dirac deltas with weights 1, -1 and that they are at the correct locations. (See Section 15.1.)

5.12 Repeat Exercise 5.11, but use the following two differentiation packages instead:

**FORWARD DIFF 1st DERIVATIVE**  
**CENTRAL DIFF 1st DERIVATIVE**

The theory behind all of these differentiation packages is contained in Section 15.3. Read it in order to become familiar with how they work.

5.13 Load the pulse shown in Figure 5.34 into the **X** vector of the FFT system using  $N = 500$ , **SAMPLED**,  $T = 10$ , **PULSE**, and then find its second derivative, using the **F** postprocessor package

**CENTRAL DIFF 2nd DERIVATIVE**

The result should be four Dirac deltas. Verify that the lines are in the correct locations and have the correct values.

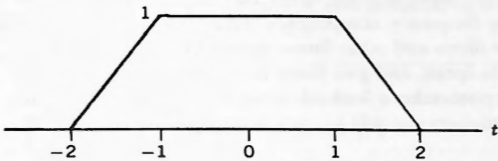


*Figure 5.34.*

# Frequency-Domain Analysis

---

## 6.1 INTRODUCTION

---

Perhaps the greatest contribution that Fourier analysis makes to engineering, and especially to electrical engineering, is the fact that it enables us to break down input signals into their frequency components. Once that has been done we can easily comprehend how filters and other linear networks operate on such signals, frequency by frequency so to speak, and give them the attributes that we want them to have.

In this chapter we take a look at three applications of Fourier analysis in the frequency domain:

- The response of an electrical network to a pulse
- The response of a network to an ac input such as  $\sin(\omega_0 t)$  or  $\cos(\omega_0 t)$
- The response of a network to any periodic signal

The second of these applications, known as **ac linear circuit analysis**, is probably the most commonly used analytical tool in electrical engineering (see, e.g., Edminster, 1972). Often taught by rote in the early years of study, students are shown that if they replace the inductors and capacitors in a network by the quantities  $j\omega_0 L$  and  $1/j\omega_0 C$  (sometimes called complex resistors) and if they use as the input to the network the quantity  $e^{j\omega_0 t}$  (called a phasor), then the response can be calculated simply by using Kirchhoff's voltage and current laws. Although there is a slight mystique to all of this, it works so well that its rules are soon accepted and the mystery is forgotten.

The method was first used by Oliver Heaviside in 1878 (Nahin, 1987), and while it can be derived using his operational mathematics, that is something that we have intentionally avoided. It also springs directly from **formal Fourier analysis**, however, but since very few beginning students have the required background, it is not surprising that they are asked simply to take things on trust. Since we now do have that background it will be one of the objectives of this chapter to show clearly how the techniques used in ac circuit analysis come about and why they work so effectively. This also provides us with a valuable opportunity to put our Fourier analysis to work.

Bear in mind while reading this chapter that its methods are applicable not only to electrical networks but also to networks comprised of other types of components—mechanical, acoustical, hydraulic, and many more. Indeed they, and all of the other

Fourier analysis applications that we are now beginning to explore, are applicable to any system whose behavior can be modeled by a **constant-coefficient linear differential equation**.

## 6.2 RESPONSE OF A LINEAR, TIME-INVARIANT SYSTEM TO A PULSE FUNCTION

As noted earlier, linear systems can be made up of many different types of components—electrical, mechanical, hydraulic, and so on—but our interest here is only in systems comprised of electrical components. Moreover, we are only concerned with linear systems whose element values do not change with time, what are called **linear, time-invariant (LTI)** systems.

For the present we ask you to interpret the word **linear** by using your intuition. In Section 6.4 we define precisely what it means.

**Definition:** An LTI system is one that can be characterized by a constant-coefficient linear differential equation (**CCL DE**).

An LTI system and its CCL DE are mathematically equivalent, and we shall use these terms interchangeably, sometimes also using the nomenclature “LTI system/CCL DE” to underscore this fact.

The amount of effort needed to arrive at the differential equation for an electrical network of more than trivial complexity is usually quite substantial, but the good news is that once we have completed this chapter we shall see that we in fact never really need to do that, as the operational method that we shall derive will make it totally unnecessary. Moreover, starting with the results obtained from the operational method, if we so desire we shall easily be able to write down the DE by inspection.

As a start, then, let's examine how the Fourier transform can be used to solve CCL DEs and in so doing, to find the response of an LTI network to various pulse inputs.

The general form of a CCL DE is as follows:

$$P_1(D)y(t) = P_2(D)x(t) \quad (6.1)$$

in which

- $P_1(D)$  and  $P_2(D)$  are polynomials in the operator  $D \equiv d/dt$  with constant coefficients
- $x(t)$  is called the **input** or the **forcing function**
- $y(t)$  is called the **output** or the **response** or the **solution**.

An example would be

$$(5D^2 + 6D + 1)y(t) = (3D + 2)x(t) \quad (\forall t) \quad (6.2)$$

in which we see that the coefficients of the two polynomials are all constants and that

the DE is linear. It is in fact a CCL DE. Note two very important items regarding (6.2):

- There is a condition attached to it that states that it is in force for all values of  $t$ . By this is meant that the solution  $y(t)$  that we hope to obtain must cause (6.2) to balance for all values of  $t$  in the range  $-\infty < t < \infty$ .
- No initial conditions have been specified. By this is meant that we are not imposing any conditions that  $y(t)$  must meet at certain specified values of  $t$ , such as  $y(0) = 1$  or  $y'(5) = 2$ , and so forth.

These two facts are always present, either implicitly or explicitly, when using the Fourier transform to solve CCL DEs.

From a system standpoint an LTI system/CCL DE can be represented by the block diagram shown in Figure 6.1. In the figure we see how the input  $x(t)$  acts on the LTI system, characterized by its CCL DE, and produces the output or response  $y(t)$ .

The statement "solve a CCL DE" means: Given the expression for the input  $x(t)$ , find the expression for the output  $y(t)$  that causes the DE to balance. Thus by solving the CCL DE associated with an LTI system we are finding what the response of the system is to a given input.

As an illustrative example we now solve (6.2) by the use of Theorem 5.1 from the previous chapter, which is ideally suited to solving differential equations of this kind. First we take the Fourier transform of both sides of the equation, obtaining

$$\int_{-\infty}^{\infty} [5D^2 + 6D + 1]y(t)e^{-j\omega t} dt = \int_{-\infty}^{\infty} [3D + 2]x(t)e^{-j\omega t} dt \quad (6.3)$$

Note the fact that the range of integration agrees with the condition that came with the DE, namely " $\forall t$ ." Note also that nowhere in the Fourier transformation process is there a place to include initial conditions (as there is with the **single-sided Laplace transform**), but since none were imposed this is clearly not a problem.

By Theorem 5.1 and its corollaries, (6.3) now becomes

$$[5(j\omega)^2 + 6j\omega + 1]Y(\omega) = [3j\omega + 2]X(\omega) \quad (6.4)$$

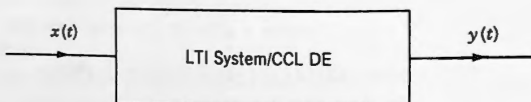


Figure 6.1.

and this is seen to be a **purely algebraic statement** involving complex quantities. We thus have the remarkable result stated in Theorem 6.1 below.

### ■ THEOREM 6.1

Fourier transformation of the time-domain CCL DE

$$P_1(D)y(t) = P_2(D)x(t) \quad (\forall t) \quad (6.5)$$

converts it to the algebraic equation

$$P_1(j\omega)Y(\omega) = P_2(j\omega)X(\omega) \quad (6.6)$$

in the frequency domain.

Solving for  $Y(\omega)$  in (6.4), we now obtain

$$Y(\omega) = \left[ \frac{3j\omega + 2}{5(j\omega)^2 + 6j\omega + 1} \right] X(\omega) \quad (6.7)$$

which we pause to examine.

- (1) The RHS of (6.7) is a product of two terms, the first in square brackets coming only from the DE and the second only from the input  $x(t)$ .
- (2) We have obtained a general expression for  $Y(\omega)$  without ever having stated what  $x(t)$  is. Thus any  $x(t)$ , which has a Fourier transform, can now be used to obtain an answer for  $Y(\omega)$  and then by inversion, for  $y(t)$ .

Figure 6.1 was in the time domain. Equation (6.7) enables us to redraw it in the frequency domain, giving us Figure 6.2.

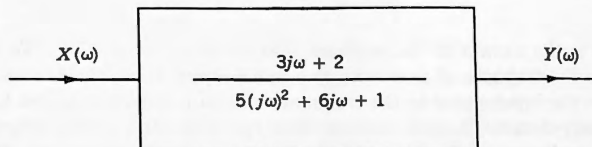


Figure 6.2.

The expression inside the box in the figure can be derived once and for all from the DE. We shall call it the **frequency response** or the **frequency transfer function** of the system and symbolize it as  $H(j\omega)$ . It is defined as follows:

**Definition:** Let the CCL DE for an LTI system be

$$P_1(D)y(t) = P_2(D)x(t) \quad (\forall t) \quad (6.8)$$

Then the **frequency response** or **frequency transfer function** of the system is

$$H(j\omega) = \frac{P_2(j\omega)}{P_1(j\omega)} \quad (6.9)$$

The CCL DE that we have been considering was

$$(5D^2 + 6D + 1)y(t) = (3D + 2)x(t) \quad (6.10)$$

and so for this system,

$$H(j\omega) = \frac{3D + 2}{5D^2 + 6D + 1} \Big|_{D \leftarrow j\omega} = \frac{3j\omega + 2}{5(j\omega)^2 + 6j\omega + 1} \quad (6.11)$$

As we shall soon see, the quantity  $H(j\omega)$  contains in it all of the information regarding the LTI system, that is, what the values of the components are and how they are interconnected. Note that it exists in the frequency domain. In the next chapter we develop a time-domain quantity called the **impulse response** and written as  $h(t)$ , which also completely characterizes the system. Not surprisingly,  $H(j\omega)$  and  $h(t)$  are closely related.

The preceding definition for  $H(j\omega)$  enables us to write it down immediately once the system's DE is given. We can then write the main response equation (6.7) in the form

$$Y(\omega) = H(j\omega)X(\omega) \quad (6.12)$$

and from this, by use of the synthesis equation,

$$y(t) = \frac{1}{2\pi} \int_{-\infty}^{\infty} H(j\omega)X(\omega)e^{j\omega t} d\omega \quad (6.13)$$

This then is the answer to the problem that we set out to solve. We now have a statement for the response of a network to a pulse input. What (6.12) tells us is that if we transform the input signal to the frequency domain and express the LTI network by its frequency-domain characterization, then the transform of the response can be found using **ordinary algebraic multiplication**. By simple inversion, as shown in (6.13), we then obtain the final answer.

Equations (6.12) and (6.13) are of fundamental importance in the analysis of LTI systems, and so we state them as Theorem 6.2 below.

### ■ THEOREM 6.2

Let the pulse  $x(t) \Leftrightarrow X(\omega)$  be the input to an LTI system whose frequency transfer function is  $H(j\omega)$ . Then the output will be

- In the frequency domain

$$Y(\omega) = H(j\omega)X(\omega) \quad (6.14)$$

- In the time domain

$$y(t) = \frac{1}{2\pi} \int_{-\infty}^{\infty} H(j\omega)X(\omega)e^{j\omega t} d\omega \quad (6.15)$$

The structure of (6.15) is best underscored by writing the following two equations:

$$\text{Input: } x(t) = \frac{1}{2\pi} \int_{-\infty}^{\infty} X(\omega)e^{j\omega t} d\omega \quad (6.16)$$

$$\text{Output: } y(t) = \frac{1}{2\pi} \int_{-\infty}^{\infty} H(j\omega)X(\omega)e^{j\omega t} d\omega \quad (6.17)$$

In the first we show the Fourier integral representation of the input pulse, in which  $x(t)$  is being synthesized from its frequency-domain representation  $X(\omega)$ . In the second we show the same for  $y(t)$ . Observe, however, how the term  $H(j\omega)$  has now insinuated itself into the second integral as a multiplier of  $X(\omega)$ , representing the action of the system on the input to produce the output.

Equations (6.16) and (6.17) are a frequency-domain summary of the way in which the Fourier transform enables us to find the response of a network, given its frequency transfer function and the input, and in Figure 6.3 we show a representation of what those equations tell us. In Chapter 7 we derive their time-domain counterpart.

The following two simple examples illustrate what we have been discussing, but their results and methodology are perfectly general.

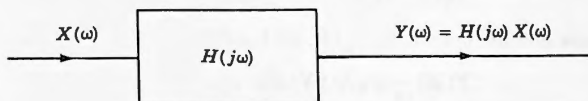


Figure 6.3.

□**EXAMPLE 6.1:** Assume that the frequency response of a network is

$$H(j\omega) = \frac{1}{2 + j\omega} \quad (6.18)$$

Find the magnitude and phase spectra of the output when the input is

$$x(t) = e^{-t}U(t) \quad (6.19)$$

**Solution:** From (6.18) we have the magnitude spectrum of  $H(j\omega)$  as

$$|H(j\omega)| = \frac{1}{\sqrt{(4 + \omega^2)}} \quad (6.20)$$

and in order to find its phase spectrum we proceed as follows. From (6.18)  $H(j\omega)$  is seen to be the quotient of two quantities, namely 1 and  $2 + j\omega$ . The phase spectrum of 1 is simply

$$\Theta_1(\omega) = 0$$

and the phase spectrum of  $2 + j\omega$  is

$$\Theta_2(\omega) = \tan^{-1} \frac{\omega}{2}$$

Since we are considering a **quotient** of two quantities, we know (see Exercise 2.9) that its phase spectrum must be the **difference** of the two spectra, and so we obtain the required result as

$$\Theta_H(\omega) = 0 - \tan^{-1} \frac{\omega}{2} = \tan^{-1} \frac{-\omega}{2} \quad (6.21)$$

Consider now the input pulse,  $x(t)$ . From Chapter 4 we recall that

$$e^{-\beta t}U(t) \Leftrightarrow \frac{1}{\beta + j\omega} \quad (6.22)$$

and so, for  $x(t)$  in (6.19),

$$X(\omega) = \frac{1}{1 + j\omega} \quad (6.23)$$

Repeating what we did earlier for  $H(j\omega)$ , we obtain the magnitude and phase spectra of  $x(t)$  as

$$|X(\omega)| = \frac{1}{\sqrt{1 + \omega^2}} \quad \text{and} \quad \theta_X(\omega) = \tan^{-1}[-\omega] \quad (6.24)$$

We can now find the output. By (6.14), its Fourier transform will be

$$\begin{aligned} Y(\omega) &= H(j\omega)X(\omega) \\ &= |H(j\omega)|e^{j\Theta_H(\omega)}|X(\omega)|e^{j\Theta_X(\omega)} \\ &= |H(j\omega)||X(\omega)|e^{j[\Theta_H(\omega) + \Theta_X(\omega)]} \end{aligned} \quad (6.25)$$

Thus from (6.25) we see that the general expression for the magnitude spectrum of  $y(t)$  will be

$$|Y(\omega)| = |H(j\omega)||X(\omega)| \quad (6.26)$$

which in this problem is

$$|Y(\omega)| = \frac{1}{\sqrt{(4 + \omega^2)\sqrt{(1 + \omega^2)}}} \quad (6.27)$$

and the general expression for the phase spectrum will be

$$\Theta_Y(\omega) = \Theta_H(\omega) + \Theta_X(\omega) \quad (6.28)$$

which for this problem is

$$\Theta_Y(\omega) = \tan^{-1} \frac{-\omega}{2} + \tan^{-1}[-\omega] \quad (6.29)$$

□

Observe in the preceding example how

- The magnitude spectra multiply
- The phase spectra add

In effect, then, a linear network acts on the incoming signal as a frequency-sensitive filter, modifying its magnitude and phase spectra to produce the output spectra according to the rules given in (6.26) and (6.28). By appropriately designing the network we can produce a desired frequency response  $H(j\omega)$ , which brings about a desired output  $y(t)$ . This is the basis of filter theory and of much of circuit design theory in electrical engineering. Theorem 6.3 summarizes these results.

### ■ THEOREM 6.3

Let the signal  $x(t) \Leftrightarrow X(\omega)$  be the input to the LTI network whose frequency response is  $H(j\omega)$ . Then the output will be  $y(t)$ , where the magnitude of  $Y(\omega)$  satisfies

$$|Y(\omega)| = |H(j\omega)||X(\omega)| \quad (6.30)$$

and the phase of  $Y(\omega)$  satisfies

$$\Theta_Y(\omega) = \Theta_H(\omega) + \Theta_X(\omega) \quad (6.31)$$

that is, the magnitudes multiply and the phases add.

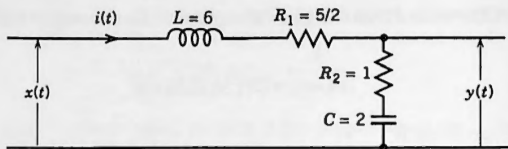


Figure 6.4. Electrical network.

■ **EXAMPLE 6.2:** The electrical network shown in Figure 6.4 is characterized by the CCL DE

$$12y''(t) + 7y'(t) + y(t) = 2x'(t) + x(t) \quad (\forall t) \quad (6.32)$$

(We shall soon see how the CCL DE for such a network can be quickly obtained.) Write the expressions for

- (1) The frequency response  $H(j\omega)$
- (2) The magnitude and phase spectra of  $y(t)$  assuming that

$$x(t) = e^{-t}U(t) \quad (6.33)$$

- (3) The time-domain expression for  $y(t)$
- (4) Prove that your answer in (3) satisfies the DE

**Solution:** Part (1): Using the  $D$  operator the DE becomes

$$[12D^2 + 7D + 1]y(t) = [2D + 1]x(t) \quad (6.34)$$

and so the frequency response is

$$H(j\omega) = \frac{2D + 1}{12D^2 + 7D + 1} \Big|_{D \leftarrow j\omega} = \frac{2j\omega + 1}{12(j\omega)^2 + 7j\omega + 1} \quad (6.35)$$

Part (2): To obtain the magnitude and phase spectra of  $H(j\omega)$  in (6.35) we proceed as follows. Multiplying out the  $(j\omega)^2$  in its denominator gives us

$$H(j\omega) = \frac{1 + 2j\omega}{(1 - 12\omega^2) + 7j\omega} \quad (6.36)$$

Then, proceeding as we did in the preceding exercise, the magnitude spectrum will be the quotient of the magnitude spectra of the two quantities in (6.36), namely

$$|H(j\omega)| = \frac{\sqrt{(1 + 4\omega^2)}}{\sqrt{[(1 - 12\omega^2)^2 + 49\omega^2]}} \quad (6.37)$$

and the phase spectrum will be the difference of their phase spectra, that is,

$$\Theta_H(\omega) = \tan^{-1}(2\omega) - \tan^{-1}\left[\frac{7\omega}{1 - 12\omega^2}\right] \quad (6.38)$$

Regarding the input signal:

$$[x(t) = e^{-t}U(t)] \Leftrightarrow [X(\omega) = \frac{1}{1 + j\omega}] \quad (6.39)$$

In the preceding example we found that for this pulse its magnitude spectrum is

$$|X(\omega)| = \frac{1}{\sqrt{(1 + \omega^2)}} \quad (6.40)$$

and its phase spectrum is

$$\Theta_X(\omega) = \tan^{-1}[-\omega] \quad (6.41)$$

By (6.30) the magnitude spectrum of the output will then be

$$\begin{aligned} |Y(\omega)| &= |H(j\omega)||X(\omega)| \\ &= \frac{\sqrt{1 + 4\omega^2}}{\sqrt{(1 - 12\omega^2)^2 + 49\omega^2}} \frac{1}{\sqrt{1 + \omega^2}} \end{aligned} \quad (6.42)$$

and by (6.31) its phase spectrum will be

$$\begin{aligned} \Theta_Y(\omega) &= \Theta_H(\omega) + \Theta_X(\omega) \\ &= \tan^{-1}(2\omega) - \tan^{-1}\left[\frac{7\omega}{1 - 12\omega^2}\right] + \tan^{-1}[-\omega] \end{aligned} \quad (6.43)$$

**Part (3):** Multiplying  $H(j\omega)$  by  $X(\omega)$  gives us the Fourier transform of  $y(t)$  as

$$\begin{aligned} Y(\omega) &= \frac{2j\omega + 1}{12(j\omega)^2 + 7j\omega + 1} \frac{1}{1 + j\omega} \\ &= \frac{2j\omega + 1}{(4j\omega + 1)(3j\omega + 1)(j\omega + 1)} \end{aligned} \quad (6.44)$$

We now find the partial fraction expansion of this expression as

$$Y(\omega) = \frac{2/3}{j\omega + 1/4} + \frac{-1/2}{j\omega + 1/3} + \frac{-1/6}{j\omega + 1} \quad (6.45)$$

which we can invert term by term by making use of the Fourier pair (4.12),

obtaining the solution to the DE as

$$y(t) = [(2/3)e^{-t/4} - (1/2)e^{-t/3} - (1/6)e^{-t}]U(t) \quad (6.46)$$

**Part (4):** To verify that (6.46) will cause the original DE to balance we proceed as follows: Using the product rule for differentiation we obtain

$$\begin{aligned} Dy(t) &= [-(1/6)e^{-t/4} + (1/6)e^{-t/3} + (1/6)e^{-t}]U(t) \\ &\quad + [(2/3)e^{-t/4} - (1/2)e^{-t/3} - (1/6)e^{-t}] \delta(t) \\ &= [-(1/6)e^{-t/4} + (1/6)e^{-t/3} + (1/6)e^{-t}]U(t) \end{aligned} \quad (6.47)$$

Differentiating a second time leads to

$$D^2y(t) = [(1/24)e^{-t/4} - (1/18)e^{-t/3} - (1/6)e^{-t}]U(t) + (1/6)\delta(t) \quad (6.48)$$

Using these results the LHS of the DE (6.34) now gives us

$$[12D^2 + 7D + 1]y(t) = 2\delta(t) - e^{-t}U(t) \quad (\forall t) \quad (6.49)$$

On the other hand, for the input  $x(t) = e^{-t}U(t)$  we obtain

$$Dx(t) = -e^{-t}U(t) + \delta(t) \quad (6.50)$$

from which the RHS of the DE (6.34) gives

$$[2D + 1]x(t) = 2\delta(t) - e^{-t}U(t) \quad (\forall t) \quad (6.51)$$

and so the DE balances  $\forall t$ , thereby validating the solution.  $\square$

Note that in this particular case we were able to obtain an explicit expression for  $y(t)$ , but that was because we selected a very simple function for  $x(t)$ , and so in the end we were able to invert the expression (6.44) for  $Y(\omega)$  conclusively. In general that will not be the case and we shall then have to content ourselves with the Fourier integral representation for  $y(t)$  shown in (6.15).

However, this is precisely where the FFT comes into play, since it can then be used very effectively to give us a numerical version of  $y(t)$ .

**EXAMPLE 6.3:** Use the FFT system to invert  $Y(\omega)$  of (6.44) numerically.

**Solution:** First we multiply out the denominator of  $Y(\omega)$  obtaining

$$Y(\omega) = \frac{2j\omega + 1}{1 - 19\omega^2 + j(8\omega - 12\omega^3)} \quad (6.52)$$

which we now rationalize,

$$\begin{aligned} Y(\omega) &= \frac{2j\omega + 1}{1 - 19\omega^2 + j(8\omega - 12\omega^3)} \frac{1 - 19\omega^2 - j(8\omega - 12\omega^3)}{1 - 19\omega^2 - j(8\omega - 12\omega^3)} \\ &= \frac{(1 - 3\omega^2 - 24\omega^4) - j(6\omega + 26\omega^3)}{(1 - 19\omega^2)^2 + (8\omega - 12\omega^3)^2} \end{aligned} \quad (6.53)$$

From this the real and imaginary parts of  $Y(\omega)$  are

$$A(\omega) = \frac{(1 - 3\omega^2 - 24\omega^4)}{(1 - 19\omega^2)^2 + (8\omega - 12\omega^3)^2} \quad (6.54)$$

and

$$B(\omega) = \frac{-(6\omega + 26\omega^3)}{(1 - 19\omega^2)^2 + (8\omega - 12\omega^3)^2} \quad (6.55)$$

We now loaded these two expressions into *F* and then ran SYNTHESIS. (When prompted, we used an alias level of 5. See Chapter 17 for the meaning of this.) In Figure 6.5 we show the resulting plot of  $y(t)$ . Note that it is everywhere continuous,

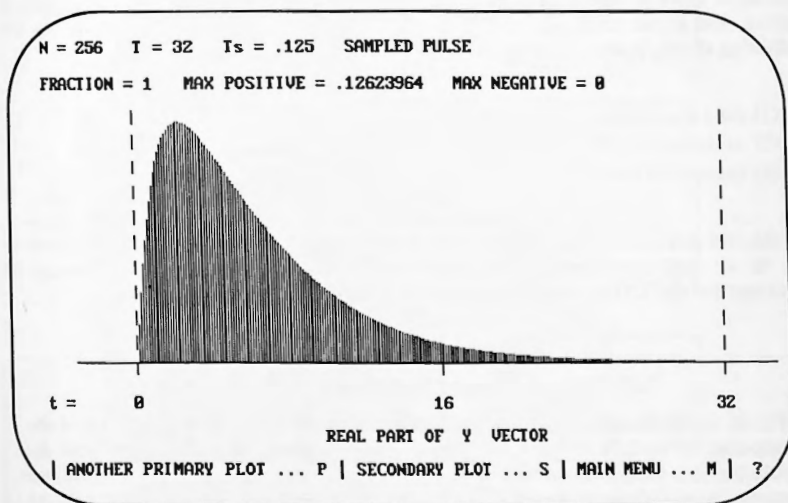


Figure 6.5. Plot of  $y(t)$  from Example 6.3.

TABLE 6.1 FFT vs. Exact

<i>k</i>	FFT	Exact	Rel Error (%)
8	0.099787509	0.099626164	0.16
32	0.110481010	0.110401785	0.07
64	0.055455353	0.055425886	0.05
96	0.024043460	0.024032535	0.05

Note:  $N = 256$ ;  $T = 32$ . Each unit of  $k$  is equal to  $32/256 = 0.125$  seconds.

but  $y'(t)$  has a discontinuity at  $t = 0$ . This was to be expected from (6.44), where we see that  $Y(\omega)$  dies out like  $1/\omega^2$ . (See Table 3.2 in Chapter 3.)

In Table 6.1 we show a comparison between the FFT values for  $y(t)$  and the exact values from (6.46). The fit is seen to be extremely close, even though we only used  $N = 256$  for the run. A larger  $N$  such as 1024 would have given even closer results. We used  $T = 32$  since the slowest decaying exponential term in (6.46) has a time constant of 4 seconds, and so this value for  $T$  ensures good decay to zero. (See the remarks in Section 17.5 on distortion and errors caused by time-domain aliasing.)  $\square$

In the preceding FFT-system demonstration it was assumed that we knew the expression for  $X(\omega)$ , and so we were able to write the complete expression for  $Y(\omega)$  in (6.44), which formed the starting point for the FFT demonstration in (6.52).

In general that will not be the case. The input pulse may be far more complex than the simple one that we just used, and so we may not be able to write its Fourier transform quite so easily, or it may even be given to us as a sequence of numerical values, and so we shall not be able to write its Fourier transform at all. As the following shows, however, we can also use the FFT system to

- (1) Find the Fourier transform of the input pulse
- (2) Multiply it by  $H(j\omega)$ , obtaining  $Y(\omega)$
- (3) Invert  $Y(\omega)$ , obtaining  $y(t)$

In this way any input pulse can be used, regardless of the form in which it comes to us. As we shall also soon see, the analytical expression for  $H(j\omega)$  can always be obtained for any LTI network, no matter how complex.

#### Accompanying Disk

Figure 6.6 shows all of the steps needed when using the FFT system to find the response of an LTI network to a pulse input. Equivalently it shows how the solution to a CCL DE can be found. Referring to the numbers in the figure, we start with two pieces of information, the details regarding the pulse  $x(t)$  and the expression for the frequency transfer function  $H(j\omega)$ .

- (1) The details for the pulse could be in one of two forms:
  - (a) An analytical expression, in which case it can be loaded directly into X starting from main menu A.
  - (b) A vector of numerical values, in which case it can be loaded from an external disk file starting from main menu B.
- (2)  $x(t)$  is Fourier transformed using ANALYSIS, thereby producing a numerical version of  $X(\omega)$  in F.
- (3) The expression for  $H(j\omega)$  is loaded into F2, starting from main menu A.
- (4) Using a procedure called COMPLEX MULTIPLY, which is one of the packages in the F postprocessor, F and F2 are multiplied together producing  $Y(\omega)$  in F.
- (5)  $Y(\omega)$  in F is inverse Fourier transformed using SYNTHESIS.
- (6) The end result is a numerical version of  $y(t)$  in Y, which is then the response of the network or the solution to the DE.

*Note:* Figure 6.6 applies to periodic inputs as well.

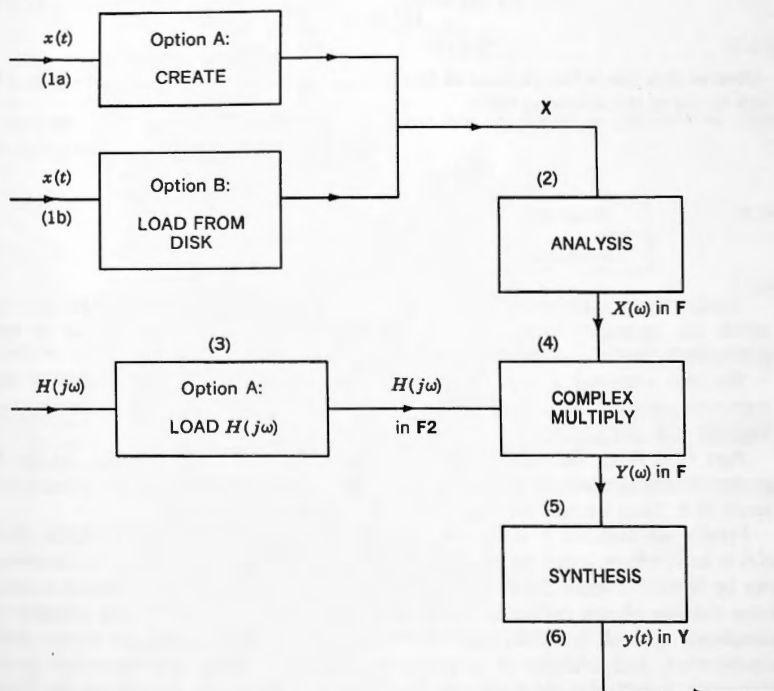


Figure 6.6. Using the FFT system to obtain the response to a pulse.

□ **EXAMPLE 6.4:** Use the FFT system to create the following:

- The Fourier transform of  $x(t)$  specified in (6.33)
- The frequency response  $H(j\omega)$  from (6.35)
- The resulting response of the network,  $y(t)$

Use  $N = 256$ , SAMPLED,  $T = 32$ , PULSE.

**Solution:** Part (a): We loaded the time-domain expression for  $x(t)$  from (6.33) into **X** starting from option A. Although  $x(t)$  had a very simple analytical form in this case, we could just as well have loaded a pulse with arbitrary analytical complexity or loaded a sequence of numerical values from a disk file without any knowledge of the analytical statement for the pulse. Indeed, such a statement may not even have existed at all, or the numbers could even have been a sequence of random values.

We then ran ANALYSIS from the main menu, thereby placing  $X(\omega)$  in **F**.

Part (b): From (6.35),

$$H(j\omega) = \frac{2j\omega + 1}{12(j\omega)^2 + 7j\omega + 1} \quad (6.56)$$

Observe that this is the quotient of two polynomials, whose essential information is contained in the following table:

	Degree	Coefficients		
Numerator	1	1	2	
Denominator	2	1	7	12

Starting from main menu A, we entered a facility called “Create  $H(j\omega)$ ,” in which the necessary tools are provided for creating such a quotient of two polynomials, either of which can be of degree up to 10.

We also executed a LOAD from this facility, thereby actually placing the numerical values of  $H(j\omega)$  in **F2**. (For “alias level” we used 20. This is discussed in Sections 12.5 and 17.5.)

Part (C): From the main menu we took Option G, which leads to the **F** postprocessor, in which there is a facility to complex multiply **F** and **F2**, placing the result in **F**. Thus we now have a numerical version of  $Y(\omega)$  in **F**.

Finally, we inverted  $Y(\omega)$  to the time domain by running SYNTHESIS. Now  $y(t)$  is in **Y**, where it can be viewed by plotting it (main menu H), or its numbers can be inspected (main menu I). The resulting plot of  $y(t)$  was indistinguishable from the one shown earlier in Figure 6.5. The method used in this example is **completely general**, however, and will work for **any** input pulse, no matter how complicated, and whether it is given to us in analytical or numerical form. Moreover, it will also work for any frequency response up to degree 10. (This number was chosen arbitrarily and could be larger.)

As with Example 6.3, we carried out a numerical comparison of the FFT values of  $y(t)$  with the exact values from (6.46). The numbers were very close to those in Table 6.1.  $\square$

### 6.3 AC CIRCUIT ANALYSIS USING THE FOURIER TRANSFORM

When the input to a CCL DE is an **eternal complex exponential** the results obtained in the preceding section undergo a dramatic simplification. This forms the basis of the method of **ac circuit analysis**, widely used in electrical engineering.

Consider the simple resistance-inductance-capacitance (RLC) electrical network shown in Figure 6.7. In this case it is easy to set up the DE relating  $y(t)$  and  $x(t)$ . Using Kirchhoff's and Faraday's laws, we see that

$$LDi(t) + Ri(t) + \frac{1}{C} \int_{-\infty}^t i(t) dt = x(t) \quad (6.57)$$

and

$$y(t) = \frac{1}{C} \int_{-\infty}^t i(t) dt \quad (6.58)$$

In order to eliminate the integrals in these two equations we differentiate them, obtaining the pair of differential equations

$$LD^2i(t) + RDi(t) + \frac{1}{C}i(t) = Dx(t) \quad (6.59)$$

$$Dy(t) = \frac{1}{C}i(t) \quad (6.60)$$

Observe the important fact that all of the coefficients in these DEs are made up from the elements of the network, namely  $R$ ,  $L$ , and  $C$ .

**Because  $R$ ,  $L$ , and  $C$  are real valued, the coefficients of any network's CCL DE will always be real valued.**

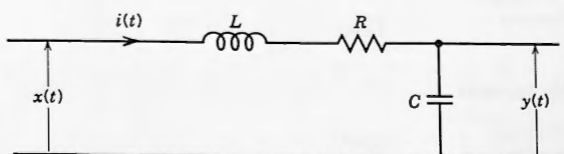


Figure 6.7. RLC network.

This statement will be true in general for any LTI network, no matter how complex. It will be a critical fact later. Factorizing (6.59) gives

$$\left[ LD^2 + RD + \frac{1}{C} \right] i(t) = Dx(t) \quad (\forall t) \quad (6.61)$$

which we pause to examine. Equation (6.61) is seen to be a CCL DE for  $i(t)$ , with  $x(t)$  as the forcing function. Observe that we have appended “ $\forall t$ ” since that is applicable. Observe also that there are no initial conditions.

Fourier transformation of (6.61) using Theorem 5.1 now leads to the algebraic equation

$$\left[ (j\omega)^2 L + (j\omega) R + \frac{1}{C} \right] I(\omega) = j\omega X(\omega) \quad (6.62)$$

which we divide through by  $j\omega$ , obtaining

$$\left[ j\omega L + R + \frac{1}{j\omega C} \right] I(\omega) = X(\omega) \quad (6.63)$$

and since this is a relationship between a current and a voltage, the term in square brackets plays the role of an impedance. In ac circuit analysis it is called the **input impedance**, and is written

$$Z(j\omega) = j\omega L + R + \frac{1}{j\omega C} \quad (6.64)$$

Solving (6.63) for  $I(\omega)$ , we obtain

$$I(\omega) = \left[ \frac{1}{j\omega L + R + 1/j\omega C} \right] X(\omega) = \frac{1}{Z(j\omega)} X(\omega) \quad (6.65)$$

Next we transform (6.60), obtaining

$$j\omega Y(\omega) = \frac{1}{C} I(\omega) \quad (6.66)$$

from which

$$Y(\omega) = \frac{1}{j\omega C} I(\omega) \quad (6.67)$$

Using (6.65) this becomes

$$Y(\omega) = \left[ \frac{1/j\omega C}{j\omega L + R + 1/j\omega C} \right] X(\omega) = H(j\omega) X(\omega) \quad (6.68)$$

Note how (6.68) has the same structure as (6.14), where the frequency transfer function in this case is

$$H(j\omega) = \frac{1/j\omega C}{j\omega L + R + 1/j\omega C} \quad (6.69)$$

Up to this point  $x(t)$  can be any voltage that has a Fourier transform, for example,  $e^{-\beta t}U(t)$ ,  $\delta(t)$ , and so forth, but in ac circuit analysis the following decision is always made:

The input voltage shall be an **eternal complex exponential** with radian frequency  $\omega_0$ , that is,

$$x(t) = e^{j\omega_0 t} \quad (6.70)$$

Such a function is called a **phasor**.

The reason for this is a simple one.

What we are really after is the network's response to either  $\cos(\omega_0 t)$  or  $\sin(\omega_0 t)$ . Using an eternal complex exponential will give us both.

To see why this is so, consider the following argument. The system DE will always have the following two attributes:

- It will be linear
- It will have real-valued coefficients

From this it follows that

- To find the response of a network to  $\cos(\omega_0 t)$ , find its response to  $e^{j\omega_0 t}$  and then take the real part
- To find the response to  $\sin(\omega_0 t)$ , find its response to  $e^{j\omega_0 t}$  and then take the imaginary part.

This is depicted in Figure 6.8.

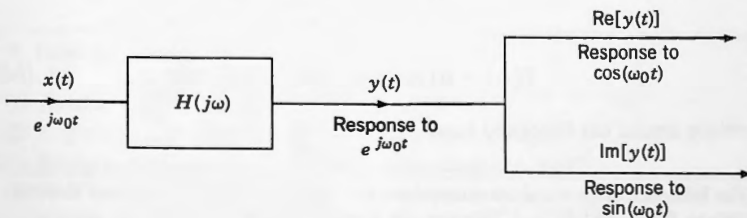


Figure 6.8.

We now give a proof of the validity of these statements.

*Proof:* Let the DE be

$$P_1(D)y(t) = P_2(D)x(t) \quad (6.71)$$

Then, if the input is  $x(t) = e^{j\omega_0 t}$ , this becomes

$$P_1(D)y(t) = P_2(D)e^{j\omega_0 t} \quad (6.72)$$

from which it is also true that

$$\operatorname{Re}[P_1(D)y(t)] = \operatorname{Re}[P_2(D)e^{j\omega_0 t}] \quad (6.73)$$

We have seen earlier, however, that the coefficients of the DE will always be real, which means that (6.73) is the same as

$$P_1(D)\operatorname{Re}[y(t)] = P_2(D)\cos(\omega_0 t) \quad (6.74)$$

This is now seen to be the same CCL DE that we have considered in (6.72), except that the input is now  $\cos(\omega_0 t)$  and the response is  $\operatorname{Re}[y(t)]$ .

A similar argument proves the result for  $\sin(\omega_0 t)$ . ■

We now apply a phasor to the circuit in Figure 6.7. First we recall from (4.85) that

$$e^{j\omega_0 t} \Leftrightarrow 2\pi\delta(\omega - \omega_0) \quad (6.75)$$

and so, when the input is the phasor  $e^{j\omega_0 t}$ , (6.65) and (6.68) become

$$I(\omega) = \frac{1}{Z(j\omega)} 2\pi\delta(\omega - \omega_0) \quad (6.76)$$

$$Y(\omega) = H(j\omega) 2\pi\delta(\omega - \omega_0) \quad (6.77)$$

Sampling by the Dirac deltas now takes place, resulting in

$$I(\omega) = \frac{1}{Z(j\omega_0)} 2\pi\delta(\omega - \omega_0) \quad (6.78)$$

and

$$Y(\omega) = H(j\omega_0) 2\pi\delta(\omega - \omega_0) \quad (6.79)$$

Something crucial has happened here.

The Dirac delta  $\delta(\omega - \omega_0)$  has sampled the functions  $Z(j\omega)$  and  $H(j\omega)$  and changed them to  $Z(j\omega_0)$  and  $H(j\omega_0)$ . They are now simply complex numbers.

Applying the synthesis equation to (6.78) and (6.79) in order to obtain  $i(t)$  and  $y(t)$  we have the two equations

$$i(t) = \frac{1}{2\pi} \int_{-\infty}^{\infty} \frac{1}{Z(j\omega_0)} 2\pi\delta(\omega - \omega_0) e^{j\omega t} d\omega \quad (6.80)$$

$$y(t) = \frac{1}{2\pi} \int_{-\infty}^{\infty} H(j\omega_0) 2\pi\delta(\omega - \omega_0) e^{j\omega t} d\omega \quad (6.81)$$

and once again **Dirac-delta sampling takes place**. These two equations become

$$i(t) = \frac{1}{Z(j\omega_0)} e^{j\omega_0 t} \int_{-\infty}^{\infty} \delta(\omega - \omega_0) d\omega = \frac{1}{Z(j\omega_0)} e^{j\omega_0 t} \quad (6.82)$$

$$y(t) = H(j\omega_0) e^{j\omega_0 t} \int_{-\infty}^{\infty} \delta(\omega - \omega_0) d\omega = H(j\omega_0 t) e^{j\omega_0 t} \quad (6.83)$$

The input current and response of the system when the input voltage is the phasor  $e^{j\omega_0 t}$  are thus

$$i(t) = \frac{1}{Z(j\omega_0)} e^{j\omega_0 t} \quad (6.84)$$

$$y(t) = H(j\omega_0 t) e^{j\omega_0 t} \quad (6.85)$$

Observe that we are now back in the time domain, which is where we want to be. Writing these equations in full, we have

$$i(t) = \left[ \frac{1}{j\omega_0 L + R + 1/j\omega_0 C} \right] e^{j\omega_0 t} \quad (6.86)$$

$$y(t) = \left[ \frac{1/j\omega_0 C}{j\omega_0 L + R + 1/j\omega_0 C} \right] e^{j\omega_0 t} \quad (6.87)$$

Referring to the circuit in Figure 6.7, these two equations now suggest the following rules.

### ■ Rules for ac Circuit Analysis

- (1) Assume that the input is the phasor  $e^{j\omega_0 t}$ .
- (2) Replace each inductor  $L$  by a complex resistor  $j\omega_0 L$ .
- (3) Replace each capacitor  $C$  by a complex resistor  $1/j\omega_0 C$ .
- (4) Find the input impedance and the output voltage using Kirchhoff's loop-voltage and nodal-current laws.

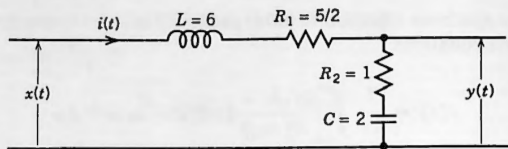


Figure 6.9.

**EXAMPLE 6.5**

Apply the rules of ac circuit analysis to the network of Figure 6.9 to find

- The input impedance as seen from the left
- The frequency transfer function
- The CCL DE for the network
- The input impedance and the response of the network when the input signals are  $\cos(3t)$  and  $\sin(3t)$

**Solution:** Using the rules stated earlier, the network becomes the one shown in Figure 6.10. The input voltage is  $x(t) = e^{j\omega_0 t}$ .

**Part (a):** For the input impedance we can immediately write

$$Z(j\omega_0) = j\omega_0 6 + \frac{7}{2} + \frac{1}{j\omega_0 2} \quad (6.88)$$

**Part (b):** The input current is

$$i(t) = \left[ \frac{1}{j\omega_0 6 + 7/2 + 1/j\omega_0 2} \right] e^{j\omega_0 t} \quad (6.89)$$

and the output voltage is

$$y(t) = \left[ 1 + \frac{1}{j\omega_0 2} \right] i(t) \quad (6.90)$$

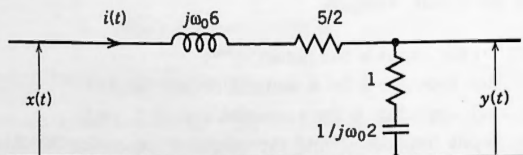


Figure 6.10. Electrical network using ac analysis.

Hence

$$\begin{aligned} y(t) &= \left[ \frac{1 + 1/j\omega_0 2}{j\omega_0 6 + 7/2 + 1/j\omega_0 2} \right] e^{j\omega_0 t} \\ &= \left[ \frac{2(j\omega_0) + 1}{12(j\omega_0)^2 + 7(j\omega_0) + 1} \right] e^{j\omega_0 t} \end{aligned} \quad (6.91)$$

and so the frequency transfer function is

$$H(j\omega_0) = \frac{2(j\omega_0) + 1}{12(j\omega_0)^2 + 7(j\omega_0) + 1} \quad (6.92)$$

**Part (c):** To find the CCL DE for the network we start from

$$\begin{aligned} Y(\omega) &= H(j\omega)X(\omega) \\ &= \frac{2(j\omega) + 1}{12(j\omega)^2 + 7(j\omega) + 1} X(\omega) \end{aligned} \quad (6.93)$$

from which

$$[12(j\omega)^2 + 7(j\omega) + 1]Y(\omega) = [2(j\omega) + 1]X(\omega) \quad (6.94)$$

In the time domain this is simply

$$[12D^2 + 7D + 1]y(t) = [2D + 1]x(t) \quad (6.95)$$

which is the required system CCL DE, obtained here by reversing the method of ac circuit analysis.

**Part (d):** When  $\omega_0 = 3$  the input impedance in (6.88) becomes

$$Z(j\omega_0)|_{\omega_0=3} = j18 + \frac{7}{2} + \frac{1}{j6} = \frac{7}{2} + j\left(18 - \frac{1}{6}\right)$$

giving

$$Z(j3) = 18.17355e^{j1.37600}$$

and the frequency transfer function in (6.92) becomes

$$H(j\omega_0)|_{\omega_0=3} = \frac{2(j3) + 1}{12(j3)^2 + 7(j3) + 1} = \frac{1 + j6}{-107 + j21} \quad (6.96)$$

which can be restated in polar form to give

$$H(j3) = 0.055784e^{-j1.54215} \quad (6.97)$$

Then the response to the phasor  $e^{j3t}$  will be

$$\begin{aligned} y(t) &= H(j3)e^{j3t} \\ &= 0.055784e^{j(3t - 1.54215)} \end{aligned} \quad (6.98)$$

The complex exponential can now be broken down into its real and imaginary parts, giving

$$y(t) = 0.055784[\cos(3t - 1.54215) + j\sin(3t - 1.54215)] \quad (6.99)$$

and so the response to  $\cos(3t)$  will be

$$\text{Re}[y(t)] = 0.055784 \cos(3t - 1.54215) \quad (6.100)$$

and the response to  $\sin(3t)$  will be

$$\text{Im}[y(t)] = 0.055784 \sin(3t - 1.54215) \quad (6.101)$$

□

We can now make the following observation: Let the frequency response of an LTI network be (in polar form)

$$H(j\omega) = |H(j\omega)|e^{j\Theta(\omega)} \quad (6.102)$$

Then the response to the phasor  $e^{j\omega_0 t}$  will be

$$y(t) = H(j\omega_0)e^{j\omega_0 t} = |H(j\omega_0)|e^{j(\omega_0 t + \Theta(\omega_0))} \quad (6.103)$$

which is seen to be another phasor with magnitude  $|H(j\omega_0)|$  and phase shift  $\Theta(\omega_0)$ . This is summarized in the following theorem.

**■ THEOREM 6.4: Fundamental Theorem of Linear Circuit Analysis**

The response of an LTI network to a phasor is another phasor of the same frequency whose magnitude and phase shift are those of the network evaluated at that frequency.

This is depicted in Figure 6.11.

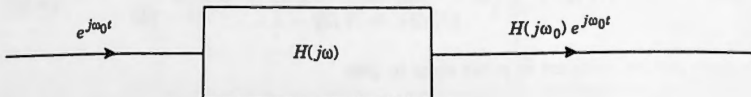


Figure 6.11. Complex exponential passing through an LTI system.

Observe from the theorem and the figure:

- A complex exponential goes in and a complex exponential comes out.
- Its form and frequency are unchanged.
- Its magnitude and phase shift are those of the network evaluated at its frequency.

**Complex exponentials (which include sines and cosines as well) are the only functions that pass through linear systems in this way. These are the central facts of LTI system behavior.**

## 6.4 RESPONSE OF A NETWORK TO A PERIODIC FUNCTION

We are dealing here with LTI systems and their associated CCL DEs of the form

$$P_1(D)y(t) = P_2(D)x(t) \quad (6.104)$$

in which  $P_1(D)$  and  $P_2(D)$  are polynomials in the operator  $D$ .

Equation (6.104) is a **linear transformation**. It takes the function  $x(t)$  and transforms it into the function  $y(t)$ , and it has the following **linearity property**:

**Definition:** "A system is linear" means: Let  $x_1(t)$  and  $x_2(t)$  have individual responses  $y_1(t)$  and  $y_2(t)$ . Then  $\alpha x_1(t) + \beta x_2(t)$  will have the response  $\alpha y_1(t) + \beta y_2(t)$ .

What this says is that a linear system can have multiple inputs acting simultaneously, and the response will be the same as if they were acting separately and then added.

The linearity of a CCL DE stems from the fact that differentiation is a linear operator. Thus, to prove that (6.104) is linear we proceed as follows: Let  $y_1(t)$  and  $y_2(t)$  be the individual responses to  $x_1(t)$  and  $x_2(t)$ , respectively, that is, let

$$P_1(D)y_1(t) = P_2(D)x_1(t) \quad (6.105)$$

$$P_1(D)y_2(t) = P_2(D)x_2(t) \quad (6.106)$$

Multiplying (6.105) by  $\alpha$  and (6.106) by  $\beta$  and adding, we obtain

$$\alpha P_1(D)y_1(t) + \beta P_1(D)y_2(t) = \alpha P_2(D)x_1(t) + \beta P_2(D)x_2(t) \quad (6.107)$$

We now use the properties of differentiation to rewrite this as

$$P_1(D)[\alpha y_1(t) + \beta y_2(t)] = P_2(D)[\alpha x_1(t) + \beta x_2(t)] \quad (6.108)$$

which shows that  $\alpha y_1(t) + \beta y_2(t)$  will be the response when the input is  $\alpha x_1(t) + \beta x_2(t)$ , and the proof is complete. ■

We saw in the preceding section that a complex exponential going into a linear circuit (or CCL DE) emerges as a complex exponential with its form unchanged. Only

its magnitude and phase may be altered. When the form of a function is unchanged by a transformation, it is called an **eigenfunction** of that transformation.

Complex exponentials are the eigenfunctions of CCL DEs and LTI electrical networks.

We now note the following central fact:

Fourier analysis has shown us that any periodic waveform can be represented as a linear combination of complex exponentials (subject to appropriate conditions).

Thus any acceptable periodic function can be represented by a Fourier series of the form

$$x_p(t) = \sum_{n=-\infty}^{\infty} X(n) e^{jn\omega_0 t} \quad (6.109)$$

Observe how (6.109) has restated  $x_p(t)$  as a sum of the **eigenfunctions** of LTI networks. Thus we should now easily be able to find the response of a network to such an input.

Consider just one of the complex exponentials in (6.109), that is  $X(n)e^{jn\omega_0 t}$  for some  $n$ . This is seen to be a **phasor**, and so we know immediately from (6.103) that the response will be

$$y_n(t) = H(jn\omega_0) X(n) e^{jn\omega_0 t} \quad (6.110)$$

We now note a critical fact: The network is linear, and so if the input is a **sum** of such phasors, then the output will be the **sum** of such responses. Since (6.109) is precisely a sum of phasors, the output must be precisely a sum of terms of the form (6.110). This gives us Theorem 6.5.

### ■ THEOREM 6.5: Response to a Periodic Waveform

Let the periodic waveform with Fourier series

$$x_p(t) = \sum_{n=-\infty}^{\infty} X(n) e^{jn\omega_0 t} \quad (6.111)$$

be the input to an LTI network whose frequency transfer function is  $H(j\omega)$ . Then the response will have Fourier series coefficients

$$Y(n) = H(jn\omega_0) X(n) \quad (\forall n) \quad (6.112)$$

and its Fourier series will be

$$y_p(t) = \sum_{n=-\infty}^{\infty} H(jn\omega_0) X(n) e^{jn\omega_0 t} \quad (6.113)$$

Observe how the frequency response, evaluated at each of the infinity of frequencies in (6.113), has insinuated itself into that equation. Compare this theorem to Theorem 6.2. They are almost identical, this one dealing with periodic waveforms, that one with pulses.

**EXAMPLE 6.6:** Find the expression for the output from the network shown in Figure 6.9 when the input is the periodic waveform

$$x_p(t) = \begin{cases} 0 & (-1 < t < -\frac{1}{2}) \\ 1 & (-\frac{1}{2} < t < \frac{1}{2}) \\ 0 & (\frac{1}{2} < t < 1) \end{cases} \quad x_p(t+2) = x_p(t)$$

**Solution:** The Fourier series for the periodic waveform is easily shown to be

$$x_p(t) = \frac{1}{2} \sum_{n=-\infty}^{\infty} \text{Sa} \frac{n\pi}{2} e^{jn\pi t} \quad (6.114)$$

and from (6.92) we know that the transfer function will be

$$H(j\omega_0) = \frac{2(j\omega_0) + 1}{12(j\omega_0)^2 + 7(j\omega_0) + 1} \quad (6.115)$$

From (6.113) the Fourier series for the output will thus be

$$\begin{aligned} y_p(t) &= \frac{1}{2} \sum_{n=-\infty}^{\infty} \left[ \frac{2(j\omega_0) + 1}{12(j\omega_0)^2 + 7(j\omega_0) + 1} \right]_{\omega_0 \leftarrow \frac{n\pi}{2}} \text{Sa} \frac{n\pi}{2} e^{jn\pi t} \\ &= \frac{1}{2} \sum_{n=-\infty}^{\infty} \frac{2(jn\pi) + 1}{12(jn\pi)^2 + 7(jn\pi) + 1} \text{Sa} \frac{n\pi}{2} e^{jn\pi t} \end{aligned} \quad (6.116)$$

It would almost certainly be impossible to sum this series in order to see what  $y_p(t)$  looks like. We know, however, that we can use the FFT system to find a numerical representation for  $y_p(t)$ . (Figure 6.6 works for periodic inputs as well. Just tell the FFT that the signal is PERIODIC.) Later we shall show a plot of the signal appearing in (6.116).  $\square$

## 6.5 FINDING THE TRANSFER FUNCTION FOR PULSES

In the first section of this chapter we showed how, given the CCL DE that describes the behavior of a network, we could find its response to any pulse that has a Fourier transform. The Fourier transform of the response was seen to be (cf. Theorem 6.2),

$$Y(\omega) = H(j\omega)X(\omega) \quad (6.117)$$

from which

$$y(t) = \frac{1}{2\pi} \int_{-\infty}^{\infty} H(j\omega) X(\omega) e^{j\omega t} d\omega \quad (6.118)$$

The expression for  $H(j\omega)$  in these equations was derived in Section 6.1 starting from the CCL DE for the network. That DE is seldom available, however, and can only be found with great effort unless the network in question is of trivial complexity.

We now show how the method of ac circuit analysis can be used to find  $H(j\omega)$  for the case when the input is any pulse that has a Fourier transform. (What we are about to do amounts to a reversal of the arguments that we used in Chapter 3 when we went from Fourier series to the Fourier integral, and so, as we did there, we shall only sketch out a sequence of plausibility arguments. A rigorous mathematical justification goes far beyond the scope of this book.)

Consider the pulse  $x(t)$  with Fourier transform  $X(\omega)$ . Then

$$x(t) = \frac{1}{2\pi} \int_{-\infty}^{\infty} X(\omega) e^{j\omega t} d\omega \quad (6.119)$$

We now revert to the form appearing in (3.13) before we let  $T_0$  there tend to  $\infty$ , namely

$$x(t) = \frac{1}{2\pi} \sum_{n=-\infty}^{\infty} X(\omega_n) e^{j\omega_n t} \delta\omega \quad (6.120)$$

from which we see once again that we are dealing with a sum of complex exponentials. The results of Sections 6.3 and 6.4 are thus immediately applicable.

Each complex exponential in (6.120) is an eigenfunction of the network that it is entering, and so each will have its response as given by the method of ac analysis. This is depicted in Figure 6.12. Observe in the figure that

- A complex exponential is going in and one comes out, multiplied by  $H(j\omega)$  evaluated at its frequency
- The expression for  $H(j\omega)$  is obtained using the method of ac circuit analysis

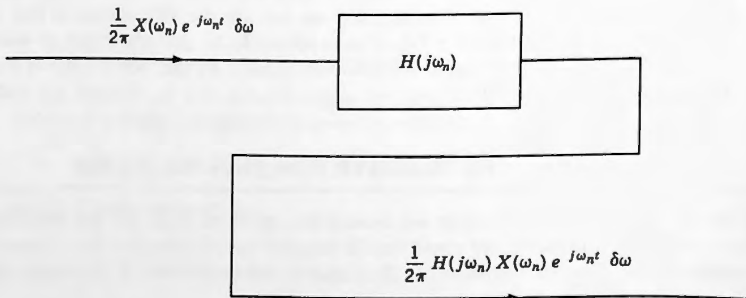


Figure 6.12.

We now invoke the linearity property of the network. If a sum of such complex exponentials is going in, then a sum will come out, each multiplied by  $H(j\omega)$  evaluated at its frequency. Thus if (6.120) is going in, then the response must be

$$y(t) = \frac{1}{2\pi} \sum_{n=-\infty}^{\infty} H(j\omega_n) X(\omega_n) e^{j\omega_n t} \delta\omega \quad (6.121)$$

As we did in Chapter 3 we now let  $\delta(\omega) \rightarrow 0$ . Then it seems reasonable that (6.121) will tend to

$$y(t) = \frac{1}{2\pi} \int_{-\infty}^{\infty} H(j\omega) X(\omega) e^{j\omega t} d\omega \quad (6.122)$$

which is the same result that we obtained earlier. However, now we know that  $H(j\omega)$  can be derived for pulses by using the ac-analysis approach, and so we are not hampered by the nonavailability of the network's CCL DE. Indeed, as we saw in Example 6.5, the DE can now be easily written down once  $H(j\omega)$  has been obtained in this way.

□EXAMPLE 6.7: For the network of Figure 6.9:

- (a) Find the expression for  $H(j\omega)$  using ac analysis
- (b) Use this result to find the CCL DE for the network
- (c) Find the response when the input is the single pulse

$$x(t) = \text{Rect}(t)$$

- (d) Find the response when the input is the same as the periodic waveform used in Example 6.6, but viewing it now as a single eternal pulse

**Solution:**

- (a) In Example 6.5 we saw that ac analysis gives us

$$H(j\omega) = \frac{2(j\omega) + 1}{12(j\omega)^2 + 7(j\omega) + 1} \quad (6.123)$$

- (b) To find the CCL DE relating the output to the input, we simply open up (6.123) and replace each  $j\omega$  by  $D$ , obtaining

$$[12D^2 + 7D + 1]y(t) = [2D + 1]x(t) \quad (6.124)$$

How do we know that this procedure is justified? Just Fourier transform (6.124) and we immediately obtain  $H(j\omega)$  as stated in (6.123).

Thus the operational rules for ac circuit analysis have now given us a quick and easy way to find the CCL DE for a network.

(c) For the single pulse input we have

$$\text{Rect}(t) \Leftrightarrow \text{Sa} \frac{\omega}{2} \quad (6.125)$$

and so, from (6.122), we have the response as

$$\begin{aligned} y(t) &= \frac{1}{2\pi} \int_{-\infty}^{\infty} H(j\omega) X(\omega) e^{j\omega t} d\omega \\ &= \frac{1}{2\pi} \int_{-\infty}^{\infty} \frac{2(j\omega) + 1}{12(j\omega)^2 + 7(j\omega) + 1} \text{Sa} \frac{\omega}{2} e^{j\omega t} d\omega \end{aligned} \quad (6.126)$$

If we so desire we can also then write

$$Y(\omega) = \frac{2(j\omega) + 1}{12(j\omega)^2 + 7(j\omega) + 1} \text{Sa} \frac{\omega}{2} \quad (6.127)$$

(d) Treating the periodic waveform of Example 6.6 as an eternal pulse, we obtain its Fourier transform (see Section 4.10) as

$$\begin{aligned} x_p(t) &= \frac{1}{2} \sum_{n=-\infty}^{\infty} \text{Sa} \frac{n\pi}{2} e^{jn\pi t} \\ \Leftrightarrow X_p(\omega) &= 2\pi \sum_{n=-\infty}^{\infty} X(n) \delta(\omega - n\omega_0) = \pi \sum_{n=-\infty}^{\infty} \text{Sa} \frac{n\pi}{2} \delta(\omega - n\pi) \end{aligned} \quad (6.128)$$

Then the transform of the response will be

$$\begin{aligned} Y_p(\omega) &= H(j\omega) X_p(\omega) \\ &= H(j\omega) \left[ \pi \sum_{n=-\infty}^{\infty} \text{Sa} \frac{n\pi}{2} \delta(\omega - n\pi) \right] \end{aligned} \quad (6.129)$$

in which each of the infinity of Dirac deltas in the square brackets samples  $H(j\omega)$ , and so we continue as

$$\cdots = \pi \sum_{n=-\infty}^{\infty} H(jn\pi) \text{Sa} \frac{n\pi}{2} \delta(\omega - n\pi) \quad (6.130)$$

We now invert to the time domain using synthesis, obtaining

$$y_p(t) = \frac{1}{2\pi} \int_{-\infty}^{\infty} \left[ \pi \sum_{n=-\infty}^{\infty} H(jn\pi) \text{Sa} \frac{n\pi}{2} \delta(\omega - n\pi) \right] e^{j\omega t} d\omega \quad (6.131)$$

in which sampling takes place once more, and so this continues as

$$\begin{aligned} \dots &= \frac{1}{2} \int_{-\infty}^{\infty} \left[ \sum_{n=-\infty}^{\infty} H(jn\pi) \text{Sa} \frac{n\pi}{2} e^{jn\pi t} \delta(\omega - n\pi) \right] d\omega \\ &= \frac{1}{2} \sum_{n=-\infty}^{\infty} H(jn\pi) \text{Sa} \frac{n\pi}{2} e^{jn\pi t} \int_{-\infty}^{\infty} \delta(\omega - n\pi) d\omega \\ &= \frac{1}{2} \sum_{n=-\infty}^{\infty} H(jn\pi) \text{Sa} \frac{n\pi}{2} e^{jn\pi t} \end{aligned} \quad (6.132)$$

which is the same as (6.116), as of course it should be.  $\square$

Observe how the method of ac circuit analysis serves as the key to finding the response of an LTI network when the input is

- A complex exponential
- A pulse
- A periodic waveform

**EXAMPLE 6.8:** Use the FFT system to plot the response of the network considered in Examples 6.6 and 6.7 for the cases where:

- The pulse input is  $x(t) = \text{Rect}(t/32)$
- The periodic input is

$$x(t) = \sum_{n=-\infty}^{\infty} \text{Rect} \frac{t - nT}{32} \quad (T = 128)$$

In Figures 6.13 and 6.14 we show plots of the responses for the two cases that we considered in Examples 6.6 and 6.7, based on the FFT block diagram of Figure 6.6, with  $N = 1024$  and  $T = 128$ .

The frequency transfer function was

$$H(j\omega) = \frac{2(j\omega) + 1}{12(j\omega)^2 + 7(j\omega) + 1}$$

- For Figure 6.13, the input was the pulse

$$x(t) = \text{Rect} \frac{t}{32}$$

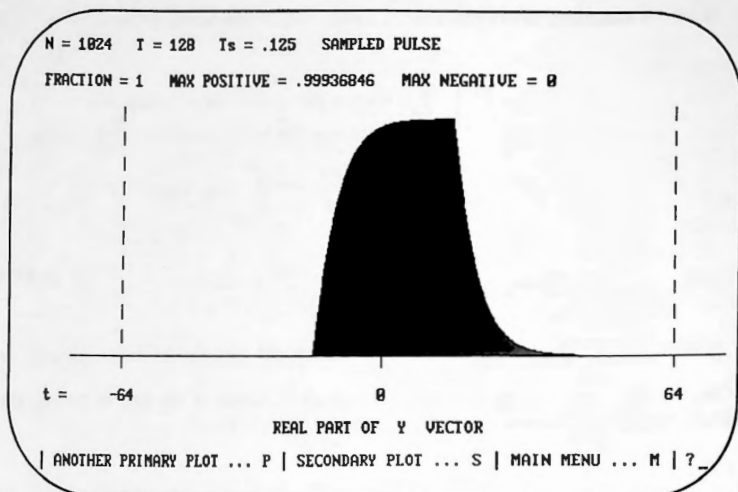


Figure 6.13. Response to pulse.

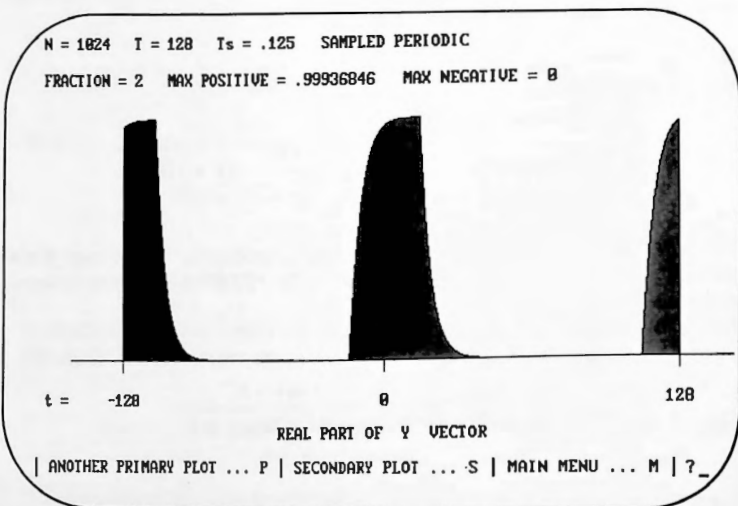


Figure 6.14. Response to periodic waveform.

- For Figure 6.14, the input was the periodic waveform

$$x_p(t) = \sum_{n=-\infty}^{\infty} \text{Rect} \frac{t - nT}{32} \quad (T = 128)$$

□

## EXERCISES

- 6.1 Theorem 5.1 enables us to prove a very powerful proposition that is applicable to linear systems, namely:

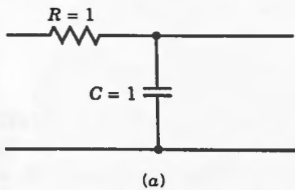
**■ THEOREM 6.6**

If  $y(t)$  is the response of a linear system to an input  $x(t)$ , then  $y'(t)$  will be the response to the input  $x'(t)$ .

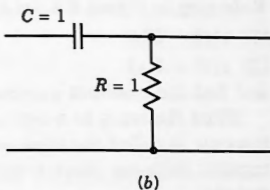
Prove this proposition.

*Hint:* Do it in the frequency domain.

- 6.2 (a) For each of the networks shown in Figure 6.15, find and sketch the response when the input is
- $\delta(t)$
  - $U(t)$
- (b) The input  $\delta(t)$  is the derivative of the input  $U(t)$ . According to Theorem 6.6 the response to  $\delta(t)$  should be the derivative of the response to  $U(t)$ . Verify that this is so for both networks in Part (a) of this exercise.



(a)



(b)

Figure 6.15.

- 6.3 The equation

$$De^{j\omega t} = j\omega e^{j\omega t} \quad (6.133)$$

is the most obvious example of the fact that  $e^{j\omega t}$  is an eigenfunction of  $D$  with eigenvalue  $j\omega$ . It has exactly the same structure as the linear algebra statement

$Ax = \lambda x$ . Prove that (6.133) and Theorem 5.1 are fully equivalent, giving us Theorem 6.7.

■ THEOREM 6.7

The eigenfunction statement

$$De^{j\omega t} = j\omega e^{j\omega t}$$

is equivalent to the statement

$$Df(t) \Leftrightarrow j\omega F(\omega)$$

Thus each implies the other.

*Hint:* Start from (6.133), multiply both sides by  $F(\omega)$ , and then apply the synthesis equation for pulses.

6.4 Solve the following CCL DEs using Fourier transforms.

(a)  $y'' + 4y' + 3y = x' + 5x \quad (\forall t)$

where  $x(t) = e^{-2t}U(t)$

(b)  $y'' + 4y' + 5y = 3x' + x \quad (\forall t)$

where  $x(t) = (1 + e^{-t})U(t)$

(c) Use the FFT system to verify the result you obtained in (a).

(d) Verify the result that you obtained in (b) analytically by applying the DE to it.

6.5 (a) Referring to Figure 6.4, let the input voltage be

(1)  $x(t) = U(t)$

(2)  $x(t) = \delta(t)$

and find the resultant expressions for  $y(t)$  in each case.

When the input to a system is the unit impulse  $\delta(t)$ , as in Part (a)(2), the response is called the **impulse response**. In the next chapter we see that the impulse response plays a central role in the **time-domain** analysis of LTI systems.

(b) Verify your solutions analytically by applying the system DE to them.

(c) Use the FFT system to verify the result you obtained in Part (a)(2) of this exercise.

6.6 (a) Derive the CCL DE that links the input and output for the network shown in Figure 6.16.

(b) Assuming that  $x(t)$  is the complex exponential  $e^{j\omega_0 t}$ , derive the expression for  $H(j\omega_0)$  from the CCL DE that you have obtained in (a), using Fourier transformation.

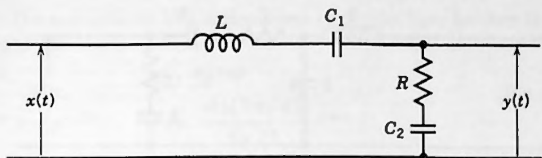
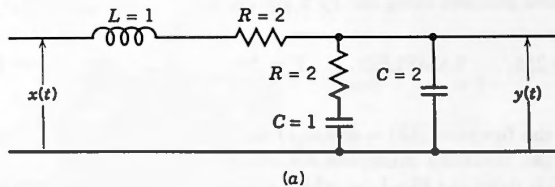


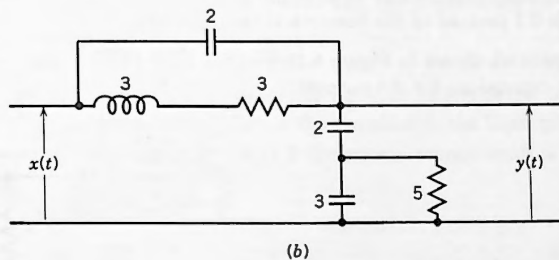
Figure 6.16.

- (c) Now find the frequency response  $H(j\omega)$  by the method of ac circuit analysis, that is, by replacing inductors by  $j\omega_0 L$  and capacitors by  $1/j\omega_0 C$ .
- (d) Starting from the frequency response obtained in (c), write the CCL DE for the system.
- 6.7 Use the method of ac circuit analysis for each of the following three LTI systems (Fig. 6.17–6.19) to obtain
- (1) The input impedance
  - (2) The frequency response
  - (3) The CCL DE that relates the output to the input



(a)

Figure 6.17.



(b)

Figure 6.18.

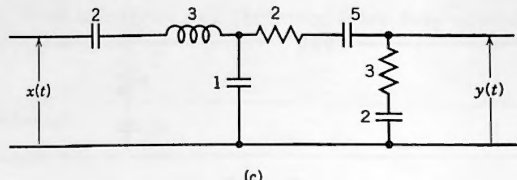


Figure 6.19.

**6.8** Referring to Figure 6.4, let the input voltage be

$$x(t) = \cos(\omega_0 t) \quad (\forall t)$$

Find the resulting expression for  $y(t)$  in two ways:

- Starting from the CCL DE and solving it with  $x(t)$  as the forcing function.
- Applying the rules of ac circuit analysis.
- Verify analytically that the result that you have obtained in (a) or (b) satisfies the system DE.
- When you have obtained the expression for  $y(t)$ , let the input frequency be 0.2 hertz and reduce the answer to the form  $y(t) = K \cos(\omega_0 t - \Theta)$ , finding the values for  $K$  and  $\Theta$ .
- Run this problem using the FFT system with the following parameters:

$$N = 256, \quad \text{SAMPLED}, \quad T = 100, \quad \omega_0 = 0.04\pi, \quad \text{PERIODIC}$$

Load the function  $x(t) = \cos(\omega_0 t)$  into X. Load  $H(j\omega)$  starting from main menu A. You'll be prompted for the required aliasing level, and because  $H(j\omega)$  is dying out like  $1/\omega$ , which is slow, you must use a fairly large value. Use 20. Then run ANALYSIS, followed by COMPLEX MULTIPLY (in the F postprocessor) followed by SYNTHESIS. A plot of Y should show you the cosine in the form  $K \cos(\omega_0 t - \Theta)$ . Determine the value of  $K$ , and from the numbers (main menu I), determine the value of  $\Theta$ . They should both be within 0.1 percent of the theoretical result in (d).

**6.9** For the network shown in Figure 6.20 and for each of the inputs shown below, write the expressions for the outputs.

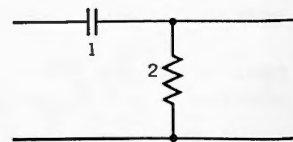


Figure 6.20.

*Note:* Do not reduce the expressions once you have written them unless you really want to.

(a)  $3e^{j7t}$

(b)  $5e^{-j3t}$

(c)  $3e^{j7t} + 5e^{-j3t}$

(d)  $\frac{\sin(5\pi/2)}{5\pi/2} e^{j5\pi t/2}$

(e) 
$$\sum_{n=-\infty}^{\infty} \frac{\sin(n\pi/2)}{n\pi/2} e^{jn\pi t/2}$$

What is the  $n = 5$  term in the series for the output in (e)? What is the  $n = -9$  term?

(f) 
$$\frac{1}{2\pi} \int_{-\infty}^{\infty} \frac{2a}{a^2 + \omega^2} e^{j\omega t} d\omega$$

(g) 
$$\sum_{n=-\infty}^{\infty} \frac{2/\pi}{(1-4n^2)} e^{j2\pi nt} + \frac{1}{2\pi} \int_{-\infty}^{\infty} e^{-a|\omega|} e^{j\omega t} d\omega$$

### 6.10 Let

$$x(t) = \sum_{n=-\infty}^{\infty} \frac{(-1)^n - 1}{1+n^2} e^{j3nt}$$

Then the complete expression for  $x_1(t)$  is

$$x_1(t) = -\frac{2}{2} e^{j3t} \quad \text{and} \quad \omega_1 = 3$$

- (a) Write the expressions for  $x_5(t)$ ,  $x_{15}(t)$ ,  $x_{-3}(t)$ , and  $x_{-7}(t)$  together with their respective values of  $\omega$ .
- (b) What is the frequency transfer function for the network of Figure 6.16 when  $L = 2$ ,  $C_1 = 2$ ,  $C_2 = 2$ , and  $R = 3$ ?
- (c) Assuming that the input voltage to the network of part (b) is each of the four terms in part (a) **individually**, write out the expressions for the resultant  $y_n(t)$ 's.

*Note:* Do not reduce the results.

- (d) What is the expression for  $y(t)$  if the four components are first added together and the resulting sum is then applied to the input port?
- (e) What is the expression for  $y(t)$  if the entire infinite series is applied as an input?

### 6.11 For the CCL DE

$$y'' + 4y' + 5y = 3x' + x \quad (\forall t)$$

the forcing function is the periodic waveform

$$x_p(t) = \begin{cases} 1 & (0 < t < 1) \\ 0 & (1 < t < 2) \end{cases} \quad x(t+2) = x(t)$$

- (a) Find the Fourier series for  $y(t)$ .
- (b) Find the values for  $A(n)$ ,  $B(n)$ ,  $|Y(n)|$ ,  $\Theta(n)$ , and  $P(n)$  [the real part, imaginary part, magnitude, phase, and power of  $Y(n)$ ] for  $-3 \leq n \leq 3$ , where  $Y(n)$  is the  $n$ th coefficient in the Fourier series of  $y(t)$ .
- (c) Use the FFT system to verify the numerical values that you obtained in (b). Use  $N = 256$ , SAMPLED,  $T = 2$ , PERIODIC, alias-level 20.
- (d) Use the FFT system to draw plots of the input and output.

**6.12** Prove that when two networks are cascaded in such a way that there is no loading, the magnitudes of their frequency responses multiply and their phases add.

- (a) Do this first using polar notation, that is,

$$H(j\omega) = |H(j\omega)|e^{j\Theta(\omega)}$$

- (b) Now prove the same result using Cartesian notation, that is,

$$H(j\omega) = A(\omega) + jB(\omega)$$

**6.13** Let  $T_1$  and  $T_2$  be the LTI transformations

$$T_1: \quad P_1(D)[\text{output}_1] = P_2(D)[\text{input}_1]$$

and

$$T_2: \quad Q_1(D)[\text{output}_2] = Q_2(D)[\text{input}_2]$$

in which  $P_1$ ,  $P_2$ ,  $Q_1$ , and  $Q_2$  represent polynomials with constant coefficients.

- (a) Prove that if the output from  $T_1$  is used as the input to  $T_2$ , the result is the overall LTI transformation

$$T_2 T_1: \quad P_1(D)Q_1(D)[\text{output}] = P_2(D)Q_2(D)[\text{input}]$$

- (b) Verify that the same result would be obtained if the output from  $T_2$  is used as the input to  $T_1$ , that is, that

$$T_1 T_2 = T_2 T_1$$

*Note:* This is an exceptional occurrence in the theory of linear transformations, since in general two such transformations do **not** commute. However, polynomials in  $D$  do commute when the coefficients are constant.

- (c) Infer that if two LTI networks with frequency responses  $H_1(j\omega)$  and  $H_2(j\omega)$  are cascaded in such a way that the second does not in any way load the first, then the order of the cascade is immaterial, that is, that the result is an LTI network with frequency response either

$$H_1(j\omega)H_2(j\omega) \quad \text{or} \quad H_2(j\omega)H_1(j\omega)$$

- 6.14 The network in Figure 6.21 comprises the two networks shown, connected together using an isolation amplifier whose gain is unity. The net result is that the second network does not impose a load on the first, and so the individual frequency responses are unaffected.

- (a) What is the frequency response for the overall network?  
 (b) For each of the inputs shown below, write the expression for the output. Note: Do not reduce the results.

$$(1) 3e^{j7t}$$

$$(2) 2e^{-j5t}$$

$$(3) 3e^{j7t} + 2e^{-j5t}$$

$$(4) j \frac{\sin(5\pi/2)}{5\pi/2} e^{j5\pi t/2}$$

$$(5) \sum_{n=-\infty}^{\infty} j \frac{\sin(n\pi/2)}{n\pi/2} e^{jn\pi t/2}$$

What is the  $n = 5$  term in the series for the output? What is the  $n = -7$  term?

$$(6) \frac{1}{2\pi} \int_{-\infty}^{\infty} \frac{2a}{a^2 + \omega^2} e^{j\omega t} d\omega$$

$$(7) \frac{1}{2\pi} \int_{-\infty}^{\infty} e^{-a|\omega|} e^{j\omega t} d\omega + \sum_{n=-\infty}^{\infty} \frac{2}{\pi(1-4n^2)} e^{j2\pi nt}$$

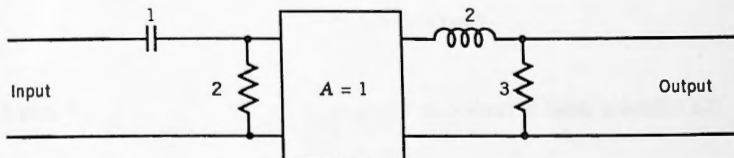


Figure 6.21.

### Two Projects Involving The FFT System

- 6.15 (a) For the periodic function

$$x_p(t) = |t| \quad (-1 < t < 1), \quad x_p(t+2) = x_p(t)$$

find  $X(\omega)$ , the Fourier transform of  $x_p(t)$ .

- (b) Sketch  $x_p(t)$ , its line spectrum  $X_p(n)$ , and its Fourier transform  $X(\omega)$ .  
 (c) Confirm what you have done in (a) and (b) by using the FFT system with  $N = 1024$ .  
 (d) Now let  $x_p(t)$  be the input to the circuit shown in Figure 6.22 and let  $y_p(t)$  be the output. Derive the expression for the Fourier series representation of  $y_p(t)$  in two ways:  
   (1) By starting from the Fourier series of  $x_p(t)$   
   (2) By starting from the Fourier transform of  $x_p(t)$   
 (e) Starting from the Fourier coefficients  $Y(n)$  obtained in (d), use a hand calculator to derive the values for

$$\operatorname{Re}[Y_p(n)], \quad \operatorname{Im}[Y_p(n)], \quad |Y_p(n)|, \quad \Theta_p(n), \quad P_p(n)$$

for  $-3 \leq n \leq 3$ .

- (f) Use the FFT system to verify the results that you obtained in (e).  
 (g) At what rate are the Fourier coefficients  $Y_p(n)$  going to zero for large  $n$ ?  
 (h) Use the FFT system to plot  $y_p(t)$ , the output from the circuit. Does the plot appear to confirm what you reported in (g)?  
 (i) Starting from main menu G, use the F postprocessor to form the second derivative of  $y_p(t)$ . (Refer to Section 17.1.) Does a plot of  $y_p''(t)$  appear to confirm what you reported in (g)? Now form the third derivative and plot it. Does it do what you expected it to?

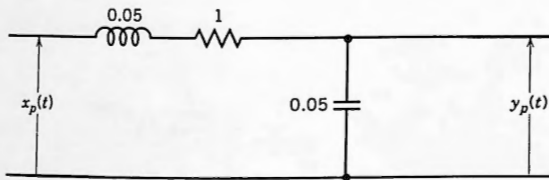


Figure 6.22. RLC integrator.

**6.16** The following pulse is applied as an input to the RLC network of Figure 6.22:

$$x(t) = \begin{cases} 1 & (0 < t < 1) \\ -1 & (1 < t < 2) \\ 0 & \text{otherwise} \end{cases}$$

- (a) Find the expressions for  $X(\omega)$ ,  $Y(\omega)$ , and  $y(t)$ .  
   (1) At what rate is  $X(\omega)$  dying out? What does this tell you about  $x(t)$ ? Is this consistent with the definition of  $x(t)$ ?  
   (2) At what rate is  $Y(\omega)$  dying out? What does this tell you about  $y(t)$ ?

- (b) Find the expressions for the real and imaginary parts of  $X(\omega)$  and of its magnitude and phase spectra. Display a table of numerical samples of these functions taken at  $\omega = n\omega_0$  for  $-3 \leq n \leq 3$ , where  $\omega_0 = 2\pi/T$  and  $T = 8$ .
- (c) Sample  $H(j\omega)$  at the same values of  $\omega$  as in (b) and display a table of numerical values of  $|H(j\omega)|$  and  $\Theta_H(\omega)$  for  $-3 \leq n \leq 3$ .
- (d) Combine the results of the two tables to give a table of  $|Y(\omega)|$  and  $\Theta_Y(\omega)$  for  $\omega = n\omega_0$  as in (b).
- (e) Using the FFT system on the disk, compare the numerical values obtained from the FFT system with those that you obtained in (d). Load the pulse using  $N = 512$  and  $T = 8$ . For  $H(j\omega)$ , use  $\text{ALPHA} = 0$ .
- (f) Obtain plots of  $y(t)$ ,  $y'(t)$ , and  $y''(t)$ , and verify that the first two are everywhere continuous but the third one is not, confirming the result from (a)(2). Use  $N = 512$ ,  $T = 8$ , but for  $H(j\omega)$ , use  $\text{ALPHA} = 50$ .

*Note:* The differentiation facilities are included in the F postprocessor. (See Section 17.1.) To investigate the continuity of  $y(t)$  at the origin you can expand the scale of the displays, using smaller values for FRACTION in the plotting facility.

# Time-Domain Analysis

## 7.1 INTRODUCTION

Fourier analysis has come a long way from the flow of heat to the response of linear, time-invariant (LTI) networks, and the techniques that Fourier discovered regarding the solution of partial differential equations (PDEs) have undergone a radical change of emphasis in order for them to be of use today in electrical engineering.

- Fourier did not require that his Fourier series be periodic, only that they be comprised of sines or cosines. For him they were initial conditions on a heated rod of finite length. For us, however, they can be made to represent repeating electrical waveforms and it is precisely their inherent periodicity that makes them so useful for that purpose.
- The functions that he transformed using his Fourier integrals were initial conditions on a heated rod of infinite length, functions of the variable  $x$ . By contrast, in our work here they are one-time pulses, functions of the variable  $t$  instead of  $x$ , and not necessarily of infinite duration.
- Theorem 5.1, namely  $f'(t) \leftrightarrow j\omega F(\omega)$ , did not form a central result for the problems that Fourier addressed, and in fact he does not appear to have used it at all. In Chapter 6, however, we saw that the entire application of Fourier analysis to LTI networks hinges on that theorem.

It is not easy to establish precisely who it was that first took Fourier's (and Laplace's) results and redirected them to the types of problems that we encounter today in electrical engineering. Clearly Kelvin applied much of what Fourier had discovered regarding the use of Fourier series and integrals to the solution of PDEs, but Kelvin's interest was in the telegraph equation and not in electrical networks.

We suspect that it was Oliver Heaviside who was the major innovator in this regard. Like Kelvin,<sup>†</sup> he was an expert in Fourier's techniques and also held him in great esteem. To quote from his writings:

No one admires Fourier more than I do. It is the only entertaining mathematical work I ever saw. Its lucidity has always been admired. But it was more than lucid. It was luminous. Its light showed a crowd of followers the way to a heap of new problems. (Nahin)

<sup>†</sup>Heaviside (1850–1925) was 26 years younger than Kelvin.

Heaviside devoted almost his entire life to the application of mathematics to electrical engineering, and among his many skills was his deep insight into the behavior of LTI networks. We know for sure that it was he who invented the method of ac circuit analysis discussed in the previous chapter, and what we now call the unit step is still known in many places as the **Heaviside function**. One cannot but help surmise that he may also have been the first to use the fact that Fourier's series and integrals, by enabling us to resolve periodic and pulse waveforms into sums of complex exponentials, can serve as ideal tools for finding the response of electrical networks to a variety of inputs.

In this chapter we shall come to know another highly important mathematical tool called the **convolution integral**. Closely related to the Fourier transform, we shall soon see why it finds such widespread application in today's world of electrical engineering.

The convolution integral comes to us from the field of probability and was first used by Laplace (Stigler), who, as we noted earlier, was also the discoverer of the complex Fourier integral, as well as of complex Fourier series. Thus Laplace scores three out of three: complex Fourier series, the complex form of the Fourier integral, and convolution. Fourier's name, however, will be forever linked to the first two because of the way in which he used their real forms to solve PDEs.

As with Fourier series and the Fourier integral, we suspect that it was also Heaviside who first applied convolution to the analysis of electrical networks.

## 7.2 THE IMPULSE RESPONSE

---

In Chapter 6 we examined how Fourier series and the Fourier transform can be applied to the analysis of LTI systems that have pulse or periodic waveforms as their inputs. Essentially all of what we did there was done in the **frequency domain**. In this chapter we examine LTI networks once again, but this time we do it in the **time domain**.

The central result of Chapter 6 was equation (6.14), namely

$$Y(\omega) = H(j\omega)X(\omega) \quad (7.1)$$

which is the frequency-domain relationship between the input, the frequency response, and the output. Let's now take another look at that equation, but this time examining it in the time domain.

We know that the time-domain representation of  $Y(\omega)$  in (7.1) is  $y(t)$ , and that the time-domain representation of  $X(\omega)$  would be  $x(t)$ , but up to now we have not thought in terms of the time-domain representation of the term  $H(j\omega)$ . Clearly there must be one, and we now investigate precisely what it is.

**Problem Statement:** What does the time domain representation of  $H(j\omega)$  in (7.1) mean?

The answer is one that is intricately bound up with LTI systems analysis in the time domain and, as we now show, will lead to some extremely valuable results. Let the

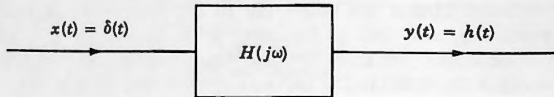


Figure 7.1.

time-domain representation of  $H(j\omega)$  be called  $h(t)$ . Then

$$H(j\omega) \leftrightarrow h(t) \quad (7.2)$$

by which we mean that  $h(t)$  is the Fourier inverse of  $H(j\omega)$ , that is,

$$h(t) = \frac{1}{2\pi} \int_{-\infty}^{\infty} H(j\omega) e^{j\omega t} d\omega \quad (7.3)$$

Referring to Figure 7.1, suppose now that we let the input to an LTI network whose frequency response is  $H(j\omega)$  be a Dirac delta, that is,  $x(t) = \delta(t)$ . Then  $X(\omega) = 1$ , and so (7.1) becomes

$$Y(\omega) = H(j\omega) \quad (7.4)$$

from which

$$y(t) = h(t) \quad (7.5)$$

Thus, when  $x(t)$  is a unit impulse the response will be the quantity that we have called  $h(t)$ . This gives us Theorem 7.1 below.

**THEOREM 7.1:** Let  $H(j\omega)$  be the frequency response of an LTI system. Then its inverse transform

$$h(t) = \frac{1}{2\pi} \int_{-\infty}^{\infty} H(j\omega) e^{j\omega t} d\omega \quad (7.6)$$

will be the network's response when the input is a unit impulse.

We encounter  $h(t)$  frequently in what lies ahead and so we give it a name.

**Definition:** The inverse transform of a network's frequency response is called the **impulse response** of the network.

**EXAMPLE 7.1:** Find the impulse responses for the two LTI networks shown in Figure 7.2.

For Network (a):

$$H(j\omega) = \frac{R}{R + j\omega L} = \frac{R}{L} \frac{1}{R/L + j\omega} = \beta \frac{1}{\beta + j\omega} \quad (7.7)$$

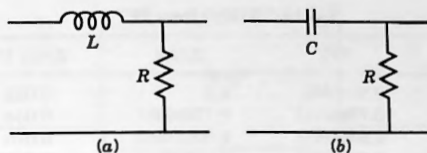


Figure 7.2. Two LTI networks.

where  $\beta = R/L$ . Since any physically realizable  $R$  and  $L$  will always both be positive, it follows that  $\beta$  will also always be positive. We can thus obtain the network's impulse response by inverting (7.7) to give

$$h(t) = \beta e^{-\beta t} U(t) = \frac{R}{L} e^{-Rt/L} U(t) \quad (7.8)$$

Thus  $h(t)$  for Network (a) is seen to be a single-sided decaying exponential.

For Network (b):

$$\begin{aligned} H(j\omega) &= \frac{R}{R + 1/j\omega C} = \frac{j\omega RC}{1 + j\omega RC} \\ &= 1 - \frac{1}{RC} \frac{1}{1/RC + j\omega} = 1 - \beta \frac{1}{\beta + j\omega} \end{aligned} \quad (7.9)$$

where  $\beta = 1/RC$  and is thus always positive for all realizable  $R$  and  $C$ . The impulse

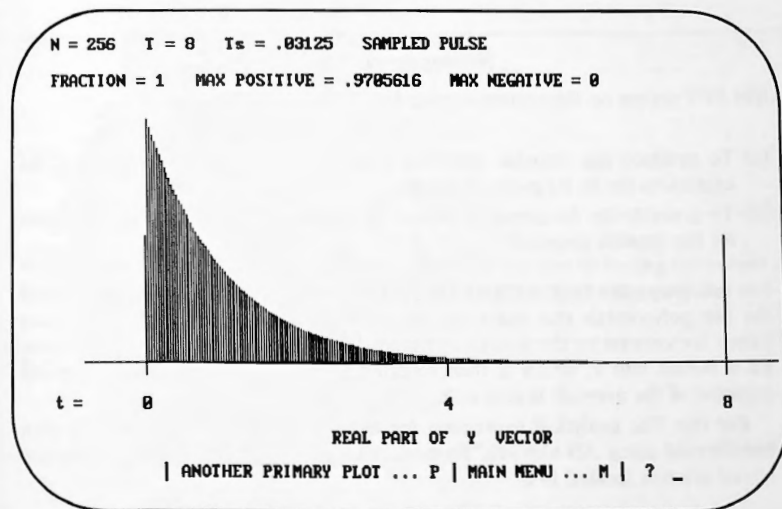
Figure 7.3. Impulse response  $h(t)$ .

TABLE 7.1  $h(t)$  from FFT

<i>k</i>	FFT	Exact	Error (%)
0	0.5001848	0.5	0.037
8	0.77846097	0.77880097	0.044
16	0.60643653	0.60653066	0.016
32	0.36785995	0.36787944	0.0053
64	0.13532149	0.13533528	0.01
128	0.018321785	0.018315639	0.034

Note: One unit on the *k*-scale equals  $T/N = 0.03125$  seconds. Also,  $N = 256$ ,  $T = 8$ .

response will be

$$h(t) = \delta(t) - \frac{1}{RC} e^{-t/RC} U(t) \quad (7.10)$$

which is seen to be a Dirac delta together with a negative single-sided decaying exponential.  $\square$

In Figure 7.3 we show a plot of  $h(t)$  for Network (a) of Figure 7.2, obtained by using the system with  $R = L = 1$ . In Table 7.1 we show a comparison between the exact and the fast Fourier transform (FFT) derived numerical values for  $h(t)$ .

#### Accompanying Disk

The FFT system on the accompanying disk can be used

- (a) To produce the impulse response of an LTI system starting from the expression for its frequency response.
- (b) To generate the frequency response, starting from an analytical expression for the impulse response.

**For (a):** Using the facility CREATE  $H(j\omega)$  (main-menu A) the coefficients of the two polynomials that make up  $H(j\omega)$  are loaded, from which numerical values are created by the system and placed in F2. Using the F postprocessor, F2 is moved into F, which is then inverted using SYNTHESIS. The impulse response of the network is now in Y.

**For (b):** The analytical expression for  $h(t)$  is loaded into X, which is then transformed using ANALYSIS. Numerical values of the frequency response  $H(j\omega)$  are now located in F.

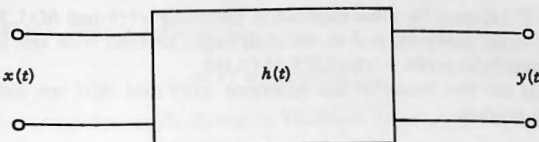


Figure 7.4. Input, output, and impulse response.

### 7.3 CONVOLUTION

The convolution integral is central to the entire field of Fourier analysis. It is simplicity itself once understood, and in what follows we shall try to explain what it is all about. Consider an LTI system with input  $x(t)$ , output  $y(t)$ , and impulse response  $h(t)$ , as shown in Figure 7.4. Here's a statement of the problem that we are setting out to solve.

**Problem Statement:** What is the time-domain expression for  $y(t)$  in terms of  $x(t)$  and  $h(t)$ ?

**Answer:** Since the network is LTI there is a constant-coefficient linear differential equation (CCL DE) that relates  $y(t)$  to  $x(t)$  of the form

$$P_1(D)y(t) = P_2(D)x(t) \quad (7.11)$$

As we saw in Chapter 6, this quickly leads to

$$Y(\omega) = H(j\omega)X(\omega) \quad (7.12)$$

where

$$H(j\omega) \leftrightarrow h(t) \quad (7.13)$$

We are seeking  $y(t)$ , so from (7.12) the answer clearly lies in finding the inverse of the product  $H(j\omega)X(\omega)$ . Here's a mathematical statement of the problem:

**Problem Statement**

$$\frac{1}{2\pi} \int_{-\infty}^{\infty} H(j\omega)X(\omega)e^{j\omega t} d\omega = ? \quad (7.14)$$

The answer to (7.14) must be some expression involving  $x(t)$  and  $h(t)$ . Its form is not immediately obvious, however, and so we shall begin instead with the known answer and work backwards to arrive at the LHS of (7.14).

Starting from the two time-domain functions  $x(t)$  and  $h(t)$  we form the rather strange looking product

$$x(\tau)h(t - \tau) \quad (7.15)$$

(We'll soon see exactly what this means.) Then we form the integral of this quantity:

$$\int_{-\infty}^{\infty} x(\tau)h(t - \tau) d\tau \quad (7.16)$$

Clearly this integral must be a function of  $t$  since  $\tau$  is a dummy variable that disappears under the integration, but for the moment we cannot see what that time function is. We now find the Fourier transform of (7.16), and on the following page we prove that it is precisely  $X(\omega)H(j\omega)$ . This enables us to state the following result:

■ THEOREM 7.2: Time-domain convolution

$$\int_{-\infty}^{\infty} x(\tau)h(t - \tau) d\tau \Leftrightarrow X(\omega)H(j\omega) \quad (7.17)$$

We have thus shown that the integral on the LHS of (7.17) is the inverse of  $H(j\omega)X(\omega)$ . By (7.12), however,  $y(t)$  is also the inverse of  $H(j\omega)X(\omega)$ , and so the answer to our question must be

$$y(t) = \int_{-\infty}^{\infty} x(\tau)h(t - \tau) d\tau \quad (7.18)$$

**Definition:** Given  $h(t)$  and  $x(t)$ , the integral shown in (7.16) is called their convolution product, and for ease of notation we use an asterisk, and write

$$x(t) * h(t) \equiv \int_{-\infty}^{\infty} x(\tau)h(t - \tau) d\tau \quad (7.19)$$

Equation (7.18) can now be written as

$$y(t) = x(t) * h(t) \quad (7.21)$$

We have thus proved the result shown as Theorem 7.3.

*Proof of Theorem 7.2*

$$\begin{aligned}
 & \int_{-\infty}^{\infty} \left[ \int_{-\infty}^{\infty} x(\tau) h(t - \tau) d\tau \right] e^{-j\omega t} dt \longrightarrow \\
 & \qquad \qquad \boxed{\text{Reverse the order of integration by bringing out } x(\tau) \text{ and } d\tau \text{ and sliding } e^{-j\omega t} \text{ and } dt \text{ to the left}} \\
 & \longrightarrow = \int_{-\infty}^{\infty} \left[ \int_{-\infty}^{\infty} h(t - \tau) e^{-j\omega t} dt \right] x(\tau) d\tau \\
 & \qquad \qquad \boxed{\text{Now let } t - \tau = z \\
 & \text{Then } t = z + \tau \\
 & \text{and } dt = dz} \\
 & \longrightarrow = \int_{-\infty}^{\infty} \left[ \int_{-\infty}^{\infty} h(z) e^{-j\omega z} dz \right] e^{-j\omega \tau} x(\tau) d\tau \\
 & \qquad = \int_{-\infty}^{\infty} [H(j\omega)] x(\tau) e^{-j\omega \tau} d\tau \\
 & \qquad = H(j\omega) \int_{-\infty}^{\infty} x(\tau) e^{-j\omega \tau} d\tau = H(j\omega) X(\omega) \quad (7.20)
 \end{aligned}$$

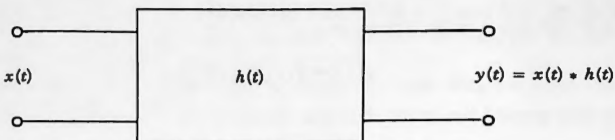


Figure 7.5. Input, output, and impulse response.

■ **THEOREM 7.3:** Let  $x(t)$  be the input to a system whose impulse response is  $h(t)$ . Then, in the frequency domain

$$Y(\omega) = H(j\omega)X(\omega) \quad (7.22)$$

and in the time domain

$$y(t) = x(t) * h(t) \quad (7.23)$$

Observe how ordinary multiplication in the frequency domain in (7.22) has been replaced by convolution in the time domain in (7.23). Thus:

Convolution gives us a complete alternative to the frequency-domain techniques of Chapter 6 for finding the response of an LTI network to an input function. As shown in (7.23), convolution does it in the time domain.

*Note:* We are only considering the case where the input is a pulse. In Chapter 14 we examine what is called "circular convolution," in which the input is a periodic function.

Our problem is now solved, and Figure 7.4 can be extended as shown in Figure 7.5.

#### 7.4 WHAT DOES THE CONVOLUTION PRODUCT MEAN?

In the preceding section we derived the time-domain statement:

$$y(t) = \int_{-\infty}^{\infty} x(\tau)h(t - \tau) d\tau \quad (7.24)$$

We now try to explain what this integral means.

Consider the pulse  $x(t)$  appearing in Figure 7.6. As shown, we have overlaid a rectangle whose left side touches  $x(t)$  at  $t = \tau_k$ , with width  $\Delta\tau$ . Then the area of the rectangle is  $x(\tau_k)\Delta\tau$ . We now create a Dirac delta located at  $t = \tau_k$  whose weight is equal to the area of that rectangle. Thus, letting that impulse be called  $x_k(t)$ , we form

$$x_k(t) = x(\tau_k)\Delta\tau\delta(t - \tau_k) \quad (7.25)$$

This is displayed in Figure 7.7. At this stage we decide to send this single impulse into the LTI system whose impulse response is  $h(t)$ . (See Fig. 7.8.) In order to obtain the

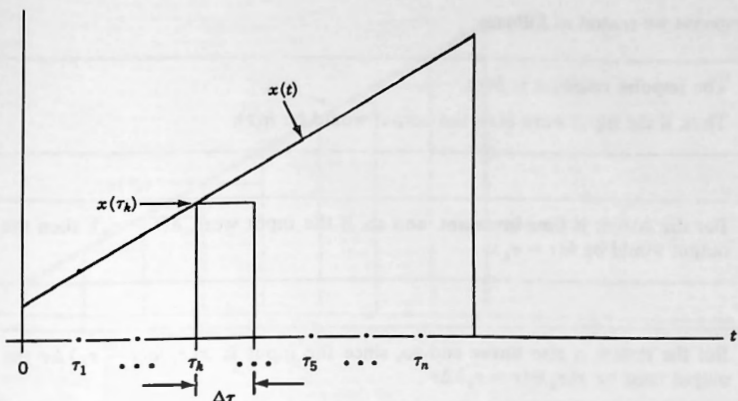
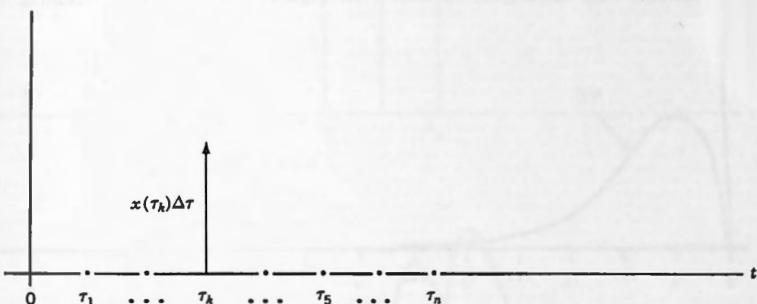
Figure 7.6. Single rectangle overlaid on  $x(t)$ .

Figure 7.7. Single impulse.

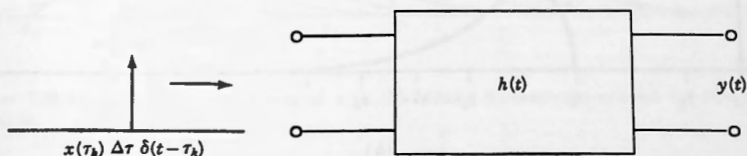


Figure 7.8. Single impulse entering a network.

response we reason as follows:

The impulse response is  $h(t)$ .

Thus, if the input were  $\delta(t)$ , the output would be  $h(t)$ .

But the system is time-invariant, and so, if the input were  $\delta(t - \tau_k)$ , then the output would be  $h(t - \tau_k)$ .

But the system is also linear and so, since the input is  $x(\tau_k)\delta(t - \tau_k)\Delta\tau$  the output must be  $x(\tau_k)h(t - \tau_k)\Delta\tau$

Notice how at each stage what was formerly a  $\delta$  becomes an  $h$ .

In Figure 7.9a we show the network's impulse response  $h(t)$  (invented for the purpose of this demonstration), and in Figure 7.9b its response  $y_k(t)$  to the delayed impulse  $x_k(t)$ .

We now return to Figure 7.6. The remainder of the pulse  $x(t)$  could also have been overlaid with rectangles, as shown in Figure 7.10a, thereby creating the

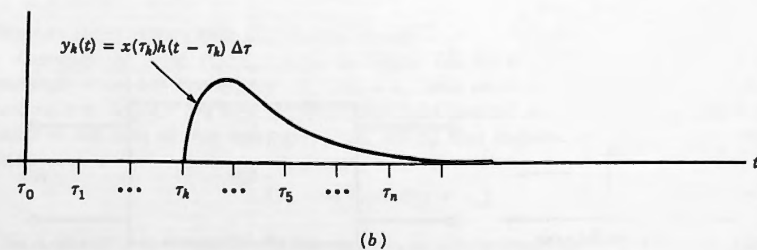
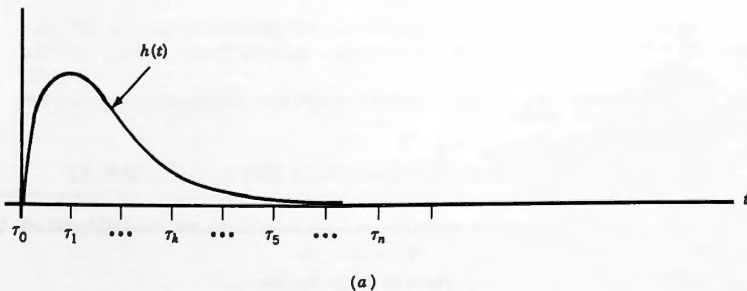


Figure 7.9. (a) Impulse response. (b) Response to delayed impulse.

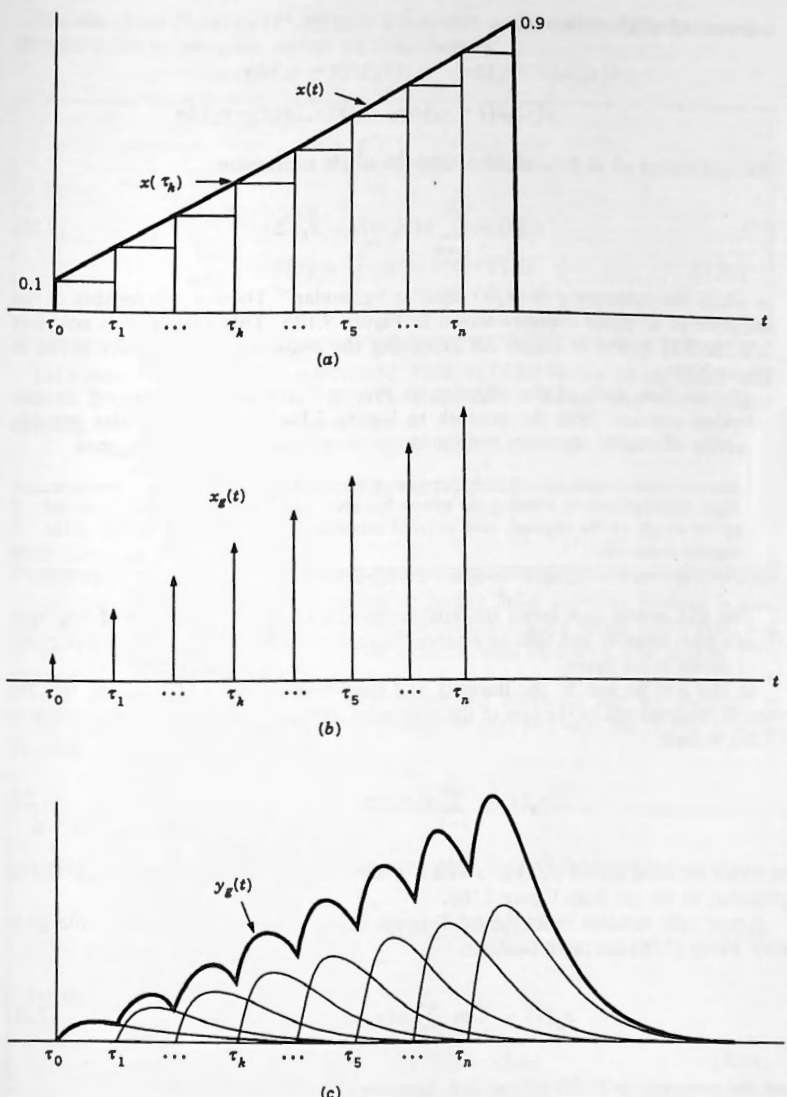


Figure 7.10. (a) Complete discretization of  $x(t)$ . (b) Impulse representation of  $x(t)$ . (c) Network's response.

sequence of weighted impulses:

$$\begin{aligned}x(\tau_0)\delta(t - \tau_0)\Delta\tau, \dots, x(\tau_k)\delta(t - \tau_k)\Delta\tau, \dots \\x(\tau_5)\delta(t - \tau_5)\Delta\tau, \dots, x(\tau_n)\delta(t - \tau_n)\Delta\tau\end{aligned}$$

We now collect all of these impulses into the single expression

$$x_g(t) = \sum_{k=0}^n x(\tau_k)\delta(t - \tau_k)\Delta\tau \quad (7.26)$$

in which the subscript  $g$  in  $x_g(t)$  signifies "granular." Then  $x_g(t)$  consists of the sequence of weighted impulses shown in Figure 7.10b. This sequence is now sent into the LTI system of Figure 7.8 producing the sequence of responses shown in Figure 7.10c.

Observe how each of the impulses in Figure 7.10b has triggered off its own individual response from the network in Figure 7.10c, with the smaller impulses triggering off smaller responses and the larger ones triggering off larger ones.

Eight weighted impulse entering the system has given rise to its own response, scaled by the weight of the impulse, each delayed according to the time of arrival of the impulse in question.

The LTI system then forms the arithmetic sum of all of these scaled responses (that's what linearity and time invariance means) and produces the overall response  $y_g(t)$  shown in the figure.

In this way we see, by the **linearity** and **time invariance** of the system, that the overall response will be the sum of the responses to each of the individual impulses in (7.26), namely

$$y_g(t) = \sum_{k=0}^n x(\tau_k)h(t - \tau_k)\Delta\tau \quad (7.27)$$

which we have shown  $y_g(t)$  also with a  $g$  subscript, although it may not in fact be granular, as we see from Figure 7.10c.

It now only remains to let the subdivisions of the time axis in Figure 7.10a go to zero. From (7.26) the input becomes

$$x_g(t) = \lim_{\Delta\tau \rightarrow 0} \sum_{k=0}^n x(\tau_k)\delta(t - \tau_k)\Delta\tau \quad (7.28)$$

and the response in (7.27) follows suit, becoming

$$y_g(t) = \lim_{\Delta\tau \rightarrow 0} \sum_{k=0}^n x(\tau_k)h(t - \tau_k)\Delta\tau \quad (7.29)$$

But equations (7.28) and (7.29) have a form that we are familiar with; they are the representation of integrals, and so we write them as

$$x(t) = \int_{-\infty}^{\infty} x(\tau) \delta(t - \tau) d\tau \quad (7.30)$$

and

$$y(t) = \int_{-\infty}^{\infty} x(\tau) h(t - \tau) d\tau \quad (7.31)$$

Let's examine what we have obtained. First, in (7.30) we see an expression that involves a Dirac delta in the RHS. To verify that it makes sense we note that sampling takes place, and so it continues as

$$\dots = \int_{-\infty}^{\infty} x(t) \delta(t - \tau) d\tau = x(t) \int_{-\infty}^{\infty} \delta(t - \tau) d\tau = x(t) \quad (7.32)$$

which is the same as the LHS.

Next we note in (7.30) that we have used a range of integration from  $-\infty$  to  $\infty$  even though the pulse was regarded earlier as having finite duration. Nothing is lost, however, by extending the interval of integration into regions where  $x(\tau)$  is zero, and in fact (7.30) covers the most general case as well, of pulses with infinite time durations.

Now let's look at (7.31). This is precisely the statement that we obtained in (7.23). It says  $y(t)$  is the convolution product of  $x(t)$  and  $h(t)$ . All of this gives us Theorem 7.4 below.

#### ■ THEOREM 7.4

Let an LTI system have impulse response  $h(t)$ . Then, if the input is

$$x(t) = \int_{-\infty}^{\infty} x(\tau) \delta(t - \tau) d\tau \quad (7.33)$$

the output will be

$$y(t) = \int_{-\infty}^{\infty} x(\tau) h(t - \tau) d\tau \quad (7.34)$$

We are now close to an understanding of what convolution means. Examining (7.33), we see on the RHS an infinite sum of Dirac deltas, each with its own weight,

each following the other, all added together (integrated) to give  $x(t)$ . Thus the input pulse  $x(t)$  is simply a train of Dirac deltas.

In (7.34) we see on the RHS almost the same integrand, except that now there is an  $h$  where in (7.33) there was a  $\delta$ . Each of the impulses in the sum in (7.33) has triggered off a response in (7.34). In (7.33) the impulses added up to  $x(t)$ . In (7.34) their responses add up to  $y(t)$ . Thus convolution is simply a mathematical statement of the fact that

Train of impulses in . . . Train of responses to each impulse out

In closing this section we make two final remarks.

- In Chapter 6 we examined a network's response to complex exponentials, what we called the eigenfunctions of LTI systems. We saw there an analogous mechanism in operation, namely

Sum of complex exponentials in . . . Sum of responses to each exponential out

All that we have done in the present case is to use a different form for representing  $x(t)$ , but nothing else has changed. The LTI network responds in precisely the same way.

We have seen that Dirac deltas and complex exponentials are closely related. In fact, as we recall from Theorem 4.1,

$$\delta(t) = \frac{1}{2\pi} \int_{-\infty}^{\infty} e^{j\omega t} d\omega \quad (7.35)$$

which says that a Dirac delta is simply a “sum” of every possible complex exponential in equal amounts. For this reason it makes no difference whether we examine the response of a network in terms of Dirac deltas or complex exponentials as the input. The underlying behavior must be the same.

- Equation (7.33) is a surprisingly powerful result, and so we shall state it as the following theorem.

**■ THEOREM 7.5:** Any pulse  $x(t)$  can be expressed as a “linear combination” of Dirac deltas in the form

$$x(t) = \int_{-\infty}^{\infty} x(\tau) \delta(t - \tau) d\tau \quad (7.36)$$

where  $x(\tau)$  is the coefficient function of the linear combination.

Starting from (7.36) we are able to show that analysis and synthesis are each other's exact inverses. This is done in Exercise 7.27 (with some assistance).

## 7.5 CONVOLUTION THE GRAPHICAL WAY

The preceding explanation of what convolution means is good for providing us with an intuitive time-domain understanding of how an LTI system responds to an input pulse. However, it doesn't provide us with a good way of arriving at the actual shape of the output, since it's too hard to add up infinitely many delayed, scaled, individual impulse responses as we attempted to do in Figure 7.10c. Here's a solution to that problem.

First we require the following theorem, which says that  $x(t)$  and  $h(t)$  play symmetric roles in the convolution integral.

■ **THEOREM 7.6:** The convolution symmetry property

$$\int_{-\infty}^{\infty} x(\tau)h(t - \tau) d\tau = \int_{-\infty}^{\infty} x(t - \tau)h(\tau) d\tau \quad (7.37)$$

Proof is given in the box below.

*Proof of Theorem 7.6*

$$\int_{-\infty}^{\infty} x(\tau)h(t - \tau) d\tau \longrightarrow$$

Let  $t - \tau = z$ .  
 Then  $\tau = t - z$ ,  
 and so  $d\tau = -dz$   
 $\tau = \infty$  becomes  $z = -\infty$   
 $\tau = -\infty$  becomes  $z = \infty$ .

$$\longrightarrow = \int_{\infty}^{-\infty} x(t - z)h(z) (-dz)$$

$$= \int_{-\infty}^{\infty} x(t - z)h(z) dz = \int_{-\infty}^{\infty} x(t - \tau)h(\tau) d\tau \quad (7.38)$$

What Theorem 7.6 tells us is that the order of the terms in the convolution product is immaterial, and so  $x(t) * h(t)$  can be used to mean either of the integrals shown in (7.37). It also then follows that we have two equivalent statements for the output from an LTI system, namely:

$$y(t) = \int_{-\infty}^{\infty} x(\tau)h(t - \tau) d\tau = \int_{-\infty}^{\infty} x(t - \tau)h(\tau) d\tau \quad (7.39)$$

Up to now we have been considering only the first of these two integrals, namely (A), and all of the analysis regarding the meaning of convolution has been based on that integral. While either form can be used in what follows, we now show that the second integral gives us a handy graphical way of actually carrying out convolution. Thus we shall now write our convolution integral as follows:

$$y(t) = \int_{-\infty}^{\infty} x(t - \tau)h(\tau) d\tau \quad (7.40)$$

First let's try to understand what  $x(t - \tau)$  means in (7.40). Consider the pulse  $x(t)$ , which we have depicted in Figure 7.11a. Suppose now that it is put onto an electrical conductor leading to the input of an LTI system. Our natural inclination is to think of it as moving to the right along the conductor as time progresses, but that is incorrect. In fact, it is the **mirror image** of this pulse that moves to the right, since it is the part at  $t = 0$  that occurs first, and hence reaches the network first.

In Figure 7.11b we show the same pulse as a function of  $\tau$ , and so we call it  $x(\tau)$ .

In Figure 7.11c we have reversed the pulse, showing it as  $x(-\tau)$ , which now has the correct orientation for movement to the right into a network.

In Figure 7.11d we show  $x(-1 - \tau)$ . Observe that the leading edge of the pulse is now located at  $\tau = -1$ .

In Figure 7.11e we show  $x(t - \tau)$ . The leading edge is now at  $\tau = t$ , with  $t$  frozen at  $-2$ .

If we now let  $t$  increase steadily, then the pulse will start to move to the right.

This is shown in Figure 7.11f at the instant when  $t = -1.75$ . In (f) we have also positioned a copy of the impulse response of an LTI system, which in this case is assumed to be

$$h(t) = \begin{cases} 2 & (0 < t < 1) \\ 0 & (\text{otherwise}) \end{cases} \quad (7.41)$$

Notice that the leading edge of the moving pulse is the one that occurs first, and so it arrives at  $h(t)$  with the correct orientation.

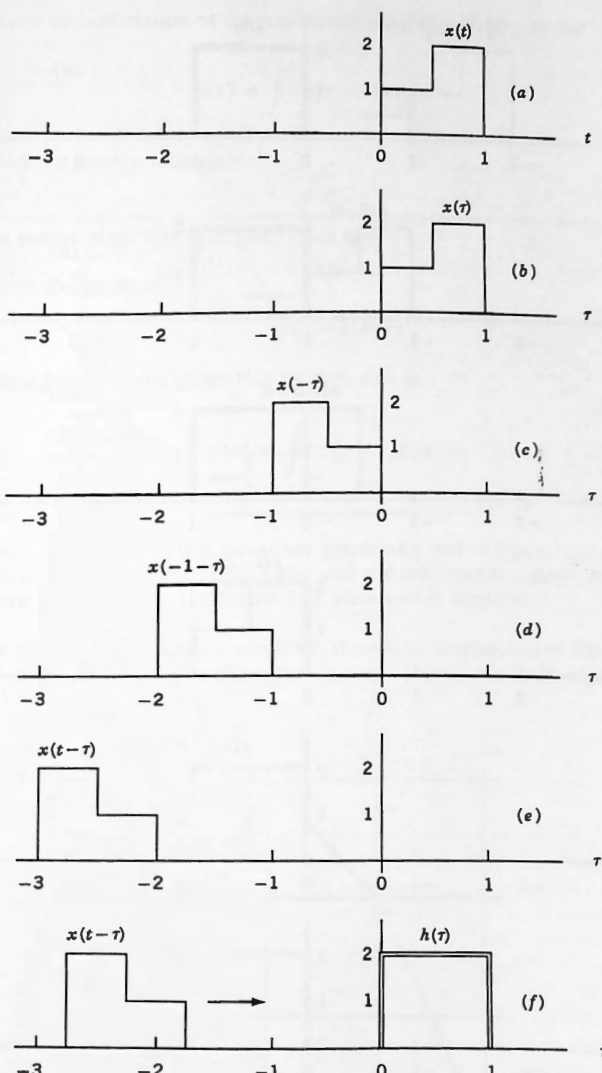


Figure 7.11.

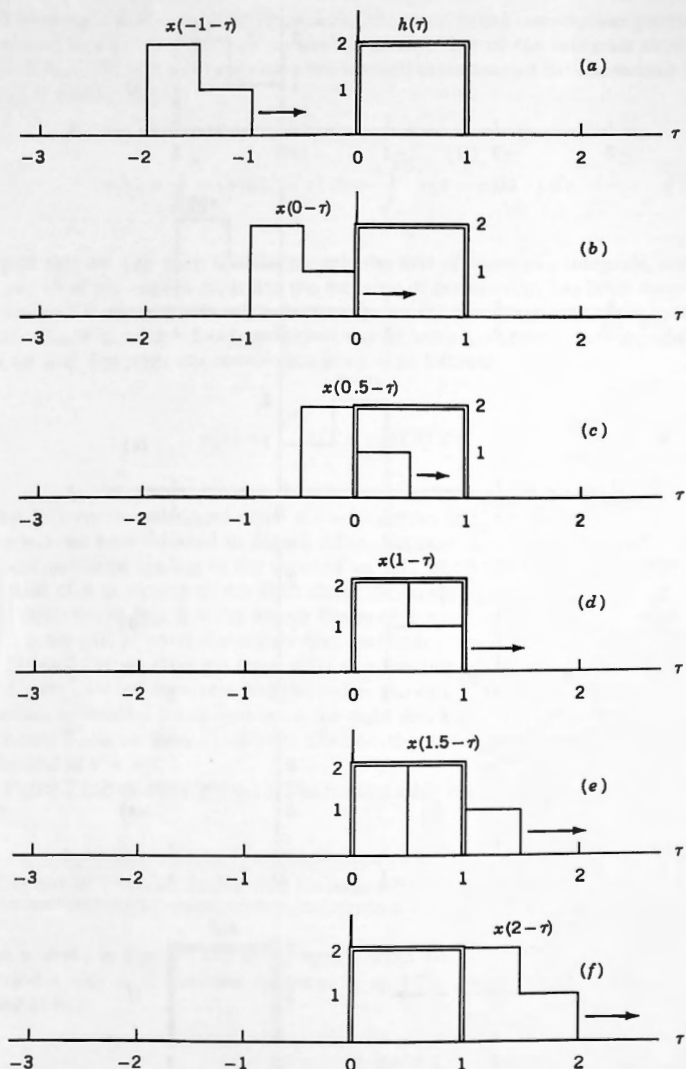


Figure 7.12. Graphical convolution.

Now, our second version of the convolution integral in (7.40) says that

$$y(t) = \int_{-\infty}^{\infty} x(t - \tau)h(\tau) d\tau \quad (7.42)$$

from which we see the following:

■ **To obtain  $y(t)$ :** For each given value of  $t$

(a) Form the product

$$x(t - \tau)h(\tau)$$

(b) Then find the area under that product, that is,

$$y(t) = \int_{-\infty}^{\infty} x(t - \tau)h(\tau) d\tau \quad (7.43)$$

We can easily perform this procedure graphically, and in Figure 7.12 we display, step by step, the convolution of the pulse  $x(t)$  and the impulse response  $h(t)$ , both of which were previously used in Figure 7.11. Here's what happens:

**Figure 7.12a ( $t < 0$ ):** Until  $t$  reaches 0, there is no overlap, and so the area under the product of the two functions is zero. This is shown in Figure 7.13 as  $y(t) = 0$  for  $t < 0$ .

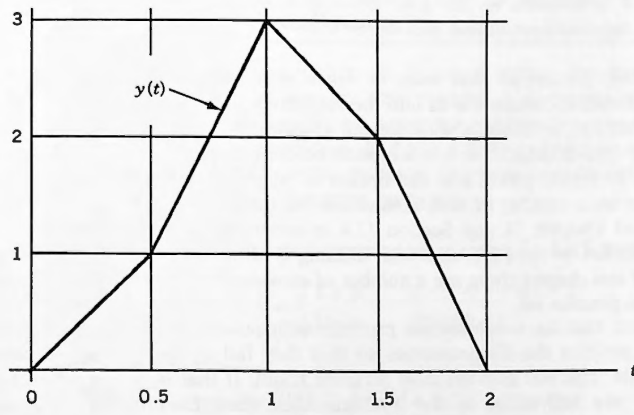


Figure 7.13.  $x(t) * h(t)$ .

**Figure 7.12b and c ( $0 < t < 0.5$ ):** The first part of the pulse with height 1 is penetrating  $h(\tau)$ , and so the area under the product of the two functions increases linearly with time. As shown in Figure 7.13,  $y(t)$  now goes linearly from  $y(0) = 0$  to  $y(0.5) = 1$ .

**Figure 7.12c and d ( $0.5 < t < 1$ ):** The second part of the pulse is entering  $h(\tau)$ , and so the area under the product continues to increase linearly, but at a greater rate, going from 1 and ending at 3.

**Figure 7.12d and e ( $1 < t < 1.5$ ):** Now the leading part of the pulse is emerging, and so the area under the product diminishes linearly from 3 to 2.

**Figure 7.12e and f ( $1.5 < t < 2$ ):** The high part of the pulse is now emerging and so the area under the product goes linearly from 2 to 0.

Thereafter there is no overlap, and so  $y(t) = 0$  for  $t > 2$ . All of this is reflected in the plot of  $y(t)$  in Figure 7.13.

#### Accompanying Disk

In addition to the other features that we have already discussed, the FFT system can also perform convolution. As (7.22) and (7.23) suggest, this is done as follows:

- The two functions  $x(t)$  and  $x_2(t)$  that are to be convolved are loaded into **X** and **X2** by the user.
- Main-menu option F, CONVOLUTION is selected. The system then
  - (1) Runs ANALYSIS on each of **X** and **X2** to produce their spectra, which are placed in **F** and **F2**
  - (2) These two spectra are then multiplied together using complex multiplication and the result is placed in **F**
  - (3) **F** is inverted to the time domain using SYNTHESIS to produce the required convolution product in **Y**

The only precaution that must be taken is to ensure that the result of the convolution operation will fit into the time range that  $N$  represents, for if not it will overflow, resulting in what we call **aliasing**.

The system detects for this condition before proceeding and warns you if it is about to occur, giving you the option of aborting or proceeding regardless. (There are a number of situations where the latter is acceptable.)

Read Chapter 14 and Section 17.4 in order to learn the full story about convolution on the FFT, and what aliasing is all about. In the exercises at the end of this chapter there are a number of convolution problems that you will be able to practice on.

When running a convolution problem with pulses that have discontinuities, try to position the discontinuities so that they fall in the **centers of sampling intervals**. This will give the most accurate result. If that is not possible, then of course use half-values at the discontinuities. (See Exercise 14.6.) Also, the greater  $N$ , the better the accuracy.

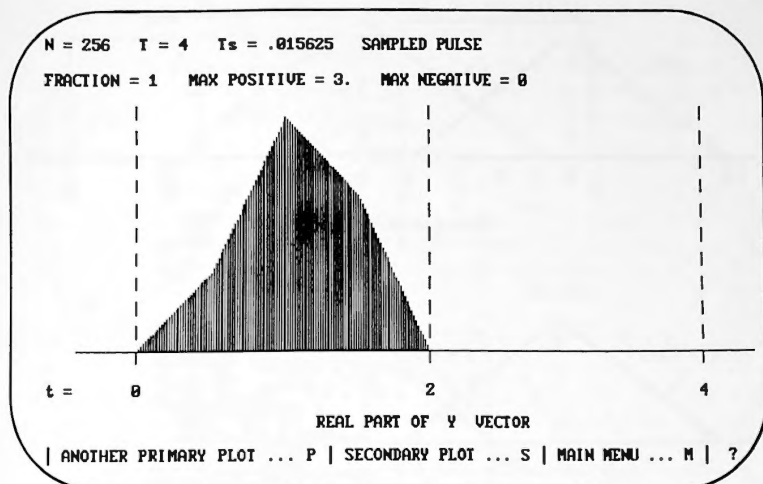


Figure 7.14. Result of convolution.

Using the FFT system, we ran the convolution example shown in Figure 7.12. In Figure 7.14 we show a plot of the result, which should be compared to Figure 7.13.

We shifted both pulses in the example to the right by half a sampling interval so that all of the discontinuities fell in the centers of the intervals. The numbers from the FFT were then in **perfect agreement** with the theoretical values.

## 7.6 EVALUATING THE CONVOLUTION INTEGRAL ANALYTICALLY

In addition to the graphical approach that we discussed earlier, the convolution integral can also be evaluated analytically. The method is demonstrated in the following example which may appear to be somewhat lengthy but was carefully selected to show all aspects of the procedure. In it you will observe that we carry out, step by step, everything that we did in the graphical approach, but now we find the areas by integration rather than by "counting squares."

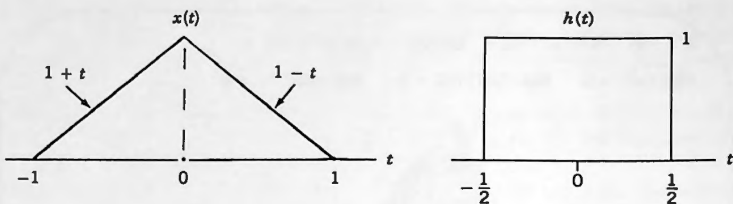
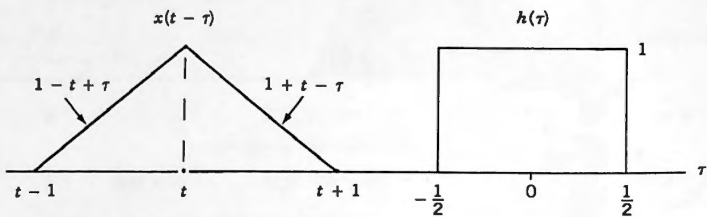
**EXAMPLE 7.2:** Find the complete expression for  $y(t) = x(t) * h(t)$ , assuming that

$$x(t) = \Lambda(t) = \begin{cases} 1 + t & (-1 < t < 0) \\ 1 - t & (0 < t < 1) \end{cases}$$

and

$$h(t) = \text{Rect}(t)$$

In Figures 7.15 we show these two pulses, together with the analytical definitions of the sectors that they contain.

Figure 7.15.  $x(t)$  and  $h(t)$ .Figure 7.16. Case 1,  $t < -\frac{3}{2}$ .

**Step 1:** Redraw  $h(t)$  as  $h(\tau)$  on the  $\tau$ -axis. This new pulse is depicted in Figure 7.16.

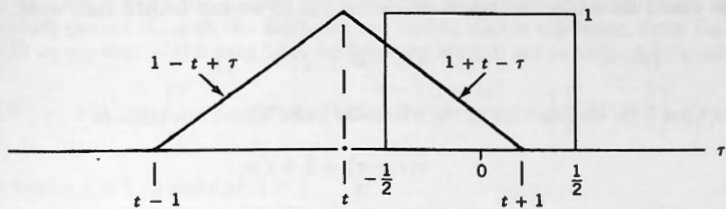
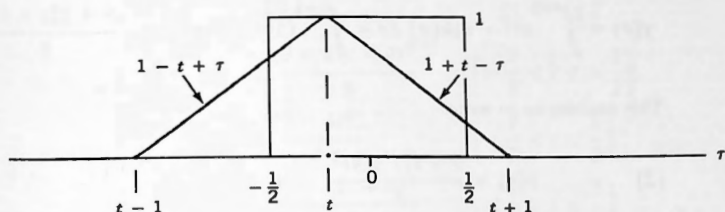
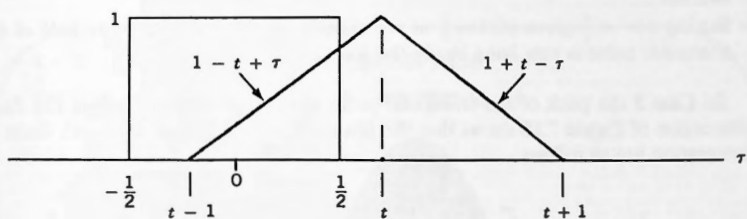
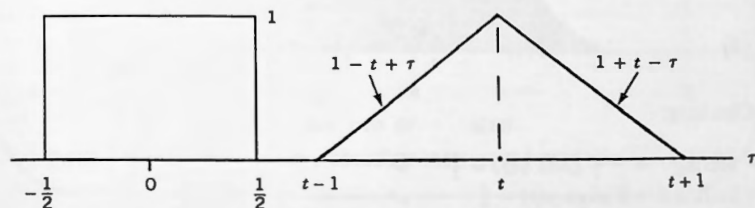
**Step 2:** Redraw  $x(t)$  as  $x(t - \tau)$  on the same  $\tau$ -axis. It is important to keep in mind that this calls for a reversal of the pulse  $x(t)$ .

We have deliberately elected to reverse the triangular pulse rather than the square one in order to show this aspect of the process. An alternative, and slightly simpler, approach would have been to keep the triangular pulse as  $x(\tau)$  and to redraw the square pulse as  $h(t - \tau)$ , but then the need for reversal of the sector definitions would not have come up.

The reversed pulse is depicted in Figure 7.16 where careful examination of the definitions of the sectors in  $x(t - \tau)$  will show that the pulse  $x(t)$  has indeed been reversed. Observe also that the point formerly located at zero is now labeled  $t$ , and that the ends of the pulse now lie at  $\tau = t + 1$  and  $\tau = t - 1$ , respectively.

**Step 3:** Identify all of the separate cases as follows:

Case 1:	$t < -\frac{3}{2}$	(Fig. 7.16)
Case 2:	$-\frac{3}{2} < t < -\frac{1}{2}$	(Fig. 7.17)
Case 3:	$-\frac{1}{2} < t < \frac{1}{2}$	(Fig. 7.18)
Case 4:	$\frac{1}{2} < t < \frac{3}{2}$	(Fig. 7.19)
Case 5:	$\frac{3}{2} < t$	(Fig. 7.20)

Figure 7.17. Case 2,  $-\frac{3}{2} < t < -\frac{1}{2}$ .Figure 7.18. Case 3,  $-\frac{1}{2} < t < \frac{1}{2}$ .Figure 7.19. Case 4,  $\frac{1}{2} < t < \frac{3}{2}$ .Figure 7.20. Case 5,  $\frac{3}{2} < t$ .

In Case 1 there is no overlap of the pulses, and so we can immediately write:

$$(1) \quad y(t) = 0 \quad (t < -\frac{3}{2})$$

In Case 2 the leading edge of the triangular pulse whose equation is

$$x(t - \tau) = 1 + t - \tau$$

has penetrated into the Rect pulse, but the peak of the triangular pulse is still not yet inside the Rect. Careful inspection of Figure 7.17 shows that the following integral with its limits will give us  $y(t)$  for this stage.

$$y(t) = \int_{-\frac{1}{2}}^{t+1} x(t - \tau) h(\tau) d\tau = \int_{-\frac{1}{2}}^{t+1} (1 + t - \tau) d\tau = \frac{9 + 12t + 4t^2}{8}$$

This enables us to write

$$(2) \quad y(t) = \frac{9 + 12t + 4t^2}{8} \quad \left( -\frac{3}{2} < t < -\frac{1}{2} \right)$$

As a sanity test on this result we have the following:

- Setting  $t = -\frac{3}{2}$  gives  $y(t) = 0$  as we should expect, since there is then no overlap.
- Setting  $t = -\frac{1}{2}$  gives  $y(t) = \frac{1}{2}$  as we should expect, since exactly half of the triangular pulse is now lying inside the Rect.

In Case 3 the peak of the triangular pulse is now somewhere inside the Rect. Inspection of Figure 7.18 shows that the integral expression for  $y(t)$  with limits of integration are as follows:

$$y(t) = \int_{-\frac{1}{2}}^t (1 - t + \tau) d\tau + \int_t^{\frac{1}{2}} (1 + t - \tau) d\tau$$

and so

$$(3) \quad y(t) = \frac{3 - 4t^2}{4} \quad \left( -\frac{1}{2} < t < \frac{1}{2} \right)$$

Checking:

- Setting  $t = -\frac{1}{2}$  gives  $y(t) = \frac{1}{2}$  ✓
- Setting  $t = 0$  gives  $y(t) = \frac{3}{4}$  ✓
- Setting  $t = \frac{1}{2}$  gives  $y(t) = \frac{1}{2}$  ✓

In Case 4 both the leading edge and the peak of the triangular pulse have already passed through the Rect, but the trailing edge is still inside. From Figure 7.19 we see that  $y(t)$  comes from the following integral and its limits of integration:

$$(4) \quad y(t) = \int_{t-1}^{\frac{1}{2}} (1 - t + \tau) d\tau = \frac{9 - 12t + 4t^2}{8} \quad \left( \frac{1}{2} < t < \frac{3}{2} \right)$$

- Setting  $t = 1/2$  gives  $y(t) = \frac{1}{2}$  ✓
- Setting  $t = 3/2$  gives  $y(t) = 0$  ✓

**Step 4:** We can now assemble the final answer as

$$y(t) = \begin{cases} 0 & \left( t < -\frac{3}{2} \right) \\ \frac{9 + 12t + 4t^2}{8} & \left( -\frac{3}{2} < t < -\frac{1}{2} \right) \\ \frac{3 - 4t^2}{4} & \left( -\frac{1}{2} < t < \frac{1}{2} \right) \\ \frac{9 - 12t + 4t^2}{8} & \left( \frac{1}{2} < t < \frac{3}{2} \right) \\ 0 & \left( \frac{3}{2} < t \right) \end{cases}$$

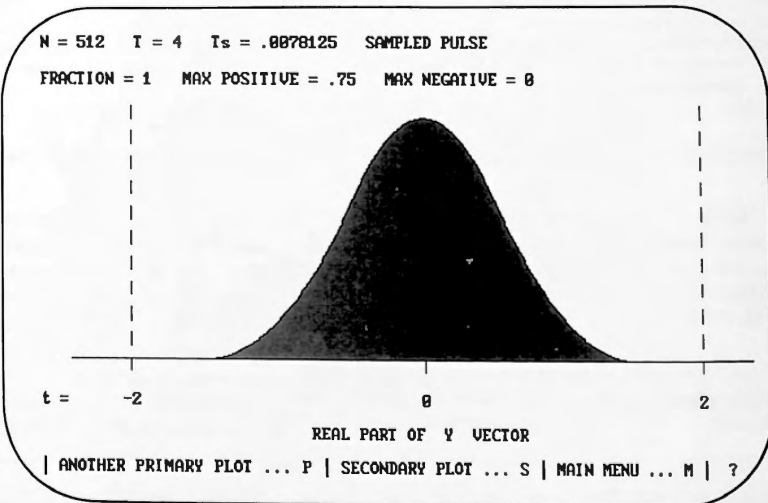


Figure 7.21.  $y(t)$  from the FFT system.

A plot of  $y(t)$  generated by the FFT system as a final check appears in Figure 7.21. The numbers obtained from the preceding theoretical result were in exact agreement with values obtained from the FFT system.  $\square$

## 7.7 CONVOLUTION IN THE FREQUENCY DOMAIN

In the preceding sections we derived a new tool that works in the time domain, what we called the convolution product and defined by either of two integrals as

$$x(t) * h(t) = \int_{-\infty}^{\infty} x(\tau)h(t - \tau) d\tau = \int_{-\infty}^{\infty} h(\tau)x(t - \tau) d\tau \quad (7.44)$$

The importance of the convolution product lies in the following fact, which we proved in Theorem 7.2

$$x(t) * h(t) \Leftrightarrow X(\omega)H(j\omega) \quad (7.45)$$

On the right of (7.45) we see two Fourier transforms that have been multiplied together. Note how their algebraic product in the frequency domain inverts to their convolution product in the time domain. We state this as follows:

Multiplication in the frequency domain corresponds to convolution in the time domain, that is,

$$x(t) * h(t) \Leftrightarrow X(\omega)H(j\omega) \quad (7.46)$$

This is an extremely powerful result. It enables us to understand and interpret results obtained from the analysis of LTI systems of the preceding chapter and to envisage them in the time domain. There is, however, a dual statement that is perhaps of even greater value.

**Question:** What happens if we reverse the order of the domains? In other words,

Multiplication in the time domain corresponds to what in the frequency domain?

Before answering, let's first make the observation that multiplication in the time domain is something that electrical engineers need to do quite frequently, three

examples of which are as follows:

- (a) **Modulation** (See Fig. 1.2.): Given a signal  $x(t)$  that we wish to send by radio transmission, one common procedure is to modulate it onto what are called carriers,  $\cos(\omega_0 t)$  or  $\sin(\omega_0 t)$ , by creating either or both of the products

$$y_1(t) = x(t)\cos(\omega_0 t) \quad (7.47)$$

and

$$y_2(t) = x(t)\sin(\omega_0 t) \quad (7.48)$$

Observe that we are forming products in the time domain.<sup>†</sup>

- (b) **Frequency division multiplexing** is another example in which the same multiplications must be carried out in order to pack more than one signal into a communication channel.
- (c) **Sampling** (See Fig. 1.3.): Given a signal  $x(t)$  we frequently need to sample it, for example to digitize it prior to transmission over a digitally coded communication link.

Mathematically this sampling is modeled by forming the time-domain product

$$y(t) = x(t)\delta_T(t) \quad (7.49)$$

where  $\delta_T(t)$  is the train of equally spaced unit impulses that was defined in Section 4.11. In (7.49) we see a product being formed in the time domain.

We now proceed to answer the question that we posed earlier, and to do that we start with the known answer and work backwards. Thus, what we propose to show is:

■ **THEOREM 7.7: Frequency domain convolution**

$$x(t)g(t) \Leftrightarrow \frac{1}{2\pi} \int_{-\infty}^{\infty} X(\Theta)G(\omega - \Theta) d\Theta \quad (7.50)$$

Let's just take a minute to examine (7.50) before we prove it. Observe that on the left we have a product in the time domain and on the right we have a convolution in the frequency domain. Note that we are now using  $\Theta$  as the dummy variable in the convolution where formerly we used  $\tau$ , and also the fact that there is a  $1/2\pi$  present here.

Thus (7.50) is the dual to the earlier convolution theorem that we derived, in which we had convolution in the time domain and a product in the frequency domain.

To prove (7.50) we start from the RHS and form its Fourier inverse, proceeding as shown on the following page.

<sup>†</sup>Without modulation, megawatts of power and antenna lengths of many hundreds of meters would be required for radio transmission, whereas with modulation the power requirements are small and antenna lengths of only a few meters or even fractions of a meter work successfully.

**Definition:** Given  $X(\omega)$  and  $G(\omega)$ , then the integral shown in (7.50) (excluding the  $1/2\pi$ ) is called their **frequency-domain convolution product**, and for ease of notation we write

$$X(\omega) * G(\omega) \equiv \int_{-\infty}^{\infty} X(\Theta)G(\omega - \Theta) d\Theta \quad (7.51)$$

Based on the proof that we gave earlier for time-domain convolution, it follows immediately that the convolution symmetry property holds here as well. (Just change the symbols.) We can thus write

$$\int_{-\infty}^{\infty} X(\Theta)G(\omega - \Theta) d\Theta = X(\omega) * G(\omega) = \int_{-\infty}^{\infty} G(\Theta)X(\omega - \Theta) d\Theta \quad (7.53)$$

*Proof of Theorem 7.7*

$$\begin{aligned}
 & \frac{1}{2\pi} \int_{-\infty}^{\infty} \left[ \frac{1}{2\pi} \int_{-\infty}^{\infty} X(\Theta)G(\omega - \Theta) d\Theta \right] e^{j\omega t} d\omega \longrightarrow \\
 & \qquad \qquad \boxed{\text{Reverse the order of integration by sliding } X(\Theta) d\Theta \text{ out and moving } e^{j\omega t} d\omega \text{ in}} \\
 & \longrightarrow = \frac{1}{2\pi} \int_{-\infty}^{\infty} \left[ \frac{1}{2\pi} \int_{-\infty}^{\infty} G(\omega - \Theta) e^{j\omega t} d\omega \right] X(\Theta) d\Theta \\
 & \qquad \qquad \qquad \boxed{\text{Let } \omega - \Theta = \beta. \\
 & \text{Then } \omega = \beta + \Theta, \\
 & \text{and } d\omega = d\beta.} \\
 & \longrightarrow = \frac{1}{2\pi} \int_{-\infty}^{\infty} \left[ \frac{1}{2\pi} \int_{-\infty}^{\infty} G(\beta) e^{j\beta t} d\beta \right] e^{j\Theta t} X(\Theta) d\Theta \\
 & = \frac{1}{2\pi} \int_{-\infty}^{\infty} G(\beta) e^{j\beta t} d\beta \frac{1}{2\pi} \int_{-\infty}^{\infty} X(\Theta) e^{j\Theta t} d\Theta \\
 & = g(t)x(t) \tag{7.52}
 \end{aligned}$$

What all of this means is that the answer to our question is:

Multiplication in the time domain corresponds to  $1/2\pi \times$  convolution in the frequency domain, that is,

$$x(t)g(t) \Leftrightarrow \frac{1}{2\pi}X(\omega)*G(\omega) \quad (7.54)$$

(Don't forget the  $1/2\pi$ .)

**EXAMPLE 7.3:** Find the Fourier transform of the product

$$y(t) = x(t)\cos(\omega_0 t) \quad (7.55)$$

Note that  $y(t)$  consists of the signal  $x(t)$  being modulated onto an eternal cosine acting as a carrier.

**Solution:** From Chapter 4 we recall that

$$\cos(\omega_0 t) \Leftrightarrow \pi[\delta(\omega - \omega_0) + \delta(\omega + \omega_0)] \quad (7.56)$$

and so, by (7.50)

$$\begin{aligned} x(t)\cos(\omega_0 t) &\Leftrightarrow \frac{1}{2\pi} \int_{-\infty}^{\infty} X(\Theta) \pi[\delta(\omega - \omega_0 - \Theta) + \delta(\omega + \omega_0 - \Theta)] d\Theta \\ &= \frac{1}{2} \int_{-\infty}^{\infty} X(\Theta) \delta(\omega - \omega_0 - \Theta) d\Theta \\ &\quad + \frac{1}{2} \int_{-\infty}^{\infty} X(\Theta) \delta(\omega + \omega_0 - \Theta) d\Theta \end{aligned} \quad (7.57)$$

In the integrations in (7.57) our independent variable is  $\Theta$ , and so, in the first integrand,  $\delta(\omega - \omega_0 - \Theta)$  is an impulse on the  $\Theta$ -axis located at  $\omega - \omega_0$ . Hence by the sampling property

$$X(\Theta)\delta(\omega - \omega_0 - \Theta) = X(\omega - \omega_0)\delta(\omega - \omega_0 - \Theta) \quad (7.58)$$

and in the same way for the second integrand

$$X(\Theta)\delta(\omega + \omega_0 - \Theta) = X(\omega + \omega_0)\delta(\omega + \omega_0 - \Theta) \quad (7.59)$$

and so (7.57) continues as

$$\begin{aligned}
 \cdots &= \frac{1}{2} \int_{-\infty}^{\infty} X(\omega - \omega_0) \delta(\omega - \omega_0 - \Theta) d\Theta \\
 &\quad + \frac{1}{2} \int_{-\infty}^{\infty} X(\omega + \omega_0) \delta(\omega + \omega_0 - \Theta) d\Theta \\
 &= \frac{1}{2} X(\omega - \omega_0) \int_{-\infty}^{\infty} \delta(\omega - \omega_0 - \Theta) d\Theta \\
 &\quad + \frac{1}{2} X(\omega + \omega_0) \int_{-\infty}^{\infty} \delta(\omega + \omega_0 - \Theta) d\Theta \\
 &= \frac{1}{2} X(\omega - \omega_0) + \frac{1}{2} X(\omega + \omega_0)
 \end{aligned} \tag{7.60}$$

Thus

$$x(t) \cos(\omega_0 t) \Leftrightarrow \frac{1}{2} X(\omega - \omega_0) + \frac{1}{2} X(\omega + \omega_0) \tag{7.61}$$

□

Let's interpret what (7.61) says. The signal  $x(t)$  is depicted in Figure 7.22a<sup>†</sup> and adjacent to it in 7.22b we show its Fourier spectrum  $X(\omega)$ . In Figure 7.22c we show the carrier  $\cos(\omega_0 t)$  onto which the signal is to be modulated, and to the right of this in 7.22d we show the spectrum of  $\cos(\omega_0 t)$ , which consists of two impulses. Finally in Figure 7.22e we show the time-domain product of the signal and the carrier,  $x(t)\cos(\omega_0 t)$ , while adjacent to that in 7.22f we show the Fourier spectrum of this product, consisting of the signal's spectrum from 7.22b, which has been convolved in the frequency domain with the spectrum of  $\cos(\omega_0 t)$  from 7.22d.

According to (7.61), the Fourier spectrum of the product  $x(t)\cos(\omega_0 t)$  consists of  $\frac{1}{2}X(\omega)$  replicated twice, once centered at  $\omega_0$  and once at  $-\omega_0$ . This is shown in Figure 7.22f.

By using modulation we have produced these two **shifted** copies of the original spectrum of  $x(t)$ . They are now centered at  $\omega = \pm\omega_0$  rather than at  $\omega = 0$ , and we find that they can be made to radiate quite easily if  $\omega_0$  is chosen to be large enough. The radiated signal  $y(t)$  then carries with it the complete spectrum of  $x(t)$ , and in this way communication is accomplished.

At the receiving end we must **demodulate** what is received and recover from it the spectrum of  $x(t)$ , which contains the information that was transmitted. To do that we simply multiply the received signal by  $\cos(\omega_0 t)$  once again. This process of demodulation is considered in one of the exercises.

<sup>†</sup>In Figure 7.22 you will observe that we have shown both  $x(t)$  and its spectrum  $X(\omega)$  as having only finite ranges over which they are nonzero. This is actually an impossibility, and was done only in order to simplify the illustration. A time-domain signal that has a finite span must have a frequency-domain counterpart with infinite span and vice versa.

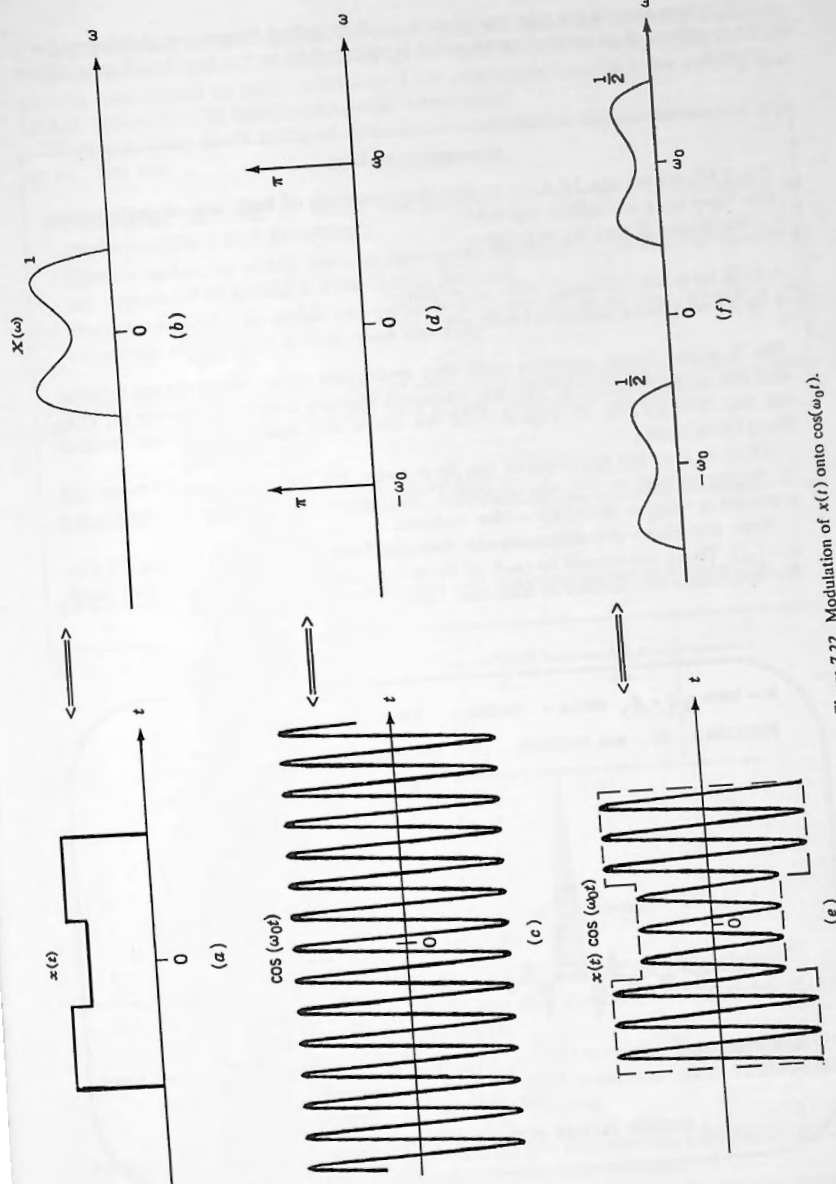


Figure 7.22. Modulation of  $x(t)$  onto  $\cos(\omega_0 t)$ .

It is now easy to see why modulation is often called **frequency shifting** and why the spectrum of an unmodulated signal is referred to as the **baseband** or **unshifted** version.

### Accompanying Disk

The FFT system can be used to find the spectrum of two time-domain signals that have been multiplied together.

We loaded X and X2 as follows:

- In X we placed  $\cos(\omega_0 t)$  with  $\omega_0 = 16\pi$
- In X2 we placed  $\text{Rect}(t/\tau)$  with  $\tau = 1$

The X postprocessor contains code that multiplies these two vectors together and places the result in X. This was executed starting from main-menu G. Then we ran ANALYSIS. In Figure 7.23 we show the spectrum of the product  $\text{Rect}(t)\cos(16\pi t)$ .

Observe how the spectrum of the Rect pulse has been duplicated twice and its height halved to 0.5. As expected, the copies of the Sa envelopes are centered at  $\pm\omega_0 = 50.26548 = 16\pi$  radians.

Note the slight distortions in the two Sa functions in the center of Figure 7.23. These are caused by each of them interfering with the other (aliasing). We investigate this further in Exercise 7.29.

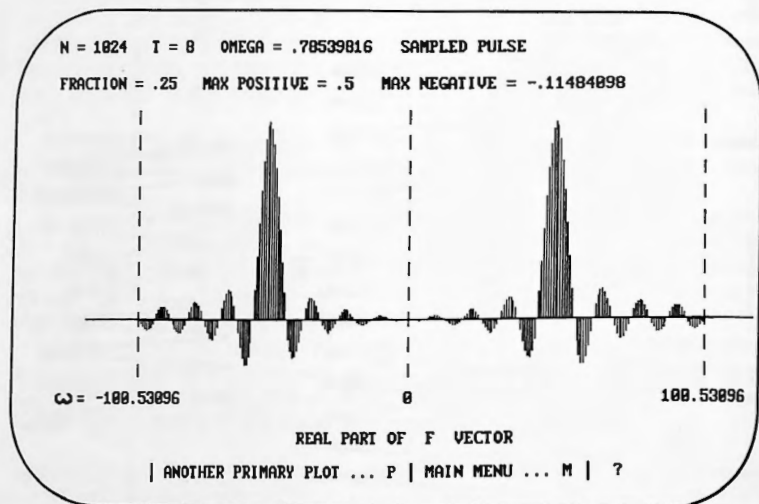


Figure 7.23. Spectrum of  $\cos(\omega_0 t)\text{Rect}(t/\tau)$ .

Before concluding this chapter on convolution we make the following comments. In all of the discussion of convolution in the time domain we were concerned only with the convolution of pulse functions of the continuous variable  $t$ . We refer to that kind of convolution as **continuous-pulse** convolution.

There are three more kinds of time-domain convolution that we discuss in Chapter 14. They are:

- **Continuous periodic**, in which two periodic functions of  $t$  are convolved to produce a third such function.
- **Discrete pulse**, in which two one-time pulse functions of the discrete variable  $k$  are convolved to produce a third such function.
- **Discrete periodic**, in which two periodic functions of the discrete variable  $k$  are convolved to produce a third such function.

The term "circular convolution" is also sometimes used when talking about convolution that involves periodic functions. In Chapter 14 we shall see why.

## EXERCISES

---

### (A) Impulse Response

7.1 Derive the impulse responses for the two networks shown in Figure 7.24.

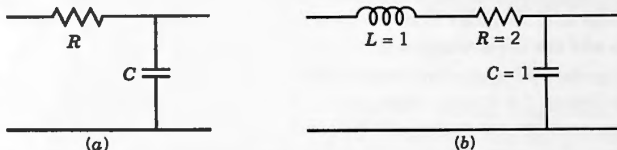


Figure 7.24.

7.2 (a) Describe an electrical network whose impulse response  $h(t)$  is

- (1)  $\delta(t)$
- (2)  $\frac{1}{2}\delta(t)$
- (3)  $\delta(t - T)$

(b) What are the frequency transfer functions for these three networks?

(c) Use time-domain convolution to find the response  $y(t)$  to a signal  $x(t)$  that is applied to each of these networks.

(d) Use frequency domain analysis per Chapter 6 to find the response  $y(t)$  to a signal  $x(t)$  that is applied to each of these networks. Verify all three results obtained in (c) by using the inversion integral.

7.3 Solve the following, by two methods: (1) use time-domain convolution and then transform the result; (2) transform first and then multiply.

A network has impulse response  $h(t) \Leftrightarrow H(j\omega)$ . What is the Fourier transform

of the output when the input is:

- A unit impulse  $\delta(t)$ ?
- The eternal cosine,  $\cos(\omega_0 t)$ ?

*Hint:* Use (2.15).

**7.4** A network has impulse response  $\delta(t)$  and input  $\delta(t)$ . Use time-domain convolution to find the response.

**7.5** (a) Two networks are cascaded, the first with impulse response  $g(t)$  and the second with  $h(t)$ , in such a way that the second does not load the first. A signal  $\delta(t)$  is then applied at the input of the first network.

- What is the time-domain expression for the output from the cascade? (Find the answer using both time-domain and frequency-domain analysis.)
- What is the time-domain expression for the impulse response of the cascade?
- If the order of the networks in (a) is reversed, what will be the expression for the impulse response of the cascade? Give reasons.

**7.6** Using  $R = L = 1$ ,  $N = 256$  and  $T = 8$ :

- Load the expression for the impulse response given in (7.8) into X and then run ANALYSIS. Verify that the resulting spectrum that you obtain is consistent with (7.7).
- Do the same starting from (7.10) and verify that the FFT spectrum comes close to (7.9). (Start from main-menu A to create the exponential and then to add the Dirac delta.)
- Use the FFT system to obtain a plot of the impulse response of network (a) in Figure 7.2 starting from its frequency response. Validate your impulse response by comparing selected values to the theoretical values obtained from (7.8). *Hint:* Main-menu A. Use  $\text{ALPHA} = 10$ .

**7.7** (a) Find the frequency transfer function  $H(j\omega)$  and then the impulse response  $h(t)$  for the network shown in Figure 7.25, using the values given.

- Starting from  $H(j\omega)$  obtained in (a), use the FFT system to plot the impulse response. Use the expression for  $h(t)$  that you obtained in (a) in order to validate your result. (Main-menu A,  $N = 512$ ,  $T = 16$ ,  $\text{ALPHA} = 10$ .)

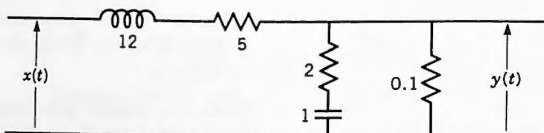


Figure 7.25.

### (B) Time-Domain Convolution/Frequency-Domain Multiplication

Read section 17.4 in order to learn enough about how the FFT system can be used to perform convolution and then use it, where asked, to run the following time-domain convolution problems. You will have to pay careful attention to how you select values for  $T$  and how you carry out your sampling in order to avoid what we call **aliasing** or **folding**, which is discussed in detail in Chapters 14 and 17.

**7.8** Convolve two copies of  $\text{Rect}(t)$ . Do this in three ways:

- By evaluating the convolution integral for the two functions analytically
- Using the graphical method
- Using the FFT system

Verify that the result is a triangular pulse of width 2 and height 1, centered on the origin. For (c), use  $N = 1024$ , and run two cases:

- $T = 4$ . There will be no aliasing.
- $T = 1.5$  **Aliasing will be present**, showing what happens when the result of a convolution does not fit into the time interval that  $N$  represents. When prompted, use “proceed regardless.”

**7.9** Convolve  $\text{Rect}(t)$  with the delayed Dirac delta  $\delta(t - 1)$ .

- Do this first theoretically, using the definition of the convolution integral and verify that your result is  $\text{Rect}(t - 1)$ .
- Generalize this result to show that

$$x(t) * \delta(t - k) = x(t - k) \quad (7.62)$$

where  $x(t)$  is any pulse. Compare (7.62) to the sampling statement

$$x(t)\delta(t - k) = x(k)\delta(t - k) \quad (7.63)$$

- Convolve  $\text{Rect}(t)$  and  $\delta(t - 1)$  using the FFT system. You should obtain the same result as in (a). In order to load a Dirac delta into the FFT system start from main-menu A. Use  $N = 256$ ,  $T = 4$ .

**7.10** A system has impulse response

$$h(t) = \begin{cases} 1 & (0 < t < 1) \\ 0 & \text{otherwise} \end{cases}$$

The input pulse is  $x(t) = e^{-t}U(t)$

- Find the response by evaluating the convolution integral.
- Validate your result using the FFT system. ( $N = 1024$ ,  $T = 8$ .)
- Fourier transform the result that you obtained in (a) and verify that it is equal to  $H(j\omega)X(\omega)$ .
- Load the expression that you have obtained in (c) into F using  $N = 1024$  and  $T = 8$ . Use level-5 aliasing. Invert the result (SYNTHESIS) and verify that the numbers in Y are acceptably close to those obtained from the exact expression in (a) for  $y(t)$ .

- 7.11 (a) Find the expression for the convolution product of the following two pulses by direct evaluation of the convolution integral:

$$x(t) = e^{-t}U(t)$$

$$x_2(t) = \begin{cases} 1-t & (0 < t < 1) \\ 0 & \text{otherwise} \end{cases}$$

- (b) Fourier transform the result obtained in (a) and verify that it is equal to  $X(\omega)X_2(\omega)$ .

- (c) Load the two expressions in (a) into **X** and **X2**, and run CONVOLUTION. Verify that the numbers in **Y** are acceptably close to those obtained from your exact expression in (a) for  $x(t)*x_2(t)$ . ( $N = 1024$ ,  $T = 8$ .)

- 7.12 (a) In the real world our signals start at time  $t = 0$ , that is, our inputs always satisfy  $x(t) = 0$  for  $t < 0$ . Moreover physical networks cannot respond before an input appears, that is, their impulse responses always satisfy  $h(t) = 0$  for  $t < 0$ . (We call such impulse responses **causal**). Prove that under these conditions the convolution product of  $x(t)$  and  $h(t)$  simplifies to

$$y(t) = \left[ \int_0^t x(\tau)h(t - \tau) d\tau \right] U(t) \quad (7.64)$$

*Hint:* Write  $x(t)$  as  $x(t)U(t)$  and  $h(t)$  as  $h(t)U(t)$ . When you form their convolution product you will obtain an integrand that contains a term  $U(\tau)U(t - \tau)$ . Plot this as a function of  $\tau$ .

- (b) A network has impulse response  $h(t) = e^{-2t}U(t)$  and input  $x(t) = e^{-3t}U(t)$ . Find the output using the convolution interval.  
 (c) Repeat (b), but this time work in the frequency domain and then invert your answer to the time domain. You should obtain the same result as in (b).

- 7.13 For the circuit in Figure 7.26:

- (a) Find the impulse response  $h(t)$ .  
 (b) Find  $y(t)$  by time-domain convolution for the case where the input is  $x(t) = e^{-t}U(t)$ .  
 (c) Find  $y(t)$  by working in the frequency domain.  
 (d) Transform the result that you obtained in (b) and verify that it is equal to  $H(j\omega)X(\omega)$ .

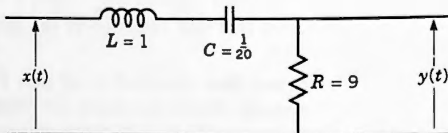


Figure 7.26.

7.14 Use Fourier transformation to prove that

$$\int_{-\infty}^{\infty} x(\tau)g(t - \tau) d\tau = \int_{-\infty}^{\infty} g(\tau)x(t - \tau) d\tau$$

**(C) Time-Domain Multiplication/Frequency-Domain Convolution**

7.15 In Example 7.3 we used frequency-domain convolution to prove that

$$x(t)\cos(\omega_0 t) \Leftrightarrow \frac{1}{2}X(\omega - \omega_0) + \frac{1}{2}X(\omega + \omega_0)$$

Obtain the same result using the frequency-shift property of Theorem 4.4, namely

$$e^{j\omega_0 t}f(t) \Leftrightarrow F(\omega - \omega_0)$$

7.16 In Figure 7.23 we showed a plot of the spectrum of  $\cos(\omega_0 t)\text{Rect}(t/\tau)$  for the case where  $\omega_0 = 16\pi$  and  $\tau = 1$ . We noted that the two Sa envelopes in that plot were slightly distorted due to the fact that they were interfering with each other. Produce that plot on the FFT system (with  $N = 1024$  and  $T = 8$ ) and verify that the numbers for the spectrum are acceptably close to

$$Y(\omega) = \frac{1}{2}\text{Sa}\left[\frac{\omega - \omega_0}{2}\right] + \frac{1}{2}\text{Sa}\left[\frac{\omega + \omega_0}{2}\right]$$

- 7.17 (a) Load the pulse shown in Figure 7.27 into X and obtain a plot of its magnitude spectrum. (Use  $N = 1024$  and  $T = 16$ .) Now load the eternal-cosine function  $\cos(2\pi 8t)$  into X2 and use the REAL-MULTIPLY package in the X postprocessor to multiply XRE and X2RE. Then run ANALYSIS. You should obtain a magnitude spectrum that has two copies of the original magnitude spectrum, halved in height, one at  $\omega = 2\pi 8$  and the other at  $\omega = -2\pi 8$ .
- (b) Repeat the plot of Figure 7.23, but this time use an eternal sine instead of a cosine. What differences do you expect in the spectrum? Are they confirmed by what you obtain from the run?

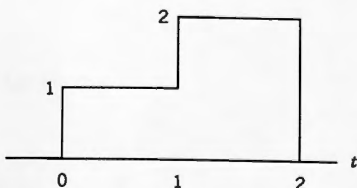
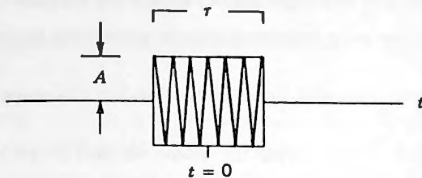


Figure 7.27.  $x(t)$ .

- 7.18 (a) Use convolution to find the Fourier transform of the single radar pulse  $x(t)$  shown in Figure 7.28. The pulse is  $\tau$  seconds long centered at  $t = 0$  and the RF carrier is  $\cos(\omega_0 t)$ . The amplitude is  $A$  volts.  
 (b) Use the inversion integral to find the Fourier inverse of the result that you obtained in (a) and verify that it is the product of  $\text{Rect}(t/\tau)$  and  $\cos(\omega_0 t)$ .

Figure 7.28. Radar pulse  $x(t)$ .

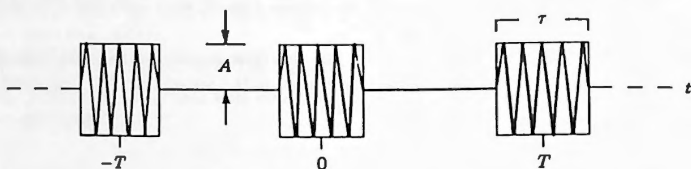
- 7.19 (a) Find the Fourier transform of the infinite train of radar pulses  $x_p(t)$  shown in Figure 7.29. There are two ways to carry this out:

Method 1: Assume that an RF oscillator is putting out  $\cos(\omega_0 t)$  that is being gated (multiplied) by an **independently operated** periodic train of  $\text{Rect}$  pulses.

Method 2: (You will only be able to do this after you have read Chapter 9.) Assume that the RF oscillator starts up whenever a  $\text{Rect}$  pulse commences, thereafter putting out  $\cos(\omega_0 t)$ . The net result is that each burst of RF is an **exact replica** of the previous one.

*Hint:* The signal is now a repetition of the pulse  $f(t) = A \cos(\omega_0 t)$  ( $0 < t < \tau$ ) period  $T$ . In Theorem 11.3 we show how to find the Fourier coefficients of a periodically repeated pulse.

- (b) Find the Fourier inverse of the expression that you obtained in (a), Method 1, and verify that it is the product of the envelope function and  $\cos(\omega_0 t)$ .

Figure 7.29. Radar pulse train  $x_p(t)$ .

- 7.20 Find the Fourier transform of  $f(t) = x(t)\sin(\omega_0 t)$

- (a) By convolution  
 (b) Using the frequency-shift property

7.21 (a) Find the Fourier transform of  $f(t) = \cos^2(\omega_0 t)$

(1) Using the analysis equation.

(2) Using frequency-domain convolution.

(b) Prove that  $2 \sin(\omega_0 t) \cos(\omega_0 t) = \sin(2\omega_0 t)$  by using frequency-domain convolution to find the Fourier transform of the LHS, and show that it is equal to the Fourier transform of the RHS.

7.22 (a) In order to demodulate the amplitude-modulated signal  $f(t) = x(t)\cos(\omega_0 t)$  we multiply it by  $\cos(\omega_0 t)$ . Find the Fourier spectrum of the result. How would you extract  $x(t)$  from it?

(b) Prove that if we demodulate  $x(t)\cos(\omega_0 t)$  by multiplication with  $\sin(\omega_0 t)$  we get zero in the baseband. Hence if the phase of the demodulating cosine in (a) drifts, the magnitude of the output falls. For this reason it is best that the demodulating cosine be phase locked to the incoming carrier, if that is possible.

7.23 (a) Prove that

$$\cos(\omega_0 t)U(t) \Leftrightarrow \frac{j\omega}{(j\omega)^2 + (\omega_0)^2} + \frac{1}{2}\pi[\delta(\omega - \omega_0) + \delta(\omega + \omega_0)] \quad (7.65)$$

by regarding the LHS as the time-domain product of  $\cos(\omega_0 t)$  and  $U(t)$ , and then applying frequency-domain convolution.

(b) From (a) we see that  $\cos(\omega_0 t)U(t)$  transforms to the sum of two terms, its odd part being the **pure imaginary and odd function**

$$P(\omega) \equiv \frac{j\omega}{(j\omega)^2 + (\omega_0)^2} \quad (7.66)$$

and its even part being the **real and even function**, one half the transform of  $\cos(\omega_0 t)$ . Sketch  $\cos(\omega_0 t)U(t)$ , its even part,  $\frac{1}{2}\cos(\omega_0 t)$ , and its odd part, and then infer that for (7.66),

$$p(t) = \begin{cases} \frac{1}{2} \cos(\omega_0 t) & (t > 0) \\ 0 & (t = 0) \\ -\frac{1}{2} \cos(\omega_0 t) & (t < 0) \end{cases} \quad (7.67)$$

(c) Infer that

$$\cos(\omega_0 t)\text{sgn}(t) \Leftrightarrow \frac{2j\omega}{(j\omega)^2 + (\omega_0)^2} \quad (7.68)$$

7.24 (a) Prove that

$$\sin(\omega_0 t)U(t) \Leftrightarrow \frac{\omega_0}{(j\omega)^2 + (\omega_0)^2} + \frac{\pi}{2j}[\delta(\omega - \omega_0) - \delta(\omega + \omega_0)] \quad (7.69)$$

by regarding the LHS as the time-domain product of  $\sin(\omega_0 t)$  and  $U(t)$ , and then applying frequency-domain convolution.

- (b) From (a) we see that  $\sin(\omega_0 t)U(t)$  transforms to the sum of two terms, its even part being the **real and even function**

$$Q(\omega) \equiv \frac{\omega_0}{(j\omega)^2 + (\omega_0)^2} \quad (7.70)$$

and its odd part being the **pure imaginary and odd function**, half the transform of  $\sin(\omega_0 t)$ . Sketch  $\sin(\omega_0 t)U(t)$ , its odd part,  $\frac{1}{2}\sin(\omega_0 t)$ , and its even part, and hence infer that for (7.70),

$$q(t) = \begin{cases} \frac{1}{2}\sin(\omega_0 t) & (t > 0) \\ 0 & (t = 0) \\ -\frac{1}{2}\sin(\omega_0 t) & (t < 0) \end{cases} \quad (7.71)$$

- (c) Infer that

$$\sin(\omega_0 t)\operatorname{sgn}(t) \Leftrightarrow \frac{2\omega_0}{(j\omega)^2 + (\omega_0)^2} \quad (7.72)$$

- 7.25 Use frequency-domain convolution to find the Fourier transforms of

(a)  $\cos(\omega_0 t)\operatorname{sgn}(t)$     (b)  $\sin(\omega_0 t)\operatorname{sgn}(t)$

Compare your results to (7.68) and (7.72).

- 7.26 For each of networks (a) and (b) shown in Figure 7.30:

- (a) Find the frequency transfer function and the CCL DE relating the output to the input.  
 (b) Fill in  $H(j\omega)$  and  $X(\omega)$  in the relationship

$$Y(\omega) = H(j\omega)X(\omega)$$

where  $x(t)$  for each network is as specified in the figure.

- (c) Invert the result obtained in (b) to obtain  $y(t)$ .  
 (d) Verify the result obtained in (c) by applying the CCL DE obtained in (a).

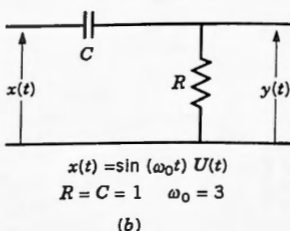
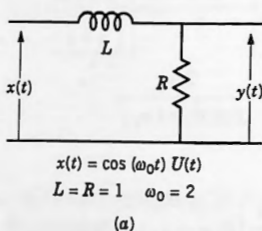


Figure 7.30.

### (D) Proof that Analysis and Synthesis Are Each Other's Inverses

7.27 (a) In (7.36)  $x(t)$  was expanded as a “sum” of sequential Dirac deltas. We repeat that equation here.

$$x(t) = \int_{-\infty}^{\infty} x(\tau) \delta(t - \tau) d\tau \quad (7.73)$$

Observe how similar this statement is to the Fourier synthesis equation where the function  $x(t)$  was expanded as a “linear combination” of complex exponentials, namely:

$$x(t) = \frac{1}{2\pi} \int_{-\infty}^{\infty} X(\omega) e^{j\omega t} d\omega \quad (7.74)$$

This is again evidence of the fact that Dirac deltas and complex exponentials are closely related. However, (7.73) is a time-domain expansion of  $x(t)$  and (7.74) is a frequency-domain expansion. Equation (7.73) is a surprisingly powerful result and we now use it to prove that

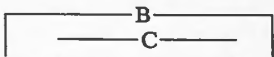
■ The Fourier analysis and synthesis transformations are each other's inverses.

First we note the following: Recall from the proof of Theorem 4.1 that (4.63) was based on the assumption that the Fourier analysis and synthesis transformations were each other's inverses, and so on that account we cannot use it to prove that very same proposition. However, (4.63) can also be derived by a totally independent method as well [see, e.g., Papoulis 1962] and so in fact we are entitled to use it in order to prove the proposition, as we shall now proceed to do.

(1) Use (4.63) in (7.73) to show that

$$x(t) = \frac{1}{2\pi} \int_{-\infty}^{\infty} x(\tau) \left[ \int_{-\infty}^{\infty} e^{j\omega t} e^{-j\omega\tau} d\omega \right] d\tau$$

(2) Now interchange the order of integration to obtain

$$x(t) = \frac{1}{2\pi} \int_{-\infty}^{\infty} \left[ \int_{-\infty}^{\infty} x(\tau) e^{-j\omega\tau} d\tau \right] e^{j\omega t} d\omega$$

(7.75)

(3) Then (7.75) is seen to consist of synthesis (B) acting on analysis (C) yielding the original function (A). Infer that they are each other's inverses. ■

(b) The complex exponential transforms as follows:

$$e^{jzt} \Leftrightarrow 2\pi\delta(\omega - z)$$

Use this fact to show that

$$\int_{-\infty}^{\infty} \left[ \frac{1}{2\pi} \int_{-\infty}^{\infty} F(z) e^{jzt} dz \right] e^{-j\omega t} dt = F(\omega)$$

Infer, once again, that synthesis and analysis are each other's inverses.

### (E) Discrete Convolution

**7.28** Given two discrete functions

$$g(n) \quad \text{and} \quad h(n) \quad (n \text{ any integer})$$

we define their **discrete convolution product**  $f(n)$  by

$$f(n) = \sum_{k=-\infty}^{\infty} g(k)h(n-k) \quad (7.76)$$

(a) Verify that the discrete convolution product satisfies the symmetry relationship

$$\sum_{k=-\infty}^{\infty} g(k)h(n-k) = \sum_{k=-\infty}^{\infty} h(k)g(n-k) \quad (7.77)$$

(b) Verify that if both  $g(n)$  and  $h(n)$  are zero for  $n < 0$ , then their convolution product simplifies to

$$f(n) = \sum_{k=0}^n g(k)h(n-k) = \sum_{k=0}^n h(k)g(n-k) \quad (7.78)$$

(c) Let  $g(n)$  and  $h(n)$  be equal to 1 for  $n = 1, \dots, 6$ , and zero otherwise. (See Fig. 7.31.) Calculate and plot  $f(n)$ , their convolution product.

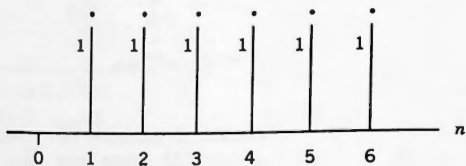


Figure 7.31.

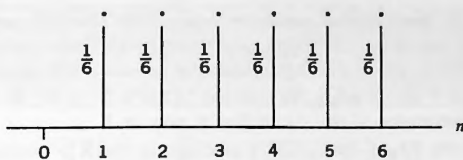


Figure 7.32.

- (d) If we modify the values shown in Figure 7.31 to  $\frac{1}{6}$ , then both  $g(n)$  and  $h(n)$  represent the probability that a single throw of a die (one dice) will come up equal to  $n$  ( $1 \leq n \leq 6$ ). This is shown in Figure 7.32. Verify that their discrete convolution product now represents the probability that a single throw of a **pair** of dice will come up equal to  $n$  ( $2 \leq n \leq 12$ ). From this we begin to see how convolution and probability are related. Laplace did extensive work in probability, and so we also begin to see why it was he who first discovered complex Fourier series, the complex Fourier integral, and convolution.
- (e) Obtain the same plots that were obtained in (c) and (d) by running this problem on the FFT system.  $N = 14$ , DISCRETE.

In Chapter 14 we carry out an operation count for discrete convolution, by two methods:

- Using the algorithm (7.76) (called the **direct method**)
- Using the FFT

and we'll see that, other than for very short sequences, it is much quicker to do discrete convolution using the FFT. The longer the sequence, the more this is true.

#### (F) An FFT Project Involving Prefiltering

- 7.29 In Figure 7.23 we saw how the two Sa functions were distorting one another because they were running into each other. This process is called **aliasing**. This aliasing could be avoided if we first **band-limit** the spectrum of the Rect signal that we are modulating onto the cosine function. Here's how to do it on the system.

- (1) Using  $N = 1024$  and  $T = 8$ , load  $\text{Rect}(t)$  into  $\mathbf{X}$  and  $\cos(16\pi t)$  in  $\mathbf{X2}$ .
- (2) Run ANALYSIS. This places the FFT spectrum of  $\mathbf{X}$  in  $\mathbf{F}$ .
- (3) Now use the system to **band-limit** this spectrum. (Go into the  $\mathbf{F}$  postprocessor via main-menu  $G$  where you will see a package called LOW-PASS FILTER. Use  $i_{\max} = 56$ . This will cut off all frequency components in  $\mathbf{F}$  for  $|\omega| > 14\pi$ .)
- (4) After running LOW-PASS FILTER, inspect the FFT spectrum to observe how the spectrum of the pulse is now zero outside of the interval  $-14\pi \leq \omega \leq 14\pi$ .

- (5) Invert this **band-limited** spectrum using **SYNTHESIS** and inspect a plot. You will see some distortion of the original Rect pulse, caused by the band-limiting, which will depend on how severely you have band-limited.
- (6) Now move Y into X using the package "COPY Y → X" in the X postprocessor. Inspect a plot of the signal that is now in X.
- (7) Now use the **REAL-MULTIPLY** package in the X postprocessor to multiply this band-limited  $\text{Rect}(t)$  pulse by the cosine in **X2**.
- (8) Run **ANALYSIS** and inspect **FRE**. You will observe that the two copies of the spectrum of the band-limited  $\text{Rect}(t)$  no longer run into each other. They are perfectly symmetrical with respect to their center frequencies.

Thus prefiltering of the signal going into the modulation process has eliminated aliasing, but has also distorted the signal somewhat. In Figure 7.33 we show a plot of the end result in which you will see how the two spectra of the Rect pulse have been truncated and no longer run into each other.

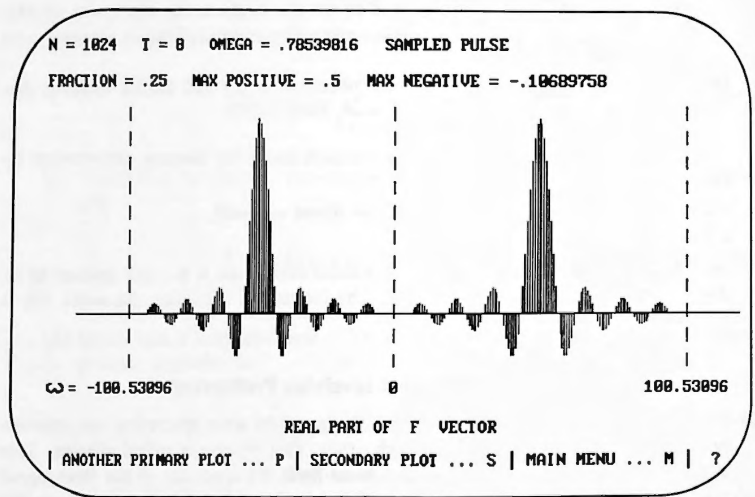


Figure 7.33. Spectrum of  $\text{Rect}(t)\cos(\omega_0 t)$  using prefiltering.

# The Properties

We have derived a number of properties of the Fourier transform in the preceding chapters. Some were displayed as theorems and others were derived as exercises. In this chapter we list them together with a few new ones that we derive here, all of which enable us to cut down significantly on the amount of work involved in finding Fourier transforms.

The properties also give us greater insight into the Fourier transform as a mathematical tool.

## 8.1 THE LINEARITY PROPERTY

---

■ **The linearity property**

$$c_1 f_1(t) + c_2 f_2(t) \Leftrightarrow c_1 F_1(\omega) + c_2 F_2(\omega) \quad (8.1)$$

This property follows immediately from the fact that integration is a linear operator, and so

$$\begin{aligned} & \int_{-\infty}^{\infty} [c_1 f_1(t) + c_2 f_2(t)] e^{-j\omega t} dt \\ &= c_1 \int_{-\infty}^{\infty} f_1(t) e^{-j\omega t} dt + c_2 \int_{-\infty}^{\infty} f_2(t) e^{-j\omega t} dt \end{aligned} \quad (8.2)$$

□**EXAMPLE 8.1:** Find the Fourier transform of

$$f(t) = \frac{1}{2}e^{-t/4}U(t) - \frac{1}{3}e^{-t/3}U(t) \quad (8.3)$$

**Solution:**

$$\begin{aligned} F(\omega) &= \frac{1}{2} \frac{1}{1/4 + j\omega} - \frac{1}{3} \frac{1}{1/3 + j\omega} \\ &= \frac{2(j\omega) + 1}{12(j\omega)^2 + 7(j\omega) + 1} \end{aligned} \quad (8.4)$$

□

**8.2 THE REALNESS PROPERTY****■ The realness property**

$$F^*(\omega) = F(-\omega) \quad \text{if and only if } f(t) \text{ is real} \quad (8.5)$$

□ **EXAMPLE 8.2:** Test the function  $F(\omega)$  in (8.4) to see if it comes from a real  $f(t)$ .**Solution:** Applying the test shown in (8.5) we have

$$\begin{aligned} F^*(\omega) &= \left[ \frac{2(j\omega) + 1}{12(j\omega)^2 + 7(j\omega) + 1} \right]^* \\ &= \frac{2(-j\omega) + 1}{12(-j\omega)^2 + 7(-j\omega) + 1} = F(-\omega) \end{aligned} \quad (8.6)$$

and so  $f(t)$  must be real. Equation (8.3) confirms this. □**8.3 THE SYMMETRY PROPERTIES****■ The symmetry properties**Let  $F(\omega) = A(\omega) + jB(\omega) = |F(\omega)|e^{j\Theta(\omega)}$ . Then, for  $f(t)$  real: $A(\omega)$  is even and  $B(\omega)$  is odd $|F(\omega)|$  is even and  $\Theta(\omega)$  is odd $f_{ev}(t) \Leftrightarrow A(\omega) \quad f_{od}(t) \Leftrightarrow jB(\omega)$  $F(\omega)$  is real and even iff  $f(t)$  is even $F(\omega)$  is imaginary and odd iff  $f(t)$  is odd

■ EXAMPLE 8.3: Consider the pulse  $f(t)$  shown in Figure 8.1, and let its Fourier transform be

$$F(\omega) = A(\omega) + jB(\omega) \quad (8.7)$$

In Figures 8.2 and 8.3 we show the even and odd parts of  $f(t)$ , which we call  $a(t)$  and  $b(t)$ . Then, without ever deriving  $F(\omega)$  we can infer quite a few of its properties. To keep score we shall append numbers inside a small circle. Thus, the Fourier inverse of  $A(\omega)$  is shown in Figure 8.2 ① and the Fourier inverse of  $jB(\omega)$  is shown in Figure 8.3. ②. □

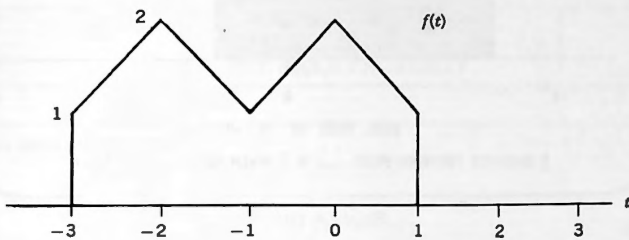


Figure 8.1.

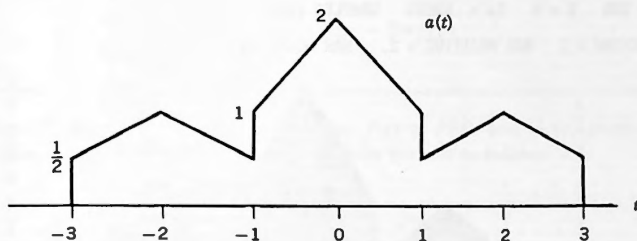


Figure 8.2.

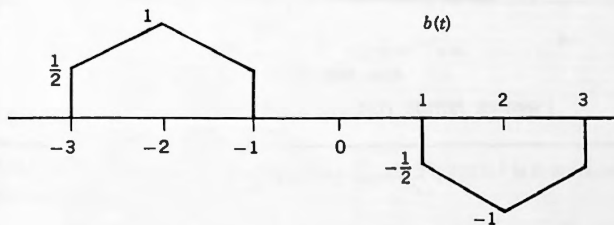
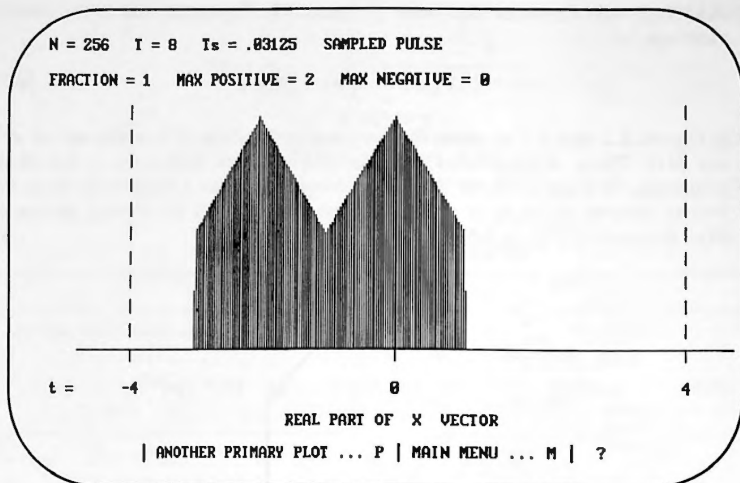
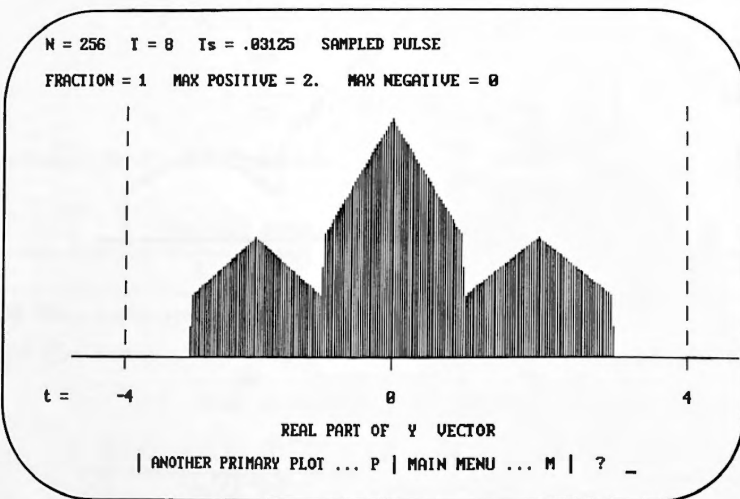


Figure 8.3.



*Figure 8.4.*  $f(t)$ .



*Figure 8.5.  $a(t)$ .*

### Accompanying Disk

In Figure 8.4 we show a plot of the pulse  $f(t)$  used previously, as it was submitted to the FFT system.

After deriving its FFT spectrum we nulled out the imaginary part  $B(\omega)$ , leaving only the real part  $A(\omega)$ . (There is a package in the F postprocessor that accomplishes this.) We then inverted  $A(\omega)$  using SYNTHESIS.

The result is plotted in Figure 8.5, which should be compared with Figure 8.2. Clearly it is the even part of  $f(t)$  that we called  $a(t)$ .

Similarly, when we nulled out  $A(\omega)$  using the F postprocessor and then inverted  $jB(\omega)$ , we obtained a plot that was identical to Figure 8.3.

## 8.4 THE AREA PROPERTY

### ■ The area property

$$\int_{-\infty}^{\infty} f(t) dt = F(0) \quad (8.8a)$$

and

$$\int_{-\infty}^{\infty} F(\omega) d\omega = 2\pi f(0) \quad (8.8b)$$

Equation (8.8a) states that the area under  $f(t)$  is  $F(0)$ , and (8.8b) states that area under  $F(\omega)$  is  $2\pi f(0)$ . These results are easily proved as follows:

$$F(\omega) = \int_{-\infty}^{\infty} f(t) e^{-j\omega t} dt \quad (8.9)$$

Setting  $\omega = 0$  gives (8.8a). Similarly

$$f(t) = \frac{1}{2\pi} \int_{-\infty}^{\infty} F(\omega) e^{j\omega t} d\omega \quad (8.10)$$

Setting  $t = 0$  gives (8.8b). ■

**EXAMPLE 8.4:** The area under the pulse  $f(t)$  in Figure 8.1 is 6 units, which means that from (8.8a)

$$F(0) = 6 \quad \textcircled{3}$$

Likewise the area under  $a(t)$  in Figure 8.2 is 6 units, and so,

$$A(0) = 6 \quad (4)$$

Since  $b(t)$  in Figure 8.3 is odd, its area is zero, and so

$$B(0) = 0 \quad (5)$$

This also follows immediately from the fact that  $B(\omega)$  is odd. □

■ **EXAMPLE 8.5:** From Figure 8.1,  $f(0) = 2$ , and so (8.8b) gives

$$\int_{-\infty}^{\infty} F(\omega) d\omega = 4\pi \quad (6)$$

From Figure 8.2,  $a(0) = 2$ , and so

$$\int_{-\infty}^{\infty} A(\omega) d\omega = 4\pi \quad (7)$$

From Figure 8.3, since  $b(t)$  is odd,  $b(0) = 0$ , and so

$$\int_{-\infty}^{\infty} B(\omega) d\omega = 0 \quad (8)$$

This also follows from the fact that  $B(\omega)$  is odd. □

There are other facts that we can infer without deriving  $F(\omega)$ , and in one of the exercises we explore some of them.

## 8.5 THE DUALITY PROPERTY

---

### ■ The duality property

$$\text{If } f(t) \Leftrightarrow F(\omega) \text{ then } F(t) \Leftrightarrow 2\pi f(-\omega) \quad (8.11)$$

First let's try to understand what this says and then we'll prove it: Referring to Figure 8.6, starting from the extreme left of (8.11), we take a given function  $f(t)$  and find its Fourier transform, which we call  $F(\omega)$ . Now take  $F(\omega)$  and substitute  $t$  in place of  $\omega$ , calling the result  $F(t)$ . Then the Fourier transform of  $F(t)$  will be  $2\pi$  times the original function  $f(t)$  with  $t$  replaced by  $-\omega$ .

What this tells us is that whenever we have found a Fourier transform it can be used immediately to produce a second one. As we shall see from the examples that

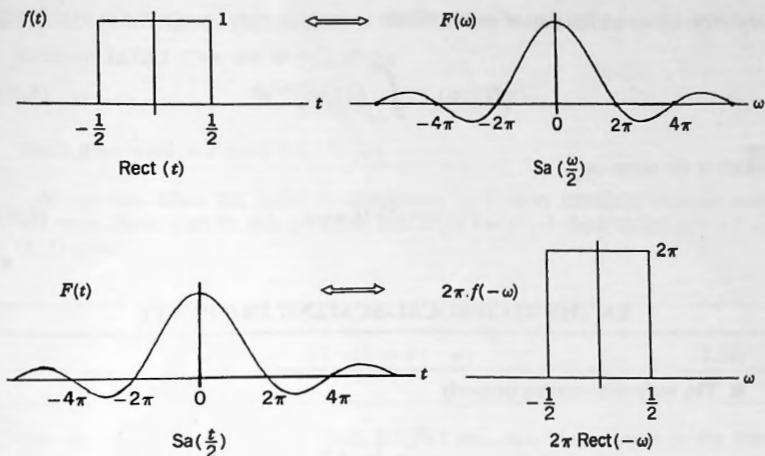


Figure 8.6. The duality property.

follow, in most cases that second transform is one that would have been extremely difficult to find by direct use of the analysis equation.

**EXAMPLE 8.6:** Find the Fourier transform of  $\text{Sa}(t/2)$ .

**Solution:** Trying to transform  $\text{Sa}(t/2)$  by using the analysis equation would be hopeless. (Just try it and you'll see why.) However, if we recall that  $\text{Rect}(t) \Leftrightarrow \text{Sa}(\omega/2)$ , then by (8.11)

$$\text{Sa}(t/2) \Leftrightarrow 2\pi \text{Rect}(-\omega) = 2\pi \text{Rect}(\omega) \quad (8.12)$$

which solves the problem immediately. Equation (8.12) is illustrated in Figure 8.6.  $\square$

*Proof of (8.11)*

$$f(t) = \frac{1}{2\pi} \int_{-\infty}^{\infty} F(\omega) e^{j\omega t} d\omega \quad (8.13)$$

Interchanging the symbols  $t$  and  $\omega$  gives

$$f(\omega) = \frac{1}{2\pi} \int_{-\infty}^{\infty} F(t) e^{j\omega t} dt \quad (8.14)$$

and now, reversing the sign of  $\omega$ , we obtain

$$2\pi f(-\omega) = \int_{-\infty}^{\infty} F(t) e^{-j\omega t} dt \quad (8.15)$$

which is the same as

$$F(t) \Leftrightarrow 2\pi f(-\omega) \quad (8.16)$$

## 8.6 THE RECIPROCAL-SCALING PROPERTY

### ■ The reciprocal-scaling property

$$f(\alpha t) \Leftrightarrow \frac{1}{|\alpha|} F\left(\frac{\omega}{\alpha}\right) \quad (8.17)$$

What this tells us is that if we compress a function on the  $t$ -axis by a factor  $\alpha$ , then we stretch it on the  $\omega$ -axis by a factor  $\alpha$  as well as multiplying by a scale-factor  $1/|\alpha|$ . (See Fig. 8.7.)

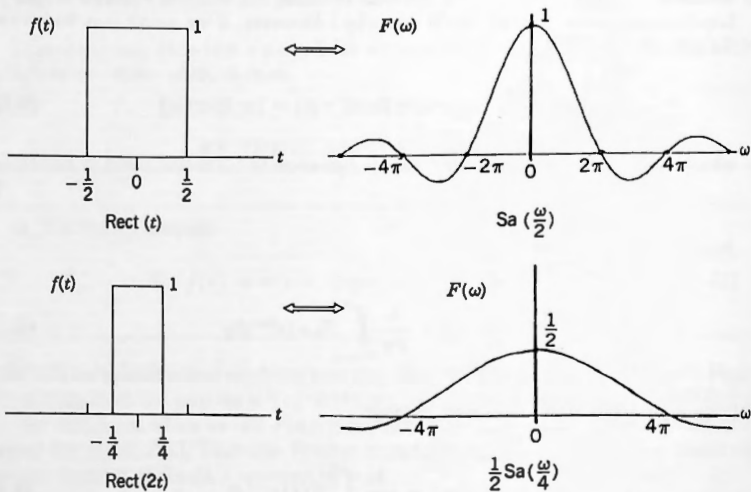


Figure 8.7. Example of reciprocal scaling.

**EXAMPLE 8.7:** Given that  $\text{Rect}(t) \Leftrightarrow \text{Sa}(\omega/2)$  find the transform of  $\text{Rect}(2t)$ .

**Solution:** In (8.17) we use  $\alpha = 2$ , giving

$$\text{Rect}(2t) \Leftrightarrow \frac{1}{2}\text{Sa}(\omega/4)$$

This is illustrated in Figure 8.7. □

Notice that when the pulse is compressed its Fourier transform expands, and vice versa. Note also by this property that if  $f(t) \Leftrightarrow F(\omega)$ , then letting  $\alpha = -1$  in (8.17) gives

$$f(-t) \Leftrightarrow F(-\omega) \quad (8.18)$$

Combining this with (8.5) means that, for  $f(t)$  real, reversing a pulse in the time domain corresponds to conjugation in the frequency domain (and vice-versa).

*Proof of (8.17):* Suppose first that  $\alpha > 0$ . Then we have the sequence in the following box:

Let  $\alpha t = z$ .  
Then  $t = z/\alpha$   
and  $dt = dz/\alpha$ .

$$\begin{aligned}
 f(\alpha t) &\Leftrightarrow \int_{-\infty}^{\infty} f(\alpha t) e^{-j\omega t} dt \longrightarrow \\
 &= \int_{-\infty}^{\infty} f(z) e^{-j\omega z/\alpha} \frac{dz}{\alpha} = \frac{1}{\alpha} \int_{-\infty}^{\infty} f(z) e^{-j(\omega/\alpha)z} dz \\
 &= \frac{1}{\alpha} F\left(\frac{\omega}{\alpha}\right)
 \end{aligned} \quad (8.19)$$

Now suppose that  $\alpha < 0$ . Then  $\alpha = -|\alpha|$  and the substitution box in (8.19) becomes,

Let  $\alpha t = z$ .  
Then  $t = z/\alpha = -z/|\alpha|$  and  $dt = dz/\alpha = -dz/|\alpha|$   
when  $t = \infty$ ,  $z = -\infty$  and when  $t = -\infty$ ,  $z = \infty$

from which we obtain

$$\begin{aligned} f(\alpha t) &\Leftrightarrow \int_{-\infty}^{\infty} f(\alpha t) e^{-j\omega t} dt = \int_{-\infty}^{-\infty} f(z) e^{-j\omega z/\alpha} \frac{-dz}{|\alpha|} \\ &= \frac{1}{|\alpha|} \int_{-\infty}^{\infty} f(z) e^{-j(\omega/\alpha)z} dz = \frac{1}{|\alpha|} F\left(\frac{\omega}{\alpha}\right) \end{aligned} \quad (8.20)$$

and so whether  $\alpha$  is positive or negative, (8.19) and (8.20) prove the proposition. ■

## 8.7 THE TIME-SHIFT PROPERTY

---

### ■ The time-shift property

If  $f(t) \Leftrightarrow F(\omega)$ , then

$$f(t - t_0) \Leftrightarrow e^{-j\omega t_0} F(\omega) \quad (8.21)$$

This was proved as Theorem 4.2.

□EXAMPLE 8.8: For pulse A shown in Figure 8.8, we have

$$e^{-\beta t} U(t) \Leftrightarrow \frac{1}{\beta + j\omega} \quad (8.22)$$

Hence for the same pulse delayed by 2 seconds (pulse B):

$$e^{-\beta(t-2)} U(t-2) \Leftrightarrow \frac{e^{-j2\omega}}{\beta + j\omega} \quad (8.23)$$

□

Equation (8.21) tells us the following: If a pulse  $f(t)$  has a Fourier transform with magnitude  $|F(\omega)|$  and phase  $\Theta(\omega)$ , then the same pulse delayed by  $t_0$  seconds will have a Fourier transform with magnitude still  $|F(\omega)|$ , but the phase will now be  $\Theta(\omega) - \omega t_0$ .

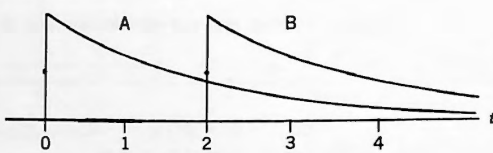


Figure 8.8. Time shift.

Thus time shifting does not affect the magnitude spectrum, but modifies the phase spectrum of a pulse, subtracting  $\omega t_0$  from the original phase spectrum. Since  $|F(\omega)|$  is unchanged, it follows that the energy spectrum is also unaffected by time shift, a property that we would totally expect.

## 8.8 THE FREQUENCY-SHIFT PROPERTY

### ■ The frequency-shift property

If  $f(t) \Leftrightarrow F(\omega)$ , then

$$f(t)e^{j\omega_0 t} \Leftrightarrow F(\omega - \omega_0) \quad (8.24)$$

This is also known as the **modulation property** or sometimes as Heaviside's shifting theorem. We have already encountered it in Theorem 4.4 and in a number of other places.

**EXAMPLE 8.9:** Given that  $U(t) \Leftrightarrow \pi\delta(\omega) + 1/j\omega$ , find the Fourier transform of  $\cos(\omega_0 t)U(t)$ .

**Solution:** In Exercise 7.23 we suggested that you solve this problem using frequency-domain convolution. We now do it using the frequency-shift property. By (8.24)

$$e^{j\omega_0 t}U(t) \Leftrightarrow \pi\delta(\omega - \omega_0) + \frac{1}{j(\omega - \omega_0)} \quad (8.25)$$

and so

$$\begin{aligned} \cos(\omega_0 t)U(t) &= \frac{1}{2}e^{j\omega_0 t}U(t) + \frac{1}{2}e^{-j\omega_0 t}U(t) \\ &\Leftrightarrow \frac{1}{2}\left[\pi\delta(\omega - \omega_0) + \frac{1}{j(\omega - \omega_0)}\right] \\ &\quad + \frac{1}{2}\left[\pi\delta(\omega + \omega_0) + \frac{1}{j(\omega + \omega_0)}\right] \\ &= \frac{1}{2}[\pi\delta(\omega - \omega_0) + \pi\delta(\omega + \omega_0)] + \frac{j\omega}{(j\omega)^2 + \omega_0^2} \end{aligned} \quad (8.26)$$

□

The function  $\cos(\omega_0 t)U(t)$  is neither odd nor even. In (8.26) we see that its even and odd parts have transformed as follows:

$$f_{ev}(t) \Leftrightarrow \frac{1}{2}[\pi\delta(\omega - \omega_0) + \pi\delta(\omega + \omega_0)] \quad (\text{real and even}) \quad (8.27)$$

$$f_{od}(t) \Leftrightarrow \frac{j\omega}{(j\omega)^2 + \omega_0^2} \quad (\text{purely imaginary and odd}) \quad (8.28)$$

*Proof of (8.24):* In Exercise 4.3 we suggested that you prove this property by direct use of the analysis equation. We now do it using frequency-domain convolution. Thus

$$\begin{aligned} f(t)e^{j\omega_0 t} &\Leftrightarrow \frac{1}{2\pi} \int_{-\infty}^{\infty} F(\Theta) 2\pi\delta(\omega - \omega_0 - \Theta) d\Theta \\ &= \int_{-\infty}^{\infty} F(\omega - \omega_0) \delta(\omega - \omega_0 - \Theta) d\Theta = F(\omega - \omega_0) \end{aligned} \quad (8.29)$$

■

## 8.9 TIME-DOMAIN DIFFERENTIATION

---

### ■ Time-domain differentiation

$$\text{If } f(t) \Leftrightarrow F(\omega) \text{ then } D^{(n)}f(t) \Leftrightarrow (j\omega)^n F(\omega) \quad (8.30)$$

This was proved as Theorem 5.1, and in Chapter 5 we made extensive use of it in the method of successive differentiation.

---

## 8.10 FREQUENCY-DOMAIN DIFFERENTIATION

---

### ■ Frequency-domain differentiation

$$\text{If } f(t) \Leftrightarrow F(\omega) \text{ then } t^n f(t) \Leftrightarrow (j)^n d^n F(\omega) / d\omega^n \quad (8.31)$$

This is the dual to time-domain differentiation just given. We established this property earlier as Theorem 4.3.

□EXAMPLE 8.10: Find the Fourier transform of

$$f(t) = te^{-\beta t} \cos(\omega_0 t)U(t) \quad (\beta > 0)$$

**Solution:** First we find the transform of  $e^{-\beta t} \cos(\omega_0 t)U(t)$ . We know that  $e^{-\beta t}U(t) \Leftrightarrow 1/(\beta + j\omega)$ , and so

$$\begin{aligned} e^{-\beta t} \cos(\omega_0 t)U(t) &= \frac{1}{2}e^{-\beta t}U(t)(e^{j\omega_0 t} + e^{-j\omega_0 t}) \\ &\Leftrightarrow \frac{1}{2} \frac{1}{\beta + j(\omega - \omega_0)} + \frac{1}{2} \frac{1}{\beta + j(\omega + \omega_0)} = \frac{j\omega + \beta}{(j\omega + \beta)^2 + \omega_0^2} \end{aligned}$$

[by frequency shift]

Then, by (8.31),

$$\begin{aligned} te^{-\beta t} \cos(\omega_0 t)U(t) \\ \Leftrightarrow j \frac{d}{d\omega} \left[ \frac{j\omega + \beta}{(j\omega + \beta)^2 + \omega_0^2} \right] = \frac{(j\omega + \beta)^2 - \omega_0^2}{[(j\omega + \beta)^2 + \omega_0^2]^2} \end{aligned} \quad (8.32)$$

□

*Proof of (8.31):* Although we proved (8.31) in Chapter 4 by direct differentiation, it can also be proved as follows (good practice in the use of these properties):

$$\begin{aligned} f(t) &\Leftrightarrow F(\omega) \\ \therefore F(t) &\Leftrightarrow 2\pi f(-\omega) \quad (\text{duality}) \\ \therefore DF(t) &\Leftrightarrow 2\pi j\omega f(-\omega) \quad (\text{time differentiation}) \\ \therefore 2\pi jtf(-t) &\Leftrightarrow 2\pi F'(-\omega) \quad (\text{duality}) \\ \therefore tf(-t) &\Leftrightarrow -jF'(-\omega) \\ \therefore -tf(t) &\Leftrightarrow -jF'(\omega) \quad (\text{reciprocal scaling}) \\ \therefore tf(t) &\Leftrightarrow jF'(\omega) \end{aligned}$$

To prove it for any  $n$  we now use the method of induction. ■

## 8.11 TIME-DOMAIN CONVOLUTION

### ■ Time-domain convolution

$$\int_{-\infty}^{\infty} f(\tau)g(t - \tau) d\tau \Leftrightarrow F(\omega)G(\omega) \quad (8.33)$$

We are completely familiar with this property from Chapter 7, which says that convolution in the time domain corresponds to multiplication in the frequency domain.

### 8.12 FREQUENCY-DOMAIN CONVOLUTION

#### ■ Frequency-domain convolution

$$f(t)g(t) \Leftrightarrow \frac{1}{2\pi} \int_{-\infty}^{\infty} F(\Theta)G(\omega - \Theta) d\Theta \quad (8.34)$$

We are also completely familiar with this property from Chapter 7, which says that multiplication in the time domain corresponds to  $1/2\pi$  times convolution in the frequency domain.

### 8.13 TWO PROPERTIES OF THE DIRAC DELTA

#### ■ Two properties of the Dirac delta

##### (a) The sampling property:

$$f(t)\delta(t - t_0) = f(t_0)\delta(t - t_0) \quad (8.35)$$

$$G(\omega)\delta(\omega - \omega_0) = G(\omega_0)\delta(\omega - \omega_0) \quad (8.36)$$

##### (b) The convolution property

$$f(t) * \delta(t - t_0) = f(t - t_0) \quad (8.37)$$

$$G(\omega) * \delta(\omega - \omega_0) = G(\omega - \omega_0) \quad (8.38)$$

We have used these four results earlier, and we display them here to reinforce the reader's awareness of their existence and their precise structure. The sampling property—(8.35) and (8.36)—was discussed in Chapter 4. Equation (8.37) follows from (8.35). Thus:

$$\begin{aligned} f(t) * \delta(t - t_0) &= \int_{-\infty}^{\infty} f(\tau)\delta(t - t_0 - \tau) d\tau \\ &= \int_{-\infty}^{\infty} f(t - t_0)\delta(t - t_0 - \tau) d\tau = f(t - t_0) \end{aligned} \quad (8.39)$$

with a similar proof for (8.38). ■

There is a second way of seeing (8.37), as follows. By the convolution property:

$$f(t) * \delta(t - t_0) \Leftrightarrow F(\omega) e^{-j\omega t_0} \quad (8.40)$$

By the time-shift property however, the RHS of (8.40) is the transform of  $f(t - t_0)$ , and so it can be continued as

$$\dots \Leftrightarrow f(t - t_0) \quad (8.41)$$

which is what (8.37) says. ■

Note that in the sampling-property statements there are impulses on both sides of the equation, whereas in the convolution-property statements there are no impulses on the RHS.

## 8.14 THE INTEGRATION PROPERTY

### ■ The integration property

If  $f(t) \Leftrightarrow F(\omega)$ , then

$$\int_{-\infty}^t f(\tau) d\tau \Leftrightarrow \frac{1}{j\omega} F(\omega) + \pi F(0) \delta(\omega) \quad (8.42)$$

A proof is constructed (with some help) in Exercise 8.35.

## EXERCISES

### 8.1 For $F(\omega)$ of Example 8.3, show that

- (a)  $\int_{-\infty}^{\infty} F(\omega) e^{-j\omega} d\omega = 2\pi$
- (b)  $\int_{-\infty}^{\infty} F(\omega) e^{j\omega} d\omega = \pi$
- (c)  $\int_{-\infty}^{\infty} |F(\omega)|^2 d\omega = 56\pi/3$
- (d)  $\int_{-\infty}^{\infty} |A(\omega)|^2 d\omega = 42\pi/3$
- (e)  $\int_{-\infty}^{\infty} |B(\omega)|^2 d\omega = 14\pi/3$

### 8.2 (a) Use reciprocal scaling followed by time shift to prove that

$$f[\alpha(t - \tau)] \Leftrightarrow \frac{1}{|\alpha|} F\left(\frac{\omega}{\alpha}\right) e^{-j\omega\tau}$$

- (b) Use time shift followed by reciprocal scaling to prove that

$$f(\alpha t - \tau) \Leftrightarrow \frac{1}{|\alpha|} F\left(\frac{\omega}{\alpha}\right) e^{-j\omega\tau/\alpha}$$

- (c) Verify these two results by direct transformation.

**8.3** Prove the time-shift property by combining frequency shift with duality.

**8.4** Prove the frequency-shift property by combining time shift with duality.

**8.5** (a) Verify by duality that

$$\delta(t + \tau/2) - \delta(t - \tau/2) \Leftrightarrow 2j \sin(\omega\tau/2)$$

- (b) Now verify the same result by direct transformation.

**8.6** (a) Verify by duality that

$$\delta(t + \tau) + \delta(t - \tau) \Leftrightarrow 2 \cos(\omega\tau)$$

- (b) Now verify the same result by direct transformation.

**8.7** Starting from  $e^{-\beta t}U(t) \Leftrightarrow 1/(\beta + j\omega)$ , ( $\beta > 0$ ), plus frequency shift, verify that

$$(a) e^{-\beta t} \cos(\omega_0 t)U(t) \Leftrightarrow \frac{j\omega + \beta}{(j\omega + \beta)^2 + \omega_0^2}$$

$$(b) e^{-\beta t} \sin(\omega_0 t)U(t) \Leftrightarrow \frac{\omega_0}{(j\omega + \beta)^2 + \omega_0^2}$$

(c) Now find the inverse of

$$\frac{8j\omega + 4}{(j\omega)^2 + 4j\omega + 20}$$

**8.8** Starting from  $e^{-\beta t}U(t) \Leftrightarrow 1/(\beta + j\omega)$  and  $\cos(\omega_0 t) \Leftrightarrow \pi\delta(\omega - \omega_0) + \pi\delta(\omega + \omega_0)$ , use convolution to prove that

$$e^{-\beta t} \cos(\omega_0 t)U(t) \Leftrightarrow \frac{j\omega + \beta}{(j\omega + \beta)^2 + \omega_0^2}$$

**8.9** (a) Is  $f(t) = 1/t$  square integrable over  $-\infty < t < \infty$ ? If not, then we are not guaranteed that it has a Fourier transform.

(b) Try to find the transform of  $1/t$  by direct transformation. Explain what the problem is.

(c) Now find the transform of  $1/t$  starting from  $\text{sgn}(t)$  by using the duality property to show that

$$\frac{1}{t} \Leftrightarrow \frac{\pi}{j} \text{sgn}(\omega)$$

Thus, by thinking of  $1/t$  as a distribution, even though it is not square integrable it nevertheless has a Fourier transform.

**8.10** Define  $\Lambda(t/k)$  as a triangular pulse from  $-k$  to  $k$  with height 1 (Figure 8.9).

(a) Make direct use of the convolution integral to verify that

$$k\Lambda(t/k) = \text{Rect}(t/k) * \text{Rect}(t/k)$$

(b) Starting from this result show that

$$\Lambda(t/k) = k \text{Sa}^2(\omega k/2)$$

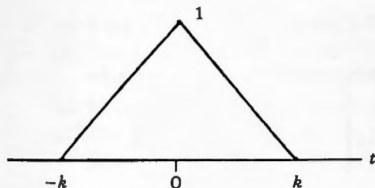


Figure 8.9.  $\Lambda(t/k)$ .

**8.11** (a) Use the transform pair that you obtained in Exercise 8.10 to find the inverse transform of  $\Lambda(\omega/k)$ .

(b) Use duality to find the Fourier transform of  $\text{Sa}^2(t)$ .

**8.12** Apply reciprocal scaling to find the transform of  $e^{-\sigma t}U(t)$  given that

$$e^{-\beta t}U(t) \Leftrightarrow 1/(\beta + j\omega) \quad (\sigma \neq \beta)$$

**8.13** Given that  $\text{Rect}(t) \Leftrightarrow \text{Sa}(\omega/2)$  find the Fourier transform of  $\text{Sa}(3t)$

**8.14** Prove by convolution that

$$f(t - t_0) \Leftrightarrow e^{-j\omega t_0}F(\omega)$$

**8.15** (a) Find the Fourier transform of the radar pulse  $\sin(\omega_0 t)\text{Rect}(t/\tau)$  by using frequency shift.

(b) Find the Fourier transform of the modulated signal  $\cos(\omega_0 t)f(t)$  by frequency shift.

**8.16** (a) Find an expression for the Fourier transform of the gated function  $f(t)\text{Rect}(t/\tau)$

(b) Using the result obtained in (a), verify the sampling property

$$f(t)\delta(t - t_0) = f(t_0)\delta(t - t_0)$$

*Hint:* Start with the box function  $B(t - t_0)$ .

8.17 (a) Using time shift, write the Fourier transform for the group of impulses shown in Figure 8.10.

(b) Using time shift, write the Fourier inverse of

- |  |                                 |
|--|---------------------------------|
| (1) $e^{-j\omega\tau}$                       | (2) $\cos(\omega\tau)$          |
| (3) $j \sin(\omega\tau)$                     | (4) $\cos^2(\omega\tau)$        |
| (5) $4j \cos(p\omega)\sin(q\omega)$          | (6) $\cos(\omega\tau)F(\omega)$ |
| (7) $[e^{j\omega\tau} + e^{j2\omega\tau}]^2$ |                                 |

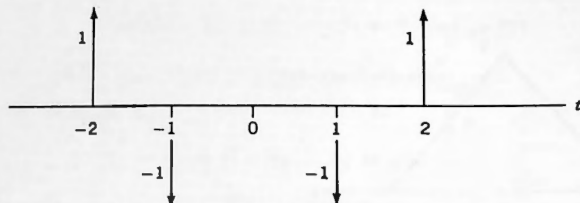


Figure 8.10.

8.18 For the pulse  $f(t)$  shown in Figure 8.11

(a) Find its Fourier transform starting from

$$\text{Rect}(t) \Leftrightarrow \text{Sa}(\omega/2)$$

followed by reciprocal scaling, followed by time shift.

- (b) Differentiate the pulse in the time domain by inspection. Find the Fourier transform of the result.
- (c) Differentiate the pulse by performing an appropriate operation in the frequency domain and reconcile the result with that obtained in (b).

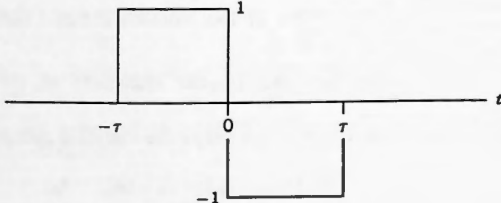


Figure 8.11.

8.19 A pulse  $x(t)$  is passed through an ideal low-pass filter whose frequency response is exactly 1 from  $-\omega_0/2$  to  $\omega_0/2$  and zero outside of that range.

- (a) Find the time-domain expression for the pulse  $y(t)$  that emerges from the filter in two ways:
  - (1) By the Fourier inversion integral
  - (2) By convolution in the time domain
- (b) Assuming that  $x(t) = \delta(t)$ , carry out the integrations specified in (a)(1) and (a)(2), and compare your answers.

8.20 A filter has frequency response

$$H(\omega) = 1 + 2k \cos(\omega T)$$

- (a) Find the impulse response of the filter.
- (b) Use time-domain convolution to find the expression for the pulse  $y(t)$  that emerges, given that  $x(t)$  is the input.
- (c) Find  $y(t)$  by making direct use of the inversion integral.
- (d) For the case where  $x(t) = \text{Rect}(t)$ ,  $k = 0.5$ , and  $T = 2$ , draw the output pulse.

8.21 For the pulse  $f(t)$  shown in Figure 8.12:

- (a) Starting from  $\Delta(t/\tau) \Leftrightarrow \tau \text{Sa}^2(\omega\tau/2)$  find its Fourier transform by treating it as the difference of two  $\Delta$  pulses. (See Exercise 8.10 for a definition of  $\Delta(t/\tau)$ ).
- (b) Find its Fourier transform by the method of successive differentiation and reconcile the result with what you obtained in (a).

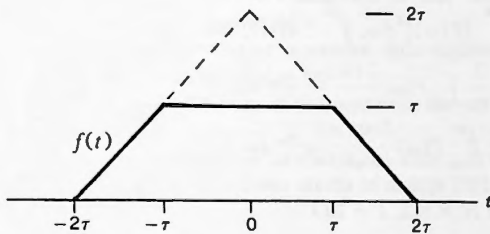


Figure 8.12.

8.22 For the two functions:

$$x(t) = e^{-2t}U(t) \quad \text{and} \quad h(t) = e^{-3t}U(t)$$

- (a) Find their convolution product in the time domain using the convolution integral.
- (b) Fourier transform the result that you obtained in (a).

- (c) Now find the Fourier transform of their convolution product using frequency-domain multiplication, and show that your result is equivalent to (b).
- (d) If  $x(t)$  is the input to a linear, time-invariant (LTI) system whose impulse response is  $h(t)$ , find the expression for  $y(t)$  and draw it.
- (e) Confirm your results using the convolution option in the FFT system on the disk. (Use  $N = 512$ ,  $T = 4$ .)

8.23 For the pulse  $f(t)$  shown in Figure 8.13:

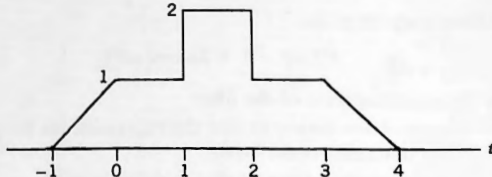


Figure 8.13.

- (a) Letting  $F(\omega) = A(\omega) + jB(\omega)$ , sketch

$$\frac{1}{2\pi} \int_{-\infty}^{\infty} A(\omega) e^{j\omega t} d\omega \quad \text{and} \quad \frac{1}{2\pi} \int_{-\infty}^{\infty} jB(\omega) e^{j\omega t} d\omega$$

- (b) Find  $F(0)$ ,  $A(0)$ , and  $jB(0)$ .

$$(c) \text{Find } \int_{-\infty}^{\infty} F(\omega) d\omega, \int_{-\infty}^{\infty} A(\omega) d\omega \quad \text{and} \quad \int_{-\infty}^{\infty} jB(\omega) d\omega$$

$$(d) \text{Find } \int_{-\infty}^{\infty} |F(\omega)|^2 d\omega, \int_{-\infty}^{\infty} |A(\omega)|^2 d\omega \quad \text{and} \quad \int_{-\infty}^{\infty} |B(\omega)|^2 d\omega$$

$$(e) \text{Sketch } \frac{1}{2\pi} \int_{-\infty}^{\infty} F(\omega) \frac{2\sin(\omega)}{\omega} e^{j\omega t} d\omega$$

$$(f) \text{Evaluate } \int_{-\infty}^{\infty} F(\omega) \frac{2\sin(\omega)}{\omega} e^{j2\omega} d\omega$$

- (g) Use the FFT system to obtain confirmation of your results from (a), (d), (e), and (f). (Use  $N = 512$ ,  $T = 16$ .)

8.24 An ideal low-pass filter has response 1 for  $-1/2 < \omega < 1/2$  and zero otherwise. A unit impulse at time  $t = 1$  is presented as its input.

- (a) Write the frequency-domain expression for the response  $y(t)$ .
- (b) Find the time-domain expression for  $y(t)$ .
- (c) The pulse  $y(t)$  is now sampled (multiplied) by a second unit impulse at  $t = 1$ , that we call  $w(t)$ , and the result is called  $z(t)$ . Find the time-domain expression for  $z(t)$ .
- (d) Write the frequency-domain expression for the operation that takes place in (c) in terms of  $Y(\omega)$  and  $W(\omega)$ . Then invert it and reconcile your result with what you obtained in (c).

8.25 Let  $y(t) = te^{-\beta t}U(t)$ . Prove that

$$y(t) * U(t) = \frac{1}{\beta^2} [1 - (1 + \beta t)e^{-\beta t}]U(t)$$

8.26 For the two pulses  $x(t)$  and  $h(t)$  shown in Figure 8.14:

- Find  $x(t) * h(t)$  analytically by evaluating the convolution integral.
- Find  $x(t) * h(t)$  graphically.
- If  $x(t)$  is the input to an LTI system whose impulse response is  $h(t)$  and output is  $y(t)$ , find the expression for  $Y(\omega)$ .
- Confirm the result that you obtained in (a) or (b) by the use of the convolution option in the FFT system. (Use  $N = 512, T = 4$ .)
- Use the FFT system to invert the expression for  $Y(\omega)$  that you obtained in (c) and reconcile the result with what you obtained in (d).

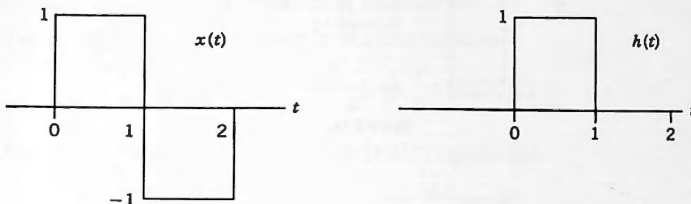


Figure 8.14.

- 8.27 (a) Use time shift plus  $\text{Rect}(t/\tau) \Leftrightarrow \tau \text{Sa}(\omega\tau/2)$  to find  $X(\omega)$ , the Fourier transform of  $x(t)$  shown in Figure 8.15.
- (b) Now find  $X(\omega)$  by the method of successive differentiation and reconcile your result with what you obtained in (a).
- (c) Sketch the even and the odd parts of  $x(t)$  and write the expressions for their Fourier transforms.
- (d) Use the FFT system on the disk to create the even and odd parts of the pulse. ( $N = 480, T = 12$ )

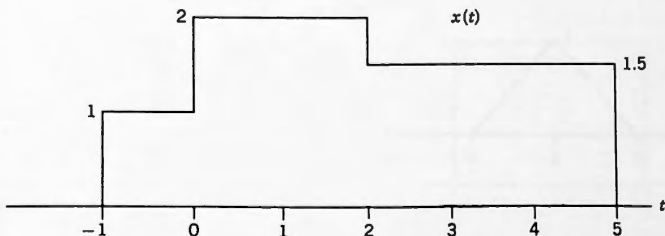


Figure 8.15.

- 8.28** (a) Find the Fourier transform for the pulse  $x(t)$  shown in Figure 8.16 by using the method of successive differentiation.  
 (b) Now find  $X(\omega)$  by regarding  $x(t)$  as a sum of four delayed Rect pulses. Reconcile your result with the one you obtained in (a).  
 (c) Find  $x(t) * h(t)$  graphically, where  $h(t)$  is shown in Figure 8.14.  
 (d) Confirm your result in (c) by using the convolution option in the FFT system on the disk. ( $N = 300$ ,  $T = 6$ .)

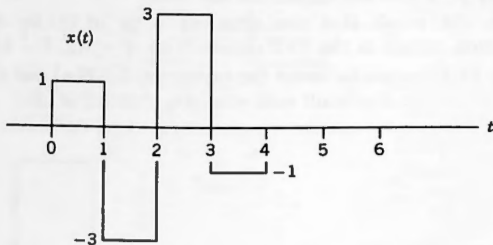


Figure 8.16.

- 8.29** (a) Use the convolution integral directly to find

$$y(t) = x(t) * h(t)$$

- where  $x(t)$  and  $h(t)$  are shown in Figure 8.17, and then sketch  $y(t)$ .  
 (b) Verify from your expression for  $y(t)$  that it is everywhere continuous and its first derivative is also everywhere continuous, but its second derivative is not. What does this suggest about  $Y(\omega)$ ?  
 (c) Find the expression for  $Y(\omega)$  and reconcile it with what you learned in (b).  
 (d) Use CONVOLUTION in the FFT system to validate (a). ( $N = 512$ ,  $T = 8$ .)

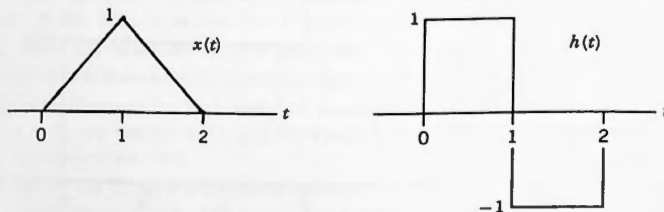


Figure 8.17.

- 8.30 In the exercises to Chapter 6 you were asked to prove the following theorem regarding differentiation of the input to a linear system and the resulting response:

**THEOREM 6.6**

If  $y(t)$  is the response of a linear system to an input  $x(t)$ , then  $y'(t)$  will be the response to the input  $x'(t)$ .

- Regarding the two pulses  $x(t)$  and  $h(t)$  of Figure 8.17, use this theorem to create sketches of  $y'(t)$  and  $y''(t)$ , where  $y(t) = x(t) * h(t)$ .
- Use the FFT system to validate your results. ( $N = 512, T = 8$ )
- In Exercise 8.29(b) you were asked to show that  $y(t)$  and  $y'(t)$  were everywhere continuous but that  $y''(t)$  was not. Reconcile what you obtained there with what you obtained in this exercise.

- 8.31 Use duality plus the first result in (4.15) to prove that

$$\frac{1}{t^2 + \beta^2} \Leftrightarrow \frac{\pi}{\beta} e^{-\beta|\omega|}$$

- 8.32 Use duality plus the second result in (4.15) to prove that

$$\frac{t}{t^2 + \beta^2} \Leftrightarrow -j\pi e^{-\beta|\omega|} \operatorname{sgn}(\omega)$$

- 8.33 Use frequency-domain differentiation to carry out Exercise 8.32 starting from Exercise 8.31.

- Sketch the convolution product of the two pulses in Figure 8.18, calling it  $f(t)$ .
- Using only the pulse that you have sketched in (a), find its Fourier transform,  $F(\omega)$ .
- How should  $F(\omega)$  be related to the transforms of the individual pulses,  $G(\omega)$  and  $H(\omega)$ ?
- Find  $G(\omega)$  and  $H(\omega)$ .
- Verify that (c) is in fact correct.

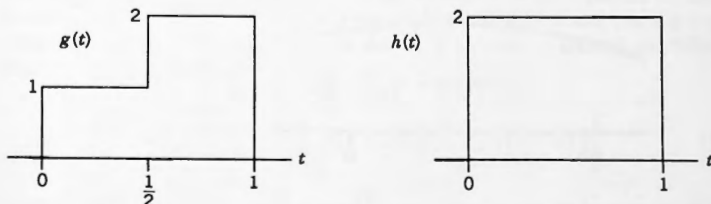


Figure 8.18.

## 8.35 Proof of the integration property (8.42), namely

$$\int_{-\infty}^t f(\tau) d\tau \Leftrightarrow \frac{1}{j\omega} F(\omega) + \pi F(0) \delta(\omega) \quad (8.43)$$

We use convolution in the time domain as follows: First we note that  $U(t - \tau)$  on the  $\tau$ -axis is the unit step shown in Figure 8.19a. Then the product  $f(\tau)U(t - \tau)$  is as shown in Figure 8.19c,  $f(\tau)$  to the left of  $t$  and zero to the right. From this it follows that the integral in (8.43) can be written as

$$\int_{-\infty}^t f(\tau) d\tau = \int_{-\infty}^{\infty} f(\tau) U(t - \tau) d\tau \quad (8.44)$$

The RHS of (8.44) is now seen to be a time-domain convolution product. Transform it to prove (8.43).

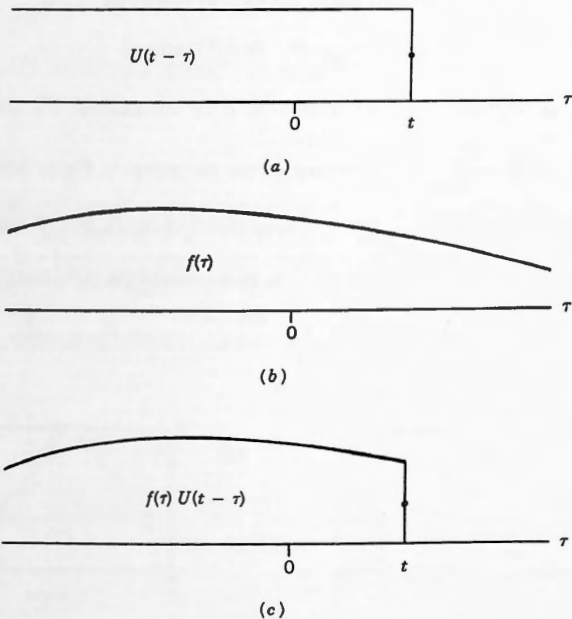


Figure 8.19. Forming  $f(\tau)U(t - \tau)$ .

8.36 We recall from Chapter 5 that

$$\int_{-\infty}^t \delta(\tau) d\tau = U(t) \quad (8.45)$$

Use the integration property to find the Fourier transform of the LHS of (8.45) and verify that it is equal to the transform of the RHS.

8.37 The pulse  $f(t)$  is shown in Figure 8.20a, and in Figure 8.20b we show its integral

$$g(t) = \int_{-\infty}^t f(\tau) d\tau$$

Find the Fourier transform of  $g(t)$  in two ways:

- (a) By the method of successive differentiation
- (b) Using the integration property

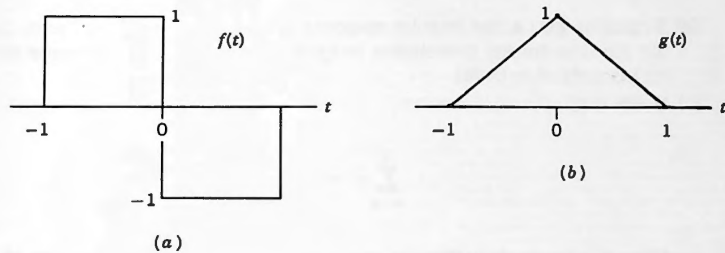


Figure 8.20.

8.38 Find the Fourier transform of  $\text{Sa}^2(t)$

8.39 **An Edge Detector:** A video camera scans a scene using a raster scan and converts it to a sequence of electronic pulses, one for each line of the scan. We call any one of those video lines  $x(t)$ . By an edge in a video picture we mean a transition from black to white, or white to black in  $x(t)$ , where black is a small value and white is a large one. To decide if an edge is present the following algorithm could be used:

$$y(t) = \frac{1}{8} \left[ \sum_{n=0}^4 x(t + nT) - \sum_{n=0}^4 x(t - nT) \right] \quad (8.46)$$

In (8.46),  $T$  is a suitably chosen time interval that is a small fraction of the total duration of the pulse  $x(t)$ .

If the picture has an edge that is going from black on the left to white on the right, then the values of  $x(t)$  in the first sum in the RHS of (8.46) will be large and the values in the second sum will be small, and so  $y(t)$  will be a large number. If the edge has white on the left and black on the right, then  $y(t)$  will still be large but with reversed sign. If there is no edge, then  $y(t) \approx 0$ .

Thus a large value for  $|y(t)|$  on any one line means that a possible edge has been detected. If the same happens on enough succeeding lines of the raster scan in roughly the same place, then it is confirmed that an edge has been detected.

Observe also that by including five (or more) samples in each of the sums in (8.46) we are incorporating a certain degree of data smoothing to counteract the effects of any noise in the signal  $x(t)$ . Consider the impulse response shown in Figure 8.21, called  $g(t)$ :

- (a) Verify that for four impulses in each group as shown, we can write the expression for  $g(t)$  as

$$g(t) = \frac{1}{8} \left[ \sum_{n=0}^4 \delta(t + nT) - \sum_{n=0}^4 \delta(t - nT) \right]$$

- (b) Regarding  $g(t)$  as the impulse response of a network with  $x(t)$  as its input, use the time-domain convolution integral to verify that the response will be  $y(t)$  as defined in (8.46).
- (c) Verify that

$$\sum_{n=0}^4 a^n = \frac{1 - a^5}{1 - a}$$

Using this result, show that the expression for the Fourier transform of  $g(t)$  in Figure 8.21 is

$$G(\omega) = j \left[ \frac{\sin(\omega T) + \sin(4\omega T) - \sin(5\omega T)}{16 \sin^2(\omega T/2)} \right]$$

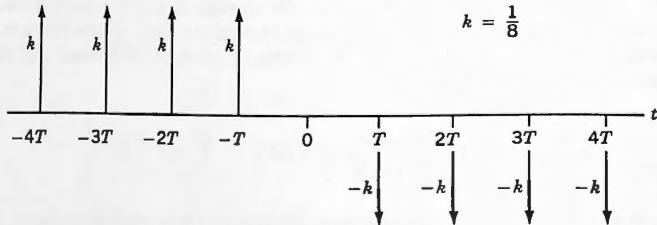


Figure 8.21. Impulse response  $g(t)$ .

- (d) Instead of just four impulses in each group with weights 1/8 in  $g(t)$ , assume that there are  $m$  impulses each with weight  $1/2m$ . Now show that the Fourier transform of  $g(t)$  is

$$G(\omega) = j \left[ \frac{\sin(\omega T) + \sin(m\omega T) - \sin[(m+1)\omega T]}{4m \sin^2(\omega T/2)} \right]$$

- (e) Use the FFT system to verify the expression for  $G(\omega)$  that you obtained in (c). ( $N = 256$ ,  $T = 16$ .)

# The Sampling Theorems

### 9.1 INTRODUCTION

---

The term “sampling” refers to a process whereby a continuous function is evaluated at discrete points, usually on a periodic basis. The continuous function may be in the time domain, such as a pulse or periodic function  $x(t)$ , in which case sampling results in the sequence of numbers

$$\dots, x(t_1), x(t_2), x(t_3), \dots$$

Alternatively the continuous function may be in the frequency domain, such as a Fourier transform  $X(\omega)$ , in which case sampling results in

$$\dots, X(\omega_1), X(\omega_2), X(\omega_3), \dots$$

In this chapter we examine how a mathematical model can be constructed to represent what we call **impulse sampling**, and we develop a number of theorems regarding the impulse sampling process. We shall also model the sampling process when the sampling waveforms are other than impulses.

### 9.2 TIME-DOMAIN IMPULSE SAMPLING

---

It is often the case that we have a continuous function of time, such as a voltage  $x(t)$ , and that we wish to transmit it over a system that accepts only discrete values. We shall then have to take samples of our waveform.

Two interrelated questions arise:

- (A) How frequently should the sampling take place?
- (B) Can we reconstruct the original function  $x(t)$  from its samples at the reception point?

In this chapter we try to provide answers to both questions.

The first form of sampling that we consider is what is known as **impulse sampling**, in which the sampling pulse is a Dirac delta. Keep in mind that impulse sampling is

only a mathematical idealization and cannot really be carried out in practice. It provides us with a basis for our modeling, however, and serves as a yardstick against which other forms of sampling can be compared.

In a later section we examine what happens when the sampling pulse is a more realistic one, such as a narrow Rect pulse, and we find that the main results that we obtain with impulse sampling still hold true although there are some secondary differences in the final picture.

In Chapter 4 we introduced the concept of a train of equally spaced unit impulses called the Dirac comb,

$$\delta_T(t) = \sum_{n=-\infty}^{\infty} \delta(t - nT_s) \quad (9.1)$$

where  $T_s$  is the time between the impulses and will now be called the **sampling interval**.

Impulse sampling is a mathematical procedure whereby we multiply the continuous function  $x(t)$  that we wish to sample by the impulse train  $\delta_T(t)$  as shown in Figure 9.1. The multiplication takes place in the time domain and so the output from the sampler is the product

$$x(t)\delta_T(t) = x(t) \sum_{n=-\infty}^{\infty} \delta(t - nT_s) \quad (9.2)$$

Then, by virtue of the Dirac-delta sampling property, each impulse in the RHS of (9.2) samples  $x(t)$ , and so it becomes

$$x_s(t) = \sum_{n=-\infty}^{\infty} x(nT_s)\delta(t - nT_s) \quad (9.3)$$

in which we now show a subscript  $s$  on the left to signify that this is a sampled version of  $x(t)$ .

All of this is depicted in Figure 9.1. Notice how the samples  $x(nT_s)$  have been formed in Figure 9.1c, and how they have been modulated onto the impulses as their weights or areas. Thus the impulses have become carriers of the sampled values of  $x(t)$ .

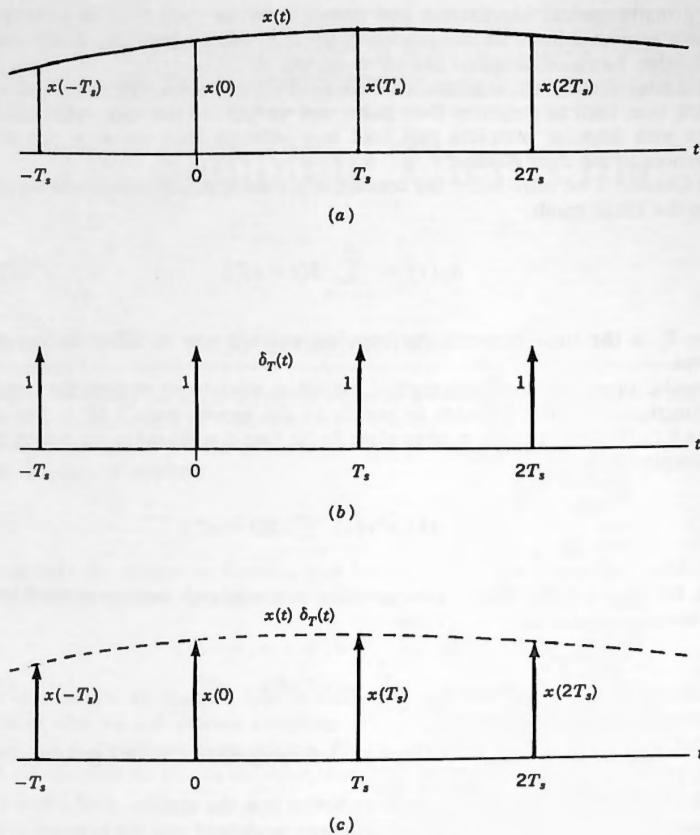
We wish to examine what the effects of impulse sampling have been, and the best way to do that is to find an expression for the Fourier transform of  $x_s(t)$  in (9.3). There are two ways of doing that, both of which will be required.

**Method 1:** By the time-shift property

$$\delta(t - nT_s) \Leftrightarrow e^{-j\omega nT_s} \quad (9.4)$$

Applying this to (9.3) gives us the first form of the Fourier transform of  $x_s(t)$  as

$$X_s(\omega) = \sum_{n=-\infty}^{\infty} x(nT_s)e^{-j\omega nT_s} \quad (9.5)$$

Figure 9.1. Sampling of  $x(t)$  by  $\delta_T(t)$ .

**Method 2:** In (9.2) multiplication of the two functions  $x(t)$  and  $\delta_T(t)$  has taken place in the time domain, which means that we can obtain the Fourier transform of their product by the use of convolution in the frequency domain. To do that we require the transforms of each of those two functions individually.

The transform of  $x(t)$  is simply  $X(\omega)$  and the transform of  $\delta_T(t)$  was derived in Chapter 4 as

$$\delta_{\Omega}(\omega) = \omega_s \sum_{n=-\infty}^{\infty} \delta(\omega - n\omega_s) \quad (9.6)$$

where  $\omega_s = 2\pi/T_s$ . The quantity  $\omega_s$  will be called the **sampling frequency**. Observe

that as  $T_s$  is made smaller so  $\omega_s$  becomes larger, and vice versa. We now carry out the frequency-domain convolution, obtaining

$$\begin{aligned} X_s(\omega) &= \frac{1}{2\pi} \int_{-\infty}^{\infty} X(\Theta) \left[ \omega_s \sum_{n=-\infty}^{\infty} \delta(\omega - n\omega_s - \Theta) \right] d\Theta \\ &= \frac{1}{T_s} \sum_{n=-\infty}^{\infty} \int_{-\infty}^{\infty} X(\Theta) \delta(\omega - n\omega_s - \Theta) d\Theta \end{aligned} \quad (9.7)$$

The independent variable in the integrand in (9.7) is  $\Theta$ , and so the impulse  $\delta(\omega - n\omega_s - \Theta)$  is on the  $\Theta$ -axis located at  $\Theta = \omega - n\omega_s$ . Thus the sampling property gives

$$X(\Theta) \delta(\omega - n\omega_s - \Theta) = X(\omega - n\omega_s) \delta(\omega - n\omega_s - \Theta) \quad (9.8)$$

and so (9.7) continues as

$$\dots = \frac{1}{T_s} \sum_{n=-\infty}^{\infty} \int_{-\infty}^{\infty} X(\omega - n\omega_s) \delta(\omega - n\omega_s - \Theta) d\Theta \quad (9.9)$$

giving us the transform of  $x_s(t)$  as

$$X_s(\omega) = \frac{1}{T_s} \sum_{n=-\infty}^{\infty} X(\omega - n\omega_s) \quad (9.10)$$

Equation (9.10) is the second form of the Fourier transform of  $x_s(t)$  and it shows us the following:

The spectrum  $X_s(\omega)$  is comprised of repeated copies of the original spectrum  $X(\omega)$ , each copy displaced by  $\omega_s$  and scaled by  $1/T_s$ . It is thus a **periodic function** located on the  $\omega$ -axis with period  $\omega_s$ .

In Figure 9.2, we depict the process that has taken place, showing the Fourier transform of  $x(t)$  before and after sampling. Observe how the spectrum  $X(\omega)$  of the unsampled signal has become, after sampling, a periodic function comprised of repeated copies of  $X(\omega)$  with period  $\omega_s$ , all multiplied by the scale factor  $1/T_s$ . This replication of the original spectrum  $X(\omega)$  under sampling is the central fact underlying the sampling theorem that we shall soon state.

As we shall also see, the replication of  $X(\omega)$  takes place even when the sampling pulses are not Dirac deltas, although we shall find then that the multiplier  $1/T_s$  is no longer a constant but varies with each copy of the replicated spectrum.

In Figure 9.2 we have actually cheated a little by showing  $X(\omega)$  being strictly **band-limited**. By this we mean that we have shown it extending over just a finite part of the  $\omega$ -axis and zero over the rest. This was done for convenience in drawing the figure, but in general that is not the case.

A more representative picture is shown in Figure 9.3 where we show  $X(\omega)$  as a spectrum that extends over a much greater portion of the  $\omega$ -axis, and we now see that

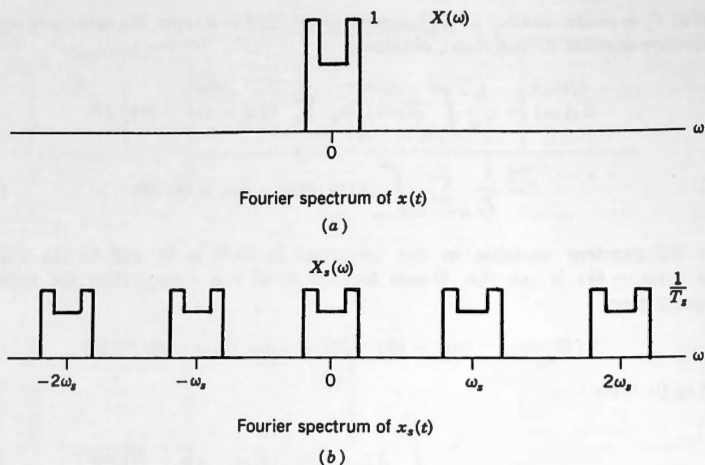


Figure 9.2. Spectrum of unsampled and sampled pulse. (a) Fourier spectrum of  $x(t)$ . (b) Fourier spectrum of  $x_s(t)$ .

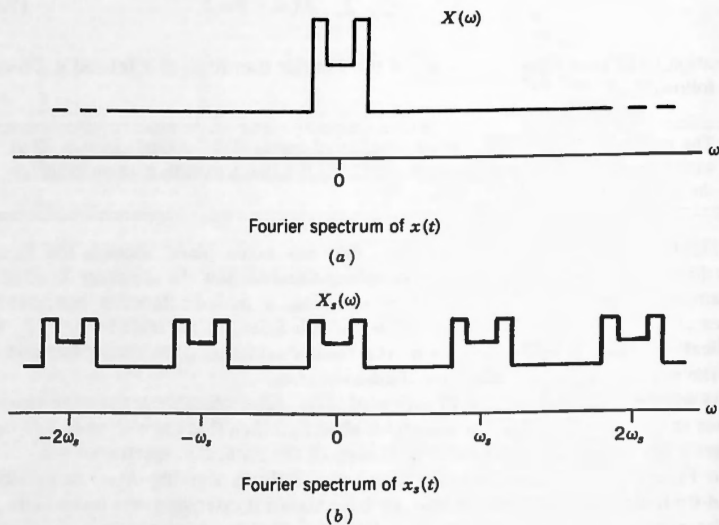


Figure 9.3. Spectrum with aliasing. (a) Fourier spectrum of  $x(t)$ . (b) Fourier spectrum of  $x_s(t)$ .

in general there will be **overlap** of the various copies of the spectra that  $X_s(\omega)$  is composed of.

Notice how  $X_s(\omega)$  now no longer consists of perfect stand-alone copies of  $X(\omega)$ . Instead, filling in and changes have taken place due to the overlap of the individual spectra, and so the spectrum of the sampled function now differs dramatically from what was shown in Figure 9.2 for the band-limited case.

This phenomenon in which the repeated copies of  $X(\omega)$  that make up  $X_s(\omega)$  overlap and change their net shape is called **aliasing**, and is generally present whenever sampling takes place. However, consider the special case where  $X(\omega)$  really is strictly band-limited. Then the situation really would be as was shown in Figure 9.2.

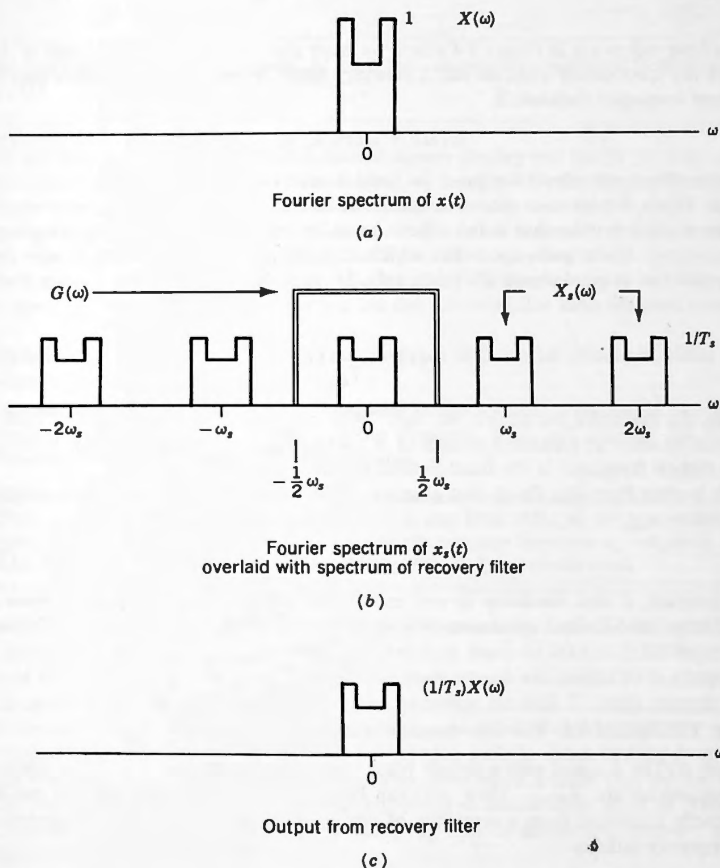


Figure 9.4. Unaliased spectrum with recovery filter. (a) Fourier spectrum of  $x(t)$ . (b) Fourier spectrum of  $x_s(t)$  overlaid with spectrum of recovery filter. (c) Output from recovery filter.

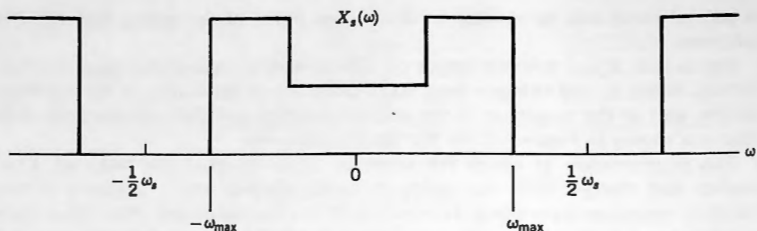


Figure 9.5. Condition for alias-free sampling.

We have redrawn it in Figure 9.4 where we have also overlaid the spectrum of  $X_s(\omega)$  with the spectrum of what we call a **recovery filter**, which is an ideal low-pass filter whose frequency response is

$$G(\omega) = \text{Rect}(\omega/\omega_s) \quad (9.11)$$

that is,  $G(\omega)$  has value 1 for  $|\omega| < \frac{1}{2}\omega_s$  and is zero otherwise.

In Figure 9.4 we also show the spectrum of the output from the recovery filter, from which it is clear that in the strictly band-limited case with proper sampling, we can recover the original spectrum, which in turn means that we have now reconstructed the original signal  $x(t)$  precisely. In fact, from the figure we see that the output from the filter will be

$$y(t) = \frac{1}{T_s} x(t) \quad (9.12)$$

In the preceding paragraph we said "with proper sampling." To see what this means we show an expanded version of  $X_s(\omega)$  in Figure 9.5, in which we have called the highest frequency in the band-limited signal  $\omega_{\max}$ .

It is clear from that figure that aliasing will be absent if and only if we satisfy the condition  $\omega_{\max} < \frac{1}{2}\omega_s$ , that is, if

$$\omega_s > 2\omega_{\max} \quad (9.13)$$

By contrast, if this condition is not met, then aliasing will take place even with a strictly band-limited spectrum. We state all of what we have just derived as Theorem 9.1.

### ■ THEOREM 9.1: The time-domain sampling theorem

Let  $x(t)$  be a signal with a strictly band-limited spectrum  $X(\omega)$  whose limiting frequencies are  $\pm\omega_{\max}$ . Then  $x(t)$  can be completely specified by and can be exactly recovered from a sequence of equally spaced samples iff the sampling frequency satisfies

$$\omega_s > 2\omega_{\max} \quad (9.14)$$

Stated in hertz, condition (9.14) becomes

$$f_s > 2f_{\max} \quad (\text{hertz}) \quad (9.15)$$

The critical sampling frequency

$$f_c = 2f_{\max} \quad (\text{hertz}) \quad (9.16)$$

is called the **Nyquist frequency**, named for its discoverer who worked at Bell Telephone Laboratories in the years before World War II. (He also left his name in the control-theory field through the Nyquist stability criterion.) The rule expressed by (9.14) or (9.15) is often stated as

**The Nyquist Sampling Criterion:** At least two samples for the highest frequency in  $x(t)$

We see then that for strictly band-limited signals aliasing will not be present, and perfect recovery will be possible if and only if we comply with the Nyquist sampling criterion. In practice, however, signals are seldom strictly band-limited. What happens then? In Figure 9.6a we show a spectrum  $X(\omega)$  that is not strictly band-limited and in Figure 9.6b we show the spectrum  $X_s(\omega)$  after sampling, where  $\omega_s$  is small (i.e., a slow sampling rate). In Figure 9.6c we show  $X_s(\omega)$  when  $\omega_s$  is large (i.e., a more rapid sampling rate). From this we see the following:

- Aliasing is not necessarily a yes/no condition and can be present at either an acceptable or an unacceptable level.
- An increase in  $\omega_s$  causes the repeated copies of the spectrum to separate further, and so the effects of aliasing diminish. That will only be the case, however, if  $X(\omega)$  eventually decays to zero.

Thus, provided that  $X(\omega)$  eventually decays to zero, the effects of aliasing can be made as small as we please simply by making the sampling frequency  $\omega_s$  sufficiently large, or equivalently, by making the sampling interval  $T_s$  sufficiently small.

We note that all finite energy signals such as the ones that we have been working with throughout this text have Fourier spectra that decay to zero at least like  $1/\omega$ , many of them even faster than that. Thus all such signals are amenable to sampling and to acceptable recovery if we make the sampling interval  $T_s$  small enough ( $\omega_s$  large enough), even though the spectrum may not be strictly band-limited.

Practical signals that we might wish to sample, such as those coming from the human voice or from telemetry systems, also have finite energy (not so for rock bands), and so they too will have spectra that decay to zero at least like  $1/\omega$ . Thus all such signals will also be amenable to sampling and to acceptable recovery given sufficiently small  $T_s$ .

However if  $x(t)$  is not strictly band-limited and  $\omega_s$  is not sufficiently large, then the repeated copies of its spectrum in  $x_s(\omega)$  may not be spread sufficiently far apart. In

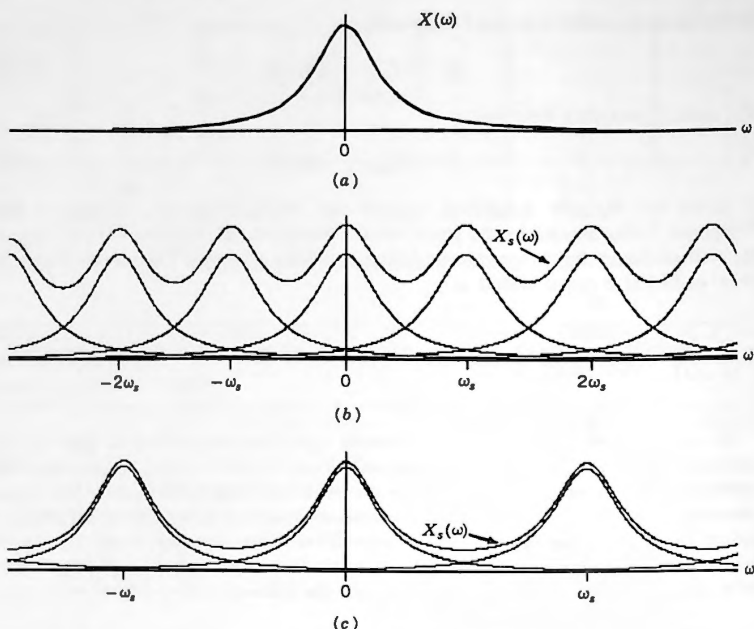


Figure 9.6. Effects of two sampling frequencies.

that case aliasing may make adequate recovery impossible. If we nevertheless wish to sample  $x(t)$  using such a value of  $\omega_s$ , then we must first band-limit it by passing it through a low-pass **conditioning filter** prior to sampling, in order to increase the falloff rate of its spectrum. Admittedly this band-limiting will modify the  $x(t)$  that we originally wished to transmit, but at least we shall then be able to recover the band-limited version that we do transmit.

The Nyquist sampling criterion as stated previously is of course only a **limiting condition**, and in practice we always sample at a rate that exceeds it, a condition known as **oversampling**, for the following reason. In practice we cannot construct a recovery filter that precisely matches the idealized one that we showed in Figure 9.4. Practical filters cannot have vertical falloff. Thus there must be at least some separation between the repeated copies of the original spectrum.<sup>†</sup>

In practice, moreover, the signals that we sample are seldom strictly band-limited and have spectra that decay to zero asymptotically rather than terminating abruptly at some value of  $\omega$ . Thus for such signals there is no clearly defined Nyquist frequency,

<sup>†</sup>Modern-technology filters can be constructed with very sharp cutoff, and so oversampling by only a few percent is all that is required. A familiar example of a system where sampling and recovery takes place is in compact-disc recording and playback, where signals are oversampled by only about 5 percent.

and, as we mentioned earlier, it is only by sampling at a sufficiently high rate that the effects of aliasing can be kept to an acceptable level. That rate is a subjective one, however, and can only be arrived at by judgment based on some knowledge of the properties of the signal being sampled and of the rate of falloff of its spectrum.

**EXAMPLE 9.1:** As an example of a pulse that has a strictly band-limited spectrum, consider the time-domain Sa pulse

$$x(t) = \frac{1}{\pi} \text{Sa}(t)$$

To find its Fourier transform we start from

$$\text{Rect}\frac{t}{\tau} \Leftrightarrow \tau \text{Sa}\frac{\omega\tau}{2}$$

Setting  $\tau = 2$  and using duality, we obtain

$$2 \text{Sa}(t) \Leftrightarrow 2\pi \text{Rect}\frac{\omega}{2}$$

giving us

$$\frac{1}{\pi} \text{Sa}(t) \Leftrightarrow \text{Rect}\frac{\omega}{2}$$

from which we note that  $x(t)$  is strictly band-limited to the range  $|\omega| < 1$ . The pulse and its spectrum are plotted in Figures 9.7 and 9.8.

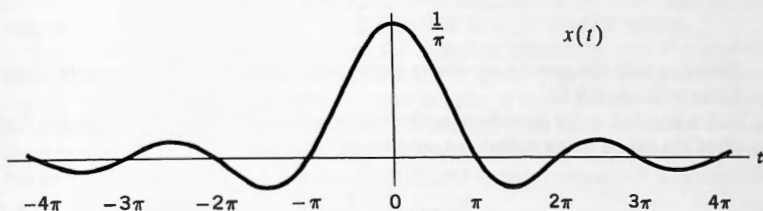


Figure 9.7.  $(1/\pi)\text{Sa}(t)$ .

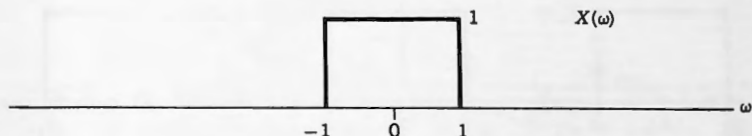
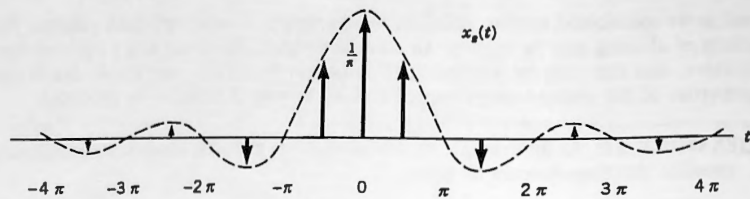


Figure 9.8. Spectrum of  $(1/\pi) \text{Sa}(t)$ .

Figure 9.9. Sampling of  $x(t)$ .

We now impulse sample  $x(t)$  at  $t = 0 \pm n\pi/2$ , as shown in Figure 9.9. Since  $T_s = \pi/2$ , it follows that  $\omega_s = 4$ , and so from (9.10) the spectrum of the samples will be

$$X_s(\omega) = \frac{1}{T_s} \sum_{n=-\infty}^{\infty} X(\omega - n\omega_s) = \frac{2}{\pi} \sum_{n=-\infty}^{\infty} \text{Rect} \frac{\omega - 4n}{2}$$

This spectrum is depicted in Figure 9.10. We see that there is no aliasing at this sampling rate and so we would easily be able to recover the original signal with the aid of a recovery filter.

By the Nyquist sampling criterion (9.14), the largest sampling interval that we can use before frequency-domain aliasing commences will be  $T_{\max}$  such that

$$\omega_s = 2\omega_{\max} = 2$$

which gives

$$T_{\max} = \frac{2\pi}{\omega_s} = \frac{2\pi}{2} = \pi \text{ seconds}$$

Sampling with this spacing we obtain the impulse sequence and spectrum shown in Figures 9.11 and 9.12.

We see that in the time domain there is now only a single sample at  $t = 0$ , with all of the others being nulled out, and so in this case  $x_s(t)$  becomes

$$x_s(t) = \frac{1}{\pi} \delta(t) \quad (9.17)$$

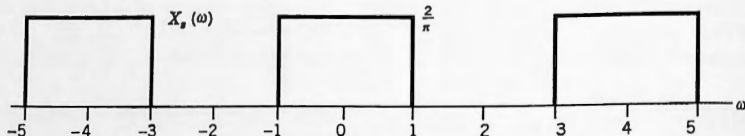


Figure 9.10. Spectrum of sampled signal.

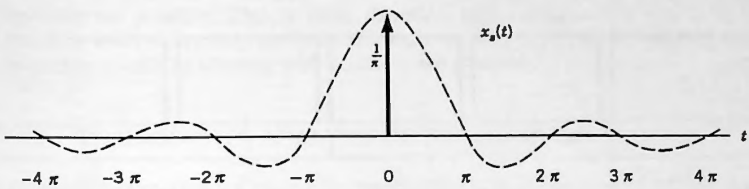


Figure 9.11. Sampling at the critical rate.

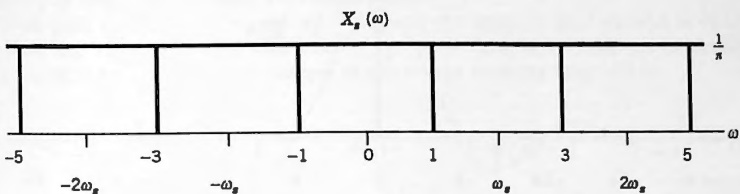


Figure 9.12. Spectrum of signal sampled at critical rate.

In the frequency domain, on the other hand, the blocks are now just touching one another, giving us a **constant value** for  $X_s(\omega)$ . In fact

$$X_s(\omega) = \frac{1}{\pi}$$

which we know to be the correct Fourier transform of the single impulse  $x_s(t)$  in (9.17). Theoretically this is the limiting condition, and we are now right on the edge of the ability to recover the original signal from its sampled version.

Suppose that we were to decrease the sampling interval by even the smallest amount from  $T_{\max}$  to say  $0.9 \times T_{\max}$ , that is, we speeded up the sampling process slightly. Then the result would be that the samples of the waveform will no longer be nulled out, and we would obtain on the average **more than one hit** on each of the cusps of  $x(t)$ . (See Fig. 9.13.) In the frequency domain the sampling frequency has now been **increased** by a factor of 1:0.9, and so the copies of the spectrum will

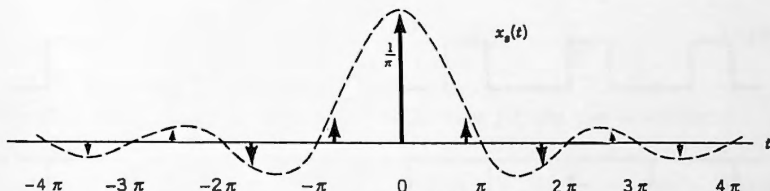


Figure 9.13. Reduced sampling interval.

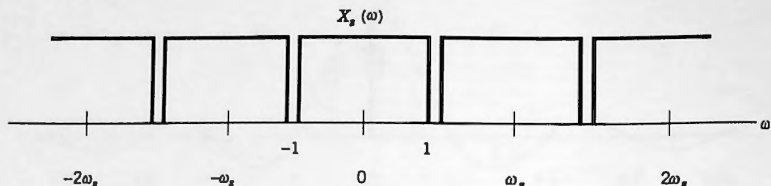


Figure 9.14. Spectrum from reduced sampling interval.

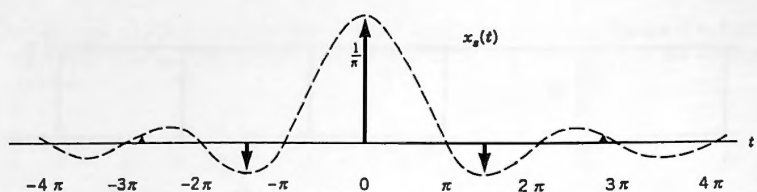


Figure 9.15. Increased sampling interval.

separate slightly as shown in Figure 9.14. Theoretically, perfect recovery of  $x(t)$  will once again be possible.

On the other hand, if we elected instead to increase our sampling interval to a value exceeding  $T_{\max}$ , then we would inevitably get less than one hit on the average for each cusp of  $x(t)$ . In Figure 9.15 we show the case where our sampling interval was increased to  $\frac{4}{3}T_{\max}$ , which is larger than that permitted by the Nyquist criterion, from which we see how we have failed to hit the fourth cusp entirely. This will happen again and again, which means that we shall obtain less than adequate information regarding the waveform  $x(t)$ .

For this case, in the frequency domain we get

$$\omega_s = \frac{2\pi}{T_{\max}} = \frac{2\pi}{4\pi/3} = 1\frac{1}{2} \text{ radian/sec.}$$

(The critical value was  $\omega_s = 2$ .) The blocks now overlap, resulting in the aliased spectrum shown in Figure 9.16, from which we see that recovery of  $x(t)$  is

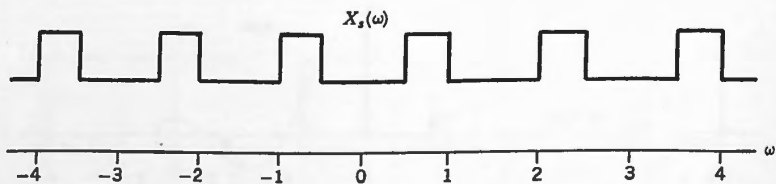


Figure 9.16. Spectrum from increased sampling interval.

definitely not possible. Clearly, then, there is a switch point at  $T_s = \pi$  or  $\omega_s = 2$ . Sampling more frequently gives no aliasing with recovery possible; sampling less frequently results in aliasing with recovery not possible.  $\square$

### 9.3 TIME-DOMAIN ANALYSIS OF THE RECOVERY PROCESS

In the preceding section we gave a frequency-domain demonstration of the fact that with an adequate sampling rate and a strictly band-limited signal all of the information in the original signal is preserved. We now examine, in the time domain, how recovery of the original signal  $x(t)$  takes place.

If we pass the sampled signal  $x_s(t)$  through the recovery filter defined in (9.11), then we are multiplying its spectrum  $X_s(\omega)$  by  $\text{Rect}(\omega/\omega_s)$ . Using the expression given in (9.5) for  $X_s(\omega)$ , the spectrum of the output from the filter will be

$$Y(\omega) = \left[ \sum_{n=-\infty}^{\infty} x(nT_s) e^{-j\omega nT_s} \right] \text{Rect}(\omega/\omega_s) \quad (9.18)$$

which we now invert by direct use of the synthesis equation. Thus

$$\begin{aligned} y(t) &= \frac{1}{2\pi} \int_{-\infty}^{\infty} \left[ \sum_{n=-\infty}^{\infty} x(nT_s) e^{-j\omega nT_s} \right] \text{Rect}(\omega/\omega_s) e^{j\omega t} d\omega \\ &= \frac{1}{2\pi} \int_{-\frac{1}{2}\omega_s}^{\frac{1}{2}\omega_s} \left[ \sum_{n=-\infty}^{\infty} x(nT_s) e^{-j\omega nT_s} \right] e^{j\omega t} d\omega \\ &= \frac{1}{2\pi} \sum_{n=-\infty}^{\infty} x(nT_s) \int_{-\frac{1}{2}\omega_s}^{\frac{1}{2}\omega_s} e^{j\omega(t-nT_s)} d\omega \\ &= \frac{1}{2\pi} \sum_{n=-\infty}^{\infty} x(nT_s) \frac{e^{j\omega(t-nT_s)}}{j(t-nT_s)} \Big|_{-\frac{1}{2}\omega_s}^{\frac{1}{2}\omega_s} \\ &= \frac{1}{2\pi} \sum_{n=-\infty}^{\infty} x(nT_s) \omega_s \frac{e^{j\frac{1}{2}\omega_s(t-nT_s)} - e^{-j\frac{1}{2}\omega_s(t-nT_s)}}{2j[\frac{1}{2}\omega_s(t-nT_s)]} \\ &= \frac{1}{T_s} \sum_{n=-\infty}^{\infty} x(nT_s) \text{Sa}[\frac{1}{2}\omega_s(t-nT_s)] \end{aligned} \quad (9.19)$$

From (9.12) we know that the output from the filter  $y(t)$  can also be written as

$$y(t) = \frac{1}{T_s} x(t) \quad (9.20)$$

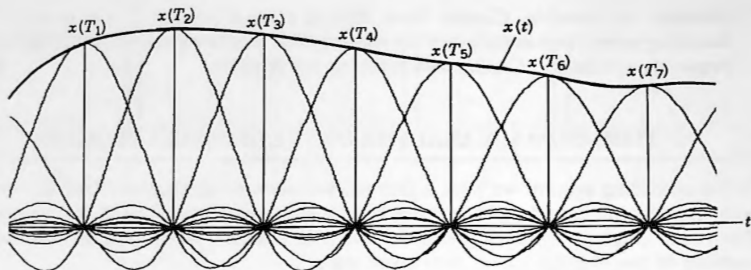


Figure 9.17. Recovery of a signal from its samples.

and so, combining (9.19) and (9.20) we obtain

$$\sum_{n=-\infty}^{\infty} x(nT_s) \text{Sa}\left[\frac{1}{2}\omega_s(t - nT_s)\right] = x(t) \quad (9.21)$$

What the LHS of (9.21) tells us is that the signal coming from the recovery filter can be viewed as an infinite sum of Sa functions, each weighted by an appropriate multiplier, with the net result being that they all add up to the original signal  $x(t)$ .<sup>†</sup> This is a new property of the Sa functions as far as we are concerned in this book, and shows us that they can be used to interpolate a signal based on its samples.

Observe how each of the Sa functions on the LHS of (9.21) is multiplied by the scale factor  $x(nT_s)$ , which is the numerical value of  $x(t)$  at the  $n$ th sampling instant. Equation (9.21) is depicted in Figure 9.17 where we show an assembly of such Sa functions, each scaled by  $x(nT_s)$  adding up precisely to  $x(t)$ . Notice in the figure how each Sa function crosses the others at precisely their zero crossings, and that all of these crossings take place at each of the original sampling points. To see that this is so we consider the one for which  $n = 0$  in (9.21), namely  $\text{Sa}(\frac{1}{2}\omega_s t)$ . It passes through zero every time that

$$\frac{1}{2}\omega_s t = k\pi \quad (k \text{ any integer}) \quad (9.22)$$

which is at

$$t = \frac{k2\pi}{\omega_s} = kT_s \quad (9.23)$$

and so it passes through zero at integral multiples of  $T_s$ . However, then so do all the others, which demonstrates the validity of the proposition.

The cumulative nonzero values of the weighted Sa functions between the sampling instants will exactly add up to give the original function  $x(t)$ . According to (9.21), perfect interpolation will take place.

<sup>†</sup>This is true for all signals that we sample and is unrelated to the Sa pulse that we used earlier in Example 9.1.

## 9.4 SAMPLING WITH PULSES OTHER THAN DIRAC DELTAS

In the preceding two sections we examined the sampling process based on the use of an impulse as the sampling waveform. We now analyze what the effect will be of using a sampling waveform that is not an impulse. The result that we shall arrive at is a surprising one. It shows that **in theory it makes virtually no difference what the shape of the sampling waveform is**, the sampling theorem and the Nyquist sampling criterion remain intact. There is, however, a practical constraint that dictates that sampling pulses of a certain kind shall be used.

Thus, let the signal  $x(t)$  be “sampled” by multiplying it by any periodic function  $f_p(t)$  whatsoever. The period is assumed to be  $T_s$ , and so the Fourier series representation of  $f_p(t)$  is

$$f_p(t) = \sum_{n=-\infty}^{\infty} F_p(n) e^{jn\omega_s t} \quad (9.24)$$

Note that the fundamental frequency of the sampling waveform is being shown as  $\omega_s \equiv 2\pi/T_s$ , and observe that we have not specified the shape of  $f_p(t)$  because  $F_p(n)$  has not been specified. After “sampling” we obtain

$$\begin{aligned} x_s(t) &= x(t) \sum_{n=-\infty}^{\infty} F_p(n) e^{jn\omega_s t} \\ &= \sum_{n=-\infty}^{\infty} F_p(n) x(t) e^{jn\omega_s t} \end{aligned} \quad (9.25)$$

which we now Fourier transform in order to find  $X_s(\omega)$ . By the frequency-shift property

$$x(t) e^{jn\omega_s t} \Leftrightarrow X(\omega - n\omega_s) \quad (9.26)$$

and so (9.25) transforms to

$$X_s(\omega) = \sum_{n=-\infty}^{\infty} F_p(n) X(\omega - n\omega_s) \quad (9.27)$$

This tells us the following (see Fig. 9.18): The spectrum of  $x_s(t)$  is comprised of the original spectrum  $X(\omega)$  replicated infinitely many times with spacing  $\omega_s$ , with the  $n$ th copy being multiplied by the Fourier series coefficient  $F_p(n)$ .

Observe in the figure how each copy of the original spectrum now has a unique scale factor  $F_p(n)$ , whereas in the previous case of impulse sampling all copies were multiplied by the same scale factor  $1/T_s$ . We see then that the particular shape of the sampling pulse affects only the **envelope** of the spectrum  $X_s(\omega)$ .

As we recall from Chapter 4, the Fourier series coefficients for a Dirac comb satisfy

$$F_p(n) = \frac{1}{T_s} \quad (9.28)$$

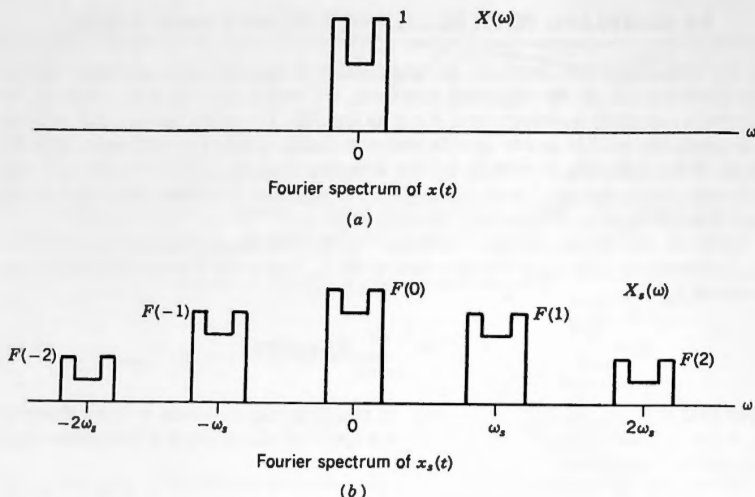


Figure 9.18. Sampling with other than an impulse train. (a) Fourier spectrum of  $x(t)$ . (b) Fourier spectrum of  $x_s(t)$ .

and so the result obtained earlier with impulse sampling is seen to be just a special case of the more general result that we have now obtained in (9.27).

Clearly from Figure 9.18 the sampling theorem that we stated earlier still holds, that is, provided that the signal  $x(t)$  is strictly band-limited, and provided that we satisfy the Nyquist sampling criterion, namely  $\omega_s > \omega_{\max}$ , we shall again be able to use an ideal recovery filter to extract the central copy of the replicated spectrum, thereby recovering the original signal  $x(t)$ .

It appears then that any sampling waveform  $f_p(t)$  will suffice, provided only that it has a Fourier series. From a practical standpoint, however, that is not quite true. In Figure 9.19a we see a signal  $x(t)$  that is being sampled by the train of pulses  $f_p(t)$  shown in Figure 9.19b resulting in the sampled signal  $x_s(t)$  in Figure 9.19c.

What we now know is that the spectrum of  $x_s(t)$  is given by (9.27), and that we can recover  $x(t)$  from  $x_s(t)$  by the use of a recovery filter. Thus if we were to transmit precisely the waveform shown in Figure 9.19c, we are assured by the sampling theorem that we can recover  $x(t)$  from it, provided that we comply with the Nyquist sampling criterion. Sending a signal like the one in Figure 9.19c, however, is seldom the objective of a system involving sampling. What we usually require is a single numerical value for each period of the sampling process, which is then encoded in some way and transmitted in digital form.

In practice therefore a sampling waveform is always very narrow in relation to the sampling interval  $T_s$ , and for that reason we usually restrict ourselves to a train of very narrow Rect pulses as the sampler. Indeed the width of the sampling pulse is usually made so small that during its on-time the signal  $x(t)$  can be regarded as being

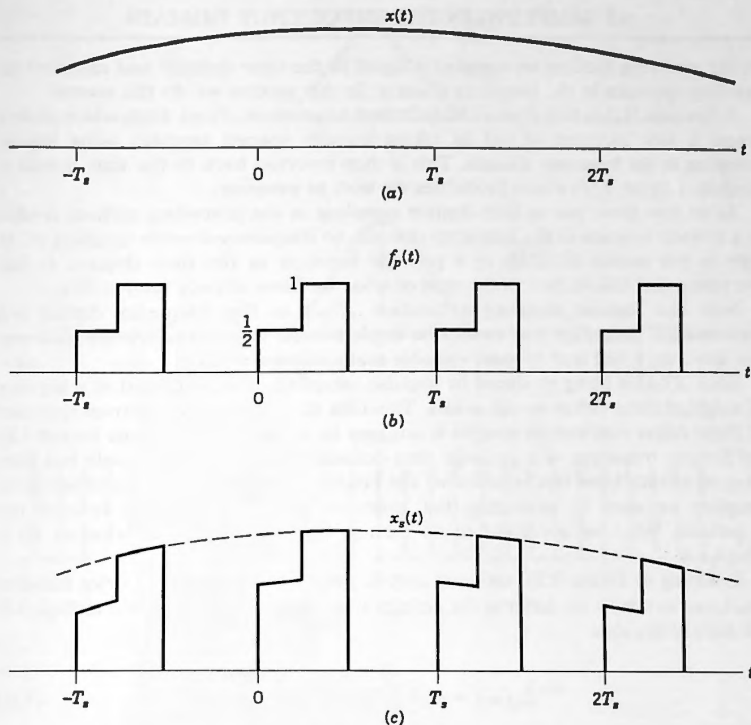


Figure 9.19. Sampling of  $x(t)$  by  $f_p(t)$ .

essentially constant, and it is that value that is captured and encoded for transmission.

Ultimately if we were to make the sampling pulse narrow enough we would arrive at a sampling window of zero width, mathematically the same as what impulse sampling gives us, and this is why the latter is usually taken to be the mathematical idealization of the perfect sampling pulse.

Keep in mind that the sampling period can be as long as many hours in practical systems or as short as microseconds or less. The essential item, however, is that the width of the sampling pulse should be a very small fraction of that sampling period.

Also keep in mind that the signals that we wish to sample are seldom strictly band-limited, and so there is seldom a precisely defined Nyquist sampling rate. From what we have seen in this section, the remarks that we made in Section 9.2 still apply, even when we are using a narrow Rect as the sampling pulse rather than a Dirac delta.

## 9.5 SAMPLING IN THE FREQUENCY DOMAIN

---

In the preceding sections we sampled a signal in the time domain and examined the resulting spectrum in the frequency domain. In this section we do the reverse.

A function  $x(t)$  is now Fourier transformed to produce  $X(\omega)$ , from which we then create a new spectrum  $X_s(\omega)$  by taking equally spaced samples **using impulse sampling in the frequency domain**. This is then inverted back to the time domain to produce a signal  $x_s(t)$  whose properties we wish to examine.

As we now show, just as time-domain sampling in the preceding sections resulted in a periodic function in the frequency domain, so frequency-domain sampling will be seen in this section to result in a periodic function in the time domain. In fact, everything that follows here is the dual of what we have already seen earlier.

Note that impulse sampling a function  $X(\omega)$  in the frequency domain is a mathematical procedure that cannot be implemented in practice. As we shall soon see, however, it will lead to some valuable mathematical results.

Since  $X_s(\omega)$  is being produced by impulse sampling, it must consist of a sequence of weighted Dirac deltas on the  $\omega$ -axis. This idea of a frequency spectrum comprised of Dirac deltas with various weights is not new to us; as we recall from Section 4.10, the Fourier transform of a periodic time-domain function has precisely that form. Thus we already know that by sampling the Fourier spectrum of a pulse using impulse sampling we must be producing the spectrum of a time-domain function that is periodic. What we are about to do then is also the reverse of what we did in Chapter 4.

Referring to Figure 9.20, we start with a pulse  $x(t)$  that has Fourier transform  $X(\omega)$ , and to sample the latter at the equally spaced points  $\omega = n\omega_0$  we multiply it by the train of impulses

$$\delta_\Omega(\omega) = \omega_0 \sum_{n=-\infty}^{\infty} \delta(\omega - n\omega_0) \quad (9.29)$$

Note that we are now using the symbol  $\omega_0$  rather than  $\omega_s$  for the spacing between the samples in the frequency domain. Note also the multiplier  $\omega_0$  that we have elected to include in front of the sigma. Then multiplication of  $X(\omega)$  by  $\delta_\Omega(\omega)$  gives us

$$X_s(\omega) = X(\omega) \left[ \omega_0 \sum_{n=-\infty}^{\infty} \delta(\omega - n\omega_0) \right] \quad (9.30)$$

which, by the sampling property, becomes

$$X_s(\omega) = \omega_0 \sum_{n=-\infty}^{\infty} X(n\omega_0) \delta(\omega - n\omega_0) \quad (9.31)$$

This sampling of  $X_s(\omega)$  is depicted in the figure where we have used as our time-domain pulse  $\Lambda(t) \Leftrightarrow \text{Sa}^2(\omega/2)$ . Note once again how impulse sampling, this time in the frequency domain, has led to the information values being modulated onto the impulses as their weights.

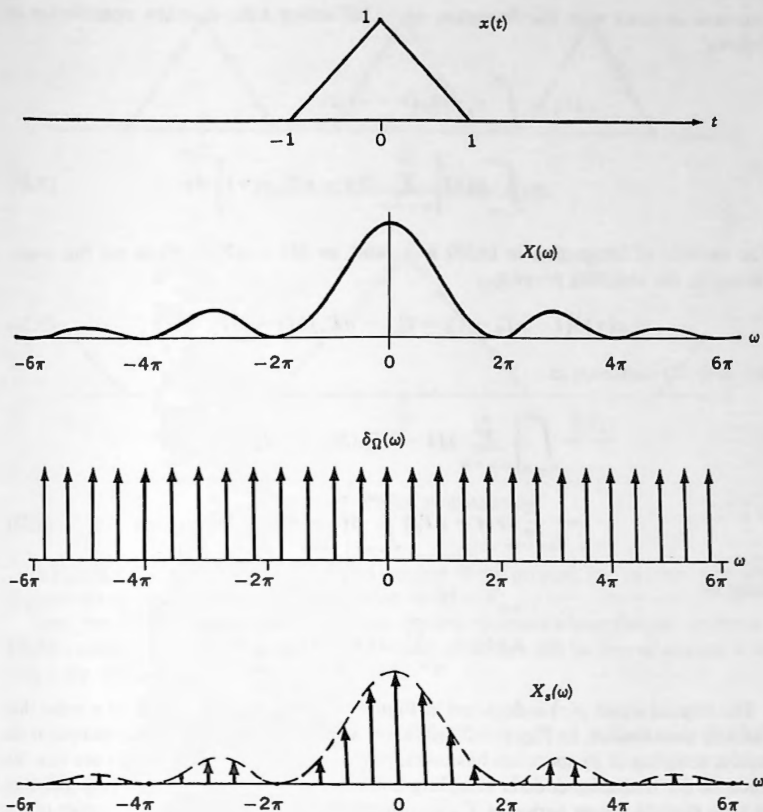


Figure 9.20. A pulse and its sampled spectrum.

To find what the effect of this sampling process has been in the time domain, we must invert  $X_s(\omega)$ . As before, there are two ways to do this.

**Method 1:** Starting from (9.30), we note that multiplication has taken place in the frequency domain, and so this corresponds to convolution in the time domain. In order to carry out that convolution we first need to invert (9.29), but that was already done in Section 4.11 where we saw that the infinite train of equally spaced impulses

$$\delta_T(t) = \sum_{n=-\infty}^{\infty} \delta(t - nT_0) \quad (9.32)$$

transformed to (9.29), and so (9.32) is the required inverse, in which  $T_0 = 2\pi/\omega_0$ . We

can now proceed with the inversion of (9.30) using time-domain convolution as follows:

$$\begin{aligned}x_s(t) &= \int_{-\infty}^{\infty} x(\tau) \delta_T(t - \tau) d\tau \\&= \int_{-\infty}^{\infty} x(\tau) \left[ \sum_{n=-\infty}^{\infty} \delta(t - nT_0 - \tau) \right] d\tau\end{aligned}\quad (9.33)$$

The variable of integration in (9.33) is  $\tau$ , and so  $\delta(t - nT_0 - \tau)$  is on the  $\tau$ -axis. Hence, by the sampling property,

$$x(\tau) \delta(t - nT_0 - \tau) = x(t - nT_0) \delta(t - nT_0 - \tau) \quad (9.34)$$

and so (9.33) continues as

$$\begin{aligned}\cdots &= \int_{-\infty}^{\infty} \left[ \sum_{n=-\infty}^{\infty} x(t - nT_0) \delta(t - nT_0 - \tau) \right] d\tau \\&= \sum_{n=-\infty}^{\infty} x(t - nT_0) \int_{-\infty}^{\infty} \delta(t - nT_0 - \tau) d\tau\end{aligned}\quad (9.35)$$

giving us

$$x_s(t) = \sum_{n=-\infty}^{\infty} x(t - nT_0) \quad (9.36)$$

The original signal  $x(t)$  is depicted in Figure 9.21 where we show it as a pulse that is strictly time-limited. In Figure 9.22 we show what happens after frequency-domain impulse sampling of its spectrum has taken place. According to (9.36) we see that the effects of the frequency-domain sampling have been to create a periodic function in the time domain whose period is  $T_0$ , comprised of an eternal train of copies of the original function  $x(t)$ , each displaced by an integral multiple of  $T_0$ . Note that there is no scale factor here as there was in Figure 9.2.

In the more general case where  $x(t)$  is not strictly time-limited, aliasing will take place in the time domain and the function  $x_s(t)$  will not appear as shown because of the overlap of the individual copies of which it is comprised.

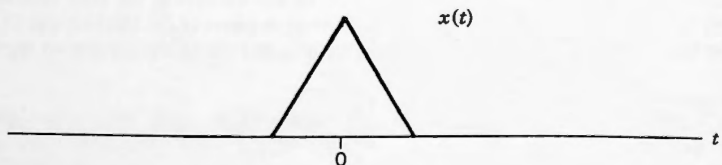


Figure 9.21. Time-domain function  $x(t)$ .

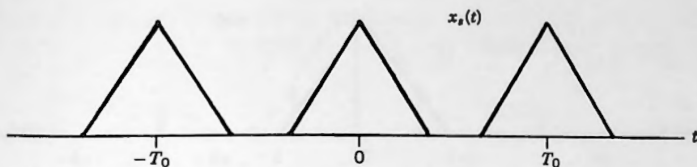
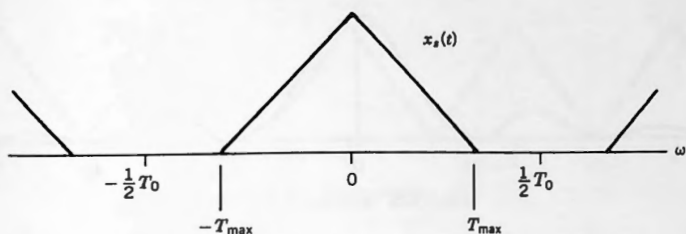
Figure 9.22. Inverse transform of  $X_s(\omega)$ .

Figure 9.23. Critical sampling period.

In Figure 9.23 we depict an enlarged version of the process, and in it we show what happens when  $x(t)$  is strictly time-limited to  $|t| < T_{\max}$ .

From the figure we see that for a time-limited function whose Fourier spectrum is impulse sampled, the inverse of that sampled spectrum will be free of aliasing if and only if we satisfy  $T_{\max} < \frac{1}{2}T_0$ , that is, iff

$$T_0 > 2T_{\max} \quad (9.37)$$

We have thus proved Theorem 9.2.

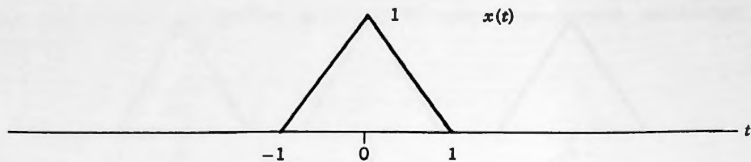
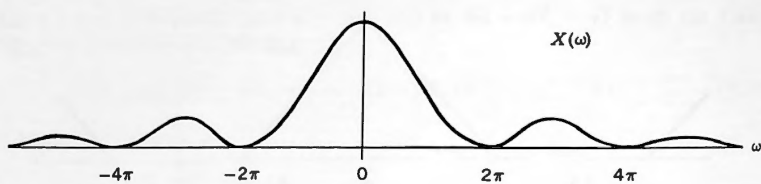
### ■ THEOREM 9.2: The frequency-domain sampling theorem

Let  $x(t)$  be a signal that is strictly time-limited to  $|t| < T_{\max}$ , and let its Fourier spectrum be impulse sampled at  $\omega = n\omega_0$  ( $n$  every integer) to produce  $X_s(\omega)$ . Then the inverse transform of  $X_s(\omega)$  will be a periodic repetition of  $x(t)$  with period  $T_0$ , and will be free of time-domain aliasing if and only if

$$T_0 \geq 2T_{\max} \quad (9.38)$$

where

$$T_0 = 2\pi/\omega_0 \quad (9.39)$$

Figure 9.24.  $\Lambda(t)$ .Figure 9.25. Spectrum of  $\Lambda(t)$ .

□ **EXAMPLE 9.2:** Let  $x(t) = \Lambda(t)$ . Then  $X(\omega) = \text{Sa}^2(\omega/2)$ . These two functions are depicted in Figures 9.24 and 9.25.

Note that  $x(t)$  is time-limited to  $T_{\max} = 1$ , and so the maximum frequency at which we can sample  $X(\omega)$  before time-domain aliasing sets in will be  $\omega_0$  such that

$$T_0 = 2T_{\max} = 2$$

from which

$$\omega_0 = \frac{2\pi}{2} = \pi$$

We now use (9.31), with  $\omega_0 = \pi$ , obtaining

$$X_s(\omega) = \omega_0 \sum_{n=-\infty}^{\infty} X(n\omega_0) \delta(\omega - n\omega_0) = \pi \sum_{n=-\infty}^{\infty} \text{Sa}^2 \frac{n\pi}{2} \delta(\omega - n\pi)$$

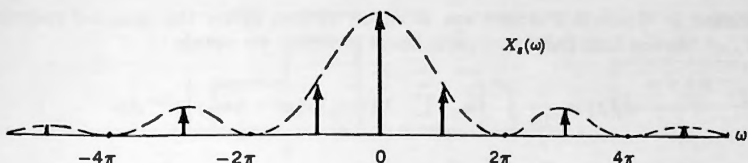
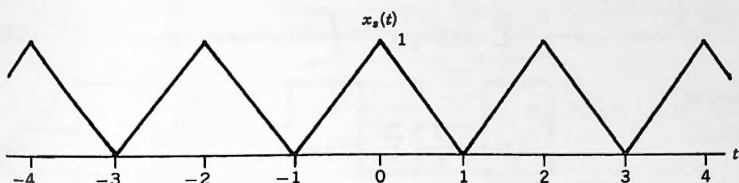
This is shown in Figure 9.26 together with its corresponding  $x_s(t)$  in Figure 9.27.

Observe how the repetitions of  $x(t)$  are now just touching each other, brought about by the fact that we have sampled in such a way that we have equality in (9.38).

If we sample at twice the critical spacing used earlier, however, that is, if we use  $\omega_0 = 2\pi$ , then we obtain

$$X_s(\omega) = 2\pi \sum_{n=-\infty}^{\infty} \text{Sa}^2(n\pi) \delta(\omega - n2\pi)$$

which is shown in Figure 9.28 with its associated  $x_s(t)$  in Figure 9.29. Extensive aliasing is now present.

Figure 9.26.  $X_s(\omega)$ .Figure 9.27. Repeated pulse  $x_s(t)$ .

There is now only a single nonzero hit in the frequency domain at  $\omega = 0$ , and so the sampled spectrum becomes

$$X_s(\omega) = 2\pi \text{Sa}^2(0)\delta(\omega) = 2\pi\delta(\omega) \quad (9.40)$$

Although the time-domain function is heavily aliased, we also see that all of the triangular pulses shown add up precisely to

$$x_s(t) = 1$$

which we know transforms to  $X_s(\omega) = 2\pi\delta(\omega)$  in (9.40).  $\square$

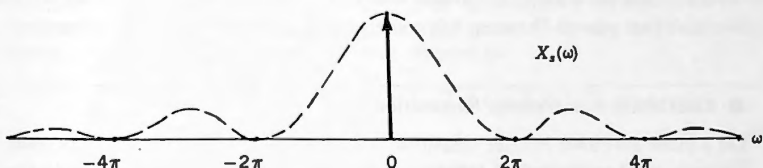
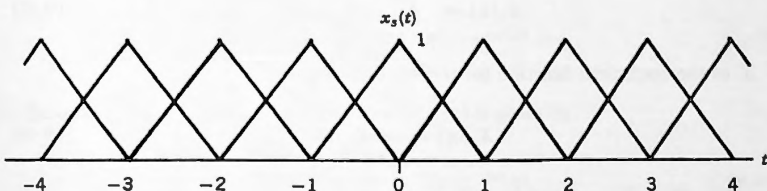
Figure 9.28.  $X_s(\omega)$ .

Figure 9.29. Aliased repeated pulses.

**Method 2:** There is a second way in which we can invert the sampled spectrum  $X_s(\omega)$ . Starting from (9.31), and using direct inversion we obtain

$$\begin{aligned} x_s(t) &= \frac{1}{2\pi} \int_{-\infty}^{\infty} \left[ \omega_0 \sum_{n=-\infty}^{\infty} X(n\omega_0) \delta(\omega - n\omega_0) \right] e^{j\omega t} d\omega \\ &= \frac{1}{T_0} \int_{-\infty}^{\infty} \left[ \sum_{n=-\infty}^{\infty} X(n\omega_0) \delta(\omega - n\omega_0) e^{jn\omega_0 t} \right] d\omega \\ &= \frac{1}{T_0} \sum_{n=-\infty}^{\infty} X(n\omega_0) e^{jn\omega_0 t} \int_{-\infty}^{\infty} \delta(\omega - n\omega_0) d\omega \end{aligned} \quad (9.41)$$

giving us

$$x_s(t) = \frac{1}{T_0} \sum_{n=-\infty}^{\infty} X(n\omega_0) e^{jn\omega_0 t} \quad (9.42)$$

This is seen to be a Fourier series with coefficients

$$X_p(n) = \frac{1}{T_0} X(n\omega_0) \quad (9.43)$$

and fundamental frequency  $\omega_0$ . We now combine (9.42) with (9.36), obtaining

$$\sum_{n=-\infty}^{\infty} x(t - nT_0) = \frac{1}{T_0} \sum_{n=-\infty}^{\infty} X(n\omega_0) e^{jn\omega_0 t} \quad (9.44)$$

Observe that the LHS of (9.44) is a periodic repetition of  $x(t)$  and the RHS is its Fourier series. Observe also that, to within the constant  $1/T_0$ , the coefficient function for the Fourier series is  $X(n\omega_0)$ , which is simply  $X(\omega)$  evaluated at the points  $\omega = n\omega_0$ .

We have thus proved Theorem 9.3, sometimes known as “Poisson Summation”:

### ■ THEOREM 9.3: (Poisson Summation)

Let a pulse  $x(t)$  have Fourier transform  $X(\omega)$ . Then we can produce a periodic function  $x_p(t)$  comprised of repeated copies of  $x(t)$  with period  $T_0 = 2\pi/\omega_0$  and Fourier series representation

$$x_p(t) = \sum_{n=-\infty}^{\infty} X_p(n) e^{jn\omega_0 t} \quad (9.45)$$

if, as the coefficient function for the series, we use

$$X_p(n) = \frac{1}{T_0} X(n\omega_0) \quad (9.46)$$

where  $X(n\omega_0)$  means  $X(\omega)$  evaluated at  $\omega = n\omega_0$ .

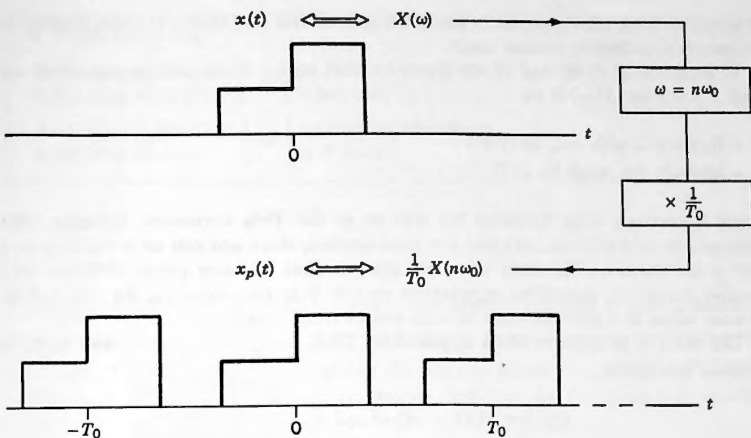


Figure 9.30. A pulse and its periodic repetition.

Theorem 9.3 tells us the following: Referring to Figure 9.30, we start with a pulse  $x(t) \Leftrightarrow X(\omega)$ . If we now wish to find the Fourier series coefficients for a periodic repetition of  $x(t)$  with period  $T_0$ , then all we need do is to replace  $\omega$  by  $n\omega_0$ , in  $X(\omega)$  and divide by  $T_0$ .

Note that in the theorem we say nothing about  $x(t)$  being time-limited or about time-domain aliasing, since the theorem holds for any  $x(t)$  that has a Fourier transform and holds regardless of whether or not time-domain aliasing is present.

If  $x(t)$  is not time-limited, then time-domain aliasing will take place. Similarly, if it is time-limited but we fail to observe (9.38), then again aliasing will take place.

In a sense Theorem 9.3 should not have come as too much of a surprise, for the following reason. Given a periodic function defined by

$$\begin{aligned} x_p(t) &= x(t) & (-T_0/2 < t < T_0/2) \\ x_p(t + T_0) &= x_p(t) \end{aligned} \quad (9.47)$$

in which  $x(t)$  is assumed to be zero outside the range shown, we know that its Fourier coefficients can be found from

$$X_p(n) = \frac{1}{T_0} \int_{-T_0/2}^{T_0/2} x(t) e^{-jn\omega_0 t} dt \quad (9.48)$$

On the other hand, the Fourier transform of  $x(t)$  is given by

$$X(\omega) = \int_{-T_0/2}^{T_0/2} x(t) e^{-j\omega t} dt \quad (9.49)$$

in which we have shown the finite limits because of the fact that  $x(t)$  was assumed to be strictly time-limited to that range.

Comparison of (9.48) and (9.49) shows us that under these circumstances we can find  $X_p(n)$  from  $X(\omega)$  if we

- Replace  $\omega$  with  $n\omega_0$  in (9.49)
- Multiply the result by  $1/T_0$

which is precisely what Theorem 9.3 tells us to do. This approach, however, while appropriate for functions  $x(t)$  that are time-limited, does not tell us what happens if that is not the case. The more complete story is that, for any pulse  $x(t)$  that has a Fourier transform, regardless of whether or not it is time-limited, we can find the Fourier series of a periodic train of such pulses from Theorem 9.3.

**The reverse process is often applicable.** Thus, suppose that we start from the periodic waveform

$$\begin{aligned}x_p(t) &= x(t) \quad (-T_0/2 < t < T_0/2) \\x_p(t + T_0) &= x_p(t)\end{aligned}\tag{9.50}$$

and let its Fourier series coefficients be  $X_p(n)$ . We now isolate the central period in  $x_p(t)$  and zero out all of the other periods, giving us the single time-limited pulse  $x(t)$ . Then we can immediately write the Fourier transform of  $x(t)$  as follows:

- In  $X_p(n)$  replace every occurrence of  $n$  with  $\omega/\omega_0$
- Multiply the result by  $T_0$

The result will be  $X(\omega)$ , the Fourier transform of  $x(t)$ . We state this as a corollary to Theorem 9.3.

### ■ COROLLARY to Theorem 9.3

Let the periodic waveform

$$\begin{aligned}x_p(t) &= x(t) \quad (-T_0/2 < t < T_0/2) \\x_p(t + T_0) &= x_p(t)\end{aligned}\tag{9.51}$$

have Fourier series coefficients  $X_p(n)$ . Then the Fourier transform of  $x(t)$  ( $-T_0/2 < t < T_0/2$ ) will usually be

$$X(\omega) = T_0 X_p(n)|_{n \leftarrow \omega/\omega_0}\tag{9.52}$$

We conclude by stating Theorem 9.4 and its corollary, which have also been proved in this chapter.

**■ THEOREM 9.4**

A function is discrete in the time domain iff [ its Fourier transform is periodic

A function is periodic in the time domain iff [ its Fourier transform is discrete

**■ COROLLARY**

A function that is discrete in both domains must be periodic in both domains.

In the next chapter we shall be studying the discrete Fourier transform (DFT), which is discrete in both the time and frequency domains. As the preceding corollary predicts, we shall find that it is also periodic in both domains.

---

**EXERCISES**

---

**9.1** Starting from the Fourier series for  $\delta_T(t)$ , namely

$$\delta_T(t) = \frac{1}{T_s} \sum_{n=-\infty}^{\infty} e^{jn\omega_s t}$$

use the frequency-shift property to find the Fourier transform of the sampled pulse

$$x_s(t) = x(t)\delta_T(t)$$

Compare your result to (9.10).

**9.2** Using the FFT system, the following exercise demonstrates very clearly the effects of time-domain impulse sampling.

- (a) With  $N = 1024$  and  $T = 4$ , load the pulse  $\text{Rect}(t)$  into  $\mathbf{X}$ . Run ANALYSIS and inspect the spectrum. There should be a single copy of  $\text{Sa}(\omega/2)$  in the display with a maximum value of unity.
- (b) Now go into the  $\mathbf{X}$  postprocessor and do the following two operations:
  - Take the SAMPLE option with  $M = 4$ , (i.e., keeping every fourth value in  $\mathbf{X}$ ).
  - To emulate **impulse sampling** we must now multiply  $\mathbf{X}$  by the weights of unit impulses, which, for  $N = 1024$  and  $T = 4$ , is  $N/T = 256$ . Use the MULTIPLY option to do this.

Exit from the postprocessor, run ANALYSIS and inspect the spectrum. There should now be four copies in the display. According to (9.10) they

should each have a maximum value of  $1/T_s$ . In our case

$$T_s = 4 \frac{T}{N} = 0.015625 \quad \text{and so} \quad \frac{1}{T_s} = 64$$

The four Sa's in your display should each have this maximum value.

- (c) Repeat all of the preceding, but now use  $M = 32$  when sampling. There will be 32 copies of the Sa in the display, but they are now clearly interfering with each other, that is, they are heavily aliased.

### 9.3 (a) Sketch the band-limited function

$$X(\omega) = \cos(\pi\omega)\text{Rect}(\omega)$$

- (b) Show that its inverse transform is

$$x(t) = \frac{\cos(t/2)}{\pi^2 - t^2}$$

- (c) Sketch this function for the range  $-7\pi \leq t \leq 7\pi$ , paying careful attention to the indeterminacy at  $t = \pm\pi$ .
- (d) Starting from your sketch in (a), what is the greatest interval  $T_{\max}$  with which we can sample  $x(t)$  before frequency-domain aliasing commences?
- (e) Assuming that we impulse sample at  $t = 0 \pm nT_{\max}$ , as determined in (d), sketch the function  $x_s(t)$ , showing the points at which sampling takes place.
- (f) Sketch  $X_s(\omega)$ , the spectrum of  $x_s(t)$  in (e).
- (g) Sampling  $x(t)$  at intervals  $\frac{1}{2}T_{\max}$ , sketch  $x_s(t)$  and  $X_s(\omega)$ , numbering all critical values.
- (h) Sampling  $x(t)$  at intervals  $\frac{3}{2}T_{\max}$  sketch  $x_s(t)$  and  $X_s(\omega)$ , numbering all critical values.
- (i) Verify your plots using the FFT system. Use  $N = 900$  and  $T = 60\pi$ .

### 9.4 (a) Starting with the same Fourier pair as in Exercise 9.2, namely:

$$\left[ x(t) = \frac{\cos(t/2)}{\pi^2 - t^2} \right] \Leftrightarrow [X(\omega) = \cos(\pi\omega)\text{Rect}(\omega)]$$

sketch  $x(t)$  and  $X(\omega)$ .

- (b) Impulse sample  $x(t)$  by multiplying it with the **shifted** Dirac comb of Exercise 4.20, namely

$$\delta_{TS}(t) = \sum_{n=-\infty}^{\infty} \delta\left(t - nT_s - \frac{T_s}{2}\right)$$

whose Fourier transform was shown to be

$$\delta_{TS}(\omega) = \omega_s \sum_{n=-\infty}^{\infty} (-1)^n \delta(\omega - n\omega_s)$$

Sketch  $\delta_{Ts}(t)$  and verify that for  $T_s = 2\pi$  there are only two nonzero hits on  $x(t)$ , with all of the remaining impulses being nulled out at the crossing points of  $x(t)$ .

- (c) Sketch the resulting  $x_s(t)$  and verify that it is

$$x_s(t) = \frac{1}{4\pi} [\delta(t - \pi) + \delta(t + \pi)]$$

- (d) Find  $X_s(\omega)$ , the Fourier transform of  $x_s(t)$  in (c), and sketch it.  
 (e) Using frequency-domain convolution, find the Fourier transform after the sampling in (b), namely of  $x_s(t) = x(t)\delta_{T_s}(t)$

Your two spectra in (d) and (e) should be the same.

9.5 A slightly spacy student thinks that he can create a train of equally spaced Dirac deltas by the use of a delay line and an ultra-high-voltage dc power supply, along the lines of what he learned in radar lectures. He manages to get the output to be a train of 1000<sup>v</sup> pulses each 1 ms wide, and so he says that "their area is equal to 1," which makes them box functions that are extremely high and very thin, supposedly very close to Dirac deltas. Over the one period  $-T_s/2 < t < T_s/2$  his pulse train is thus:

$$f_p(t) = \begin{cases} 1/\tau & (|t| < \tau/2) \\ 0 & \text{otherwise} \end{cases} \quad (\tau = 1e-3)$$

He then feeds this pulse train and a signal  $x(t)$  whose Fourier spectrum is  $X(\omega)$  into a multiplier, creating the product

$$x_s(t) = x(t)f_p(t)$$

The student claims that he has now successfully sampled  $x(t)$  and that  $X_s(\omega)$  is an endless repetition of the spectrum of  $X(\omega)$ , each copy multiplied by  $1/T_s$  and spaced  $\omega_s = 2\pi/T_s$  radians apart.

- (a) Derive the true expression for the spectrum of what he obtained and prove to him that unless he can get  $\tau$  to equal zero he will never be precisely correct.

He then claims that for  $T_s = 1$  s and  $\tau = 1$  ms the first 1100 copies of the repeated spectra on each side of  $\omega = 0$  that he obtained are within 1 percent of the central spectrum's value.

- (b) Prove to him that only the first 78 copies of his spectrum on each side of  $\omega = 0$  are within 1 percent of the central one, and that he must get  $\tau$  to equal about  $71 \mu\text{s}$  for his statement to be true.

He replies by saying that he would then have to have the height of his pulses equal to about 14,084.5 volts for that to be true, so that the area of his pulses equals 1. Your answer is that the height of the pulses is of no consequence, and if he used 1-volt pulses he would burn out fewer multipliers. Pulse height is just

a scale factor and the only thing that matters for accurate sampling is the smallness of  $\tau/T_s$ .

**9.6** Using the FFT system, the following exercise demonstrates very clearly the effects of frequency-domain impulse sampling.

- With  $N = 1024$  and  $T = 4$ , load the pulse  $\text{Rect}(t)$  into  $\mathbf{X}$ . Run ANALYSIS and inspect  $\mathbf{F}$ . There should be a copy of  $\text{Sa}(\omega/2)$  in the display with a maximum value of unity. Invert to the time domain using SYNTHESIS. There should be a single  $\text{Rect}(t)$  in the display (with height unity).
- To emulate **impulse sampling**, go into the  $\mathbf{F}$  postprocessor and do the following two operations:
  - Take the SAMPLE option with  $M = 2$ , (i.e., keeping every second value in  $\mathbf{F}$ ).
  - Multiply  $\mathbf{F}$  by the weights of the impulses appearing in (9.30). In this case  $\omega_0$  is the spacing between the impulses and in our sampling we spaced them  $2\Omega = 2(2\pi/T)$  radians apart. Thus,  $\omega_0 = 4\pi/T$ . According to (15.7), to emulate a Dirac delta in the frequency domain with weight  $\mu$  we must use a single value  $V = \mu T/2\pi$ . In this case

$$\mu = \frac{4\pi}{T} \quad \text{and so} \quad V = 2$$

Thus use the multiply option in the  $\mathbf{F}$  postprocessor to multiply  $\mathbf{F}$  by 2.

- Return to the main menu and run SYNTHESIS. There should now be two copies of  $\text{Rect}(t)$  in the display, and according to (9.36) they should have a height of unity.
- Repeat all of the preceding, but now use  $M = 4$  when sampling. Inspect  $\mathbf{F}$ . It has a single nonzero value at  $\omega = 0$ . After running SYNTHESIS there should be four copies of the  $\text{Rect}(t)$  in the display. They are now touching each other, precisely as expected.

- 9.7** (a) Find the Fourier transform of the pulse shown in Figure 9.31.  
 (b) Now use Theorem 9.3 to produce the Fourier series for the two functions in Figures 9.32 and 9.33.  
 (c) Validate (b) by finding values for the first five Fourier series coefficients from the formulas and compare them to FFT values.

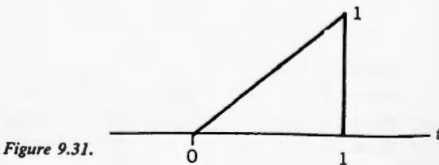


Figure 9.31.

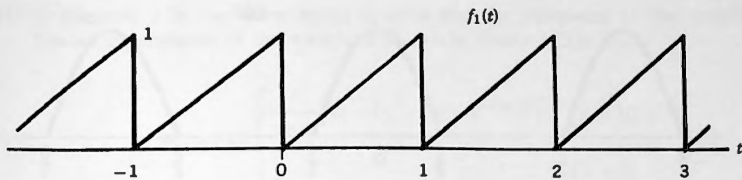


Figure 9.32.

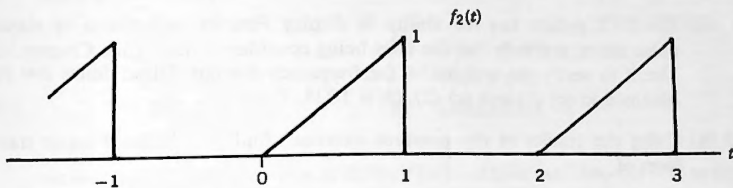


Figure 9.33.

9.8 (a) Sketch the time-domain function

$$f(t) = \cos(\pi t)\text{Rect}(t)$$

(b) Find  $F(\omega)$  in four ways:

- (1) By duality using the results of Exercise 9.3
  - (2) By frequency-domain convolution
  - (3) By successive differentiation
  - (4) By direct integration of the analysis equation
- (c) Using your results from (a) and (b) find the Fourier transforms of the following two periodic functions:
- (1) The full-wave rectified cosine  $f_1(t)$  shown in Figure 9.34
  - (2) The half-wave rectified cosine  $f_2(t)$  shown in Figure 9.35

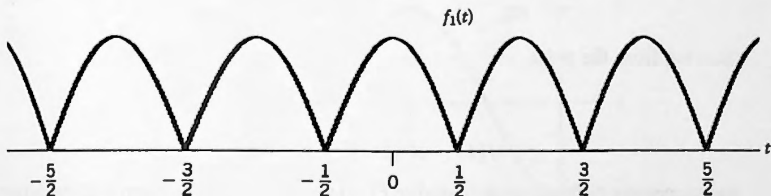


Figure 9.34.

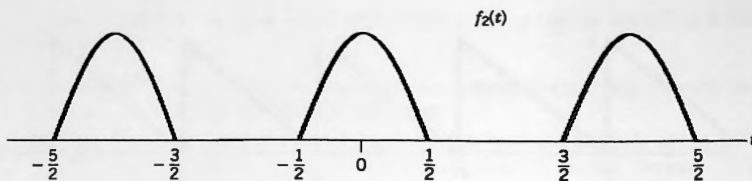


Figure 9.35.

- (d) The FFT system has the ability to display Fourier transforms of eternal pulse trains, precisely like the ones being considered here. (See Chapter 16.) Use it to verify the weights of the frequency-domain Dirac deltas that you obtained in (c) (1) and (c) (2). ( $N = 1024$ ,  $T = 1$ .)

- 9.9** (a) Using the results of the previous exercise, find  $F(\omega)$ , the Fourier transform of

$$f(t) = |\cos(\pi t)| \quad (t \in \mathbb{R})$$

- (b) Now find  $F_2(\omega)$  the Fourier transform of  $f''(t)$ .

- (c) Invert  $F_2(\omega)$  to the time domain and sketch what you obtain.

*Hint:* See Exercise 4.20.

- (d) Now differentiate  $f(t)$  twice in the time domain and sketch the result. Your sketches from (c) and (d) should be the same.

- 9.10** Starting from  $\delta(t) \Leftrightarrow 1$  use Theorem 9.3 to derive the Fourier series for the periodic function  $\delta_T(t)$ .

- 9.11** In Exercise 2.17 you were asked to find the complex Fourier coefficients  $F_p(n)$  for the periodic waveform

$$f_p(t) = \begin{cases} 0, & (-1 < t < 0) \\ e^t, & (0 < t < 1) \end{cases} \quad f_p(t+2) = f_p(t)$$

Starting from the pulse

$$f(t) = e^t \quad (0 < t < 1)$$

use successive differentiation to derive  $F(\omega)$  and then use Theorem 9.13 to derive the result obtained earlier for  $F_p(n)$ .

- 9.12 In Exercise 2.26 you were asked to show that the expression for the complex Fourier coefficients of the waveform shown in Figure 2.23 is

$$F_p(n) = \begin{cases} \frac{j}{4n\pi} [2(-1)^n - 1 - e^{-jn\pi/2}] & (n \neq 0) \\ \frac{3}{8} & (n = 0) \end{cases}$$

Starting from the pulse

$$f(t) = \begin{cases} \frac{1}{2} & (0 < t < 1) \\ 1 & (1 < t < 2) \\ 0 & (\text{otherwise}) \end{cases}$$

use successive differentiation to derive  $F(\omega)$  and then use Theorem 9.13 to derive the result shown for  $F_p(n)$ .

*Hint:* The term  $(-1)^n$  appearing in  $F_p(n)$  came from  $e^{-jn\pi}$

- 9.13 (a) Find the Fourier transform of the gated cosine pulse

$$f(t) = \cos(2\pi t/\tau) \text{Rect}(t/\tau)$$

shown in Figure 9.36 by two methods:

- (1) Frequency-domain convolution
- (2) Successive differentiation

- (b) Now use Theorem 9.3 to find the Fourier series of an infinite train of such pulses laid end to end, where the separation of the centers of the pulses is equal to

$$T_0 > \tau$$

- (c) Show that when  $T_0 \rightarrow \tau$  all coefficients in your Fourier series tend to zero except for the two associated with the fundamental, and that the final result

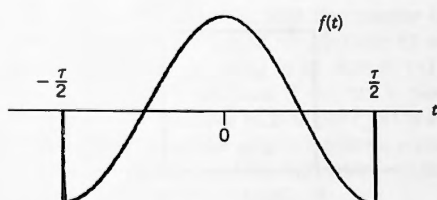


Figure 9.36.

becomes the two-term series

$$f_p(t) = \frac{1}{2}e^{j\omega_0 t} + \frac{1}{2}e^{-j\omega_0 t}$$

in which  $\omega_0 = 2\pi/T_0$ .

- (d) Express the two-term series in (c) as a sine/cosine series.
- (e) Sketch the train of pulses as they would appear when  $T_0 = \tau$ . Does your sketch agree with what you obtained in (d)?

**9.14** The spectrum of the pulse  $x(t) = \Lambda(t)$  is impulse sampled with spacing  $\omega_0 = 4\pi/3$  to produce a new spectrum  $X_s(\omega)$ .

- (a) Sketch the result in the time domain.
- (b) Now find the Fourier series of what you have sketched.

**9.15** (a) Sketch the pulse  $f(t) = e^{-\beta t}U(t)$ , where  $\beta = 1$ .

- (b) Now sketch the periodic function

$$f_p(t) = \sum_{n=-\infty}^{\infty} f(t - nT) \quad (T = 1)$$

- (c) Use Theorem 9.3 to find the Fourier series for  $f_p(t)$ .

- (d) Find the average value and the peak value of  $f_p(t)$ .

### A Project Involving the FFT System

**9.16** (a) Use time-shift to write the Fourier transform of the pulse  $x(t)$  shown in Figure 9.37.

(b) Use your result to find the Fourier series coefficients of the periodic waveform

$$x_p(t) = \begin{cases} 1 & (0 < t < 1) \\ 0 & (1 < t < 3) \end{cases} \quad x_p(t+3) = x_p(t)$$

(c) Load the expression that you obtained in (b) into F. Use  $N = 864$ , SAMPLED,  $T = 3$ , PERIODIC, ALPHA = 10. Then run SYNTHESIS. You should obtain a periodic waveform consisting of repetitions of the pulse shown in Figure 9.37, with period equal to 3.

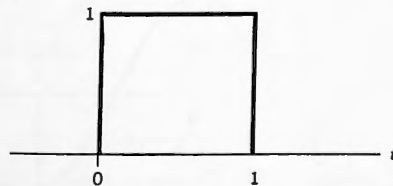


Figure 9.37.

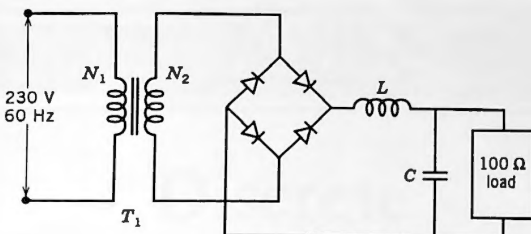


Figure 9.38. dc power supply.

### Design Project for a Power Supply

9.17 The dc power supply shown in Figure 9.38 consists of the following:

- (1) An ideal transformer  $T_1$ , turns ratio  $N_2 : N_1$  and zero internal resistance
- (2) A full-wave diode-rectifier bridge. (Assume perfect diodes with zero threshold voltages and zero internal impedances.)
- (3) An ideal series inductor, inductance  $L$  henrys with zero internal resistance
- (4) A shunt capacitor  $C$ , capacitance  $10,000 \mu\text{F}$ .
- (5) A pure resistive load of  $100 \Omega$  connected across the output.
- (6) The input voltage is a cosine.

**Find the answers to the following questions:**

- (a) What should the turns ratio be in order for there to be 1000 V dc across the resistive load?
- (b) If the peak-to-peak of the first harmonic of the ripple across the load shall not exceed 0.1 percent of the dc voltage, find the value required for the inductor.
- (c) What are the amplitudes (peak to zero) of the first five harmonics in the ripple. At what rate are they converging?

**Validate all results using the FFT system as follows:**

- (1) When you have obtained the Fourier coefficients for the full-wave rectified cosine, validate them by transforming such a periodic waveform using ANALYSIS.
- (2) The turns ratio that you obtain should give the zeroth harmonic in the series a value of 1000.
- (3) Once you have found a value for  $L$ , load the transfer function of the  $LC$  smoothing network (including the load resistor) into F2 using main-menu A, CREATE H(jw). This places  $H(jn\omega_0)$  in F2. Run ANALYSIS on the input waveform, thereby loading its spectrum  $F_p(n)$  into F. Now use COMPLEX-MULTIPLY in the F postprocessor to multiply  $F_p(n)$  in F by  $H(jn\omega_0)$  in F2. This produces the spectrum of the output waveform across the load resistor, placing it in F. The FFT's values of the harmonics can then be compared to the values that you obtained theoretically.



---

**PART 2**

---

# Discrete Fourier Analysis



# The Discrete Fourier Transform

## 10.1 INTRODUCTION

The discrete Fourier transform (DFT) is the primary tool that is used when computers are employed in Fourier analysis. To run the DFT on a computer one uses an ingenious algorithm known as the fast Fourier transform (FFT), which is a highly efficient implementation of the DFT, described in 1965 by Cooley and Tukey.<sup>†</sup> In this chapter we examine the DFT and some of its key properties, and in the next one we take a brief look at what goes on inside the FFT, just enough for us to understand some of its remarkable properties and why it is so effective when we use it to evaluate the DFT.

## 10.2 THE DISCRETE COMPLEX EXPONENTIALS

In Part 1 we encountered two sets of complex exponentials

$$S_1 = \{e^{jn\omega_0 t} \mid n \in I\} \quad (10.1)$$

and

$$S_2 = \{e^{j\omega t} \mid \omega \in \mathbb{R}\} \quad (10.2)$$

in both of which  $t$  was a continuous variable. The first set formed the basis for complex Fourier series and the second the basis for the Fourier transform. In both cases the underlying mechanism that makes analysis and synthesis possible is their respective orthogonality properties, the first set satisfying

$$\frac{1}{T_0} \int_{-T_0/2}^{T_0/2} e^{jn\omega_0 t} e^{jm\omega_0 t^*} dt = \begin{cases} 0 & \text{if } n \neq m \\ 1 & \text{if } n = m \end{cases} \quad (10.3)$$

<sup>†</sup>For a history of the FFT, see Cooley et al. See also Heidemann et al., which traces the FFT all the way back to Gauss.

and the second set (see Theorem 4.5)

$$\int_{-\infty}^{\infty} e^{j\omega_1 t} e^{j\omega_2 t^*} dt = 2\pi\delta(\omega_2 - \omega_1) \quad (10.4)$$

In this chapter we consider a third set called the **discrete complex exponentials of order  $N$** , namely

$$S = \{e^{j2\pi m/N} \mid m \in I\} \quad (10.5)$$

in which the independent variable  $m$  is now discrete. As we shall soon see, this set also satisfies an orthogonality condition, and it is on that property that we shall build the DFT.

The key to understanding the discrete complex exponentials lies in understanding **modulo- $N$**  arithmetic: Two integers  $a$  and  $b$  can be said to be “equal modulo  $N$ ,” where  $N$  is some positive integer. This is written as  $|a|_N = b$  and read as “ $a$  modulo  $N$  equals  $b$ .” As examples,

$$|13|_5 = 3, \quad |8|_7 = 1, \quad |9|_3 = 0 \quad \text{and} \quad |-13|_5 = 2$$

The rules are as follows: Consider the number 13 with  $N = 5$ . Dividing 13 by 5 we obtain a remainder of 3. Then  $|13|_5 = 3$ .

Negative integers can also be included: Consider the number  $-13$  with  $N = 5$ . Dividing  $-13$  by 5 we obtain a remainder of  $-3$  to which we then add 5, giving us 2. Then  $|-13|_5 = 2$ .

As an example, modulo-8 equivalence works according to the truth table shown in Table 10.1. In the first line we show  $m$  running linearly from  $-\infty$  to  $\infty$ , and beneath it we show its value modulo-8. Observe how all of the integers are mapped into the central period 0 to 7.

When two integers are multiplied together their product is again an integer, and if we are operating under the modulo- $N$  rule, then that product is mapped into an integer lying in the range 0 to  $N - 1$ . As examples,

$$|7 \times 9|_5 = 3, \quad |3 \times 27|_3 = 0 \quad \text{and} \quad |-2 \times 15|_{32} = 2$$

Now let's return to the complex exponentials  $e^{j2\pi m/N}$ . The first thing that we note is the fact they all lie on the unit circle. As an example let  $N = 8$  and  $m = 1$  (see Fig. 10.1). Then  $e^{j2\pi/8}$  has modulus 1 and argument  $2\pi/8$ . Thus it lies at unit distance from the origin, and the line from it to the origin makes an angle  $2\pi/8$  with the positive real axis.

As we let  $m$  increase from 1 to 7 we see that we are jumping from point to point around the unit circle, each time increasing our angle with the real line by  $2\pi/8$ .

TABLE 10.1 Modulo-8 Truth Table

$m$	...	-5	-4	-3	-2	-1	0	1	2	3	4	5	6	7	8	9	10	...
$ m _8$	...	3	4	5	6	7	0	1	2	3	4	5	6	7	0	1	2	...

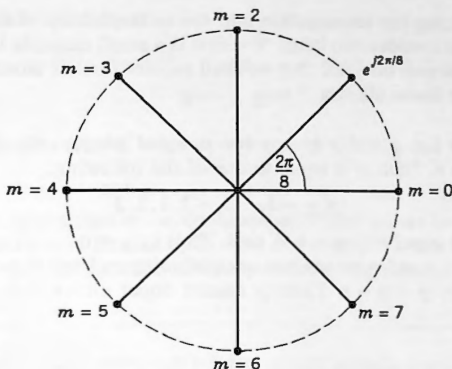


Figure 10.1. The numbers  $e^{j2\pi m/N}$ .

When  $m$  increases beyond 7 we have returned to our starting point and are now going around the unit circle again; in fact, no matter how large  $m$  becomes, we always arrive at one of the eight points appearing in the figure. The same is true if  $m$  takes on negative values.

Clearly, then, there is a modulo-8 equivalence at work, and we can write

$$e^{j2\pi m/N} = e^{j2\pi|m|_N/N} \quad (10.6)$$

Thus, for  $m = 53$ ,  $|53|_8 = 5$ , and so (10.6) gives

$$e^{j2\pi 53/8} = e^{j2\pi|53|_8/8} = e^{j2\pi 5/8}$$

We refer to (10.6) as the **circularity property** of the complex exponentials, and from it others will soon follow.

**EXAMPLE 10.1:** Let  $n$  and  $k$  be integers. Then  $nk$  is also an integer, and so (10.6) gives

$$e^{j2\pi nk/N} = e^{j2\pi|nk|_N/N}$$

Letting  $n = 13$ ,  $k = 27$ , and  $N = 32$  we have

$$nk = 351 \quad \text{and} \quad |351|_{32} = 31$$

and so (10.6) gives us

$$e^{j2\pi 13 \times 27/32} = e^{j2\pi 31/32}$$

**EXAMPLE 10.2:** Let  $q$  be any multiple of  $N$ . Then  $|q|_N = 0$ , and so

$$e^{j2\pi q/N} = e^{j2\pi 0/N} = 1$$

Before commencing our investigation into the orthogonality of the complex exponentials we need to consider two items. The first is a small example that demonstrates a result (perhaps already obvious) that we shall require further along, and the second is a definition from linear algebra.

**□EXAMPLE 10.3:** Let  $q$  and  $r$  be any two **unequal** integers equal to 0, 1, 2, or 3, and let  $p = q - r$ . Then  $p$  is equal to one of the following:

$$p = -3, -2, -1, 1, 2, 3$$

and so  $p$  cannot equal either  $-4$ ,  $0$ , or  $4$ . Thus  $|p|_4 \neq 0$ .

In general, let  $q$  and  $r$  be any two unequal integers lying between  $0$  and  $N - 1$  inclusive, and let  $p = q - r$ . Then  $p$  cannot equal either  $-N$ ,  $0$  or  $N$ , that is,  $|p|_N \neq 0$ .  $\square$

We recall from linear algebra that to test for the orthogonality of complex vectors we use what is known as the **inner product**, defined as follows:

**Definition:** The **inner product** of two complex  $N$ -vectors  $\mathbf{a}$  and  $\mathbf{b}$  is written as  $(\mathbf{a}, \mathbf{b})$  and has the following meaning:

$$(\mathbf{a}, \mathbf{b}) \equiv \sum_{k=0}^{N-1} a_k b_k^* \quad (10.7)$$

**□EXAMPLE 10.4:** Let

$$\mathbf{a} = \begin{bmatrix} 1+j \\ 2-j \\ j \end{bmatrix} \quad \text{and} \quad \mathbf{b} = \begin{bmatrix} j \\ 1+2j \\ -j \end{bmatrix}$$

Then  $N = 3$  and (10.7) gives us

$$(\mathbf{a}, \mathbf{b}) = \sum_{k=0}^2 a_k b_k^* = (1+j)(-j) + (2-j)(1-2j) + (j)(j) = -6j \quad \square$$

**Definition:** Two vectors are said to be **orthogonal** if their inner product is equal to zero.

Before stating the orthogonality property of  $S$  on which the DFT is based we make the following definition that will enable us to conserve energy.

**Definition:** The quantity  $W$  is defined by

$$W = e^{-j2\pi/N} \quad (10.8)$$

Using (10.8), we have the following:

$$e^{-j2\pi k/N} = W^k \quad \text{and} \quad e^{j2\pi n/N} = W^{-n} \quad (10.9)$$

$$W^{k*} = W^{-k} \quad (10.10)$$

■ **EXAMPLE 10.5:** For  $N = 4$

$$W^0 = 1, \quad W^1 = -j, \quad W^2 = -1 \quad \text{and} \quad W^3 = j \quad \square$$

Please note the minus sign in the definition of  $W$  and always keep it in mind. The quantity  $W$  will recur very frequently in what lies ahead. We now come to Theorem 10.1, which states the orthogonality property of the discrete complex exponentials.

### ■ THEOREM 10.1

Let  $q$  and  $r$  be any two integers in the range 0 to  $N - 1$  inclusive. Then the discrete complex exponentials of order  $N$  satisfy the orthogonality condition

$$\sum_{k=0}^{N-1} e^{j2\pi qk/N} e^{j2\pi rk/N*} = \begin{cases} 0 & \text{if } q \neq r \\ N & \text{if } q = r \end{cases} \quad (10.11a)$$

$$\sum_{k=0}^{N-1} W^{-qk} W^{-rk*} = \begin{cases} 0 & \text{if } q \neq r \\ N & \text{if } q = r \end{cases} \quad (10.11b)$$

Stating (10.11) in terms of  $W$ , the orthogonality property is:

$$\sum_{k=0}^{N-1} W^{-qk} W^{-rk*} = \begin{cases} 0 & \text{if } q \neq r \\ N & \text{if } q = r \end{cases} \quad (10.12a)$$

$$\sum_{k=0}^{N-1} W^{-qk} W^{-rk*} = \begin{cases} 0 & \text{if } q \neq r \\ N & \text{if } q = r \end{cases} \quad (10.12b)$$

Observe first, by comparing the LHS of (10.12) to the RHS of (10.7), that we are dealing here with the **inner product of two complex vectors**. This becomes clear in the following example where we demonstrate the validity of (10.11). After that we'll prove it in general.

■ **EXAMPLE 10.5:** For simplicity we let  $N = 5$  and consider the two complex exponentials appearing on the LHS of (10.11), namely  $W^{-qk}$  and  $W^{-rk}$ .

**Case 1:**  $q$  and  $r$  are unequal.

Then according to (10.11a) the sum shown should be equal to zero. As an example take  $q = 2$  and  $r = 3$ , and form the following two vectors by letting  $k$  run from 0 to  $N - 1$  in the two complex exponentials.

$$\begin{array}{lll} & q = 2 & r = 3 \\ k = 0 & \left[ \begin{matrix} W^0 \\ W^{-2} \\ W^{-4} \\ W^{-6} \\ W^{-8} \end{matrix} \right] & \left[ \begin{matrix} W^0 \\ W^{-3} \\ W^{-6} \\ W^{-9} \\ W^{-12} \end{matrix} \right] \\ k = 1 & & \\ k = 2 & \mathbf{a} = & \\ k = 3 & & \\ k = 4 & & \end{array} \quad (10.13)$$

Forming the inner product of  $\mathbf{a}$  and  $\mathbf{b}$ , we start with the sum shown in (10.7). Thus

$$(\mathbf{a}, \mathbf{b}) = \sum_{k=0}^4 W^{-2k} W^{-3k} \quad (10.14)$$

which we see is precisely the LHS of (10.11), and so it is indeed the inner product of two complex  $N$ -vectors. Expanding (10.14) we now continue as

$$\begin{aligned} \dots &= W^0 W^0 + W^{-2} W^3 + W^{-4} W^6 + W^{-6} W^9 + W^{-8} W^{12} \\ &= 1 + W^1 + W^2 + W^3 + W^4 \end{aligned} \quad (10.15)$$

which is the sum of the five distinct values that  $e^{-j2\pi m/5}$  can assume around the unit circle. We now draw a line from the origin to each of those five numbers and think of them as vectors in two-space (see Fig. 10.2). Then, by virtue of their symmetric positions, their sum must be equal to zero. (For a more rigorous proof see the lemma in Notes and Comments.) Thus the vectors  $\mathbf{a}$  and  $\mathbf{b}$  in (10.13) are orthogonal, and so (10.11a) has been shown to hold.

**Case 2:**  $q$  and  $r$  are equal.

According to (10.11b) the sum on the LHS should now be equal to 5, regardless of the choice of values for  $q$  and  $r$ . As an example we let both  $q$  and  $r$  equal 2 and generate the following two vectors, starting as before from  $W^{-qk}$  and  $W^{-rk}$ :

$$\begin{array}{ll} q = 2 & r = 2 \\ \begin{matrix} k = 0 \\ k = 1 \\ k = 2 \\ k = 3 \\ k = 4 \end{matrix} & \mathbf{a} = \begin{bmatrix} W^0 \\ W^{-2} \\ W^{-4} \\ W^{-6} \\ W^{-8} \end{bmatrix} \quad \mathbf{b} = \begin{bmatrix} W^0 \\ W^{-2} \\ W^{-4} \\ W^{-6} \\ W^{-8} \end{bmatrix} \end{array} \quad (10.16)$$

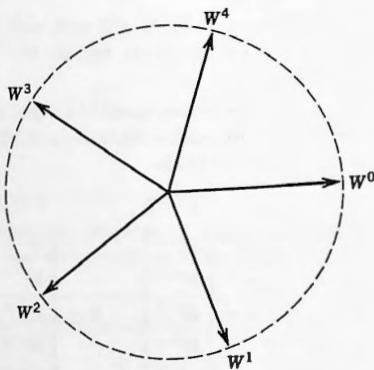


Figure 10.2.

Once again we form the inner product of  $\mathbf{a}$  and  $\mathbf{b}$ , using (10.7) obtaining

$$(\mathbf{a}, \mathbf{b}) = \sum_{k=0}^4 W^{-2k} W^{-2k} \quad (10.17)$$

and again we see that this is precisely the LHS of (10.11). Continuing (10.17), we have

$$\dots = \sum_{k=0}^4 W^{-2k} W^{2k} = \sum_{k=0}^4 W^0 = 5 \quad (10.18)$$

and so (10.11b) has been validated □

As we have now seen, the LHS of (10.11) is the inner product of two vectors, and what that equation is saying is that pairs of vectors such as those that we created in (10.13) and (10.16) will give us zero if we form the inner-product of any of them with another, and will give us a value of  $N$  if we form the inner-product of any of them with itself. We now prove that (10.11) is true in general.

*Proof of Theorem 10.1:* Starting from the LHS of (10.11) we have

$$\sum_{k=0}^{N-1} W^{-qk} W^{-rk} = \sum_{k=0}^{N-1} W^{-(q-r)k} = \sum_{k=0}^{N-1} W^{-pk} \quad (10.19)$$

where  $p = q - r$ .

**Case 1:**  $q \neq r$ . Recall that  $q$  and  $r$  both lie in the range 0 to  $N - 1$ , and that here they are unequal. Thus  $p = q - r$  is some integer that cannot be equal to either  $-N$ , 0, or  $N$  (see Example 10.3), and so  $W^{-p} \neq 1$ . Then (10.19) continues as

$$\dots = \sum_{k=0}^{N-1} [W^{-p}]^k$$

which is the sum of  $N$  terms of a geometric progression that we then sum, continuing as

$$\dots = \frac{1 - [W^{-p}]^N}{1 - W^{-p}} = \frac{1 - W^{-pN}}{1 - W^{-p}} = \frac{1 - 1}{1 - W^{-p}} = 0 \quad (10.20)$$

**Case 2:**  $q = r$ . Then  $q - r = 0$ , and so (10.19) continues as

$$\dots = \sum_{k=0}^{N-1} 1 = N \quad (10.21)$$

Thus Theorem 10.1 is proved. ■

**Accompanying Disk**

It is tempting to think that the discrete sines and cosines

$$\cos \frac{2\pi nk}{N} \quad \text{and} \quad \sin \frac{2\pi nk}{N}$$

form orthogonal sets, as was the case with the continuous sines and cosines in Chapter 2. That is almost true, but not quite.

In H of the program PLOTS we demonstrate the nonorthogonality property of the discrete sines and cosines.

We also point out there that the discrete complex exponentials

$$e^{j2\pi nk/N} = \cos \frac{2\pi nk}{N} + j \sin \frac{2\pi nk}{N}$$

definitely do possess orthogonality, as was proved in Theorem 10.1.

---

### 10.3 THE DISCRETE FOURIER TRANSFORM

---

The orthogonality property of the discrete complex exponentials will now enable us to create the DFT. Thus, suppose that we have a discrete function  $f_k$  ( $0 \leq k \leq N - 1$ ) that we wish to restate as a linear combination of the discrete complex exponentials of order  $N$ . The function  $f_k$  could come to us either as an analytical statement, for example,  $f_k = e^{-2k+3}$ , or else simply as a vector of  $N$  explicit values. We are thus in the same situation as in Chapter 2 where we had the analytical definition of a periodic function of  $t$  that we wished to restate as a linear combination of the set of continuous complex exponentials  $\{e^{jn\omega_0 t}\}$ .

Following what we did in Chapter 2 we now assert that  $f_k$  can in fact be written as the following linear combination

$$f_k = \frac{1}{N} \sum_{n=0}^{N-1} F_n e^{j2\pi nk/N} \quad (0 \leq k \leq N - 1) \quad (10.22)$$

in which the numbers  $F_n$  are the constants of the combination and are yet to be determined. Regarding (10.22) we note that

- It is actually  $N$  separate statements, one for each value of  $k$ .
- There are  $N$  constants  $F_n$  involved whose values must be specified.
- We have elected to include the multiplier  $1/N$  as shown.

Then, as we did in Chapter 2, to find expressions for the  $F_n$  we now multiply both sides of (10.22) by  $e^{-j2\pi mk/N}$ , obtaining

$$f_k e^{-j2\pi mk/N} = \left[ \frac{1}{N} \sum_{n=0}^{N-1} F_n e^{j2\pi nk/N} \right] e^{-j2\pi mk/N} \quad (10.23)$$

which we then sum over  $k$  as follows:

$$\sum_{k=0}^{N-1} f_k e^{-j2\pi mk/N} = \sum_{k=0}^{N-1} \left[ \frac{1}{N} \sum_{n=0}^{N-1} F_n e^{j2\pi nk/N} \right] e^{-j2\pi mk/N} \quad (10.24)$$

We now interchange the order of summation on the right (no problem here as there was in Chapter 2 because here the series is of finite length), and so we continue as

$$\dots = \frac{1}{N} \sum_{n=0}^{N-1} F_n \sum_{k=0}^{N-1} e^{j2\pi nk/N} e^{-j2\pi mk/N} \quad (10.25)$$

Then, by the orthogonality property (10.11), we see that the second sum in (10.25) is equal to zero for  $n \neq m$ , and equal to  $N$  for  $n = m$ , and so (10.25) collapses down to the single term  $F_m$ , giving us

$$\sum_{k=0}^{N-1} f_k e^{-j2\pi mk/N} = F_m \quad (10.26)$$

We now replace  $m$  with  $n$ , obtaining

$$F_n = \sum_{k=0}^{N-1} f_k e^{-j2\pi nk/N} \quad (0 \leq n \leq N-1) \quad (10.27)$$

and this is the required expression for the  $N$  constants  $F_n$  in (10.22). All of this is summarized in Theorem 10.2.

### ■ THEOREM 10.2: The discrete Fourier transform

Let  $f_k$  ( $0 \leq k \leq N-1$ ) be a function of the discrete variable  $k$ , defined either analytically or else as a given  $N$ -vector of (possibly complex) numbers. Then  $f_k$  can be stated as a sum of discrete complex exponentials in the form

$$f_k = \frac{1}{N} \sum_{n=0}^{N-1} F_n e^{j2\pi nk/N} \quad (0 \leq k \leq N-1) \quad (10.28)$$

where the  $N$  numbers  $F_n$  can be found from the numbers  $f_k$  by

$$F_n = \sum_{k=0}^{N-1} f_k e^{-j2\pi nk/N} \quad (0 \leq n \leq N-1) \quad (10.29)$$

- Equation (10.28) is called the **DFT synthesis equation**, often also referred to as the **inverse discrete Fourier transform** (IDFT).
- Equation (10.29) is called the **DFT analysis equation**. The numbers  $F_n$  that it produces form the **DFT line spectrum** of the vector  $f_k$ .
- Together they form a pair called the **discrete Fourier transform**, which is now our third example of an analysis/synthesis system.

We'll soon see how the DFT can be used to find estimates for the Fourier series coefficients and Fourier transforms of Part 1.

Consider now the following basic property of the DFT.

■ **COROLLARY 1 to Theorem 10.2**

The two transformations defined by (10.28) and (10.29) are each other's exact inverses.

This means that the vector  $\mathbf{f}$  generated by (10.28) is exactly the vector  $\mathbf{f}$  whose elements were used in (10.29). To verify this we suppose that (10.28) produces a number that we call  $g_k$ , whatever it may be. Then, using (10.29) in (10.28), we obtain

$$\begin{aligned} g_k &= \frac{1}{N} \sum_{n=0}^{N-1} F_n W^{-nk} = \frac{1}{N} \sum_{n=0}^{N-1} \left[ \sum_{r=0}^{N-1} f_r W^{nr} \right] W^{-nk} \\ &= \frac{1}{N} \sum_{r=0}^{N-1} f_r \sum_{n=0}^{N-1} W^{nr} W^{-nk} \end{aligned} \quad (10.30)$$

However, by the orthogonality property (10.11) the final sum in (10.30) is equal to zero if  $r \neq k$ , and is equal to  $N$  if  $r = k$ , and so it continues as

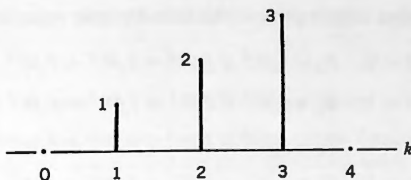
$$\cdots = \frac{1}{N} f_k N = f_k \quad (10.31)$$

Thus  $g_k$  is in fact  $f_k$  and so the proposition is proved. ■

Suppose next that we start with the following sequence of  $N$  complex numbers for  $f_k$ :

$$f_0, f_1, f_2, \dots, f_k, \dots, f_{N-1}$$

and assume that, by the use of (10.29), we have found the set of  $N$  complex numbers  $F_n$ . Then, when  $n$  goes through the values  $0 \leq n \leq N - 1$ , (10.29) will generate the numbers  $F_0, \dots, F_{N-1}$ . When  $n$  takes on integer values outside of the range  $0 \leq n \leq N - 1$ , however, the exponentials inside the summation sign in (10.29) will recycle because of their circularity, and will simply repeat themselves with period  $N$ . Thus the values of  $F_n$  being generated must also be periodic repetitions of the original set, and so (10.29) is seen to be an **inherently periodic** function of  $n$  with period  $N$ .

Figure 10.3.  $f_k = k$ .

Clearly, the same is also true for (10.28)—the sequence of numbers  $f_0, \dots, f_{N-1}$  generated by that equation will repeat with period  $N$  as  $k$  ranges through all of the integers, a direct result of the circularity property of the discrete complex exponentials. We state this as a second corollary to Theorem 10.2.

### ■ COROLLARY 2 to Theorem 10.2

The numbers generated by both the DFT analysis and synthesis equations are inherently periodic with period  $N$ .

We now work an example which illustrates the complete operation of the DFT from end to end.

■**EXAMPLE 10.6:** The analytical definition of a discrete pulse is

$$f_k = \begin{cases} k & (0 \leq k \leq 3) \\ 0 & (\text{otherwise}) \end{cases} \quad (10.32)$$

We display  $f_k$  in Figure 10.3. Our objectives in this example are threefold, as follows:

- To transform the given function  $f_k$  using the DFT analysis equation, thereby producing the DFT line spectrum  $F_n$ .
- To invert the line spectrum obtained in (a) using the DFT synthesis equation, thereby recreating the original input vector  $f_k$ .
- To show that the given function  $f_k$  has been restated as a linear combination of complex exponentials.

Using  $N = 4$  the input data calculated from the analytical definition in (10.32) become the vector

$$\mathbf{f} = (0, 1, 2, 3) \quad (10.33)$$

For part (a): Expanding (10.29) gives us the four analysis equations

$$n = 0: F_0 = f_0W^0 + f_1W^0 + f_2W^0 + f_3W^0 \quad (10.34)$$

$$n = 1: F_1 = f_0W^0 + f_1W^1 + f_2W^2 + f_3W^3 \quad (10.35)$$

$$n = 2: F_2 = f_0W^0 + f_1W^2 + f_2W^4 + f_3W^6 \quad (10.36)$$

$$n = 3: F_3 = f_0W^0 + f_1W^3 + f_2W^6 + f_3W^9 \quad (10.37)$$

Using the values for  $f$  from (10.33), and substituting the numerical values of the powers of  $W$ , these four equations then give us the DFT coefficients as follows:

$$n = 0: F_0 = 0 + 1 + 2 + 3 = \boxed{6} \quad (10.38)$$

$$n = 1: F_1 = 0 - j1 - 2 + j3 = \boxed{-2 + j2} \quad (10.39)$$

$$n = 2: F_2 = 0 - 1 + 2 - 3 = \boxed{-2} \quad (10.40)$$

$$n = 3: F_3 = 0 + j1 - 2 - j3 = \boxed{-2 - j2} \quad (10.41)$$

These results can then be assembled to form the DFT spectrum vector

$$\mathbf{F} = (6, -2 + j2, -2, -2 - j2) \quad (10.42)$$

For part (b): Expanding (10.28) gives us the four synthesis equations

$$k = 0: f_0 = \frac{1}{4}[F_0W_0 + F_1W^0 + F_2W^0 + F_3W^0] \quad (10.43)$$

$$k = 1: f_1 = \frac{1}{4}[F_0W^0 + F_1W^{-1} + F_2W^{-2} + F_3W^{-3}] \quad (10.44)$$

$$k = 2: f_2 = \frac{1}{4}[F_0W^0 + F_1W^{-2} + F_2W^{-4} + F_3W^{-6}] \quad (10.45)$$

$$k = 3: f_3 = \frac{1}{4}[F_0W^0 + F_1W^{-3} + F_2W^{-6} + F_3W^{-9}] \quad (10.46)$$

To verify that these four equations do in fact give us back the original function  $f_k$ , we now substitute the numerical values for the powers of  $W$  and use the values for  $F_n$  appearing in (10.42), obtaining

$$\begin{aligned} f_0 &= \frac{1}{4}[F_0 + F_1 + F_2 + F_3] \\ &= \frac{1}{4}[6 + (-2 + j2) + (-2) + (-2 - j2)] = \boxed{0} \end{aligned} \quad (10.47)$$

$$\begin{aligned} f_1 &= \frac{1}{4}[F_0 + jF_1 - F_2 - jF_3] \\ &= \frac{1}{4}[6 + j(-2 + j2) - (-2) - j(-2 - j2)] = \boxed{1} \end{aligned} \quad (10.48)$$

$$\begin{aligned} f_2 &= \frac{1}{4}[F_0 - F_1 + F_2 - F_3] \\ &= \frac{1}{4}[6 - (-2 + j2) + (-2) - (-2 - j2)] = \boxed{2} \end{aligned} \quad (10.49)$$

$$\begin{aligned} f_3 &= \frac{1}{4}[F_0 - jF_1 - F_2 + jF_3] \\ &= \frac{1}{4}[6 - j(-2 + j2) - (-2) + j(-2 - j2)] = \boxed{3} \end{aligned} \quad (10.50)$$

These results can then be assembled to give us the output vector

$$\mathbf{f} = (0, 1, 2, 3) \quad (10.51)$$

which is seen to be the same as  $\mathbf{f}$  in (10.33) that we started out with.

**For part (c):** To show that we have been able to restate  $\mathbf{f}$  as a linear combination of complex exponentials we rewrite (10.43) through (10.46) using the values of  $\mathbf{F}$  from part (a) as follows:

$$\begin{bmatrix} 0 \\ 1 \\ 2 \\ 3 \end{bmatrix} = \frac{6}{4} \begin{bmatrix} W^0 \\ W^0 \\ W^0 \\ W^0 \end{bmatrix} + \frac{-2+j2}{4} \begin{bmatrix} W^0 \\ W^{-1} \\ W^{-2} \\ W^{-3} \end{bmatrix} - \frac{2}{4} \begin{bmatrix} W^0 \\ W^{-2} \\ W^{-4} \\ W^{-6} \end{bmatrix} + \frac{-2-j2}{4} \begin{bmatrix} W^0 \\ W^{-3} \\ W^{-6} \\ W^{-9} \end{bmatrix} \quad (10.52)$$

Reading across the first line of (10.52) we obtain (10.43), across the second line we obtain (10.44), and so on. Equation (10.52) shows us a great deal that we may otherwise have missed. Observe the following:

- On the LHS we have the vector  $\mathbf{f}$ , while on the RHS we see four vectors of complex exponentials in a linear combination, with the values of  $\mathbf{F}$  as the constants of that combination. This is the discrete counterpart to the two synthesis statements from Part 1, namely,

$$f_p(t) = \sum_{n=-\infty}^{\infty} F_n e^{jn\omega_0 t} \quad (10.53)$$

and

$$f(t) = \int_{-\infty}^{\infty} F(\omega) e^{j\omega t} dt \quad (10.54)$$

The structures of (10.52), (10.53), and (10.54) are mathematically identical, in the sense that in each case a given function has been restated as a “linear combination” of complex exponentials.

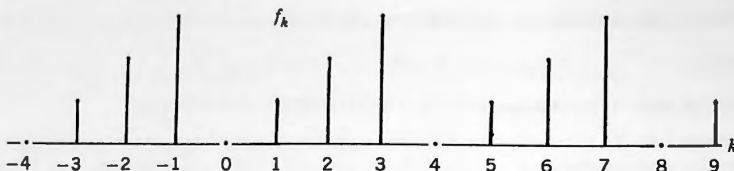
- The vectors on the RHS of (10.52) form an orthogonal set in the sense of linear algebra. They are the quantities that the orthogonality property of Theorem 10.1 was concerned with. It is the inner product of each of these vectors with another that is zero, each with itself that is equal to  $N$ . (See also Exercise 10.2.)
- Each of the vectors in (10.52) represents a sampling of a “complete” complex exponential. They are the discrete counterparts of the countably infinite set of quantities

$$\dots e^{j0\omega_0 t}, \quad e^{j1\omega_0 t}, \quad e^{j2\omega_0 t}, \quad e^{j3\omega_0 t}, \dots$$

and of the uncountably infinite set of quantities

$$S = \{e^{j\omega t} \mid \omega \in \mathbb{R}\}$$

which formed the bases for the expansions in Chapters 2 and 3.

Figure 10.4. Periodic extension of  $f_k = k$ .

- In this simple example we used  $N = 4$ , which is a very small number. This led to four vectors appearing in (10.52), to four elements in  $\mathbf{F}$  and to four in  $\mathbf{f}$ . There are only four discrete complex exponentials at work here. Had we used a larger value for  $N$ , say 10,000, then there would have been that many vectors on the RHS of (10.52), each with that many elements.  $\mathbf{F}$  and  $\mathbf{f}$  would have been of dimension 10,000, and that is the number of complex exponentials that would have been at work. (It is clear why we used  $N = 4$  and not  $N = 10,000$ . The book publisher would not have liked 10,000.)

As we increase  $N$  the discrete complex exponentials begin to look more and more like their continuous counterparts, and so the numbers coming from DFT begin to look more and more like those coming from (10.53) and (10.54). In Chapter 12 we shall see how the DFT's results can in fact be made to serve as estimates of those two from the earlier chapters, with startling accuracy for  $N$  only a relatively small number such as 512 or 1024.  $\square$

In all of this we only considered values for  $n$  and  $k$  in the range 0 to 3. By Corollary 2 to Theorem 10.2, however, we know that the numbers generated by both the DFT and the IDFT are inherently periodic with period  $N$ . Thus if we were to redo computations (10.34) through (10.37), letting  $n$  range over  $-8$  to  $11$ , say, we would obtain precisely the same answers repeated over and over again because the complex exponentials would recycle.

Likewise if we were to redo (10.43) through (10.46), letting  $k$  range over  $-4$  to  $9$  we would obtain precisely the same answers repeated over and over again for the same reason—the complex exponentials are circular. This is depicted in Figure 10.4.

Starting from the single-period statement of  $F_n$  appearing in (10.42) we can now assemble the array of numbers appearing in Table 10.2 in which we show all of the essential features of the DFT line spectrum.

TABLE 10.2 DFT Line Spectrum of Example 10.6

$n$	$FRE(n)$	$FIM(n)$	$ F(n) $	$\theta(n)$	$ F(n) ^2$
-2	-2	0	2	*****	4
-1	-2	-2	2.8284	-2.3562	8
0	6	0	6	0	36
1	-2	2	2.8284	2.3562	8
2	-2	0	2	*****	4

The table shows the way in which the FFT system on the disk displays numerical values of  $F$ . Observe that  $\text{FRE}(n)$ ,  $|F(n)|$ , and  $|F(n)|^2$  are all even, and that  $\text{FIM}(n)$  and  $\theta(n)$  are odd. We shall return to this later. (For the significance of the rows of asterisks see “Anomalous Points of the Arctangent Function” in Notes and Comments later in the chapter.)

We draw the reader’s attention to the following: There is a multiplier  $1/N$  that appears in (10.28) in front of the sigma. This is needed either in that equation or else in (10.29) in order that those two equations shall be each other’s inverses.

- Some authors prefer to place the  $1/N$  in (10.29) rather than in (10.28) as we have done.
- Others use  $1/\sqrt{N}$  in each equation.

#### Accompanying Disk

The FFT system on the accompanying disk implements the discrete Fourier transform equations of Theorem 10.2 without any deviations. On the disk the transformation shown in (10.29) is called ANALYSIS and the inverse transformation shown in (10.28) is called SYNTHESIS.

The numerical results that would be obtained from these equations are precisely the same numbers as those obtained using the disk. The periodicity of the DFT that we discussed in Corollary 2 to Theorem 2 is present in the FFT system as are all of the other properties of the DFT.

To implement the DFT equations exactly as they are shown in Theorem 10.2 would result in unacceptably long execution times when  $N$  is large, because the number of complex multiplications required is of the order of  $N^2$ .

When  $N$  is a power of 2, however, the number of complex multiplies can be reduced to  $\frac{1}{2}N \log_2(N)$ , which is a very much smaller number than  $N^2$ . This is the breakthrough that the FFT gives us that has led to the use of Fourier analysis on computers and specially designed chips on an ever-increasing scale in modern technology. All of this is discussed in the next chapter.

Just as we saw in the continuous world, Figure 10.5 illustrates the relationships between what we call the  $k$ -domain (time) and the  $n$ -domain (frequency) in the discrete world. Here’s what the figure shows:

- As with the continuous-world case, we start with an analytical definition of a time-domain function, but in this case the independent variable is the discrete variable  $k$ . Here, however, we can also accept a data vector without having any idea of how it was generated, and in fact it may even have come from a random process in which the rules are stochastic rather than deterministic.
- We transform the data vector using a discrete analysis equation in which integration, difficult on a computer, has been replaced by computationally trivial summation and multiplication.

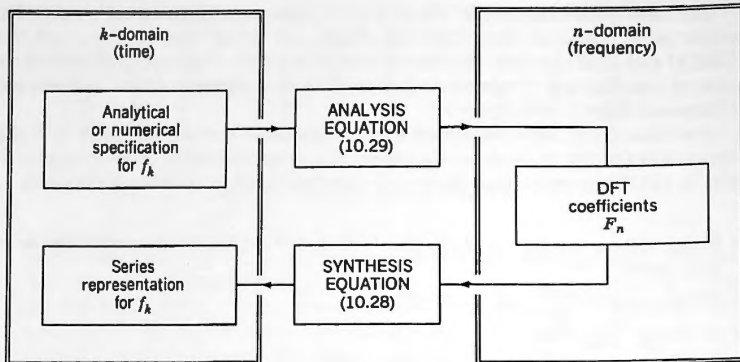


Figure 10.5.

- In the *n*-domain we now have a finite-length vector of numbers that we call the DFT line spectrum. A large and ever-growing number of techniques has been developed for accomplishing desired results by working on this finite-length vector.
- Once we have carried out desired operations in the *n*-domain we can, if we so desire, invert the result and return to the *k*-domain. Again this is accomplished only by summation and multiplication. In fact, in any implementation of the FFT analysis and synthesis procedures, precisely the same code or hardware is used for both the forward and reverse transformations. This is discussed further in Section 11.7.
- When we are finished, we end up with a finite-length vector of numbers back in the *k*-domain, rather than an infinite sum or an integral. This means that we can immediately apply the results to real-world situations, rather than having to undertake further numerical work to achieve what we want.

These are some of the many reasons why the FFT that implements the DFT has found such rapidly expanding acceptance in the world of modern technology. However, perhaps the single most important reason is the following:

The FFT gives us approximations for Fourier series coefficients and for Fourier transforms that can be made as accurate as we please.

#### 10.4 PROPERTIES OF THE DFT

In Chapters 12 and 13 we delve more deeply into the precise relationships between the DFT, Fourier series, and the Fourier integral. From those investigations we shall come to understand how the results of the DFT can be used as approximations for

either Fourier series or for Fourier integrals, and we shall find that the accuracy of the approximations can be made as good as we please subject only to the availability of memory space and computation time.

Keep in mind, however, that there are many situations in which we use the DFT to transform functions that are inherently discrete, and so we should not only think of the DFT as being a numerical approximation for the continuous transforms of periodic or pulse waveforms that we considered in Part 1. When we transform such inherently discrete functions there is no question of "accuracy of the approximation." The resulting spectrum is exact, subject only to the round-off errors in the arithmetic functions of the computer on which the DFT/FFT was run.

As we did with Fourier series and the Fourier integral, we now introduce the following notation regarding the DFT:

**Definition:** The expression

$$f_k \leftrightarrow F_n$$

will be used to represent Theorem 10.2, stating that the DFT of  $f_k$  is  $F_n$  per (10.29) and the IDFT of  $F_n$  is  $f_k$  per (10.28).

We also introduce the following notation regarding the DFT coefficients  $F_n$ . (It is the same as the notation that we used for continuous periodic and pulse spectra.)

In **Cartesian form**,

$$F_n = A_n + jB_n \quad (10.55)$$

and in **polar form**,

$$F_n = |F_n|e^{j\theta_n} \quad (10.56)$$

where

$$|F_n| = (A_n^2 + B_n^2)^{1/2} \quad (10.57)$$

and

$$\theta_n = \arctan \frac{B_n}{A_n} \quad (10.58)$$

In the preceding section we saw that the mathematical structure of the DFT is identical to the structure of the transformations for both the periodic and pulse functions of Part 1. This results in the same theorems and symmetries for the DFT as for those earlier transformations, and so we list them without proof. (Proof in every case involves a repetition of what was done in Chapter 2.)

■ Properties of  $F_n$  for  $f_k$  real

$$F_n^* = F_{-n} \quad (10.59)$$

$$(f_k)_{ev} \Leftrightarrow A_n \quad \text{and} \quad (f_k)_{od} \Leftrightarrow jB_n$$

$A_n$  is even,  $B_n$  is odd,  $|F_n|$  is even,  $\theta_n$  is odd

$F_n$  is real and even iff  $f_k$  is even

$F_n$  is imaginary and odd iff  $f_k$  is odd

In closing, we need to bring to the attention of the reader the ranges over which the symmetries in the preceding box are applicable.

Up to now we have talked about the values of  $k$  and  $n$  as integers in the range 0 to  $N - 1$ . Thus for  $N = 8$  we have what we call our **primary period** with the values

$$0, 1, 2, 3, 4, 5, 6, 7, 8$$

where the 8 is shown for completeness, although 8 and 0 are equivalent by virtue of the periodicity involved. (Thus  $F_8$  and  $F_0$  are always equal when  $N = 8$ .)

Consider now the period of numbers immediately to the left of the primary period, namely

$$-8, -7, -6, -5, -4, -3, -2, -1, 0$$

If we place these two periods on top of each other, we obtain

$$\begin{array}{cccccccccc} 0, & 1, & 2, & 3, & 4, & 5, & 6, & 7, & 8 \\ -8, & -7, & -6, & -5, & -4, & -3, & -2, & -1, & 0 \end{array} \quad (10.60)$$

Then, by the periodicity properties of the DFT, the sequence of numbers  $f_k$  that the synthesis equation produces will have the same values over either of the ranges shown in (10.60), and the same is also true for the sequence of numbers  $F_n$  produced by the analysis equation.

If we now place these two sets of numbers end to end, we obtain two full periods as follows:

$$\begin{array}{cccccccccc} -8, & -7, & -6, & -5, & \underbrace{-4, -3, -2, -1,}_{-N/2 \leq n \leq N/2} 0, & 1, & 2, & 3, & 4, & 5, & 6, & 7, & 8 \end{array}$$

and, as shown, we can also mark out a central period in which the values range from -4 to 4, namely

$$-4, -3, -2, -1, 0, 1, 2, 3, 4 \quad (10.61)$$

This period is symmetric about the origin, and is the one that the first line in the preceding box is concerned with. What that statement asserts is that the numbers  $F_n^*$

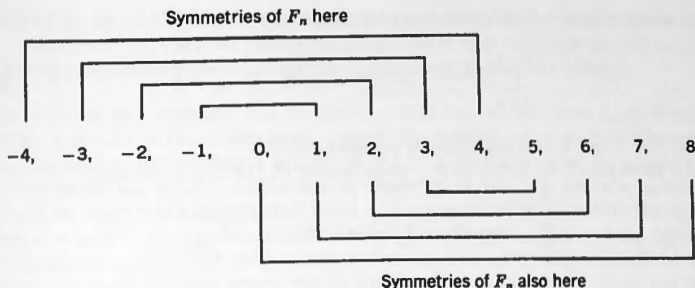


Figure 10.6.

and  $F_{-n}$  lying in the range marked out in (10.61) are equal, that is, that

$$F_0^* = F_0, \quad F_1^* = F_{-1}, \quad F_2^* = F_{-2}, \quad F_3^* = F_{-3}, \quad F_4^* = F_{-4} \quad (10.62)$$

As (10.60) shows, however, periodicity means that

$$F_{-1} = F_7, \quad F_{-2} = F_6, \quad F_{-3} = F_5, \quad F_{-4} = F_4 \quad (10.63)$$

and so, combining the preceding two sets of equations, we see that the theorem is also saying that

$$F_0^* = F_0, \quad F_1^* = F_7, \quad F_2^* = F_6, \quad F_3^* = F_5, \quad F_4^* = F_4 \quad (10.64)$$

This means that the center of the primary period (and indeed any other period) acts as a **pivot point** and that pairs of values that are equidistant from it are also linked by the theorem. This is depicted in Figure 10.6.

## NOTES AND COMMENTS

---

(A) **Lemma** The discrete complex exponentials satisfy the following property:

$$\sum_{n=0}^{N-1} e^{j2\pi n/N} = 0 \quad (10.65)$$

*Proof:* We have here the sum of all of the discrete complex exponentials of order  $N$ . Since they occupy symmetric positions around the unit circle they must add up to zero from geometric considerations.

As a second proof, by the orthogonality property

$$\sum_{n=0}^{N-1} e^{j2\pi nb/N} e^{j2\pi na/N} = 0 \quad \text{if } a \neq b \quad (10.66)$$

Setting  $b = 1$  and  $a = 0$  immediately proves (10.65).

As a third proof, we can sum the series shown in (10.65), obtaining

$$\sum_{n=0}^{N-1} e^{j2\pi n/N} = \sum_{n=0}^{N-1} e^{(j2\pi/N)^n} = \frac{1 - e^{j2\pi N/N}}{1 - e^{j2\pi/N}} \quad (10.67)$$

Now  $e^{j2\pi/N} \neq 1$ . Hence the denominator on the RHS of (10.66) is nonzero. On the other hand

$$e^{j2\pi N/N} = e^{j2\pi} = 1 \quad (10.68)$$

and so the numerator is equal to zero, which again proves the proposition. ■

**(B) Anomalous Points of the Arctangent Function** The arctangent function has an anomalous situation under the following circumstances: Letting  $z = x + jy$  we define  $\arg(z) = \arctan(y/x)$

- (a) When both  $y = 0$  and  $x = 0$ , then  $\arctan(y/x)$  has no meaning, and so neither does  $\arg(0)$ .
- (b) When  $y = 0$  and  $x < 0$ , then  $z$  is a negative real number.  $\text{Arg}(z)$  can be taken as either  $\pi$  or  $-\pi$ , and in all of the figures in the text the choice, while entirely arbitrary, was made on the basis of the additional fact that  $\arg(z)$  shall be an odd function. However if  $z$  is also periodic (as  $F_n$  is in the DFT), then we can arrive at a situation where a contradiction arises as the following shows:

Let  $z = e^{j2\pi n/N}$ , where for definiteness we take  $N = 4$ . Then  $z$  is a periodic function of  $n$  with period 4.

Starting from  $n = -4$  and letting it increase through the integers gives the following sequence of numbers:

$n$	-4	-3	-2	-1	0	1	2	3	4
$z$	1	$j$	-1	$-j$	1	$j$	-1	$-j$	1
$\arg(z)$	0	$\pi/2$	AAA	$-\pi/2$	0	$\pi/2$	AAA	$-\pi/2$	0

Since  $z$  is periodic we would like all of its attributes to be periodic as well, including  $\arg(z)$ . That is not entirely possible, however, because of the anomalous situation at  $n = -2$  and  $n = 2$  where  $y = 0$  and  $x = -1$ . If we use  $\pi$  for  $\arg(z)$  at both of the points AAA (or we use  $-\pi$  at both of them), then we satisfy the periodicity requirement. However, we cannot then satisfy the requirement that

$\arg(z)$  be an odd function. On the other hand, if we use  $\pi$  at one of them and  $-\pi$  at the other, then we satisfy the requirement that  $\arg(z)$  be an odd function. However, we cannot then satisfy the requirement that it be periodic.

The root of the problem lies in the fact that we do not have a good way of designating  $\arg(z)$  at those locations. Clearly the position of  $z$  on the unit circle is unique, regardless of whether it arrived at  $-1$  by a clockwise or by an anticlockwise path. Yet we do not have a symbol for its argument at  $z = -1$ , which is unique.

Ideally we would like to call that value of the argument by a symbol that satisfies both  $* = *$  and  $* = -*$ , which would meet both the periodicity and the odd-function requirements. But the only number that we have that satisfies both of those conditions is zero, and that would not be appropriate for the cases where  $y = 0$  and  $x < 0$ . Accordingly, in the numerical displays generated by the FFT disk: For anomaly (a) we display  $\arg(0/0)$  as zero; for anomaly (b)

- Whenever  $y = 0$  and  $x < 0$  we blank out the value of the arctan by the symbol \*\*\*\*\* (which, fortunately, does not happen very often).
- At  $n = 0$  we display the arctan as zero no matter what the values of  $x$  and  $y$  are, since that is an essential attribute of an odd phase plot.

## EXERCISES

10.1 Calculate the following:

- (a)  $|19|_4$     (b)  $| - 35|_8$     (c)  $|59|_{16}$     (d)  $| - 99|_{32}$   
 (e)  $|67|_{25}$     (f)  $| - 213|_{13}$     (g)  $|214|_{45}$     (h)  $| - 956|_{72}$

10.2 Verify that the four vectors appearing in (10.52) form an orthogonal set in the sense of Theorem 10.1.

10.3 (a) From the definition of  $F_n$  given in Theorem 10.2, prove:

When the input is a real function of  $k$ , then  $F_n$  is always real for  $n = 0$  and  $n = N/2$

(b) Prove the same proposition starting from (10.59).

### Accompanying Disk

When transforming discrete functions, the FFT system gives exact results. Thus your "pencil and paper" numbers should be exactly the same as those obtained from the FFT, regardless of the value of  $N$  that was used.

This is not the case when the FFT is being used to derive estimates of Fourier series coefficients, and of sampled values of a Fourier transform. In those cases the values obtained are not exact, but their accuracy can be made as good as we desire, simply by making  $N$  sufficiently large. This is discussed in Chapters 12 and 13.

When transforming discrete functions using the FFT system, remember to use the mode "DISCRETE" when prompted for TYPE.

Also remember that we never use half-values with discrete functions. There is no such thing as a discontinuity here and no convergence to half-values as there is with functions of  $t$ .

- 10.4** (a) Sketch each of the following discrete functions over the range  $-N \leq k \leq 2N$

$$\begin{array}{ccccc} k = 0 & 1 & 2 & 3 & N = 4 \end{array}$$

$$(1) x_k = \begin{matrix} 1 & 1 & 1 & 1 \end{matrix} \quad \text{pulse}$$

$$(2) x_k = \begin{matrix} 1 & 0 & 0 & 0 \end{matrix} \quad \text{periodic}$$

$$(3) x_k = \begin{matrix} 1 & -1 & 1 & -1 \end{matrix} \quad \text{pulse}$$

$$(4) x_k = \begin{matrix} 1 & j & 1 & j \end{matrix} \quad \text{periodic}$$

$$\begin{array}{ccccccc} k = 0 & 1 & 2 & 3 & 4 & 5 & N = 6 \end{array}$$

$$(5) x_k = \begin{matrix} 1 & 2 & 3 & 4 & 5 & 6 \end{matrix} \quad \text{periodic}$$

- (b) Find the DFT of each of these discrete functions by making direct use of Theorem 10.2 and sketch two periods of the resulting spectrum.

*Suggestion:* Prepare a table showing  $e^{-j2\pi m/N}$  and  $e^{j2\pi m/N}$  for  $m = 0, 1, \dots, N$ .

- (c) Invert the spectra that you obtain using (10.28) and verify that you have recreated the original function.

- (d) Run the same problems using the FFT system on the accompanying disk and compare your results obtained here with those obtained from the FFT.

*Note:* Start from main-menu C and load the functions from the keyboard. Use DISCRETE as the MODE.

- 10.5** When finding complex coefficients for a Fourier series in Chapter 2 we had to be able to integrate. For the DFT we have to be able to sum. Sketch the following discrete functions, and then use Theorem 10.2 to find the expressions for their DFT coefficients, verifying your results using the FFT system on the accompanying disk. (If you need help, see the hint at the end of the problem.)

$$(a) f_k = 1 \quad (0 \leq k \leq N/2 - 1) \quad (\text{pulse})$$

$$(b) f_k = \begin{cases} 1 & (0 \leq k \leq N-2) \\ 0 & (k = N-1) \end{cases} \quad (\text{pulse})$$

$$(c) f_k = 1 \quad (0 \leq k \leq N/4 - 1), \quad f_{k+N} = f_k, \quad f_k \text{ is even}$$

*Hint:* Starting from (10.29) and using  $W = e^{-j2\pi/N}$ , we obtain

$$F_n = \sum_{k=0}^{B-1} f_k W^{nk}.$$

When  $f_k = 1$ , this reduces to  $(1 - W^{nB})/(1 - W)$ .

10.6 (a) Sketch the following discrete periodic function:

$$f_k = k \quad (0 \leq k \leq N-1) \quad f_{k+N} = f_k$$

(b) Prove that

$$\sum_{k=0}^{N-1} kW^k = W \frac{d}{dW} \left[ \frac{1 - W^N}{1 - W} \right]$$

(c) Now use Theorem 10.2 to show that the expression for the DFT coefficients of  $f_k$  is

$$F_n = \frac{-N}{2} + j \frac{N \sin(2\pi n/N)}{2[1 - \cos(2\pi n/N)]}$$

(d) Verify this result using the FFT system. (Use  $N = 10$ )

*Hint:*

$$\sum_{k=0}^{N-1} kW^k = W \sum_{k=0}^{N-1} kW^{k-1} = W \sum_{k=0}^{N-1} \frac{d}{dW} W^k = W \frac{d}{dW} \sum_{k=0}^{N-1} W^k$$

10.7 Find the expressions for the DFT coefficients of the following discrete periodic functions, in each case verifying your results using the FFT system on the accompanying disk. (Use  $\beta = 0.1$ ,  $N = 20$ .)

- (a)  $f_k = e^{\beta k}$  ( $0 \leq k \leq N-1$ ) (pulse)
- (b)  $f_k = \sin(2\pi k/N)$  ( $0 \leq k \leq N-1$ )  $f_{k+N} = f_k$
- (c)  $f_k = \cos(10\pi k/N)$  ( $0 \leq k \leq N-1$ ) (pulse)

*Hint:* Use (2.15) and (2.16) for (b) and (c).

10.8 (a) Prove the time-shift property for the DFT:

$$\text{If } f_k \Leftrightarrow F_n \text{ then } f_{k-m} \Leftrightarrow F_n W^{nm} \quad (10.69)$$

(b) Prove the frequency-shift property for the DFT:

$$\text{If } f_k \Leftrightarrow F_n \text{ then } f_k W^{mk} \Leftrightarrow F_{n+m} \quad (10.70)$$

(c) Show that the duality property for the DFT is

$$\text{If } f_k \Leftrightarrow F_n \text{ then } F_k \Leftrightarrow Nf_{-n} \quad (10.71)$$

*Hint:* Start from the DFT synthesis equation and repeat the "Proof of (8.11)" in Chapter 8.

**10.9** Define  $g_k$  as follows:

$$g_k = \frac{f_{k+1} - f_{k-1}}{2T_s} \quad (10.72)$$

This is called the divided central difference of  $f_k$ ; it is discussed in Section 15.3.

(a) Prove that

$$g_k \Leftrightarrow \frac{F_n(W^{-n} - W^n)}{2T_s} \quad (10.73)$$

(b) Now use the definition for  $W$  to show further that

$$g_k \Leftrightarrow F_n \left[ \frac{j \sin(2\pi n/N)}{T_s} \right] \quad (10.74)$$

**10.10** Define the **backward shifting operator**  $B$  as follows:

$$Bf_k \equiv f_{k-1} \quad (10.75)$$

(a) Apply DFT time shift (Exercise 10.8) to show that

$$Bf_k \Leftrightarrow W^n F_n \quad (10.76)$$

(b) Generalize this result to show that if

$$B^m f_k \equiv f_{k-m} \quad (10.77)$$

then

$$B^m f_k \Leftrightarrow W^{nm} F_n \quad (10.78)$$

From this we conclude the following:

■ **THEOREM 10.3**

Backward shifting by  $m$  steps in the time domain corresponds to multiplication by  $W^{nm}$  in the frequency domain

Theorem 10.3 is the counterpart in the discrete world to Theorem 5.1 in the continuous.

**10.11** Consider the **constant-coefficient linear difference equation**

$$P_1(B)y_k = P_2(B)x_k \quad (\forall k) \quad (10.79)$$

in which  $P_1(B)$  and  $P_2(B)$  are polynomials in the  $B$ -operator with constant coefficients. As an example, consider the constant-coefficient linear (CCL) difference equation

$$y_k - \alpha y_{k-1} = x_k - \beta x_{k-1} \quad (\forall k) \quad (10.80)$$

in which  $x_k$  is the **forcing function** and  $y_k$  is the **response** that causes (10.80) to balance for all values of  $k$ . Using the  $B$ -operator, this becomes

$$[1 - \alpha B]y_k = [1 - \beta B]x_k \quad (\forall k) \quad (10.81)$$

which is seen to be of the same form as (10.79). Apply the DFT plus time shift to (10.79) to show that

$$P_1(W^n)Y_n = P_2(W^n)X_n \quad (10.82)$$

This enables us to write the following:

### ■ THEOREM 10.4

Discrete Fourier transformation of the CCL difference equation

$$P_1(B)y_k = P_2(B)x_k \quad (10.83)$$

converts it to the algebraic equation

$$P_1(W^n)Y_n = P_2(W^n)X_n \quad (10.84)$$

10.12 Discrete Fourier transform (10.79) to show the following:

### ■ COROLLARY to Theorem 10.4

If

$$P_1(B)y_k = P_2(B)x_k \quad (\forall k) \quad (10.85)$$

then

$$Y_n = \frac{P_2(W^n)}{P_1(W^n)}X_n \quad (10.86)$$

These two equations are the duals to (6.8) and (6.9). The expression that is multiplying  $X_n$  on the RHS of (10.86) is called the **discrete-frequency transfer function**. The FFT system could be used to solve CCL difference equations of the form (10.85) in exactly the same way that it was used in Chapter 6 to solve CCL differential equations. However, we have not implemented the necessary code for this in the current version of the disc.

---

---

## CHAPTER 11

---

# Inside The Fast Fourier Transform

### 11.1 INTRODUCTION

---

We now take a very brief look at what goes on inside the radix-2 Fast Fourier Transform (FFT) (i.e., when  $N$  is an exact power of 2) and attempt to understand why it is so efficient computationally.

In what follows we present a few examples of the FFT algorithm for small values of  $N$  and urge you to take the time to understand them fully, concentrating on how they work rather than why. In the later parts of this chapter we develop the general theory for radix-2, and it will become extremely clear what lay behind these simple examples.

If you wish to learn more about the details of the FFT you are referred to Bergland; Brigham; Brigham and Morrow; Cochran et al.; Oppenheim and Schaeffer; and Stremler.

### 11.2 THE FFT FOR SMALL VALUES OF $N$

---

From (10.29) we recall that the analysis equation of the discrete Fourier transform (DFT) is

$$F_n = \sum_{k=0}^{N-1} f_k e^{-j2\pi nk/N} \quad (0 \leq n \leq N - 1) \quad (11.1)$$

We now need to place special emphasis on the subscripts appearing in (11.1), and so we shall restate that equation as

$$F(n) = \sum_{k=0}^{N-1} f_0(k) W^{nk} \quad (0 \leq n \leq N - 1) \quad (11.2)$$

Observe the following regarding (11.2):

- We are now using the symbol  $F(n)$  for the  $n$ th DFT spectral element rather than  $F_n$ . This will only apply in this chapter, after which we shall revert to  $F_n$ .
- We are using  $f_0(k)$  rather than  $f_k$  as the symbol for the  $k$ th element of the data vector. The zero subscript shows that this is part of what we shall call the **stage-zero vector**, something that will soon become clear.
- The quantity inside the brackets in  $F(n)$  or  $f_0(k)$ , that is, the  $n$  or the  $k$ , will henceforth be known as the **index** of the term.
- We are using the same compact symbol for the exponential that we used in Chapter 10, namely

$$W \equiv e^{-j2\pi/N} \quad (11.3)$$

and so

$$e^{-j2\pi nk/N} = (e^{-j2\pi/N})^{nk} = W^{nk} \quad (11.4)$$

Always keep in mind the minus sign in the exponent inside the  $W$ .

Now consider the case  $N = 2$ . Then (11.2) gives us

$$\begin{bmatrix} F(0) \\ F(1) \end{bmatrix} = \begin{bmatrix} W^0 & W^0 \\ W^0 & W^1 \end{bmatrix} \begin{bmatrix} f_0(0) \\ f_0(1) \end{bmatrix} \quad (11.5)$$

and since

$$W^0 = 1 \quad \text{and} \quad W^1 = e^{-j2\pi 1/2} = -1 \quad (11.6)$$

(11.5) simplifies to

$$\begin{bmatrix} F(0) \\ F(1) \end{bmatrix} = \begin{bmatrix} 1 & 1 \\ 1 & -1 \end{bmatrix} \begin{bmatrix} f_0(0) \\ f_0(1) \end{bmatrix} \quad (11.7)$$

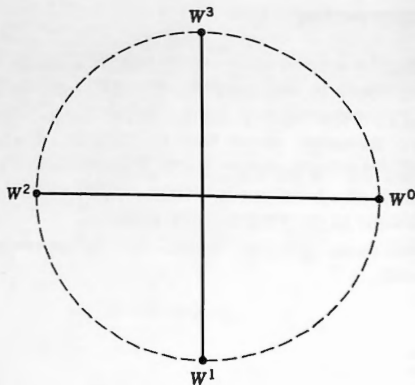
from which

$$\left. \begin{aligned} F(0) &= f_0(0) + f_0(1) \\ F(1) &= f_0(0) - f_0(1) \end{aligned} \right\} \quad (11.8)$$

Thus, for  $N = 2$ , the DFT coefficients are simply the sum and difference of the two given data values.

Consider next what happens when  $N = 4$ . Then (11.2) gives us

$$\begin{bmatrix} F(0) \\ F(1) \\ F(2) \\ F(3) \end{bmatrix} = \begin{bmatrix} W^0 & W^0 & W^0 & W^0 \\ W^0 & W^1 & W^2 & W^3 \\ W^0 & W^2 & W^4 & W^6 \\ W^0 & W^3 & W^6 & W^9 \end{bmatrix} \begin{bmatrix} f_0(0) \\ f_0(1) \\ f_0(2) \\ f_0(3) \end{bmatrix} \quad (11.9)$$

Figure 11.1.  $N = 4$ .

From Chapter 10 we recall that the discrete complex exponentials possess the circular property of repeating themselves with period  $N$ . This was summed up there by the modulo- $N$  statement

$$e^{-j2\pi nk/N} = e^{-j2\pi|nk|_N/N} \quad (11.10)$$

and so, in terms of  $W$ , we can write (11.10) as

$$W^{nk} = W^{nk(\text{modulo } N)} \quad (11.11)$$

For  $N = 4$  this means that  $W^4 = W^0$ ,  $W^6 = W^2$ , and  $W^9 = W^1$ . Moreover, as we see from Figure 11.1, when  $N$  is any even number (as it will always be in this chapter), then each value of  $W^{nk}$  is always equal to the negative of one that is opposite to it. Thus when  $N = 4$ ,  $W^2 = -W^0$  and  $W^3 = -W^1$ , and so (11.9) reduces further to

$$\begin{bmatrix} F(0) \\ F(1) \\ F(2) \\ F(3) \end{bmatrix} = \begin{bmatrix} W^0 & W^0 & W^0 & W^0 \\ W^0 & W^1 & -W^0 & -W^1 \\ W^0 & -W^0 & W^0 & -W^0 \\ W^0 & -W^1 & -W^0 & W^1 \end{bmatrix} \begin{bmatrix} f_0(0) \\ f_0(1) \\ f_0(2) \\ f_0(3) \end{bmatrix} \quad (11.12)$$

Observe the significant fact, already apparent, that only  $W^0$  and  $W^1$  need to be evaluated, and that the remaining distinct values of  $W$ , namely  $W^2$  and  $W^3$  do not appear in (11.12). Thus only half of all of the possible values of  $W^{nk}$  will occur in what lies ahead. (In this case, since  $W^0 = 1$ , we see that in fact we only need to evaluate  $W^1$ , which is equal to  $-j$ .)

We now factorize the matrix on the RHS of (11.12) as follows:

$$\begin{bmatrix} F(0) \\ F(2) \\ F(1) \\ F(3) \end{bmatrix} = \begin{bmatrix} 1 & W^0 & 0 & 0 \\ 1 & -W^0 & 0 & 0 \\ 0 & 0 & 1 & W^1 \\ 0 & 0 & 1 & -W^1 \end{bmatrix} \begin{bmatrix} 1 & 0 & W^0 & 0 \\ 0 & 1 & 0 & W^0 \\ 1 & 0 & -W^0 & 0 \\ 0 & 1 & 0 & -W^0 \end{bmatrix} \begin{bmatrix} f_0(0) \\ f_0(1) \\ f_0(2) \\ f_0(3) \end{bmatrix} \quad (11.13)$$

Note first that the indices of the vector on the LHS are no longer in their natural order. This reordering is an inherent part of the factorization process.

Do not be concerned with how the factorization was derived. The answer to that goes to the very heart of the FFT, and at a later stage it will become perfectly clear. For now, all that you should do is to multiply out the matrices in (11.13) in order to verify that their product is in fact the same as the matrix in (11.12), keeping in mind the resequencing of  $F(n)$  on the LHS.

We now split (11.13) into the following **two-stage procedure** plus a third stage that is called the **bit reversal**.

#### Stage 1

$$\begin{bmatrix} f_1(0) \\ f_1(1) \\ f_1(2) \\ f_1(3) \end{bmatrix} = \begin{bmatrix} 1 & 0 & W^0 & 0 \\ 0 & 1 & 0 & W^0 \\ 1 & 0 & -W^0 & 0 \\ 0 & 1 & 0 & -W^0 \end{bmatrix} \begin{bmatrix} f_0(0) \\ f_0(1) \\ f_0(2) \\ f_0(3) \end{bmatrix} \quad (11.14)$$

#### Stage 2

$$\begin{bmatrix} f_2(0) \\ f_2(1) \\ f_2(2) \\ f_2(3) \end{bmatrix} = \begin{bmatrix} 1 & W^0 & 0 & 0 \\ 1 & -W^0 & 0 & 0 \\ 0 & 0 & 1 & W^1 \\ 0 & 0 & 1 & -W^1 \end{bmatrix} \begin{bmatrix} f_1(0) \\ f_1(1) \\ f_1(2) \\ f_1(3) \end{bmatrix} \quad (11.15)$$

#### Bit reversal

$$\begin{bmatrix} F(0) \\ F(1) \\ F(2) \\ F(3) \end{bmatrix} = \begin{bmatrix} f_2(0) \\ f_2(2) \\ f_2(1) \\ f_2(3) \end{bmatrix} \quad (11.16)$$

Let's take a look at the preceding three operations:

- In Stage 1 we start with  $\mathbf{f}_0$ , the data vector obtained from the analytical definition of the input function. This is transformed in (11.14) to produce the Stage-1 vector  $\mathbf{f}_1$ .
- In Stage 2 the vector  $\mathbf{f}_1$  is transformed to produce the Stage-2 vector  $\mathbf{f}_2$ .
- Finally, in the bit reversal,  $\mathbf{f}_2$  is resequenced to produce the output vector  $\mathbf{F}$ .

We now write out the computations that would have to be performed to carry out Stage 1. From (11.14) we obtain the two pairs of equations

$$\left. \begin{aligned} f_1(0) &= f_0(0) + W^0 f_0(2) \\ f_1(2) &= f_0(0) - W^0 f_0(2) \end{aligned} \right\} \quad (11.17)$$

and

$$\left. \begin{aligned} f_1(1) &= f_0(1) + W^0 f_0(3) \\ f_1(3) &= f_0(1) - W^0 f_0(3) \end{aligned} \right\} \quad (11.18)$$

and from these we can already begin to see how the computational efficiency of the FFT arises. Observe how, in (11.17), only a **single** complex multiplication needs to be performed, since once the product  $W_0 f_0(2)$  has been obtained we need only add it to  $f_0(0)$  for the first result and then subtract it from  $f_0(0)$  to obtain the second. The same happens again in (11.18).

It is one of our objectives to compare the number of computer operations required to execute the FFT against the number for executing the DFT directly, and so we now start to keep count. On the basis of the preceding, the FFT operation count stands as follows:

Complex multiplications: 2

Complex additions: 2

Complex subtractions: 2

(See Notes and Comments for remarks concerning these operations.)

Repeating the same expansion for Stage 2 we obtain the two pairs of equations

$$\left. \begin{aligned} f_2(0) &= f_1(0) + W^0 f_1(1) \\ f_2(1) &= f_1(0) - W^0 f_1(1) \end{aligned} \right\} \quad (11.19)$$

and

$$\left. \begin{aligned} f_2(2) &= f_1(2) + W^1 f_1(3) \\ f_2(3) &= f_1(2) - W^1 f_1(3) \end{aligned} \right\} \quad (11.20)$$

in which we see the identical structure to the previous one. Thus the FFT operation count now becomes

Complex multiplications: 4

Complex additions: 4

Complex subtractions: 4

Finally, consider the bit-reversal stage shown in (11.16). If we rewrite those equations expressing the indices in binary rather than decimal, then here is what we obtain:

$$\begin{bmatrix} F(00) \\ F(01) \\ F(10) \\ F(11) \end{bmatrix} = \begin{bmatrix} f_2(00) \\ f_2(10) \\ f_2(01) \\ f_2(11) \end{bmatrix} \quad (11.21)$$

Observe how each index is the mirror inverse of the one opposite to it. Thus 00 is opposite 00, 01 is opposite 10, and so forth. This gives us the following rule (and also explains why the procedure is referred to as "bit reversal"):

**Rule 1:** To obtain  $\mathbf{F}$  in correct sequence, place  $f_2(ij)$  in  $F(ji)$ .

Thus  $f_2(00)$  is sent to  $F(00)$ ,  $f_2(01)$  is sent to  $F(10)$ , and so on. At a later stage we shall see how a more efficient way can be found to accomplish this with the least number of operations.

The bit reversal imposes an overhead on the FFT that must be added to its overall operation count when comparing it to the direct method. However, the number of operations involved in the bit reversal is proportional to  $N$ , and so it soon becomes insignificant when compared to the number of operations for the direct method.

Let's now take a look at that number. If we were to evaluate (11.9) directly, without devoting any prior attention to the values of the various powers of  $W$ , the required number of operations would be as follows:

Complex multiplications:  $4^2 = 16$

Complex additions:  $4(4 - 1) = 12$

Already there is a startling difference between direct and FFT.

We now derive the operation count for the FFT for  $N$  any power of 2, that is,

$$N = 2^\nu \quad (11.22)$$

where  $\nu$  is some positive integer. For example if  $\nu = 10$ , then  $N = 2^{10} = 1024$ , and so on.

When  $N$  was equal to 4 in the previous example, then the value of  $\nu$  was 2. We were then able to factor the original  $W$ -matrix of (11.9) into a product of two matrices, each  $4 \times 4$  in size, each of which computed four intermediate values using two complex multiplications and four addition/subtractions.

The general radix-2 FFT algorithm, as we shall see later, enables us to factor the  $W$ -matrix into a product of  $\nu$  matrices, each  $N \times N$  in size, each of which computes  $N$  intermediate values using  $N/2$  complex multiplications and  $N$  addition/subtractions. Thus the general power-of-2 FFT operation count will be

Complex multiplications:  $\frac{1}{2}N\nu$

Complex add/subtracts:  $N\nu$

(Observe that this is consistent with the preceding count where  $N$  was 4 and  $\nu$  was 2.)

TABLE 11.1 Operation Count

<i>Operation</i>	<i>Direct</i>	<i>FFT</i>	<i>Ratio</i>
Complex multiplications	$N^2$	$\frac{1}{2}N \log_2 N$	$2N/\log_2 N$
Complex add/subtracts	$N(N - 1)$	$N \log_2 N$	$(N - 1)/\log_2 N$

TABLE 11.2 Multiplication Count

<i>N</i>	<i>Direct</i>	<i>FFT</i>	<i>Ratio</i>
4	16	4	4 : 1
64	4096	192	21 : 1
1024	1048576	5120	205 : 1
32768	1073741824	245760	4369 : 1

Using the fact that  $v = \log_2 N$ , we state these results in Table 11.1, where we also show the formulas for the direct approach and for the ratio of direct to FFT. As we see from Table 11.2, the ratio of the number of multiplications soon becomes dramatic.

□EXAMPLE 11.1: Based only on multiplication count, a machine that takes one minute to run the radix-2 FFT for  $N = 32,768$  would take 4369 minutes to evaluate the conventional DFT for the same value of  $N$ .

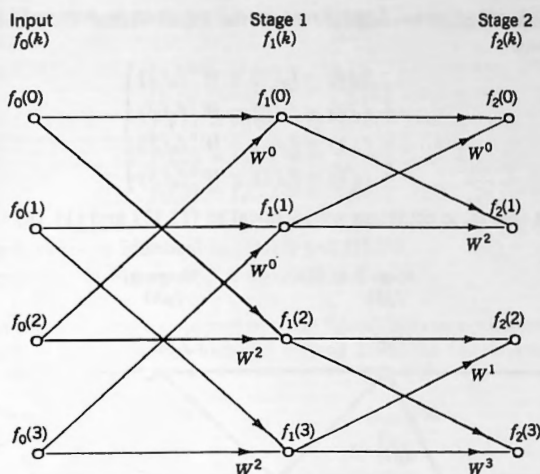
This equates to a full three days! □

In addition to the advantage of speed, the FFT also brings with it the advantage of accuracy, since the fewer operations that we employ to obtain our final results, the smaller will be the truncation errors and so the better the final accuracy.

### 11.3 THE GENERAL RADIX-2 FFT ALGORITHM

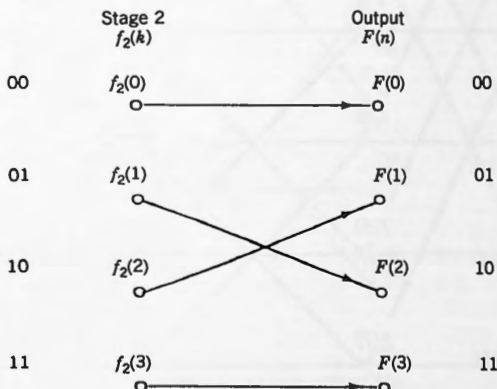
The FFT algorithm can best be comprehended by making use of what are called **signal flow graphs**. For  $N = 4$  the flow graphs are shown in Figures 11.2 and 11.3. The basic idea of a signal flow graph is that **nodes**, shown as small circles in the two figures, have **inputs** and **outputs** (information pipes) as shown by the lines with arrows entering and leaving them. The rules are as follows:

- Multiple inputs entering a node are added.
- The arrowheads may have values associated with them, shown in Figure 11.2 as various powers of  $W$ . The information flowing along any one of those lines is multiplied by the power of  $W$  shown next to it.
- If no explicit multiplier is shown, then multiplication by unity is implied.

Figure 11.2. FFT signal flow graph ( $N = 4$ ).

Here's what we see in Figure 11.2:

- Every node is computed from precisely two inputs, the upper of which always has a multiplier of 1 and the lower of which always appears with a multiplier  $W^p$  with various values of  $p$ .

Figure 11.3. Bit reversal ( $N = 4$ ).

- The Stage-1 vector is computed from the input vector by the following four equations:

$$\begin{cases} f_1(0) = f_0(0) + W^0 f_0(2) \\ f_1(2) = f_0(0) - W^0 f_0(2) \\ f_1(1) = f_0(1) + W^0 f_0(3) \\ f_1(3) = f_0(1) - W^0 f_0(3) \end{cases} \quad (11.23)$$

Observe that these equations are identical to (11.17) and (11.18).

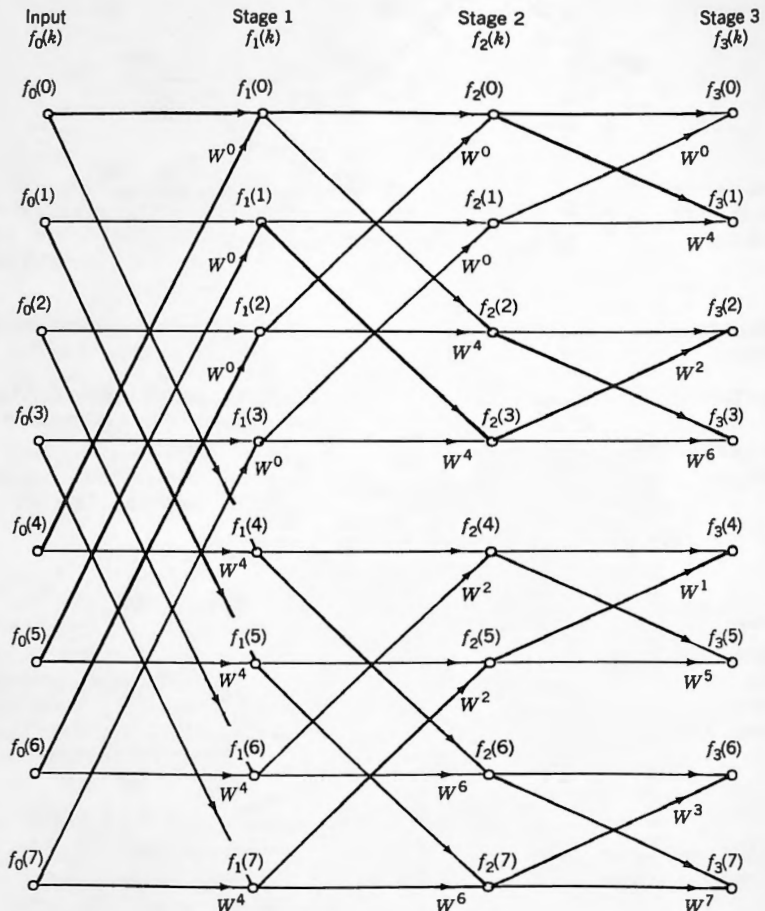


Figure 11.4. FFT flow graph for  $N = 8$ .

- The Stage-2 vector is computed from the Stage-1 vector by the following four equations:

$$\left. \begin{aligned} f_2(0) &= f_1(0) + W^0 f_1(1) \\ f_2(1) &= f_1(0) - W^0 f_1(1) \\ f_2(2) &= f_1(2) + W^1 f_1(3) \\ f_2(3) &= f_1(2) - W^1 f_1(3) \end{aligned} \right\} \quad (11.24)$$

which are seen to be identical to (11.19) and (11.20).

- The unscrambler in Figure 11.3 is identical to (11.21).

Clearly then the procedure depicted in these figures is a correct implementation of the FFT algorithm for  $N = 4$ , which we arrived at by the factorization shown in

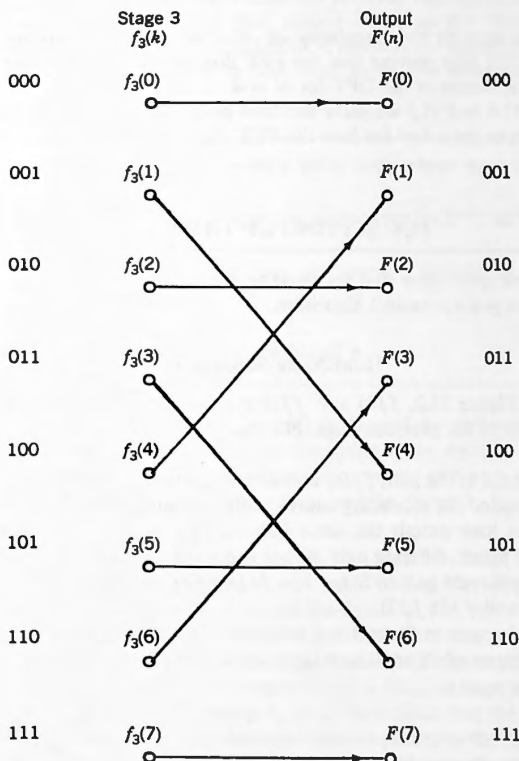


Figure 11.5. Bit reversal  $N = 8$ .

(11.13). Indeed, we can now begin to see how that factorization was arrived at. Just write the four equations appearing in (11.23) in matrix form and you will obtain (11.14). Do the same for (11.24) and you will have (11.15). Combine these into a single equation and you will have the factored form shown in (11.13).

There is another way of looking at the procedure of Figures 11.2 and 11.3. Careful inspection shows that there is precisely one path from every input node to every output node. By tracing the paths from each of the input nodes to a given output node we find the following:

$$\left. \begin{aligned} F(0) &= f_0(0) + W^0 f_0(1) + W^0 f_0(2) + W^0 W^0 f_0(3) \\ F(1) &= f_0(0) + W^1 f_0(1) + W^2 f_0(2) + W^2 W^1 f_0(3) \\ F(2) &= f_0(0) + W^2 f_0(1) + W^0 f_0(2) + W^0 W^2 f_0(3) \\ F(3) &= f_0(0) + W^3 f_0(1) + W^2 f_0(2) + W^2 W^3 f_0(3) \end{aligned} \right\} \quad (11.25)$$

Taking into account the circularity of  $W$  this set of equations is seen to be identical to (11.9), thus proving that the FFT flow graph shown in the figures gives a correct implementation of the DFT for  $N = 4$ .

In Figures 11.4 and 11.5 we show the flow graph and bit reversal for  $N = 8$  from which we begin to get a feel for how the FFT algorithm generalizes.

## 11.4 SETTING UP THE RULES

---

There are a few more rules that we need to establish before we can put together a flowchart of the general radix-2 algorithm.

### Dual-Node Separation

In Stage 1 of Figure 11.2,  $f_1(0)$  and  $f_1(2)$  are both computed from the same two inputs coming from the previous stage. For this reason they are known as a **dual-node pair**.

The upper input to the pair,  $f_0(0)$ , is called the **primary source node**, and the lower input,  $f_0(2)$ , is called the **secondary source node**. Observe that the dual-node pair and its source nodes have exactly the same indices, that is, they have the same vertical positions in the figure, differing only in that the source nodes are in a previous stage.

The other dual-node pair in Stage 1 is  $f_1(1), f_1(3)$ . In Stage 2 the dual-node pairs are  $f_2(0), f_2(1)$  and  $f_2(2), f_2(3)$ .

The dual-node pairs in Stage 1 are two nodes apart, and in Stage 2 they are one node apart. In terms of  $N$  and the stage number, which we shall call  $\sigma$ , we have the following rule:

**Rule 2:** Dual node separation =  $N/2^\sigma$

(11.26)

**EXAMPLE 11.2:**

Checking (11.26), in Figure 11.2 where  $N = 4$ :

- Stage-1 separation =  $N/2^\sigma = 4/2^1 = 2 \quad \checkmark$
- Stage-2 separation =  $N/2^\sigma = 4/2^2 = 1 \quad \checkmark$

In Figure 11.4 where  $N = 8$ ,

- Stage-1 separation =  $N/2^\sigma = 8/2^1 = 4 \quad \checkmark$
- Stage-2 separation =  $N/2^\sigma = 8/2^2 = 2 \quad \checkmark$
- Stage-3 separation =  $N/2^\sigma = 8/2^3 = 1 \quad \checkmark$

□

**Power of  $W$** 

We have pointed out earlier that every node has precisely two inputs, a primary and a secondary. Examination of the two flow graphs shows us that the signal from a primary source node always has a multiplier of 1, whereas the signal from a secondary always has a multiplier  $W^p$ , where  $p$  has some value. We now state the rule for determining that value of  $p$ .

**Rule 3:** To calculate the value of  $p$  for a given node whose stage number is  $\sigma$ :

- Divide the decimal representation of the node index by  $2^{\nu-\sigma}$  and retain only the integer part.
- Convert that decimal number to binary and reverse the order of the bits.
- Convert back to decimal.

The result will be the required binary value of  $p$ .

In the first operation, although we are still in decimal, by performing the division we are in fact shifting the **binary** value of the index to the right by  $\nu - \sigma$  bits and filling in with zeros on the left. In the second we convert to binary and flip the bits end to end, and finally, in the third we convert back to decimal.

**EXAMPLE 11.3:** Consider  $f_2(6)$  in Figure 11.4. In binary its index is  $110_2$ . Its stage number is  $\sigma = 2$  and  $\nu = 3$ , and so  $\nu - \sigma = 1$ . Dividing 6 by  $2^1$  gives 3, which is equivalent to shifting the binary form of the index to the right by one position, which would give us  $011_2$ . We then flip end to end, obtaining  $p = 110_2 = 6_{10}$ . In the figure we see the multiplier on the lower input path appearing as  $W^6$ .

Consider  $f_1(5)$  in Figure 11.4. Its binary index is  $101_2$ , its stage number is  $\sigma = 1$ , and  $\nu = 3$ . Thus  $\nu - \sigma = 2$ . Dividing  $5_{10}$  by  $2^2$  and discarding the remainder gives  $1_{10}$  or  $001_2$ . This is equivalent to shifting  $101_2$  two places to the right and filling in with zeros on the left. Flipping  $001_2$  gives  $100_2$ , which is the same as  $4_{10}$ . This agrees with  $W^4$  appearing on the lower input path in the figure. □

**Dual-node Power-of- $W$** 

From either of the figures we can see the following rule:

**Rule 4:** If a given node has power-of- $W$  given by  $p$ , then its dual node will have power  $p + N/2$ .

□ **EXAMPLE 11.4:** From Figure 11.4 we see that  $f_2(0)$  has  $W^0$  as its multiplier, and so  $p = 0$  for this node. Rule 4 requires that its dual node shall have power  $p = 0 + \frac{8}{2} = 4$ . In the figure we see that the dual node  $f_2(2)$  does indeed have  $W^4$  as its multiplier.

Node  $f_3(6)$  has  $W^3$  as its multiplier, and so  $p = 3$ . By Rule 4 the dual node should have  $p = 3 + \frac{8}{2} = 7$ . This agrees with the figure where we see that the dual node  $f_3(7)$  does in fact have  $W^7$  as its multiplier. □

By the circularity of  $W$  we know that  $W^{p+N/2} = -W^p$  (provided that  $N$  is even), and so Rule 4 is equivalent to the following:

**Rule 5:** If a given node has multiplier given by  $W^p$ , then its dual node will have multiplier  $-W^p$ .

This, together with the fact that dual nodes derive their inputs from the same dual pair in the previous stage, gives us the following algorithm for any node pair:

$$\left. \begin{aligned} f_\sigma(k) &= f_{\sigma-1}(k) + W^p f_{\sigma-1}(k + N/2^\sigma) \\ f_\sigma(k + N/2^\sigma) &= f_{\sigma-1}(k) - W^p f_{\sigma-1}(k + N/2^\sigma) \end{aligned} \right\} \quad (11.27)$$

The equations appearing in (11.27) are of critical importance, incorporating almost all of what we have discussed thus far, and so we need to take a little time to understand them completely.

On the RHS of (11.27) we see the primary and secondary source nodes,  $f_{\sigma-1}(k)$  and  $f_{\sigma-1}(k + N/2^\sigma)$ , being used to compute values for the dual-node pair  $f_\sigma(k)$  and  $f_\sigma(k + N/2^\sigma)$  on the left. The value of  $p$  is computed according to Rule 3.

Observe that only a **single** complex multiplication needs to be done in the RHS of (11.27), namely to form the quantity  $W^p f_{\sigma-1}(k + N/2^\sigma)$ . This quantity is then added to  $f_{\sigma-1}(k)$  in the first equation and subtracted from it in the second.

Thus once that multiplication has been performed on the source data from Stage- $(\sigma - 1)$ , we can immediately fill in both of the values in the Stage- $\sigma$  vector that we are currently computing.

Thereafter the source values are no longer required since there are no further nodes to which their values flow, and so the latest results can simply be overlaid on top of them. **We thus require only one storage vector throughout the entire FFT**

**computation.** Since storage requirements grow in direct proportion to  $N$ , which doubles every time we go to the next power of 2, this is a saving that is of considerable value.

In practice we must rearrange (11.27) slightly in order to take full advantage of this overlay process, for the following reason: As it stands,  $f_\sigma(k)$  overlays  $f_{\sigma-1}(k)$  in the first equation, and so the latter will no longer be available for use in the second. Accordingly, we reverse the order of (11.27) obtaining

$$\left. \begin{aligned} f_\sigma(k + N/2^\sigma) &= f_{\sigma-1}(k) - W^p f_{\sigma-1}(k + N/2^\sigma) \\ f_\sigma(k) &= f_{\sigma-1}(k) + W^p f_{\sigma-1}(k + N/2^\sigma) \end{aligned} \right\} \quad (11.28)$$

in which the problem no longer exists— $f_{\sigma-1}(k)$  is not overlaid in the first equation, and so it is available for use in the second.

In the course of working our way down the vector of computations that we must perform for a given stage we see that once a value has been computed for a given node according to the first line of (11.28), then its dual node is always done at the same time according to the second line. Thus later, when we come to that dual node, nothing further needs to be done, and so we shall need a **rule for skipping**. Here is that rule:

**Rule 6:** Starting from the top of the Stage- $\sigma$  vector, execute (11.28) for the first  $N/2^\sigma$  nodes and then skip over the next  $N/2^\sigma$ , repeating this alternating process until we reach a node whose index exceeds  $N - 1$ .

□ **EXAMPLE 11.5:** Consider Stage 2 in Figure 11.4. We have  $v = 3$  and  $\sigma = 2$ .

Computing for the dual nodes  $f_2(4)$  and  $f_2(6)$ , we first require their values of  $p$ .

By Rule 3 we obtain the value of  $p$  for  $f_2(4)$  as follows: Dividing the node index by  $2^{v-\sigma}$ , namely  $2^1$ , we obtain  $4/2 = 2$ . Converting to binary gives  $010_2$ , which we reverse, obtaining  $010_2$ . In decimal this is  $2_{10}$ , which is the value of  $p$ . Just below  $f_2(4)$  we see the multiplier  $W^2$  as required, and for  $f_2(6)$  we see  $W^6$  (by Rule 4).

Referring to (11.28) we have  $k = 4$ ,  $k + N/2^\sigma = 4 + 8/2^2 = 6$  and  $p = 2$ , and so (11.28) becomes the pair of equations

$$\left. \begin{aligned} f_2(6) &= f_1(4) - W^2 f_1(6) \\ f_2(4) &= f_1(4) + W^2 f_1(6) \end{aligned} \right\} \quad (11.29)$$

which we see agrees with Figure 11.4. □

Observe that all dual-node computations according to (11.28) in a given stage could be executed simultaneously since none contributes to any other. Thus the ability to do parallel processing would be a great advantage in a hardware implementation for computing the FFT.

### Bit Reversal

The flow-graph structure of the FFT produces a final-stage vector that is incorrectly sequenced, and if we wish to obtain the correct output, then the values in that final-stage vector must be resequenced using what we have termed **bit reversal**.

There are two aspects of the resequencing that need to be examined. The first is how to carry out the bit reversal and the second is a practical matter that we shall consider later.

Bit reversal of the final-stage vector requires that, for each element of the vector, we must

- Express the index of the element in binary
- Reverse the binary bits
- Convert back to decimal
- Move the value in the element into the location of the output vector whose index is specified by that new decimal number

Note that bit reversal was also required for calculating the value of  $p$  when we were considering the power-of- $W$  calculation earlier, and so clearly an efficient bit-reversal algorithm is needed.

Given the decimal value of an index it is a straightforward matter to find its binary equivalent, as the following example shows:

**EXAMPLE 11.6:** Let  $N = 32$ . Then  $\nu = 5$ . To find the 5-bit binary value  $b_4b_3b_2b_1b_0$  of the index of  $f_5(13)$  we proceed as follows:

- Initialize by setting  $k_{\text{old}} = 13$ . Divide  $k_{\text{old}}$  by 2 and truncate, retaining only the integer part of the quotient, calling the latter  $k_{\text{new}} = 6$ .
- Multiply  $k_{\text{new}}$  by 2 obtaining 12 and subtract from  $k_{\text{old}}$ , giving a result of 1. Then this is the least significant bit, which we shall call  $b_0$ .
- Let  $k_{\text{old}} = k_{\text{new}}$  and cycle a total of  $\nu = 5$  times. Each cycle will produce a bit.

In this way the binary equivalent of 13 is found to be

$$b_4b_3b_2b_1b_0 = 01101$$

The decimal equivalent of the reversed bit sequence is

$$D = b_0 \times 2^4 + b_1 \times 2^3 + b_2 \times 2^2 + b_3 \times 2^1 + b_4 \times 2^0 = 22 \quad (11.30)$$

Thus  $f_5(13)$  must be placed in  $F(22)$ . □

In the preceding example we saw that the least-significant bit was the first to emerge, which means that  $D$  in (11.30) can be calculated concurrently with the bit analysis preceding it.

The practical matter that we referred to earlier is the following: We are trying to do all of the FFT computations using a **single** data vector in order to minimize the

storage required. Thus the data move that we talked about earlier is actually an interchange of two values in the same vector, namely of  $f_5(13)$  and  $f_5(22)$ .

In Figure 11.5 we saw that when we started from the top of the final-stage vector:

- The first value  $f_3(0)$  was interchanged with itself, that is, it stayed where it was.
- Next we came to  $f_3(1)$ , which we interchanged with  $f_3(4)$ .
- Next was  $f_3(2)$ , which stayed where it was.
- Then  $f_3(3)$ , which was interchanged with  $f_3(6)$ .
- Then we came to  $f_3(4)$ , which our algorithm tells us must be interchanged with  $f_3(1)$ . If we did that, however, **then we would have undone the interchange that we did earlier**, and so we need a rule to tell us when to skip.

Here is that rule:

**Rule 7:** If the decimal value coming out of the bit-reversal subroutine is less than the decimal value going into it, then skip.

This rule and all of the others that have been enunciated will be incorporated into the overall flowchart that we are now able to assemble.

## 11.5 THE COMPLETE FFT FLOWCHART

In Figure 11.6 we show a complete flowchart of the radix-2 FFT algorithm as implemented on the accompanying disk. Here is what we see from the flowchart.

- Box 1:** The data consist of the input vector  $f(k)$  derived from the analytical definition of the function to be transformed. The value of  $N$  must be given, together with  $\nu = \log_2 N$ , which can either come in as a datum or else can be derived from  $N$ .
- Box 2:** Initialization consists of setting  $\sigma = 1$ ,  $k = 0$ ,  $N2 = N/2$ , and  $NU2 = \nu - 1$ .
- Box 3:** The stage number is started at  $\sigma = 1$  and incremented. This box tests to see if it has exceeded  $\nu$ . If YES then go to the final bit reversal. If NO then go to Box 4, which is the beginning of the master loop of the FFT algorithm.
- Box 4:** Enter a loop in which  $Q$  runs from 1 to  $N2$ . These are the values of the dual-node computations that must be carried out for the present stage before skipping commences according to Rule 6, when  $Q$  exceeds  $N2$ .
- Box 5:** Calculate the value of  $p$  required in (11.28). The actions here are the implementation of Rule 3.
- Box 6:** With the required value of  $p$  from Box 5, carry out the computation and overlay per (11.28).
- Box 7:** Increment the node index by 1.
- Box 8:** Perform a test according to Rule 6. If no skip is called for, then  $Q$  is incremented in Box 9 and the next node-pair computation is carried out. However, if a skip is called for, then go to Box 10.

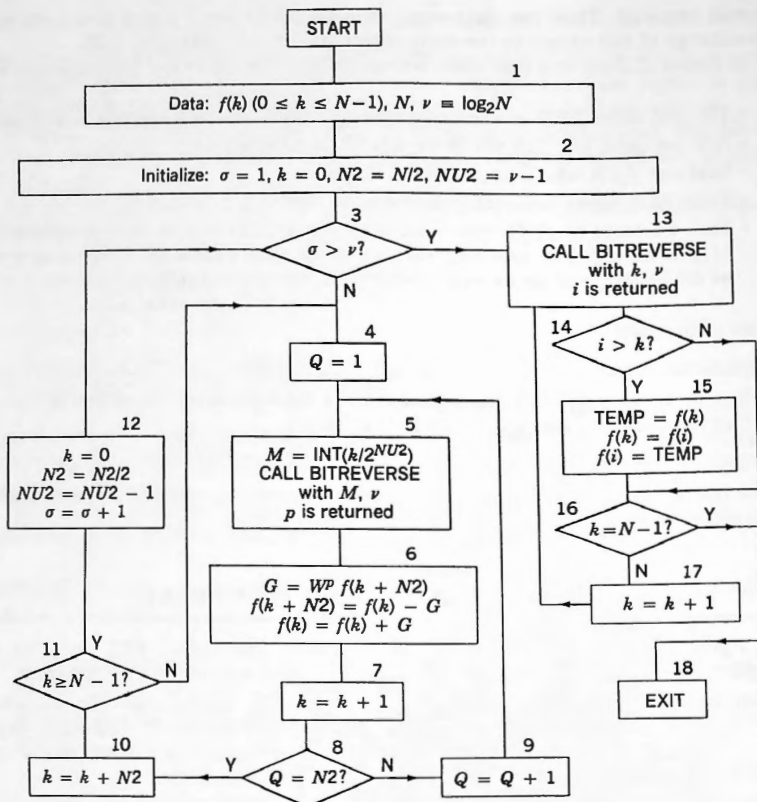


Figure 11.6. Power-of-2 FFT flowchart. (Adapted from E. Oran Brigham, *The Fast Fourier Transform and Its Applications*, p. 143, 1988, by kind permission of Prentice-Hall, Englewood Cliffs, N.J.)

- Box 10:** Increment the node index  $k$  by  $N2$ , which is the skip distance prescribed by Rule 6.
- Box 11:** Test to see if the end of the current stage has been reached, according to Rule 6. If NO then return to Box 4 and resume the node-pair calculations below the skip. If YES then go to Box 12, where we initialize for the next stage.
- Box 12:** The node index  $k$  is set to zero, the skip distance  $N2$  is halved, the variable  $NU2 = \nu - \sigma$  is decremented by 1, and the stage number  $\sigma$  is incremented by 1. Then return to Box 3 and test to see if the final stage has been completed. If NO then go to Box 4. If YES then go to Box 13 for the final bit reversal.

- Box 13:** Starting with  $k = 0$  from Box 12, send the final-stage node index  $k$  to the bit-reversal subroutine and return with  $i$ .
- Box 14:** Test to see if  $i > k$ .
- Box 15:** If YES then interchange  $f(k)$  and  $f(i)$ . If NO then skip. (See Rule 7.)
- Box 16:** Test to see if  $k = N - 1$ . If YES then EXIT. If NO then increment  $k$  and return to Box 13.

We have not provided a flowchart of the BITREVERSE subroutine. However, the reader should have no difficulty in constructing one based on what we did earlier in Example 11.6. Two values are always sent to BITREVERSE, and in the example we sent 13, which was the number to be bit-reversed and  $v = 5$ . The subroutine then returns the bit-reversed value, which in the example was 22.

## 11.6 COOLEY-TUKEY DERIVATION OF THE RADIX-2 ALGORITHM

---

We now turn our attention to the theoretical derivation of the radix-2 FFT algorithm. Rather than doing it for  $N$  any power of 2, however, we shall content ourselves with only the case  $N = 2^3$ , but it will be quite obvious how it generalizes. The method that we use follows the procedure devised by Cooley and Tukey, where they did it for the general mixed-radix case.

Suppose then that  $N = 8$ . The DFT becomes

$$F(n) = \sum_{k=0}^7 f_0(k)W^{nk} \quad (0 \leq n \leq 7) \quad (11.31)$$

Representing both  $n$  and  $k$  as binary numbers, we have

$$n = 4a + 2b + c \quad \text{and} \quad k = 4x + 2y + z \quad (11.32)$$

in which  $a, b, c$  and  $x, y, z$  take on the values 0 or 1, and in so doing  $n$  and  $k$  take on all values from 0 to 7. Keep in mind that  $a$  is the most significant binary bit in  $n$  and  $c$  is the least significant. Similarly  $x$  is the most significant in  $k$  and  $z$  the least. With this representation of  $n$  and  $k$ , (11.31) becomes

$$F(a, b, c) = \sum_{z=0}^1 \sum_{y=0}^1 \sum_{x=0}^1 f_0(x, y, z)W^{(4a+2b+c)(4x+2y+z)} \quad (11.33)$$

Observe the order of summation,  $x$  first on the inside, then  $y$  second, and finally  $z$  on the outside. This choice has been made deliberately because of what follows later. By breaking up  $k = 4x + 2y + z$  in (11.33) we now write  $W$  with its exponent as follows:

$$W^{(4a+2b+c)(4x+2y+z)} = W^{(4a+2b+c)x}W^{(4a+2b+c)y}W^{(4a+2b+c)z} \quad (11.34)$$

Observe again that a choice has been made. We have broken up the value of  $k$  into its binary components, but an alternate and completely valid approach would have been to break up  $n$ . However, that would have led to a slightly different FFT algorithm than the one in which we are interested (there are many others).

Rearranging the exponents of the first two  $W$ 's on the RHS of (11.34) we now see that

$$W^{(4a+2b+c)4x} = \left[ (W^8)^{(2a+b)x} \right] W^{4cx} \quad (11.35)$$

and

$$W^{(4a+2b+c)2y} = \left[ (W^8)^{ay} \right] W^{(2b+c)2y} \quad (11.36)$$

However, for  $N = 8$ ,

$$W^8 = 1 \quad (11.37)$$

and so the terms in square brackets in both (11.35) and (11.36) are simply 1. Thus they disappear and (11.34) becomes

$$W^{(4a+2b+c)(4x+2y+z)} = W^{4cx} W^{(2b+c)2y} W^{(4a+2b+c)z} \quad (11.38)$$

This means that (11.33) can be written as

$$F(a, b, c) = \sum_{z=0}^1 \sum_{y=0}^1 \sum_{x=0}^1 f_0(x, y, z) W^{4cx} W^{(2b+c)2y} W^{(4a+2b+c)z} \quad (11.39)$$

The inner sum that has been separated out by bracket (1) no longer involves the variable  $x$ , since  $x$  sums out. Instead it depends on the value of  $c$ , and so we give it a name as follows:

$$f_1(c, y, z) \equiv \sum_{x=0}^1 f_0(x, y, z) W^{4cx} \quad (11.40)$$

Observe how  $x$  has been replaced by  $c$  on the left.

Similarly, in (11.39) we name the sum separated out by bracket (2) as follows:

$$f_2(c, b, z) \equiv \sum_{y=0}^1 f_1(c, y, z) W^{(2b+c)2y} \quad (11.41)$$

Observe first that (11.40) has been put to use in this equation. Secondly, we see that the sum in (11.41) no longer depends on  $y$  since it sums out, but depends instead on  $b$ , and so  $b$  has replaced  $y$  on the left.

Finally, consider the sum marked by bracket (3) in (11.39). We see that it can be named

$$f_3(c, b, a) = \sum_{z=0}^1 f_2(c, b, z) W^{(4a+2b+c)z} \quad (11.42)$$

Taking all of this together with the LHS of (11.39) then means that the DFT spectrum vector and our newly defined vector  $f_3(c, b, a)$  are one and the same, that is, that

$$F(a, b, c) = f_3(c, b, a) \quad (11.43)$$

showing that the output vector  $F$  can be obtained from the Stage-3 vector  $f_3$  by interchanging values based on reversing the bits in the indices.

Let's now write out (11.40) in full, in order better to understand exactly what it means. Since  $c$ ,  $y$ , and  $z$  can each take on the values 0 or 1, and since summation is over  $x$  from 0 to 1, (11.40) expands to (11.44).

$$\left. \begin{array}{lllll} cyz & xyz & W^{4cx} & xyz & W^{4cx} \\ f_1(0, 0, 0) = f_0(0, 0, 0) & W^0 & +f_0(1, 0, 0) & W^0 \\ f_1(0, 0, 1) = f_0(0, 0, 1) & W^0 & +f_0(1, 0, 1) & W^0 \\ f_1(0, 1, 0) = f_0(0, 1, 0) & W^0 & +f_0(1, 1, 0) & W^0 \\ f_1(0, 1, 1) = f_0(0, 1, 1) & W^0 & +f_0(1, 1, 1) & W^0 \\ f_1(1, 0, 0) = f_0(0, 0, 0) & W^0 & +f_0(1, 0, 0) & W^4 \\ f_1(1, 0, 1) = f_0(0, 0, 1) & W^0 & +f_0(1, 0, 1) & W^4 \\ f_1(1, 1, 0) = f_0(0, 1, 0) & W^0 & +f_0(1, 1, 0) & W^4 \\ f_1(1, 1, 1) = f_0(0, 1, 1) & W^0 & +f_0(1, 1, 1) & W^4 \end{array} \right\} \quad (11.44)$$

- On the right of each row, there is a sum of two terms. That is the summation over  $x$  from 0 to 1, with every first term showing  $x = 0$  and every second one  $x = 1$ .
- The variables  $c$ ,  $y$ , and  $z$  in the first three columns on the left make up all of the binary numbers from 0 to 7 since those are all the possible cases that we must consider.
- The values of  $c$ ,  $y$ , and  $z$  in the first three columns are carried over to the right of each equation.
- The exponent of  $W$  is  $4cx$ , whose value can be computed row by row since the values of  $x$  and  $c$  have been established. The results are as shown.

Comparison with Figure 11.4 shows that the preceding eight equations are identical to the first stage of the base-8 FFT algorithm. Similarly, writing out (11.41) in full gives us the eight equations numbered (11.45).

$$\left. \begin{array}{ll} cbz & cyz \quad W^{(2b+c)2y} \\ f_2(0,0,0) = f_1(0,0,0)W^0 & + f_1(0,1,0)W^0 \\ f_2(0,0,1) = f_1(0,0,1)W^0 & + f_1(0,1,1)W^0 \\ f_2(0,1,0) = f_1(0,0,0)W^0 & + f_1(0,1,0)W^4 \\ f_2(0,1,1) = f_1(0,0,1)W^0 & + f_1(0,1,1)W^4 \\ f_2(1,0,0) = f_1(1,0,0)W^0 & + f_1(1,1,0)W^2 \\ f_2(1,0,1) = f_1(1,0,1)W^0 & + f_1(1,1,1)W^2 \\ f_2(1,1,0) = f_1(1,0,0)W^0 & + f_1(1,1,0)W^6 \\ f_2(1,1,1) = f_1(1,0,1)W^0 & + f_1(1,1,1)W^6 \end{array} \right\} \quad (11.45)$$

As before, the reader can verify that these are in fact the expansion of (11.41) by cross checking values of  $c$ ,  $b$ , and  $z$  and the exponents of  $W$ , and by verifying that  $y = 0$  in every first term on the right and  $y = 1$  everywhere in every second one. Examination of Figure 11.4 shows that the preceding eight equations are identical to the second stage of the base-8 FFT algorithm.

Finally, when (11.42) is written out in full we obtain eight equations that will be seen to be identical to the third stage of Figure 11.4. Thus the very compact notation shown in (11.39) expands out exactly to the base-8 FFT algorithm.

## 11.7 FINAL COMMENTS

---

### Using the FFT for Synthesis

Thus far we have only paid attention to the analysis equation of the DFT, namely

$$F_n = \sum_{k=0}^{N-1} f_k e^{-j2\pi nk/N} \quad (0 \leq n \leq N-1) \quad (11.46)$$

However, the synthesis equation

$$f_k = \frac{1}{N} \sum_{n=0}^{N-1} F_n e^{j2\pi nk/N} \quad (0 \leq k \leq N-1) \quad (11.47)$$

can be restated as follows:

$$f_k = \frac{1}{N} \left[ \sum_{n=0}^{N-1} F_n^* e^{-j2\pi nk/N} \right]^* \quad (11.48)$$

showing us the following: If we wish to run synthesis on the vector  $F_n$  using the FFT analysis transformation that we have been discussing, then all that we have to do is

- Conjugate  $F_n$  to give  $F_n^*$ , which is sent to the FFT
- Conjugate the vector that comes out of the FFT
- Divide the result by  $N$

Thus with a small amount of pre- and postprocessing the same FFT code can carry out both the analysis and the synthesis operations.

### Economizing When the Input is Real and $N$ is Even

In almost all cases the input vector  $f_k$  consists of only real numbers. The FFT, on the other hand, is perfectly general and assumes that the input vector is complex. That being the case, most of the time the imaginary part of the input vector being sent to the FFT is all zeros, and this is a wasteful situation that need not be accepted.

It is possible to load the  $N$  numbers of a real input vector into a vector of length  $N/2$  using both the real and imaginary input slots, to then run the FFT transformation based on  $N/2$ , and then finally to construct from the resulting spectrum vector of length  $N/2$  a spectrum vector of length  $N$  that is the exact DFT of the original input vector of length  $N$ . The time and storage savings are substantial.

In our implementation on the accompanying disc we included this feature, and so, whenever the input vector is real and the value of  $N$  is even, you will observe the message,

NOW RUNNING POWER-OF-2 ANALYSIS USING N = xxx

in which  $xxx$  is half of the current value of  $N$ .

It is not possible to use this approach when running SYNTHESIS since the starting vector there is  $F_n$ , which is almost always complex. Full details on all of this are given in Brigham.

### The FFT for $N$ Composite

When  $N$  is not an exact power of 2, then the FFT algorithm that we have discussed in this chapter is no longer applicable. It is still possible, however, to apply the type of theory that we used in the previous section in order to develop an FFT for this situation and to gain a significant advantage over the straight DFT (although not as great an advantage as when  $N$  is a power of 2).

Cooley and Tukey in their original paper started out assuming that  $N$  was a general composite number (one that can be factored into a product of primes, not necessarily all equal to 2), and only later in the paper specialized to the case where all factors were equal to 2. The paper is hard to understand at first, but it's all there, and once one has some familiarity based on other references it becomes surprisingly easy to follow. The remarkable thing is that it was only  $4\frac{1}{2}$  pages in length (perhaps that's why it's not so easy to read at first), and yet much of what we know today about the FFT is contained in it.

In addition to the general power-of-2 we also implemented the composite capability on our disk, and so it will accept any value of  $N$ , power-of-2, composite, or prime, the last of which is just a special case of composite and identical to the good old DFT without any advantages at all. Full details are given in Brigham.

### NOTES AND COMMENTS

---

Complex multiplication, addition, and subtraction involve the following: Let  $c = a + jb$  and  $w = u + jv$  be two complex numbers with real and imaginary parts as shown. Then their product, formed by **complex multiplication**, is

$$cw = (a + jb)(u + jv) = (au - bv) + j(bu + av) \quad (11.49)$$

and so their product has real and imaginary parts

$$\begin{cases} [cw]_{\text{Re}} = au - bv \\ [cw]_{\text{Im}} = bu + av \end{cases} \quad (11.50)$$

**Complex addition** of  $c$  and  $w$  is

$$c + w = (a + jb) + (u + jv) = (a + u) + j(b + v) \quad (11.51)$$

whose real and imaginary parts are

$$\begin{cases} [c + w]_{\text{Re}} = a + u \\ [c + w]_{\text{Im}} = b + v \end{cases} \quad (11.52)$$

**Complex subtraction** is defined similarly.

In the present context we are typically required to form the complex product of  $W^p$  with  $x_\sigma(k)$ . Since  $W^p$  can be expanded as follows,

$$W^p = (e^{-j2\pi/N})^p = e^{-j2\pi p/N} = \cos \frac{2\pi p}{N} - j \sin \frac{2\pi p}{N} \quad (11.53)$$

and since, in general,  $x_\sigma(k)$  is a complex quantity, that is,

$$x_\sigma(k) = a + jb \quad (11.54)$$

we see that

$$\begin{aligned} W^p x_\sigma(k) &= \left[ \cos \frac{2\pi p}{N} - j \sin \frac{2\pi p}{N} \right] [a + jb] \\ &= a \cos \frac{2\pi p}{N} + b \sin \frac{2\pi p}{N} \\ &\quad - j \left[ a \sin \frac{2\pi p}{N} - b \cos \frac{2\pi p}{N} \right] \end{aligned} \quad (11.55)$$

whose real and imaginary parts are

$$\left. \begin{aligned} [W^p x_\sigma(k)]_{\text{Re}} &= a \cos \frac{2\pi p}{N} + b \sin \frac{2\pi p}{N} \\ [W^p x_\sigma(k)]_{\text{Im}} &= -a \sin \frac{2\pi p}{N} + b \cos \frac{2\pi p}{N} \end{aligned} \right\} \quad (11.56)$$

The pair of expressions in (11.56) can be readily computed using only real arithmetic. Once done, it can then be used in subsequent computations involving complex quantities.

# The Discrete Fourier Transform as an Estimator

## **12.1 INTRODUCTION**

---

In Chapter 10 we developed a new mathematical tool that we called the discrete Fourier transform (DFT), and we pointed out that it exists in its own right, independently of any of the tools that we developed in Part 1. However the DFT can also be used [via the fast Fourier transform (FFT)] to obtain numerical estimates of both Fourier transforms and Fourier series coefficients. Indeed this is probably the main reason why the FFT is now in such widespread use. In this chapter we commence the study of how these estimation operations are carried out.

To underscore the fact that the FFT is the algorithm that is used in practice to evaluate the DFT we shall now begin to use the designation **FFT** whenever referring to the DFT. Thus:

**FFT** will refer to the synthesis and analysis equations of the discrete Fourier transform.

We shall also need to make reference to the transformations from Part 1. In order to distinguish between them and the FFT we shall henceforth begin referring to those of Part 1 as the **continuous Fourier transforms**, using the designation **CFT**. Thus

**CFT** will refer to the synthesis and analysis equations for

- complex Fourier series
- Fourier transforms

It will usually be clear from the context which of the CFTs we are referring to, but where this may not be the case we shall use specific designations such as **CFT** (Fourier series) or **CFT** (pulse).

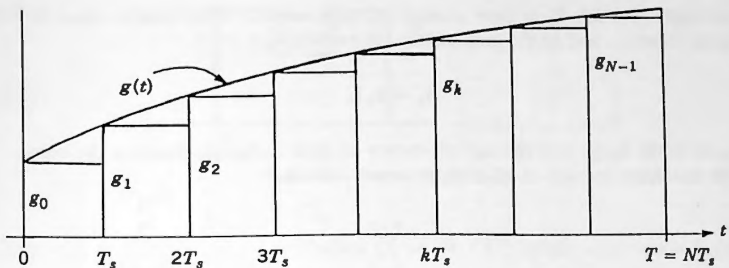


Figure 12.1. Rectangular-rule integration.

## 12.2 RELATIONSHIPS BASED ON THE RECTANGULAR RULE

The value of a definite integral can almost always be estimated by what is known as the **rectangular rule**, which is perhaps the simplest method of carrying out numerical integration. There are many approaches to implementing this rule, but the one that we now present is about as simple and as basic as they come. The pleasant surprise is that, when applied to the derivation of CFT spectra for either periodic waveforms or pulses, it leads directly to the FFT.

Here's how the rectangular rule works. Referring to Figure 12.1, we wish to find the area under  $g(t)$  over the range shown, and so we set up the integral

$$I = \int_0^T g(t) dt \quad (12.1)$$

If we can evaluate  $I$  it will give us precisely the area that we are looking for. It is often not possible to carry out that integration, however, and so our approach will instead be to find a **numerical estimate** for  $I$ . To do that we break up the range of integration into  $N$  equal intervals. (In Fig. 12.1 we show the case where  $N = 8$ .) Then each interval will have length  $T_s$ , where

$$T_s = \frac{T}{N} \quad (12.2)$$

This creates  $N$  sampling points on the  $t$ -axis located at

$$t_k = kT_s \quad (0 \leq k \leq N - 1). \quad (12.3)$$

The function  $g(t)$  that we wish to integrate is now numerically sampled at each of these points, giving the sequence of values:

$$g_k = g(kT_s) \quad (0 \leq k < N - 1) \quad (12.4)$$

A rectangle of width  $T_s$  is then created in each section with height equal to the sampled value  $g_k$ , and so the area of the  $k$ th rectangle is

$$A_k = g_k T_s \quad (12.5)$$

Observe in the figure how the top left corner of each rectangle touches the curve.

We now form the sum of all of these areas, namely

$$S_N = \sum_{k=0}^{N-1} g_k T_s \quad (12.6)$$

and because of the way in which we have sampled, (12.6) is known in mathematical terms as a **left-endpoint uniform Riemann sum**, and the mode of sampling that we have employed is known as **left-endpoint uniform sampling**.

As shown,  $S_N$  is approximately equal to the area under  $g(t)$ . Then, as  $N$  becomes larger and larger and the number of sampling points increases,  $S_N$  tends to the area under  $g(t)$  exactly. This is stated in calculus texts as

$$\int_0^T g(t) dt = \lim_{N \rightarrow \infty} \sum_{k=0}^{N-1} g_k T_s \quad (12.7)$$

(In fact, versions of (12.7) are usually used as definitions of what is meant by integration.) In computational work we cannot actually let a variable tend to infinity, and so we assign to  $N$  in (12.7) some large but finite value and then evaluate the sum shown. The result is then only an approximation of the integral on the left, but by the meaning of the term **limit** it follows that the approximation can be made as good as we please simply by making  $N$  sufficiently large. Thus, formally stated, the rectangular rule is as shown in the following box.

### ■ Rectangular Rule for Numerical Integration

$$\int_0^T g(t) dt \approx \sum_{k=0}^{N-1} g_k T_s \quad (12.8)$$

with the approximation errors being made as small as we please by making  $N$  sufficiently large.

We now show that applying (12.8) to the derivation of the CFT transform of a pulse using left-endpoint uniform sampling leads directly to the FFT. Thus consider a pulse  $f(t)$  that has what we call a **finite span**, that is, its duration on the  $t$ -axis is finite. Assume that the pulse can be bracketed in the interval  $0 \leq t < T$ , as shown in Figure 12.2.

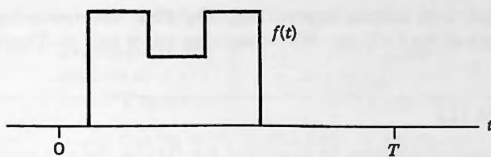


Figure 12.2. Pulse with finite span.

We wish to transform  $f(t)$  and so we set up the CFT analysis equation as follows:

$$F(\omega) = \int_0^T f(t) e^{-j\omega t} dt \quad (12.9)$$

in which we have used a finite range of integration because of the nature of the pulse. (We shall have a great deal more to say about how  $T$  for a pulse is actually arrived at.)

Instead of carrying out the integration as it stands (we may in fact not be able to) we now apply the rectangular rule, obtaining

$$F(\omega) \approx \sum_{k=0}^{N-1} f_k e^{-j\omega k T_s} T_s \quad (12.10)$$

which we see is a function of the continuous variable  $\omega$ . In order to be able to utilize this formula on a computer we then select specific numerical values of  $\omega$ , and for that purpose we elect to sample at the points  $\omega_n = n\omega_0$  ( $-N/2 \leq n \leq N/2$ ), where

$$\omega_0 = \frac{2\pi}{T} \quad (12.11)$$

Thus (12.10) becomes

$$\begin{aligned} F(n\omega_0) &\approx \sum_{k=0}^{N-1} f_k e^{-jn\omega_0 k T_s} T_s \\ &= T_s \sum_{k=0}^{N-1} f_k e^{-jn(2\pi/T)k T_s} \quad \left( \text{where } T_s = \frac{T}{N} \right) \\ &= \frac{T}{N} \sum_{k=0}^{N-1} f_k e^{-j2\pi n k / N} \quad \left( \frac{-N}{2} \leq n \leq \frac{N}{2} \right) \end{aligned} \quad (12.12)$$

Except for the scale factor  $T/N$ , we see that the RHS of (12.12) is precisely the FFT analysis formula.

By making  $N$  sufficiently large, that is, by subdividing the range of integration 0 to  $T$  into sufficiently many subintervals, we can make the errors in the rectangular rule, and hence also in the approximation shown in (12.12), as small as we please. This

then tells us that, with appropriate scaling, the FFT spectrum can be used for estimates of values of the CFT one. We summarize all of this as Theorem 12.1.

### ■ THEOREM 12.1

Let the CFT analysis equation be evaluated for  $f(t)$  by the use of the rectangular rule with left-endpoint uniform sampling at  $N$  points over  $0 \leq t < T$ , and let the variable  $\omega$  be sampled at the  $N$  points  $n\omega_0$  ( $-N/2 \leq n \leq N/2$ ) where  $\omega_0 = 2\pi/T$ . Then, to within the constant  $T/N$ , the spectral elements so obtained are identical to those that would be obtained if we had used the FFT analysis equation on the same  $N$  samples taken from  $f(t)$ , that is,

$$\left. \begin{array}{l} \text{Rectangular rule} \\ \text{applied to } f(t) \\ \text{for CFT spectrum} \end{array} \right\} = \frac{T}{N} \times \left\{ \begin{array}{l} \text{FFT applied} \\ \text{to } f(t) \text{ for} \\ \text{FFT spectrum} \end{array} \right\}$$

Moreover these values can be used as estimates of  $F(\omega)$  sampled at  $n\omega_0$ , that is,

$$F(n\omega_0) \approx \frac{T}{N} F_n \quad \left( -\frac{N}{2} \leq n \leq \frac{N}{2} \right) \quad (12.13)$$

where the errors in (12.13) can be made as small as we please by making  $N$  sufficiently large.

Of course, in practice we do not use the rectangular rule for obtaining DFT line spectra since the FFT is far more efficient and is always used for that purpose. We merely demonstrated this approach in order to begin to provide some insight into some of the relationships between the CFT and the FFT.

In Chapter 13 we give specific formulas for the values of the errors involved in (12.13) when using the FFT spectral elements as estimates for their CFT counterparts.

Consider next a periodic waveform  $f_p(t)$ . Applying the rectangular rule to the CFT analysis equation in order to derive its complex coefficients leads to a result that is similar to the one given earlier. In Exercise 12.3 we ask you to show that to within the scale factor  $1/N$ , the values so obtained for the CFT coefficients are precisely equal to the spectral elements that would have been obtained had we used the same set of data points in the FFT. We state this as Theorem 12.2.

### ■ THEOREM 12.2

Let the CFT analysis equation be evaluated for  $f_p(t)$  by the use of the rectangular rule with left-endpoint uniform sampling at  $N$  points over one period. Then, to within the constant  $1/N$ , the spectral elements so obtained are identical to those that would be obtained if we had used the FFT analysis

equation on the same  $N$  samples taken from  $f_p(t)$ , that is,

$$\left. \begin{array}{l} \text{Rectangular rule applied to } f_p(t) \\ \text{for CFT spectrum} \end{array} \right\} = \frac{1}{N} \times \left\{ \begin{array}{l} \text{FFT applied to } f_p(t) \text{ for} \\ \text{FFT spectrum} \end{array} \right\}$$

Moreover, these values can be used as estimates of the complex Fourier series coefficients of  $f_p(t)$ , that is,

$$F_p(n) \approx \frac{1}{N} F_n \quad \left( \frac{-N}{2} \leq n \leq \frac{N}{2} \right) \quad (12.14)$$

where the errors in (12.14) can be made as small as we please by making  $N$  sufficiently large.

In summary: The rectangular rule can give us values for definite integrals that are as accurate as we want them to be, and the rectangular rule has led us directly to the FFT. Thus it follows that (with appropriate scaling) the FFT can give us estimates of the CFT spectra for periodic and pulse functions that can be made as accurate as we want them to be.

We remind the reader of the following two facts that emerge from the two preceding theorems:

- If we want the FFT to give us a valid estimate of the CFT spectrum of a pulse or a periodic waveform, then we must always use left-endpoint uniform sampling, because that is how the FFT is connected to the CFT.
- If we have a sampling instant that coincides with a discontinuity, then we must use the half-value at that point as the number that we submit to the FFT, because in the Fourier sense, that is the function's value there.

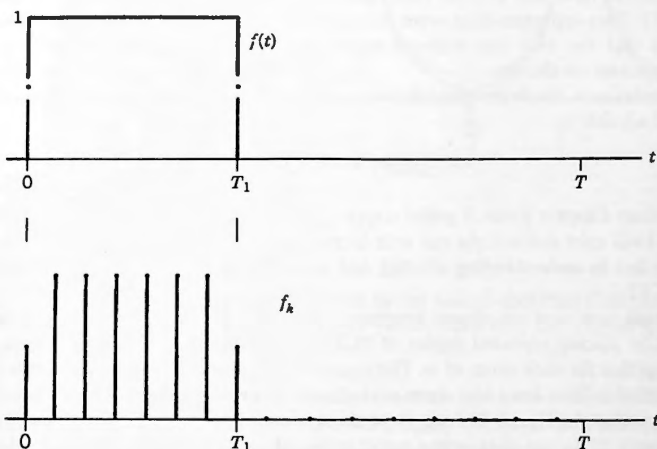


Figure 12.3.

These two statements are depicted in Figure 12.3 where we show a pulse  $f(t)$  and the sequence of samples that must be taken if correct FFT estimation is to take place. Note how left-endpoint sampling and half-values are being used. (See also Fig. 12.6.)

### 12.3 ALIASING

---

In what follows we shall be talking about a certain periodic waveform and about a related pulse. In order to make perfectly clear which of the two we are referring to we shall use the following notation:

$$\begin{cases} \text{per}(t) & \text{will be the given periodic waveform} \\ \text{PER}(n) & \text{will be the CFT line spectrum of per}(t) \\ \\ \text{pul}(t) & \text{will be the given pulse} \\ \text{PUL}(\omega) & \text{will be the Fourier transform of pul}(t) \end{cases}$$

The pulses with which we are concerned all have finite spans and finite energy. We refer to them as finite-span, finite-energy pulses.

Whenever we use the subscript  $n$ , we are referring to an FFT line spectrum. Thus:

$$\begin{cases} \text{PER}_n & \text{is the FFT line spectrum obtained from sampled values of per}(t). \\ \text{PUL}_n & \text{is the FFT line spectrum obtained from sampled values of pul}(t). \end{cases}$$

Earlier we have seen how the rectangular rule connects the FFT and the spectra of the CFT. Two approximations were obtained by its use in (12.13) and (12.14), which showed that the FFT can estimate values for either a Fourier transform or for Fourier series coefficients.

Consider now the finite-span, finite-energy pulse  $\text{pul}(t)$ , whose Fourier transform is  $\text{PUL}(\omega)$ , that is,

$$\text{pul}(t) \Leftrightarrow \text{PUL}(\omega) \quad (12.15)$$

Recall from Chapter 3 that if  $\text{pul}(t)$  contains finite energy, then its Fourier transform  $\text{PUL}(\omega)$  will exist and will die out with increasing values of  $\omega$  at least like  $1/\omega$ . This is a key fact in understanding aliasing and how the FFT can give us approximations of the CFT.

Suppose now that an aliased spectrum, which we shall call  $\text{PUL}_a(\omega)$ , has been created by placing repeated copies of  $\text{PUL}(\omega)$  of (12.15) on the  $\omega$ -axis and adding them together for each value of  $\omega$ . The copies that we have positioned in this manner are assumed to have been laid down periodically, every  $\omega_s$  radians, which is called the aliasing period. In Figure 12.4 we show three examples.

In Figure 12.4a we start with a small value of  $\omega_s$  (small in relation to the speed with which  $\text{PUL}(\omega)$  is dying out). Notice how there is heavy interference between the

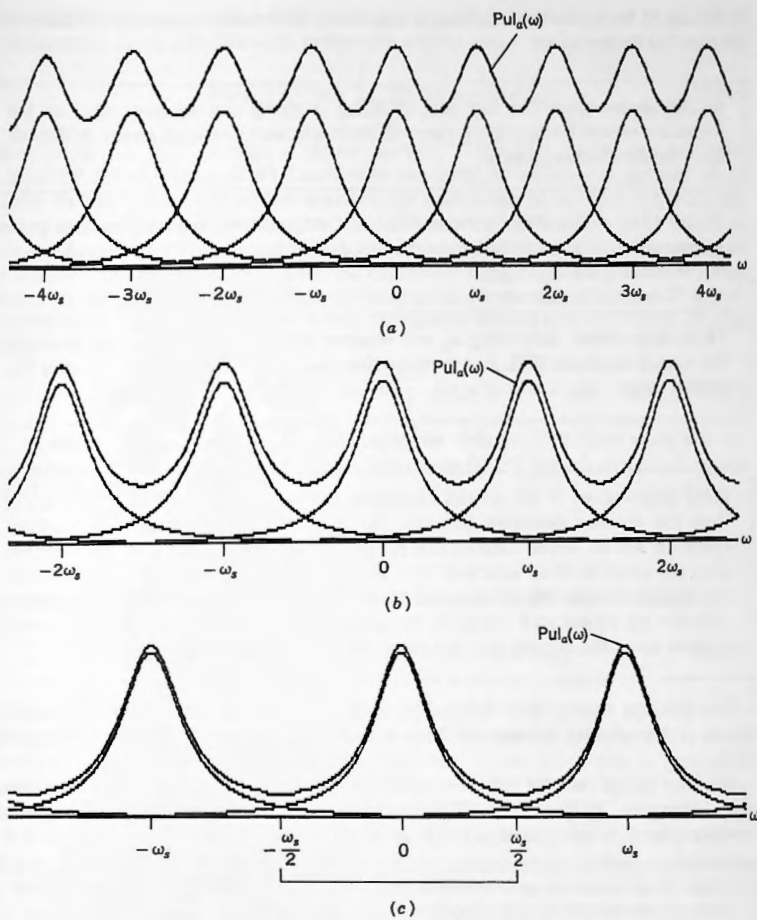


Figure 12.4.

various copies of the spectra, and so all parts of the aliased spectrum  $PUL_a(\omega)$  differ radically from the single spectrum  $PUL(\omega)$ . Notice also that the aliased spectrum  $PUL_a(\omega)$  is periodic.

**First observation:** Every aliased spectrum  $PUL_a(\omega)$  will be periodic with period  $\omega_s$ , even though the original spectrum  $PUL(\omega)$  was not.

In Figure 12.4b  $\omega_s$  has been increased somewhat, and so the copies of  $PUL(\omega)$  have been pulled further apart.

**Second observation:** The fact that  $PUL(\omega)$  is dying out ensures that as the copies are moved further apart, they will have less and less interaction with each other in the aliasing process.

In Figure 12.4c  $\omega_s$  has been increased further yet, and we see that as this process continues we are constantly reducing the amount of interaction between the various copies of the original spectrum.

**Third observation:** Increasing  $\omega_s$  will improve the degree of accuracy to which the aliased spectrum  $PUL_a(\omega)$  matches the original spectrum  $PUL(\omega)$  over the central range  $-\omega_s/2 \leq \omega \leq \omega_s/2$ .

**Final observation:** If we restrict ourselves to the range  $-\omega_s/2 \leq \omega \leq \omega_s/2$ , then the greatest deviation between the aliased spectrum and the original spectrum will be at the ends of this range. The central copy and the adjacent ones are equal at those locations, and so we expect the relative error between the aliased version and the original to be about 100 percent at those points. Likewise we expect such errors to be smallest in the neighborhood of  $\omega = 0$  because there the central copy is largest and the adjacent ones least.

The key fact here is that  $PUL(\omega)$  is dying out. Thus by increasing the aliasing period  $\omega_s$  the aliasing process will have a steadily diminishing effect on the central copy.

We have talked thus far only about  $PUL(\omega)$ , the CFT spectrum of a finite-energy pulse. However,  $PER(n)$ , the CFT spectrum of a finite-average-power periodic function, also dies out at least like  $1/n$  as we move away from its central region.

Hence all of the preceding observations regarding Fourier spectra of pulses will also hold true for the line spectra of periodic functions.

The aliasing mechanism that we have been discussing is central to understanding how the results of the FFT are related to the CFTs, both pulse and periodic, and in due course we shall be making use of all of the observations that we have just noted.

We now examine how one builds a mathematical model for the aliasing process. Again, this is something that we need to be completely familiar with in order to understand the proofs that are presented later in the chapter.

Given a Fourier spectrum  $PUL(\omega)$ , we modify its argument to give  $PUL(\omega - \omega_s)$ . This is then the original spectrum, shifted  $\omega_s$  radians to the right along the  $\omega$ -axis. Further modification of the argument gives  $PUL(\omega - m\omega_s)$  where  $m$  is any integer. If

$m$  is positive, then this copy will be shifted  $m\omega_s$  radians to the right of  $F(\omega)$ , and if  $m$  is negative, to its left. We now create the infinite sum

$$\text{PUL}_a(\omega) = \sum_{m=-\infty}^{\infty} \text{PUL}(\omega - m\omega_s) \quad (12.16)$$

where, as before, the subscript  $a$  means "aliased." Then  $\text{PUL}_a(\omega)$  is seen to consist of infinitely many copies of  $\text{PUL}(\omega)$ , each displaced by an integral multiple of  $\omega_s$  radians on the  $\omega$ -axis, all added together for each value of  $\omega$ . Thus (12.16) is the required mathematical expression to represent the aliasing of  $\text{PUL}(\omega)$ .

We still need to take one more step and that is to include numerical sampling of the spectrum. As it stands in (12.16) the expression for  $\text{PUL}_a(\omega)$  is a function of the continuous variable  $\omega$ . Suppose that we were to take numerical samples of  $\text{PUL}_a(\omega)$  at points spaced  $\omega_0$  radians apart, where the sample spacing is related to the aliasing period by

$$\omega_0 = \frac{\omega_s}{N} \quad (12.17)$$

and in which the parameter  $N$  remains to be defined. (We shall soon see the motivation for selecting  $\omega_0$  in this way.) Then from (12.16) the  $n$ th numerical sample of  $\text{PUL}_a(\omega)$  would be

$$\text{PUL}_a(n\omega_0) = \sum_{m=-\infty}^{\infty} \text{PUL}(n\omega_0 - m\omega_s) \quad (12.18)$$

and with  $\omega_0$  selected as shown in (12.17), we see that (12.18) can also be written as

$$\text{PUL}_a(n\omega_0) = \sum_{m=-\infty}^{\infty} \text{PUL}[(n - mN)\omega_0] \quad (12.19)$$

Plotting (12.18) on the  $\omega$ -axis for various values of  $n$  would give us a line spectrum of the kind shown in Figure 12.5a. In Figure 12.5b we show the same spectrum on the  $n$ -axis for comparison. Observe that the step-size  $\omega_0$  on the  $\omega$ -axis is present by implication when we are on the  $n$ -axis. Thus the point  $N\omega_0$  on the  $\omega$ -axis corresponds to the point  $N$  on the  $n$ -axis.

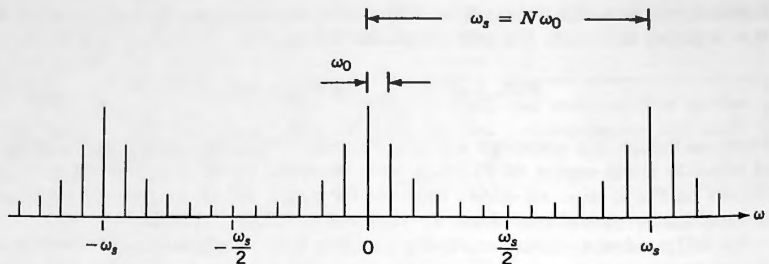
We observed earlier (see third observation) that increasing the aliasing period  $\omega_s$  will improve the degree of accuracy to which the aliased spectrum  $\text{PUL}_a(\omega)$  matches the original spectrum  $\text{PUL}(\omega)$  over the central period  $-\omega_s/2 \leq \omega \leq \omega_s/2$ . For the case of the numerically sampled version of the aliased spectrum shown in (12.18) this now gives us the following:

### ■ Approximation for a CFT (pulse) spectrum $\text{PUL}(\omega)$

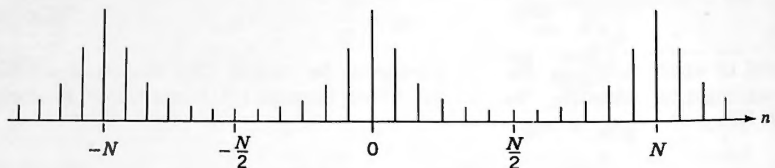
If  $\omega_s$  is sufficiently large, then over the range  $-N/2 \leq n \leq N/2$

$$\sum_{m=-\infty}^{\infty} \text{PUL}(n\omega_0 - m\omega_s) \approx \text{PUL}(n\omega_0) \quad (12.20)$$

with the approximation errors being made smaller as we increase  $\omega_s$ .

Numerically sampled aliased spectrum on the  $\omega$ -axis.

(a)

Numerically sampled aliased spectrum on the  $n$ -axis.

(b)

Figure 12.5. (a) Numerically sampled aliased spectrum on the  $\omega$ -axis. (b) Numerically sampled aliased spectrum on the  $n$ -axis.

We shall show in the next section that (to within a constant) the quantity on the LHS of (12.20) is precisely what we obtain from the FFT. Thus (12.20) will be the critical approximation statement that permits us to use the FFT to obtain CFT transforms of pulses over the range shown.

The preceding mathematical model for the aliasing of a pulse's CFT spectrum can now be quickly restated for the CFT spectrum of a periodic waveform. Thus, starting with a periodic function  $\text{per}(t)$  whose CFT line spectrum is assumed to be  $\text{PER}(n)$ , we modify the argument to give  $\text{PER}(n - N)$ . Then this is a copy of  $\text{PER}(n)$  shifted  $N$  units on the  $n$ -axis to the right. We then form infinitely many shifted copies  $\text{PER}(n - mN)$ , where  $m$  is any integer, positive or negative, and add them all together, obtaining

$$\text{PER}_a(n) = \sum_{m=-\infty}^{\infty} \text{PER}(n - mN) \quad (-\infty < n < \infty) \quad (12.21)$$

where, as before, the subscript  $a$  means aliased. This then is the mathematical statement for an aliased version of  $\text{PER}(n)$ . Note that  $\text{PER}_a(n)$  in (12.21) will be periodic with aliasing period  $N$ , even though the original copy  $\text{PER}(n)$  was not, because the results of aliasing are always periodic. Recall also that  $\text{PER}(n)$  always

dies out at least like  $1/n$ . Hence, as the copies making up the aliased spectrum are pulled further apart, the central portion of  $\text{PER}_a(n)$  and the unaliased original spectrum  $\text{PER}(n)$  will become more and more like each other over the range  $-N/2 \leq n \leq N/2$ . Thus, for the statement corresponding to (12.20), we now have:

**■ Approximation for a CFT (periodic) spectrum  $\text{PER}(n)$**

If  $N$  is sufficiently large, then over the range  $-N/2 \leq n \leq N/2$

$$\sum_{m=-\infty}^{\infty} \text{PER}(n - mN) \approx \text{PER}(n) \quad (12.22)$$

with the approximation errors being made smaller as we increase  $N$ .

We shall see the next section that (to within a constant) the spectrum on the LHS of (12.22) is precisely what we obtain from the FFT. Thus (12.22) will be the critical approximation statement that permits us to use the FFT to obtain CFT spectra of periodic waveforms.

## 12.4 THE FFT AS AN ESTIMATOR FOR THE CFTs

In Section 12.2 we showed that the FFT can serve as an estimator for CFT spectra by using the rectangular rule to evaluate the CFT analysis equations. In this section we demonstrate that fact again, but here we base our analysis on the aliasing that comes into play when we use the FFT.

The results in this section complement those of Section 12.2 and provide us with a much more complete picture of what is taking place, and we shall need both when we come to the next chapter.

We start with a periodic train of Dirac deltas spaced  $T_s$  seconds apart that we call  $\delta_T(t)$ , defined as follows:

$$\delta_T(t) \equiv T_s \sum_{k=-\infty}^{\infty} \delta(t - kT_s) \quad (12.23)$$

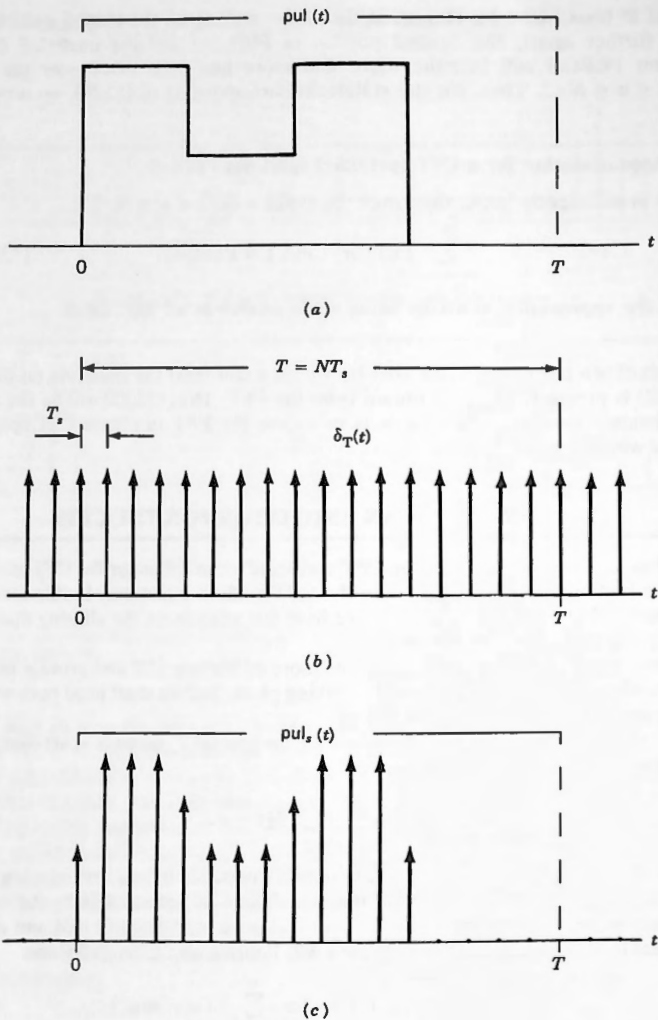
Observe that the impulses in (12.23) are not unit impulses but all have weights  $T_s$ , and so this Dirac comb differs from the one considered in Section 4.11 by the constant multiplier  $T_s$ . In order to find the CFT of  $\delta_T(t)$  we start from (4.105) and multiply both sides by  $T_s$ . Then  $\delta_T(t)$  just defined will Fourier transform as follows:

$$T_s \sum_{k=-\infty}^{\infty} \delta(t - kT_s) \Leftrightarrow 2\pi \sum_{m=-\infty}^{\infty} \delta(\omega - m\omega_s) \quad (12.24)$$

where

$$\omega_s = \frac{2\pi}{T_s}. \quad (12.25)$$

Consider next a finite-span pulse  $\text{pul}(t)$  that is assumed to lie within the time interval  $0 \leq t < T$  as shown in Figure 12.6a, and in which the parameter  $T$  and the

Figure 12.6.  $\text{pul}(t)$  and its impulse-sampled version  $\text{pul}_s(t)$ .

spacing  $T_s$  of the impulse train of (12.23) satisfy

$$T = NT_s \quad (12.26)$$

We now impulse sample  $\text{pul}(t)$  by multiplying it by  $\delta_T(t)$ . The sampled version of  $\text{pul}(t)$  that is produced in this way will be called  $\text{pul}_s(t)$  (where the subscript  $s$  designates sampled) and is depicted in Figure 12.6c. Then

$$\text{pul}_s(t) = \text{pul}(t) \times T_s \sum_{k=-\infty}^{\infty} \delta(t - kT_s) \quad (12.27)$$

There are now two ways in which we can find the CFT of  $\text{pul}_s(t)$ .

**Method A:** By the impulse sampling property we have

$$\begin{aligned} \text{pul}_s(t) &= \text{pul}(t) \times T_s \sum_{k=-\infty}^{\infty} \delta(t - kT_s) \\ &= T_s \sum_{k=-\infty}^{\infty} \text{pul}(kT_s) \delta(t - kT_s) \\ &= T_s \sum_{k=-\infty}^{\infty} \text{pul}_k \delta(t - kT_s) \end{aligned} \quad (12.28)$$

in which we have written  $\text{pul}_k$  as an abbreviation for  $\text{pul}(kT_s)$ . Then, using time-shift, we obtain the CFT of  $\text{pul}_s(t)$  as

$$\text{PUL}_s(\omega) = \frac{T}{N} \sum_{k=0}^{N-1} \text{pul}_k e^{-j\omega kT_s} \quad (12.29)$$

**Method B:**  $\text{pul}_s(t)$  has been formed by multiplication in the time domain, and so its CFT can be obtained by convolution in the frequency domain. Thus

$$\begin{aligned} \text{PUL}_s(\omega) &= \frac{1}{2\pi} \text{PUL}(\omega) * 2\pi \sum_{m=-\infty}^{\infty} \delta(\omega - m\omega_s) \\ &= \int_{-\infty}^{\infty} \text{PUL}(\Theta) \sum_{m=-\infty}^{\infty} \delta(\omega - m\omega_s - \Theta) d\Theta \\ &= \sum_{m=-\infty}^{\infty} \text{PUL}(\omega - m\omega_s) \int_{-\infty}^{\infty} \delta(\omega - m\omega_s - \Theta) d\Theta \\ &= \sum_{m=-\infty}^{\infty} \text{PUL}(\omega - m\omega_s) \end{aligned} \quad (12.30)$$

Hence a second version of the Fourier transform of  $\text{pul}_s(t)$  is

$$\text{PUL}_s(\omega) = \sum_{m=-\infty}^{\infty} \text{PUL}(\omega - m\omega_s) \quad (12.31)$$

(This result is not new to us, and was in fact derived in Chapter 9 when we examined time-domain impulse sampling.) The CFTs that we have derived by these two methods must be equal and so we can combine them, giving

$$\sum_{m=-\infty}^{\infty} \text{PUL}(\omega - m\omega_s) = \frac{T}{N} \sum_{k=0}^{N-1} \text{pul}_k e^{-j\omega kT_s} \quad (\forall \omega) \quad (12.32)$$

We now numerically sample both sides of this equation by setting  $\omega = n\omega_0$  in which it is assumed that the quantity  $\omega_0$  is related to  $\omega_s$  as shown in (12.17), namely  $\omega_0 = \omega_s/N$ . Then (12.32) becomes

$$\sum_{m=-\infty}^{\infty} \text{PUL}(n\omega_0 - m\omega_s) = \frac{T}{N} \sum_{k=0}^{N-1} \text{pul}_k e^{-jn\omega_0 kT_s} \quad (\forall n) \quad (12.33)$$

Consider now the following: Earlier in this section [see (12.25)] we had the relationship  $\omega_s = 2\pi/T_s$ , and in (12.26) we stated that  $T_s$  and  $T$  were related by  $T = NT_s$ . Then, when we sampled (12.33) we selected  $\omega_0$  so that  $\omega_0 = \omega_s/N$ . Combining all three gives us

$$\omega_0 = \frac{\omega_s}{N} = \frac{2\pi}{NT_s} = \frac{2\pi}{T} \quad (12.34)$$

and so we see that  $\omega_0$ , the sampling interval on the  $\omega$ -axis, and  $T$ , the time-domain extent of  $\text{pul}(t)$ , are related by

$$\omega_0 = \frac{2\pi}{T} \quad (12.35)$$

Returning to (12.33), on the RHS the exponential term now reduces as follows:

$$e^{-jn\omega_0 kT_s} = e^{-jnk(2\pi/T)(T/N)} = e^{-j2\pi nk/N} \quad (12.36)$$

and so (12.33) becomes

$$\sum_{m=-\infty}^{\infty} \text{PUL}(n\omega_0 - m\omega_s) = \frac{T}{N} \sum_{k=0}^{N-1} \text{pul}_k e^{-j2\pi nk/N} \quad (12.37)$$

The RHS of this equation is precisely the FFT of  $\text{pul}(t)$  multiplied by the scale factor  $T/N$ , and so we can write it as

$$\sum_{m=-\infty}^{\infty} \text{PUL}(n\omega_0 - m\omega_s) = \frac{T}{N} \text{PUL}_n \quad (\forall n) \quad (12.38)$$

Let's take a minute to examine what we have obtained:

- On the left we have the **CFT spectrum** of  $\text{pul}(t)$ , namely  $\text{PUL}(\omega)$ , which has been aliased with period  $\omega_s$  and then sampled at values of  $\omega_0 = \omega_s/N$ . We know that such a spectrum is periodic all along the  $\omega$ -axis with period  $\omega_s$ .
- On the right we have the **FFT spectrum** of  $\text{pul}(t)$ , namely  $\text{PUL}_n$ , which we know is also periodic with period  $N$  on the  $n$ -axis, and so it is periodic with period  $N\omega_0$  on the  $\omega$ -axis.

Observe that (12.38) is true for  $n$  any integer. It tells us precisely how the CFT of  $\text{pul}(t)$  and the FFT obtained from numerical samples of  $\text{pul}(t)$  are related. All of this is summarized in Theorem 12.3.

### ■ THEOREM 12.3

Let  $\text{pul}(t)$  ( $0 \leq t < T$ ) be transformed to give its CFT spectrum  $\text{PUL}(\omega)$ . Let  $\text{pul}(t)$  also be numerically sampled over  $0 \leq t < T$  at intervals of  $T_s = T/N$  to give the sequence of  $N$  samples  $\text{pul}_k$ , from which its FFT spectrum  $\text{PUL}_n$  is derived. Then  $\text{PUL}(\omega)$  and  $\text{PUL}_n$  are related as follows:

$$\sum_{m=-\infty}^{\infty} \text{PUL}(n\omega_0 - m\omega_s) = \frac{T}{N} \text{PUL}_n \quad (\forall n) \quad (12.39)$$

in which  $\omega_s = 2\pi/T_s$  and  $\omega_0 = 2\pi/T$ . Thus, if we alias  $\text{PUL}(\omega)$  with period  $\omega_s$  and then sample it at intervals of  $\omega_0 = \omega_s/N$ , the result is equal to  $\text{PUL}_n$  multiplied by the scale factor  $T/N$ .

We now recall from (12.20) that, by making  $\omega_s$  sufficiently large, we have the **restricted-range approximation**

$$\sum_{m=-\infty}^{\infty} \text{PUL}(n\omega_0 - m\omega_s) \approx \text{PUL}(n\omega_0) \quad (-N/2 \leq n \leq N/2) \quad (12.40)$$

Taken together with (12.39) this then gives us the corollary to Theorem 12.3 in the box below.

### ■ COROLLARY to Theorem 12.3

**Using the FFT to obtain estimates of a Fourier transform**

$$\text{PUL}(n\omega_0) \approx \frac{T}{N} \text{PUL}_n \quad \left( \frac{-N}{2} \leq n \leq \frac{N}{2} \right) \quad (12.41)$$

in which the estimation errors become smaller as we increase the value of  $N$ .

A brief comment on the ranges of  $n$  over which (12.39) and (12.41) are valid: As we pointed out earlier, the two spectra appearing on the opposite sides of (12.39) are

equal for  $n$  any integer from  $-\infty$  to  $\infty$ . On the other hand, in (12.41) we show a restricted range of validity. This arose when we derived (12.20), because it is only over the central range  $-N/2 \leq n \leq N/2$  that the aliased spectrum appearing on its LHS approaches the CFT spectrum  $PUL(n\omega_0)$  on the RHS. Outside of this range the two begin to diverge dramatically, the former continuing forever in a periodic manner and the latter decaying at least like  $1/\omega$ .

Equation (12.41) is the second time that we have shown that the FFT can be used to provide estimates of the CFT of a pulse. (The first was in (12.13) based on the rectangular rule.) In the next chapter we make detailed and precise statements regarding the magnitude of the estimation errors and we shall make use of both derivations that we have carried out in this chapter.

We make the following observations regarding the preceding corollary:

- (1) The FFT system on the accompanying disc enables us to do precisely what is stated there.
  - Numerical samples of a given pulse  $pul(t)$  are loaded into the **X** vector by the user. **X** is then transformed using **ANALYSIS** to produce the spectrum vector **F**.
  - Prior to displaying the numbers in **F** the system multiplies it by the scale-factor  $T/N$ . The result is a vector of values that can be used as estimates of samples of  $PUL(\omega)$ , the Fourier transform of the pulse, where the sampling points are at  $\omega = n\omega_0$ , and the range of validity is  $-N/2 \leq n \leq N/2$ .
- (2) Either by virtue of the aliasing mechanism by which the FFT numbers and the exact samples of  $F(\omega)$  are related, or else by the results of Theorem 12.1 based on rectangular-rule integration, we know that
  - The smaller we make  $T_s$ , that is, the larger we make  $\omega_s$ , the smaller will be the errors in the estimates.
  - Making  $T_s$  smaller means making  $N$  larger for a given value of  $T$ .

In the statement of Theorem 12.3 we have said that  $pul(t)$  is sampled at  $N$  points over the interval  $0 \leq t < T$ , thereby implying that it is a pulse with finite time span. As we point out in the *User's Manual* (Section 17.2), in addition to the samples taken from  $pul(t)$  itself, we must also include a number of zeros in that interval in order to obtain a satisfactory set of values for  $PUL(\omega)$ . This process is known as zero padding, or adding white space, and is discussed in detail in that section.

We also show in Chapter 17 that we can use the FFT to analyze pulses with infinite spans such as  $e^{-\beta t}U(t)$ . The previous theorem and its corollary are still the key result that we use in that process. ■

We can now quickly complete this section by extending our results to include the estimation of CFT coefficients. Let the periodic function  $per(t)$  be comprised of repeated copies of the pulse  $pul(t)$  with period  $T_0$ . Then, by Theorem 9.3 in Chapter 9, the CFT coefficients for  $per(t)$  will be given by

$$PER(n) = \frac{1}{T_0} PUL(n\omega_0) \quad (12.42)$$

Replacing  $n$  by  $n - mN$  gives

$$\text{PER}(n - mN) = \frac{1}{T_0} \text{PUL}[(n - mN)\omega_0] = \frac{1}{T_0} \text{PUL}(n\omega_0 - m\omega_s) \quad (12.43)$$

from which

$$\sum_{m=-\infty}^{\infty} \text{PER}(n - mN) = \frac{1}{T_0} \sum_{m=-\infty}^{\infty} \text{PUL}(n\omega_0 - m\omega_s) \quad (12.44)$$

and so, by (12.39) this now means that

$$\sum_{m=-\infty}^{\infty} \text{PER}(n - mN) = \frac{1}{N} \text{PUL}_n \quad (\forall n) \quad (12.45)$$

In the defining interval of the periodic function we have

$$\text{per}(t) = \text{pul}(t) \quad (0 \leq t < T_0) \quad (12.46)$$

and so, after numerical sampling,

$$\text{per}_k = \text{pul}_k \quad (0 \leq k \leq N - 1) \quad (12.47)$$

Thus the FFT spectra of these two functions are one and the same, and so (12.45) can be replaced by

$$\sum_{m=-\infty}^{\infty} \text{PER}(n - mN) = \frac{1}{N} \text{PER}_n \quad (\forall n) \quad (12.48)$$

We have thus proved Theorem 12.4 stated below.

#### ■ THEOREM 12.4

Let  $\text{per}(t)$ , a periodic function with period  $T_0$ , be transformed to give its CFT line spectrum  $\text{PER}(n)$ . Let  $\text{per}(t)$  also be numerically sampled over one period at intervals of  $T_s = T_0/N$  to give the sequence of  $N$  samples  $\text{per}_k$  from which its FFT line spectrum  $\text{PER}_n$  is derived. Then  $\text{PER}(n)$  and  $\text{PER}_n$  are related as follows:

$$\sum_{m=-\infty}^{\infty} \text{PER}(n - mN) = \frac{1}{N} \text{PER}_n \quad (\forall n) \quad (12.49)$$

Thus if we alias  $\text{PER}(n)$  with period  $N$ , the result is equal to  $\text{PER}_n$  multiplied by the scale factor  $1/N$ .

Thus the aliased CFT line spectrum of a periodic function has been shown to be equal to  $1/N$  times its FFT spectrum.

We now recall from (12.22) that when  $N$  is sufficiently large we have the restricted-range approximation

$$\sum_{m=-\infty}^{\infty} \text{PER}(n - mN) \approx \text{PER}(n) \quad \left( \frac{-N}{2} \leq n \leq \frac{N}{2} \right) \quad (12.50)$$

Taken together with (12.49) this then gives us the following corollary to Theorem 12.4.

■ COROLLARY to Theorem 12.4

Using the FFT to obtain estimates of the coefficients of a Fourier Series:

$$\text{PER}(n) \approx \frac{1}{N} \text{PER}_n \quad \left( \frac{-N}{2} \leq n \leq \frac{N}{2} \right) \quad (12.51)$$

in which the estimation errors become smaller as we increase the value of  $N$ .

Again (12.51) is not new. In (12.14) we derived it based on an approach using the rectangular rule and here we have derived it based on aliasing. In the next chapter we make some very detailed and precise statements regarding the magnitude of the estimation errors that arise from the approximation shown in (12.51), and in order to carry that out we shall need both approaches.

The FFT system on the accompanying disc also enables us to do what is stated in this corollary, and we make the following observations:

- (1) • Numerical samples of a given periodic function  $\text{per}(t)$  are loaded into the  $\mathbf{X}$  vector by the user.  $\mathbf{X}$  is then transformed using ANALYSIS to produce the spectrum vector  $\mathbf{F}$ .
- Prior to displaying the numbers of  $\mathbf{F}$ , the system multiplies it by the scale-factor  $1/N$ . The result is a vector of values that can be used as estimates of  $\text{PER}(n)$ , the CFT coefficients of the periodic function, over the range  $-N/2 \leq n \leq N/2$ .
- (2) Either by virtue of the aliasing mechanism by which the FFT numbers and the exact values of  $\text{PER}(n)$  are related, or else by the results of Theorem 12.1 based on rectangular-rule integration, we know that the smaller we make the sample spacing  $T_s$ , the smaller will be the errors in the estimates. Making  $T_s$  smaller is equivalent to making  $N$  larger.
- (3) In the case of a periodic function the interval  $T_0$  is fixed by the problem statement, and the value of  $T_s$  is simply  $T_s = T_0/N$ .

## 12.5 INVERTING CFT SPECTRA USING THE FFT

We have shown how the FFT can be used to obtain approximations for CFT spectra. We now comment on an associated problem, namely **the inversion to the time domain of CFT spectra** by the use of the FFT.

Suppose that we were given the CFT formula for either

- The coefficients of a Fourier series, PER( $n$ ), or
- a Fourier transform, PUL( $\omega$ )

and that we wished to invert it to the time domain, for example, in order to examine the original function from which it was derived. As an example we may wish to invert either of the following two CFT spectra to the time domain:

$$\text{PER}(n) = \frac{1}{2} \frac{\sin(n\pi/2)}{n\pi/2} \quad (\forall n) \quad (12.52)$$

$$\text{PUL}(\omega) = \frac{1}{5 + j\omega} \quad (\forall \omega) \quad (12.53)$$

Clearly, neither of these is an FFT spectrum—first, neither is periodic, and second, (12.53) is a function of the continuous variable  $\omega$ .

In Figure 12.7 we show a plot of what comes out of the FFT system when we inverted  $\text{Sa}(\omega/2)$  to the time domain without taking any precautions. We simply loaded it, and the system then sampled at  $\omega = n\omega_0$  for  $-N/2 \leq n \leq N/2$  in the usual way, placing those samples in  $\mathbf{F}$ . Then we ran SYNTHESIS. By contrast, in Figure 12.8 we show a plot of the same inverse, but this time using what we shall call an “alias level” of 20. The errors in  $\mathbf{Y}$  that were evident in the first approach are now largely gone (and can, in fact, be made to disappear entirely).

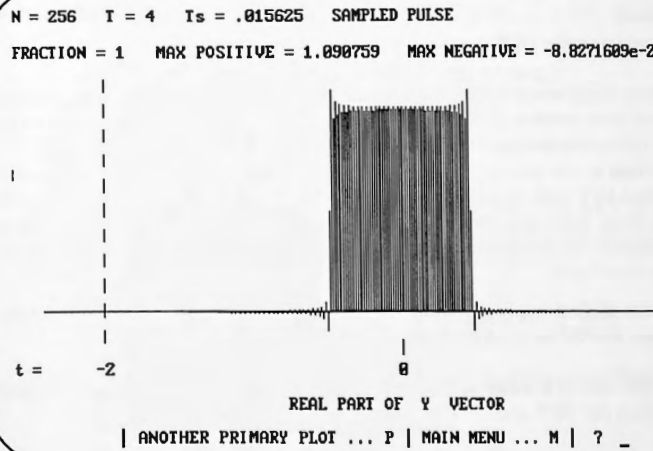


Figure 12.7. Inverse of  $\text{Sa}(\omega/2)$  without precautions.

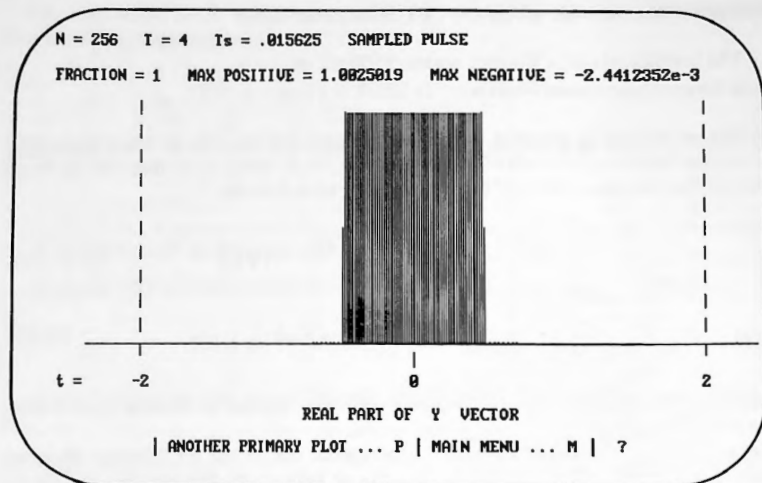


Figure 12.8. Same inverse using alias level 20.

Here's the problem. Simply extracting  $N$  numerical samples from a given formula, loading them into  $\mathbf{F}$ , and then running SYNTHESIS amounts to a **hybrid operation** in which a spectrum that was derived from the CFT analysis equation is now being

- Sampled
- Truncated
- Inverted using the DFT synthesis equation

None of these three would have been involved had we carried out the inversion as we really should have, namely, by the use of the **CFT synthesis equation**. It is thus hardly surprising that errors should be present in the end result.

One solution to the problem might be to use as large a value for  $N$  as possible, in which case the CFT and the FFT become more and more like each other. That would be a brute-force approach, however, and even then there would always be some vestigial evidence of the hybrid operation, thereby making the time-domain values numerically unreliable.

A far more elegant approach would be to start with the given CFT formula and then to create its FFT equivalent using aliasing, as follows:

- (A) For the case of **Fourier series coefficients**, we know that the exact relationship between the FFT and CFT spectra is [see (12.49)]

$$\text{PER}_n = N \sum_{m=-\infty}^{\infty} \text{PER}(n - mN) \quad (\forall n) \quad (12.54)$$

in which it is assumed that the CFT formula for  $\text{PER}(n)$  on the RHS is given. As (12.54) shows, we can produce the FFT spectrum on the left by aliasing  $\text{PER}(n)$ , which in practice comes down to performing the following summation:

$$\text{PER}_n \approx N \sum_{m=-\alpha}^{\alpha} \text{PER}(n - mN) \quad (12.55)$$

where  $\alpha$  is chosen to be suitably large, depending on how much computation time we wish to expend.

**Definition:**  $\alpha$  is called the **aliasing level** and its value specifies how many pairs of the repeated and shifted spectra shall be added to the central copy.

In the case of the example cited in (12.52) the algorithm becomes

$$\text{PER}_n \approx N \sum_{m=-\alpha}^{\alpha} \frac{1}{2} \frac{\sin[(n - mN)\pi/2]}{(n - mN)\pi/2} \quad \left( -\frac{N}{2} \leq n \leq \frac{N}{2} \right) \quad (12.56)$$

Then, once  $N$  and  $\alpha$  are selected, the summation can be carried out for each value of  $n$ . (Observe the multiplication by  $N$  on the RHS of (12.56). The system does this automatically any time the spectrum of a sampled periodic waveform is loaded, and so the user is not required to do it.) In this way we can create as good an approximation as we please for any of the values on the LHS of (12.56), starting from the given CFT formula. Care must also be taken, however, to ensure that the resulting FFT spectrum has the correct symmetries that we referred to earlier, real part even and imaginary part odd.

(B) Similarly for a Fourier transform [see (12.39)]

$$\begin{aligned} \text{PUL}_n &= \frac{N}{T} \sum_{m=-\infty}^{\infty} \text{PUL}(n\omega_0 - m\omega_s) \\ &= \frac{N}{T} \sum_{m=-\infty}^{\infty} \text{PUL}[(n - mN)\omega_0] \end{aligned} \quad (12.57)$$

in which it is assumed that we are given the CFT formula for  $\text{PUL}(\omega)$  on the RHS of (12.57). For example, starting from (12.53) we first separate out the real and imaginary parts, obtaining

$$A(\omega) = \frac{5}{5^2 + \omega^2} \quad \text{and} \quad B(\omega) = \frac{-\omega}{5^2 + \omega^2} \quad (12.58)$$

Then, considering only  $A(\omega)$ , we now replace every occurrence of  $\omega$  by  $(n - mN)\omega_0$ , obtaining

$$A[(n - mN)\omega_0] = \frac{1}{5^2 + [(n - mN)\omega_0]^2} \quad (12.59)$$

which we then sum as follows:

$$\sum_{m=-\alpha}^{\alpha} A[(n - mN)\omega_0] = \sum_{m=-\alpha}^{\alpha} \frac{1}{5^2 + [(n - mN)\omega_0]} \quad (12.60)$$

Once  $\omega_0$ ,  $N$ , and  $\alpha$  have been selected, the summation can be carried out for each value of  $n$ , with a similar summation being carried out for  $B(\omega)$ . From (12.57) we can then write

$$PUL_n \approx \frac{N}{T} \left[ \sum_{m=-\alpha}^{\alpha} A[(n - mN)\omega_0] + j \sum_{m=-\alpha}^{\alpha} B[(n - mN)\omega_0] \right] \quad (12.61)$$

If we have selected  $\alpha$  to be sufficiently large, the result shown in (12.61) will be a very close approximation to the required  $n$ th FFT spectral element. (Observe the multiplication by  $N/T$  on the RHS of (12.61), something which the system does automatically for us whenever we load the FFT spectrum of a sampled pulse.) Again, care must be taken to ensure that the FFT spectrum that has been created in this way has the correct symmetries, real part even and imaginary part odd. ■

In either case, periodic or pulse, using aliasing in this way we can create as good an approximation as we desire for the corresponding FFT spectrum. Thereafter the FFT operation SYNTHESIS can be run, and if we have made  $\alpha$  large enough and selected our other parameters appropriately, a very satisfactory presentation will be obtained of a sampled version of the original time-domain waveform from which the CFT formula originated. Numerically, these results can be made as accurate as we want them to be by making  $N$  and  $\alpha$  sufficiently large, of course at the cost of computation time.<sup>†</sup>

Keeping in mind the time-domain periodicity of the FFT, when inverting a CFT (pulse) spectrum care must especially be taken with the selection of  $T$  in order to ensure that the waveform that is produced in this way is not aliased in the time domain.

The FFT system on the accompanying disk enables us to carry out these operations, and whenever the expression for a CFT spectrum is loaded into F, the user is prompted for a value of the aliasing level,  $\alpha$ . The aliasing summations are then carried out.

All of this is discussed in further detail in the *User's Manual* in Chapter 17, where we also discuss how the required symmetries of the FFT spectrum are created.

<sup>†</sup>The author has run aliasing calculations with values of  $\alpha$  up to 2,000,000 in order to satisfy himself that the errors in the inverted waveform can be made as small as we please. In this instance, the RMS error computed across the entire result was less than 1e-6. The aliasing computation with  $\alpha = 2e6$  took 60 hours on a 486/60.

---

**EXERCISES**


---

**12.1** Use the rectangular rule to find the area under

$$y = t^2 \quad \text{from } t = 0 \quad \text{to } t = 1$$

Set up the approximation according to (12.8) and then let  $N$  tend to infinity. Verify that you obtain the correct answer of  $\frac{1}{3}$ .

**12.2** Repeat Exercise 1 to find the area under

$$y = e^t \quad \text{from } t = 0 \quad \text{to } t = 1$$

After letting  $N$  tend to infinity, you should get the correct answer  $e - 1$ .

**12.3** Derive the results shown in Theorem 12.2 by repeating the steps used for Theorem 12.1, but this time applying them to a periodic function  $f_p(t)$ .

**12.4** (a) Apply the rectangular rule to find the Fourier coefficients for the following periodic function:

$$f_p(t) = 1 \quad (0 < t < 4), \quad f_p(t + 8) = f_p(t)$$

*Hint:* Remember to use half-values at the discontinuities. Divide the period into eight sampling intervals and verify that you obtain the following:

$$\begin{aligned} F_p(0) &= \frac{1}{2}, & F_p(1) &= \frac{-j(1 + \sqrt{2})}{8}, & F_p(2) &= 0, \\ F_p(3) &= \frac{j(1 - \sqrt{2})}{8}, & F_p(4) &= 0 \end{aligned}$$

- (b) Using the symmetry properties of the DFT, write down the remaining coefficients.  
 (c) Verify your results using the FFT system.

**12.5** (a) Apply the rectangular rule to find values for the Fourier transform of the following pulse:

$$f(t) = t \quad (0 < t < 4)$$

Remember to use half-values at any discontinuities. Use  $T = 8$  and divide the range of integration into eight sampling intervals. Verify that you obtain:

$$\begin{aligned} F(0) &= 8, & F(\omega_0) &= -(2 + \sqrt{2}) - j2(1 + \sqrt{2}), & F(2\omega_0) &= j2, \\ F(3\omega_0) &= (\sqrt{2} - 2) + j2(1 - \sqrt{2}), & F(4\omega_0) &= 0 \end{aligned}$$

where  $\omega_0 = \pi/4$ .

- (b) Using the symmetry properties of the DFT, write down the remaining coefficients.  
 (c) Verify your results using the FFT system.

- 12.6 Load the following spectrum into  $\mathbf{F}$  starting from main-menu A. Use  $N = 256$ , SAMPLED,  $T = 4$ , PULSE.

$$F(\omega) = \frac{\omega \sin(\omega) + 1 - \cos(\omega)}{\omega^2} + j \frac{\omega \cos(\omega) - \sin(\omega)}{\omega^2}$$

Use an alias level of zero and then run it again with 20. There will be a division-by-zero error for  $A(\omega)$ . Use  $A(0) = 1.5$  or else let the system find its value for you. (The value 1.5 can be obtained by l'Hôpital's rule.) Now run SYNTHESIS and plot  $\mathbf{Y}$ .

You will observe the following:

- With  $\alpha = 0$ , ringing is present before and after the discontinuity.
- With  $\alpha = 20$ , most of the ringing has been removed
- With higher values of  $\alpha$ , the ringing can be removed entirely

- 12.7 Use the FFT system to invert the spectrum

$$F(\omega) = \frac{1}{1 + j\omega} \quad (12.62)$$

following the method described in Section 12.5. Use  $N = 256$ . Initially use  $T = 2$  and  $\alpha = 0$ . Compare numbers from the inverted pulse to the original pulse whose inverse you can obtain analytically from (12.62). You will find that there are two sources of error present:

- (1) The inverted pulse has an infinite span, and yet here we are trying to force it into a window that is 2 seconds wide, by which time it has only died down to about 13 percent of its maximum value. Thus there is significant time-domain aliasing present caused by the copies from the periodic extension interacting with each other.
- (2) You will also observe significant ringing immediately before and after the discontinuity. Since we have used  $\alpha = 0$ , it means that the spectrum that we are inverting is the CFT version that (i) has been truncated by taking 256 samples, and (ii) is then being inverted using the DFT inversion equation, both of which give rise to the ringing and to numerical errors.

To fix these two problems:

- (a) Increase the value of  $T$  to, say, 10, which means that the pulse will have died down to about 0.005 percent of its maximum value at the end of the window, thereby significantly reducing the time-domain aliasing.
- (b) Increase the value of  $\alpha$  to 5, then repeat with 20 and then 50. Because the spectrum (12.62) is dying out only like  $1/\omega$ , you will find that it takes a great deal of frequency-domain aliasing in (12.61) to convert the CFT spectrum to a DFT version that inverts to a waveform that is free of ringing.

12.8 We can alias a value from a CFT spectrum by hand to produce its FFT counterpart, as the following shows. Consider the pulse  $f(t)$  whose analytical definition is

$$f(t) = \begin{cases} 4 + 4t + t^2 & (-2 < t < -1) \\ 2 - t^2 & (-1 < t < 1) \\ 4 - 4t + t^2 & (1 < t < 2) \end{cases} \quad (12.63)$$

- (a) Sketch  $f(t)$  and verify that it is continuous everywhere up to and including its first derivative. Hence we can expect that its Fourier transform will die out like  $1/\omega^3$ .

(b) Verify that

$$F(\omega) = (4/\omega^3)[2\sin(\omega) - \sin(2\omega)] \quad (12.64)$$

- (c) Load this pulse into  $\mathbf{X}$  starting from (12.63) using  $N = 256$  and  $T = 8$ , and verify that the FFT's estimate of  $F(\omega)$  at  $\omega = 23\omega_0$  is

$$F_{23} = -2.8095879e-4 \quad (12.65)$$

where  $\omega_0 = 2\pi/T = \pi/4$ . Then (12.65) is the exact DFT value of  $F_{23}$  for this pulse.

- (d) Verify that (12.64) gives

$$F(23\omega_0) = -2.8108077e-4 \quad (12.66)$$

which of course differs from (12.65). Thus simply sampling (12.64) over  $-N/2 \leq n \leq N/2$  and loading the results into  $\mathbf{F}$  would give us incorrect values for the DFT spectrum.

- (e) We can convert the CFT values from (12.65) to their FFT values as follows. Starting from

$$\frac{T}{N} F_n = \sum_{m=-\alpha}^{\alpha} F[(n-mN)\omega_0] \quad (\forall n) \quad (12.67)$$

we know that (12.66) can be moved closer to the FFT value in (12.65), depending on how large a value we use for  $\alpha$ . By summing the RHS of (12.67) using  $n = 23$  and  $N = 256$ , verify the results in the following table, showing how successively larger values of  $\alpha$  are leading to the value shown in (12.65).

$\alpha$	Value of RHS
0	$-2.8108078e-4$
1	$-2.8096789e-4$
2	$-2.8096098e-4$
3	$-2.8095962e-4$
4	$-2.8095919e-4$
5	$-2.8095901e-4$

*Note:* We deliberately selected a pulse whose Fourier transform goes to zero very quickly in order to display the convergence of the RHS of (12.67). In general the rate of convergence will not be as fast as this and we shall have to use much larger values for  $\alpha$ .

- (f) Use the FFT system to invert the spectrum

$$F(\omega) = (4/\omega^3)[2\sin(\omega) - \sin(2\omega)]$$

following the method described in Section 12.5. Use

$$N = 256 \quad \text{and} \quad T = 8.$$

- (1) Use values for  $\alpha$  of 0, 1, 2, 3, 4, and 5 and verify all of the values in (e).
- (2) Compare numbers from the inverted pulse to the original pulse in (12.63). You will see that very small values of  $\alpha$  will give a very satisfactory result because the CFT spectrum is converging so quickly.

# The Errors in Fast Fourier Transform Estimation

## 13.1 INTRODUCTION

---

We have shown in the preceding chapter that the fast Fourier transform (FFT) is related to its continuous Fourier transform (CFT) counterparts by the following alias statements:

- For pulses

$$\sum_{m=-\infty}^{\infty} F[(n - mN)\omega_0] = \frac{T}{N}F_n \quad (\forall n) \quad (13.1)$$

- For periodic functions

$$\sum_{m=-\infty}^{\infty} F_p(n - mN) = \frac{1}{N}F_n \quad (\forall n) \quad (13.2)$$

In these two equations the symbols have the following meanings:

- $F(\omega)$  is the CFT of a pulse  $f(t)$ , which has a finite span that lies in the range  $0 \leq t \leq T$
- $F_p(n)$  is the CFT transform of a periodic function  $f_p(t)$
- $F_n$  is the FFT spectrum obtained by taking  $N$  samples from either  $f(t)$  over  $0 \leq t < T$  or from  $f_p(t)$  over one period

The author is indebted to Professor R. I. Becker of the University of Cape Town for extensive conversation regarding the material in this chapter. A version has been submitted to a technical journal under their joint names.

Based on (13.1) we then derived the following estimation statements:

- For  $F(\omega)$

$$F(n\omega_0) \approx \frac{T}{N} F_n \quad \left( -\frac{N}{2} \leq n \leq \frac{N}{2} \right) \quad (13.3)$$

- For  $F_p(n)$

$$F_p(n) \approx \frac{1}{N} F_n \quad \left( -\frac{N}{2} \leq n \leq \frac{N}{2} \right) \quad (13.4)$$

Certain empirical rules have been devised for bounding the errors in these estimates (see, e.g., Walker). In this chapter we show that algebraic formulas can be derived that give the relative errors exactly when FFT estimation is performed for a certain class of pulse or periodic functions.

For functions that are outside of this class<sup>†</sup> we show that the same algebraic error formulas hold in an asymptotic sense. We also show that the estimation errors can be reduced by appropriately positioning the FFT sampling points.

## 13.2 THE ERRORS IN THE ESTIMATES

---

The relative error in an estimate is defined by

$$\text{Relative error} = \frac{\text{estimate} - \text{exact}}{\text{exact}} \quad (13.5)$$

For the present case we thus have the relative error for pulses as

$$E_N(n) = \frac{\sum_{m=-\infty}^{\infty} F[(n-mN)\omega_0] - F(n\omega_0)}{F(n\omega_0)} \quad (13.6)$$

and for periodic functions as

$$E_N(n) = \frac{\sum_{m=-\infty}^{\infty} F_p(n-mN) - F_p(n)}{F_p(n)} \quad (13.7)$$

For the case  $m = 0$  the numerators in (13.6) and (13.7) are zero. Moreover, the denominators do not depend on  $m$ . Thus they can be restated as follows.

<sup>†</sup>Always assuming that such functions are CFT transformable.

For pulses:

$$E_N(n) = \sum_{\substack{m=-\infty \\ m \neq 0}}^{\infty} \frac{F[(n - mN)\omega_0]}{F(n\omega_0)} \quad \left( \frac{-N}{2} \leq n \leq \frac{N}{2} \right) \quad (13.8)$$

For periodic functions:

$$E_N(n) = \sum_{\substack{m=-\infty \\ m \neq 0}}^{\infty} \frac{F_p(n - mN)}{F_p(n)} \quad \left( \frac{-N}{2} \leq n \leq \frac{N}{2} \right) \quad (13.9)$$

In what follows we assume that the denominators of (13.8) and (13.9) are nonzero.

### 13.3 CANONICAL PULSES AND ORDER OF CONTINUITY

**Definition:** Let a pulse that is to be FFT-transformed have a  $(k + 1)$ -th derivative that consists of only Dirac deltas, each of which would coincide with a sampling instant. Then such a pulse will be said to be **canonical- $k$** .

*Note:* As always, it is assumed that the sampling of the pulse is left-endpoint uniform, and that wherever a sampling instant coincides with a discontinuity in the pulse the value sent to the FFT is the average of the values immediately on each side of it. (We have been referring to these as the half-values.) The value sent to the FFT for the sample at  $t = 0$  is the average of  $f(0)$  and  $f(T)$ .

In Figure 13.1 we show an example of a canonical-0 pulse. The first derivative of this pulse consists of only Dirac deltas. Since every discontinuity lies at a sampling instant, it follows that each of the Dirac deltas in the first derivative would coincide with an FFT sampling instant. Thus the pulse is indeed canonical-0.

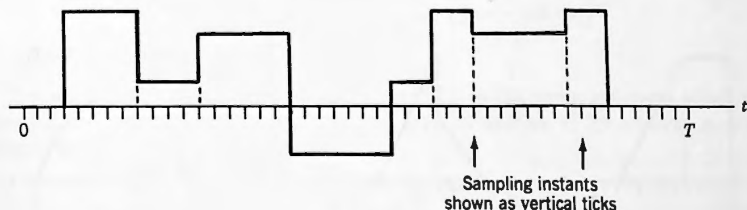


Figure 13.1. Canonical-0 pulse.

**EXAMPLE 13.1:** Every Rect pulse whose endpoints lie at an FFT sampling instant is canonical-0. □

In Figure 13.2 we show an example of a canonical-1 pulse. The first derivative of this pulse is canonical-0 and the second derivative consists of only Dirac deltas. For the pulse shown, each of those Dirac deltas would coincide with an FFT sampling instant. The pulse is thus canonical-1.

In Figure 13.3 we show three examples of noncanonical pulses. The first pulse has a first-degree section and a discontinuity. The second has two first-degree sections and a discontinuity. The third has a sinusoidal section. No derivative of any of these three pulses would consist of only Dirac deltas.

Any periodic function  $f_p(t)$  can be regarded as a periodic repetition of a one-time pulse  $f(t)$  defined over  $0 \leq t \leq T$ , and so, depending on the properties of  $f(t)$ , we can also talk of a periodic function as being canonical- $k$ .

If any of the discontinuities in the pulse in Figure 13.1 did not coincide with a sampling instant, then the pulse would not be canonical-0. Similarly for the pulse in Figure 13.2, if any of its break points (changes from ramps to constants) did not coincide with a sampling instant, then the pulse would not be canonical-1.

We now introduce a second concept, called the **order of continuity**, something that we are already familiar with from Chapter 2.

**Definition:** Let a pulse be everywhere continuous up to and including its  $(k - 1)$ -th derivative, but let its  $k$ th derivative be discontinuous. Then such a pulse will be said to be **continuous of order  $k$** , or simply **continuous- $k$** .

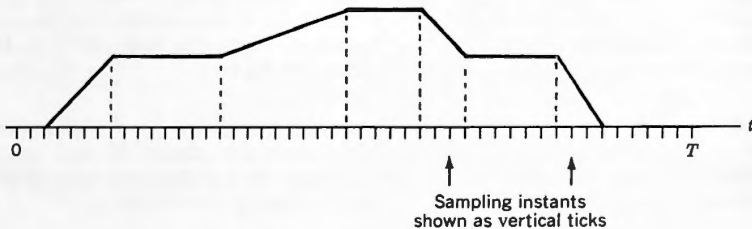


Figure 13.2. A canonical-1 pulse.

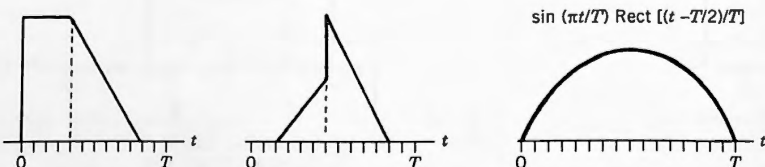


Figure 13.3. Three noncanonical pulses.

**EXAMPLE 13.2**

- Rect pulses are continuous-0.
- Canonical- $k$  pulses are continuous- $k$ .
- The three noncanonical pulses shown in Figure 13.3 have orders of continuity as follows:
  - Pulses 1 and 2 are continuous-0
  - Pulse 3 is continuous-1
- Every pulse that is continuous-0 has a Fourier transform that dies out like  $1/\omega$ .
- Every pulse that is continuous-1 has a Fourier transform that dies out like  $1/\omega^2$ .

□

**13.4 THE ERROR EXPRESSIONS**

**Case I, pulses:** Consider first a canonical- $k$  pulse  $f(t)$  whose  $(k + 1)$ -th derivative consists of  $r$  Dirac deltas, and assume that an FFT spectrum has been derived from it. As always, the length of the vector of samples submitted to the FFT is  $N$ .

We need to find the CFT of  $f(t)$ , and so we differentiate it  $k + 1$  times obtaining

$$f^{(k+1)}(t) = \sum_{i=1}^r \mu_i \delta(t - g_i T_s) \quad (13.10)$$

in which  $\mu_i$  is the weight of the  $i$ th Dirac delta,  $T_s$  is the FFT sampling interval,  $g_i T_s$  is the instant at which the  $i$ th Dirac delta is located, and each  $g_i$  is an integer in the range 0 to  $N - 1$  inclusive. CFT transformation of (13.10) then gives

$$F(\omega) = \frac{1}{(j\omega)^{k+1}} \sum_{i=1}^r \mu_i e^{-j\omega g_i T_s} \quad (13.11)$$

Using (13.11) in (13.8) we now obtain

$$E_N(n) = \sum_{\substack{m=-\infty \\ m \neq 0}}^{\infty} \frac{(jn\omega_0)^{k+1}}{\sum_{i=1}^r \mu_i e^{-jn\omega_0 g_i T_s}} \frac{\sum_{i=1}^r \mu_i e^{-j(n-mN)\omega_0 g_i T_s}}{[j(n-mN)\omega_0]^{k+1}} \quad (13.12)$$

—A—

The expression  $mN\omega_0 g_i T_s$  appearing in (13.12) in the upper summand, which we have marked with an A, will always be an integral multiple of  $2\pi$  because  $g_i$  is an integer, and so

$$mN\omega_0 g_i T_s = mg_i N \frac{2\pi}{T} \frac{T}{N} = mg_i 2\pi \quad (13.13)$$

From this it follows that  $e^{jmN\omega_0 g_i T_s} = 1$ , and so (13.12) will always simplify to

$$E_N(n) = \sum_{m=-\infty}^{\infty} \frac{(jn\omega_0)^{k+1}}{\sum_{i=1}^r \mu_i e^{-jn\omega_0 g_i T_s}} \frac{\sum_{i=1}^r \mu_i e^{-jn\omega_0 g_i T_s}}{[j(n - mN)\omega_0]^{k+1}} \quad (13.14)$$

Cancellations will now take place and the end result will be

$$E_N(n) = \sum_{m=-\infty}^{\infty} \frac{n^{k+1}}{(n - mN)^{k+1}} \quad \left( \frac{-N}{2} \leq n \leq \frac{N}{2} \right) \quad (13.15)$$

**Case II, periodic functions:** Consider next any periodic function

$$f_p(t) = f(t) \quad (0 \leq t < T_0) \quad f_p(t + T_0) = f_p(t) \quad (13.16)$$

Thus we are assuming that the defining pulse of  $f_p(t)$  is  $f(t)$ . Let  $f(t)$  be canonical- $k$  and let it transform to  $F(\omega)$ , and assume that an FFT spectrum has been derived from it.

We need to find the expression for its CFT coefficients, and so we proceed as we did with the pulse in (13.10) and (13.11), obtaining

$$F_p(n) = \frac{1}{T_0} F(n\omega_0) = \frac{1}{T_0 (jn\omega_0)^{k+1}} \sum_{i=1}^r \mu_i e^{-jn\omega_0 g_i T_s} \quad (13.17)$$

Then, using (13.9) and following the previous argument for pulses again leads to (13.15), and so, for  $E_N(n)$  for either pulses or periodic functions to have the form shown in (13.15) it is sufficient that the pulse be canonical- $k$ . (We believe that it is also necessary that the pulse be canonical- $k$ , but we do not offer a proof of that fact.) All of this is summarized as Theorem 13.1.

### ■ THEOREM 13.1

Let either a pulse  $f(t)$  or a periodic function  $f_p(t)$ , whose single-period defining function is  $f(t)$ , be sampled and transformed using the FFT, and let the spectrum so derived be used as an estimate of the CFT spectrum of  $f(t)$  or  $f_p(t)$ , as the case may be. Then the error in the  $n$ th spectral estimate will be given by (13.15) if  $f(t)$  is canonical- $k$ .

## 13.5 SOME PROPERTIES OF $E_N(n)$

For  $k = 0$ , (13.15) becomes

$$E_N(n) = \sum_{m=-\infty}^{\infty} \frac{n}{n - mN} \quad \left( \frac{-N}{2} \leq n \leq \frac{N}{2} \right) \quad (13.18)$$

This is the expression for the errors incurred in using the FFT to estimate values for a CFT spectrum when the pulse is canonical-0. Observe that (13.18) is valid only over the restricted range shown, outside of which the FFT spectrum repeats periodically, whereas in general the CFT spectrum is not periodic and so the two begin to diverge dramatically.

In order to assess the rate of convergence of the series appearing in (13.18) we proceed as follows. Define the quantity  $Z$  by

$$Z = \frac{n}{N} \quad (13.19)$$

Observe that if we divide the statement  $-N/2 \leq n \leq N/2$  by  $N$ , we obtain  $-\frac{1}{2} \leq Z \leq \frac{1}{2}$ , which can then be written as  $|Z| \leq \frac{1}{2}$ .

Equation (13.18) can now be rearranged as follows:

$$\begin{aligned} \sum_{\substack{m=-\infty \\ m \neq 0}}^{\infty} \frac{n}{n - mN} &= \sum_{\substack{m=-\infty \\ m \neq 0}}^{\infty} \frac{Z}{Z - m} = \sum_{m=1}^{\infty} \left[ \frac{Z}{Z - m} + \frac{Z}{Z + m} \right] \\ &= \sum_{m=1}^{\infty} \frac{2Z^2}{Z^2 - m^2} \quad (|Z| \leq \frac{1}{2}) \end{aligned} \quad (13.20)$$

from which we see that the terms in the series die out like  $1/m^2$ , and so convergence is guaranteed (something that we knew intuitively anyway). Repeating this process for each of  $k = 0, 1, 2, 3$  gives us the following results:

Canonical-0:

$$\sum_{\substack{m=-\infty \\ m \neq 0}}^{\infty} \frac{Z}{Z - m} = \sum_{m=1}^{\infty} \frac{2Z^2}{Z^2 - m^2} \quad (|Z| \leq \frac{1}{2}) \quad (13.21)$$

Canonical-1:

$$\sum_{\substack{m=-\infty \\ m \neq 0}}^{\infty} \frac{Z^2}{(Z - m)^2} = \sum_{m=1}^{\infty} \frac{2Z^2(Z^2 + m^2)}{(Z^2 - m^2)^2} \quad (|Z| \leq \frac{1}{2}) \quad (13.22)$$

Canonical-2:

$$\sum_{\substack{m=-\infty \\ m \neq 0}}^{\infty} \frac{Z^3}{(Z - m)^3} = \sum_{m=1}^{\infty} \frac{2Z^3(Z^3 + 3Zm^2)}{(Z^2 - m^2)^3} \quad (|Z| \leq \frac{1}{2}) \quad (13.23)$$

Canonical-3:

$$\sum_{\substack{m=-\infty \\ m \neq 0}}^{\infty} \frac{Z^4}{(Z - m)^4} = \sum_{m=1}^{\infty} \frac{2Z^4(Z^4 + 6Z^2m^2 + m^4)}{(Z^2 - m^2)^4} \quad (|Z| \leq \frac{1}{2}) \quad (13.24)$$

From these four statements we can infer the following regarding the error expressions for canonical- $k$  pulses:

- Their series converge like  $1/m^2$  for  $k = 0, 1$ , and like  $1/m^4$  for  $k = 2, 3$ .
- The errors resulting from canonical pulses are all real.
- The errors resulting from all canonical pulses are precisely zero when  $n = 0$ , regardless of the value of  $N$ .
- The errors are all negative for  $k$  even, and positive for  $k$  odd.
- The error expressions are all even in  $Z$  (and hence even in  $n$ ).

### 13.6 THE LOG-LINEAR Z-CURVES

---

We now consider how to carry out the summation in (13.15), which we restate here in terms of  $Z$  as

$$E(Z, k) = \sum_{\substack{m=-\infty \\ m \neq 0}}^{\infty} \frac{Z^{k+1}}{(Z - m)^{k+1}} \quad (13.25)$$

First, it can be shown by the use of residue theory from complex analysis (see, e.g., Ahlfors or MacRobert) that

$$\sum_{m=1}^{\infty} \frac{2Z^2}{Z^2 - m^2} = \pi Z \cot(\pi Z) - 1 \quad (13.26)$$

The LHS of this equation is the same as the RHS of (13.20), and so it follows that

$$\sum_{m=-\infty}^{\infty} \frac{Z}{Z - m} = \pi Z \cot(\pi Z) \quad (13.27)$$

from which

$$\sum_{m=-\infty}^{\infty} \frac{1}{Z - m} = \pi \cot(\pi Z) \quad (13.28)$$

Differentiation of (13.28) with respect to (wrt)  $Z$  now gives us

$$\sum_{m=-\infty}^{\infty} \frac{1}{(Z - m)^2} = \frac{\pi^2}{\sin^2(\pi Z)} \quad (13.29)$$

after which repeated differentiation wrt  $Z$  gives

$$\sum_{m=-\infty}^{\infty} \frac{1}{(Z - m)^3} = \frac{\pi^3 \cot(\pi z)}{\sin^2(\pi Z)} \quad (13.30)$$

$$\sum_{m=-\infty}^{\infty} \frac{1}{(Z - m)^4} = \frac{\pi^4 [1 + 3 \cot^2(\pi z)]}{3 \sin^2(\pi Z)} \quad (13.31)$$

and so on. These formulas now give us Theorem 13.2.

**■ THEOREM 13.2: The closed-form error expressions**

**Canonical-0:** From (13.27)

$$E(Z, 0) = \sum_{\substack{m=-\infty \\ m \neq 0}}^{\infty} \frac{Z}{Z - m} = \pi Z \cot(\pi Z) - 1 \quad \left( |Z| \leq \frac{1}{2} \right) \quad (13.32)$$

**Canonical 1:** From (13.29)

$$E(Z, 1) = \sum_{\substack{m=-\infty \\ m \neq 0}}^{\infty} \frac{Z^2}{(Z - m)^2} = \frac{(\pi Z)^2}{\sin^2(\pi Z)} - 1 \quad \left( |Z| \leq \frac{1}{2} \right) \quad (13.33)$$

**Canonical-2:** From (13.30)

$$E(Z, 2) = \sum_{\substack{m=-\infty \\ m \neq 0}}^{\infty} \frac{Z^3}{(Z - m)^3} = \frac{(\pi Z)^3 \cot(\pi Z)}{\sin^2(\pi Z)} - 1 \quad \left( |Z| \leq \frac{1}{2} \right) \quad (13.34)$$

**Canonical-3:** From (13.31)

$$E(Z, 3) = \sum_{\substack{m=-\infty \\ m \neq 0}}^{\infty} \frac{Z^4}{(Z - m)^4} = \frac{(\pi Z)^4 [1 + 3 \cot^2(\pi Z)]}{3 \sin^2(\pi Z)} - 1 \quad \left( |Z| \leq \frac{1}{2} \right) \quad (13.35)$$

In Figure 13.4 we show plots of  $E(Z, 0)$  through  $E(Z, 3)$  for  $0 \leq Z \leq \frac{1}{2}$ , obtained from these closed-form expressions, using a logarithmic vertical scale and a linear horizontal scale. The values for  $E(Z, 0)$  and  $E(Z, 2)$  are negative, and so we have shown their magnitudes in the plots. To see how to make use of these log-linear Z curves we consider the following two simple examples.

**EXAMPLE 13.3:** For any periodic function whose FFT-derived spectrum is canonical-0, find the error in the FFT's estimate of  $F_p(n)$  when  $n = 53$  and  $N = 1024$ .

**Solution:** We note that the value of  $T_0$  is not involved in using the error curves for periodic functions. All that we require is that they be canonical and of course we must be given the values of  $n$  and  $N$ . In this case

$$Z = \frac{n}{N} = \frac{53}{1024} = 0.05176 \approx 0.052$$

and so, entering the horizontal axis in Figure 13.4 at  $Z = 0.052$ , we obtain the relative error in  $F_p(n)$  from the  $E(Z, 0)$  line as about 0.9 percent in magnitude. The formula value from (13.32) is -0.883 percent.  $\square$

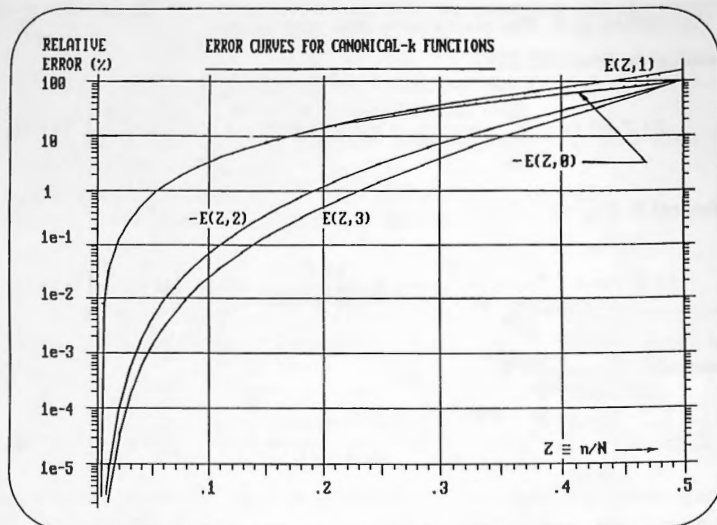


Figure 13.4.

■ **EXAMPLE 13.4:** For a canonical-0 pulse, find the error in the estimate of  $F(\omega)$  at  $\omega = 240$ , assuming that  $N = 2000$  and  $T = 5$ .

**Solution:** For pulses we require the value of  $T$ . In this case  $\omega_0 = 2\pi/T = 2\pi/5$ , and so  $\omega = 240$  corresponds to  $n = 240/\omega_0 = 190.986$ , which is closest to  $n = 191$ . Then  $Z = n/N = 191/2000 = 0.0955 \approx 0.096$ .

Entering the horizontal axis in Figure 13.4 at  $n/N = 0.096$ , we obtain the relative error in  $F(\omega)$  for  $\omega = 240$  from the canonical-0 line as about 3 percent in magnitude. Formula (13.32) gives -3.018 percent. □

Here are some observations that we can make:

- (1) The values of the  $E(Z, 1)$  plot are always **slightly larger** than those of the  $E(Z, 0)$ , as we see from Figure 13.4 and Table 13.1. This is a surprising result since the CFT spectra of canonical-1 pulses die out like  $1/\omega^2$ , whereas for canonical-0 ones they die out like  $1/\omega$ , and so one might have thought that the aliasing effect in (13.1), and hence also the errors in (13.3) for canonical-1 pulses would have been less. However, we see that they are in fact greater.
- (2) If  $n$  is preselected to have a specific value independent of  $N$ , then  $Z = n/N$  can be made arbitrarily small simply by making  $N$  sufficiently large. Since the error curves all decrease monotonically to zero with decreasing  $Z$ , this then means that the error in the  $n$ th estimate for fixed  $n$  can be made as small as we please. If we select  $n$  to be a given fraction of  $N$ , however, then  $Z = n/N$

TABLE 13.1

Z	$E(Z, 0)$ (%)	$E(Z, 1)$ (%)
0.05	0.8238	0.8265
0.1	3.3117	3.3558
0.15	7.5142	7.7429
0.2	13.5194	14.2674

TABLE 13.2

$n/N$	$E(Z, 0)$ (%)	$E(Z, 1)$ (%)	$E(Z, 2)$ (%)	$E(Z, 3)$ (%)
0.5	100	146.740	100	102.936

is a fixed number, and no matter how large we make  $N$  the error in the  $n$ th estimate will be fixed at the value obtained from the appropriate error curve. Thus for  $n = N/2$  the errors are as shown in Table 13.2. No matter how large we make  $N$  the relative errors will always be as shown.

- (3) While the  $E(Z, 3)$  curve in Figure 13.4 lies below  $E(Z, 2)$  over most of the range, they cross at  $n/N \approx 0.49192$  and end up as shown in Table 13.2 with  $E(Z, 3)$  slightly higher than  $E(Z, 2)$ .

### 13.7 ASYMPTOTIC BEHAVIOR OF NONCANONICAL FUNCTIONS

Thus far we have considered only canonical functions, either pulses or periodic waveforms, and we have seen how error curves can be derived for them.

Suppose now that we have a noncanonical function that has one or more discontinuities. Let it be made up piecewise from sections with a variety of analytical definitions, with all points of change from one such section to another (which we call the break points) located at sampling instants. Then Theorem 13.3 can be shown to hold. The proof is beyond the level assumed for this text and so we omit it, merely demonstrating the proposition by considering an example. (Proof is given in the paper referred to on the first page of this chapter.)

#### ■ THEOREM 13.3

Let  $f(t)$  be piecewise continuous of order zero and twice continuously differentiable on each interval of continuity, and let it be zero outside the range  $0 \leq t \leq T$ . Let all of its discontinuities lie at FFT sampling instants. Let  $E_N(Z)$  denote the relative error in the FFT's estimate of  $F(n\omega_0)$  when a vector of samples of length  $N$  is sent to the FFT. Finally, assume that  $F(n\omega_0) \neq 0$ . Then for constant  $Z$ ,

$$\lim_{N \rightarrow \infty} E_N(Z) = E(Z, 0) \quad (13.36)$$

The result contained in the theorem is significant. What it tells us is that when a pulse or periodic function of continuity order zero is noncanonical, we can still use the error expression  $E(Z, 0)$  that we derived earlier. Here the errors are not given exactly by that formula, however, but are given by it approximately with the accuracy of the approximation becoming steadily better as  $N$  is increased.

The reader might argue that as  $N$  is increased we know that the errors themselves go to zero, and so we do not require an error curve to give us their values. That is only true, however, in the sense that we pointed out earlier, which we restate here.

The error in the  $n$ th spectral element becomes steadily smaller with increasing  $N$  only if  $n$  is preselected and then kept fixed. If the ratio  $Z = n/N$  is kept fixed, however, then as we increase  $N$ , Theorem 10.3 is applicable. The error in the  $n$ th estimate does not then go to zero, but tends instead to the value given by  $E(Z, 0)$  as  $N$  tends to infinity.

*Note:* We have stated the theorem in terms of pulses. Just like Theorem 13.1, it applies also for periodic functions.

□EXAMPLE 13.5: Consider the noncanonical pulse of continuity order zero, shown in Figure 13.5, in which we assume that both  $T_1 = g_1 T_s$  and  $T_2 = g_2 T_s$  are FFT sampling points, and so both  $g_1$  and  $g_2$  are integers. Using successive differentiation we find its Fourier transform as

$$F(\omega) = \frac{1 - e^{-j\omega g_1 T_s} - j\omega e^{-j\omega g_2 T_s}}{(j\omega)^2}$$

Forming the error function (13.8) now gives us  $E_N(n)$ , which is the quotient of the following two terms:

Term 1:

$$\sum_{\substack{m=-\infty \\ m \neq 0}}^{\infty} \frac{1 - e^{-j(n-mN)\omega_0 g_1 T_s} - [j(n-mN)\omega_0] e^{-j(n-mN)\omega_0 g_2 T_s}}{[j(n-mN)\omega_0]^2} \overbrace{P}^{P}$$

Term 2:

$$\frac{1 - e^{-jn\omega_0 g_1 T_s} - [jn\omega_0] e^{-jn\omega_0 g_2 T_s}}{(jn\omega_0)^2} \overbrace{Q}^{Q}$$

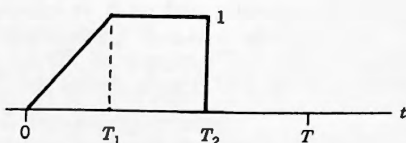


Figure 13.5.

Even though  $mN\omega_0 g_1 T_s$  and  $mN\omega_0 g_2 T_s$  appearing in the exponentials above are integral multiples of  $2\pi$ , the cancellations that earlier led to (13.15) cannot now take place because of the terms  $j(n - mN)\omega_0$  labeled  $P$  and  $jn\omega_0$  labeled  $Q$ .

We now divide the numerators of both Term 1 and Term 2 by  $N$  and divide both of their denominators by  $N^2$ , and then replace  $n/N$  by  $Z$ , obtaining the following.

Term 1:

$$\sum_{\substack{m=-\infty \\ m \neq 0}}^{\infty} \frac{(1 - e^{-j(n-mN)\omega_0 g_1 T_s})/N - j(Z-m)\omega_0 e^{-jn\omega_0 g_2 T_s}}{[j(Z-m)\omega_0]^2}$$

Term 2:

$$\frac{(1 - e^{-jn\omega_0 g_1 T_s})/N - jZ\omega_0 e^{-jn\omega_0 g_2 T_s}}{(jZ\omega_0)^2}$$

Then, keeping  $Z$  fixed and letting  $N \rightarrow \infty$ , the terms tend to the following:

Term 1:

$$\sum_{\substack{m=-\infty \\ m \neq 0}}^{\infty} \frac{-j(Z-m)\omega_0 e^{-jn\omega_0 g_2 T_s}}{[j(Z-m)\omega_0]^2}$$

Term 2:

$$\frac{-jZ\omega_0 e^{-jn\omega_0 g_2 T_s}}{(jZ\omega_0)^2}$$

The error is the quotient of these two terms, and cancellations can now take place. We obtain, for  $Z$  fixed and  $N \rightarrow \infty$ , the following limit for the error:

$$E_N(Z) = \sum_{\substack{m=-\infty \\ m \neq 0}}^{\infty} \frac{Z}{Z-m}$$

whose RHS is precisely  $E(Z, 0)$ , as predicted by Theorem 13.3. □

In Figure 13.6 we show the error curves for the (noncanonical) decaying exponential pulse

$$f(t) = e^{-5t} \quad (0 \leq t \leq 8)$$

for the cases  $N = 16, 32, \dots, 512$ . Here  $f(t)$  has a jump at  $t = 0$ , and so its continuity order is zero. According to the preceding theorem, the error curves for this pulse should approach  $E(Z, 0)$  for fixed  $Z$  as  $N \rightarrow \infty$ . In the figure we see how the curves do precisely that.

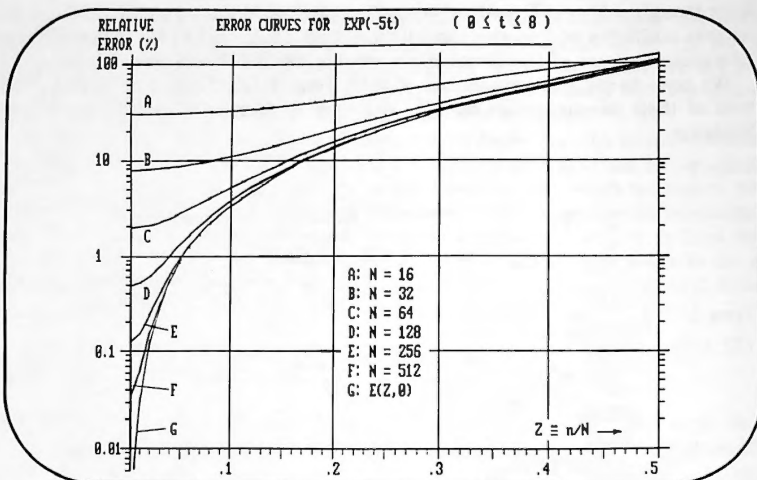


Figure 13.6.

Theorem 13.3 was for noncanonical functions of continuity order zero. Similar results hold true for noncanonical functions of higher continuity orders as well. We state this as Theorem 13.4.

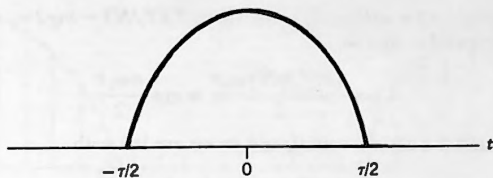
#### ■ THEOREM 13.4

Let  $f(t)$  be piecewise continuous of order  $k$  and  $(k+2)$  times continuously differentiable on each interval of continuity of the  $(k-1)$ -st derivative, and let it be zero outside the range  $0 \leq t \leq T$ . Let all of its break points lie at FFT sampling instants. Let  $E_N(Z)$  denote the relative error in the FFT's estimate of  $F(n\omega_0)$  when an  $N$ -vector of samples is sent to the FFT, and assume that  $F(n\omega_0) \neq 0$ . Then, for constant  $Z$ ,

$$\lim_{N \rightarrow \infty} E_N(Z) = E(Z, k) \quad (13.37)$$

□ EXAMPLE 13.6: Consider the gated cosine pulse shown in Figure 13.7, namely

$$f(t) = \cos \frac{\pi t}{\tau} \operatorname{Rect} \frac{t}{\tau}$$

Figure 13.7.  $\cos(\pi t/\tau) \operatorname{Rect}(t/\tau)$ .

In this case  $f(t)$  is noncanonical and of continuity order 1. According to Theorem 13.4 its error function should tend to  $E(Z, 1)$  for fixed  $Z$  as  $N \rightarrow \infty$ .

The Fourier transform of  $f(t)$  is

$$F(\omega) = \frac{2\pi\tau \cos(\omega\tau/2)}{\pi^2 - (\omega\tau)^2}$$

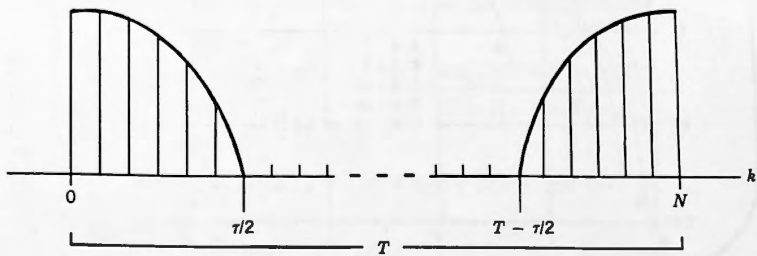
In order to sample  $f(t)$  for submission to the FFT we now redraw it as shown in Figure 13.8 where we also show a value for  $T$  that exceeds  $\tau$ .

We are assuming that the endpoints of the pulse are sampling instants, and so we must have

$$\frac{\tau}{2} = gT_s \quad \text{and} \quad T - \frac{\tau}{2} = (N - g)T_s$$

in which  $g$  is an integer. Then, using (13.8) to form the error function we obtain

$$E_N(n) = \sum_{\substack{m=-\infty \\ m \neq 0}}^{\infty} \frac{\pi^2 - (n\omega_0\tau)^2}{\cos(n\omega_0\tau/2)} \frac{\cos[(n-mN)\omega_0\tau/2]}{\pi^2 - [(n-mN)\omega_0\tau]^2}$$

Figure 13.8.  $\cos(\pi t/\tau) \operatorname{Rect}(t/\tau)$  in the FFT's data window.

However,  $mN\omega_0\tau/2 = mN\omega_0gT_s = mgN(2\pi/T)(T/N) = mg2\pi$ , which is an integral multiple of  $2\pi$ , and so

$$\cos \frac{(n - mN)\omega_0\tau}{2} = \cos \frac{n\omega_0\tau}{2}$$

This means that the cosines cancel, and so we are left with

$$E_N(n) = \sum_{\substack{m=-\infty \\ m \neq 0}}^{\infty} \frac{\pi^2 - (n\omega_0\tau)^2}{\pi^2 - [(n - mN)\omega_0\tau]^2}$$

We now divide numerator and denominator by  $N^2$  and replace  $n/N$  by  $Z$ , obtaining

$$E_N(Z) = \sum_{\substack{m=-\infty \\ m \neq 0}}^{\infty} \frac{(\pi/N)^2 - (Z\omega_0\tau)^2}{(\pi/N)^2 - [(Z - m)\omega_0\tau]^2}$$

Then, for constant  $Z$ , as  $N \rightarrow \infty$  we obtain the limit as

$$E_N(Z) = \sum_{\substack{m=-\infty \\ m \neq 0}}^{\infty} \frac{Z^2}{(Z - m)^2} = E(Z, 1)$$

□

In Figure 13.9 we show the error curves for the pulse of the preceding example with  $\tau = 1$  and  $T = 1$ , for the cases  $N = 4, 8, 16, 64$ , and  $128$ . We also show a plot of

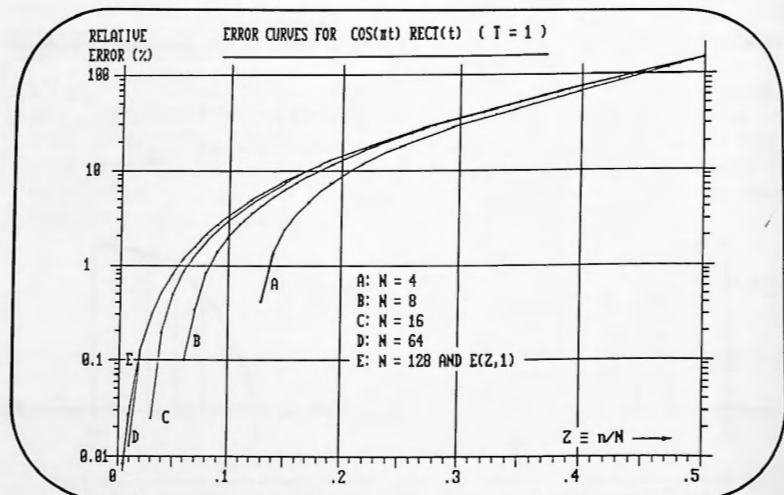
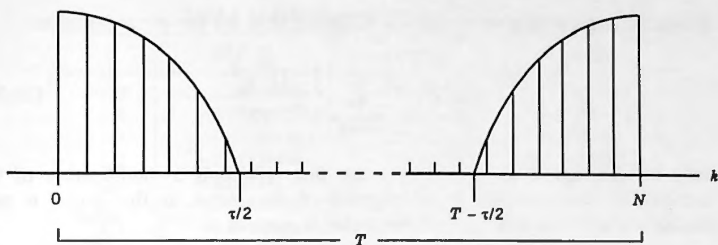


Figure 13.9.

Figure 13.10.  $\cos(\pi t/\tau) \operatorname{Rect}(t/\tau)$  in the FFT's data window.

$E(Z, 1)$ . Observe how the error curves all tend to  $E(Z, 1)$  for a given value of  $Z$  as  $N \rightarrow \infty$ , precisely as predicted by the theorem.

### 13.8 BREAK POINTS NOT AT A SAMPLING INSTANT

Thus far we have assumed that all of the break points (changes from one analytically defined section to another, etc.) coincide with a sampling instant. We have seen that under such circumstances we can use the canonical error functions to give us values for the errors, either precisely or else approximately. We now examine what happens when the break points are not at sampling instants.

□ **EXAMPLE 13.7:** Consider once again the cosine pulse of Example 13.6, namely  $f(t) = \cos(\pi t/\tau) \operatorname{Rect}(t/\tau)$ . We now select  $T$  and  $N$  such that the endpoints are in the centers of sampling intervals rather than coinciding with sampling points, and so in Figure 13.10 we have the following relationships:

$$\frac{\tau}{2} = \left(g + \frac{1}{2}\right)T_s \quad \text{and} \quad T - \frac{\tau}{2} = \left(N - g - \frac{1}{2}\right)T_s$$

where  $g$  is an integer.

Once again we form the error function as we did earlier, obtaining

$$E_N(n) = \sum_{\substack{m=-\infty \\ m \neq 0}}^{\infty} \frac{\pi^2 - (n\omega_0\tau)^2}{\cos(n\omega_0\tau/2)} \frac{\cos[(n-mN)\omega_0\tau/2]}{\pi^2 - [(n-mN)\omega_0\tau]^2}$$

However,  $mN\omega_0\tau/2 = mN\omega_0(g + \frac{1}{2})T_s = mg2\pi + m\pi$ , and so

$$\cos \frac{(n-mN)\omega_0\tau}{2} = \cos \frac{n\omega_0\tau}{2} \cos(m\pi) = (-1)^m \cos \frac{n\omega_0\tau}{2}$$

Under these conditions we obtain the following limit for the error function;

$$E_N(Z) = \sum_{\substack{m=-\infty \\ m \neq 0}}^{\infty} \frac{(-1)^m Z^2}{(Z^2 - m^2)^2} \quad (13.38)$$

valid for constant  $Z$  as  $N \rightarrow \infty$ . We see that (13.38) is a modification of the canonical-1 error function in which each of the terms in the series is now multiplied by the factor  $(-1)^m$ . Rearranging it gives us

$$E_N(Z) = \sum_{m=1}^{\infty} \frac{(-1)^m 2Z^2(Z^2 + m^2)}{(Z^2 - m^2)^2} \quad (13.39)$$

in which the terms are seen to alternate in sign, and so now (13.39) must be less than (13.22) for any given  $Z$ .  $\square$

In Table 13.3 we show the canonical-1 error values from (13.33) to serve as a reference, together with numerical values from two computer runs for the cosine pulse with  $N = 1024$ ,  $\tau = 2$ , and  $T$  selected as follows:

**Case (a):**  $T = 4$  (Sampling so that the endpoints are at  $\pm 256$ ).

**Case (b):**  $T = 3.992202728$  (Sampling so that the endpoints are at  $\pm 256.5$ )

Here's what we see from the table:

- Once  $n$  has reached a value of 8, that is,  $n/N = 0.0078$ , **the first two columns are virtually identical**. This is consistent with Theorem 13.4, and shows how the error function for the cosine pulse has tended to the  $E(Z, 1)$  function. Here  $N = 1024$ , which is large, and so the "tending" is almost complete.
- For most of the range of values for  $n$  **the Case (b) figures are about one half those of Case (a)**. This is consistent with (13.38), and shows that if we sample so that the endpoints are halfway between sampling instants, then the errors can be reduced to about 50 percent relative to Case (a).

TABLE 13.3 Percentage Errors in FFT Estimates for Cosine Pulse

$n$	$E(Z, 1)$	<i>Case (a)</i>	<i>Case (b)</i>
0	0.000000	0.000318	0.000154
1	0.000314	0.000000	0.00000724
2	0.00126	0.000942	0.000470
4	0.00502	0.00471	0.00235
8	0.0201	0.0198	0.00989
16	0.0804	0.0800	0.0400
32	0.322	0.322	0.161
64	1.295	1.295	0.651
128	5.303	5.303	2.712
256	23.370	23.370	12.764
512	146.740	146.740	100.000

TABLE 13.4 Percentage Errors for Rect Pulse

<i>n</i>	$E(Z, 0)$	Case (a)	Case (b)
0	0.00000000	0.00000000	+ 0.000000
1	- 0.00031376	- 0.000309842	+ 0.000156
3	- 0.00282373	- 0.002823098	+ 0.001411
7	- 0.01537406	- 0.015373737	+ 0.007687
63	- 1.24837138	- 1.248370160	+ 0.625357
255	- 21.28546896	- 21.285468973	+ 10.979218
511	- 99.51902542	- 99.519025434	+ 56.791075

■ EXAMPLE 13.8: Consider the canonical-0 pulse  $\text{Rect}(t/\tau)$  whose transform is  $\tau \text{Sa}(\omega\tau/2)$ . This pulse was sampled in two ways using  $\tau = 2$  and  $N = 1024$ :

Case (a):  $T = 4$ , which means that the endpoints coincided with sampling instants where a value of  $\frac{1}{2}$  was used. A value of 1 was used at all other sampling points.

Case (b):  $T = 3.992202728$ , which means that the endpoints were at the centers of sampling intervals and so they were not sampled. A value of 1 was used for all other samples.

The results of two computer runs are shown in Table 13.4. Here's what we see from the table:

- The Case (a) column is almost identical to  $E(Z, 0)$  for all values of  $n$  as expected, because the Rect pulse is canonical-0 if sampling includes the endpoints of the pulse. What slight differences exist are due to finite-length-arithmetic computational errors.
- The Case (b) figures are very close to one-half of those of Case (a), showing that the estimation errors can be cut in half if we sample so that the ends of the pulse lie in the centers of sampling intervals. [The sign of  $E(Z, 0)$  and Case (a) is negative, whereas for Case (b) it is positive.] □

We can explain the reduction in estimation errors in Case (b) as follows. In the same way as what took place in (13.38), if we sample so that the ends of the pulse are located at the centers of sampling intervals, each term in the series (13.21) becomes multiplied by  $(-1)^m$ , giving us

$$E = \sum_{m=1}^{\infty} \frac{(-1)^m 2Z^2}{Z^2 - m^2} \quad (13.40)$$

Once again the terms are alternating in sign and so the sum must be reduced relative to (13.21). (The reader can easily start generating the numbers in the Case (b) column of Table 13.4 by using a hand calculator to sum (13.40) for various values of  $Z$ .)

In both of the preceding examples we saw that, with sampling at the endpoints, the terms being summed always have the same sign, whereas when we sampled so that the break points fall at the center of a sampling interval, the terms are multiplied by  $(-1)^m$ . This is a **consistent outcome**, that is, it will always occur for any pulse or periodic function. Thus we can say that placing the sampling points so that all break points fall at the centers of sampling intervals will always lead to a reduction in the estimation errors.

### 13.9 ERROR CORRECTION OF FAST FOURIER TRANSFORM ESTIMATES

---

Because we now have an expression for the errors it follows that we can apply a correction to the results that we obtain from the FFT and thus obtain exact values for pulse or periodic spectra. However, this is only applicable to pulses and periodic functions that are canonical. For them we have the exact error expressions, but for noncanonical functions we do not. Theorem 13.4 tells us that the error formulas of Theorem 13.2 apply only in an asymptotic sense.

□**EXAMPLE 13.9:** Use  $E(Z, 0)$  to remove the errors for a Rect pulse.

**Solution:** From (13.1),

$$\sum_{m=-\infty}^{\infty} F[(n - mN)\omega_0] = \frac{T}{N} F_n \quad (\forall n) \quad (13.41)$$

and from (13.6) and (13.32), for canonical-0 pulses,

$$\frac{\sum_{m=-\infty}^{\infty} F[(n - mN)\omega_0] - F(n\omega_0)}{F(n\omega_0)} = \pi Z \cot(\pi Z) - 1 \quad (13.42)$$

Combining these two statements we obtain

$$F(n\omega_0) = \frac{(T/N)F_n}{\pi Z \cot(\pi Z)} \quad (13.43)$$

The numerator of the RHS is the FFT's estimate of  $F(n\omega_0)$ , and so, after division by  $\pi Z \cot(\pi Z)$  we should have the exact value of the LHS.

The pulse  $f(t) = \text{Rect}(t)$  transforms to  $F(\omega) = \text{Sa}(\omega/2)$ . Loading  $f(t)$  into X with  $N = 64$  and  $T = 4$  and then running ANALYSIS we obtained the values appearing in Table 13.5. Observe that we have deliberately used a very small value for  $N$ .

In the second column of the table we show the FFT's estimate of  $F(n\omega_0)$ . In the third we show the value of  $\pi Z \cot(\pi Z)$ , where  $Z = n/N$ . The fourth column

TABLE 13.5 Error Correction for a Rect Pulse

$n$	FFT Value	$\pi Z \cot(\pi Z)$	$FFT/\pi Z \cot(\pi Z)$	$F(n\omega_0)$
0	1.00000000	1.000000000	1.000000000	1.000000000
1	0.89959307	0.999196680	0.900316312	0.900316316
7	-0.12351444	0.960330358	-0.128616615	-0.128616616
15	-4.8760757e-2	0.812393753	-6.0021088e-2	-6.0021087e-2
31	-2.1711205e-3	7.4757765e-2	-2.9042461e-2	-2.9042461e-2

is the second divided by the third according to (13.43). In the fifth column we show the exact value, computed from  $\text{Sa}(n\omega_0/2)$ , where  $\omega_0 = 2\pi/T$ . The fourth column is almost identical to the fifth, showing that we have indeed been able to correct the FFT's estimates to give the true values to 8-digit precision.  $\square$

### 13.10 CONFIRMATION OF THEORETICAL RESULTS

The theory that was developed earlier in the chapter appears to be new. Most of it was first observed by use of the accompanying disc and was later investigated theoretically. Proofs for the theorems were then developed.

In the exercises that follow we include most of the numerical values that the reader is asked to derive by using the disc. Even without carrying out the exercises one can observe from those numbers a total confirmation of the theoretical results of this chapter.

### 13.11 ZERO PADDING INCREASES THE ESTIMATION ERRORS

It is frequently the case that a pulse has been sampled so that the number of those samples is not an exact power of 2. What is then often done is to append a string of zeros in order to bring the total number to the next power of 2. This process is known as **padding with zeros or adding white space**.

There is a second reason why zeros are sometimes appended, and that is to produce a **better representation of the spectrum** of the pulse on the FFT.

While both of these lead to their desired results, if the FFT is being used in order to estimate values for the continuous Fourier transform, then we must bear in mind the following incontrovertible fact:

The more zeros we append, the greater will be the errors between the FFT's estimates of the continuous Fourier transform and the exact values of that transform.

This fact is easily verified using the accompanying disc, and in Chapter 17 we provide a general proof of its veracity.

**EXERCISES**

**13.1** Verify that the error series for canonical spectra can be rearranged as shown in (13.21) through (13.24). Verify the following regarding the error expressions for canonical- $k$  pulses:

- Their series converge like  $1/m^2$  for  $k = 0, 1$  and like  $1/m^4$  for  $k = 2, 3$ .
- The errors for canonical pulses are all real.
- The errors for canonical pulses are precisely zero when  $n = 0$ , regardless of the value of  $N$ .
- The errors are all negative for  $k$  even, and positive for  $k$  odd.
- The error expressions are all even in  $Z$  and hence even in  $n$ .

**13.2** The pulse

$$f(t) = \begin{cases} 1 & (0 < t < T/8) \\ 0 & \text{otherwise} \end{cases} \quad (T = 8)$$

- is canonical-0 because its first derivative is only Dirac deltas, assuming that its endpoints are at sampling instants.
  - has a complex Fourier transform.
- (a) Find the exact expressions for the real and imaginary parts of its Fourier transform.
- (b) Load this pulse into X with  $N = 256$  and  $T = 8$  and run ANALYSIS.
- (c) Calculate the errors for  $n = 5$  and  $n = 71$  from the FFT data and the exact expressions, and verify that they are real and negative.

*Hint:* For a complex estimate we must use

$$\text{Relative error} \equiv \frac{[A_{\text{est}} - A_{\text{exact}}] + j[B_{\text{est}} - B_{\text{exact}}]}{A_{\text{exact}} + jB_{\text{exact}}} \quad (13.44)$$

Thus you must verify that, for this pulse and the values of  $n$  and  $N$  in (b) and (c), the quotient in (13.44) gives values that are real and negative.

- (d) Reconcile the errors that you obtain with the values given by Figure 13.4 as well as with (13.32), namely

$$E(Z, 0) = \pi Z \cot(\pi Z) - 1$$

**13.3** (a) Sketch the following pulse:

$$f(t) = \begin{cases} 0 & (t < 0) \\ t & (0 < t < 1) \\ 1 & (1 < t < 3) \\ 4 - t & (3 < t < 4) \\ 0 & (4 < t) \end{cases}$$

- (b) Assuming that we sample so that all breakpoints are at sampling instants, is the pulse canonical, and if so, of what order?
- (c) Find the expressions for the real and imaginary parts of its Fourier transform.
- (d) What should be the value of  $F(\omega)$  for  $\omega = 0$ ? Load this pulse into **X** and verify that for  $N = 8, 40, 224$ , and  $512$  (all of these values are exact multiples of 8) with  $T = 8$ , the zeroth element of the FFT spectrum is an **exact estimate** of  $F(0)$ . Infer that using the rectangular rule to find the area under this pulse would give the correct answer for any  $N$ , provided only that the transition points  $t = 0, 1, 3$ , and  $4$  are sampling points for the numerical integration.
- (e) Use (13.44) plus FFT data to find the relative errors in the following spectral elements (use  $T = 8$  for all three):

$$n = 137 \quad \text{with } N = 800$$

$$n = 60 \quad \text{with } N = 200$$

$$n = 226 \quad \text{with } N = 512$$

and verify that all are real and positive.

- (f) Reconcile your results in (e) with Figure 13.4 as well as with (13.33), namely

$$E(Z, 1) = \frac{(\pi Z)^2}{\sin^2(\pi Z)} - 1$$

#### 13.4 (a) Sketch the pulse

$$f(t) = \begin{cases} 0 & (t < 0) \\ t^2/2 & (0 < t < 1) \\ (-2t^2 + 6t - 3)/2 & (1 < t < 2) \\ (t^2 - 6t + 9)/2 & (2 < t < 3) \\ 0 & (3 < t) \end{cases}$$

- (b) Verify that its zeroth and first derivatives are everywhere continuous and that its second derivative is discontinuous. Verify that its third derivative is only Dirac deltas, and hence infer that it is canonical-2 if we sample so that  $t = 0, 1, 2$ , and  $3$  are sampling instants.
- (c) Using successive differentiation, find the real and imaginary parts of  $F(\omega)$  for this pulse.
- (d) Load  $f(t)$  into **X** and verify that for  $N = 4, 40, 224$ , and  $500$  (all exact multiples of 4) with  $T = 4$ , the zeroth element of the FFT spectrum is an **exact estimate** of  $F(\omega)$  for  $\omega = 0$ . Infer that using the rectangular rule to find the area under this pulse would give the correct answer for any  $N$ , provided only that the transition points  $t = 0, 1, 2$ , and  $3$  are sampling points for the integration.

- (e) Use (13.44) plus FFT data to calculate the relative errors in the following spectral elements:

$$\begin{aligned} n &= 7, & N &= 100, & T &\equiv 4 \\ n &= 38, & N &= 200, & T &\equiv 4 \\ n &= 151, & N &= 500, & T &= 4 \end{aligned}$$

and verify that they are all real and negative.

- (f) Reconcile your results in (e) with Figure 13.4 as well as with (13.34), namely

$$E(Z, 2) = \frac{(\pi Z)^3 \cot(\pi Z)}{\sin^2(\pi Z)} - 1$$

- 13.5 Starting from (13.28), use differentiation to verify (13.32) through (13.35).

- 13.6 For the pulse  $f(t) = e^{-\beta t}U(t)$ :

- (a) Write its Fourier transform.
- (b) Form the error expression (13.8).
- (c) Following Examples 13.5 and 13.6 show that for fixed  $Z$ , the error expression in (b) tends to  $E(Z, 0)$  as  $N \rightarrow \infty$ , thereby validating Theorem 13.3.

- 13.7 For the pulse  $f(t) = \sin^2(\pi t)$  ( $0 \leq t \leq 1$ ):

- (a) Find its Fourier transform.
- (b) Form the error expression (13.8).
- (c) Following Examples 13.5 and 13.6, show that for fixed  $Z$ , the error expression in (b) tends to  $E(Z, 2)$  as  $N \rightarrow \infty$ , thereby validating Theorem 13.4.

- 13.8 (a) Load the pulse  $f(t) = e^{-t}U(t)$  into  $\mathbf{X}$  using  $N = 1024$  and  $T = 16$ , and verify the values for  $A_n$  and  $B_n$  in Table 13.6.  
 (b) Compute the error in the FFT estimates in the table, and then use (13.44) to verify the percent error shown.  
 (c) Use the formula  $E(Z, 0) = \pi Z \cot(\pi Z) - 1$  to compute the error values for a canonical-0 pulse, using the same values of  $n$  and  $N$  as in the table.  
 (d) Observe how closely the complex error in the table and the error obtained in (c) agree, as predicted by Theorem 13.3.

TABLE 13.6

$n$	$A_n$ (FFT)	$B_n$ (FFT)	Error (%)
0	1.00002020	0	0.002020000 + $j0$
4	0.28842075	-0.45298634	-0.002997092 + $j0.006391469$
16	2.4724875e-2	-0.15509523	-0.078305442 + $j0.025574163$
64	1.6011437e-3	-0.03921320	-1.286364741 + $j0.102793030$
256	1.2206037e-4	-7.8115455e-3	-21.45757300 + $j0.445930127$
512	6.1033908e-5	0	-99.99389600 + $j1.227159600$

## 13.9 (a) Sketch one period of the periodic waveform

$$f_p(t) = \begin{cases} e^t & (0 < t < 1) \\ 0 & (1 < t < 2) \end{cases} \quad f_p(t+2) = f_p(t)$$

- (b) Use successive differentiation plus Theorem 9.3 to find the expression for the CFT spectrum of  $f_p(t)$  and then find the expressions for  $A(n)$  and  $jB(n)$ , that is, the spectra of  $f_{ev}(t)$  and  $f_{od}(t)$ , respectively.
- (c) Sketch the even and odd parts of  $f_p(t)$ , verifying that
- $f_{ev}(t)$  is everywhere continuous
  - $f_{od}(t)$  has discontinuities
- Neither  $f_{ev}(t)$  nor  $f_{od}(t)$  is a canonical waveform. According to Theorem 13.4, if we sample so that the break points are located at sampling instants, then the errors for noncanonical waveforms tend asymptotically to the associated canonical error curves as  $N$  is made larger. We would thus expect that the errors in the FFT spectrum of  $f_{ev}(t)$  will tend to the canonical-1 error curve and those of  $f_{od}(t)$  will tend to the canonical-0 error curve.
- (d) Use the system on the disk to find the FFT spectrum of  $f_p(t)$  for the following values:

$$N = 32, 128, 512, 2048$$

For each case find the relative error in the FFT's estimate of  $A(n)$  and  $jB(n)$  for  $n = N/2 - 1$ , and confirm the values shown in Tables 13.7 and 13.8.

*Note:* We suggest that you use  $N/2 - 1$  rather than  $N/2$  because  $B(N/2)$  is zero for all values of  $N$ .

- (e) Use the formula for the errors, (13.33) for  $A$ , and (13.32) for  $jB$ , and verify the final two columns and the bottom lines of the tables. (The final column is the relative error in column 2 vs. column 3.) As the tables

TABLE 13.7

$N$	Actual Error in $A$ (%)	Formula Value (%)	Error (%)
32	118.9903548	118.9651015	0.02
128	139.2350258	139.2338049	0.0009
512	144.8255068	144.8254355	0.00005
2048	146.2590189	146.2590104	0.000006
$\infty$	—	146.7401101	—

TABLE 13.8

<i>N</i>	<i>Actual Error in jB (%)</i>	<i>Formula Value (%)</i>	<i>Error (%)</i>
32	85.50371083	85.49594371	0.009
128	96.20429775	96.20416281	0.001
512	99.03992654	99.03992441	0.000002
2048	99.75927802	99.75927798	0.00000004
$\infty$	—	100.00000000	—

clearly show, the error curves of these two noncanonical cases are tending to the canonical values as derived from the closed-form expressions for the errors. For the case  $N = \infty$  we used  $n/N = \frac{1}{2}$  in the formula.

- 13.10** Assuming that a canonical-0 pulse is sampled so that all of its discontinuities are at the centers of sampling intervals, show that the expression for the relative error is

$$E_N(n) = \sum_{\substack{m=-\infty \\ m \neq 0}}^{\infty} \frac{(-1)^m n}{n - mN} \quad \left( \frac{-N}{2} \leq n \leq \frac{N}{2} \right)$$

*Hint:* Form (13.6) and use the fact that if a discontinuity is located at  $g_i T_s$ , then  $g_i = h_i + \frac{1}{2}$  where  $h_i$  is an integer.

Infer that if a canonical- $k$  pulse is sampled so that the discontinuities are all at the centers of sampling intervals, then the expression for the relative error is

$$E_N(n) = \sum_{\substack{m=-\infty \\ m \neq 0}}^{\infty} \frac{(-1)^m n^{k+1}}{(n - mN)^{k+1}} \quad \left( \frac{-N}{2} \leq n \leq \frac{N}{2} \right)$$

- 13.11** (a) Sketch the pulse

$$f(t) = e^{-5(t-T_s/2)} U(t - T_s/2)$$

You will observe that it is a slightly shifted decaying exponential that starts at  $t = T_s/2$  and falls off exponentially as  $t$  increases.

- (b) Verify that  $f(t)$  transforms to

$$F(\omega) = \frac{1}{5 + j\omega} e^{-j\omega T_s/2}$$

**TABLE 13.9 Percentage Errors for Decaying Exponential**

<i>n</i>	$E(Z, 0)$	$e^{-5t}U(t)$	$f(t)$
0	0.00000000	0.003180000	0.001590000
1	0.00031376	0.003490020	0.001746043
8	0.02008056	0.023259396	0.011629877
32	0.32148281	0.324661914	0.162407097
128	5.19405510	5.197232988	2.61880370
256	21.46018365	21.46333095	12.52010254
512	100.00000000	100.0022287	57.08049875

- (c) If we sample starting at  $t = 0$  with sampling interval  $T_s$ , then the discontinuity in  $f(t)$  at  $t = T_s/2$  is not at a sampling instant, and instead falls halfway between two such instants. We can therefore expect that the FFT-estimation errors will be less than for the pulse  $e^{-5t}U(t)$  whose discontinuity coincides with a sampling instant. Load both  $f(t)$  as well as  $e^{-5t}U(t)$  into  $\mathbf{X}$  using  $N = 1024$  and  $T = 4$ , and verify the FFT estimation errors displayed in Table 13.9 where we also show values for a canonical-0 spectrum computed from  $E(Z, 0) = \pi Z \cot(\pi Z) - 1$ . We have used the magnitudes of all of the complex errors involved.
- (d) Observe that
- Other than for very small values of  $n$ , the error values for  $e^{(-5t)}U(t)$  are almost the same as the canonical-0 values. This is to be expected from Theorem 13.3.
  - The error values for the shifted exponential  $f(t)$  are approximately one-half of the canonical-0 values.

- 13.12** The pulse of Exercise 13.3 is canonical-1. Thus we should be able to apply a correction factor to the FFT-derived values of its spectrum in order to obtain exact values. Load the pulse into  $\mathbf{X}$  using  $N = 32$  and  $T = 8$ , and fill in Table 13.10.

*Hint:* See Example 13.9 in the chapter. The final two columns in your table should be virtually identical, showing that we have been able to correct the FFT estimation errors completely.

**TABLE 13.10 Error Correction for a Canonical-1 Pulse**

<i>n</i>	<i>FFT Value</i>	<i>Factor</i>	<i>FFT/Factor</i>	<i>F(nω₀)</i>
0				
1				
2				
3				
4				

In the following three exercises we demonstrate that the error expressions

$$E(Z, 0) = \pi Z \cot(\pi Z) - 1 \quad (|Z| \leq \frac{1}{2}) \quad (13.45)$$

and

$$E(Z, 1) = \frac{(\pi Z)^2}{\sin^2(\pi Z)} - 1 \quad \left( |Z| \leq \frac{1}{2} \right) \quad (13.46)$$

can be derived by direct means, without recourse to the series appearing in (13.15) or to residue theory. (These exercises are somewhat more challenging than the previous ones. Accordingly, we mark them with an asterisk.)

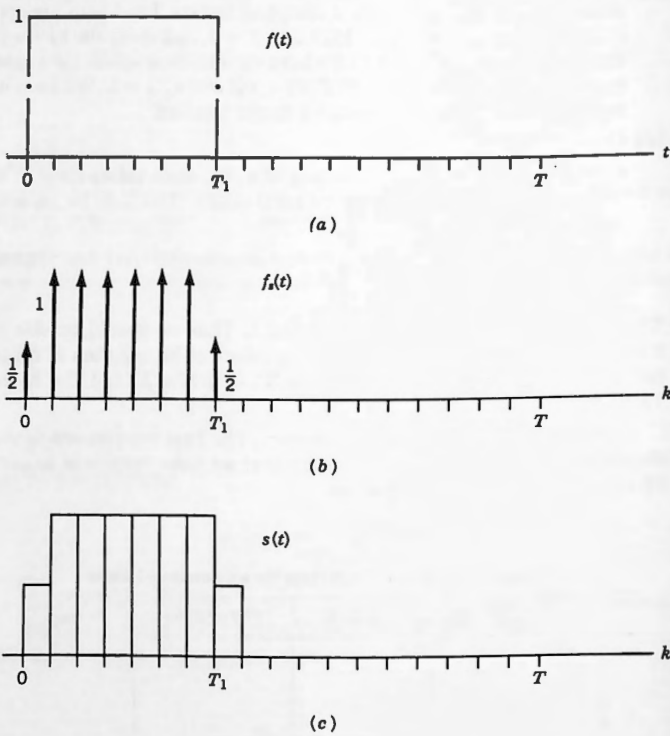


Figure 13.11.

- \*13.13 Consider the pulse  $f(t)$  shown in Figure 13.11a. Multiplying it by the train of impulses

$$\delta_T(t) = \sum_{k=-\infty}^{\infty} \delta(t - kT_s) \quad (T_s = T/N) \quad (13.47)$$

and using half-values at its discontinuities gives us the sequence of impulses shown in Figure 13.11b, namely

$$f_s(t) = \sum_{k=-\infty}^{\infty} f(kT_s) \delta(t - kT_s) \quad (13.48)$$

(It is assumed that all discontinuities coincide with sampling instants.) We now use (13.48) as the input to a network whose impulse response is shown in Figure 13.12. Verify that:

- (a)  $h(t) \Leftrightarrow H(j\omega) = e^{-j\omega T_s/2} T_s \text{Sa}(\omega T_s/2)$  (13.49)
- (b) The response to the input  $f_s(t)$  will be the pulse  $s(t)$  appearing in Figure 13.11c.
- (c) The response of the network is  $s(t)$ . Verify that

$$s(t) \Leftrightarrow S(n\omega_0) = e^{-jn\pi z} \text{Sa}(\pi Z)(T/N)F_n \quad (13.50)$$

- where  $\omega_0 = 2\pi/T$ ,  $Z = n/N$  and  $F_n$  is the discrete Fourier transform (DFT) of  $f(t)$  sampled at the points  $kT_s$ .
- (d) Observe that any pulse, canonical or otherwise, can be sampled in this way to give its version of (13.48) and its version of  $s(t)$ , which is called its **left-endpoint uniform rectangular replacement**.
  - (e) Observe also that (13.50) is a completely general formula for any pulse  $f(t)$  that has a DFT.

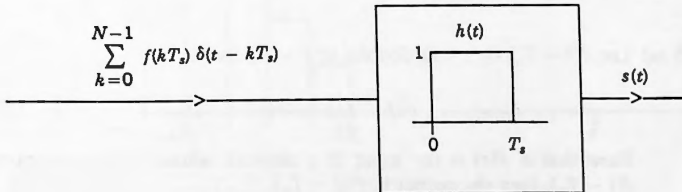


Figure 13.12.

- \*13.14 (a) Verify that if the canonical-0 pulse  $f(t)$  of Figure 13.11 is the input to the network shown in Figure 13.13 whose impulse response is called  $m(t)$ , then the response is  $s(t)$  of Figure 13.11c, that is, its left-endpoint uniform rectangular replacement.

*Hint:* Do it graphically.

- (b) Verify that

$$S(\omega) = F(\omega)M(j\omega) \quad (13.51)$$

where  $m(t) \Leftrightarrow M(j\omega)$ , and

$$M(j\omega) = \frac{1}{2}(1 + e^{-j\omega T_s}) \quad (13.52)$$

- (c) Using (13.50) and (13.51), form the quantity

$$E(Z, 0) = \frac{(T/N)F_n - F(n\omega_0)}{F(n\omega_0)}$$

which we know is the statement for the relative error of the FFT's estimate of  $F(\omega)$ . Now show that this leads to

$$E(Z, 0) = \pi Z \cot(\pi Z) - 1 \quad (13.53)$$

- (d) Observe that we have verified (13.32) and that what we have done here applies to any canonical-0 pulse.

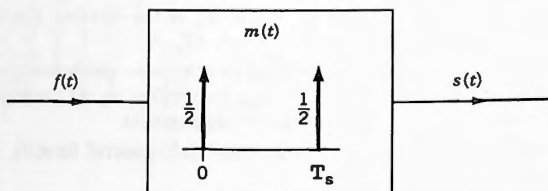


Figure 13.13.

- \*13.15 (a) Let  $d(t - T_0)$  be a unit doublet at  $t = T_0$ , that is,

$$d(t - T_0) = D\delta(t - T_0) \quad (13.54)$$

Show that if  $f(t)$  is the input to a network whose impulse response is  $d(t - T_0)$ , then the output is  $f'(t - T_0)$ .

*Hint:* Use Fourier transformation.

- (b) Extend (a) to show that if  $f(t)$  is the input to a network that has impulse response

$$m(t) = T_s \sum_{k=1}^{\infty} d(t - kT_s) \quad (13.55)$$

then the output will be

$$y(t) = T_s \sum_{k=1}^{\infty} f'(t - kT_s) \quad (13.56)$$

- (c) Verify that for the canonical-1 pulse of Figure 13.14a,

$$T_s f'(t) = \begin{cases} 0 & (t < 0) \\ \frac{1}{4} & (0 < t < 4T_s) \\ -\frac{1}{4} & (4T_s < t < 8T_s) \\ 0 & (8T_s < t) \end{cases}$$

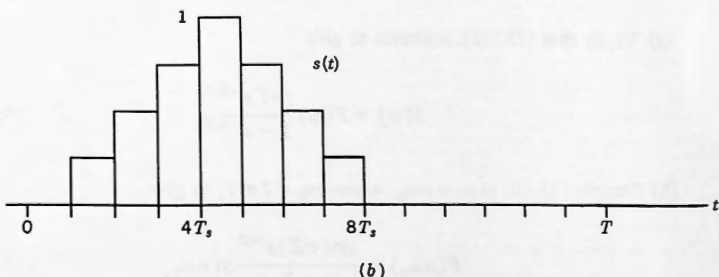
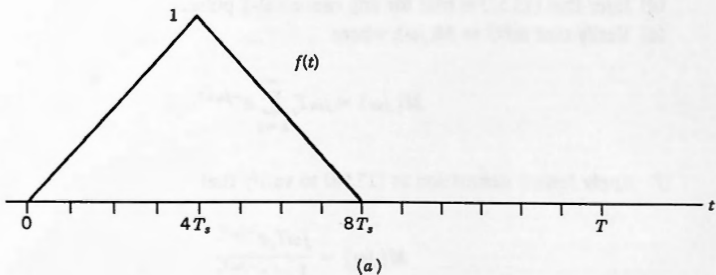


Figure 13.14.

Using a graphical construction sketch the following:

$$\text{line 1: } f(t)$$

$$\text{line 2: } T_s f'(t - 1T_s)$$

$$\text{line 3: } T_s f'(t - 2T_s)$$

$$\text{line 4: } T_s f'(t - 3T_s)$$

...      ...

$$\text{line 12: } T_s f'(t - 11T_s)$$

$$\text{line 13: Sum of lines 2 through 12.}$$

If you have done this correctly you will find that line 13 is the same as  $s(t)$  of Figure 13.14b, that is, you will have verified that

$$s(t) = T_s \sum_{k=1}^{\infty} f'(t - kT_s) \quad (13.57)$$

is the left-endpoint uniform rectangular replacement for  $f(t)$ .

(d) Infer that (13.57) is true for any canonical-1 pulse.

(e) Verify that  $m(t) \Leftrightarrow M(j\omega)$ , where

$$M(j\omega) = j\omega T_s \sum_{k=1}^{\infty} e^{-j\omega kT_s} \quad (13.58)$$

(f) Apply formal summation to (13.58) to verify that

$$M(j\omega) = \frac{j\omega T_s e^{-j\omega T_s}}{1 - e^{-j\omega T_s}} \quad (13.59)$$

(g) Verify that (13.57) transforms to give

$$S(\omega) = F(\omega) \frac{j\omega T_s e^{-j\omega T_s}}{1 - e^{-j\omega T_s}} \quad (13.60)$$

(h) Sample (13.60) at  $\omega = n\omega_0$ , where  $\omega_0 = 2\pi/T$ , to give

$$F(n\omega_0) = \frac{\sin(\pi Z)e^{j\pi Z}}{\pi Z} S(n\omega_0) \quad (13.61)$$

where  $Z = n/N$ .

- (i) Using (13.50) (which applies to any pulse that has a DFT) and (13.61) (which applies to any canonical-1 pulse), form the quantity

$$E(Z, 1) \equiv \frac{(T/N)F_n - F(n\omega_0)}{F(n\omega_0)}$$

which we know is the statement for the relative error of the FFT's estimate of  $F(\omega)$ . Call it  $E(Z, 1)$ . Now show that this leads to

$$E(Z, 1) = \frac{(\pi Z)^2}{\sin^2(\pi Z)} - 1 \quad (13.62)$$

- (j) Observe that we have verified (13.33) and that what we have done here applies to any canonical-1 pulse.

# The Four Kinds of Convolution

## 14.1 INTRODUCTION

---

In Chapter 7 we introduced the concept of convolution in which two pulses were combined according to a certain integral to produce a third. We also examined some of the relationships between that process and the Fourier transform. We now extend the idea of convolution and consider how it relates to the fast Fourier transform (FFT).

The first thing that we shall have to come to terms with is the fact that there is not just one kind of convolution that we must concern ourselves with. There are four.

In the investigations that we are about to undertake we shall constantly be referring to one or another of those four kinds, and so it is perhaps best if we now enumerate them so that their names can begin to become rooted in our minds. They are:

- (1) Continuous linear convolution
- (2) Continuous circular convolution
- (3) Discrete linear convolution
- (4) Discrete circular convolution

- **Continuous linear convolution** is the kind that we were talking about in Chapter 7 where the two pulses  $g(t)$  and  $h(t)$  were combined to produce a third, in which  $t$  is a continuous variable.
- **Continuous circular convolution** is the kind that would be used if we were combining two periodic waveforms  $g_p(t)$  and  $h_p(t)$  to produce a third.
- **Discrete linear convolution** is the kind that would be involved if we were combining two pulses  $g_k$  and  $h_k$ , in which  $k$  is a discrete variable. In Exercise 7.28 at the end of Chapter 7 we examined this kind of convolution very briefly.
- **Discrete circular convolution** is the kind that the FFT performs in which two periodic functions of the discrete variable  $k$  are combined to produce a third. As we shall soon see, this kind of convolution can be used to compute values for the other three.

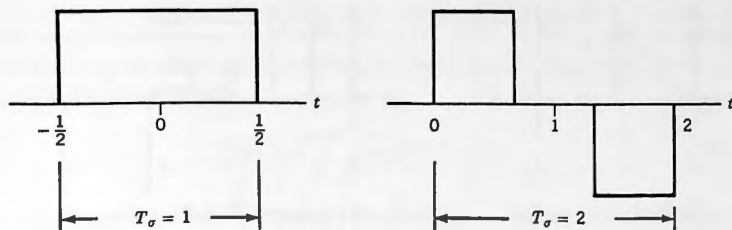


Figure 14.1. Two time-domain pulses and their spans.

There are three other new concepts that we shall require, and so we now consider their definitions.

- (A) In Chapter 12 we introduced the concept of the **span** of a pulse, and we now define formally what is meant by that term.

**Definition 1:** The **span time** of a finite-length time-domain pulse is the elapsed time from the beginning to the end of the pulse.

We shall use the symbol  $T_\sigma$  ( $T$ -sigma) for the span of a time-domain pulse in which  $T$  stands for time and  $\sigma$  stands for span.

Examples of time-domain pulses with their span times are shown in Figure 14.1.

- (B) For discrete sequences we have the counterpart to span time, which we call the **span count** of a pulse, and we now define what is meant by that term.

**Definition 2:** The **span count** of a finite-length discrete sequence is the number of elements in the sequence from beginning to the end. We include internal elements with value zero in the count.

We shall use the symbol  $C_\sigma$  ( $C$ -sigma) for the span of a discrete sequence in which  $C$  stands for count and  $\sigma$  stands for span.

Examples of discrete sequences with their span counts are shown in Figure 14.2. In the first sequence there are three nonzero elements and two with value zero for a total of five. In the second the total is eight.

- (C) There have been a number of places in earlier chapters where we referred to a quantity  $T$  in relation to  $f(t)$ , a finite-span pulse. While we know exactly what  $T_0$  means when it comes to periodic waveforms, in the case of single pulses there is no period, and so  $T$  needs to be properly defined (even though we have already been using it).

Referring to Figure 14.3, suppose that a pulse  $f(t)$  is numerically sampled over its span at instants spaced  $T_s$  seconds apart to give a sequence with a span count of  $m$ . As we point out in Section 17.2 in the *User's Manual*, we

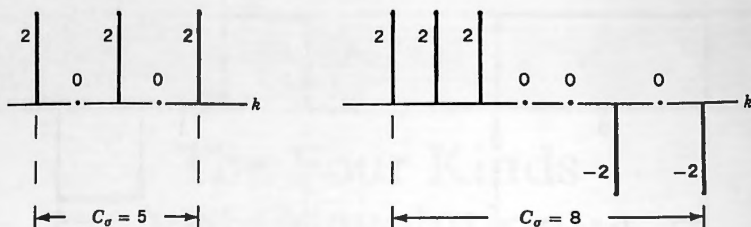


Figure 14.2. Two discrete sequences and their span counts.

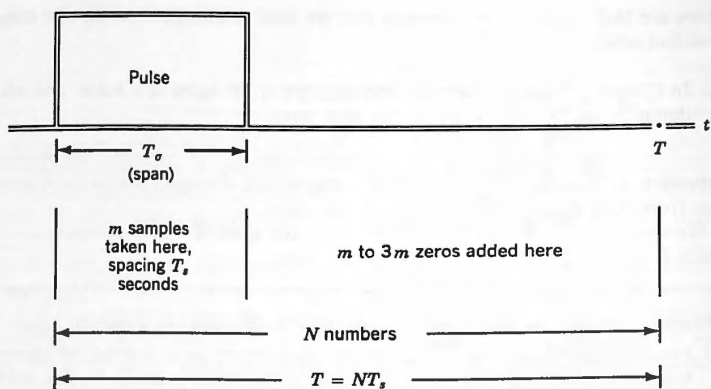


Figure 14.3.

must usually include a number of zeros (typically between  $m$  and  $3m$ ) with those samples, and then place them all in the FFT's data window as an extended sequence. (This process is called **adding white space** or **padding with zeros**.<sup>†</sup>) There will thus be  $N$  numbers placed in the FFT's window, the first  $m$  being samples of the pulse and the remaining  $N - m$  being zeros for the padding. From this we compute the value of  $T$  for the pulse as

$$T = NT_s \quad (14.1)$$

Thus  $T$  for a sampled pulse is equal to the amount of time that the  $N$  sampling intervals add up to.

<sup>†</sup>See Section 17.2 for a discussion on the effects of zero padding and how it increases the FFT's estimation errors.

## 14.2 THE FOUR KINDS OF CONVOLUTION

---

Two time-domain pulses  $g(t)$  and  $h(t)$  can be convolved to produce a third pulse  $f(t)$  by using the transformation

$$f(t) = \int_{-\infty}^{\infty} g(\tau)h(t - \tau) d\tau \quad (14.2)$$

From our theoretical work in Chapter 7 we recall that the Fourier transforms of  $f(t)$ ,  $g(t)$ , and  $h(t)$  will then satisfy

$$F(\omega) = G(\omega)H(\omega) \quad (14.3)$$

This is continuous linear convolution—"continuous" because  $g(t)$  and  $h(t)$  are functions of the continuous variable  $t$  and "linear" because the two pulses are moving past each other along a straight-line axis.

When two periodic functions of  $t$  are convolved, then we adopt a slightly different approach, namely continuous circular convolution, and a little later in this chapter we shall see exactly how it is done.

There are discrete-world counterparts to continuous linear and circular convolution. They are, respectively, discrete linear and discrete circular convolution, and it is the objective of this section to explore those processes and to establish how they work. A bit later we shall derive the scale factors so that discrete circular convolution, when done on the FFT, can be made to give values for the other three kinds.

From Exercise 7.28, we recall that discrete linear convolution is defined by the expression

$$f_k = \sum_{m=-\infty}^{\infty} g_m h_{k-m} \quad (14.4)$$

in which two sequences  $g_k$  and  $h_k$  are being convolved to produce a third sequence  $f_k$ . To better understand how it works and what "linear" means we consider the following example.

**EXAMPLE 14.1:** Let the two sequences  $g_k$  and  $h_k$  be defined as shown in Table 14.1 with their values continuing to be zero outside the table. Note that we have placed boxes around the sequences, the better to accentuate them in relation to the zeros that go to infinity in each direction.

TABLE 14.1

$k$	...	-4	-3	-2	-1	0	1	2	3	4	5	6	...
$g_k$	...	0	0	0	2	1	1	0	0	0	0	0	...
$h_k$	...	0	0	0	0	1	0	1	1	0	0	0	...

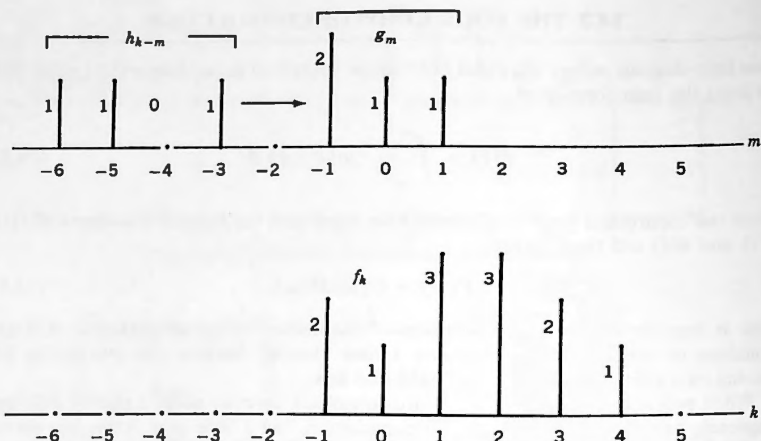


Figure 14.4. Linear convolution of discrete sequences.

In Figure 14.4 we show the portions of  $g_k$  and  $h_k$  appearing in the boxes, but now on the  $m$ -axis. Observe that the sequence  $h_k$  has been reversed and is now  $h_{k-m}$ , which is what we shall need to carry out the convolution process defined in (14.4).

Then, following the graphical convolution procedure used in Chapter 7, if for each value of  $k$  we

- Bring  $h_{k-m}$  forward one discrete step
- Multiply the pulses together element by element in their current positions
- Add the products so obtained

we obtain the current value of  $f_k$ . This results in the sequence  $f_k$  shown in the figure, with the numerical values given in Table 14.2.

To the left and right of both Tables 14.1 and 14.2 stretches an infinity of zeros. Movement of one sequence past the other is along a straight line, that is, linear,

TABLE 14.2

$k$	...	-4	-3	-2	-1	0	1	2	3	4	5	6	7	...
$f_k$	...	0	0	0	[ 2 1 3 3 2 1 ]					0	0	0	...	

and once the pulses being convolved have passed through each other along that line, the process ceases entirely. For all of these reasons, this type of convolution is called linear convolution.  $\square$

Convolving two periodic waveforms cannot be done in quite the same way, because now the waveforms repeat over and over again and never terminate. As soon as one period of one has passed through the other, the next period appears and the convolution process starts up all over again. In fact, it is constantly going on in every one of the periods all the time.

In order to convolve two periodic waveforms we therefore have to use a process known as circular convolution, which differs slightly from linear convolution. This is true regardless of whether the periodic waveforms being convolved have discrete  $k$  or continuous  $t$  as their independent variables, although in the theory that now follows we shall at first consider only the discrete case. In a later section of this chapter we examine continuous circular convolution.

As we recall from Chapter 10 the FFT is inherently periodic, and so if we use it to carry out convolution for pulses, as we intend to do, then we must recognize that it will inherently be discrete circular convolution that we are doing.

The picture that we must now keep in mind for discrete circular convolution is one in which the periodic sequences  $g_k$  and  $h_k$  are laid out on the circumferences of coaxial circles, rather than along a linear  $k$ -axis.

As shown in Figure 14.5, we assume for simplicity that the circles each have eight points on their circumferences (numbered from  $m = 0$  to  $m = 7$ ), and that one period of each of the sequences is now positioned on each of those circumferences. The values are once again those shown in Table 14.1.

However, we now have only eight slots that must be filled with numbers and so, to create periodic sequences, we must extract from the infinite linear sequences of Table 14.1 precisely eight numbers in each case, if necessary together with some of the adjacent zeros. We must also be sure that

- (a) One period of each of our sequences will fit into eight slots,
- (b) And that one period of the result of the convolution will also fit into eight slots.

If condition (b) is not satisfied, then aliasing will take place. We shall return to that possibility presently, but assume for now that both (a) and (b) are satisfied, that is, that  $g_k$ ,  $h_k$ , and  $f_k$  can all be represented on a circle with eight slots.

Starting from  $k = 0$  and proceeding to  $k = 7$ , we thus obtain the numbers shown in Table 14.3. Observe that the numbers  $g_k$  in the table are now  $g_m$  on the circle, and also that the element of  $g_k$  that was located at  $k = -1$  in Table 14.1 is now  $g_7$  at  $m = 7$  in the figure. That is an inherent implication of the circularity of the process. Observe also that we have reversed  $h_k$  in the figure, that is, we show  $h_{-m}$  and not  $h_m$ .

As shown in the figure, the counter  $m$  now refers to a position on a circle rather than to a position on a linear axis. Notice that as soon as we reach a value of  $m = 7$ , the next value  $m = 0$  appears. In Table 14.3 this is symbolized by the recirculating path with arrows.

Being circular there is now implicitly an infinite number of repetitions of the same sequences of numbers on each side of the table, which is easy to imagine when

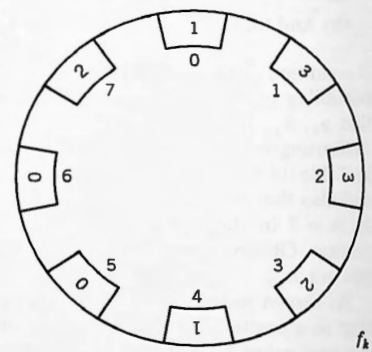
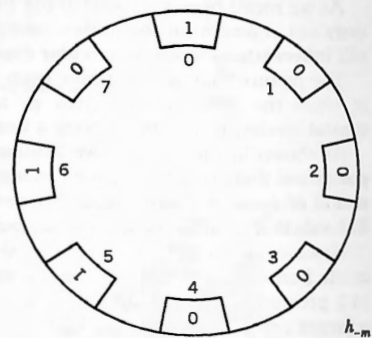
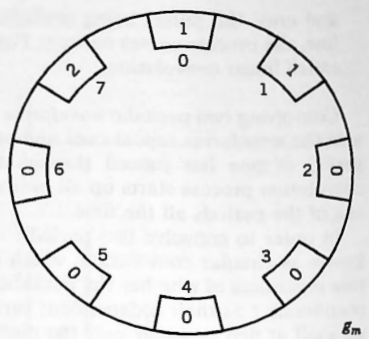


**Figure 14.5.** Circular convolution of two discrete periodic sequences.

TABLE 14.3							
$k$	0	1	2	3	4	5	6
$g_k$	1	1	0	0	0	0	2
$h_k$	1	0	1	1	0	0	0

looking at the circles in the figure. In this way the periodicity of the sequences is precisely modeled.

To perform circular convolution we reverse one of the sequences (as has already been done in the figure), place the two circles on top of each other, and then rotate one of them, step by step. For each step we multiply the numbers together that lie in the same positions on the circumferences and add the products, thereby obtaining the current value of  $f_k$ . The steps are repeated until we have returned to the initial position and a period is completed, ending the convolution process.

Since all periods are represented by the set of numbers on the circles, we shall have implicitly obtained the values of  $f_k$  for all of the periods at the same time. However, there is one major computational change necessary.

When carrying out discrete circular convolution numerically (rather than graphically using the circles) we must use a different set of arithmetic rules regarding the values of the subscript  $k$ .

In this case where the period is assumed to be 8, we must use modulo-8 arithmetic when considering the subscripts of the sequences.

Modulo- $N$  arithmetic was examined briefly in Section 10.2, and we shall assume that the reader is familiar with the discussion that we presented there. We are now in a position to define discrete circular convolution.

#### Definition of discrete circular convolution

Let  $g_k$  and  $h_k$  be two discrete sequences with definitions for  $0 \leq k \leq N - 1$ , which are repeated periodically with period  $N$ . Then their **discrete circular convolution product** is defined by

$$f_k = \sum_{m=0}^{N-1} g_m h_{k-m} \quad (14.5)$$

with the understanding that the values of the subscripts shall be computed modulo- $N$ .

Once the values of the subscripts have been obtained, we then use the given definitions of the sequences to calculate the value of  $f_k$  by ordinary arithmetic according to (14.5).

□EXAMPLE 14.2: We now perform discrete circular convolution **numerically** for the pair of sequences shown in Table 14.3 to see how it works. For our little problem the value of  $N$  is 8, and so (14.5) becomes

$$f_k = \sum_{m=0}^7 g_m h_{k-m} \quad (14.6)$$

Note that the format in (14.6) is already performing the reversal of  $h_k$  and sliding it past  $g_k$ . We now calculate the value of  $f_k$  from (14.6) for  $k = 0$  and  $k = 1$ , using  $g_k$  and  $h_k$  from Table 14.3. Modulo-8 arithmetic is used to manipulate the subscripts.

Observe how the subscripts are first written down exactly as they appear in (14.6). Then they are recomputed modulo-8. Finally, the values of the functions  $g$  and  $h$  are inserted and the values of  $f_0$  and  $f_1$  are obtained.

$k = 0:$

$$\begin{aligned} f_0 &= g_0 h_0 + g_1 h_{-1} + g_2 h_{-2} + g_3 h_{-3} + g_4 h_{-4} + g_5 h_{-5} + g_6 h_{-6} + g_7 h_{-7} \\ &= g_0 h_0 + g_1 h_7 + g_2 h_6 + g_3 h_5 + g_4 h_4 + g_5 h_3 + g_6 h_2 + g_7 h_1 \\ &= 1 + 0 + 0 + 0 + 0 + 0 + 0 + 0 + 0 \\ &= [1] \end{aligned}$$


---

$k = 1:$

$$\begin{aligned} f_1 &= g_0 h_1 + g_1 h_0 + g_2 h_{-1} + g_3 h_{-2} + g_4 h_{-3} + g_5 h_{-4} + g_6 h_{-5} + g_7 h_{-6} \\ &= g_0 h_1 + g_1 h_0 + g_2 h_7 + g_3 h_6 + g_4 h_5 + g_5 h_4 + g_6 h_3 + g_7 h_2 \\ &= 0 + 1 + 0 + 0 + 0 + 0 + 0 + 0 + 2 \\ &= [3] \end{aligned}$$

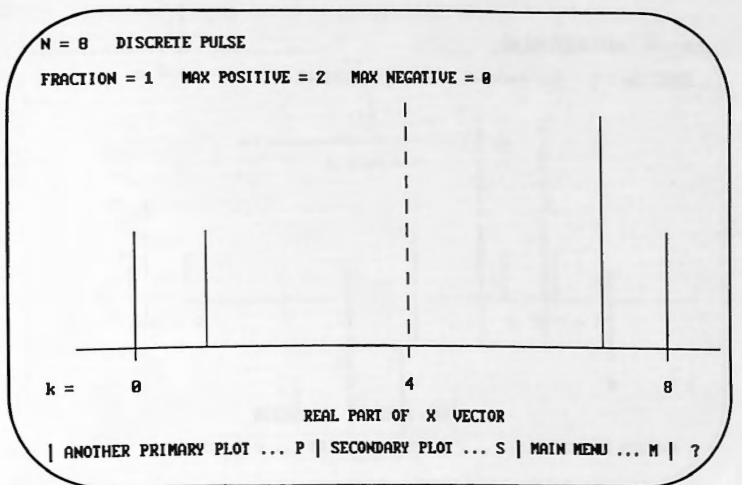
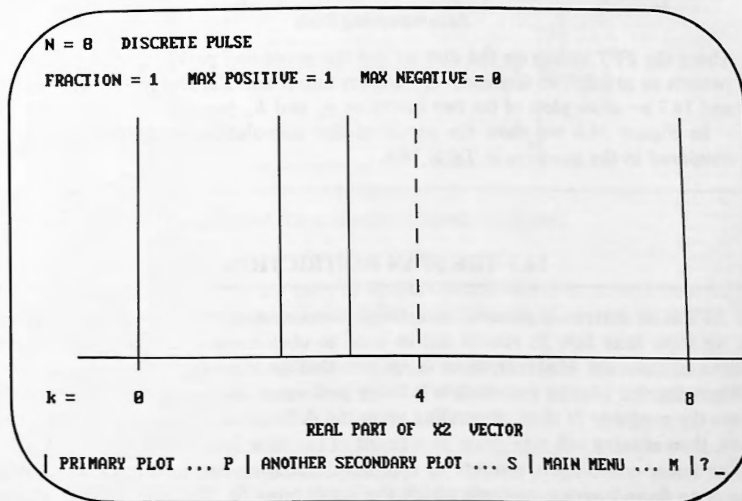
The reader should now continue this for  $k = 2, \dots, 7$ . It will be found that the overall result for one period is as shown in Table 14.4.

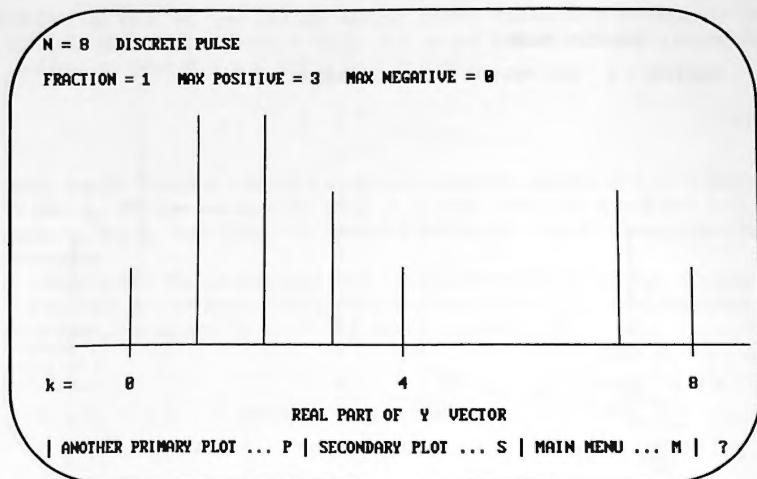
Note that  $f_k$  obtained here is the same as  $f_k$  shown in Table 14.2, except that the final value in Table 14.4 is located at  $k = 7$ , whereas in Table 14.2 that value was at  $k = -1$ , a consequence of the circularity in which  $| - 1|_8$  is equal to 7.

The reader should also do the process **graphically** using Figure 14.5. One minute of visualization will yield the same numbers as those shown in Table 14.4.

TABLE 14.4

$k$	0	1	2	3	4	5	6	7
$f_k$	1	3	3	2	1	0	0	2

Figure 14.6.  $g_k$ .Figure 14.7.  $h_k$ .

Figure 14.8. Convolution of  $g_k$  and  $h_k$ .

#### Accompanying Disk

Using the FFT system on the disk we ran the preceding problem. The system permits us to load two sequences of numbers into X and X2, and in Figures 14.6 and 14.7 we show plots of the two functions  $g_k$  and  $h_k$  just given.

In Figure 14.8 we show the result of the convolution, which should be compared to the numbers in Table 14.4.

### 14.3 THE SPAN RESTRICTION

The FFT is an extremely powerful tool for performing discrete circular convolution, and we show later how its results can be used to obtain values for the other three kinds of convolution. However, there is an item that we must first attend to.

When discrete circular convolution is being performed the output may or may not fit into the available  $N$  slots, depending upon the definitions of the inputs. If it does not fit, then aliasing will take place as a result of overflow into adjacent periods.

With linear convolution, discrete or continuous, aliasing can never occur because there is no finite-length range into which the result must fit. This means that in any runs in which discrete circular convolution is being used to emulate linear convolution we must never allow aliasing to take place. Accordingly we must be able to detect for it in order to warn the user if it is about to occur, and in what now follows we establish how that detection is done.

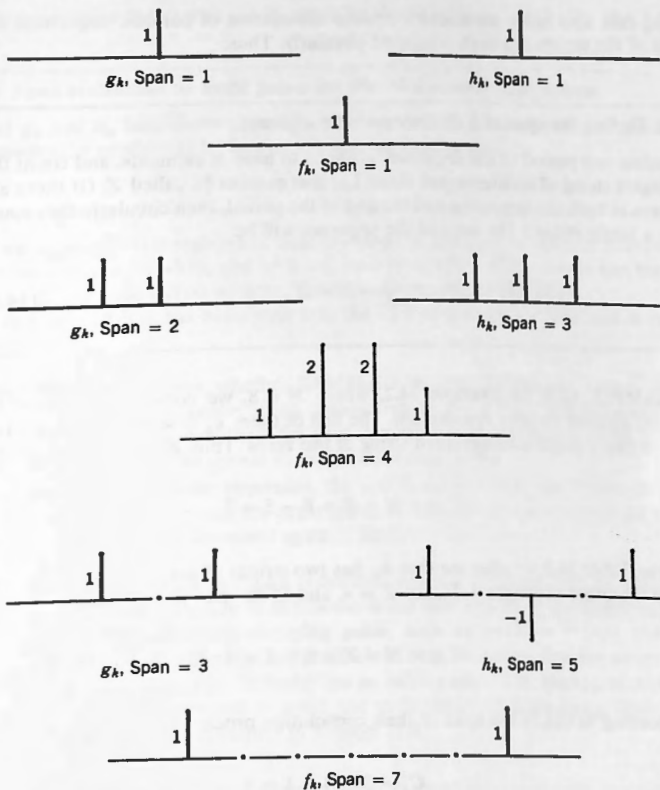


Figure 14.9. Three examples of discrete convolution.

In Figure 14.9 we show a few pairs of simple discrete linear sequences from which we will be able to derive a basic result linking the span of the output to that of the two inputs.

Examining each of the examples in the figure we see that the following rule holds true.

#### ■ Span of a discrete convolution product

If  $g_k$  has span  $p$  and  $h_k$  has span  $q$ , then their convolution product  $f_k$  will have span equal to

$$C_o = p + q - 1. \quad (14.7)$$

The rule also holds for discrete circular convolution of periodic sequences if the spans of the inputs are both computed **circularly**. Thus:

■ **To find the span of a discrete periodic sequence**

Isolate one period of the sequence, assumed to have  $N$  elements, and count the **longest string of uninterrupted zeros**. Let that number be called  $Z$ . (If there are zeros at both the beginning and the end of the period, then circularly they count as a single string.) The span of the sequence will be

$$p = N - Z \quad (14.8)$$

□ **EXAMPLE 14.3:** In Example 14.2, where  $N = 8$ , we convolved two sequences using discrete circular convolution. The first of them  $g_k$  is seen from Table 14.3 to have had a single uninterrupted string of five zeros. Thus  $Z = 5$ , and so its span is

$$p = N - Z = 8 - 5 = 3$$

From Table 14.3 we also see that  $h_k$  has two strings of zeros, the first of length 1 and the other of length 4. Hence  $Z = 4$ , and so its span is

$$q = N - Z = 8 - 4 = 4$$

According to (14.7) the span of their convolution product should be

$$C_\sigma = 3 + 4 - 1 = 6$$

Examining Table 14.4 we find that to be the case (in the circular sense). □

Here's a statement of the condition that we wish to ensure:

■ **Condition for no aliasing**

When  $g_k$  and  $h_k$  are circularly convolved, if we desire that the result  $f_k$  should fit into  $N$  slots, then its span must satisfy

$$C_\sigma \leq N \quad (14.9)$$

We now combine (14.7) with (14.9), obtaining the following:

■ **Span restriction on input pulses for alias-free circular convolution**

Let  $g_k$  and  $h_k$  have spans  $p$  and  $q$ , respectively. Then for their discrete circular convolution product to be free of aliasing, we require that

$$p + q \leq N + 1 \quad (14.10)$$

If we adhere to this restriction, then the result of the discrete circular convolution will always fit into  $N$  slots, and so it will be free of aliasing. Its results can then be used for linear convolution without fear that aliasing might take place.

A test based on it has been built into the FFT system on the disk and is run as follows:

- In the case of pulses, whether SAMPLED or DISCRETE, the system always tests them prior to commencing convolution to see if their spans comply with (14.10). If they do not, then the user is notified that aliasing is about to take place and is given the option to either abort or proceed.
- In the case of periodic sequences, the test is skipped and the results obtained from the convolution run are regarded as being correct regardless of the values of  $p$  and  $q$ . (This is discussed again in Section 14.6.)

One situation in which the span restriction might be violated, but in which one would want to proceed anyway, is as follows: When one or both of the functions being convolved is an exponentially decaying pulse, such as  $g(t) = e^{-\beta t}U(t)$ , then the sampled values of  $g(t)$  will never fall precisely to zero no matter how far we go along the  $t$ -axis, and so such a pulse in theory has an infinite span. The span restriction test, however, has been constructed to avoid just such situations from being declared as violations. This is discussed further in Section 17.4.

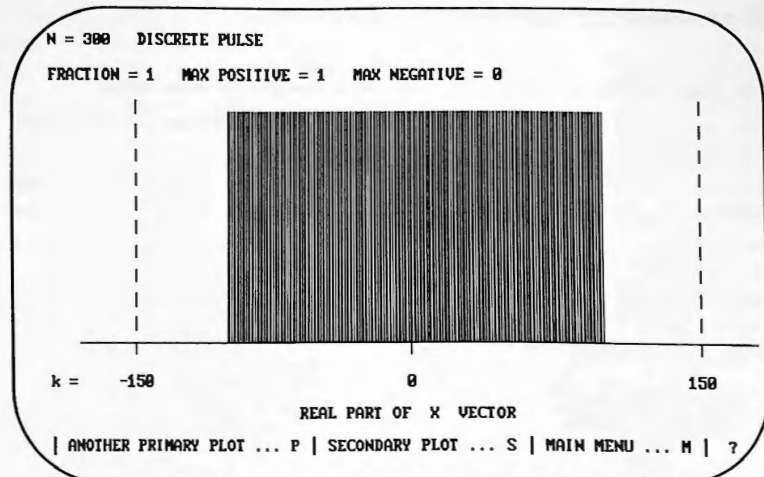
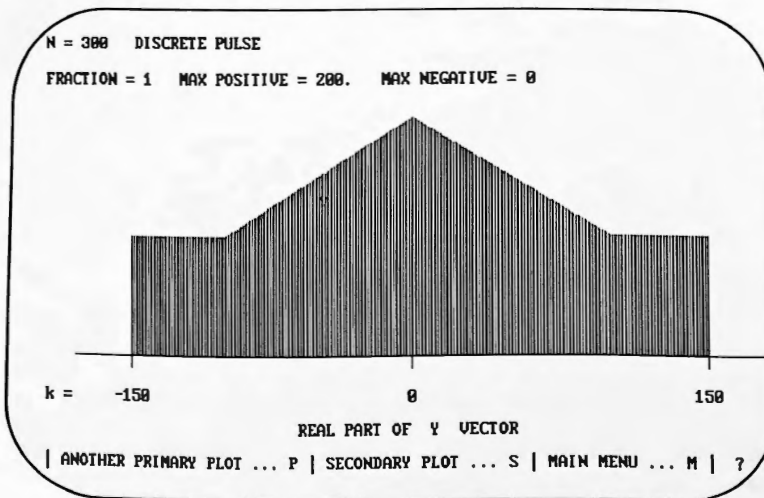
#### Accompanying Disk

Using the FFT system on the disk, we ran the following problem to demonstrate aliasing.

In Figure 14.10 we show a pulse  $g_k$  as it was loaded into the  $X$  vector. The same pulse was also loaded into  $X2$ . Both pulses were discrete Rect functions, with span counts deliberately selected so that the span restriction would be violated. Thus  $C_\sigma$  for both pulses is 200, and a value of  $N = 300$  was used.

In Figure 14.11 we show the result of the convolution run. Had the span restriction not been violated, we know that it should have been a triangular pulse. Instead we see how each period has overflowed into the adjacent one, resulting in the badly aliased pulse displayed in the figure.

In Figure 14.12 we show a run using  $N = 500$ . Aliasing is now not present because the span restriction is not being violated.

Figure 14.10.  $g_k$  and  $h_k$ .Figure 14.11. Convolution of  $g_k$  and  $h_k$  with aliasing.

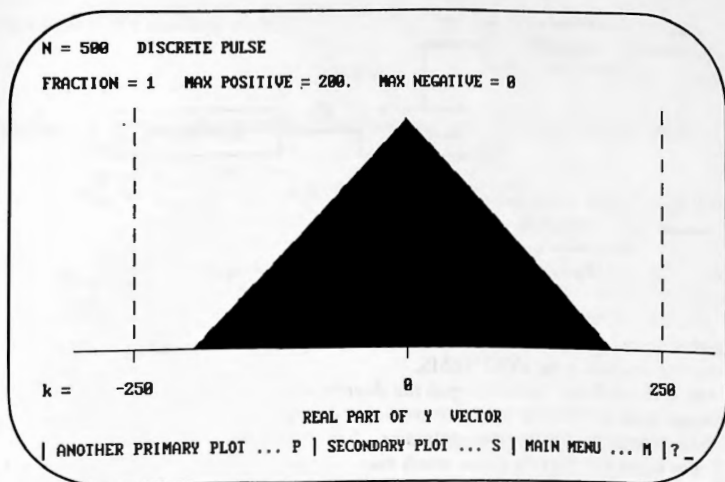


**Figure 14.12.** Convolution of  $g_k$  and  $h_k$  without aliasing.

## 14.4 DISCRETE CIRCULAR CONVOLUTION ON THE FAST FOURIER TRANSFORM

Before commencing the examination of how discrete circular convolution is run on the FFT, we make the following observation:

Referring to (14.4) the reader may well wonder why we need the FFT at all, and why we don't just carry out the convolution of the two given discrete sequences using the formula exactly as it stands. After all, we did it in Example 14.1, and so surely a computer could be programmed to do for us what we did there by hand. Moreover the computer could be programmed to do **linear** convolution rather than **circular**, thereby avoiding all possibility of aliasing, and thus eliminating the need for the span restriction.

The answer lies in the fact that direct application of (14.4) leads to very long execution times when  $N$  is large, and as we shall see, the FFT is a far more efficient way of carrying out convolution. The price that we must pay, however, is that the convolution will then be circular instead of linear, but that is not as restrictive as the reader might think.

In the final section of this chapter we compare the number of computer operations required by the two methods, direct and FFT, and it will be seen there how much more costly the direct approach becomes for large  $N$ .

Here's how discrete circular convolution is performed using the FFT. Referring to Figure 14.13, first we transform the individual discrete sequences  $g_k$  and  $h_k$  using ANALYSIS to obtain their FFT line spectra  $G_n$  and  $H_n$ , then we multiply these

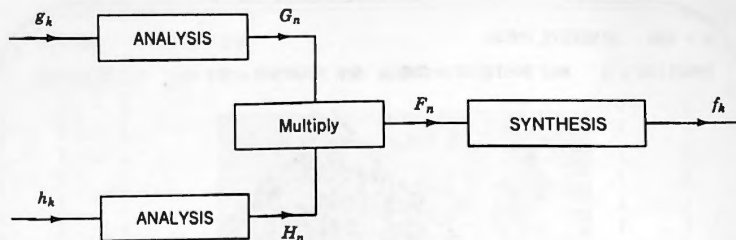


Figure 14.13. Convolution of discrete sequences using the FFT.

together (using complex multiplication) as the counterpart to (14.3), and finally we invert the product using SYNTHESIS.

The end result will correctly equal the discrete sequence  $f_k$  that would have been obtained from the discrete circular convolution definition given in (14.5). Moreover, if we have complied with the span restriction, then the discrete circular result of (14.5) will also equal the discrete linear result that would have been obtained from (14.4).

To prove that the procedure shown in Figure 14.13 is a correct representation of circular convolution we must show that if we apply the FFT to both sides of (14.5), then the resulting spectra will satisfy the expression

$$F_n = G_n H_n \quad (0 \leq n \leq N - 1) \quad (14.11)$$

because that is what the procedure in the figure accomplishes. For convenience, as in previous chapters, we define

$$W = e^{-2\pi/N} \quad (14.12)$$

Then the FFT analysis equation becomes

$$F_n = \sum_{k=0}^{N-1} f_k W^{nk} \quad (14.13)$$

We now use this to transform (14.5), obtaining

$$F_n = \sum_{k=0}^{N-1} \left[ \sum_{m=0}^{N-1} g_m h_{k-m} \right] W^{nk}$$

Interchanging the order of summation gives

$$F_n = \sum_{m=0}^{N-1} g_m \left[ \sum_{k=0}^{N-1} h_{k-m} W^{nk} \right] \quad (14.14)$$

Now define the auxiliary variable

$$r = k - m \quad (14.15)$$

Then, if we use  $r$  as the variable of summation in place of  $k$ , (14.14) becomes

$$F_n = \sum_{m=0}^{N-1} g_m \left[ \sum_{r=-m}^{N-1-m} h_r W^{n(r+m)} \right] = \sum_{m=0}^{N-1} g_m W^{nm} \left[ \sum_{r=-m}^{N-1-m} h_r W^{nr} \right] \quad (14.16)$$

At first sight it would appear as though the final sum in square brackets in (14.16) depends in some way on  $m$ , but we now show that that is not the case. For simplicity assume that  $N = 8$  and  $m = 5$ . Writing out the sum in square brackets we obtain

$$\begin{aligned} \sum_{r=-m}^{N-1-m} h_r W^{nr} &= \sum_{r=-5}^2 h_r W^{nr} \\ &= h_{-5} W^{n(-5)} + h_{-4} W^{n(-4)} + h_{-3} W^{n(-3)} + h_{-2} W^{n(-2)} \\ &\quad + h_{-1} W^{n(-1)} + h_0 W^{n(0)} + h_1 W^{n(1)} + h_2 W^{n(2)} \end{aligned} \quad (14.17)$$

However, we now note the following two facts regarding (14.17):

- Convolution here is circular, and so the subscripts of  $h_k$  must be computed modulo-8.
- The function  $W^{nr}$  repeats modulo-8 because that is an essential property of the discrete complex exponentials of order 8.

Thus (14.17) continues as follows:

$$\begin{aligned} \dots &= h_3 W^{n(3)} + h_4 W^{n(4)} + h_5 W^{n(5)} + h_6 W^{n(6)} \\ &\quad + h_7 W^{n(7)} + h_0 W^{n(0)} + h_1 W^{n(1)} + h_2 W^{n(2)} \end{aligned} \quad (14.18)$$

which can then be reordered, and so it continues further as

$$\begin{aligned} \dots &= h_0 W^{n(0)} + h_1 W^{n(1)} + h_2 W^{n(2)} + h_3 W^{n(3)} \\ &\quad + h_4 W^{n(4)} + h_5 W^{n(5)} + h_6 W^{n(6)} + h_7 W^{n(7)} \\ &= \sum_{r=0}^{N-1} h_r W^{nr} \end{aligned} \quad (14.19)$$

We have thus demonstrated that in fact the sum in square brackets does not depend on  $m$ , and that it can be replaced by the sum shown in the final line of (14.19). Indeed, if we now go back to (14.16) and picture everything on a circle, we soon see that it does not matter where on the circle we begin, as long as we go round

it once, completely. In this way (14.16) becomes

$$F_n = \left[ \sum_{m=0}^{N-1} g_m W^{nm} \right] \left[ \sum_{r=0}^{N-1} h_r W^{nr} \right] \quad (14.20)$$

which can then be stated as

$$F_n = G_n H_n \quad (14.21)$$

All of this is summarized in Theorem 14.1.

### ■ THEOREM 14.1

Let  $f_k$  be the circular discrete convolution product of  $g_k$  and  $h_k$ , that is, let

$$f_k = \sum_{m=0}^{N-1} g_m h_{k-m} \quad (0 \leq k \leq N-1) \quad (14.22)$$

in which the subscripts are computed modulo- $N$ . Then their FFT spectra satisfy

$$F_n = G_n H_n \quad (0 \leq n \leq N-1) \quad (14.23)$$

Note that (14.23) is the dual to (14.3). In the following box we give a verbal statement of what we have proved.

### ■ Discrete circular convolution

Let the two sequences  $g_k$  and  $h_k$  have FFT spectra  $G_n$  and  $H_n$ . Let the product  $G_n H_n$  be formed, and then let that product be inverted using the FFT synthesis equation. Then the result will be equal to the sequence  $f_k$ , which is the discrete circular convolution product of the sequences  $g_k$  and  $h_k$ .

Observe that in the box we say nothing about the span restriction on the input sequences  $g_k$  and  $h_k$  because it does not enter into it—the preceding theorem is true regardless of what the two spans are. However, only if the span restriction is satisfied will we obtain an unaliased spectrum  $f_k$  from the procedure described in the box and shown in Figure 14.13, and if it is violated, then  $f_k$  will be aliased.

Obviously in any practical situation involving pulses we shall want to limit  $g_k$  and  $h_k$  in accordance with the span restriction so that aliasing does not occur, although it would be instructive to create pulses whose spans do violate (14.10) and then to convolve them using the system on the disk in order to see the aliasing that inevitably takes place. This is done in some of the exercises.

## 14.5 DISCRETE LINEAR CONVOLUTION USING THE FAST FOURIER TRANSFORM

---

Given two discrete pulses that we wish to convolve using discrete linear convolution as defined in (14.4), it is now a simple matter to see how the FFT can be used.

From the results of the preceding section we now know that the FFT's convolution is discrete circular. If the inputs have finite span counts, however, and we adhere to the span restriction, then there will be no aliasing. Its results will be exactly the same as if discrete linear convolution had been run directly on the two input pulses.

The only difference is that the results of the FFT are always periodic, whereas the result of (14.4) is aperiodic. That is of little or no importance, however, since when we inspect the output of the FFT run, we need only look at one of its periods, each of which will correctly contain the result that we are seeking, namely the discrete linear convolution of our two finite-span input pulses without aliasing.

## 14.6 CONTINUOUS LINEAR CONVOLUTION USING THE FAST FOURIER TRANSFORM

---

So far we have been able to show how the FFT can be used to perform **discrete** convolution, both circular and linear. However, that does not necessarily mean that the vector  $f_k$  coming out of that convolution computation is scaled correctly to serve as a sequence of estimates for either **continuous linear** or **continuous circular** convolution. In this section we consider continuous linear convolution on the FFT, and in the next we examine continuous circular.

In the case of continuous linear convolution we start with two pulses  $g(t)$  and  $h(t)$ , and we wish to use the FFT to obtain numerical values of their convolution product, namely of

$$f(t) = \int_0^T g(\tau)h(t - \tau) d\tau \quad (14.24)$$

where  $T$  for pulses was defined at the beginning of this chapter, and where we are assuming that the pulses

- Both have spans  $\leq T$
- Are both zero for  $t < 0$

Hence the limits of integration appearing in (14.24). (See Exercise 7.12.)

*Note:* In the definition of  $T$  we talked about the need to append zeros in order to obtain a good representation of the Fourier transform of a pulse. In the case of convolution we are usually less interested in the spectra, and so the only reason we would append zeros is to be able to adhere to the span restriction. Also, in (14.24) we are showing a finite range of integration that implies that we are convolving pulses with finite spans. In Section 17.4 we show that infinite-span pulses can also be convolved using the FFT if proper precautions are taken.

Discretizing (14.24) with sampling interval  $T_s$ , and using the rectangular rule for integration (see Section 12.2), now gives us

$$f(t_k) = \sum_{m=0}^{N-1} g(\tau_m)h(t_k - \tau_m)T_s \quad (14.25)$$

in which  $t_k = kT_s$  and  $\tau_m = mT_s$ . We then abbreviate this equation as follows,

$$f_k = \sum_{m=0}^{N-1} g_m h_{k-m} T_s \quad (14.26)$$

and comparing this to (14.5), which we restate here for convenience

$$f_k = \sum_{m=0}^{N-1} g_m h_{k-m} \quad (14.27)$$

shows us that we must multiply the output of the FFT convolution computation (14.27) by  $T_s$  if we want it to give us properly scaled estimates of  $f(t_k)$  in (14.25). As we recall,  $T_s = T/N$ . Thus multiplication of the FFT's output vector by  $T/N$  will serve to accomplish the scaling correctly. We have thus proved the result shown in the following box.

### ■ Using the FFT to emulate continuous linear convolution

Let the two pulses  $g(t)$  and  $h(t)$  have finite spans, and let them be numerically sampled at  $N$  points spaced  $T_s$  seconds apart over the range 0 to  $T$  to give the discrete sequences  $g_k$  and  $h_k$ , where  $0 \leq k \leq N - 1$ . Let these sequences satisfy the span restriction (14.10). Let  $g_k$  and  $h_k$  be FFT-transformed to give  $G_n$  and  $H_n$ , and let those two FFT spectra then be multiplied together, term by term, to give the spectrum  $F_n$ , that is,

$$F_n = G_n H_n \quad (0 \leq n \leq N - 1) \quad (14.28)$$

Then if  $F_n$  is inverted using the FFT synthesis equation and the result multiplied by the scale factor  $T_s = T/N$ , we shall have obtained a sequence of estimates of the continuous linear convolution product of  $g(t)$  and  $h(t)$ , properly scaled.

Moreover, for the FFT spectrum to correctly represent the spectrum of the output  $f(t)$ , we must multiply the product  $G_n H_n$  by  $(T/N)^2$  prior to displaying it.

Because the accuracy of the result will depend on how well rectangular-rule integration approximates the continuous convolution integral (14.24), it can be made as good as we please by making  $N$  sufficiently large.

The scale factor  $(T/N)^2$  in the second paragraph in the box arises as follows. In Chapter 12 [see (12.41)] we saw that the raw values of an FFT spectrum must be

multiplied by  $T/N$  in order for them to be the approximations of a continuous Fourier transform (CFT) (pulse) spectrum. Two spectra are being multiplied together here, hence  $(T/N)^2$ .

Note that in the box we have included the span restriction, since if it were to be violated, then aliasing would take place during the FFT convolution, and aliasing is a process that could not ever occur when performing linear convolution of one-time pulses.

## 14.7 CONTINUOUS CIRCULAR CONVOLUTION USING THE FAST FOURIER TRANSFORM

We now consider how the FFT can be used to compute the convolution product of two periodic waveforms  $g_p(t)$  and  $h_p(t)$ .

In one of the exercises we ask you to prove the following basic result for periodic functions, which corresponds to (14.3).

### ■ THEOREM 14.2

Let  $f_p(t)$  be the circular convolution product of  $g_p(t)$  and  $h_p(t)$ , whose periods are  $T_0$  and whose CFT line spectra are  $G_p(n)$  and  $H_p(n)$ . Then the CFT line spectrum of  $f_p(t)$  will satisfy

$$F_p(n) = T_0 G_p(n) H_p(n) \quad (\forall n) \quad (14.29)$$

Based on Theorem 14.2 we then have the procedure shown in the following box. Note that we say nothing about the span restriction because, with circular convolution of periodic functions, aliasing has no meaning. What comes out is strictly a reflection of what went in, and so we do not require the span restriction.

### ■ Using the FFT to emulate continuous circular convolution

Let the two periodic functions  $g_p(t)$  and  $h_p(t)$  be numerically sampled at  $N$  points over one period to give the discrete sequences  $g_k$  and  $h_k$ , where  $0 \leq k \leq N - 1$ .

Let  $g_k$  and  $h_k$  be FFT-transformed to give  $G_n$  and  $H_n$ , and let those two FFT spectra then be multiplied together, term by term, to give the spectrum  $F_n$ , that is,

$$F_n = G_n H_n \quad (0 \leq n \leq N - 1) \quad (14.30)$$

Then if  $F_n$  is inverted using the FFT synthesis equation and the result multiplied by the scale factor  $T_s = T_0/N$ , we shall have obtained a sequence of estimates of the continuous circular convolution product of  $g_p(t)$  and  $h_p(t)$ , properly scaled.

Moreover, for the FFT spectrum to correctly represent the spectrum of the output  $f_p(t)$ , we must multiply the product  $G_n H_n$  by  $T_0/N^2$  prior to displaying it.

Where did the two scale factors in the box come from?

- The first one,  $T_s = T_0/N$ , is the same as the one that we used in the preceding section and arises from the  $T_s$  in (14.25) that came from the rectangular rule.
- The second one,  $T_0/N^2$ , arises as follows: In (14.29) we see that the discrete spectrum  $F_p(n)$  is produced from the product of the two spectra  $G_p(n)$  and  $H_p(n)$  and the result then multiplied by  $T_0$ . In Chapter 12 [see (12.51)] we saw that the raw values of an FFT spectrum must be multiplied by  $1/N$  in order for them to be the approximation of a Fourier series spectrum. Two spectra are being multiplied together here; hence  $1/N^2$ . Taking both of these together gives us the final scale factor for the spectrum as  $T_0/N^2$ .

Thus to use the FFT for continuous circular convolution we simply sample one period of the time-domain statement of each of the two given periodic functions and send the numbers to the FFT as input sequences to its (inherently circular) convolution algorithm. If we scale according to the preceding box, then what we get back will be a valid estimate of what we are seeking, and by making  $N$  sufficiently large, we can achieve any desired degree of accuracy.

We stated earlier that the system on the accompanying disk checks the spans of the sequences being convolved to see if they comply with the span restriction. That is only done, however, when those sequences are declared to be pulses, and is skipped when they are declared to be periodic, since in the periodic case aliasing has no meaning, and so what you get is what you want.

## 14.8 OPERATION COUNT TO PERFORM CONVOLUTION

---

Convolution of two discrete sequences can be done in two ways, either directly or else using the FFT. We close this chapter with an examination of the number of operations required to carry out this convolution directly, and we compare that number to how many are required if we use the FFT. The difference is substantial and grows rapidly as the length of the sequences increases, with the advantage being strongly in favor of the FFT.

By **direct convolution** of two sequences  $g_k$  and  $h_k$  we of course mean producing their convolution product  $f_k$  by the use of the algorithm

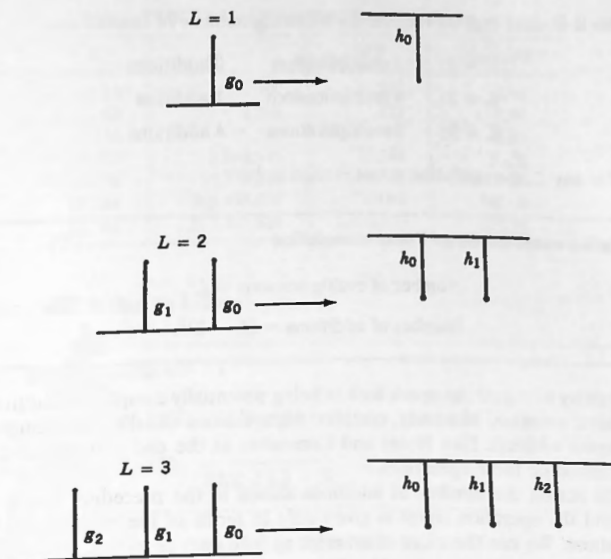
$$f_n = \sum_{k=-\infty}^{\infty} g_k h_{n-k} \quad (14.31)$$

Without loss of generality we can assume that both sequences are zero for  $k < 0$ , which means that  $g_k$  zeros out the products in (14.31) when  $k$  is negative, and so it becomes

$$f_n = \sum_{k=0}^{\infty} g_k h_{n-k} \quad (14.32)$$

Similarly, when  $k$  exceeds  $n$ , we see that the subscript of  $h$  in (14.32) becomes negative, and so it then zeros out the products as well, resulting in

$$f_n = \sum_{k=0}^n g_k h_{n-k} \quad (14.33)$$

Figure 14.14. Linear convolution,  $L = 1, 2, 3$ .

The span counts of the two sequences  $g_k$  and  $h_k$  may not be equal, but as a worst case we shall assume that they are, a quantity that we call  $L$ . (The case where either or both of them is exponentially decaying, i.e.,  $L = \infty$ , is considered in Section 17.4.) Then, (14.33) can be expanded by keeping in mind the picture shown in Figure 14.14, in which we show the two sequences being moved past each other for the three cases  $L = 1, 2$ , and  $3$ .

For the three values of  $L$  shown in the figure, we obtain the following expansions for  $f_n$ :

$$L = 1: f_0 = g_0 h_0$$

$$L = 2: f_0 = g_0 h_0$$

$$f_1 = g_0 h_1 + g_1 h_0$$

$$f_2 = g_1 h_1$$

$$L = 3: f_0 = g_0 h_0$$

$$f_1 = g_0 h_1 + g_1 h_0$$

$$f_2 = g_0 h_2 + g_1 h_1 + g_2 h_0$$

$$f_3 = g_1 h_2 + g_2 h_1$$

$$f_4 = g_2 h_2$$

From this it is clear that we require the following number of operations:

$L = 1$ :	1 multiplication	0 additions
$L = 2$ :	4 multiplications	1 addition
$L = 3$ :	9 multiplications	4 additions

and so for any  $L$ , the operation count is seen to be

#### Operation count for direct linear convolution

$$\text{Number of multiplications} = L^2.$$

$$\text{Number of additions} = (L - 1)^2.$$

It is customary to regard the operations as being potentially complex, since that is the most general situation. Moreover, complex multiplication usually takes much longer than complex addition. (See Notes and Comments at the end of Chapter 11 for a brief discussion on these operations.)

For this reason the number of additions shown in the preceding box is usually ignored and the operation count is given only in terms of the number of complex multiplications. We can therefore summarize as follows:

#### Operation count for direct linear convolution

$$\text{Number of complex multiplications} = L^2.$$

Now let's see what it would take, using the FFT. In Chapter 11 we saw that the FFT's complex multiplication count is as follows:

#### Operation count for the FFT or IFFT

$$\text{Number of complex multiplications} = \frac{1}{2}N \log_2 N.$$

To run a convolution using the FFT requires two passes through ANALYSIS and then a pass through SYNTHESIS, for a total of  $3 \times \frac{1}{2}N \log_2 N$  complex multiplications. There are also  $N$  complex multiplications required to form  $\mathbf{F} \times \mathbf{F2}$ . Taking all of this into account, we see that convolution via the FFT requires approximately  $(3/2)(N)(\log_2 N) + N$  complex multiplications.

To convolve two pulses each of length  $L$  we would use  $N = 2L - 1$  in order to avoid a violation of the span restriction. For simplicity we use  $N = 2L$  (which is on the safe side), and so the operation count using the FFT for convolution becomes

$$C_{\text{FFT}} = 3L \log_2(2L) + 2L = L[3 \log_2(L) + 5] \quad (14.34)$$

TABLE 14.5 Convolution Operation Counts

<i>L</i>	<i>Direct</i>	<i>FFT</i>	<i>Direct : FFT</i>
16	256	272	0.94
64	4,096	1,472	2.78
256	65,536	7,424	8.83
1,024	1,048,576	35,840	29.26
4,096	16,777,216	167,936	99.90
16,384	268,435,456	770,048	348.60
32,768	1,073,741,824	1,638,400	655.36

Our comparison is thus as follows:

Direct linear convolution:  $L^2$

Convolution via the FFT:  $L[3 \log_2(L) + 5]$

Ratio of Direct to FFT:  $\frac{L}{3 \log_2(L) + 5}$

This leads to the numbers displayed in Table 14.5.

Observe from the final column how rapidly the advantage is moving to the FFT. For example, a convolution run with  $L = 32,768$  requiring seven minutes of machine time for the FFT would take a full three days on the same machine if done by the direct method.

## EXERCISES

14.1 Consider the two discrete pulses  $g_k$  and  $h_k$  defined in the following table:

<i>k</i>	0	1	2	3	4	5	6	7	8	9
$g_k$	1	0	1	0	0	2	0	0	0	0
$h_k$	2	1	2	3	1	0	0	0	0	0
$f_k$	2	1	4	4	3	7	3	4	6	2

- Convolve them using linear convolution by hand, and verify that your result is the same as  $f_k$  in the table.
- Using a value of  $N = 10$ , convolve them by hand using circular convolution for  $0 \leq k \leq 9$ . Compare the result that you obtain with  $f_k$  in the table.
- Load them into  $X$  and  $X2$  of the FFT system. (Use  $N = 10$ , DISCRETE. Then Both X, Real, 10 intervals.) Run CONVOLUTION to verify the result that you obtained in (b). Inspect the numbers by taking Option I. They should be identical to (b).

- (d) What is the value of  $C_\sigma$  for each of  $g_k$  and  $h_k$ ? What is the value of  $C_\sigma$  for  $f_k$ ? Are the values consistent with (14.7)? Do the two sequences comply with the span restriction (14.10) when  $N = 10$ ?
- (e) If we were to change  $h_5$  from 0 to 4, what would be the value of  $C_\sigma$  for  $h_k$ ? Do the sequences still comply with the span restriction when  $N = 10$ ?
- (f) Repeat the linear convolution by hand with the new value of  $h_5 = 4$ .
- (g) Repeat the circular convolution both by hand as well as by using the FFT system with  $N = 10$ , and compare the result to (f).

*Note:* On the FFT system you can change  $h_5$  by “using the old-problem,” starting from main-menu A. When you run CONVOLUTION you will be told that the span restriction is being violated. Use “RUN CONVOLUTION REGARDLESS.” (Only with Version 1.30 and later.)

Your result should be inconsistent with (f) because of aliasing. Observe how two of the elements in  $f_k$  have become added together.

- (h) Now change  $N$  to 12 and rerun the circular convolution both by hand as well as by using the FFT system. The result should now be consistent with (f). Verify that the span restriction is no longer being violated.
- (i) Infer that by increasing  $N$  so that the span restriction is no longer violated, circular convolution can again be successfully used to emulate linear convolution.

The above exercise involved pulses that did not straddle the origin, and so they were extremely simple to handle circularly. In the next exercise we consider pulses that do straddle the origin.

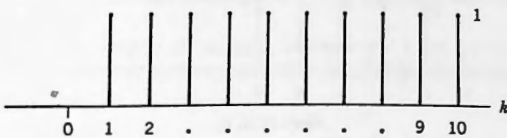
**14.2** Consider the two discrete pulses  $g_k$  and  $h_k$  defined in the following table:

$k$	-5	-4	-3	-2	-1	0	1	2	3	4
$g_k$	0	1	0	1	0	0	2	0	0	0
$h_k$	0	0	0	0	2	1	2	3	1	0
$f_k$	2	1	4	4	3	7	3	4	6	2

We note that they are the same pulses as in Exercise 1, but here they have been shifted so that now they both straddle the origin.

- (a) Convolve them using linear convolution by hand. Verify that the result agrees with  $f_k$  as shown in the table.
- (b) Using a value of  $N = 10$ , convolve them by hand using circular convolution for  $0 \leq k \leq 9$ . Compare the result that you obtain with  $f_k$  in the table.
- (c) Load them into X and X2 of the FFT system with  $N = 10$ , and run CONVOLUTION to verify the result that you obtained in (b). (Use  $N = 10$ , DISCRETE. Then Both X, Real, 10 intervals.)
- (d) What is the value of  $C_\sigma$  for each of  $g_k$  and  $h_k$ ? What is the value of  $C_\sigma$  for  $f_k$ ? Are the values consistent with (14.7)? Do the two sequences comply with the span restriction (14.10) when  $N = 10$ ?
- (e) If we were to change  $h_4$  from 0 to 4, what would be the value of  $C_\sigma$  for  $h_k$ ? Are the sequences now still in compliance with the span restriction?

- (f) Repeat the linear convolution using the new value of  $h_4 = 4$ .
- (g) Repeat the circular convolution both by hand as well as by using the FFT system with  $N = 10$ . (See Note in Exercise 14.1(g).) Your result should be inconsistent with (f) because of aliasing.
- (h) If we now change  $N$  to 12, then the span restriction would no longer be violated and aliasing should disappear. Rerun the circular convolution both by hand as well as by the use of the FFT system with  $N = 12$ . The result should now be consistent with (f), but only if you loaded the pulses properly, taking into account the note of caution just given.

Figure 14.15.  $g_k$ .

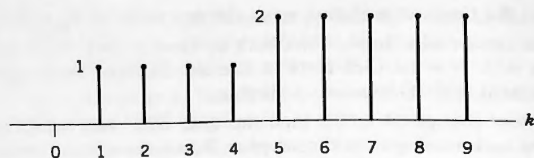
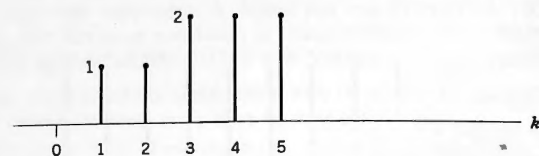
**14.3** The discrete pulse shown in Figure 14.15 has the following definition:

$$g_k = 1 \quad (1 \leq k \leq 10)$$

- (a) Use the FFT system to find the spectrum of  $g_k$  using  $N = 24$ . Let it be called  $G_n$ .
- (b) Write down the real and imaginary parts of  $G_n$  for  $n = 1, 5$  and  $9$ , that is,  $G_1$ ,  $G_5$ , and  $G_9$ .
- (c) By hand, find the convolution product of  $g_k$  with itself, calling the result  $f_k$ . Then use the FFT system to find the spectrum of  $f_k$ , using  $N = 24$ . Let it be called  $F_n$ .
- (d) Verify that  $F_1 = G_1^2$ ,  $F_5 = G_5^2$ , and  $F_9 = G_9^2$ , thereby verifying (14.23).
- (e) Load  $g_k$  into both X and X2, and run CONVOLUTION. Compare your result to what you obtained in (c) by hand. The values should be identical.

*Note:* You can read the values for the spectrum of a convolution run by starting from main-menu I.

- 14.4** (a) Referring to Figures 14.16 and 14.17, apply linear graphical convolution to the two discrete pulses  $g_k$  and  $h_k$ , calling the result  $f_k$ .
- (b) Load  $g_k$  into X and  $h_k$  into X2 of the FFT system using  $N = 16$ . Find the spectra of  $g_k$  and  $h_k$  and let them be called  $G_n$  and  $H_n$ . Write down their values for  $n = 1, 5, 7$ .

Figure 14.16.  $g_k$ .Figure 14.17.  $h_k$ .

*Hint:* After transforming  $g_k$ , use the package in the F postprocessor (main-menu G) that swaps X and X2 as well as F and F2.

- (c) Using the values from (b), use a hand calculator to find the values of  $G_n H_n$  for each of  $n = 1, 5, 7$ .
- (d) Now use the complex-multiply package in the F postprocessor to multiply  $G_n$  and  $H_n$  together. Check the results for  $n = 1, 5, 7$  against the values obtained in (c).
- (e) Use SYNTHESIS to invert the result of the multiplication. Is the result that you obtain the same as what you obtained in (a)?

- 14.5 (a) Use circular convolution by hand with  $N = 10$  to convolve the two discrete pulses of Exercise 14.4.
- (b) Carry out the convolution of the same two pulses using the formal definition of circular convolution (14.5), that is, computing the subscripts modulo-10, and account for every value that you obtained in (a).
- (c) Convolve the two pulses using the FFT with  $N = 10$  and verify your results in (a).

- 14.6 **Convolution of pulses with discontinuities.** When a pulse  $f(t)$  has a discontinuity, then we always define its value at that point to be what we have called the “half-value,” and if the pulse is sampled at the discontinuity, then the half-value is what is sent to the FFT. When we are running convolution involving such pulses, the half-values can cause slight errors. There is a way in which to fix the problem and in this exercise we explore how that is done.

- (a) Consider first the problem itself. Let the two inputs be

$$g(t) = h(t) = \text{Rect}(t - \frac{1}{2}) \quad (14.35)$$

Verify (using graphical convolution) that their convolution product is

$$f(t) = \Lambda(t - 1) \quad (14.36)$$

- (b) Now load  $g(t)$  and  $h(t)$  into **X** and **X2** using  $N = 256$ , SAMPLED,  $T = 4$ , PULSE. (The system will automatically create half-values at  $t = 0$  and  $t = 1$ , since those points are FFT sampling instants.) Then run CONVOLUTION. Observe that the **Y** vector agrees with a sampled version of (14.36) everywhere except at  $t = 0, 1$ , and 2 where there are slight errors. At  $t = 0$  and  $t = 2$  the exact values are 0, but the FFT gives 0.00390625. At  $t = 1$  the exact value is 1, but the FFT gives 0.9921875. These three errors are caused by the half-values that were present in the data that were loaded into the system.
- (c) To fix the problem: If possible, redefine the input pulses so that the discontinuities fall midway between sampling points. In this case we use as the inputs

$$g(t) = h(t) = \text{Rect}(t - \frac{1}{2} - T_s/2) \quad (14.37)$$

Use time shift to verify that the theoretical result should now be

$$f(t) = \Lambda(t - 1 - T_s) \quad (14.38)$$

- (d) Now load the pulses of (14.37) into **X** and **X2**. This time half-values will not be visible since we are not sampling at any discontinuities. Run CONVOLUTION once more. The result should now agree with a sampled version of (14.38) at every point.

**14.7** Repeat Exercise 14.6, but now use as the inputs

$$g(t) = \begin{cases} \frac{1}{2} & (0 < t < \frac{1}{2}) \\ 1 & (\frac{1}{2} < t < 1) \end{cases} \quad h(t) = \text{Rect}(t - \frac{1}{2})$$

- (a) Find and sketch their convolution product using the graphical approach.
- (b) Load the pulses into **X** and **X2** using  $N = 256$  and  $T = 4$ . Half-values will be present. Run CONVOLUTION and identify all of the errors in the output. (There are five.)
- (c) Now redo the problem, but delay the inputs by half a sampling interval. This time the result should be error free.

**14.8** Prove the result shown in Theorem 14.2.

#### 14.9 Circular convolution of periodic time functions.

- (a) Carry out the following convolution operation graphically:

$$f_p(t) = g_p(t) * h_p(t)$$

where

$$g_p(t) = h_p(t) = \sum_{k=-\infty}^{\infty} \text{Rect}(t - \frac{1}{2} - kT_0) \quad (T_0 = 4)$$

- (b) Find the expressions for the CFT coefficients of  $g_p(t)$ ,  $h_p(t)$ , and  $f_p(t)$ , calling them  $G_p(n)$ ,  $H_p(n)$ , and  $F_p(n)$ .
- (c) According to Theorem 14.2

$$F_p(n) = T_0 G_p(n) H_p(n)$$

Using the spectra from (b), verify that this is true.

- (d) Load  $g_p(t)$  and  $h_p(t)$  into X and X2 of the FFT system, using  $N = 256$ , SAMPLED,  $T = 4$ , PERIODIC, and then run CONVOLUTION. The spectrum  $H_p(n)$  is now in F2 and the spectrum  $F_p(n)$  is now in F. For each of these two spectra, fill in the following table, thereby verifying all your results, including the scale factor  $T_0/N^2$  below equation (14.30) in the box.

$n$	FFT Value		Formula Value	
	$A_n$	$B_n$	$A(n)$	$B(n)$
0				
1				
2				
3				

# Emulating Dirac Deltas and Differentiation on the Fast Fourier Transform

---

## 15.1 TIME-DOMAIN DIRAC DELTAS ON THE FAST FOURIER TRANSFORM

---

We have seen how valuable the Dirac delta is in Fourier analysis, and so it would be most unfortunate if we could not somehow also emulate it on the FFT system. At first glance one might think that this is not possible since  $\delta(t - t_0)$  has an undefined value at  $t = t_0$ , and so one has to wonder what to load into the  $X$  vector for a sample taken at that point. In this chapter we show how all of the essential attributes of the Dirac delta can in fact be implemented, in both the time and frequency domains.

After its mystique has been stripped away, we come to realize that a time-domain Dirac delta does two things:

- It nulls out a function that it multiplies at points not located at its own position on the  $t$ -axis.
- It samples the function at the point that coincides with its position and then multiplies its weight by that value.

We now discuss what we call the **Dirac function**,  $D_k$ , which can easily be implemented on the FFT system and yet possesses these two essential properties of the Dirac delta. In this section we concern ourselves with the emulation of Dirac deltas in the time domain, and in the next one we'll examine how things work in the frequency domain.

Clearly the Dirac function must be zero at all sample points on the time axis other than the one at which the “spike” is located. That's the easy part. The question still remains regarding the value that must be used at the critical sampling point.

For the Dirac function  $D_k$  to emulate the Dirac delta it would have to possess the following three properties:

- (1) In Section 4.11 we examined the function  $\delta_T(t)$ , which was a train of equally spaced unit impulses, and we found that the coefficients of its Fourier series all had the same value, namely  $1/T$ , where  $T$  is the spacing between the impulses. We can state this as

$$\delta_T(t) \Leftrightarrow \frac{1}{T} \quad (15.1)$$

If we were attempting to emulate  $\delta_T(t)$  on the FFT, we would want the same result to emerge. This in turn means that if we were to send our Dirac function to the FFT system using PERIODIC with period  $T$  and weight equal to unity, then the resulting FFT-derived Fourier series coefficients must have a value of  $1/T$  for all values of  $n$ , that is,

$$F_n = \frac{1}{T} \quad \left( -\frac{N}{2} \leq n \leq \frac{N}{2} \right) \quad (15.2)$$

- (2) We also know that the Dirac delta, when viewed as a pulse, transforms to unity in the frequency domain, that is,

$$\delta(t) \Leftrightarrow 1 \quad (15.3)$$

Thus if we were to send the Dirac function to the FFT system using PULSE with weight unity, then the resulting FFT-derived samples of its Fourier transform must have a value of 1 for all values of  $n$ , that is,

$$F_n = 1 \quad \left( -\frac{N}{2} \leq n \leq \frac{N}{2} \right) \quad (15.4)$$

- (3) Finally, when performing CONVOLUTION, if we were to convolve two Dirac functions in the time domain with weights  $\mu_1$  and  $\mu_2$ , then the result must be a Dirac function at the appropriate location with weight  $\mu_1\mu_2$ . This follows because

$$\mu_1\delta(t - t_1) * \mu_2\delta(t - t_2) = \mu_1\mu_2\delta(t - t_1 - t_2) \quad (15.5)$$

By careful consideration of the FFT analysis and synthesis equations and the way in which we implemented the various scale factors, it became clear to us that the rule stated in the following box would give us all of the desired attributes for the Dirac function  $D_k$ .

■ **The Dirac function: Emulating a Dirac delta in the time domain**

To emulate the Dirac delta  $\mu\delta(t - kT_s)$ , load into X the single value

$$XRE(k) = \frac{\mu N}{T} \quad (15.6)$$

with zeros for all other values, where

- $\mu$  is the weight of the impulse
- $N$  and  $T$  have their usual meanings
- $T_s = T/N$

Then properties (1) to (3) just listed will be present.

□ **EXAMPLE 15.1**

- (a) Load the impulse  $3\delta(t - 1)$  using  $N = 256$  and  $T = 16$ .  
 (b) Find values for  $A_n$ ,  $B_n$ , and  $|F_n|$  for  $0 \leq n \leq 4$ .

**Solution:**

- (a) The required sequence of steps is as follows: Starting from the main-menu A we enter  $N = 256$ , SAMPLED,  $T = 16$ , PULSE. Then we take the option "CREATE ONLY DIRAC DELTAS". When prompted for the location on the  $t$ -axis we enter "1", and when prompted for the weight we enter "3". In this case  $\mu = 3$ , and  $kT_s = 1$ . Since  $T_s = T/N = 1/16$ , it follows that  $k = 16$ . The system loads a value  $V = \mu N/T = 48$  into XRE(16). Taking either main-menu H or I enables us to confirm this.

- (b) Since  $3\delta(t - 1) \Leftrightarrow 3e^{-j\omega}$  and  $\omega_0 = 2\pi/T = \pi/8$ , we have

$$\begin{aligned} F(n\omega_0) &= 3e^{-jn\omega_0} \\ &= 3 \cos(n\pi/8) - j3 \sin(n\pi/8) = A(n\omega_0) + jB(n\omega_0) \end{aligned}$$

We thus expect the values for  $A_n$ ,  $B_n$ , and  $|F_n|$  to be as shown in Table 15.1. When we ran this on the FFT the results were precisely as expected. □

TABLE 15.1

$n$	$A_n$	$B_n$	$ F_n $
0	3	0	3
1	2.7716386	-1.1480503	3
2	2.1213203	-2.1213203	3
3	1.1480503	-2.7716386	3
4	0	-3	3

## 15.2 FREQUENCY-DOMAIN DIRAC DELTAS ON THE FAST FOURIER TRANSFORM

In the preceding section we saw that we were able to represent a Dirac delta in the time domain, and we now show how it can also be done in the frequency domain. The rule that we must use here is shown in the following box.

**■ The Dirac function: Emulating a Dirac delta in the frequency domain**

To emulate the Dirac delta  $\mu\delta(\omega - n \text{ OMEGA}_s)$ , load into **F** the single value

$$\text{FRE}(n) = \frac{\mu T}{2\pi} \quad (15.7)$$

with zeros for all other values, where

- $\mu$  is the required weight of the impulse.
- $T$  has its usual meaning and  $\text{OMEGA}_s = 2\pi/T$

□ **EXAMPLE 15.2:** Load the spectrum of  $2 e^{j8\pi t}$  into **F** and invert it to the time domain. Use  $N = 256$ ,  $T = 4$ .

**Solution:** We know that  $2 e^{j8\pi t} \Leftrightarrow 4\pi\delta(\omega - 8\pi)$ . Thus we are required to load a frequency-domain Dirac delta whose weight is  $\mu = 4\pi$  at the point  $\omega = 8\pi$ .

Starting from main-menu A, we enter  $N = 256$ , SAMPLED,  $T = 4$ , PULSE. Then we take the option "CREATE ONLY DIRAC DELTAS". When the system prompts us for the location on the  $\omega$ -axis we enter "8π", and when prompted for the weight we enter "4π".

In this case,  $\text{OMEGA}_s = 2\pi/T = \pi/2$ . Since the impulse is at  $\omega = 8\pi = n \text{ OMEGA}_s$ , it follows that  $n = 16$ . The system thus loads a value  $V = \mu T/2\pi = 8$  into FRE(16). Taking main-menu H or I enables us to confirm this.

Inverting to the time domain give us

$$4\pi\delta(\omega - 8\pi) \Leftrightarrow 2\cos(8\pi t) + j2\sin(8\pi t)$$

After running SYNTHESIS this is precisely what we found in YRE and YIM. □

Please note that the programs on the disk **do not** make use of this representation of the Dirac delta in order to display the Fourier transforms of periodic waveforms. (These were discussed in Section 4.10.)

□ **EXAMPLE 15.3:** Consider the eternal periodic function

$$x_p(t) = \begin{cases} 1 & (0 < t < 1) \\ 0 & (1 < t < 2) \end{cases} \quad x_p(t+2) = x_p(t)$$

We know from Section 4.10 that the Fourier transform of such a waveform, if

TABLE 15.2 Weights of Dirac Deltas

<i>n</i>	<i>A<sub>FFT</sub></i>	<i>A<sub>exact</sub></i>	<i>B<sub>FFT</sub></i>	<i>B<sub>exact</sub></i>
0	3.1415927	3.1415927	0	0
1	0	0	-1.9999749	-2.0000000
2	0	0	0	0
3	0	0	-0.6665914	-0.6666666
4	0	0	0	0
5	0	0	-0.3998745	-0.4000000
6	0	0	0	0
7	0	0	-0.2855386	-0.2857143

regarded as a single eternal pulse, will consist of an infinite sum of weighted Dirac deltas of the form

$$X(\omega) = \sum_{n=-\infty}^{\infty} W(n)\delta(\omega - n\omega_0)$$

in which  $\omega_0 = 2\pi/T_0$  and  $W(n)$  is the weight of the  $n$ th Dirac delta. It was also shown there that the weight  $W(n)$  will be equal to  $2\pi X(n)$ , where  $X(n)$  is the  $n$ th complex Fourier coefficient for  $x_p(t)$ .

In this case the continuous Fourier transform (CFT) coefficients are

$$X(n) = \frac{1}{2} \left( \cos \frac{n\pi}{2} - j \sin \frac{n\pi}{2} \right) \text{Sa} \frac{n\pi}{2}$$

and so

$$W(n) = 2\pi X(n) = \pi \left( \cos \frac{n\pi}{2} - j \sin \frac{n\pi}{2} \right) \text{Sa} \frac{n\pi}{2}$$

We loaded the single-period statement of  $f_p(t)$  just given using N = 512, SAM-PLED, T = 2, PULSE. After running ANALYSIS we took main-menu option I, then F, and displayed ETERNAL TRAIN, which shows the weights of the Dirac deltas that the spectrum is composed of. In Table 15.2 we show both the FFT values for the weights as well as the exact values, obtained from the preceding formula.  $\square$

### 15.3 DIFFERENTIATION ON THE FAST FOURIER TRANSFORM

In discrete signal processing the situation sometimes arises where we have the FFT line spectrum of a signal and we would like to have the FFT spectrum of its first or second derivative. It would be time-consuming to invert the given spectrum to the time domain, then obtain a derivative by numerical means, and then retransform the result back to the frequency domain.

In this section we consider such situations and show how they can be handled very effectively by performing an appropriate operation directly on the FFT spectrum, that is, in the frequency domain.

In continuous Fourier analysis we have the pivotal Theorem 5.1 concerning time-domain differentiation, namely

■ If

$$f(t) \Leftrightarrow F(\omega)$$

then

$$\frac{d}{dt} f(t) \Leftrightarrow j\omega F(\omega) \quad (15.8)$$

There is no exact counterpart to this theorem in the discrete world because differentiation is not defined for a function of a discrete variable. Instead we have the following, based on algorithms that come close to the concept of differentiation, and can be used to obtain acceptable estimates of the differentiation operation.

Let the function  $f(t)$  be numerically sampled at intervals spaced  $T_s$  seconds apart to produce the sequence of numbers

$$\dots, f(-2T_s), \quad f(-T_s), \quad f(0), \quad f(T_s), \quad f(2T_s), \dots, f(kT_s), \dots$$

Define the **backward divided difference** of  $f(kT_s)$  by

$$g_b(kT_s) \equiv \frac{f[kT_s] - f[(k-1)T_s]}{T_s} \quad (15.9)$$

(Note the subscript  $b$  in  $g_b(kT_s)$ , which signifies **backward**.) Then as we know from the calculus,

$$\lim_{T_s \rightarrow 0} g_b(kT_s) = f'(kT_s) \quad (15.10)$$

What this means is that, for  $T_s$  sufficiently small,

$$g_b(kT_s) \approx f'(kT_s) \quad (15.11)$$

that is, if  $T_s$  is sufficiently small, then the  $k$ th backward divided difference of a sequence of samples can be used as an estimate of the derivative of the original function  $f(t)$  at time  $t = kT_s$ . This gives us the following rule.

■ Estimating the derivative using backward differences

For  $T_s$  sufficiently small

$$f'(kT_s) \approx g_b(kT_s) \equiv \frac{f[kT_s] - f[(k-1)T_s]}{T_s} \quad (15.12)$$

In the same way we can form the **forward divided difference** of  $f(kT_s)$  defined by

$$g_f(kT_s) \equiv \frac{f[(k+1)T_s] - f[kT_s]}{T_s} \quad (15.13)$$

from which we can obtain a second rule for estimating the derivative.

■ **Estimating the derivative using forward differences**

For  $T_s$  sufficiently small

$$f'(kT_s) \approx g_f(kT_s) \equiv \frac{f[(k+1)T_s] - f[kT_s]}{T_s} \quad (15.14)$$

As a third possibility we can take the average of the backward and forward divided differences, giving us what is called the **central divided difference**, from which we obtain a third rule:

■ **Estimating the derivative using central differences**

For  $T_s$  sufficiently small

$$f'(kT_s) \approx g_c(kT_s) \equiv \frac{f[(k+1)T_s] - f[(k-1)T_s]}{2T_s} \quad (15.15)$$

It can be shown that for functions with acceptable smoothness, the central difference estimate has the smallest error of the three.

Consider now the **second derivative**. As with the first derivative there are many algorithms for estimating the second derivative from a sequence of numerical samples of a function, usually based on a double application of one of the preceding rules. Perhaps the one most widely used is based on forming the divided difference of the forward and backward divided differences, as follows:

$$\begin{aligned} h_c(kT_s) &\equiv \frac{g_f(kT_s) - g_b(kT_s)}{T_s} \\ &= \frac{f[(k+1)T_s] - 2f[kT_s] + f[(k-1)T_s]}{T_s^2} \end{aligned} \quad (15.16)$$

This gives us the following rule:

■ Estimating the second derivative using central differences

For  $T_s$  small

$$f''(kT_s) \approx h_c(kT_s) \equiv \frac{f[(k+1)T_s] - 2f[kT_s] + f[(k-1)T_s]}{T_s^2} \quad (15.17)$$

Observe that every one of the preceding rules leads to a **linear combination of sampled values of  $f(t)$** . Here's the key fact regarding such combinations:

They can all be implemented on the FFT.

We shall work only one of the algorithms, but the reader will then readily be able to apply the method to any algorithm whatsoever, as long as it is based on a linear combination of sampled values of a function.

**(A) FFT Implementation of First Derivative Estimation Based on Central Differences**

Starting from the divided central difference of  $f(t)$ , we have

$$g_c(kT_s) = \frac{f[(k+1)T_s] - f[(k-1)T_s]}{2T_s} = \frac{f_{k+1} - f_{k-1}}{2T_s} \quad (15.18)$$

From the time-shift property for the discrete Fourier transform (DFT) [see Exercise 10.8(a)] we recall that if  $f_k \Leftrightarrow F_n$ , then

$$f_{k-m} \Leftrightarrow F_n W^{nm} \quad (15.19)$$

Applying this to (15.18), we obtain

$$g_c(kT_s) \Leftrightarrow \frac{F_n(W^{-n} - W^n)}{2T_s} \quad (15.20)$$

We have thus obtained the expression for the FFT spectrum of  $g_c(kT_s)$  in terms of the spectrum of  $f_k$ . We now expand  $W^{-n}$  and  $W^n$ , obtaining

$$W^{-n} = e^{j2\pi n\pi/N} = \cos \frac{2\pi n}{N} + j \sin \frac{2\pi n}{N} \quad (15.21)$$

$$W^n = e^{-j2\pi n\pi/N} = \cos \frac{2\pi n}{N} - j \sin \frac{2\pi n}{N} \quad (15.22)$$

and then the RHS of (15.20) becomes

$$\frac{F_n(W^{-n} - W^n)}{2T_s} = F_n \left[ \frac{j \sin(2\pi n/N)}{T_s} \right] \quad (15.23)$$

which gives us the rule shown in the following box.

■ Using the FFT to estimate the derivative by central differences

Let a pulse  $f(t)$  be sampled at intervals of  $T_s$  to give  $f_k$  for  $0 \leq k \leq N - 1$ , and let  $f_k$  have as its FFT spectrum  $F_n$ . Then the central divided difference of  $f(t)$  will have spectrum

$$F_n \left[ \frac{j \sin(2\pi n/N)}{T_s} \right] \quad (0 \leq n \leq N - 1)$$

whose inverse can be used as a vector of estimates of  $f'(kT_s)$  ( $0 \leq k \leq N - 1$ ).

Table 15.3 shows the various algorithms that we have considered and the multiplier to use in order to create the required modified spectrum.

Since the FFT is a periodic system it follows that all of the algorithms in Table 15.3 act on the data vector in a circular sense. Thus the first and last elements in the Y vector are computed on that basis.

If we were starting from a time-domain pulse and wished to end up in the time domain with estimates of its derivative, then the required sequence of steps would be as shown in the block diagram of Figure 15.1.

TABLE 15.3

Function	Multiplier
(A) First derivative by backward differences	$\frac{(1 - W^n)/T_s}{1 - \cos(2\pi n/N) + j \sin(2\pi n/N)}$
(B) First derivative by forward differences	$\frac{(W^{-n} - 1)/T_s}{\cos(2\pi n/N) - 1 + j \sin(2\pi n/N)}$
(C) First derivative by central differences	$\frac{(W^{-n} - W^n)/2T_s}{j \sin(2\pi n/N)}$
(D) Second derivative by central differences	$\frac{(W^{-n} - 2 + W^n)/T_s^2}{2 \frac{\cos(2\pi n/N) - 1}{T_s^2}}$

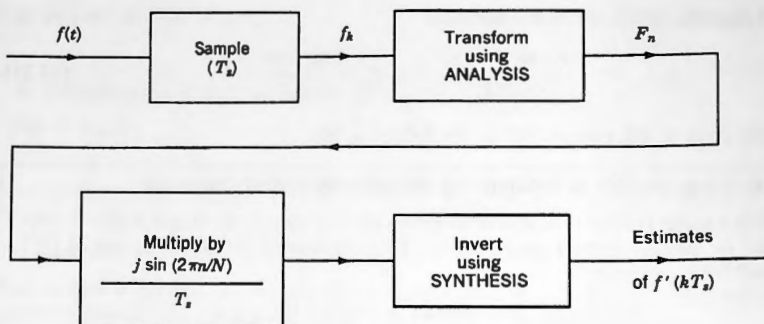


Figure 15.1. First derivative using central differences.

The algorithms just given have all been included in the **F** postprocessor. To invoke any of them, take main-menu option **G** followed by **F**. A submenu will then be displayed offering the preceding four as well as a number of other useful algorithms. All of this is discussed further in Section 17.1.

The pulse shown in Figure 15.2 was used to demonstrate the differencing algorithms. Using values  $N = 256$  and  $T = 1$ , we first differentiated it once by operating on its FFT spectrum using the backward difference rule, (A) of Table 15.3. The result when inverted gave the function shown in Figure 15.3.

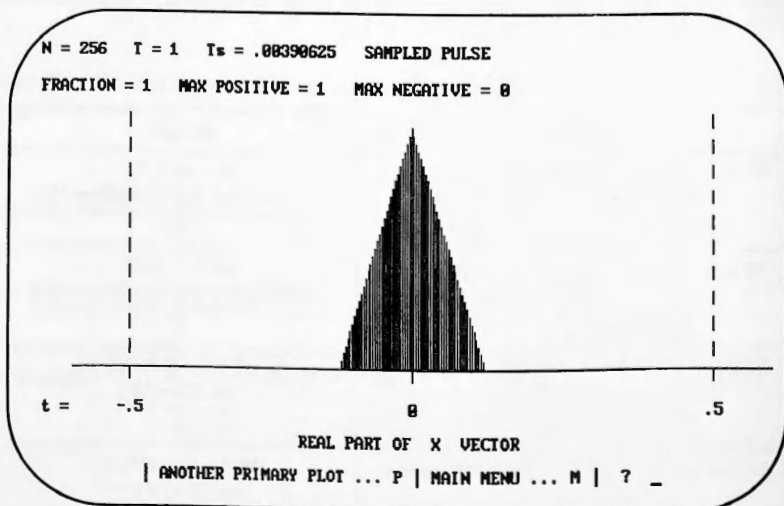
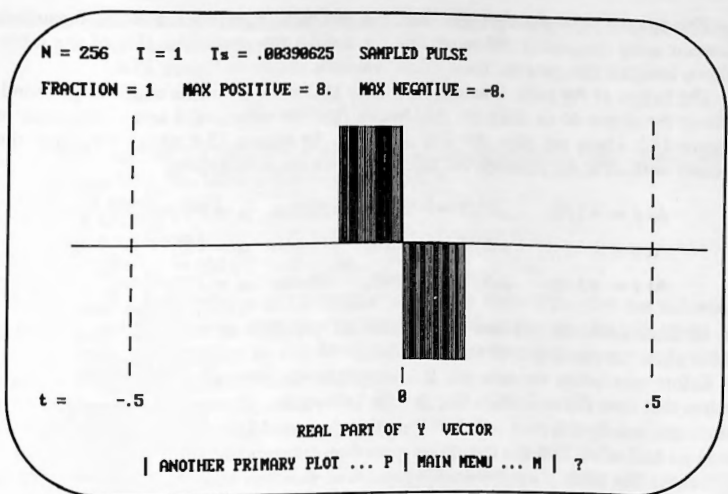
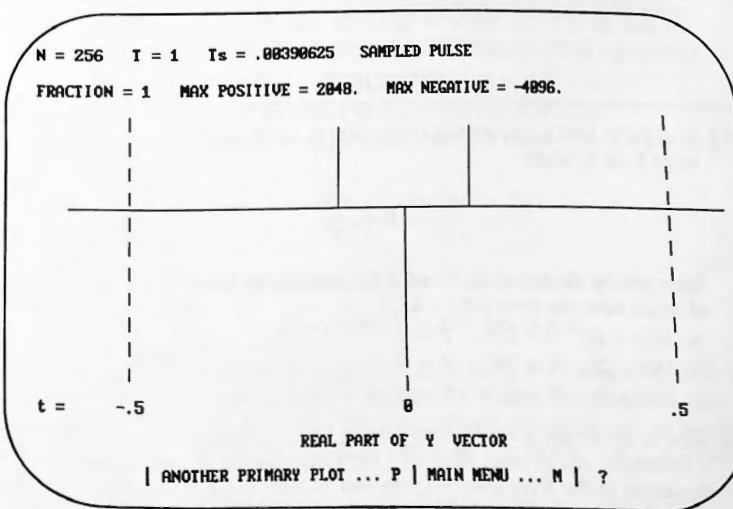


Figure 15.2. Triangular pulse.



**Figure 15.3.** First derivative of triangular pulse.



**Figure 15.4.** Second derivative of triangular pulse.

The original pulse was then also differentiated twice by operating in the frequency domain using the central difference rule for double differentiation, (D) of the table. When inverted this gave the three Dirac functions shown in Figure 15.4.

The height of the pulse is seen from Figure 15.2 to be 1 and its width is  $\frac{1}{4}$  second. Hence the slopes of its sides are  $\pm 8$ . Notice that the values of 8 and  $-8$  appear in Figure 15.3 where we show the first derivative. In Figure 15.4 where we show the second derivative, we obtained the following three Dirac functions:

$$\begin{aligned} \text{At } t = -1/8: \quad \mu N/T &= 2048. \quad \text{Hence } \mu = VT/N = 8. \\ \text{At } t = 0: \quad \mu N/T &= -4096. \quad \text{Hence } \mu = VT/N = -16. \\ \text{At } t = +1/8: \quad \mu N/T &= 2048. \quad \text{Hence } \mu = VT/N = 8. \end{aligned}$$

In all three cases the locations and weights are precisely as expected when viewing these pulses as emulations of the Dirac delta.

Before concluding we note the following: On occasion we have to differentiate pulses that have discontinuities that include half-values. The result will be two Dirac functions, side-by-side each with half the value that would have come about had there been no half-value. This is a fact of life regarding differencing and cannot be avoided. Whenever this takes place the double-line Dirac function should be thought of as a single one with value equal to the sum of the two half-values.

The same remarks apply when there are three adjacent Dirac functions, and so forth. Just add all of the values into a single value when calculating the weight of the Dirac delta that the adjacent Dirac functions represent. In the exercises we consider cases where all of these anomalies occur.

## EXERCISES

---

- 15.1** In order to load a time-domain Dirac delta of weight  $\mu$  the system must place a value  $V$  in  $\mathbf{X}$ , where

$$V = \frac{\mu N}{T}$$

What will be the values of  $V$  and  $k$  for loading the following Dirac deltas, all of which have the form  $\mu\delta(t - kT_s)$ :

- (a)  $2\delta(t - 1)$ ,  $N = 256$ ,  $T = 2$
- (b)  $5\delta(t - 2)$ ,  $N = 100$ ,  $T = 10$
- (c)  $3\delta(t + 5)$ ,  $N = 1024$ ,  $T = 20$

- 15.2** What is the weight  $\mu$  of the time-domain Dirac delta that the following values  $V$  represent, and at what value of  $t$  does the impulse lie? Write its complete expression in the form  $\mu\delta(t - t_a)$  as well as  $\mu\delta(t + t_b)$ , where both  $t_a$  and  $t_b$  are positive.

- (a)  $V = 256$ ,  $k = 32$ ,  $N = 256$ ,  $T = 2$
- (b)  $V = 10,240$ ,  $k = 40$ ,  $N = 512$ ,  $T = 0.1$
- (c)  $V = 108$ ,  $k = 56$ ,  $N = 72$ ,  $T = 2$

- 15.3 In order to load a frequency-domain Dirac delta of weight  $\mu$  the system must place a value  $V$  in  $\mathbf{F}$ , where

$$V = \frac{\mu T}{2\pi}$$

What will be the values of  $V$  and  $n$  for loading the following Dirac deltas, all of which have the form  $\mu\delta(\omega - n \text{ OMEGA}_s)$ :

- (a)  $2\pi\delta(\omega - 4\pi)$ ,  $N = 256$ ,  $T = 4$
- (b)  $16\delta(\omega - \pi)$ ,  $N = 64$ ,  $T = 10$
- (c)  $20\pi\delta(\omega + 400\pi)$ ,  $N = 80$ ,  $T = 0.1$

- 15.4 What is the weight  $\mu$  of the frequency-domain Dirac delta that the following values  $V$  represent, and at what value of  $\omega$  does the impulse lie? Write its complete expression in the form  $\mu\delta(\omega - \omega_a)$  as well as  $\mu\delta(\omega + \omega_b)$ , where both  $\omega_a$  and  $\omega_b$  are both positive.

- (a)  $V = 2$ ,  $n = 20$ ,  $N = 256$ ,  $T = 2$
- (b)  $V = 100$ ,  $n = 48$ ,  $N = 400$ ,  $T = 4$
- (c)  $V = 1$ ,  $n = 56$ ,  $N = 72$ ,  $T = 0.02$

- 15.5 Considering the following two time-domain Dirac deltas

$$3\delta(t - 2) \quad \text{and} \quad 2\delta(t - 3)$$

- (a) If they were convolved, what is the result that would be obtained?
- (b) Load them into  $\mathbf{X}$  and  $\mathbf{X2}$  using  $N = 400$  and  $T = 16$ , and then run CONVOLUTION. Verify that the result that you obtain agrees with what you expected in (a).

- 15.6 Consider the Fourier transform of  $\cos(2t)$  for two situations:

- (1) When regarded as a single pulse over the range  $-\pi/2 < t < \pi/2$ , its spectrum is

$$F(\omega) = \frac{2\omega \sin(\omega\pi/2)}{4 - \omega^2}$$

- (2) When regarded as an eternal pulse train (period  $\pi$ ), its spectrum is

$$F(\omega) = \pi\delta(\omega - 2) + \pi\delta(\omega + 2)$$

- (a) Load  $\mathbf{X}$  with  $\cos(2t)$  ( $-\pi/2 < t < \pi/2$ ) using  $N = 256$  and  $T = 4\pi$ . Run ANALYSIS and then view the spectral values (main-menu I, then F). Verify that (1) is correct. We have padded with zeros and so we obtain improved resolution of the spectrum of the pulse. This is discussed in Section 17.2
- (b) Now load  $\mathbf{X}$  with the same signal using  $N = 256$ , but this time use  $T = \pi$ . Run ANALYSIS and then view the spectral values.
  - If viewed as a single pulse, the spectrum values are

$$F_n = \pi/2 \quad \text{for } n = \pm 1 \quad \text{and zero elsewhere}$$

- If viewed as an **eternal pulse train**, the spectrum values are

$$F_n = \pi \quad \text{for } n = \pm 1 \quad \text{and zero elsewhere}$$

Show that these are consistent with Section 15.2.

- 15.7** (a) Find the Fourier transform of the eternal complex exponential  $f(t) = e^{j2\pi t}$

- (b) Now load one period of this function into **X** using  $N = 256$  and  $T = 1$ , and transform it. Verify that the result that you obtained in (a) is correct.

- 15.8** (a) Find the Fourier transform of the eternal train of pulses

$$f_p(t) = \sum_{k=-\infty}^{\infty} \text{Rect}(t - kT_0) \quad (T_0 = 4)$$

- (b) Now load this function into **X** with  $N = 1024$ , SAMPLED,  $T = 4$ , PULSE. Display its FFT spectrum using ETERNAL TRAIN. Verify that the weights of the Dirac deltas in the frequency domain in the display are in acceptable agreement with those obtained in (a) for  $n = 0, 1, 5, 25$ .

- 15.9** (a) Load  $\cos(2t)$  as a SAMPLED PULSE with  $N = 256$  and  $T = \pi$ , and view a plot of the result assuming that it is an ETERNAL TRAIN.

- (b) Verify that the numerical values of the spectrum are

$$\text{FRE}(n) = \pi \quad \text{for } n = \pm 1 \quad \text{and zero elsewhere}$$

Are these the correct weights of an eternal cosine pulse?

- (c) What is the derivative of the eternal cosine  $\cos(2t)$ ?  
 (d) Differentiate this function using the **F** postprocessor package

#### CENTRAL-DIFF 1st

and verify the resulting spectrum. (Use ETERNAL TRAIN.)

- (e) Invert the spectrum to the time domain and examine a plot of the result. Is it what you would expect?

- 15.10** (a) Find  $F_p(\omega)$ , the Fourier transform of

$$f_p(t) = |\sin(\pi t)|$$

- (b) Load the function  $\sin(\pi t)$  ( $0 < t < 1$ ) into **X** and obtain its spectrum. Verify the expression that you obtained in (a). Use  $N = 256$ , SAMPLED,  $T = 1$ , PULSE. View the spectrum using ETERNAL TRAIN.

- (c) Now use Theorem 5.1 to find  $F_2(\omega)$  the Fourier transform of  $f_p''(t)$ .  
 (d) Invert  $F_2(\omega)$  to the time domain analytically, and sketch what you have derived.  
 (e) Now differentiate  $f_p(t)$  twice in the time domain and sketch the result. Your sketches from (d) and (e) should be the same.  
 (f) Use the waveform that you created in (b) and the **F** postprocessor

#### CENTRAL-DIFF 2nd

to differentiate the waveform twice. Now invert it using SYNTHESIS. Verify that the weights of the Dirac deltas that appear in  $\mathbf{Y}$  are consistent with what you obtained in (d) and (e). Also verify that the values lying between the Dirac deltas are consistent with what you obtained in (d) and (e).

- 15.11** Load the pulse shown in Figure 15.5 into  $\mathbf{X}$  using  $N = 32$ . Do this in the two ways stated in (a) and (b):

- Without half-values at the discontinuities by using  $T = 2\pi$ , which means that the ends of the pulse will fall between sampling instants.
- With half-values at the discontinuities, using  $T = 4$ .
- For each case form the FFT spectrum of the pulse and then use the  $\mathbf{F}$  postprocessor to differentiate it, using each of the following:
  - Backward difference derivative
  - Forward difference derivative
  - Central difference derivative

In each case then invert the result back to the time domain.

- Observe at what values of  $k$  the Dirac deltas occur in Cases (a)(1), (2), and (3).

For (a)(1) backward differencing **delays** both Dirac deltas by about one half-count, and each has the correct value of 5.0929582. Thus  $\mu = VT/N = 1$ .

For (a)(2) forward differencing **advances** both Dirac deltas by about one half-count, and again each has the correct value of 5.0929582, and so  $\mu = 1$ .

For (a)(3) central differencing **doubles** the lines that then straddle the ends of the pulse, each with a value of 2.5464791. Adding them gives  $V = 5.0929582$  and so  $\mu = 1$ .

- Observe at what values of  $k$  the Dirac deltas occur in Cases (b) (1), (2), and (3).

For (b)(1) backward differencing produces two lines moved to the right, each with a value of 4. Adding them gives  $V = 8$ , and so  $\mu = VT/N = 1$ .

For (b)(2) forward differencing produces two lines moved to the left, each with a value of 4. Adding them gives  $V = 8$ , and so  $\mu = 1$ .

For (b)(3) central differencing produces **three** lines straddling the ends of the pulse, with value 2, 4, 2. Adding them gives  $V = 8$ . and so  $\mu = 1$ .

All of this is a fact of life regarding these algorithms.

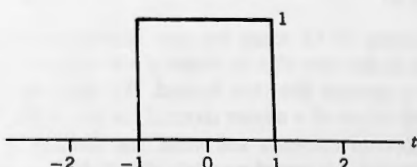


Figure 15.5. Pulse for differentiation.

- 15.12** In the text we derived one of the differentiation procedures, namely (C) of Table 15.3. Derive the remaining three shown in the table.

### Filtering and Differentiation Projects Using the FFT

- 15.13** (a) Load **X** with a signal plus noise as follows:

$$x(t) = 1 + 0.2 \sin(16\pi t) + 0.02 (\text{RND} - 0.5)$$

*Note:* RND produces a pseudorandom number lying in the range 0 to 1. Ideally, the average value of RND is  $\frac{1}{2}$ .

Use  $N = 128$ , SAMPLED,  $T = 1$ , PULSE. Plot **X** and observe the signal perturbed by the noise.

- (b) Run ANALYSIS to produce **F** and examine the numbers of
  - Its **real part**: You will observe a strong spectral line at  $n = 0$  coming from the dc part of the signal, and small random-looking lines at all other values of  $n$  that come from the noise.
  - Its **imaginary part**: You will observe strong spectral lines at  $n = \pm 8$  coming from the sinusoid, and random-looking lines from the noise.
  - Its **magnitude**: Now you see the line at  $n = 0$ , two lines at  $n = \pm 8$ , and the lines from the noise at the other frequencies.
- (d) Try to obtain the **second derivative** of the signal using the appropriate package in the **F** postprocessor. Then run SYNTHESIS and inspect what you have obtained. It will be seen to be totally useless as a representation of the second derivative of the signal.
- (e) Now start again by obtaining the FFT spectrum of the signal. Then use the **F** postprocessor package

### LOW-PASS FILTER

to zero out all values of the spectrum whose spectral numbers exceed that of the sinusoid. Then invoke the second derivative package in the **F** postprocessor, and invert the result using SYNTHESIS.

- (f) Examine **Y** and verify that it is now a fairly good representation of the second derivative of the sinusoid that we started with.
- (g) Start again with the raw data in **X** and filter out **both the noise and the sine wave**, leaving only the dc component. Invert the result to the time domain using SYNTHESIS. Is the value that you obtain precisely equal to one? If not, why not?

- 15.14** Regarding Exercise 15.13, using low-pass filtering we cannot eliminate the spectral values of the noise that lie between  $n = 0$  and the value of  $n$  at which the sine wave's spectral lines are located. We can only eliminate the noise spectrum whose values of  $n$  exceed those of the sine wave. However, we could examine the spectral elements and make the decision to retain **only those values whose magnitudes exceed a certain threshold**.

The F postprocessor package SHAVE F enables you to do precisely that. Load X with the function in Exercise 15.13 and obtain its spectrum. Then clean up the latter using SHAVE with various values of the parameter CLIP. After inverting the modified spectrum, compare the values that you obtain with the original signal

$$x(t) = 1 + 0.2 \sin(16\pi t)$$

Do this with increasing values of  $N$ . As  $N$  increases, the agreement should improve steadily.



# The User's Manual for the Accompanying Disk

There are two 3.5" disks which go with your book—a Macintosh version and a DOS version, both of which are fully executable and require no further software in order to run. The User's Manual is contained in Chapters 16, 17, and 18, which are located in README files on the disks.

### (A) Macintosh disk

Your Macintosh disk contains a single file of about 713 Kbytes, entitled "FFTMMxx.CC" where the xxx is a three-digit number showing the software version. For example "131" means "Version 1.31". The "CC" means "double click", that is, executable.

#### IMPORTANT

Install your MAC software with all extensions off. In the event of a problem running your software, try rebooting and running your MAC with all extensions off. Also, read the file README\_FIRST

Double click on the icon on your disk and then click on "Continue". You should now have a dialog box on your screen showing the path (starting from Macintosh HD) and ending with the message:

Install software into folder

FOURIER SYSTEMS folder

Edit the path to your requirements so that the FOURIER SYSTEMS folder is placed where you want it to be. Then click on "SAVE" (or else edit the folder name to be whatever name you want, and then click on "SAVE").

The de-archiving process should now run and, when done, a dialog box stating "Installation was successful..." should appear. Click on "QUIT", eject your disk from your Macintosh, and the installation is now complete. If you open the FOURIER SYSTEMS folder you should find in it the following five items:

FFT.CC

PLOTS.CC

BEDIT 3.1 Demo

README\_FIRST

USER'S MANUAL

**WARNING**

It is essential that you assign sufficient memory before attempting to start FFT.CC or PLOTS.CC. Here's how to do it.

- (1) Click one on FFT.CC to highlight it.
- (2) Pull down the FILE menu and open GET INFO.
- (3) Go to the lower right-hand corner of the box which is now on your screen and make the following entries:

Minimum size:	1500	K
---------------	------	---

Preferred size:	4096	K
-----------------	------	---

- (4) Exit and repeat for PLOTS.CC.
- (5) You should now be able to run FFT.CC and PLOTS.CC. The MINIMUM SIZE entry can be somewhat less than the value shown above but if it is too small your programs will not run. The PREFERRED SIZE entry can be as large as you like, and if you intend to run the FFT with very large values of N such as 32768 then PREFERRED SIZE should be of the order of 8192 K.

The folder USER'S MANUAL contains Chapters 16, 17 and 18. Read them using BBEDIT, and if you so desire, user BBEDIT to print them in order to create a hard-copy version of the manual. They contain most of the information that you will require for a full understanding of how to operate your software.

**(B) DOS disk**

Your DOS disk contains a single file of about 550 Kbytes, entitled "FFTNMxxx.EXE" where the xxx is a three-digit number showing the software version. For example "131" means "Version 1.31".

In your root directory, create a directory called FFT (or any other name of your choice). Change to the directory FFT so that your DOS prompt now reads C:\ FFT > place your DOS disk in your B: drive and then type

```
COPY B:\ *.*
```

Your DOS disk should now be copied into the FFT directory.

At the DOS prompt C:\ FFT > type FFTNMxxx using for xxx whatever number appears on your disk. The file will now de-archive giving you two further files

INSTALL.EXE and README1.TXT

Please read README1.TXT. It contains essential information regarding CONFIG.SYS and many other items needed for successful operation of the FFT system

When done, run the file INSTALL.EXE. It will de-archive to give you the following three executable files

FFT.EXE FFTMAX.EXE PLOTS.EXE

as well as two more directories

README'S ABOUTLHA

plus the files CARD.EXE and COLORS.TRU

The directory README'S contains three README files which are Chapters 16, 17, and 18 of your book. If you so desire, you can make yourself a hardcopy version of the User's Manual by printing the four README files.

The files CARD.EXE and COLORS.TRU must always be present in the same directory as the EXE files or else the latter will only run in a degraded mode.

Always start your EXE modules from inside the FFT directory or else it will appear as though CARD.EXE and COLORS.TRU are missing.



## References and Further Reading

- Ahlfors, L., *Complex Analysis*, McGraw-Hill, New York, 1979, p. 189.
- Bell, E. T., *Men of Mathematics*, Simon & Schuster, New York, 1965.
- Bergland, G. D., "A Guided Tour of the Fast Fourier Transform," *IEEE Spectrum*, 6(7) (July), 41-52 (1969).
- Bracewell, R., *The Fourier Transform and its Applications*, McGraw-Hill, New York, 1978.
- Bracewell, R., "The Hartley Transform," *Proceedings of the Institute of Radio Engineers*, 30(3) (March), 144-150 (1972).
- Bracewell, R., *The Hartley Transform*, Oxford University Press, New York, 1986.
- Brigham, E. O., *The Fast Fourier Transform and Its Applications*, Englewood Cliffs, N.J., Prentice-Hall, 1988.<sup>†</sup>
- Brigham, E. O., and Morrow, R. E., "The fast Fourier transform," *IEEE Spectrum* 4(12) (December) 63-70 (1967).
- Burkhardt, H., "Trigonometrische Reihen und Integrale," *Encyklopädie der Mathematischen Wissenschaften*, Vol. 2, Teubner, Leipzig, 1904-1916.
- Campbell, G. A., and Foster, R. M., *Fourier Integrals for Practical Applications*, Van Nostrand, Princeton, N.J., 1948.
- Carslaw, H. S., *Introduction to the Theory of Fourier's Series and Integrals*, Cambridge University Press, Cambridge, England, 1930 (Dover, 1952).
- Chipman, R. A., *Theory and Problems of Transmission Lines* (Schaum's Outline Series), McGraw-Hill, New York, 1968.
- Churchill, R. V., and Brown, J. W., *Fourier Series and Boundary Value Problems*, 3rd ed., McGraw-Hill, New York, 1978, pp. 149-161.
- Close, C. M., *The Analysis of Linear Circuits*, Harcourt, Brace & World, New York, 1966.
- Cochran, W. T., et al., "What is the Fast Fourier Transform?" *IEEE Trans. Audio and Electroacoustics*, AU-15 (June) 45-55, (1967).
- Cooley, J. W., and Tukey, J. W., "An Algorithm for the Machine Calculation of Complex Fourier Series," *Mathematics of Computation*, 19(90), 297-301 (1965).

<sup>†</sup>Brigham's book contains a list of references on the FFT that is 50 pages in length.

- Cooley, J. W., et al., "Application of the Fast Fourier Transform to Computation of Fourier Integrals, Fourier Series, and Convolution Integrals," *IEEE Trans. Audio and Electroacoustics*, AU-15 (June) 79-84 (1967).
- Cooley, J. W., et al., "Historical Notes on the FFT," *Proceedings of the IEEE*, 55(10) (October), 1675-1677 (1967).
- Coppel, W. A., "J. B. Fourier—On the Occasion of His Two Hundredth Birthday," *American Mathematical Monthly*, 76, 468-483 (1969).
- Davis, H. F., *Fourier Series and Orthogonal Functions*, Allyn & Bacon, Boston, 1963.
- Davis, R. J., and Hersh, R., *The Mathematical Experience*, Penguin Books, Baltimore, MD., 1980.
- Dirac, P. A. M., *The Principles of Quantum Mechanics*, Oxford University Press, London, 1947.
- Dym, H., and McKean, H. P., *Fourier Series and Integrals*, Academic Press, New York, 1972.
- Edminster, J. A., *Electric Circuits*, Schaum's Outline Series, McGraw-Hill, New York, 1972.
- Encyclopedia Britannica*, 13th edition, 1926, London.
- Fourier, J. B. J., *The Analytical Theory of Heat*, A. Freeman, transl., Dover, New York, 1955.
- Franklin, P., *An Introduction to Fourier Methods and the Laplace Transformation*, Dover, New York, 1958.
- Franks, L. E., *Signal Theory*, Prentice-Hall, Englewood Cliffs, N.J., 1969.
- Gabel, R. A., and Roberts, R. A., *Signals and Linear Systems*, 3d ed., Wiley, New York, 1987.
- Gentleman, W. M., and Sande, G., "Fast Fourier Transforms for Fun and Profit," *1966 Fall Joint Computer Conference, AFIPS Proc.* 29, 563-578 (1966).
- Guillemin, E. A., *The Mathematics of Circuit Analysis*, Wiley, New York, 1949.
- Haberman, R., *Elementary Applied Partial Differential Equations*, Prentice-Hall, Englewood Cliffs, N.J., 1983.
- Haykin, S., *Communication Systems*, Wiley, New York, 1983.
- Heidemann, M. T., Johnson, D. H., and Burrus, C. S., "Gauss and the History of the Fast Fourier Transform," *IEEE ASSP Magazine*, 1(4) (October), 14-21 (1984).
- Helms, H. D., "Fast Fourier transform method of computing difference equations and simulating filters," *IEEE Trans. Audio and Electroacoustics*. AU-15 (June) 85-90 (1967).
- Hobson, E. W., "JBJ Fourier," in *Encyclopedia Britannica*, 13th ed., 1926. See also—"On the Theory of Functions of a Real Variable and on the Theory of Fourier's Series," Cambridge Univ. Press, London, 1907.
- Hsu, H. P., *Applied Fourier Analysis*, Harcourt Brace Jovanovich College Outline Series, Harcourt Brace Jovanovich, New York, 1984.
- Jaeger, J. C., *An Introduction to the Laplace Transformation*, Methuen's Monographs, Methuen, London, 1949.
- Kirchhoff, G. R., "On the Motion of Electricity in Wires," *Philosophical Magazine*, Ser. 4, 13 (June), 395-412 (1857) (transl. from German).
- Kelvin, (William Thomson) Baron, *Collected Works*, Vol. III, Cambridge University Press, London 1911, p. 192. See also Article on Heat, *Encyclopedia Britannica*, 9th Edition, 1878.
- Lathi, B. P., *Signals, Systems and Communication*, Wiley, New York, 1965.
- Lathi, B. P., *An Introduction to Random Signals and Communication Theory*, International Textbook Company, Scranton, PA., 1968.
- Lighthill, M. J., *Fourier Analysis and Generalized Functions*, Cambridge University Press, Cambridge, England, 1959.
- MacRobert, T. A., *Functions of a Complex Variable*, Macmillan, London, 1958, p. 116.

- Mason, S. J., and Zimmerman, H. J., *Electronic Circuits, Signals and Systems*, Wiley, New York, 1960.
- McGillem, C. D., and Cooper, G. R., *Continuous and Discrete Signal and System Analysis*, Holt, Rinehart & Winston, New York, 1984.
- Nahin, P. J., *Oliver Heaviside: Sage in Solitude*, IEEE Press, New York, 1988.
- Oppenheim, A. V., and Schafer, R. W., *Digital Signal Processing*, Prentice-Hall, Englewood Cliffs, N.J., 1975.
- Oppenheim, A. V., Willsky, A. S., and Young, I. T., *Signals and Systems*, Prentice-Hall, Englewood Cliffs, N.J., 1983.
- Papoulis, A. (1), *Circuits and Systems: A Modern Approach*, Holt, Rinehart & Winston, New York, 1980.
- \_\_\_\_\_, (2), *The Fourier Integral and its Applications*, McGraw-Hill, New York, 1962.
- Parseval, M.-A., in *Mémoires de Mathématique et de Physique Présentées à l'Académie Royal de Sciences, par Divers Savants, et Lu dans ses Assemblées* (Mém. des sav. étrangers, 2(1), 639–648 (1805) proof demonstrated in 1799.
- Poisson, S.-D., "Mémoire sur la Théorie Des Ondes," in *Mémoires de l'Académie des Sciences*, Vol. 1, Paris, 1818, pp. 85–87.
- Rabiner, L. R., and Gold, B., *Theory and Application of Digital Signal Processing*, Prentice-Hall, Englewood Cliffs, N.J., 1975.
- Rayleigh, *Philosophical Magazine*, 5(27) 460–469 (1889).
- Seeley, R. T., *An Introduction to Fourier Series and Integrals*, Benjamin, New York, 1966.
- Schwartz, L., *Mathematics for the Physical Sciences*, (transl. from *Méthodes mathématiques pour les sciences physiques*, Hermann, Paris) Addison-Wesley, Reading, Mass., 1966.
- Schwartz, L., *Théorie des Distributions*, 2 vols., Hermann, Paris, 1959.
- Stearns, S. D., and Hush, D. R., *Digital Signal Analysis*, Prentice-Hall, Englewood Cliffs, N.J., 1990.
- Stigler, S. M., *The History of Statistics*, Belknap Press, Cambridge, Mass., 1986, pp. 136–138.
- Strang, G., *Introduction to Applied Mathematics*, Wellesley Cambridge Press (M.I.T.), Cambridge, Mass., 1986.
- Stremler, F. G., *Introduction to Communication Systems*, Addison Wesley, Reading, Mass., 3d ed., 1990.
- Stroud, K. A., *Fourier Series and Harmonic Analysis*, Stanley Thornes, London, 1984.
- Titchmarsh, E. C., *Introduction to the Theory of Fourier Integrals*, 2d ed., Oxford, England, 1937.
- Walker, J. S., *Fast Fourier Transforms*, CRC Press, Boca Raton, Fl., 1991. (Contains an FFT disk.)
- Wylie, C. R., and Barrett, L. C., *Advanced Engineering Mathematics*, 5th ed., McGraw-Hill, New York, 1986.
- Ziemer, R. E., Tranter, W. H., and Fannin, D. R., *Signals and Systems*, MacMillan, London, 1983.

---

---

**APPENDIX 2**

---

## A. Three Short Tables of Fourier Transforms

Table (1)

$f(t)$	$F(\omega)$
$\text{Rect}(t/\tau)$	$\tau \text{Sa}(\omega\tau/2)$
$\Lambda(t/\tau)$	$\tau \text{Sa}^2(\omega\tau/2)$
$e^{-\beta t }$ ( $\beta > 0$ )	$2\beta/(\beta^2 + \omega^2)$
$\text{sgn}(t)$	$\frac{2}{j\omega}$
$\frac{1}{t}$	$\frac{\pi}{j} \text{sgn}(\omega)$
$\delta(t)$	1
$\delta(t - \tau)$	$e^{-j\omega\tau}$
1	$2\pi\delta(\omega)$
$U(t)$	$\frac{1}{j\omega} + \pi\delta(\omega)$
$e^{j\omega_0 t}$	$2\pi\delta(\omega - \omega_0)$
$\cos(\omega_0 t)$	$\pi[\delta(\omega - \omega_0) + \delta(\omega + \omega_0)]$
$\sin(\omega_0 t)$	$\frac{\pi}{j}[\delta(\omega - \omega_0) - \delta(\omega + \omega_0)]$
$\cos(\pi t/\tau)\text{Rect}(t/\tau)$	$\frac{2\tau}{\pi} \frac{\cos(\omega\tau/2)}{1 - (\omega\tau/\pi)^2}$
$\cos^2(\pi t/\tau)\text{Rect}(t/\tau)$	$\frac{\sin(\omega\tau/2)}{\omega[1 - (\omega\tau/2\pi)^2]}$
$\sum_{n=-\infty}^{\infty} F_n e^{jn\omega_0 t}$	$2\pi \sum_{n=-\infty}^{\infty} F_n \delta(\omega - n\omega_0)$
$\delta_T(t) \equiv \sum_{n=-\infty}^{\infty} \delta(t - nT)$	$T = \frac{2\pi}{\omega_0}$
	$\delta_\Omega(\omega) \equiv \omega_0 \sum_{m=-\infty}^{\infty} \delta(\omega - m\omega_0)$
	$\omega_0 = \frac{2\pi}{T}$

Table (2)

$f(t)$	$F(\omega)$
$\cos(\omega_0 t)U(t)$	$\frac{\pi}{2}[\delta(\omega - \omega_0) + \delta(\omega + \omega_0)] + \frac{j\omega}{(j\omega)^2 + \omega_0^2}$
$\sin(\omega_0 t)U(t)$	$\frac{\pi}{2j}[\delta(\omega - \omega_0) - \delta(\omega + \omega_0)] + \frac{\omega_0}{(j\omega)^2 + \omega_0^2}$
$\cos(\omega_0 t)\text{sgn}(t)$	$\frac{2j\omega}{(j\omega)^2 + \omega_0^2}$
$\sin(\omega_0 t)\text{sgn}(t)$	$\frac{2\omega_0}{(j\omega)^2 + \omega_0^2}$
$\frac{1}{t^2 + \beta^2}$	$\frac{\pi}{\beta}e^{-\beta \omega } \quad (\beta > 0)$
$\frac{t}{t^2 + \beta^2}$	$-j\pi e^{\beta \omega } \text{sgn}(\omega) \quad (\beta > 0)$

Table (3)

$f(t)$	$F(\omega)$
$e^{-\beta t}U(t)$	$\frac{1}{\beta + j\omega} \quad (\beta > 0)$
$te^{-\beta t}U(t)$	$\frac{1}{(\beta + j\omega)^2} \quad (\beta > 0)$
$t^n e^{-\beta t}U(t)$	$\frac{n!}{(\beta + j\omega)^{n+1}} \quad (\beta > 0)$
$e^{-\beta t} \cos(\omega_0 t)U(t)$	$\frac{j\omega + \beta}{(j\omega + \beta)^2 + \omega_0^2} \quad (\beta > 0)$
$e^{-\beta t} \sin(\omega_0 t)U(t)$	$\frac{\omega_0}{(j\omega + \beta)^2 + \omega_0^2} \quad (\beta > 0)$

Note: These last five Fourier transforms look very similar to their Laplace transform counterparts with  $s$  replaced by  $j\omega$ . However, it is not generally true that we can obtain a Fourier transform from a Laplace transform simply by replacing  $s$  with  $j\omega$ . For example, the Fourier transforms of  $\cos(\omega_0 t)U(t)$  and  $\sin(\omega_0 t)U(t)$  are not derivable from their Laplace counterparts by setting  $s = j\omega$ .

## B. The Properties

Properties of the Fourier Transform for Real Functions

$f(t)$	$F(\omega) = A(\omega) + jB(\omega)$
$af(t) + bg(t)$	$aF(\omega) + bG(\omega)$
$f(t)$ even	$F(\omega)^* = F(-\omega)$
$f(t)$ odd	$A(\omega)$ even $B(\omega)$ odd $ F(\omega) $ even $\Theta(\omega)$ odd
$f(t)$ neither odd nor even	$f_{ev}(t)$ $f_{od}(t)$
$F(t)$	$A(\omega)$ $jB(\omega)$
$f(\alpha t)$	$2\pi f(-\omega)$ $\frac{1}{ \alpha } F\left(\frac{\omega}{\alpha}\right)$
$f(-t)$	$F(-\omega)$
$f(t - \tau)$	$e^{-j\omega\tau} F(\omega)$
$e^{j\omega_0 t} f(t)$	$F(\omega - \omega_0)$
$Df(t)$	$j\omega F(\omega)$
$tf(t)$	$j \frac{dF(\omega)}{d\omega}$
$\int_{-\infty}^{\infty} f(\tau) g(t - \tau) d\tau$	$F(\omega) G(\omega)$
$f(t)g(t)$	$\frac{1}{2\pi} \int_{-\infty}^{\infty} F(\Theta) G(\omega - \Theta) d\Theta$
$\int_{-\infty}^t f(t) dt$	$\frac{1}{j\omega} F(\omega) + \pi F(0) \delta(\omega)$

**The Area Property**

$$\int_{-\infty}^{\infty} f(t) dt = F(0) \quad \text{and} \quad \int_{-\infty}^{\infty} F(\omega) d\omega = 2\pi f(0)$$

**Parseval's Theorem**

$$\int_{-\infty}^{\infty} |f(t)|^2 dt = \frac{1}{2\pi} \int_{-\infty}^{\infty} |F(\omega)|^2 d\omega$$

**The Sampling Property of the Unit Impulse**

<i>Time Domain</i>	<i>Frequency Domain</i>
$\Phi(t)\delta(t - \tau) = \Phi(\tau)\delta(t - \tau)$	$F(\omega)\delta(\omega - \omega_0) = F(\omega_0)\delta(\omega - \omega_0)$

**The Convolution Property of the Unit Impulse**

<i>Time Domain</i>	<i>Frequency Domain</i>
$\Phi(t)*\delta(t - \tau) = \Phi(t - \tau)$	$F(\omega)*\delta(\omega - \omega_0) = F(\omega - \omega_0)$

**The Unit Impulse and the Unit Step**

<i>Differentiation</i>	<i>Integration</i>
$DU(t) = \delta(t) \quad (\forall t)$	$\int_{-\infty}^t \delta(\tau) d\tau = U(t) \quad (\forall t)$

---

# Answers to the Exercises

**CHAPTER 2**

2.2. (a)  $\frac{\sin(1 + 2\omega_0)}{1 + 2\omega_0} + \frac{\sin(1 - 2\omega_0)}{1 - 2\omega_0}$

(b) 0

(c)  $(2/\pi)[n/(n^2 - 1)]$  ( $n$  even); 0 ( $n$  odd)

(d)  $\sin(2)[2n\pi/(1 - n^2\pi^2)]$

2.3.

$$f_1(t) = \begin{cases} 1 & (0 < t < 1) \\ 2 & (1 < t < 2) \\ 0 & (2 < t < 3) \end{cases} \quad f_1(t+3) = f_1(t)$$

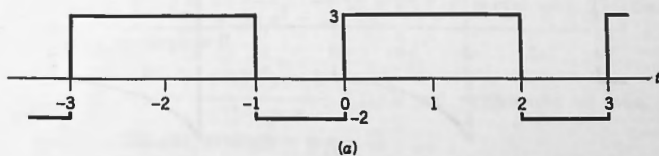
$$f_2(t) = \begin{cases} 2t & (0 < t < 1) \\ 0 & (1 < t < 2) \end{cases} \quad f_2(t+4) = f_2(t) \quad f_2(t) \text{ is odd}$$

$$f_3(t) = \begin{cases} 1 & (0 < t < 1) \\ 0 & (1 < t < 3) \\ t-3 & (3 < t < 4) \end{cases} \quad f_3(t+4) = f_3(t)$$

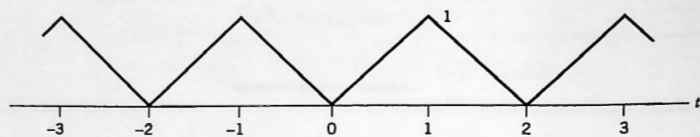
$$f_4(t) = \begin{cases} 5(1 - t/4) & (0 < t < 4) \\ 0 & (4 < t < 6) \end{cases} \quad f_4(t+12) = f_4(t) \quad f_4(t) \text{ is even}$$

$$f_5(t) = 3(1 - t/4) \quad (0 < t < 6) \quad f_5(t+6) = f_5(t)$$

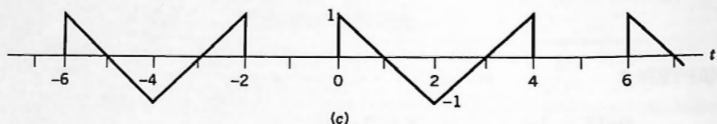
2.4. See all the following sketches.



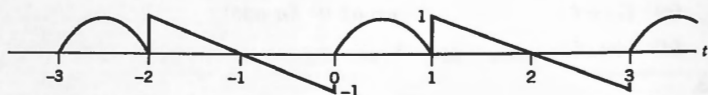
(a)



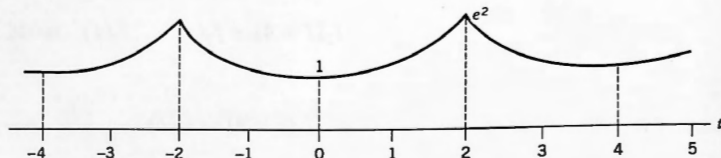
(b)



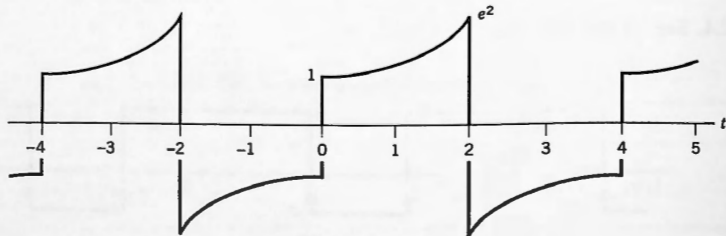
(c)



(d)



(e)



(f)

- 2.5.** (a)  $\omega_0 = 2\pi$ ;  $T_0 = 1$ ;  $F(-1) = 1/2$ ;  $F(1) = 1/2$
- (b)  $\omega_0 = 1$ ;  $T_0 = 2\pi$ ;  $F(-2) = j/2$ ;  $F(-1) = j/2$ ;  $F(0) = 1$ ;  $F(1) = -j/2$ ;  $F(2) = -j/2$
- (c)  $\omega_0 = \pi$ ;  $T_0 = 2$ ;  $F(-5) = 3$ ;  $F(-2) = -1$ ;  $F(-1) = 2$ ;  $F(0) = 3$ ;  $F(1) = 2$ ;  $F(2) = -1$ ;  $F(5) = 3$
- (d)  $\omega_0 = 2$ ;  $T_0 = \pi$ ;  $F(-5) = 5j/2$ ;  $F(-4) = j$ ;  $F(-1) = -3j/2$ ;  $F(0) = 5$ ;  $F(1) = 3j/2$ ;  $F(4) = -j$ ;  $F(5) = -5j/2$
- (e)  $\omega_0 = 1$ ;  $T_0 = 2\pi$ ;  $F(-5) = 2j$ ;  $F(-3) = -j$ ;  $F(-2) = 3/2$ ;  $F(0) = 4$ ;  $F(2) = 3/2$ ;  $F(3) = j$ ;  $F(5) = -2j$
- (f)  $\omega_0 = 10\pi$ ;  $T_0 = 0.2$ ;  $F(-10) = 3/2$ ;  $F(-7) = 5j/2$ ;  $F(7) = -5j/2$ ;  $F(10) = 3/2$
- (g)  $\omega_0 = \pi/3$ ;  $T_0 = 6$ ;  $F(-5) = 1$ ;  $F(-2) = 1/2$ ;  $F(2) = 1/2$ ;  $F(5) = 1$
- (h)  $\omega_0 = 1/6$ ;  $T_0 = 12\pi$ ;  $F(-3) = 1/2$ ;  $F(-2) = -j$ ;  $F(2) = j$ ;  $F(3) = 1/2$
- (i) Not periodic. No  $\omega_0$ , no  $T_0$ . No Fourier series.
- (j)  $\omega_0 = 1/5$ ;  $T_0 = 10\pi$ ;  $F(n) = (1/2n^2) - j[(-1)^n/2(2n+1)^2]$   
 $F(0) = 1/4$ ;  $F(-n) = (1/2n^2) + j[(-1)^n/2(2n+1)^2]$ ; ( $n = 1, 2, 3, 4$ )
- (k)  $\omega_0 = 2\pi$ ;  $T_0 = 1$ ;  $F(0) = 1/2$ ;  $F(k) = -j/\pi(2k-1)$   
 $F(-k) = j/\pi(2k-1)$  ( $k = 1, 2, 3$ )
- 2.6.** (a)  $\omega_0 = 3$ ;  $T_0 = 2\pi/3$ ;  $F(-1) = j$ ;  $F(1) = -j$ ;  $P(-1) = 1$ ;  $P(1) = 1$ ;  $P_{\text{tot}} = 2$
- (b)  $\omega_0 = 2$ ;  $T_0 = \pi$ ;  $F(-1) = 3/2 = F(1)$ ;  $P(-1) = 9/4 = P(1)$ ;  $P_{\text{tot}} = 4.5$ . As a voltage across  $100 \Omega$ ,  $P_{\text{tot}} = 0.045$ . As a current through  $100 \Omega$ ,  $P_{\text{tot}} = 450$ .
- (c)  $\omega_0 = 1$ ;  $T_0 = 2\pi$ ;  $F(-6) = 7/2$ ;  $F(-5) = 5j/2$ ;  $F(0) = 3$ ;  $F(5) = -5j/2$ ;  $F(6) = 7/2$ ;  $P(-6) = 49/4$ ;  $P(-5) = 25/4$ ;  $P(0) = 9$ ;  $P(5) = 25/4$ ;  $P(6) = 49/4$ ;  $P_{\text{tot}} = 46$ . As a voltage across  $10 \text{ k}\Omega$ ,  $P_{\text{tot}} = 4.6 \cdot 10^{-3}$ . As a current through  $0.01 \Omega$ ,  $P_{\text{tot}} = 0.46$ .
- 2.7.** (a)  $T_0 = 4$ ;  $F(n) = \text{Sa}(n\pi/2)$ ;  $f_p(t)$  is real, even, discontinuous, average = 1
- (b)  $T_0 = 1$ ;  $F(0) = \frac{1}{2}$ ;  $F(n) = (j/2\pi n)[(-1)^n - 1]$  ( $n \neq 0$ );  $f_p(t)$  is real, neither odd nor even, discontinuous, average = 1/2
- (c)  $T_0 = \pi/2$ ;  $F(n) = \frac{\cos(n\pi/2)}{n(n^2 - 4)} - j\frac{\sin(n\pi/2)}{n(n^2 - 4)}$  ( $n \neq 0$ );  $f_p(t)$  is complex
- (d)  $T_0 = 2\pi$ ;  $F(n) = \frac{2j}{\pi} \frac{1 - (-1)^n}{n(n^2 - 4)}$  ( $n \neq 0$ );  $f_p(t)$  is real, odd;  $f_p''(t)$  discontinuous, average = 0
- (e)  $T_0 = 2$ ;  $F(n) = \frac{1}{2} \frac{(-1)^n e - 1}{1 - jn\pi}$ ;  $f_p(t)$  is real, neither odd nor even;  $f_p(t)$  is discontinuous, average =  $\frac{1}{2}(e - 1)$

2.8. (a)  $f_p(t) = \frac{1}{2} + \sum_{\substack{n=-\infty \\ n \neq 0}}^{\infty} [\cos(n\pi) - 1]/(n\pi)^2 e^{jn\pi t}$ ; real; average =  $\frac{1}{2}$ ;

(b)  $f_p(t) = j \sum_{\substack{n=-\infty \\ n \neq 0}}^{\infty} [(n \cos(n\pi/2) - \sin(n\pi/2))/n^2] e^{jn2t}$ ; real; average = 0

(c)  $f_p(t) = \frac{1}{2} \sum_{\substack{n=-\infty}}^{\infty} [(\sin(n\pi/2) - jn \cos(n\pi/2))/(n\pi/2)] e^{jn\pi t/2}$ ; complex;  
average =  $1/2 - j/\pi$

2.9. (b) (1)  $|F(n)| = 2/|n|\pi$ ;  $\Theta(n) = (\pi/2)(1-n)$  ( $n > 0$ );  
 $-(\pi/2)(1+n)$  ( $n < 0$ )

(2)  $|F(n)| = [(1 - \cos(n) - n \sin(n))^2 + (\sin(n) - n \cos(n))^2]^{1/2}/n^2$ ;  
 $\Theta(n) = \tan^{-1}[(n \cos(n) - \sin(n))/(\cos(n) + n \sin(n) - 1)] + n$

(3)  $|F(n)| = \left[ \frac{(1+n^2)(4+9n^2)(16+25n^2)}{(36+49n^2)(64+81n^2)(100+121n^2)} \right]^{1/2}$ ;  
 $\Theta(n) = \tan^{-1}(n/1) + \tan^{-1}(-3n/2) + \tan^{-1}(5n/4) - \tan^{-1}(7n/6)$   
 $- \tan^{-1}(9n/8) - \tan^{-1}(11n/10) + n$

(c)	mag	arg	mag	arg
(1)	3.1623	0.3218	(11)	$\pi$
(2)	3.1623	-1.2490	(12)	$-\pi/2$
(3)	2.2361	-2.0344	(13)	$-\pi/2$
(4)	5	2.2143	(14)	0.4636
(5)	1	$\pi$	(15)	0.7854
(6)	$\pi$	0	(16)	-2.3562
(7)	$\pi$	$\pi/2$	(17)	1.8925
(8)	$\pi/5$	$-\pi/2$	(18)	2.3721
(9)	$1/\pi$	$-\pi/2$	(19)	-1.2146
(10)	$2/\pi$	$\pi/2$	(20)	-1.8176

2.10. (a)  $f_p(t) = \begin{cases} 1 & (0 < t < 1) \\ 0 & (1 < t < 2) \end{cases} \quad f_p(t+2) = f_p(t), \quad T_0 = 2, \omega_0 = \pi$

(b)  $F(0) = 1/2$ ;  $F(n) = (j/2n\pi)[(-1)^n - 1]$  ( $n \neq 0$ );  $A(0) = 1/2$ ;  $A(1) = 0$ ;  
 $A(2) = 0$ ;  $A(3) = 0$ ;  $A(4) = 0$ ;  $A(5) = 0$ ;  $B(0) = 0$ ;  $B(1) = -1/\pi$ ;  
 $B(2) = 0$ ;  $B(3) = -1/3\pi$ ;  $B(4) = 0$ ;  $B(5) = -1/5\pi$

(c)  $f_p(t) = \dots + (j/3\pi)e^{-j3\pi t} + (j/\pi)e^{-j\pi t} + 1/2 - (j/\pi)e^{j\pi t} - (j/3\pi)e^{j3\pi t} - \dots$

(d) 1/2, same    (e) Like  $1/n$

2.11. (a)  $f_p(t) = \begin{cases} -\frac{1}{2} & (-2 < t < -1) \\ \frac{1}{2} & (-1 < t < 1) \\ -\frac{1}{2} & (1 < t < 2) \end{cases} \quad f_p(t+4) = f_p(t), \quad f_p(t) \text{ is even}$

(b)  $F(0) = 0; F(n) = \frac{1}{2} \sin(n\pi/2)/(n\pi/2)$  or  $\frac{1}{2} \text{Sa}(n\pi/2)$  ( $n \neq 0$ );  
 $f_p(t) = \dots + \frac{1}{2} \text{Sa}(-3\pi/2)e^{-j3\pi t/2} + \frac{1}{2} \text{Sa}(-\pi/2)e^{-j\pi t/2}$   
 $+ \frac{1}{2} \text{Sa}(\pi/2)e^{j\pi t/2} + \frac{1}{2} \text{Sa}(3\pi/2)e^{j3\pi t/2} + \dots$

(c) Should converge to 0. Does converge to zero.

(d) Like  $1/n$ . (f) Because  $f_p(t)$  is real and even.

2.12. (a)  $f_p(t) = t$  ( $0 < t < 1$ )  $f_p(t+1) = f_p(t)$ ;  $F(0) = \frac{1}{2}$ ;  $F(n) = j/2\pi n$  ( $n \neq 0$ )

(b)  $f_p(t) = \frac{1}{2} - (1/\pi)[\sin(2\pi t) + \frac{1}{2} \sin(4\pi t) + (1/3)\sin(6\pi t) + 1/4 \sin(8\pi t) + \dots]$

(c)  $\frac{1}{2}$  (d) Like  $1/n$

2.14. (a)  $T_0 = 2\pi$

(b) 36 watts

(c)  $F(-9) = -7/2$ ;  $F(-5) = j$ ;  $F(-4) = -\frac{1}{2}$ ;  $F(0) = 3$ ;  $F(4) = -\frac{1}{2}$ ;  $F(5) = -j$ ;  $F(9) = -7/2$

(d)  $P(-9) = 49/4$ ;  $P(-5) = 1$ ;  $P(-4) = 1/4$ ;  $P(0) = 9$ ;  $P(4) = 1/4$ ;  $P(5) = 1$ ;  $P(9) = 49/4$

2.16. (a)  $f_p(t) = \frac{1}{2} - (j/\pi) \sum_{n=-\infty}^{\infty} (1/n)e^{jn2\pi t}$  ( $n$  odd)

(b)  $f_p(0) = \frac{1}{2}$ ;  $f_p(\frac{1}{2}) = \frac{1}{2}$

(c)  $p = 1$

(d)  $P(n) = (1/n\pi)^2$  ( $n$  odd);  $P(0) = 1/4$

(e)

←	$n$	0	1	2	3	4	5
Even	$ F(n) $	$\frac{1}{2}$	$1/\pi$	0	$1/3\pi$	0	$1/5\pi$
Odd	$\Theta(n)$	0	$-\pi/2$	0	$-\pi/2$	0	$-\pi/2$
Even	$P(n)$	$\frac{1}{4}$	$1/\pi^2$	0	$1/9\pi^2$	0	$1/25\pi^2$

Power in these terms = 0.48326 watts.

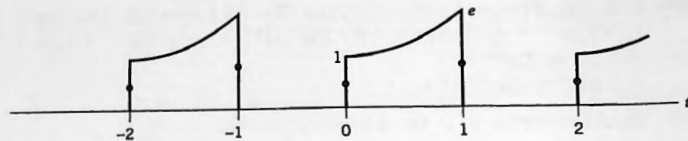
(f)  $P_{\text{tot}} = \frac{1}{2}$ . Power in (e) is 96.65% of  $P_{\text{tot}}$

2.17. (a)  $F(n) = \frac{1}{2} \frac{(-1)^n e - 1}{(1 - jn\pi)}$

(b)  $f_p(-1) = e/2$ ;  $f_p(0) = \frac{1}{2}$ ;  $f_p(1) = e/2$ . Not obvious

(c) See the following sketch.

(d)  $p = 1$



(e)

$\leftarrow$	$n$	0	1	2	3	4	5
Even	$ F(n) $	0.8591	0.5639	0.1350	0.1962	0.0682	0.1181
Odd	$\Theta(n)$	0	-1.880	1.413	-1.677	1.491	-1.634
Even	$P(n)$	0.7381	0.3180	0.0182	0.0385	0.0046	0.0140

(f)  $P(n) = \frac{[(-1)^n e - 1]^2}{4(1 + n^2\pi^2)}$ ;  $P_{\text{tot}} = 1.5973$ ;  $P_{\text{table}} = 95.45\%$

2.19. (a)

$$f_p(t) = \begin{cases} 0 & (-2 < t < -1) \\ 1+t & (-1 < t < 0) \\ 1 & (0 < t < 1) \\ 0 & (1 < t < 2) \end{cases} \quad f_p(t+4) = f_p(t)$$

$$a(n) = \frac{1}{2} \frac{\sin(n\pi/2)}{n\pi/2} + \frac{1}{2} \frac{1 - \cos(n\pi/2)}{(n\pi/2)^2} \quad (n \neq 0), \quad a(0) = 3/4$$

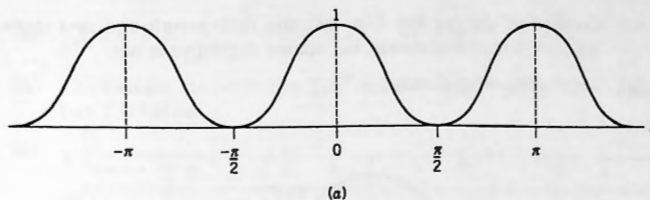
$$b(n) = \frac{1}{2} \frac{-\cos(n\pi/2)}{n\pi/2} + \frac{1}{2} \frac{\sin(n\pi/2)}{(n\pi/2)^2} \quad (n \neq 0)$$

$$f_p(t) = a(0)/2 + \sum_{n=1}^{\infty} [a(n)\cos(n\pi t/2) + b(n)\sin(n\pi t/2)]$$

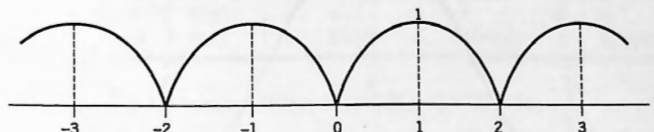
(b) Both  $a(n)$  and  $b(n)$  go to zero like  $1/n$ .(c) Series should converge to  $\frac{1}{2}$ , but this is not obvious.(d)  $A(n) = \frac{1}{2}a(n)$ ;  $B(n) = -\frac{1}{2}b(n)$ ;  $A(0) = 3/8$ 

(e) Total average power = 0.33333.

2.21. (a)  $f_p(t) = \frac{1}{2} + \frac{1}{2}\cos(2t)$ . See the following sketch.(b)  $a(n) = 4/\pi(1 - 4n^2)$ ;  $f_p(t) = 2/\pi - (4/\pi)[(1/3)\cos(\pi t) + (1/15)\cos(2\pi t) + (1/35)\cos(3\pi t) + (1/63)\cos(4\pi t) + \dots]$ . See the following sketch.



(a)

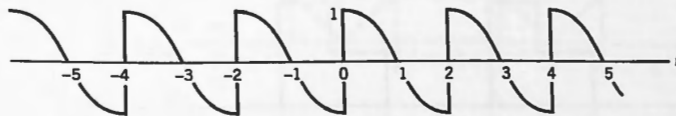


(b)

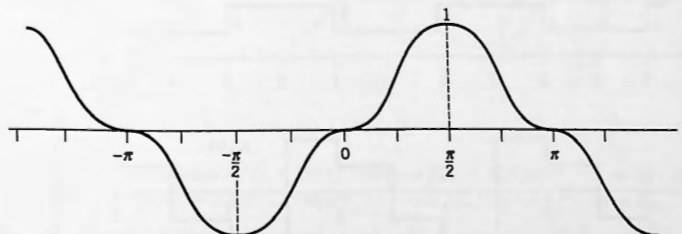
- (c) Coefficients in (b) converge like  $1/n^2$ . The waveform is everywhere continuous, but its first derivative is not.

(d)  $P = 1/2$

- 2.22. (a)  $b(n) = 8n/\pi(4n^2 - 1)$ ;  $f_p(t) = (8/\pi)[(1/3)\sin(\pi t) + (2/15)\sin(2\pi t) + (3/35)\sin(3\pi t) + (4/63)\sin(4\pi t) + \dots]$ . See the following sketch.  
 (b)  $b(n) = 4[(-1)^n - 1]/\pi(n^3 - 4n)$ ;  $f_p(t) = (8/\pi)[(1/3)\sin(t) - (1/15)\sin(3t) - (1/105)\sin(5t) - (1/315)\sin(7t) - \dots]$ ; See the following sketch.



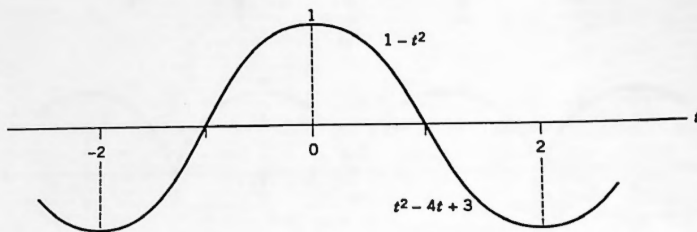
(a)



(b)

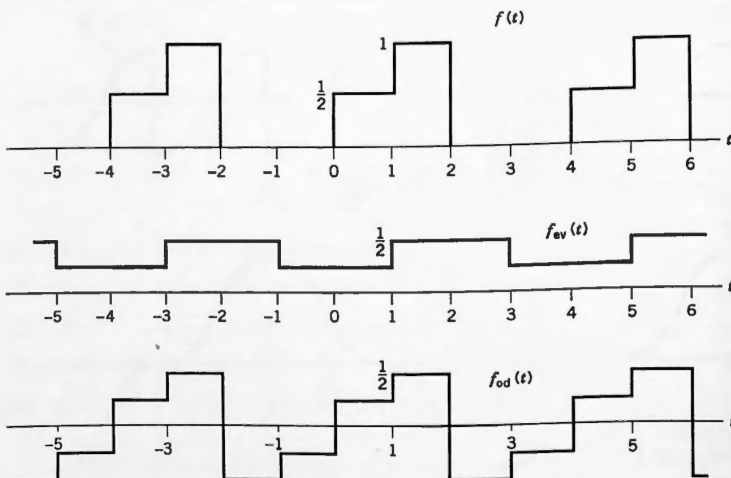
- (c) Coefficients die out like  $1/n^3$  because both zeroth and first derivatives are everywhere continuous, but second derivative is not.

**2.23.** (a) See the following sketch.



- (c) Coefficients should converge like  $1/n^3$  because zeroth and first derivatives are everywhere continuous, but second derivative is not.
- 2.26.** (b) See the following sketches.

For even part:  $A(0) = 3/8$ ;  $A(n) = -(1/4\pi n)\sin(n\pi/2)$ . For odd part:  $B(0) = 0$ ;  $jB(n) = (j/4\pi n)[2(-1)^n - 1 - \cos(n\pi/2)]$



2.27. (a)  $f_p(t) = \frac{1}{2} + \sum_{n=-\infty}^{\infty} \frac{(-1)^n - 1}{n^2 \pi^2} e^{jn\pi t}$  ( $n \neq 0$ )

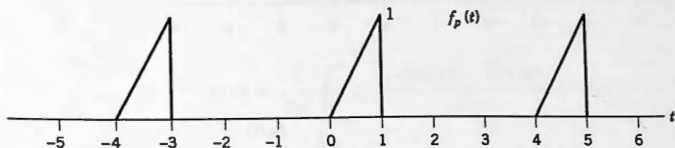
(b) Coefficients converge like  $1/n^2$  because  $f_p(t)$  is everywhere continuous but  $f'_p(t)$  is not.

(c)

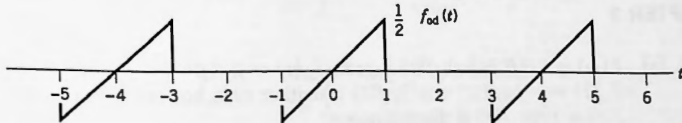
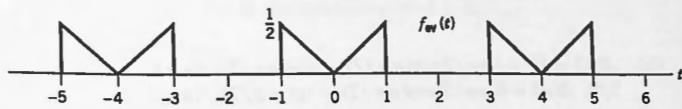
$\leftarrow$	$n$	0	1	2	3	4	5
Even	$ F(n) $	$\frac{1}{2}$	0.2026	0	0.0225	0	0.0081
Odd	$\Theta(n)$	0	$\pi$	0	$\pi$	0	$\pi$
Even	$P(n)$	$\frac{1}{4}$	0.0411	0	0.000507	0	0.000066

(d)  $P_{\text{tot}} = 0.3333$  watts;  $P(0) + P(1) + P(-1) = 99.64\%$

- 2.29. (a) See the following sketch.  $F(n) = -[1 - (\cos(n\pi/2) - j\sin(n\pi/2))(1 + jn\pi/2)]/(n\pi)^2$



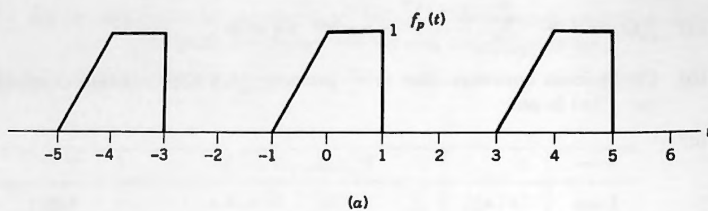
(a)



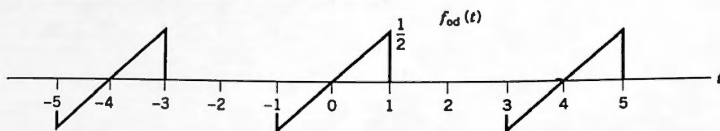
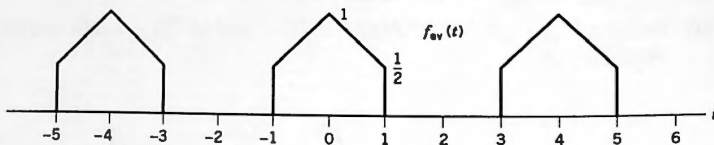
(b)

(b)  $A(n) = [\cos(n\pi/2) + (n\pi/2)\sin(n\pi/2) - 1]/(n\pi)^2$  ( $n \neq 0$ );  $A(0) = 1/8$ ;  $B(n) = [(n\pi/2)\cos(n\pi/2) - \sin(n\pi/2)]/(n\pi)^2$  ( $n \neq 0$ )

- 2.30. (a) See the following sketches.  $F(n) = [1 + j(n\pi/2)e^{-jn\pi/2} - e^{jn\pi/2}]/(n\pi)^2$  ( $n \neq 0$ );  $F(0) = 3/8$



(a)



(b)

(b)  $A(n) = [1 + (n\pi/2)\sin(n\pi/2) - \cos(n\pi/2)]/(n\pi)^2$  ( $n \neq 0$ );  $A(0) = 3/8$ ;  $B(n) = [(n\pi/2)\cos(n\pi/2) - \sin(n\pi/2)]/(n\pi)^2$  ( $n \neq 0$ )

## CHAPTER 3

- 3.3. (a)  $F(\omega) = 1/(\beta + j\omega)$ ;  $f(t)$  is real;  $f_{ev}(t) \Leftrightarrow \beta/(\beta^2 + \omega^2)$ ;  $f_{od}(t) \Leftrightarrow -j\omega/(\beta^2 + \omega^2)$ ;  $f(t)$  is neither even nor odd; area under  $f(t) = 1/\beta$ ;  $f(t)$  is discontinuous
- (b)  $F(\omega) = j2\pi[\omega \cos(\omega) - \sin(\omega)]/\omega^2$ ;  $f(t)$  is real;  $f_{ev}(t) \Leftrightarrow 0$ ;  $f_{od}(t) \Leftrightarrow j2\pi[\omega \cos(\omega) - \sin(\omega)]/\omega^2$ ;  $f(t)$  is odd; area under  $f(t) = 0$ ;  $f(t)$  discontinuous
- (c)  $F(\omega) = 2\pi[\omega \sin^2(\omega) - 2\cos(\omega)]/\omega^2$ ;  $f(t)$  is not real
- (d)  $F(\omega) = 1$ ;  $f(t)$  is real;  $f_{ev}(t) \Leftrightarrow 1$ ;  $f_{od}(t) \Leftrightarrow 0$ ;  $f(t)$  is even; area = 1; cannot say

- (e)  $F(\omega) = e^{-\beta|\omega|}$ ;  $f(t)$  is real;  $f_{ev}(t) \Leftrightarrow e^{-\beta|\omega|}$ ;  $f_{od}(t) \Leftrightarrow 0$ ;  $f(t)$  is even; area = 1; cannot say
- (f)  $F(\omega) = (j\omega + 2)/[(j\omega)^2 + \omega + 1]$ ;  $f(t)$  is not real

**3.4.** (a)  $f(t)$  is real;  $f(t) = (1/2\pi) \int_{-\infty}^{\infty} \text{Sa}(\omega/4)e^{j\omega t} d\omega$ ;  
 $f_{ev}(t) = (1/2\pi) \int_{-\infty}^{\infty} \text{Sa}(\omega/4)e^{j\omega t} d\omega$ ;  $f_{od}(t) = 0$ ;  $f(t)$  is even;  $f(t)$  is discontinuous; area = 1

(b)  $f(t)$  is real;  $f(t) = (1/2\pi) \int_{-\infty}^{\infty} e^{-j\omega/2} \text{Sa}(\omega/4)e^{j\omega t} d\omega$ ;  
 $f_{ev}(t) = (1/2\pi) \int_{-\infty}^{\infty} \cos(\omega/2)\text{Sa}(\omega/4)e^{j\omega t} d\omega$ ;  
 $f_{od}(t) = (1/2\pi) \int_{-\infty}^{\infty} (-j)\sin(\omega/2)\text{Sa}(\omega/4)e^{j\omega t} d\omega$ ;  
 Neither odd nor even;  $f(t)$  is discontinuous; area = 1

(c)  $f(t)$  is real;

$$f(t) = \frac{1}{2\pi} \int_{-\infty}^{\infty} 2j \frac{\omega \cos(\omega) - \sin(\omega)}{\omega^2} e^{j\omega t} d\omega$$

$$f_{ev}(t) = 0; \quad f_{od}(t) = \frac{1}{2\pi} \int_{-\infty}^{\infty} 2j \frac{\omega \cos(\omega) - \sin(\omega)}{\omega^2} e^{j\omega t} d\omega$$

$f(t)$  is odd;  $f(t)$  is discontinuous; area = 0

(d)  $f(t)$  is real,

$$f(t) = \frac{1}{2\pi} \int_{-\infty}^{\infty} \frac{1 - e^{-j\omega} - j\omega e^{-j\omega}}{(j\omega)^2} e^{j\omega t} d\omega$$

$$f_{ev}(t) = \frac{1}{2\pi} \int_{-\infty}^{\infty} \frac{\cos(\omega) + \omega \sin(\omega) - 1}{\omega^2} e^{j\omega t} d\omega$$

$$f_{od}(t) = \frac{1}{2\pi} \int_{-\infty}^{\infty} j \frac{\omega \cos(\omega) - \sin(\omega)}{\omega^2} e^{j\omega t} d\omega$$

$f(t)$  is neither even nor odd;  $f(t)$  is discontinuous; area =  $\frac{1}{2}$

(e)  $f(t)$  is real

$$f(t) = \frac{1}{2\pi} \int_{-\infty}^{\infty} \frac{1 + j\omega}{1 + j\omega + (j\omega)^2} e^{j\omega t} d\omega$$

$$f_{ev}(t) = \frac{1}{2\pi} \int_{-\infty}^{\infty} \frac{1}{1 - \omega^2 + \omega^4} e^{j\omega t} d\omega$$

$$f_{od}(t) = \frac{1}{2\pi} \int_{-\infty}^{\infty} \frac{-j\omega^3}{1 - \omega^2 + \omega^4} e^{j\omega t} d\omega$$

 $f(t)$  is neither even nor odd;  $f(t)$  is discontinuous; area = 1

$$(f) f(t) \text{ is real; } f(t) = (1/2\pi) \int_{-\infty}^{\infty} [\cos(\omega) - j \sin(\omega/4)] e^{j\omega t} d\omega;$$

$$f_{ev}(t) = (1/2\pi) \int_{-\infty}^{\infty} \cos(\omega) e^{j\omega t} d\omega;$$

$$f_{od}(t) = (-1/2\pi) \int_{-\infty}^{\infty} j \sin(\omega/4) e^{j\omega t} d\omega;$$

Neither even nor odd; cannot say if discontinuous or not; area = 1

- 3.5. (a) Real    (b) Complex    (c) Real    (d) Complex

$$3.6. (b) (1) |F(\omega)| = [(\omega \sin(\omega) + 1 - \cos(\omega))^2 + (\omega \cos(\omega) - \sin(\omega))^2]^{1/2}/\omega^2; \\ \Theta(\omega) = \arctan[(\omega \cos(\omega) - \sin(\omega))/(\omega \sin(\omega) + 1 - \cos(\omega))] - \omega$$

$$(2) |F(\omega)| = [(1 - \cos(\omega))^2 + (\sin(\omega) - \omega)^2]^{1/2}/\omega^2; \\ \Theta(\omega) = \arctan[(\sin(\omega) - \omega)/(1 - \cos(\omega))] - 3\omega$$

$$(3) F(\omega) = \left[ \frac{(4 + 9\omega^2)(16 + 25\omega^2)(36 + 49\omega^2)}{(64 + 81\omega^2)(100 + 121\omega^2)(144 + 169\omega^2)} \right]^{1/2}; \\ \Theta(\omega) = \tan^{-1}(-3\omega/2) + \tan^{-1}(5\omega/4) + \tan^{-1}(7\omega/6) - \tan^{-1}(9\omega/8) - \tan^{-1}(11\omega/10) - \tan^{-1}(13\omega/12)$$

- 3.7. (a) Guaranteed

(b) Not guaranteed

(c) Guaranteed

(d) Guaranteed

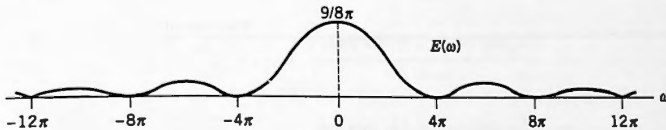
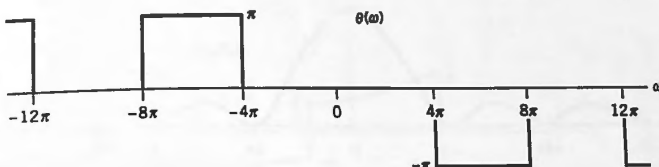
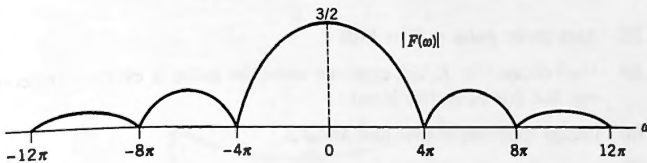
(e) Not guaranteed

(f) Not guaranteed

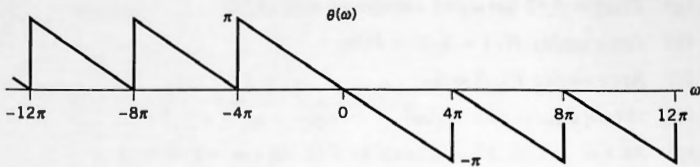
(g) Not guaranteed

(h)  $F(\omega) = 1/(\beta + j\omega)$

- 3.8. (a)  $F(\omega) = 3/2 \operatorname{Sa}(\omega/4)$ , consistent with (3.24)  
 (b) Area under  $f(t) = 3/2 = F(0)$   
 (c) Area under  $F(\omega) = 6\pi$   
 (d)  $|F(\omega)|$  decays like  $K/|\omega|$   
 (e) At  $t = \pm 1/4$ ,  $F(\omega)$  inverts to  $3/2$ . At  $t = -1/8$ , to 3  
 (f)  $E(\omega) = (9/8\pi)\operatorname{Sa}^2(\omega/4)$ , area under  $E(\omega)$  = total energy =  $9/2$   
 (g) See the following sketches.



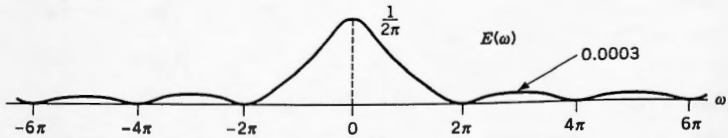
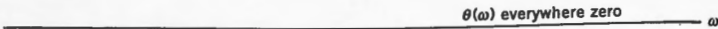
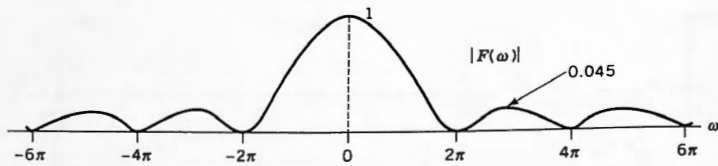
- 3.9. (a)  $F(\omega) = e^{-j\omega/4}[3/2 \operatorname{Sa}(\omega/4)]$   
 (b)  $|F(\omega)| = (3/2)|\operatorname{Sa}(\omega/4)|$ , which is the same as for Exercise 3.8  
 (c)  $E(\omega) = (9/8\pi)\operatorname{Sa}^2(\omega/4)$ , which is the same as for Exercise 3.8  
 (d) Magnitude and energy plots are the same as for Exercise 3.8  
 (e) See the following sketch of phase spectrum. Differs from Exercise 3.8 by the term  $-\omega/4$ , which came from the exponential.



Magnitude and energy spectra are the same as for exercise 3.8

- 3.10. (b) Area under pulse =  $\tau = F(0)$

- (c)  $F(\omega)$  decays like  $K/\omega^2$ , expected since the pulse is everywhere continuous, but first derivative is not.
- (d) Energy spectrum decays like  $M/\omega^4$ .
- (f) See the following sketches.



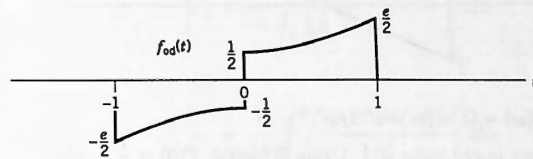
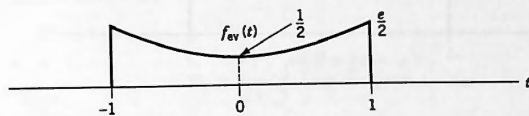
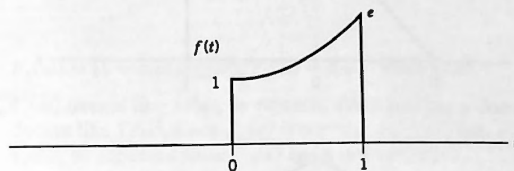
- (g) Values are 0, 0,  $\frac{1}{2}$ , 1,  $\frac{1}{2}$ , 0, 0

3.11. (a)  $F(\omega) = \frac{e^{1-j\omega} - 1}{1 - j\omega}$

(b)  $f(0) = \frac{1}{2}; f(\frac{1}{2}) = e^{\frac{1}{2}}; f(1) = e/2$

(c)  $F(0) = \text{area under pulse} = e - 1$

(d) See the following sketches.



$$f_{ev}(t) \Leftrightarrow \frac{e \cos(\omega) - 1 + \omega e \sin(\omega)}{1 + \omega^2}$$

$$f_{od}(t) \Leftrightarrow j \frac{-e \sin(\omega) + \omega e \cos(\omega) - \omega}{1 + \omega^2}$$

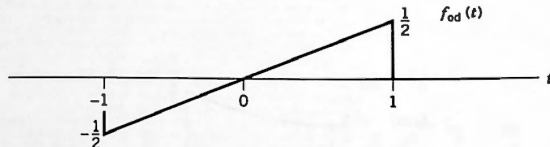
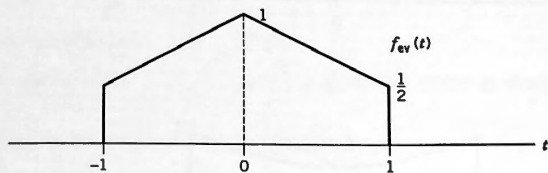
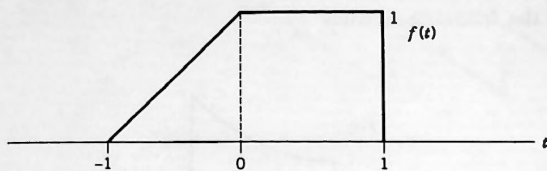
(e) Both transforms in (d) decay like  $1/\omega$ .

**3.12.** (b)  $F(\omega)$  decays like  $1/\omega^2$

$$(c) \int_{-\infty}^{\infty} A(\omega) e^{j\omega t} d\omega = 2\pi e^{-B|t|}; \int_{-\infty}^{\infty} B(\omega) e^{j\omega t} d\omega = 0$$

$$(d) E(\omega) = (1/2\pi) 4\beta^2 / (\beta^2 + \omega^2)^2; \int_{-\infty}^{\infty} E(\omega) d\omega = 1/\beta$$

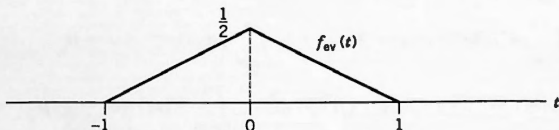
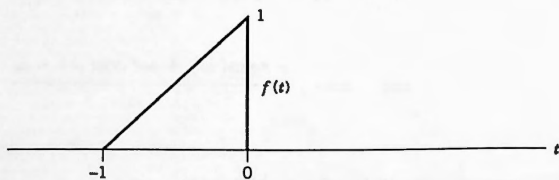
3.13. (b) See the following sketches.

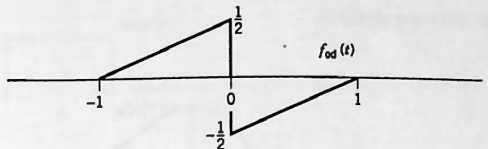


3.14. (a)  $F_1(\omega) = (1 + j\omega - e^{j\omega})/\omega^2$

(b) Area under pulse =  $\frac{1}{2}$ . Using l'Hôpital,  $F(0) = \frac{1}{2}$

(c) See the following sketches.





- (d)  $F_2(\omega) = [1 - \cos(\omega)]/\omega^2$ ;  $F_3(\omega) = j[\omega - \sin(\omega)]/\omega^2$   
 (e)  $F_1(\omega)$  decays like  $1/|\omega|$ , as expected since  $f(t)$  has a discontinuity.  $F_2(\omega)$  decays like  $1/\omega^2$ , since  $f_{ev}(t)$  is continuous,  $f'_{ev}(t)$  not.  $F_3(\omega)$  decays like  $1/|\omega|$ , as expected since  $f_{od}(t)$  has a discontinuity.  
 (f)  $E[f(t)] = 1/3$ ;  $E[f_{ev}(t)] = 1/6$ ;  $E[f_{od}(t)] = 1/6$   
 (g)

$$E_1 = \frac{1}{2\pi} \int_1^2 \left| \frac{1 + j\omega - e^{j\omega}}{\omega^2} \right|^2 d\omega$$

$$E_2 = \frac{1}{2\pi} \int_1^2 \left[ \frac{(1 - \cos(\omega))}{\omega^2} \right]^2 d\omega$$

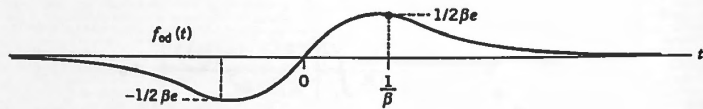
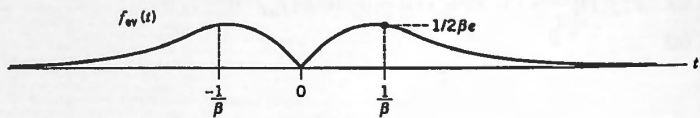
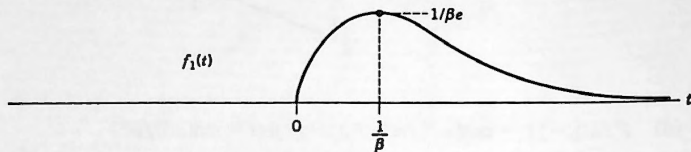
$$E_3 = \frac{1}{2\pi} \int_1^2 \left[ \frac{(\omega - \sin(\omega))}{\omega^2} \right]^2 d\omega$$

(h)  $\int_{-\infty}^{\infty} F_1(\omega) d\omega = \pi$ ;  $\int_{-\infty}^{\infty} F_2(\omega) d\omega = \pi$ ;  $\int_{-\infty}^{\infty} F_3(\omega) d\omega = 0$

## CHAPTER 4

- 4.1. (a)  $E[f_1(t)] = 1/4\beta^3$ . Since  $\beta > 0$ , energy is finite, and so  $F_1(\omega)$  exists and inverts to  $f_1(t)$ .  
 (b)  $F_1(\omega) = 1/(\beta + j\omega)^2$   
 (d) Same  
 (f)  $F_2(\omega) = 2/(\beta + j\omega)^3$   
 (h)  $E_1(\omega) = (1/2\pi)/( \beta^2 + \omega^2)^2$ ;  $E_2(\omega) = (1/2\pi)4/( \beta^2 + \omega^2)^3$

4.2. See the following sketches.



$$f_{ev}(t) \Leftrightarrow \frac{\beta^2 - \omega^2}{(\beta^2 - \omega^2)^2 + (2\beta\omega)^2}$$

$$f_{od}(t) \Leftrightarrow \frac{-j2\beta\omega}{(\beta^2 - \omega^2)^2 + (2\beta\omega)^2}$$

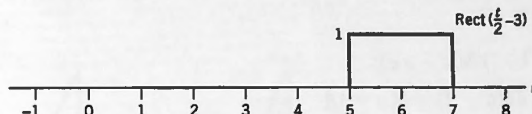
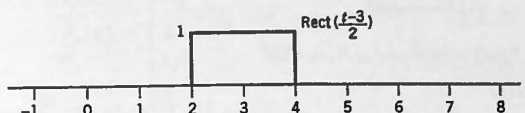
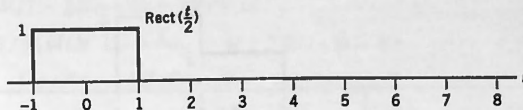
4.3. (d)  $F(\omega) \Leftrightarrow e^{-2t}[8 \cos(4t) - 3 \sin(4t)]U(t)$

4.5. (a)  $F(\omega) = \frac{2\beta}{\beta^2 + \omega^2} + e^{-\beta k/2} \left[ \frac{e^{-j\omega k/2}}{\beta + j\omega} - \frac{e^{j\omega k/2}}{\beta - j\omega} \right]$

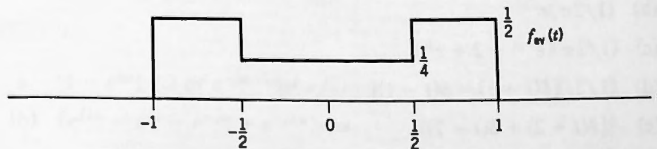
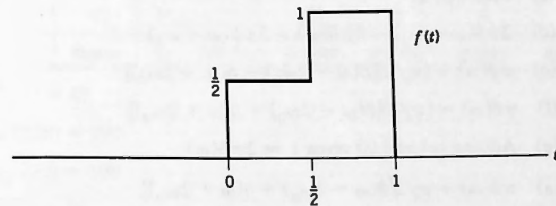
(b)  $F(\omega) = [2\beta/(\beta^2 + \omega^2)]$

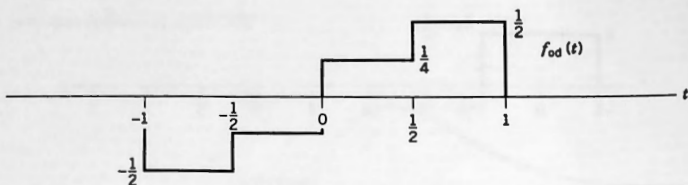
4.6.  $\text{sgn}(t) \Leftrightarrow 2/j\omega$

4.7. (a) See the following sketches.



- 4.8. (a)  $F(\omega) = (\frac{1}{2} + \frac{1}{2}e^{-j\omega/2} - e^{-j\omega})/j\omega$   
 (b)  $A(\omega) = [2 \sin(\omega) - \sin(\omega/2)]/(2\omega); B(\omega) = [2 \cos(\omega) - \cos(\omega/2) - 1]/(2\omega); |F(\omega)| = [A^2(\omega) + B^2(\omega)]^{1/2}; \Theta(\omega) = \tan^{-1}[B(\omega)/A(\omega)]$   
 (c) See the following sketches.  $f_{ev}(t) \Leftrightarrow A(\omega); f_{od}(t) \Leftrightarrow jB(\omega)$





**4.9.** (c)  $F_k(\omega) = [\sin(\omega k/2)/(\omega k/2)]^2$

**4.10.** (a)  $\delta(t)$

(b)  $\frac{1}{2}[e^{3\delta}(t+1) + e^{-3\delta}(t-1)]$

(c)  $\delta(t - \pi/2)$

(d)  $0$

(e)  $(-1)^n \delta(\omega - n\pi)$

(f)  $j[\delta(\omega - 1) + \delta(\omega + 1)]$

**4.11.** (a)  $1$

(b)  $0$

(c)  $1/\sqrt{2}$

(d)  $\pi/2\sqrt{2}$

(e)  $(-1)^n e^{jn\pi t/2}$

**4.12.** (a)  $e^{-j\omega}$

(b)  $3e^{j2\omega}$

(c)  $4\cos^2(\omega/2)$

(d)  $2\pi\delta(\omega - \omega_0) - 4\pi\delta(\omega) + 2\pi\delta(\omega + \omega_0)$

(e)  $\pi\delta(\omega) + (\pi/2)[\delta(\omega - 2\omega_0) + \delta(\omega + 2\omega_0)]$

(f)  $\pi\delta(\omega) - (\pi/2)[\delta(\omega - 2\omega_0) + \delta(\omega + 2\omega_0)]$

(g) Adding (e) and (f) gives  $1 \Leftrightarrow 2\pi\delta(\omega)$

**4.13.** (a)  $\pi\delta(\omega) + \pi/2[\delta(\omega - 2\omega_0) + \delta(\omega + 2\omega_0)]$

(b)  $\pi\delta(\omega) - \pi/2[\delta(\omega - 2\omega_0) + \delta(\omega + 2\omega_0)]$

(c)  $(\pi/2j)[\delta(\omega - 2\omega_0) - \delta(\omega + 2\omega_0)]$

**4.14.** (a)  $(1/2\pi)e^{-jt}$

(b)  $(1/2\pi)e^{j3t}$

(c)  $(1/2\pi)(e^{-jt} - 2 + e^{jt})$

(d)  $(1/2j)[\delta(t+1) - \delta(t-1)]$

(e)  $\frac{1}{2}[\delta(t+2) + \delta(t-2)]$

(f)  $\frac{1}{2}\delta(t) - \frac{1}{4}\delta(t+6) - \frac{1}{4}\delta(t-6)$

(g)  $(1/8)[\delta(t+12) + 3\delta(t+4) + 3\delta(t-4) + \delta(t-12)]$

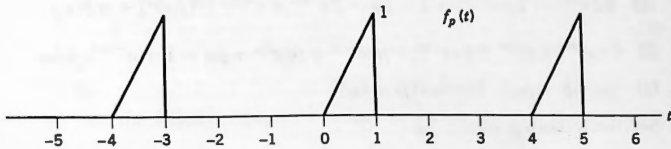
- 4.15.** (a) 1 (b)  $e^{j\omega_0 t}$  (c)  $\cos(\omega_0 t)$  (d)  $\sin(\omega_0 t)$

**4.17.**  $\omega_0 = \pi/2$ , and from Exercise 2.26:

$$F_p(n) = \begin{cases} \frac{j}{4n\pi} [2(-1)^n - 1 - e^{-jn\pi/2}] & (n \neq 0) \\ 3/8 & (n = 0) \end{cases}$$

$$f_p(t) = \sum_{n=-\infty}^{\infty} F_p(n) e^{jn\pi t/2} \text{ and so } F(\omega) = 2\pi \sum_{n=-\infty}^{\infty} F_p(n) \delta(\omega - n\pi/2)$$

- 4.18.** (a) See the following sketch.



$$F(\omega) = 2\pi \sum_{n=-\infty}^{\infty} F_p(n) \delta(\omega - n\pi/2), \text{ where (from Exercise 2.29)}$$

$$F_p(n) = [1/4(jn\pi/2)^2][1 - (1 + jn\pi/2)e^{-jn\pi/2}]$$

Relative Energies in Fourier Transform

←	n	0	1	2	3	4	5
Even	Ratio	1	0.8711	0.5695	0.2728	0.1013	0.0504

- 4.22.** (a) XRE(0) = 40  
 (b) XRE(128) = 192  
 (c) XRE(220) = 100
- 4.23.** (a) FRE(0) = 15  
 (b) FRE(24) = 8  
 (c) FRE(226) = 6/PI; FIM(226) = 12/PI

## CHAPTER 5

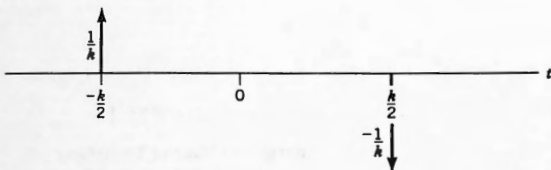
- 5.1.** (a)  $[1 - e^{j\omega}]/j\omega$  or  $e^{-j\omega/2} \text{Sa}(\omega/2)$

$$(b) (e^{j2\omega} - e^{j\omega} - e^{-j\omega} + e^{-j2\omega})/j\omega$$

- (c)  $(e^{j\omega} + e^{-j\omega} - e^{-j2\omega} - e^{-j4\omega})/(j\omega)$   
 (d)  $(e^{j2\omega} - 2e^{j\omega} + 2e^{-j\omega} - e^{-j2\omega})/(j\omega)^2$   
 (e)  $(e^{j\omega} - e^{-j\omega} - j\omega e^{j\omega} - j\omega e^{-j\omega})/(j\omega)^2$   
 (f)  $2(j\omega e^{j\omega} - e^{j\omega} + j\omega e^{-j\omega} + e^{-j\omega})/(j\omega)^3$   
 (g)  $(e^{j\omega} - 1 + j\omega e^{-j\omega} - j\omega e^{-j2\omega} - e^{-j3\omega} + e^{-j4\omega})/(j\omega)^2$   
 (h)  $(e^{-j\omega} - 2j\omega e^{-j\omega} + 2j\omega e^{-j2\omega} - e^{-j3\omega} - 2j\omega e^{-j3\omega})/(j\omega)^2$   
 (i)  $[(j\omega + 1 - e^{-j\omega} - e^{-j2\omega} + e^{-j3\omega})/(j\omega)^2] + \pi\delta(\omega)$   
 (j)  $[(1 - e^{-j\omega} - j\omega e^{-j2\omega})/(j\omega)^2] + 2\pi\delta(\omega)$   
 (k)  $[(2e^{j2\omega} - 2j\omega e^{j2\omega} - 1 - j\omega - 2e^{-j\omega} + e^{-j2\omega})/(j\omega)^2] + \pi\delta(\omega)$   
 (l)  $(-e^{j4\omega} + e^{j3\omega} + j\omega e^{j3\omega} + j\omega e^{j2\omega} + j\omega e^{j\omega} + j\omega - 1 + e^{-j\omega})/(j\omega)^2$

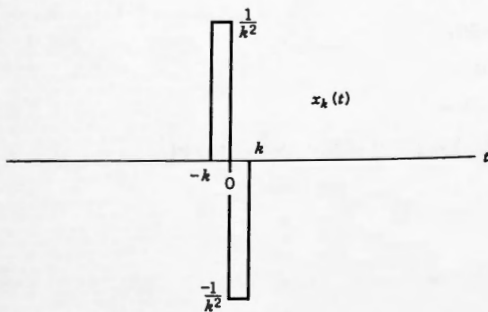
5.2. (a)  $j\omega/(\beta + j\omega)$  (b)  $j\omega/(\beta + j\omega)^2$

5.3. See the following sketch;  $j\omega$



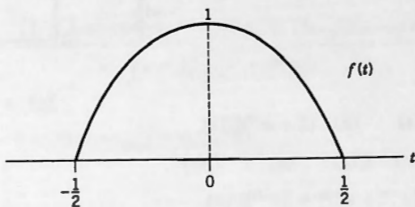
5.4.  $-D^2\delta(t)$

5.5. (d) See the following sketch.

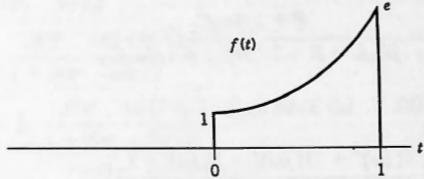


5.7.  $F(\omega) = 1/(\beta + j\omega)$ . No frequency-domain Dirac delta is required because the average over the entire  $t$ -axis is zero.

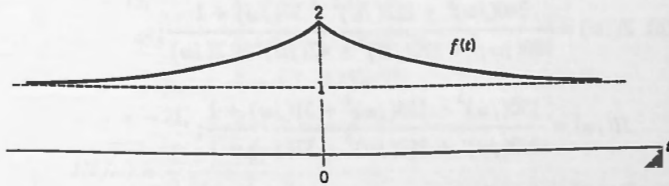
5.8. See the following sketch.  $F(\omega) = 2\pi \frac{\cos(\omega/2)}{\pi^2 - \omega^2}$



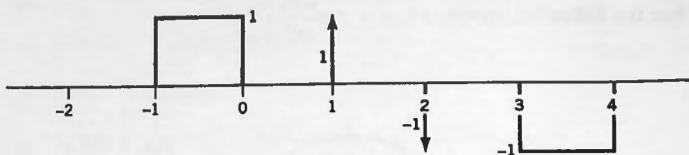
5.9. (a) See the following sketch. (b)  $F(\omega) = \frac{e^{1-j\omega} - 1}{1 - j\omega}$



5.10. (a) See the following sketch. (b)  $F(\omega) = \frac{2\beta}{\beta^2 + \omega^2} + 2\pi\delta(\omega)$



5.11. See the following sketch.



## CHAPTER 6

6.2. (a) (i)  $e^{-t}U(t)$       (ii)  $(1 - e^{-t})U(t)$

(b) (i)  $\delta(t) - e^{-t}U(t)$       (ii)  $e^{-t}U(t)$

6.4. (a)  $y(t) = [2e^{-t} + e^{-3t} - 3e^{-2t}]U(t)$

(b)  $y(t) = [1/5 - e^{-t} + (4/5)e^{-2t} \cos(t) + (33/5)e^{-2t} \sin(t)]U(t)$

6.5. (a) (1)  $y(t) = [1 + e^{-t/3} - 2e^{-t/4}]U(t)$

(2)  $y(t) = [\frac{1}{2}e^{-t/4} - (1/3)e^{-t/3}]U(t)$

6.6. (a)  $[LD^2 + RD + (1/C_1 + 1/C_2)]y(t) = [RD + 1/C_2]x(t)$

(b)  $H(j\omega_0) = \frac{R + 1/j\omega_0 C_2}{j\omega_0 L + R + 1/j\omega_0 C_1 + 1/j\omega_0 C_2}$

(c) Same as (b).      (d) Same as (a).

6.7. (a)  $Z(j\omega) = \frac{4(j\omega)^3 + 11(j\omega)^2 + 8(j\omega) + 1}{4(j\omega)^2 + (j\omega)}$ ;

$$H(j\omega) = \frac{2(j\omega) + 1}{4(j\omega)^3 + 11(j\omega)^2 + 8(j\omega) + 1};$$

$$[4D^3 + 11D^2 + 8D + 1]y(t) = [2D + 1]x(t)$$

(b)  $Z(j\omega) = \frac{240(j\omega)^3 + 252(j\omega)^2 + 37(j\omega) + 1}{180(j\omega)^4 + 192(j\omega)^3 + 42(j\omega)^2 + 2(j\omega)}$ ;

$$H(j\omega) = \frac{150(j\omega)^3 + 156(j\omega)^2 + 31(j\omega) + 1}{240(j\omega)^3 + 252(j\omega)^2 + 37(j\omega) + 1};$$

$$[240D^3 + 252D^2 + 37D + 1]y(t) = [150D^3 + 156D^2 + 31D + 1]x(t)$$

$$(c) \quad Z(j\omega) = \frac{300(j\omega)^3 + 102(j\omega)^2 + 150(j\omega) + 31}{100(j\omega)^2 + 34(j\omega)};$$

$$H(j\omega) = \frac{60(j\omega) + 10}{300(j\omega)^3 + 102(j\omega)^2 + 150(j\omega) + 31};$$

$$[300D^3 + 102D^2 + 150D + 31]y(t) = [60D + 10]x(t)$$

$$6.8. (a) \quad y(t) = \frac{(1 + 2\omega_0^2)\cos(\omega_0 t) + (5\omega_0 + 24\omega_0^3)\sin(\omega_0 t)}{(1 - 12\omega_0^2)^2 + 49\omega_0^2}$$

(b) Same as (a).

$$(d) \quad y(t) = 0.86204 \cos(\omega_0 t - 0.58006)$$

$$6.9. (a) \quad 3 \frac{j14}{1 + j14} e^{j7t}$$

$$(b) \quad 5 \frac{-j6}{1 - j6} e^{-j3t}$$

$$(c) \quad 3 \frac{j14}{1 + j14} e^{j7t} + 5 \frac{-j6}{1 - j6} e^{-j3t}$$

$$(d) \quad \frac{j5\pi}{1 + j5\pi} \frac{\sin(5\pi/2)}{5\pi/2} e^{j5\pi t/2}$$

$$(e) \quad \sum_{n=-\infty}^{\infty} \frac{jn\pi}{1 + jn\pi} \frac{\sin(n\pi/2)}{n\pi/2} e^{jn\pi t/2},$$

$$n = 5: \frac{j5\pi}{1 + j5\pi} \frac{\sin(5\pi/2)}{5\pi/2} e^{j5\pi t/2},$$

$$n = -9: \frac{-j9\pi}{1 - j9\pi} \frac{\sin(-9\pi/2)}{-9\pi/2} e^{-j9\pi t/2}$$

$$(f) \quad \frac{1}{2\pi} \int_{-\infty}^{\infty} \frac{j2\omega}{1 + j2\omega} \frac{2a}{a^2 + \omega^2} e^{j\omega t} d\omega$$

$$(g) \quad \sum_{n=-\infty}^{\infty} \frac{j4\pi n}{1 + j4\pi n} \frac{2/\pi}{(1 - 4n^2)} e^{j2\pi nt} + \frac{1}{2\pi} \int_{-\infty}^{\infty} \frac{2j\omega}{1 + 2j\omega} e^{-a|\omega|} e^{j\omega t} d\omega$$

$$6.10. (a) \quad \omega_5 = 15, \quad x_5 = (-1/13)e^{j15t};$$

$$\omega_{15} = 45, \quad x_{15} = (-1/113)e^{j45t};$$

$$\omega_{-3} = -9, \quad x_{-3} = (-1/5)e^{-j9t};$$

$$\omega_{-7} = -21, \quad x_{-7} = (-1/25)e^{-j21t}$$

$$(b) \quad H(j\omega) = \frac{1}{2} \frac{6(j\omega) + 1}{2(j\omega)^2 + 3(j\omega) + 1}$$

- (c)  $y_5(t) = \frac{1}{2} \frac{6(j15) + 1}{2(j15)^2 + 3(j15) + 1} (-1/13)e^{j15t};$   
 $y_{15}(t) = \frac{1}{2} \frac{6(j45) + 1}{2(j45)^2 + 3(j45) + 1} (-1/113)e^{j45t};$   
 $y_{-3}(t) = \frac{1}{2} \frac{6(-j9) + 1}{2(-j9)^2 + 3(-j9) + 1} (-1/5)e^{-j9t};$   
 $y_{-7}(t) = \frac{1}{2} \frac{6(-j21) + 1}{2(-j21)^2 + 3(-j21) + 1} (-1/25)e^{-j21t}$
- (d)  $y(t) = \frac{1}{2} \frac{6(j15) + 1}{2(j15)^2 + 3(j15) + 1} (-1/13)e^{j15t}$   
 $+ \frac{1}{2} \frac{6(j45) + 1}{2(j45)^2 + 3(j45) + 1} (-1/113)e^{j45t}$   
 $+ \frac{1}{2} \frac{6(-j9) + 1}{2(-j9)^2 + 3(-j9)} (-1/5)e^{-j9t}$   
 $+ \frac{1}{2} \frac{6(-j21) + 1}{2(-j21)^2 + 3(-j21) + 1} (-1/25)e^{-j21t}$
- (e)  $y(t) = \frac{1}{2} \sum_{n=-\infty}^{\infty} \frac{6(j3n) + 1}{2(j3n)^2 + 3(j3n) + 1} \frac{(-1)^n - 1}{1 + n^2} e^{j3nt}$

- 6.11. (a)  $x_p(t) = \frac{1}{2} + \frac{j}{2\pi} \sum_{n=-\infty}^{\infty} \frac{(-1)^n - 1}{n} e^{jn\pi t} \quad (n \neq 0);$   
 $y_p(t) = \frac{1}{10} + \frac{j}{2\pi} \sum_{\substack{n=-\infty \\ n \neq 0}}^{\infty} \frac{2(jn\pi) + 1}{(jn\pi)^2 + 4(jn\pi) + 5} \frac{(-1)^n - 1}{n} e^{jn\pi t}$
- (b)  $n = 0: A(0) = 0.1, B(0) = 0, |Y(0)| = 0.1, \Theta(0) = 0, P(0) = 0.01;$   
 $n = 1: A(1) = -0.102456365, B(1) = -0.199029466,$   
 $|Y(1)| = 0.223852708, \Theta(1) = -2.046197808, P(1) = 0.050110035;$   
 $n = 2: \text{All values zero};$   
 $n = 3: A(3) = -0.030241057, B(3) = -0.012334505,$   
 $|Y(3)| = 0.032659785, \Theta(3) = -2.754317834, P(3) = 0.001066662;$   
 $n = -1: A(-1) = A(1), B(-1) = -B(1), |Y(-1)| = |Y(1)|,$   
 $\Theta(-1) = -\Theta(1), P(-1) = P(1);$   
 $n = -2: \text{All values zero};$   
 $n = -3: A(-3) = A(3), B(-3) = -B(3), |Y(-3)| = |Y(3)|,$   
 $\Theta(-3) = -\Theta(3), P(-3) = P(3)$

**6.14.** (a)  $H(j\omega) = \frac{6(j\omega)}{4(j\omega)^2 + 8(j\omega) + 3}$

(b) (1)  $\frac{6(j7)}{4(j7)^2 + 8(j7) + 3} 3e^{j7t}$

(2)  $\frac{6(-j5)}{4(-j5)^2 + 8(-j5) + 3} 2e^{-j5t}$

(3)  $\frac{6(j7)}{4(j7)^2 + 8(j7) + 3} 3e^{j7t} + \frac{6(-j5)}{4(-j5)^2 + 8(-j5) + 3} 2e^{-j5t}$

(4)  $\frac{6(j5\pi/2)}{4(j5\pi/2)^2 + 8(j5\pi/2) + 3} \frac{\sin(5\pi/2)}{5\pi/2} e^{j5\pi t/2}$

(5)  $\sum_{n=-\infty}^{\infty} \frac{6(jn\pi/2)}{4(jn\pi/2)^2 + 8(jn\pi/2) + 3} \frac{\sin(n\pi/2)}{n\pi/2} e^{jn\pi t/2};$

$n = 5: \frac{6(j5\pi/2)}{4(j5\pi/2)^2 + 8(j5\pi/2) + 3} \frac{\sin(5\pi/2)}{5\pi/2} e^{j5\pi t/2};$

$n = -7: \frac{6(-j7\pi/2)}{4(-j7\pi/2)^2 + 8(-j7\pi/2) + 3} \frac{\sin(-7\pi/2)}{-7\pi/2} e^{-j7\pi t/2}$

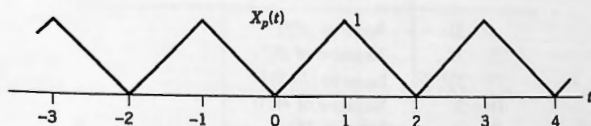
(6)  $\frac{1}{2\pi} \int_{-\infty}^{\infty} \frac{6(j\omega)}{4(j\omega)^2 + 8(j\omega) + 3} \frac{2a}{a^2 + \omega^2} e^{j\omega t} d\omega$

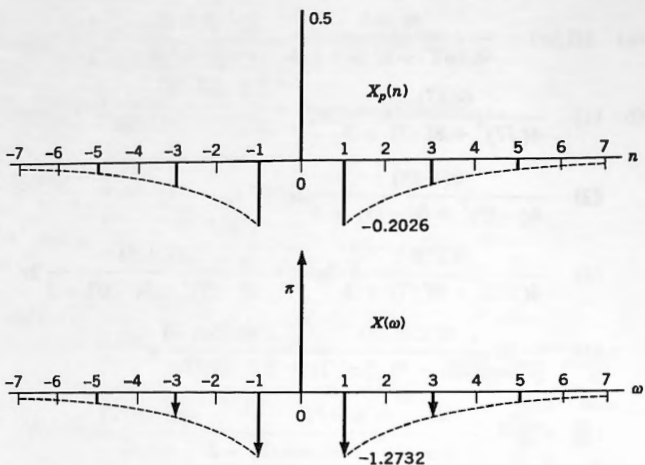
(7)  $\frac{1}{2\pi} \int_{-\infty}^{\infty} \frac{6(j\omega)}{4(j\omega)^2 + 8(j\omega) + 3} e^{-a|\omega|} e^{j\omega t} d\omega$

$$+ \sum_{n=-\infty}^{\infty} \frac{6(j2\pi n)}{4(j2\pi n)^2 + 8(j2\pi n) + 3} \frac{2}{\pi(1-4n^2)} e^{j2\pi nt}$$

**6.15.** (a)  $X(\omega) = \pi\delta(\omega) + (2/\pi) \sum_{n=-\infty}^{\infty} [((-1)^n - 1)/n^2] \delta(\omega - n\pi) \quad (n \neq 0)$

(b) See the following sketches.





$$(d) \quad y_p(t) = \frac{1}{2} + \sum_{\substack{n=-\infty \\ n \neq 0}}^{\infty} \frac{400}{(jn\pi)^2 + 20(jn\pi) + 400} \frac{(-1)^n - 1}{n^2} e^{jn\pi t}$$

(e)

Item	Exact Value	Item	Exact Value
$A(0)$	$\frac{1}{2}$	$A(1)$	-0.202515955
$B(0)$	0	$B(1)$	0.032615897
$ F(0) $	$\frac{1}{2}$	$ F(1) $	0.205125593
$\Theta(0)$	0	$\Theta(1)$	2.981910389
$P(0)$	$\frac{1}{4}$	$P(1)$	0.042076509
$A(2)$	0	$A(3)$	-0.021173620
$B(2)$	0	$B(3)$	0.012826068
$ F(2) $	0	$ F(3) $	0.024755407
$\Theta(2)$	0	$\Theta(3)$	2.596950823
$P(2)$	0	$P(3)$	0.000612830
$A(-1)$	Same as $A(1)$	$A(-2)$	0
$B(-1)$	Negative of $B(1)$	$B(-2)$	0
$ F(-1) $	Same as $ F(1) $	$ F(-2) $	0
$\Theta(-1)$	Negative of $\Theta(1)$	$\Theta(-2)$	0
$P(-1)$	Same as $P(1)$	$P(-2)$	0
$A(-3)$	Same as $A(3)$		
$B(-3)$	Negative of $B(3)$		
$ F(-3) $	Same as $ F(3) $		
$\Theta(-3)$	Negative of $\Theta(3)$		
$P(-3)$	Same as $P(3)$		

- (g) Coefficients are going to zero like  $1/n^4$ . This means that the zeroth, first, and second derivatives will all be continuous and the third derivative will be discontinuous.

**6.16.** (a)  $X(\omega) = [1 - 2e^{-j\omega} + e^{-j2\omega}]/j\omega$ ; Converging like  $1/\omega$ ;  $H(j\omega) = 400/[(j\omega)^2 + 20(j\omega) + 400]$ ;  $Y(\omega) = H(j\omega)X(\omega)$ ; Converging like  $1/\omega^3$ ; Means that  $y(t)$ ,  $y'(t)$  are continuous and that  $y''(t)$  is discontinuous;  $y(t) = x(t) - [g(t) - 2g(t-1) + g(t-2)]$ , where  $g(t) = [\cos(10t\sqrt{3}) + (1/\sqrt{3})\sin(10t\sqrt{3})]e^{-10t}U(t)$

(b)  $A_X(\omega) = \omega \sin(\omega) \text{Sa}^2(\omega/2)$ ;  $B_X(\omega) = \omega \cos(\omega) \text{Sa}^2(\omega/2)$ ;  $|X(\omega)| = [A(\omega)^2 + B(\omega)^2]^{1/2}$ ;  $\Theta_X(\omega) = \arctan(B_X(\omega)/A_X(\omega))$

$X(\omega)$  Sampled at Multiples of  $\omega_0 = \pi/4$

Item	Exact Value	Item	Exact Value
$A(0\omega_0)$	0	$A(1\omega_0)$	0.527393088
$B(0\omega_0)$	0	$B(1\omega_0)$	0.527393088
$ X(0\omega_0) $	0	$ X(1\omega_0) $	0.745846457
$\Theta(0\omega_0)$	0	$\Theta(1\omega_0)$	0.785398164
$E(0\omega_0)$	0	$E(1\omega_0)$	0.088535816
$A(2\omega_0)$	1.273239545	$A(3\omega_0)$	1.024624058
$B(2\omega_0)$	0	$B(3\omega_0)$	-1.024624058
$ X(2\omega_0) $	1.273239545	$ X(3\omega_0) $	1.449037240
$\Theta(2\omega_0)$	0	$\Theta(3\omega_0)$	-0.785398164
$E(2\omega_0)$	0.258012276	$E(3\omega_0)$	0.334179054
$A(-1\omega_0)$	Same as $A(1\omega_0)$	$A(-2\omega_0)$	Same as $A(2\omega_0)$
$B(-1\omega_0)$	Negative of $B(1\omega_0)$	$B(-2\omega_0)$	Negative of $B(2\omega_0)$
$ X(-1\omega_0) $	Same as $ X(1\omega_0) $	$ X(-2\omega_0) $	Same as $ X(2\omega_0) $
$\Theta(-1\omega_0)$	Negative of $\Theta(1\omega_0)$	$\Theta(-2\omega_0)$	Negative of $\Theta(2\omega_0)$
$E(-1\omega_0)$	Same as $E(1\omega_0)$	$E(-2\omega_0)$	Same as $E(2\omega_0)$
$A(-3\omega_0)$	Same as $A(3\omega_0)$		
$B(-3\omega_0)$	Negative of $B(3\omega_0)$		
$ X(-3\omega_0) $	Same as $ X(3\omega_0) $		
$\Theta(-3\omega_0)$	Negative of $\Theta(3\omega_0)$		
$E(-3\omega_0)$	Same as $E(3\omega_0)$		

(c)

 $H(j\omega)$  Sampled at Multiples of  $\omega_0 = \pi / 4$ 

Item	Exact Value	Item	Exact Value
$A(0\omega_0)$	1	$A(1\omega_0)$	0.999997618
$B(0\omega_0)$	0	$B(1\omega_0)$	-0.039330467
$ H(0\omega_0) $	1	$ H(1\omega_0) $	1.000770764
$\Theta(0\omega_0)$	0	$\Theta(1\omega_0)$	-0.039310300
$E(0\omega_0)$	0.159154940	$E(1\omega_0)$	0.159400379
$A(2\omega_0)$	0.999961715	$A(3\omega_0)$	0.999804697
$B(2\omega_0)$	-0.079024271	$B(3\omega_0)$	-0.119444502
$ H(2\omega_0) $	1.003079392	$ H(3\omega_0) $	1.006914307
$\Theta(2\omega_0)$	-0.078863393	$\Theta(3\omega_0)$	-0.118904282
$E(2\omega_0)$	0.160136653	$E(3\omega_0)$	0.161363444
$A(-1\omega_0)$	Same as $A(1\omega_0)$	$A(-2\omega_0)$	Same as $A(2\omega_0)$
$B(-1\omega_0)$	Negative of $B(1\omega_0)$	$B(-2\omega_0)$	Negative of $B(2\omega_0)$
$ H(-1\omega_0) $	Same as $ H(1\omega_0) $	$ H(-2\omega_0) $	Same as $ H(2\omega_0) $
$\Theta(-1\omega_0)$	Negative of $\Theta(1\omega_0)$	$\Theta(-2\omega_0)$	Negative of $\Theta(2\omega_0)$
$E(-1\omega_0)$	Same as $E(1\omega_0)$	$E(-2\omega_0)$	Same as $E(2\omega_0)$
$A(-3\omega_0)$	Same as $A(3\omega_0)$		
$B(-3\omega_0)$	Negative of $B(3\omega_0)$		
$ H(-3\omega_0) $	Same as $ H(3\omega_0) $		
$\Theta(-3\omega_0)$	Negative of $\Theta(3\omega_0)$		
$E(-3\omega_0)$	Same as $E(3\omega_0)$		

(d)

 $Y(\omega)$  Sampled at Multiples of  $\omega_0 = \pi / 4$ 

Item	Exact Value	Item	Exact Value
$ Y(0) $	0	$ Y(1) $	0.746421329
$\Theta(0)$	0	$\Theta(1)$	0.746087864
$ Y(2) $	1.277160349	$ Y(3) $	1.459056328
$\Theta(2)$	-0.078863393	$\Theta(3)$	-0.904302446

 $Y(\omega)$  Sampled at Multiples of  $\omega_0 = \pi / 4$ 

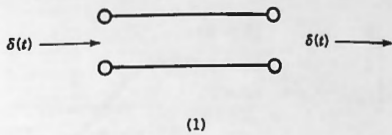
Item	FFT Value	Item	FFT Value
$ Y(0) $	0	$ Y(1) $	0.74641196
$\Theta(0)$	0	$\Theta(1)$	0.74608786
$ Y(2) $	1.27709620	$ Y(3) $	1.45889150
$\Theta(2)$	-0.078863393	$\Theta(3)$	-0.90430245

**CHAPTER 7**

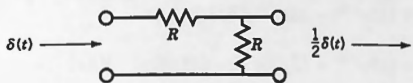
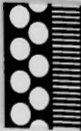
7.1. (a)  $h(t) = (1/RC)e^{-t/RC}U(t)$

(b)  $h(t) = te^{-t}U(t)$

7.2. (a) (1) Two perfect conductors

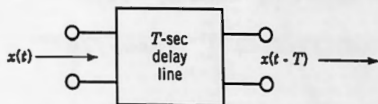


(2) A voltage divider



(2)

(3) An ideal  $T$ -second delay line



(3)

(b) (1)  $H(j\omega) = 1$ ; (2)  $H(j\omega) = \frac{1}{2}$ ; (3)  $H(j\omega) = e^{-j\omega T}$

(c) (1)  $y(t) = x(t)$ ; (2)  $y(t) = \frac{1}{2}x(t)$ ; (3)  $y(t) = x(t - T)$

7.3. (a)  $Y(\omega) = H(j\omega)$       (b)  $\pi[H(j\omega_0)\delta(\omega - \omega_0) + H(-j\omega_0)\delta(\omega + \omega_0)]$

7.4. (a)  $y(t) = \delta(t)$

7.5. (a) (1)  $y(t) = g(t) * h(t)$ ; (2) Same as (1)

(b) Order is immaterial because  $g(t) * h(t) = h(t) * g(t)$

7.7. (a)  $H(j\omega) = \frac{2(j\omega) + 1}{252(j\omega)^2 + 227(j\omega) + 51};$   
 $h(t) = [(1/77)e^{-3t/7} - (1/198)e^{-17t/36}]U(t)$

7.8. (a)  $y(t) = \Lambda(t)$

7.9. (a)  $y(t) = \text{Rect}(t - 1)$

7.10. (a)  $y(t) = \begin{cases} 0 & (t < 0) \\ 1 - e^{-t} & (0 < t < 1) \\ (e - 1)e^{-t} & (1 < t) \end{cases}$

7.11.  $y(t) = \begin{cases} 0 & (t < 0) \\ 2 - t - 2e^{-t} & (0 < t < 1) \\ (e - 2)e^{-t} & (1 < t) \end{cases}$

7.12. (b)  $y(t) = (e^{-2t} - e^{-3t})U(t)$

7.13. (a)  $h(t) = (45e^{-5t} - 36e^{-4t})U(t)$

(b)  $y(t) = [12e^{-4t} - (3/4)e^{-t} - (45/4)e^{-5t}]U(t)$

7.18. (a)  $X(\omega) = \frac{1}{2}A\tau[\text{Sa}((\omega - \omega_0)\tau/2) + \text{Sa}((\omega + \omega_0)\tau/2)]$

(b)  $x(t) = A \cos(\omega_0 t) \text{Rect}(t/\tau)$

7.19. Method 1: (a)  $X(\omega) = (\tau A \pi / T) \sum_{n=-\infty}^{\infty} \text{Sa}(n\omega_1 \tau / 2) [\delta(\omega - n\omega_1 - \omega_0) + \delta(\omega - n\omega_1 + \omega_0)],$  where  $\omega_1 = 2\pi/T$

(b)  $x(t) = \cos(\omega_0 t)(\tau A / T) \sum_{n=-\infty}^{\infty} \text{Sa}(n\omega_1 \tau / 2) e^{jn\omega_1 t} = \cos(\omega_0 t) f_p(t)$

Method 2: (a)  $X(\omega) = 2\pi \sum_{n=-\infty}^{\infty} F_p(n) \delta(\omega - n\omega_1),$  where

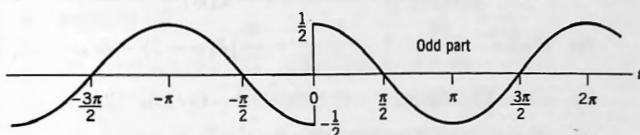
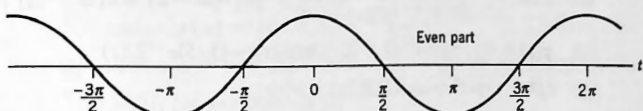
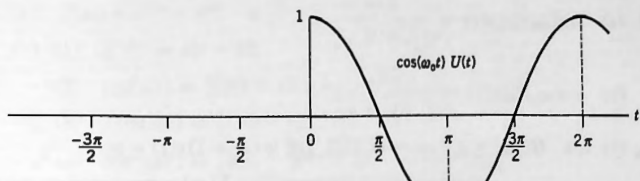
$$F_p(n) = (A\tau/2T)[\text{Sa}((n\omega_1 - \omega_0)\tau/2)e^{-j(n\omega_1 - \omega_0)\tau/2} + \text{Sa}((n\omega_1 + \omega_0)\tau/2)e^{-j(n\omega_1 + \omega_0)\tau/2}]$$

7.20.  $F(\omega) = (1/2j)[X(\omega - \omega_0) - X(\omega + \omega_0)]$

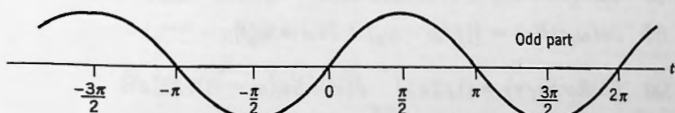
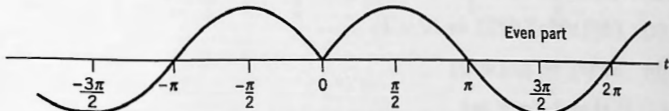
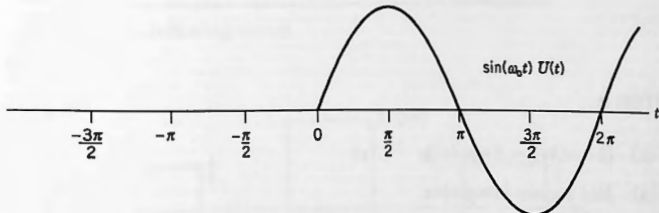
7.21.  $F(\omega) = (\pi/2)[\delta(\omega - 2\omega_0) + 2\delta(\omega) + \delta(\omega + 2\omega_0)]$

7.22.  $x(t)\cos(\omega_0 t) \Leftrightarrow \frac{1}{2}[X(\omega - \omega_0) + X(\omega + \omega_0)];$  To demodulate we multiply again by  $\cos(\omega_0 t),$  obtaining  $[x(t)\cos(\omega_0 t)]\cos(\omega_0 t) \Leftrightarrow \frac{1}{4}X(\omega - 2\omega_0) + \frac{1}{2}X(\omega) + \frac{1}{4}X(\omega + 2\omega_0).$  Now extract the baseband portion using an ideal lowpass filter that excludes  $\frac{1}{4}X(\omega - 2\omega_0)$  and  $\frac{1}{4}X(\omega + 2\omega_0)$  and passes  $\frac{1}{2}X(\omega).$

7.23. (b) See the following sketches.



7.24. (b) See the following sketches.



7.25. (a)  $\cos(\omega_0 t)\text{sgn}(t) \Leftrightarrow \frac{2j\omega}{(j\omega)^2 + \omega_0^2}$

(b)  $\sin(\omega_0 t)\text{sgn}(t) \Leftrightarrow \frac{2\omega_0}{(j\omega)^2 + \omega_0^2}$

7.26. (1) (a)  $H(j\omega) = 1/(j\omega + 1)$ ; CCL DE is  $(D + 1)y(t) = x(t)$

$$(b) Y(\omega) = \frac{1}{j\omega + 1} \left( \frac{j\omega}{((j\omega)^2 + 4)} + \frac{1}{2}\pi[\delta(\omega - 2) - \delta(\omega + 2)] \right)$$

(c)  $y(t) = [(1/5)\cos(2t) + (2/5)\sin(2t) - (1/5)e^{-t}]U(t)$

(d)  $(D + 1)y(t) = \cos(2t)U(t) = x(t)$

(2) (a)  $H(j\omega) = j\omega/(j\omega + 1)$ ; CCL DE is  $(D + 1)y(t) = Dx(t)$

$$(b) Y(\omega) = \frac{j\omega}{j\omega + 1} \left( \frac{3}{(j\omega)^2 + 9} + \frac{\pi}{2j}[\delta(\omega - 3) - \delta(\omega + 3)] \right)$$

(c)  $y(t) = [(3/10)\cos(3t) + (9/10)\sin(3t) - (3/10)e^{-t}]U(t)$

(d)  $(D + 1)y(t) = 3\cos(3t)U(t) = Dx(t)$

7.28. (c)

$n$	1	2	3	4	5	6	7	8	9	10	11	12	13
$f(n)$	0	1	2	3	4	5	6	5	4	3	2	1	0

## CHAPTER 8

8.7. (c)  $[8\cos(4t) - 3\sin(4t)]e^{-2t}U(t)$

8.9. (a) Not square integrable.

(b) Cannot evaluate analysis equation.

8.11. (a)  $(k/2\pi)\text{Sa}^2(tk/2) \Leftrightarrow \Lambda(\omega/k)$

(b)  $\text{Sa}^2(t) \Leftrightarrow \pi\Lambda(\omega/2)$

8.12.  $e^{-\sigma t}U(t) \Leftrightarrow 1/(\sigma + j\omega)$

8.13.  $\text{Sa}(3t) \Leftrightarrow (\pi/3)\text{Rect}(\omega/6)$

8.15. (a)  $\sin(\omega_0 t)\text{Rect}(t/\tau) \Leftrightarrow (\tau/2j)[\text{Sa}((\omega - \omega_0)\tau/2) - \text{Sa}((\omega + \omega_0)\tau/2)]$

(b)  $\cos(\omega_0 t)f(t) \Leftrightarrow \frac{1}{2}[F(\omega - \omega_0) + F(\omega + \omega_0)]$

8.16. (a)  $f(t)\text{Rect}(t/\tau) \Leftrightarrow (1/2\pi)\int_{-\infty}^{\infty} F(\Theta)\tau \text{Sa}[(\omega - \Theta)\tau/2] d\Theta$

- 8.17.** (a)  $f(\omega) = e^{j2\omega} - e^{j\omega} - e^{-j\omega} + e^{-j2\omega}$
- (b) (1)  $e^{-j\omega\tau} \Leftrightarrow \delta(t - \tau);$   
(2)  $\cos(\omega\tau) \Leftrightarrow \frac{1}{2}[\delta(t + \tau) + \delta(t - \tau)];$   
(3)  $j \sin(\omega\tau) \Leftrightarrow \frac{1}{2i}[\delta(t + \tau) - \delta(t - \tau)];$   
(4)  $\cos^2(\omega\tau) \Leftrightarrow \frac{1}{2}\delta(t) + \frac{1}{4}\delta(t + 2\tau) + \frac{1}{4}\delta(t - 2\tau);$   
(5)  $4j \cos(p\omega)\sin(q\omega) \Leftrightarrow \delta(t + p + q) - \delta(t - p - q) - \delta(t + p - q) + \delta(t - p + q);$   
(6)  $\cos(\omega\tau)F(\omega) \Leftrightarrow \frac{1}{2}f(t + \tau) + \frac{1}{2}f(t - \tau);$   
(7)  $(e^{j\omega\tau} + e^{j2\omega\tau})^2 \Leftrightarrow \delta(t + 2\tau) + 2\delta(t + 3\tau) + \delta(t + 4\tau)$

**8.18.** (a)  $f(t) \Leftrightarrow 2j\tau \text{Sa}(\omega_0\tau/2)\sin(\omega_0\tau/2)$

(b)  $f'(t) \Leftrightarrow -4 \sin^2(\omega_0\tau/2)$

(c) Same as (b)

**8.19.** (a) (1)  $y(t) = 1/(2\pi) \int_{-\omega_0/2}^{\omega_0/2} X(\omega)e^{j\omega t} d\omega;$

(2)  $y(t) = \omega_0/2\pi \int_{-\infty}^{\infty} x(\tau)\text{Sa}[\omega_0(t - \tau)/2] d\tau$

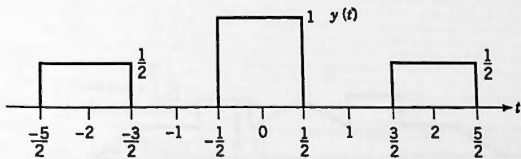
(b) Both give  $y(t) = (\omega_0/2\pi)\text{Sa}(\omega_0 t/2)$

**8.20.** (a)  $h(t) = \delta(t) + k\delta(t + T) + k\delta(t - T)$

(b)  $y(t) = x(t) + kx(t + T) + kx(t - T)$

(c) Same as (b)

(d) See the following sketch.



**8.21.** (a)  $y(t) \Leftrightarrow \tau^2[4 \text{Sa}^2(\omega\tau) - \text{Sa}^2(\omega\tau/2)]$

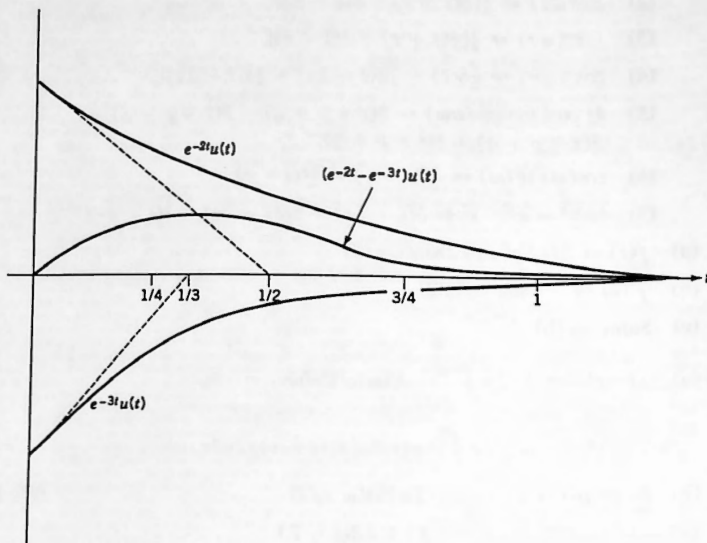
(b) Same as (a).

**8.22.** (a)  $y(t) = (e^{-2t} - e^{-3t})U(t)$

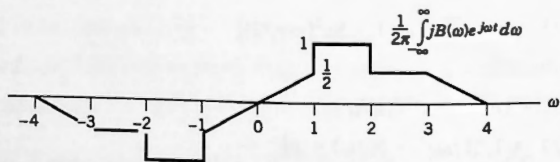
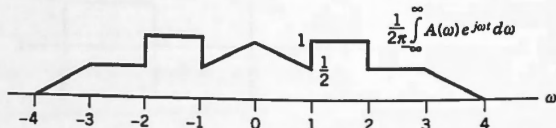
(b)  $y(t) \Leftrightarrow 1/[(j\omega)^2 + 5(j\omega) + 6]$

(c) Same as (b).

(d) Same as (a). See the following sketch.



8.23 (a) See the following sketches.

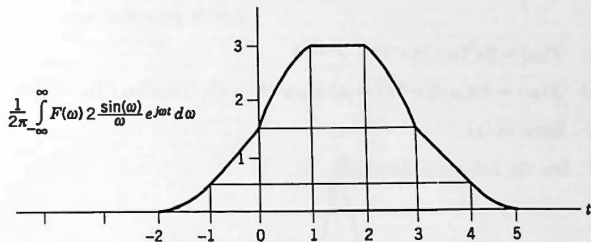
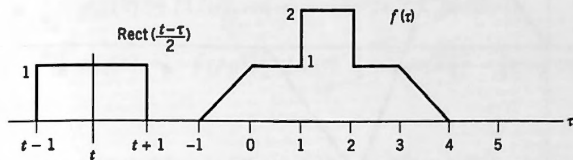


(b)  $F(0) = 5, A(0) = 5, jB(0) = 0$

(c)  $2\pi, 2\pi, 0$

(d)  $40\pi/3, 23\pi/3, 17\pi/3$

(e) See the following sketches.



(f)  $6\pi$

**8.24.** (a)  $Y(\omega) = \text{Rect}(\omega)e^{-j\omega}$

(b)  $y(t) = (1/2\pi)\text{Sa}[(t-1)/2]$

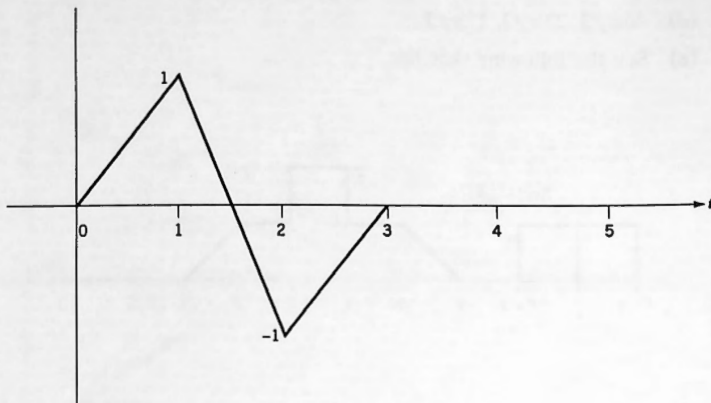
(c)  $z(t) = (1/2\pi)\delta(t-1)$

(d) Same as (c)

**8.26.** (a)

$$y(t) = \begin{cases} t & (0 < t < 1) \\ 3 - 2t & (1 < t < 2) \\ t - 3 & (2 < t < 3) \end{cases}$$

(b) Same as (a). See the following sketch.

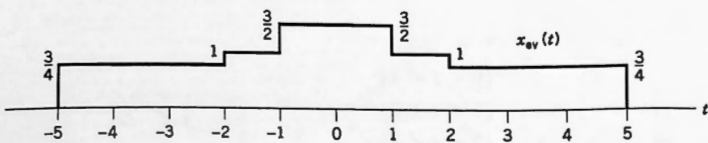
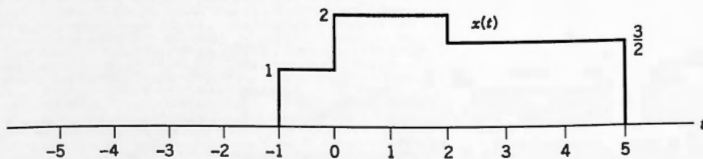


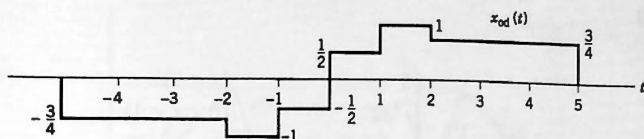
(c)  $Y(\omega) = \text{Sa}^2(\omega/2)(e^{-j\omega} - e^{-j2\omega})$

8.27. (a)  $X(\omega) = \text{Sa}(\omega/2)e^{j\omega/2} + 4\text{Sa}(\omega)e^{-j\omega} + (9/2)\text{Sa}(3\omega/2)e^{-j\omega 7/2}$

(b) Same as (a).

(c) See the following sketches.





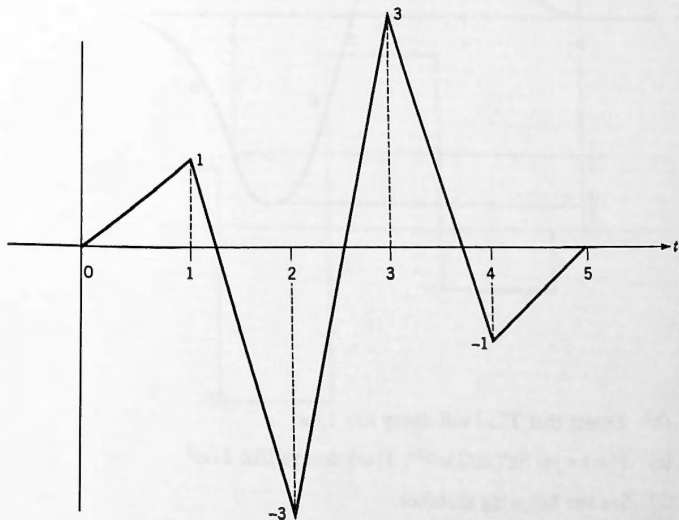
$$x_{cv}(t) \Leftrightarrow (1/\omega) [\sin(\omega) + \frac{1}{2}\sin(2\omega) + \frac{3}{2}\sin(5\omega)]$$

$$x_{od}(t) \Leftrightarrow -(j/\omega) [\cos(\omega) + 1 - \frac{1}{2}\cos(2\omega) - \frac{3}{2}\cos(5\omega)]$$

- 8.28.** (a)  $X(\omega) = (1/j\omega)(1 - 4e^{-j\omega} + 6e^{-j2\omega} - 4e^{-j3\omega} + e^{-j4\omega})$   
 or  $X(\omega) = (j\omega)^3 e^{-j2\omega} [\text{Sa}(\omega/2)]^4$

(b) Same as (a).

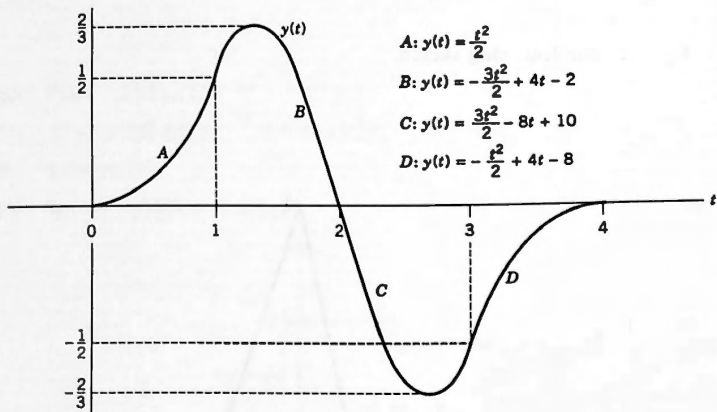
(c) See the following sketch.



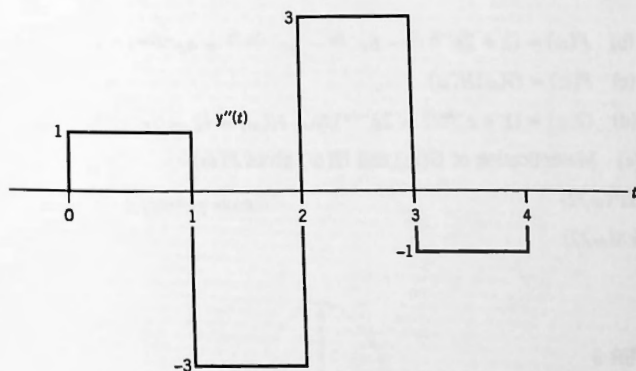
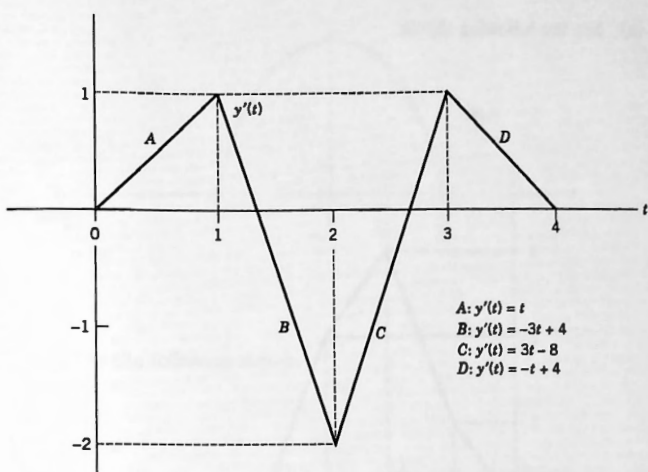
8.29. (a)

$$y(t) = \begin{cases} 0 & (t < 0) \\ t^2/2 & (0 < t < 1) \\ -3t^2/2 + 4t - 2 & (1 < t < 2) \\ 3t^2/2 - 8t + 10 & (2 < t < 3) \\ -t^2/2 + 4t - 8 & (3 < t < 4) \\ 0 & (4 < t) \end{cases}$$

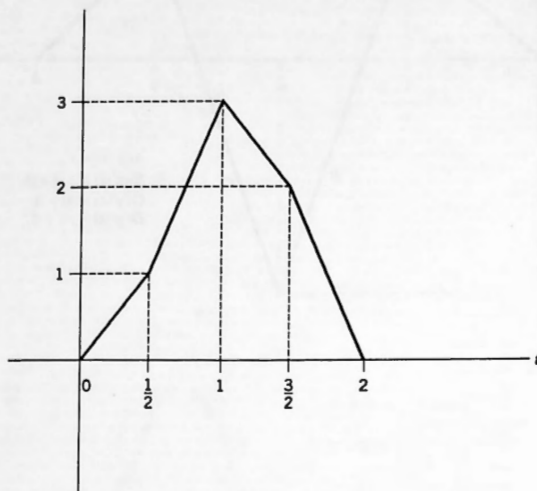
See the following sketch.

(b) Expect that  $Y(\omega)$  will decay like  $1/\omega^3$ (c)  $Y(\omega) = j\omega \operatorname{Sa}^4(\omega/2)e^{-j2\omega}$ ,  $Y(\omega)$  decays like  $1/\omega^3$ 

8.30. (a) See the following sketches.



**8.34.** (a) See the following sketch.



(b)  $F(\omega) = (2 + 2e^{-j\omega/2} - 6e^{-j\omega} - 2e^{-j3\omega/2} + 4e^{-j2\omega})/(j\omega)^2$

(c)  $F(\omega) = G(\omega)H(\omega)$

(d)  $G(\omega) = (1 + e^{-j\omega/2} - 2e^{-j\omega})/j\omega; H(\omega) = (2 - 2e^{-j\omega})/(j\omega)$

(e) Multiplication of  $G(\omega)$  and  $H(\omega)$  gives  $F(\omega)$ .

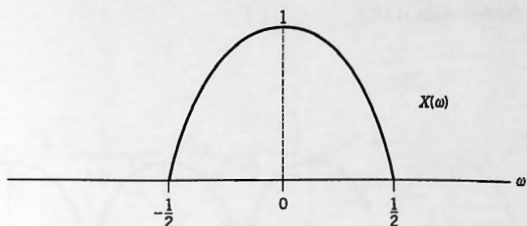
**8.37.**  $\text{Sa}^2(\omega/2)$

**8.38.**  $\pi\Lambda(\omega/2)$

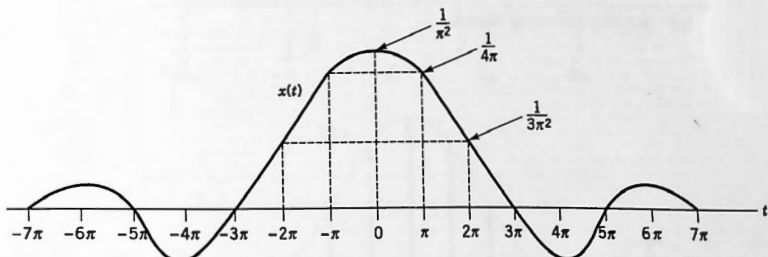
## CHAPTER 9

**9.1.**  $X_s(\omega) = (1/T_s) \sum_{n=-\infty}^{\infty} X(\omega - n\omega_s)$

**9.3.** (a) See the following sketch.

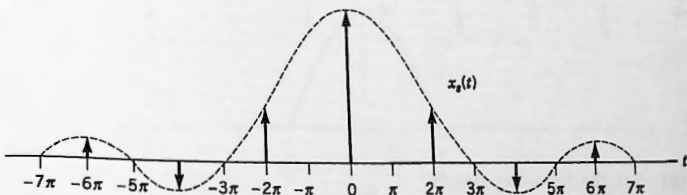


(c) See the following sketch.

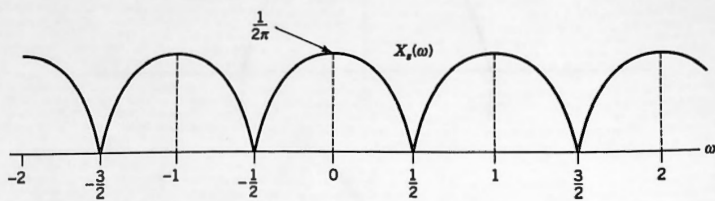


(d)  $T_{\max} = 2\pi$ .

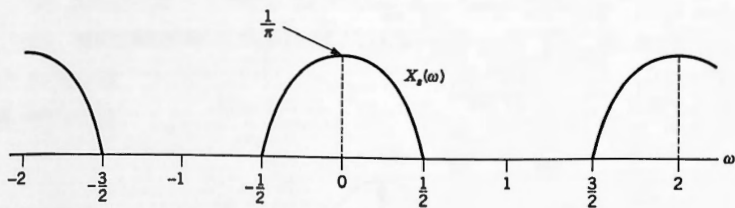
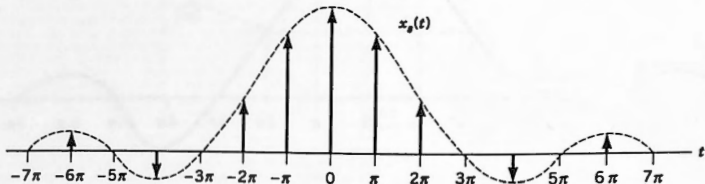
(e) See the following sketch.



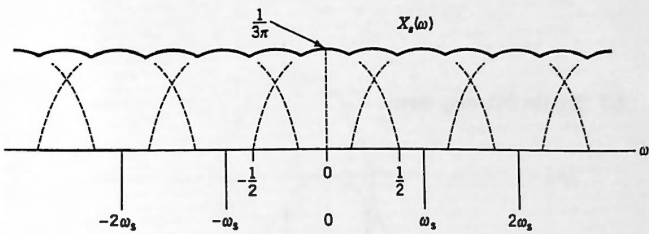
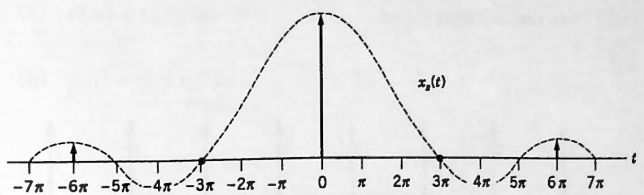
(f) See the following sketch.



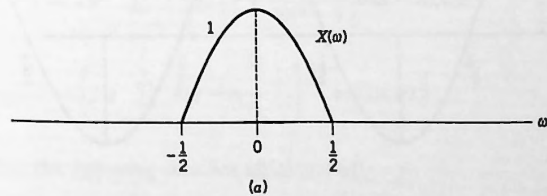
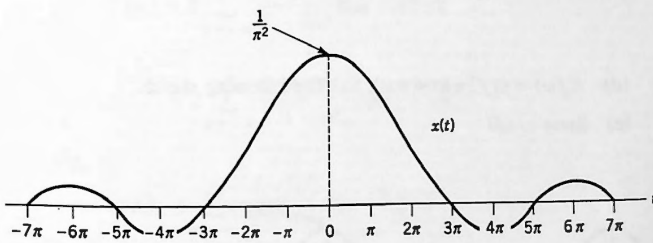
(g) See the following sketch.



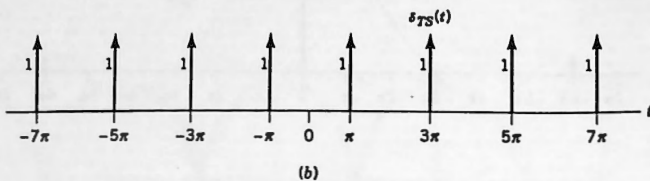
(h) See the following sketch.



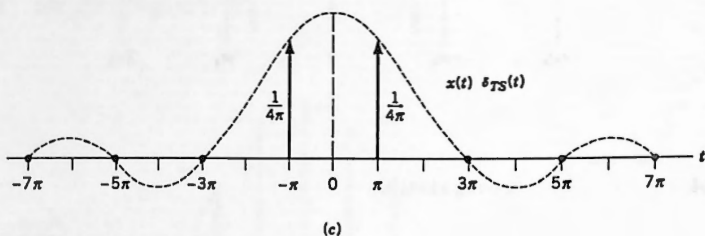
9.4. (a) See the following sketch.



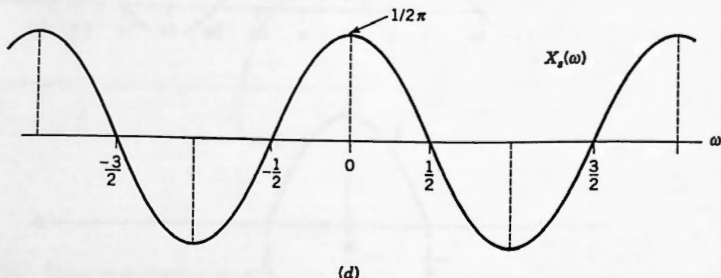
(b) See the following sketch.



(c) See the following sketch.

(d)  $X_s(\omega) = (1/2\pi)\cos(\pi\omega)$ . See the following sketch.

(e) Same as (d)

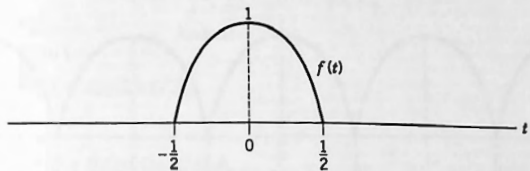


9.7. (a)  $F(\omega) = (1/\omega^2)(e^{-j\omega} - 1 + j\omega e^{-j\omega})$

(b)  $f_1(t) = \frac{1}{2} + (j/2\pi) \sum_{n=-\infty}^{\infty} (1/n)e^{jn2\pi t} \quad (n \neq 0)$

$$f_2(t) = \frac{1}{4} + (1/2\pi^2) \sum_{n=-\infty}^{\infty} \frac{(-1)^n - 1 + jn\pi(-1)^n}{n^2} e^{jn\pi t} \quad (n \neq 0)$$

9.8. (a) See the following sketch.



(b)  $F(\omega) = 2\pi \frac{\cos(\omega/2)}{\pi^2 - \omega^2}$

(c) (1)  $F_1(\omega) = 4 \sum_{n=-\infty}^{\infty} \frac{(-1)^n}{1-4n^2} \delta(\omega - n2\pi);$

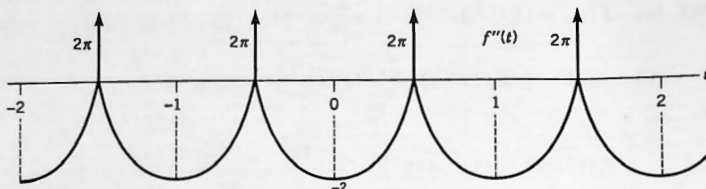
(2)  $F_2(\omega) = 2 \sum_{n=-\infty}^{\infty} \frac{\cos(n\pi/2)}{1-n^2} \delta(\omega - n\pi)$

9.9. (a)  $|\cos(\pi t)| \Leftrightarrow 4 \sum_{n=-\infty}^{\infty} \frac{(-1)^n}{1-4n^2} \delta(\omega - n2\pi)$

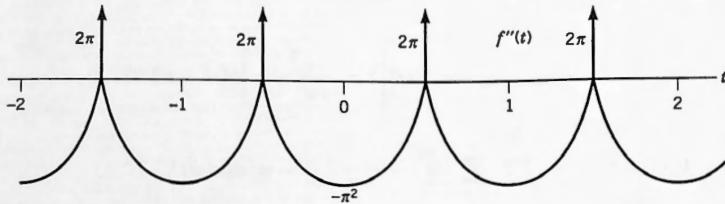
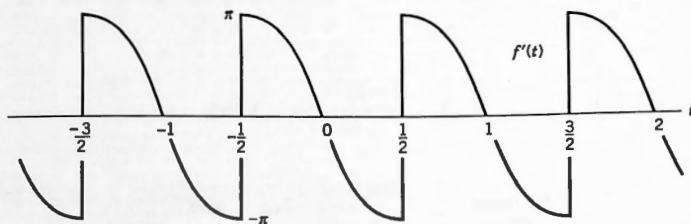
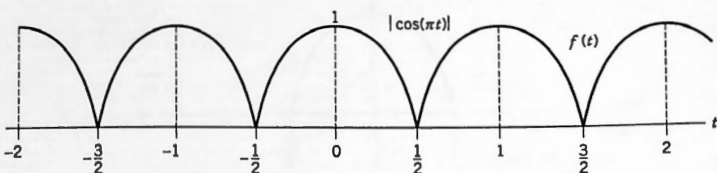
(b)  $f''(t) \Leftrightarrow 4\pi^2 \sum_{n=-\infty}^{\infty} (-1)^n \left[ 1 + \frac{1}{4n^2-1} \right] \delta(\omega - n2\pi)$

(c)  $F_2(\omega) \Leftrightarrow \left[ 2\pi \sum_{n=-\infty}^{\infty} \delta\left(t - n - \frac{1}{2}\right) \right] - \pi^2 |\cos(\pi t)|$

See the following sketches of (c) and (d).



(c)



(d)

9.10.  $\delta_T(t) = (1/T) \sum_{n=-\infty}^{\infty} e^{jn\omega_0 t} \quad (\omega_0 = 2\pi/T)$

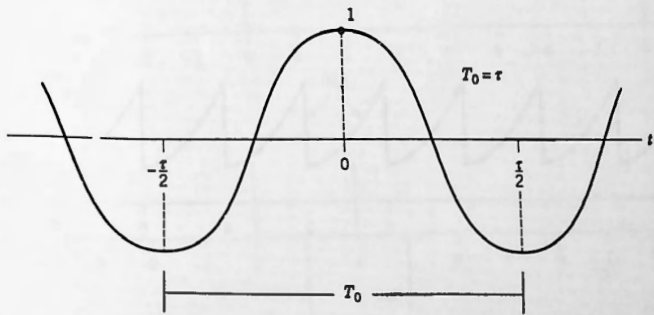
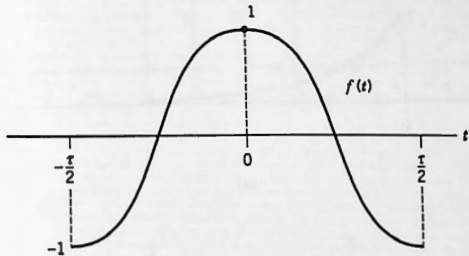
9.11.  $F_p(n) = \frac{1}{2} \frac{e(-1)^n - 1}{1 - jn\pi}$

9.13. (a)  $F(\omega) = \frac{2\omega \sin(\omega\tau/2)}{4(\pi/\tau)^2 - \omega^2}$

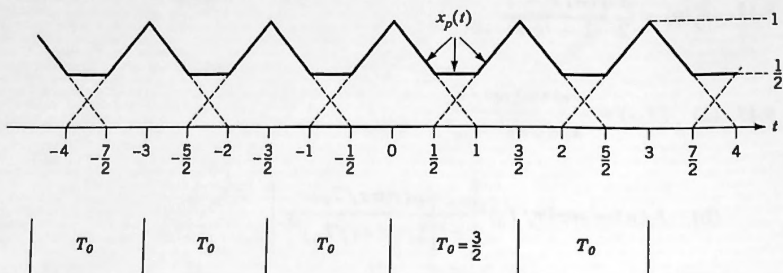
(b)  $F_p(n) = n\pi(\tau/T_0)^2 \left[ \frac{\sin(n\pi\tau/T_0)}{\pi^2 [1 - (n\tau/T_0)^2]} \right]$

(d)  $f_p(t) = \cos(2\pi t/T_0)$

(e) See the following sketch.

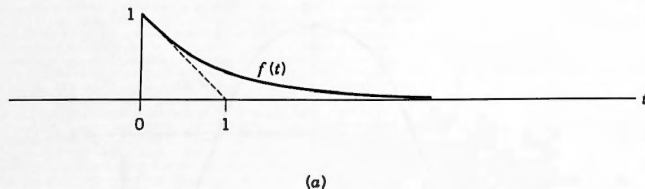


**9.14.** (a) See the following sketch.



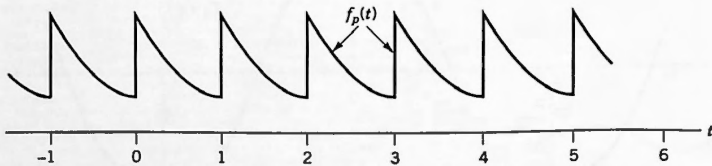
$$(b) \quad x_p(t) = (2/3) \sum_{n=-\infty}^{\infty} \text{Sa}^2(n2\pi/3) e^{jn4\pi t/3}$$

**9.15.** (a) See the following sketch.



(a)

(b) See the following sketch.



(b)

(c)  $f_p(t) = \sum_{n=-\infty}^{\infty} \frac{1}{1+jn2\pi} e^{jn2\pi t}$

(d) Average value is  $F(0) = 1$ . Peak value is  $1 + e^{-1} + e^{-2} + e^{-3} + \dots = 1/(1 + e^{-1}) = 1.58198$

9.16. (a)  $X(\omega) = \text{Sa}(\omega/2)e^{-j\omega/2}$

(b)  $x_p(t) = (1/3)\text{Sa}(n\pi/3)e^{-jn\pi/3}$

9.17. Turns ratio = 4.829,  $L = 0.235$  henrys

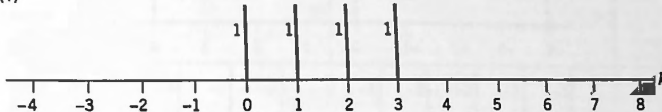
$$\left. \begin{array}{l} H_1 = 0.5^\circ \\ H_2 = 0.024985956^\circ \\ H_3 = 0.004758735^\circ \\ H_4 = 0.001487051^\circ \\ H_5 = 0.000605625^\circ \end{array} \right\} \text{converging like } 1/n^3$$

## CHAPTER 10

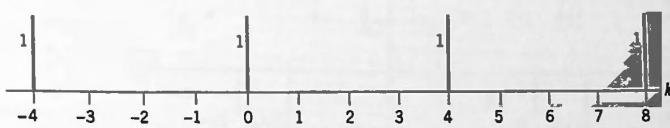
10.1. (a) 3     (b) 5     (c) 11     (d) 29     (e) 17     (f) 8     (g) 34     (h) 52

10.4. (a) See the following sketches.

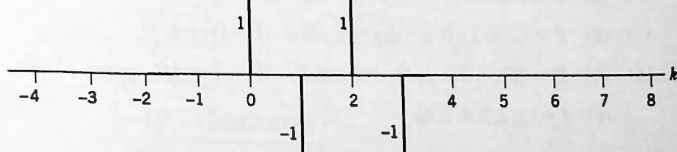
(1)

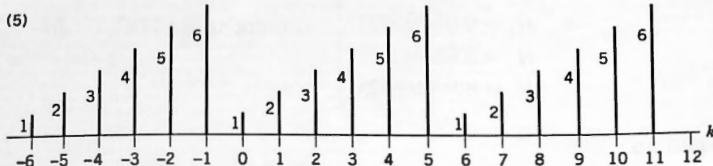
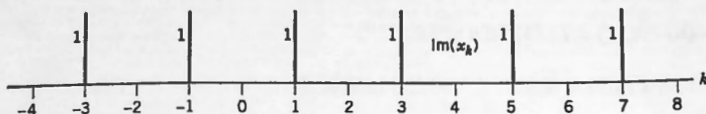
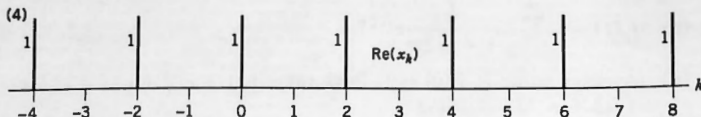


(2)

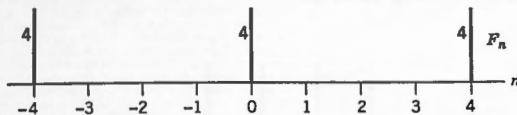


(3)





(b) (1)



(2)



(1) (b)  $\mathbf{F} = (4, 0, 0, 0)$  (c)  $\mathbf{f} = (1, 1, 1, 1);$

(2) (b)  $\mathbf{F} = (1, 1, 1, 1)$  (c)  $\mathbf{f} = (1, 0, 0, 0);$

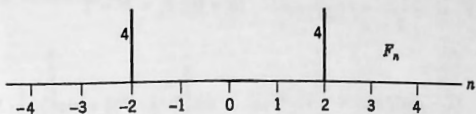
(3) (b)  $\mathbf{F} = (0, 0, 4, 0)$  (c)  $\mathbf{f} = (1, -1, 1, -1);$

(4) (b)  $\mathbf{F} = (2 + 2j, 0, 2 - 2j, 0)$  (c)  $\mathbf{f} = (1, j, 1, j),$

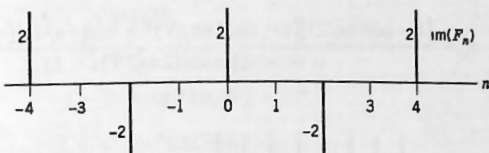
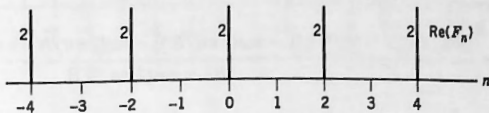
(5) (b)  $\mathbf{F} = (21, -3 + j3\sqrt{3}, -3 + j\sqrt{3}, -3, -3 - j\sqrt{3}, -3 - j3\sqrt{3})$

(c)  $\mathbf{f} = (1, 2, 3, 4, 5, 6)$

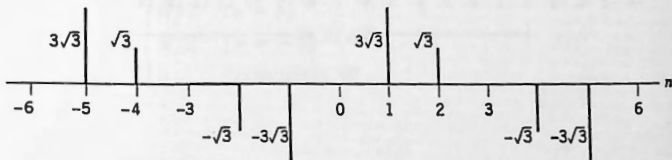
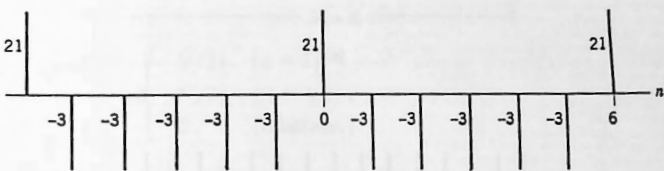
(3)



(4)



(5)



**10.5.** (a)  $F_n = \frac{1 - (-1)^n}{1 - e^{-j2\pi n/N}} \quad (n \neq 0); F_0 = N/2;$

$$A_n = \frac{1}{2}[1 - (-1)^n];$$

$$B_n = \frac{[(-1)^n - 1]\sin(2\pi n/N)}{2[1 - \cos(2\pi n/N)]}$$

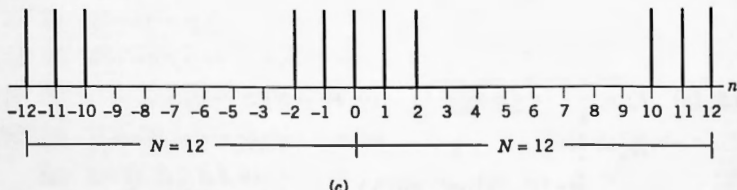
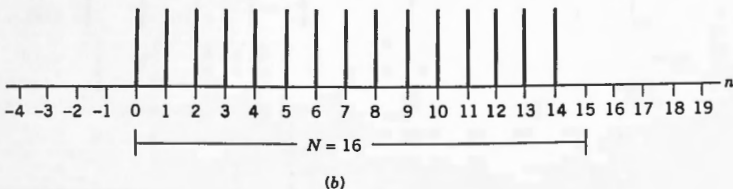
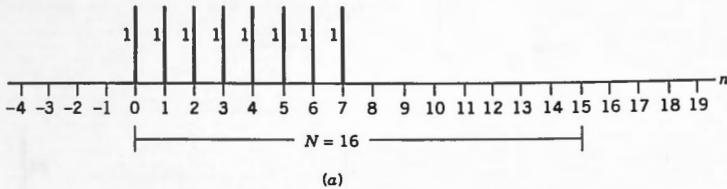
$$(b) \quad F_n = \frac{1 - e^{-j2\pi n(N-1)/N}}{1 - e^{-j2\pi n/N}} \quad (n \neq 0); \quad F_0 = N - 1$$

$$A_n = \frac{(1 - \cos[2\pi n(N-1)/N])[1 - \cos(2\pi n/N)] + \sin[2\pi n(N-1)/N]\sin(2\pi n/N)}{2[1 - \cos(2\pi n/N)]}$$

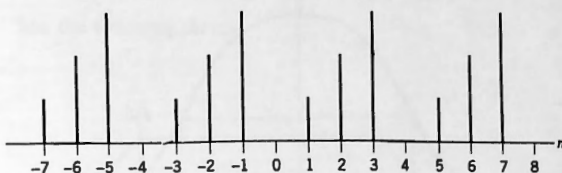
$$B_n = \frac{(\sin[2\pi n(N-1)/N])[1 - \cos(2\pi n/N)] - \sin(2\pi n/N)[1 - \cos(2\pi n(N-1)/N)}}{2[1 - \cos(2\pi n/N)]}$$

$$(n \neq 0) \quad F_0 = (N - 2)/2$$

$$(c) \quad F_n = \frac{[1 - \cos(\pi n/2)][1 - \cos(2\pi n/N)] + [\sin(\pi n/2)][\sin(2\pi n/N)]}{1 - \cos(2\pi n/N)} - 1$$



**10.6. (a)** See the following sketch.



**10.7. (a)**

$$F_n = \frac{1 - e^{-\beta N}}{1 - e^{\beta - j2\pi n/N}}$$

$$A_n = \frac{(1 - e^{\beta N})[1 - e^{\beta} \cos(2\pi n/N)]}{1 - 2e^{\beta} \cos(2\pi n/N) + e^{2\beta}}$$

$$B_n = \frac{-(1 - e^{\beta N})e^{\beta} \sin(2\pi n/N)}{1 - 2e^{\beta} \cos(2\pi n/N) + e^{2\beta}}$$

(b)

$$F_n = \begin{cases} N/2j & (n = 1) \\ -N/2j & (n = -1) \\ 0 & (\text{otherwise}) \end{cases}$$

(c)

$$F_n = \begin{cases} N/2 & (n = 5) \\ N/2 & (n = -5) \\ 0 & (\text{otherwise}) \end{cases}$$

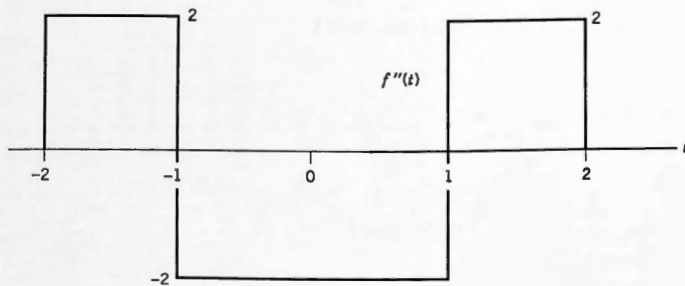
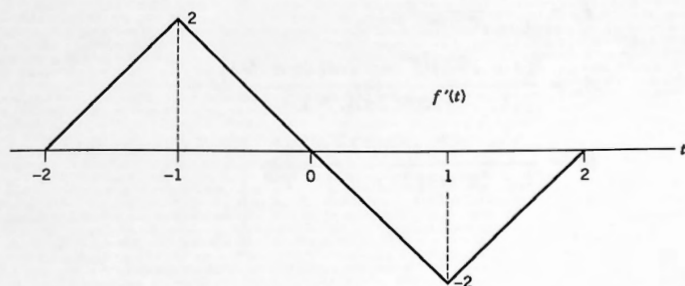
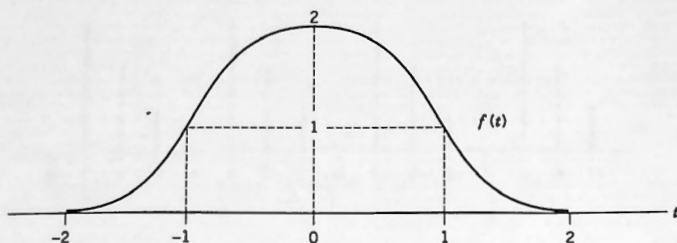
## CHAPTER 12

**12.4. (b)**  $F_p(5) = -F_p(3)$ ,  $F_p(6) = F_p(4)$ ,  $F_p(7) = -F_p(1)$

**12.5. (b)**  $F(5\omega_0) = F(3\omega_0)^*$ ,  $F(6\omega_0) = F(2\omega_0)^*$ ,  $F(7\omega_0) = F(1\omega_0)^*$ , where  $\omega_0 = \pi/4$

**12.7.**  $f(t) = e^{-t}U(t)$

- 12.8. (a) See the following sketch.



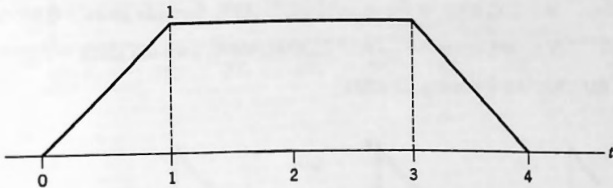
## CHAPTER 13

- 13.2. (a)  $A(\omega) = \sin(\omega)/\omega$ ,  $B(\omega) = [\cos(\omega) - 1]/\omega$   
 (c) and (d) For  $n = 5$ : actual error  $-0.12552981\%$ ;  
 For  $n = 5$ : formula gives  $-0.12553003\%$ ;

For  $n = 71$ : actual error -26.686485%;

For  $n = 71$ : formula gives -26.6864712%

- 13.3.** (a) See the following sketch.



- (b) Canonical-1

$$(c) A(\omega) = -(1/\omega^2)[1 - \cos(\omega) - \cos(3\omega) + \cos(4\omega)];$$

$$B(\omega) = -(1/\omega^2)[\sin(\omega) + \sin(3\omega) - \sin(4\omega)]$$

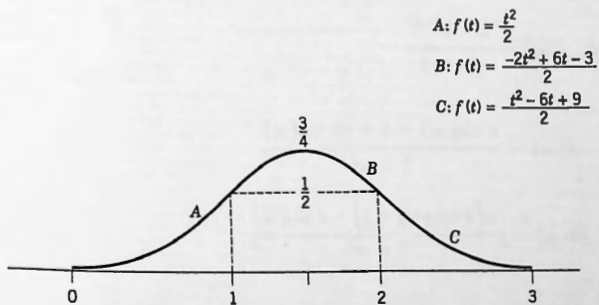
$$(d) F(0) = 3$$

(e) and (f)  $N = 800$ , error in  $F_{137}$  10.2332960%, formula gives 10.2333018%;

$N = 200$ , error in  $F_{60}$  35.7147314%, formula gives 35.7147234%;

$N = 512$ , error in  $F_{226}$  98.9649111%, formula gives 98.9648968%

- 13.4.** (a) See the following sketch.



$$(c) \quad F(\omega) = (1/j\omega)^3(1 - 3e^{-j\omega} + 3e^{-j2\omega} - e^{-j3\omega}),$$

$$A(\omega) = \cos(3\omega/2)\text{Sa}^3(\omega/2);$$

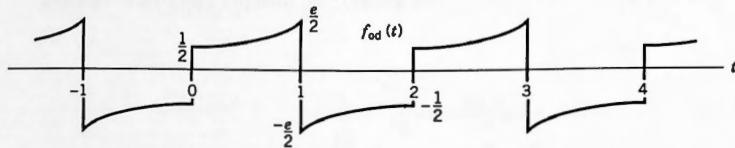
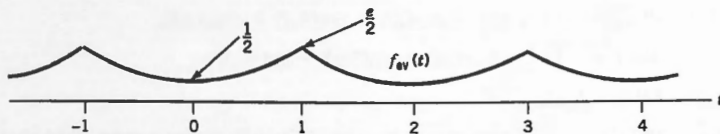
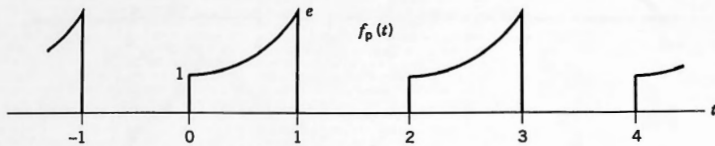
$$B(\omega) = -\sin(3\omega/2)\text{Sa}^3(\omega/2)$$

(e) and (f)  $N = 100$ , error in  $F_7 = -0.015836142\%$ , formula gives  $-0.015833660\%$ ;

$N = 200$ , error in  $F_{38} = -0.949645443\%$ , formula gives  $-0.949649930\%$ ;

$N = 500$ , error in  $F_{151} = -7.289903364\%$ , formula gives  $-7.289922230\%$

13.9. (a) See the following sketches.

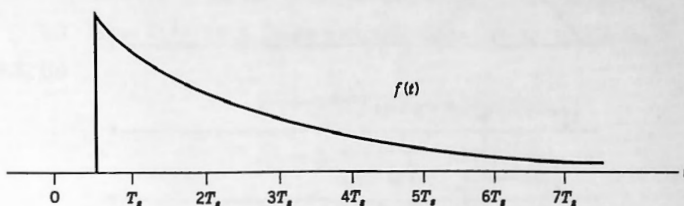


$$(b) \quad F(\omega) = \frac{1 - e^{1-j\omega}}{j\omega - 1}$$

$$A(\omega) = \frac{e \cos(\omega) - 1 + e\omega \sin(\omega)}{1 + \omega^2}$$

$$jB(\omega) = j \frac{\omega[e \cos(\omega) - 1] - e \sin(\omega)}{1 + \omega^2}$$

**13.11.** (a) See the following sketch.

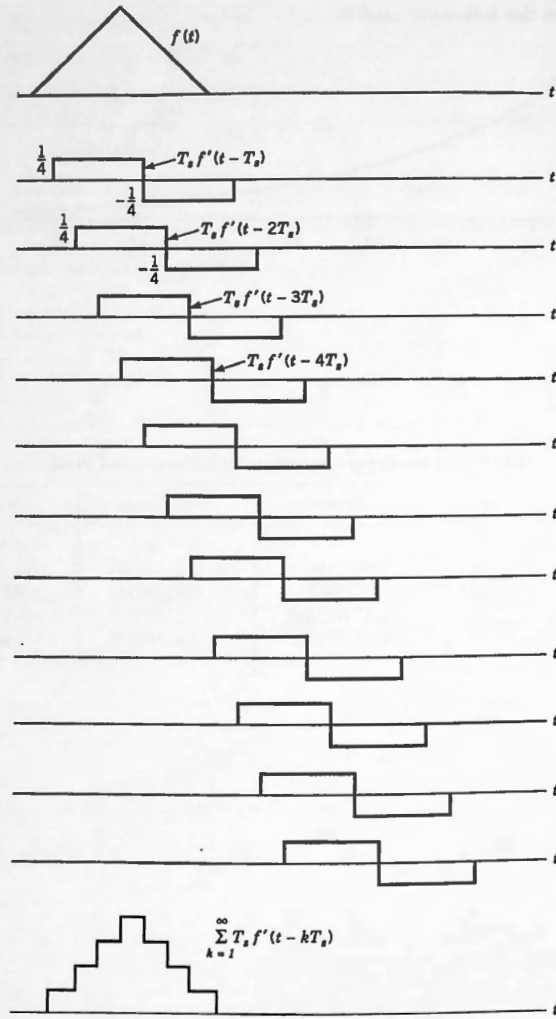


**13.12.**

TABLE 13.10: Error Correction for a Canonical-1 Pulse

<i>n</i>	FFT Value	Factor	FFT/Factor	$F(n\omega_0)$
0	$3 + j0$	1	$3 + j0$	$3 + j0$
1	$-j2.3000166$	1.003218964	$-j2.29263669$	$-j2.29263667$
2	$-0.82106695$	1.012950747	$-0.81056947$	$-0.81056949$
3	$-j0.26223267$	1.029423491	$-j0.25473741$	$-j0.25473741$
4	$-0.42677670$	1.053029288	$-0.40528474$	$-0.40528473$

**13.15.** (c) See the following sketch.



## CHAPTER 14

- 14.1. (d)  $C_\sigma(g_k) = 6$ ,  $C_\sigma(h_k) = 5$ ,  $C_\sigma(f_k) = 10 = 6 + 5 - 1$ ; Thus consistent with (14.7); The two pulses do comply with the span restriction.
- (e) Gives  $C_\sigma(h_k) = 6$ . Pulses no longer comply with span restriction.

- 14.2. (d)  $C_\sigma(g_k) = 6$ ,  $C_\sigma(h_k) = 5$ ; for  $C_\sigma(f_k) = 10 = 6 + 5 - 1$ ; Thus consistent with (14.7); The two pulses do comply with the span restriction.

(e) Gives  $C_\sigma(h_k) = 6$ . Pulses no longer comply with span restriction.

- 14.3. (b)

$$G_1 = 0.96592583 - j7.33693510;$$

$$G_5 = 0.25881905 - j0.33729955;$$

$$G_7 = -0.70710678 + j0.29289322$$

- 14.4. (a)  $f_k = 0 \quad 0 \quad 1 \quad 2 \quad 4 \quad 6 \quad 9 \quad 10 \quad 12 \quad 14 \quad 16 \quad 14 \quad 12 \quad 8 \quad 4 \quad 0$

- (b)

$$G_1 = -5.86142880 - j6.27564240;$$

$$G_5 = -1.06872250 + j1.34549110;$$

$$G_7 = 0.44721525 - j3.3001686e-2;$$

$$H_1 = 1.63098630 - j6.78530830;$$

$$H_5 = -1.08979020 - j0.68603902;$$

$$H_7 = -0.21677275 - j1.37109480$$

- (c)

$$G_1 H_1 = -52.142078530 + j29.536114710 = F_1;$$

$$G_5 H_5 = 2.087742703 - j0.733117678 = F_5;$$

$$G_7 H_7 = -0.142192520 - j0.606020638 = -F_7$$

- 14.5. (a)  $f_k = 16 \quad 14 \quad 13 \quad 10 \quad 8 \quad 6 \quad 9 \quad 10 \quad 12 \quad 14$

- 14.7. The five errors are at the points where the first derivative of the pulse is discontinuous, that is, at the five "corners."

- 14.9. (b)  $G_p(n) = \frac{1}{4}(1 - e^{-jn\pi/2})/(jn\pi/2) = H_p(n);$   
 $F_p(n) = \frac{1}{4}[1 - e^{-jn\pi/2}]^2/(jn\pi/2)^2$

- (d) Values of  $H_p(n)$   $N = 256, T = 4$

$n$	FFT Value		Formula Value	
	$A_n$	$B_n$	$A_p(n)$	$B_p(n)$
0	0.25	0	0.25	0
1	0.15914695	-0.15914695	0.159154943	-0.159154943
2	0	-0.15912298	0	-0.159154943
3	-5.302768e-2	-5.295574e-2	-5.3051647e-2	-5.3051647e-2

Values of  $F_p(n)$   $N = 256$ ,  $T = 4$ 

$n$	FFT Value		Formula Value	
	$A_n$	$B_n$	$A_p(n)$	$B_p(n)$
0	0.25	0	0.25	0
1	0	-0.20262202	0	-0.20264236
2	-0.1012805	0	-0.101321184	0
3	0	2.249548e-2	0	2.2515818e-2

## CHAPTER 15

- 15.1.** (a)  $\text{XRE}(128) = 256$   
 (b)  $\text{XRE}(20) = 50$   
 (c)  $\text{XRE}(768) = 153.6$
- 15.2.** (a)  $2\delta(t - 0.25)$  or  $2\delta(t + 1.75)$   
 (b)  $2\delta(t - 0.0078125)$  or  $2\delta(t + 0.0921875)$   
 (c)  $3\delta(t - 14/9)$  or  $3\delta(t + 4/9)$
- 15.3.** (a)  $\text{FRE}(8) = 4$   
 (b)  $\text{FRE}(5) = 80/\pi$   
 (c)  $\text{FRE}(60) = 1$
- 15.4.** (a)  $2\pi\delta(\omega - 20\pi)$  or  $2\pi\delta(\omega + 236\pi)$   
 (b)  $50\pi\delta(\omega - 24\pi)$  or  $2\pi\delta(\omega + 176\pi)$   
 (c)  $100\pi\delta(\omega - 5600\pi)$  or  $100\pi\delta(\omega + 1600\pi)$
- 15.5.** (a)  $6\delta(t - 5)$
- 15.7.** (a)  $e^{j2\pi t} \Leftrightarrow 2\pi\delta(\omega - 2\pi)$
- 15.8.** (a)  $F(\omega) = (\pi/2) \sum_{n=-\infty}^{\infty} \text{Sa}(n\pi/4)\delta(\omega - n\pi/2)$
- 15.9.** (c)  $-2\sin(2t)$
- 15.10.** (a)  $|\sin(\pi t)| \Leftrightarrow 4 \sum_{n=-\infty}^{\infty} [1/(1 - 4n^2)]\delta(\omega - n2\pi)$   
 (c)  $D^2|\sin(\pi t)| \Leftrightarrow -4\pi^2 \sum_{n=-\infty}^{\infty} [4n^2/(1 - 4n^2)]\delta(\omega - n2\pi)$   
 (d)  $-\pi^2|\sin(\pi t)| + 2\pi\delta_T(t)$   
 (e) See the sketch for Ex. 9.9(c) with all items shifted one-half second to right.

---

# Index

- Ac circuit analysis, *see* Analysis  
Acoustical components, 172  
Algebraic:  
  equation, 188  
  product, 238  
Algorithm, 323, 348  
  base-8 FFT, 368  
  FFT, 348  
  mixed-radix FFT, 365  
  node pair, 360  
  radix-2 FFT, 348, 354, 363, 365  
Alias statement:  
  for periodic functions, 399  
  for pulses, 399  
Aliasing, 289, 291, 292, 294, 304, 306, 378,  
  390, 437, 450, 451, 453  
  condition for no, 444  
  frequency-domain, 294  
  level, 393  
  period, 378, 380  
  time-domain, 184, 309  
Alpha, definition of, 393  
Amplitude spectrum, 22  
Analysis, 226, 323  
  ac circuit, 123, 172, 187, 193, 198, 199, 213  
  rules for, 191  
  equation, 14, 15, 16, 27, 63, 65, 67, 76, 82,  
    86, 106, 115, 120, 124, 127, 130, 133,  
    145, 153, 155, 268, 338  
  CFT, 375  
  DFT, 332, 348  
  FFT, 368  
  complex, 406  
Fourier, 11, 14, 62, 71, 97, 98, 109, 127,  
  172, 196, 212, 217, 323  
frequency-domain, 172  
LTI system, 177  
synthesis system, 332  
time-domain, 212  
Analytical definition, 13, 15, 16, 33, 37, 67,  
  68, 71, 76, 80, 86, 105, 106, 131, 161,  
  184, 330, 338  
Antenna length, 239  
Approximation, 338  
  restricted-range, 387  
Arc tangent, anomalous points of, 337, 342  
Area, 110, 285  
  under a Fourier transform, 53  
  under an impulse, 114, 148  
  property, definition of, 261  
  under a function, 373  
  under Sa, 99  
  numerical estimate of, 373  
Argument, 73. *See also* Phase  
  of Fourier coefficient, 22  
Asymptotic, 400, 419  
  behavior of noncanonical functions,  
    409  
  bounds, 86  
Average, 160  
  power, 33  
    finite, 33  
    total, 34, 37  
value, 17, 160, 161, 163  
Backward divided difference, 468  
Band-limited, 287, 291, 293, 300  
  signal, 297  
  strictly, 287, 290  
Base band, 244  
Base frequency, 68, 69  
Base-8 FFT algorithm, *see* Algorithm  
Basis, 9  
Bell Telephone Labs, 291  
Binary, 353, 359, 362  
Bit reversal, 351, 353, 362  
Box function, 110, 113, 115, 121  
Break-point, 402, 409, 412, 415

- Calculus, 374  
 Camera, 114  
 Canonical, 418  
   pulses, 401  
   -0, 401, 402, 405, 407, 408, 417  
   -1, 402, 405, 407, 408, 416  
   -2, 405, 407  
   -k, 402, 403, 404  
     definition of, 401  
     pulse, error expression for, 406  
 Capacitor, 172, 191  
 Carrier, 239  
 Cartesian, 339  
   form, 73, 102  
   representation, 22  
 CCL DE, 173, 174, 180, 187, 190, 192, 198, 199, 217  
 Central copy, 380  
 Central:  
   divided difference, 469, 470  
   period, 340  
   range, 388  
   result, 14, 69  
 CFT, 372  
   (Fourier series), 372  
   (pulse), 372  
   analysis equation, *see* Analysis  
   coefficients, estimation of, 389  
   spectrum, approximation of, 381, 383  
 Circuit analysis, *see* Analysis  
 Circular, 336, 350, 471  
   convolution, *see* Convolution, circular  
 Circularity, 332, 358, 360  
 Coaxial circles, 437  
 Coefficient function, 66, 69, 226  
 Coefficients, 131  
 Comb, *see* Dirac comb  
 Communication, 242  
   channel, 239  
 Compact disk, 292  
 Complex:  
   addition, 352, 353, 370  
   algebra, 10  
   analysis, *see* Analysis  
   coefficient, 29, 30, 33  
     properties of, 21  
   exponential, 10, 11, 13, 15, 16, 19, 69, 70, 98, 119, 130, 131, 132, 144, 194, 195, 196, 198, 201, 213, 226, 350  
   continuous, 330  
   discrete, 323, 330  
     sets of, 323  
   form, 84  
   Fourier integral, 213  
   Fourier series, 131, 213, 372  
   Fourier spectrum, 78  
   multiplication, 186, 352, 353, 360, 370, 448, 456  
   plane, 10  
   pulse, 127  
   resistor, 172, 191  
   subtraction, 352, 370  
 Composite FFT, 369  
 Computers, 323  
 Conditioning filter, 292  
 Constant-coefficient linear DE, *see* CCL DE  
 Continuity order, 410  
 Continuous:  
   Fourier transform, *see* CFT  
   function, 284  
   spectrum, 23, 73  
   -0, 403  
   -k, definition of, 402  
 Convergence, 97  
   at a discontinuity, 38  
   point by point, 69  
   rate of, 38, 82, 405  
 Convolution, 213, 217, 220, 225, 286, 303, 385  
   circular, 220, 245, 437, 439, 453  
 continuous:  
   circular, 432, 435, 453  
   linear, 432, 435, 451, 452  
   periodic, 245  
   pulse, 245  
 discrete:  
   circular, 432, 435, 437, 442, 444, 450  
     definition of, 439  
     on the FFT, 447  
   linear, 432, 435, 451  
   periodic, 245  
   pulse, 245  
 four kinds of, 432, 435  
 frequency domain, 238  
   definition of, 240  
 graphical, 230  
 integral, 217, 227, 228, 231  
   analytical evaluation of, 233  
 linear, 442, 453, 455  
 operation count, 454  
 of periodic waveforms, 437  
 product, 225, 238  
   definition of, 218  
   meaning of, 220  
   span of, 443

- related to FFT, 432
- symmetry property, 227, 240
- the graphical way, 227
- time domain, 217
- Cooley, 323, 365, 369
- Cosine:
  - oscillator, 18
  - pulse, gated, 412
- D* operator, 145, 147
- d'Alembert, 39
- DE, 173. *See also* CCL DE
- Decaying exponential, 163, 411
- Decimal, 350, 353, 362
- Definite integral, estimation of, 373
- Delayed:
  - impulse, 222
  - unit step, 150
- Demodulation, 242
- Derivative, 151, 153, 155
  - first, 468
  - FFT estimation of, 470
  - second, 469
  - FFT estimation of, 471
- Deterministic, 337
- DFT, 135, 311, 323, 326, 330, 336, 338, 368
  - analysis equation, *see* Analysis as an estimator, 372
  - coefficients, 334, 338
  - inherent periodicity of, 332
  - line spectrum, 333, 336, 376
  - properties of, 338
  - spectrum vector, 334
  - synthesis equation, 333
- Difference:
  - backward-divided, *see* Backward
  - central-divided, *see* Central
  - forward-divided, *see* Forward
- Differential equation, 173. *See also* CCL DE
- Differentiation, 145, 147
  - emulation, 463, 467
  - property, 145
  - theorem, 468
- Digital, 300
- Digitally coded communication link, 239
- Digitization, 239
- Dirac, 97, 109, 149
  - comb, 133, 135, 285, 299, 383
  - delta, 97, 109, 114, 118, 121, 127, 128, 132, 149, 150, 151, 156, 163, 190, 200, 214, 216, 220, 225, 226, 284, 299, 302, 401. *See also* Unit impulse
- analytical definition of, 110
- convolution property, 270
- definition of, 111
- delayed, 116
- emulation:
  - frequency domain, 466
  - time domain, 463
- Fourier transform of, 112
- magnitude spectrum of, 112
- phase spectrum of, 112
- sampling, 191
- sampling property, 113, 116, 270. *See also* Unit impulse
- deltas, periodic train of, 383
- function, 463
- Dirichlet, 43, 44, 97, 105, 110
  - conditions, 43, 85
  - for pulses, 85
  - criterion, 97
  - Jordan criterion, 85
- Discontinuity, 147, 151
- Discrete complex exponential, 323, 330, 333, 336, 341
  - circularity property of, 325
  - linear combination of, 335
  - orthogonality property of, 326
- Discrete Fourier transform, 135, 311, 323, 330
  - definition of, 331
  - inverse, 332
- Distribution, 106, 107, 109, 110, 113, 128, 133, 134. *See also* Generalized function
  - definition of, 106
  - fundamental property of, 107
  - theory, 98, 108, 127
- Double-sided decaying exponential, 104
- Doublet, 156, 157
- Dual-node pair, 358
  - power-of-*W*, 360
  - separation, 358
- Duality, 269, 293
  - property, definition of, 262
- Dummy variable, 218, 239
- Ecole Polytechnique, 98
- Economizing on the FFT, 369
- Eigenfunction, 196, 198, 204, 226
- Einstein, 45
- Electrical:
  - conductor, 228
  - engineering, 97, 98, 149, 172, 187, 212, 213
  - network, 20, 173, 212
- Encoding, 300

- Energy, 32, 128, 131, 132  
 1-ohm, 32, 79  
 content, 79  
 finite, 42, 100, 107, 130, 291, 378  
 infinite, 97, 105, 108, 112, 120, 129, 130,  
     133  
 pulse, 79, 80, 85, 100, 105, 129  
 spectrum, 77, 81, 82, 83, 87  
 total, 79
- Engineering, 145
- Envelope, 299
- Equivalence, 324
- Error:  
     correction of FFT estimate, 418  
     curve, 407, 409, 411  
     expression, 403  
         for canonical- $k$  pulse, *see* Canonical  
         closed form, 407  
         for periodic functions, 404, 410  
         properties of, 404  
         for pulses, 404  
     formula, 400  
     function, 410  
     in FFT estimate, 399, 400, 407, 408  
     in  $n$ -th spectral estimate, 404, 409  
     incurred in using FFT, 405  
     relative, 400, 408, 409  
     relative, for periodic functions, 400  
     relative, for pulses, 400
- Estimation errors, 388
- Estimation of CFT coefficients, *see* CFT
- Eternal:  
     complex exponential, 98, 127, 129, 187,  
     189  
     transform of, 128  
     constant, 98, 121, 160, 161, 163  
     transform of, 120  
     cosine, 98, 129, 241  
     transform of, 129  
     sine, 98, 129  
     transform of, 130  
     train of unit impulses, 131, 133
- Euler, 39
- Even, 30, 76, 102, 103, 104  
     function, 24, 28, 82  
         examples of, 25  
     integrand, 25  
     part, 27, 102, 124
- Execution time, 447
- Exponential, 100. *See also* Complex;  
     Discrete complex; Double-sided;  
     Single-sided
- Faraday's laws, 187
- Fast Fourier transform, *see* FFT
- FFT, 135, 182, 184, 323, 338  
     algorithm, *see* Algorithm  
     analysis equation, *see* Analysis  
     applied to synthesis, 368  
     as an estimator, 372  
     detailed workings of, 348  
     estimate of Fourier coefficients, 390  
     estimate of Fourier transform, 387  
     estimation of CFTs, 383  
     flow graph, 358  
     flowchart, 363  
     inversion of CFT spectra, 390  
     operation count, 353  
     periodicity of, 394
- Filter, 172, 179, 290
- Finite:  
     energy signals, 291  
     span, 160, 374, 378  
     span pulse, 383  
     time duration, 162
- Flash, 114
- Flow graph, 359
- Forcing function, 173, 188
- Forward divided difference, 469
- Fourier, 84, 97, 98, 109, 212  
     analysis, *see* Analysis  
     integral, 62, 66, 68, 69, 86, 97, 198, 212,  
     338  
     existence of, 83  
     representation, 71, 177, 182  
     pair, 67, 68, 71, 108, 112, 116, 121, 124,  
     128, 129, 130, 135  
     series, 86, 97, 130, 131, 133, 145, 196, 198,  
     212, 213, 308, 338  
     coefficients, 33, 37, 82, 196, 299, 392  
     argument of, *see* Argument  
     complex, 14, 15, 18, 35, 39, 223  
     estimate of, 372  
     real and imaginary parts of, 22  
     magnitude and phase of, 22  
     of periodic functions, 15  
     polar representation, 22  
     real, 39  
     convergence of, 37, 44  
     spectral density, 66  
     spectrum, 380  
     transform, 66, 73, 82, 86, 97, 103, 106,  
     110, 114, 125, 133, 145, 147, 153, 161,  
     186, 197, 213, 218, 238, 287, 293, 295,  
     309, 372, 393, 403, 413, 432

- of a doublet, 156
- estimates of, 372
- of a Fourier series, 132
- of pulses which are not time-limited, 160
- of sampled waveform, 285
- properties of, 73, 257
- transforms without integration, 154
- Fourier's theorem, 44**
- Frequency:**
  - analyzer, 15
  - division multiplexing, 239
  - domain, 15, 67, 71, 116, 121, 127, 129, 135, 137, 163, 175, 177, 213, 220
  - aliasing, *see* Aliasing
  - analysis, *see* Analysis
  - convolution, 241, 267, 270, 286, 287, 385
  - differentiation, 136
  - theorem, 268
  - multiplication, 146, 238
- representation, 34**
  - response, 176, 180, 186, 213
  - sampling, 302, 305
  - shift, 136, 269, 299
  - shifting, 244
  - transfer function, 176, 189, 192
  - shift property, 267
  - definition of, 267
- Function, 110**
  - definition of, 105
  - ordinary, 106
- Functions with discontinuities, 147**
- Fundamental, 14, 299, 308**
- Gate pulse, 98**
- Gated cosine, 163**
- Gauss, 43**
- Generalized function, 106, 109, 118, 120, 124, 129, 130, 148. *See also* Distribution**
  - definition of, 106
  - theory, 98
- Geometric progression, 329**
- Gibbs, 38, 45**
- Granular, 224**
- Growing single-sided exponential, 102**
- Half-value, 88, 232, 377, 401, 474**
  - definition of, 44
- Hardware, 338**
- Harmonic, 14, 17, 41, 131**
- Heated rod, 212**
- Heaviside, 45, 98, 123, 149, 172, 212**
  - function, 123, 213
  - shifting theorem, 137, 267
  - step function, 98
- Hertz, 291**
- Hybrid, 392**
- Hydraulic, components, 172**
- Ideal filter, 81**
- IDFT, 332, 336**
- Imaginary, 82, 104, 108**
  - part, 27, 73, 76, 183
- Impedance, 188**
- Impulse, 220, 295. *See also* Dirac delta**
  - response, 176, 213, 217, 220, 228
  - definition of, 214
- sampling:**
  - frequency domain, 302
  - time domain, 284
- sequence, 294**
- train, 135, 239**
  - Fourier transform of, 133. *See also* Dirac delta
- Independent variable, 73**
- Index, 349**
- Inductor, 172, 191**
- Infinite:**
  - countably, 335
  - series, 16, 18
    - representation, 16
  - span, 160, 388
  - sum, 381
  - uncountably, 335
- Initial condition, 174, 188, 212**
- Inner product, 9, 335**
  - definition of, 326
- Input, 173, 213, 220**
  - impedance, 188, 192
- Inside the FFT, 348**
- Integer, 324**
- Integral:**
  - representation, 67
  - of unit impulse, 148
- Integration, 148, 154**
  - definition of, 374
  - numerical, 373
  - property, definition of, 271
- Interpolation, 298**
- Inverse, *see also* IDFT**
  - discrete Fourier transform, 332, 336
  - Fourier transform, 66
  - transform, 214

- Inversion, 308  
of CFT spectra by FFT, 390
- Jump discontinuity, 38
- k*-domain, 338  
Kelvin, 20, 98, 172, 212  
Kirchhoff, 172, 187, 191
- Laplace, 39, 84, 97, 212  
Leading edge, 228  
Left-endpoint, 374  
uniform sampling, 401
- Limit, 374  
of a sequence of functions, 106, 111
- Line spectrum, 22, 64, 73, 332  
DFT, 333
- Linear, 174, 222  
algebra, 326, 335  
circuit, 195  
combination, 10, 69, 70, 129, 196, 226,  
330, 470  
network, 172, 179  
operator, 195, 257  
property, 195, 199  
definition of, 257
- system, 127, 173  
time-invariant system, 173. *See also* LTI  
transformation, 195
- Log-linear *Z*-curves, 406
- LTI, 173, 174, 177, 184, 201, 212, 213, 217,  
220, 228  
system analysis, *see* Analysis
- Magnitude, 73, 102  
line-spectrum, 23  
plot, 23  
spectrum, 22, 73, 83, 108, 117, 178, 180
- Mathematical probability, 84
- Matrix factorization, 353
- Maxwell, 45
- Mechanical components, 172
- Method:  
of induction, 269  
of successive differentiation, 268
- Michalson, 45
- Mixed-radix FFT algorithm, *see* Algorithm
- Modulation, 239, 242, 285  
property, 137, 267
- Modulo-8, 449
- Modulo-N, 324, 350, 439
- Multiplication count, table of, 354
- n*-domain, 338  
Natural order, 351  
Necessary and sufficient conditions, 38, 84,  
97
- Nineteenth century, 97
- Nobel, 97
- Node, 354
- Noncanonical, 403, 409, 410, 412, 418  
pulses, examples of, 402
- Nonpolynomial sections, 163
- Numerical:  
estimate of area, *see* Area  
estimates, 372  
integration, 373  
sampling, 373, 381  
specification, 338
- Nyquist, 292  
criterion, 291, 296  
frequency, 291, 296  
sampling rate, 301
- Odd, 30, 76, 102, 104, 108  
function, 25, 28, 81, 82  
examples of, 25
- integrand, 26, 30  
part, 27, 102, 108, 124
- Operation count:  
convolution, 454  
FFT, 353  
table of, 354, 457
- Operational:  
mathematics, 172  
method, 173
- Order of continuity, 401, 410, 413  
definition of, 402
- Order of summation, 331
- Order of summation and integration, 13, 37
- Orthogonal, 9  
set, 10
- Orthogonality, 9, 11, 12, 144, 326  
condition, 324  
property, 331, 335  
of vectors, definition of, 326
- Output, 173, 177, 213, 220
- Over-sampling, 292
- Parallel processing, 361
- Paris Academy, 37
- Parseval, 32
- Parseval's:  
lemma, 80  
theorem, 34, 112

- theorem for periodic waveforms, 33, 79, 81  
 theorem for pulses, 78, 80  
 Partial fractions, 181  
 PDE, 212  
 $\text{PER}(n)$ , 378  
 $\text{per } (t)$ , 378  
 Period, 12, 13, 16  
 Periodic:  
     extension, 20  
     function, 69, 133, 220, 330  
         Fourier transform of, 130  
     waveform, 10, 15, 32, 33, 38, 78, 98, 201  
 Periodicity property, 340  
 Phase, 102. *See also* Argument  
     line spectrum, 23  
     plot, 23  
     spectrum, 22, 73, 108, 117, 178, 180  
 Phasor, 172, 189, 196  
     response to, 194  
 Physically realizable, 14, 33, 38, 69, 79, 215  
 Pivot point, 341  
 Poisson, 108  
     summation, 308  
 Polar, 339  
     form, 73, 108  
 Polynomial, 186  
     in  $D$ , 147, 173  
     sections, 160  
 Postprocessor, 186  
 Power, 32, 41  
     average, *see* Average  
     finite average, *see* Average  
     instantaneous, 79  
     line spectrum, 34  
     1-ohm, 32, 36  
     series, 19  
     signal, 33  
     spectrum, 78  
     total average, *see* Average  
 Primary period, 340  
 Probability, 213  
 Product rule for differentiation, 151, 182  
 $\text{PUL}(\omega)$ , 378  
 $\text{pul}(t)$ , 378  
 Pulse, 10, 62, 69, 82, 87, 201  
     discrete, 333  
     even, 76  
     odd, 76  
     reversed, 234  
 Pulses with polynomial sections, 154  
 Quantum mechanics, 97, 109  
 Radio transmission, 239  
 Radix-2 FFT algorithm, *see* Algorithm  
 Random values, 186  
 Range of integration, 375  
 Rates of convergence, table of, 41, 86  
 Rayleigh, 108  
 Real, 103  
     function, 103  
     line, 325  
     part, 27, 73, 76, 183  
     valued coefficients, 189  
 Realness property, definition of, 258  
 Reciprocal scaling, 269  
     property, definition of, 264  
 Recovery, 291  
     filter, 290, 294, 297, 300  
 Rect, 70, 71, 98, 110, 113, 127, 128, 153,  
     157, 236, 290, 300, 402, 403, 419  
     Fourier transform of, 99  
     shifted, 153  
 Rectangular:  
     pulse, 70, 373, 378, 383, 390  
     rule, definition of, 374  
     integration, 452  
 Repeated differentiation, 146  
 Replicated spectrum, 287  
 Residue theory, 406  
 Response, 173, 186  
     to a periodic signal, 172  
     to a pulse, 172, 176, 197  
     to a sinusoid, 172  
 Riemann, 374  
 RLC network, 187  
 Round-off error, 339  
 Royal Society, 97  
 Sa, 18, 71, 99, 118, 121, 293, 298  
     function, interpolation, 298  
 Sampler, 285  
 Samples, 285  
 Sampling, 150, 190, 239, 284, 291, 299  
     frequency, 286, 290  
     frequency domain, 302  
     instant, 401, 402, 409, 413, 415, 418  
     interval, 285, 294, 295, 300, 403, 415  
     period, 301  
     point, 400, 410  
     property, 113, 114, 116, 126, 134, 150, 151,  
         241, 285, 287, 302, 304, 385  
     definition of, 114

- Sampling (*Continued*)  
 theorem, 135, 284, 287, 299, 300  
 time domain, 284  
 window, 301
- Scale factor, 375, 376, 386, 387, 388, 389
- Schrödinger, 97
- Schwartz, 98, 109
- Sequence:  
 function, 107, 108, 111, 118, 120, 128  
 of functions, 110  
 of pulses, 111
- Series representation, 15, 33, 338
- Set of functions, 10
- Sgn, 98, 105, 107, 108, 110, 124. *See also*  
 Signum
- Sifting property, 114
- Sign, 105
- Signal, 172, 239  
 flow graph, 354  
 processing, 15, 467
- Signum function, *see* Sgn  
 definition of, 106  
 Fourier transform of, 108
- Sinc, 44
- Sine-cosine formulation, 84
- Single-period definition, 62
- Single-sided:  
 decaying exponential, 99, 108, 215  
 Fourier transform of, 101  
 Laplace transform, 174
- Skipping rule, 361
- Solution, 173
- Source node, 358
- Span, 160, 374, 443, 451, 455  
 count, definition of, 433  
 of discrete periodic sequence, 444  
 of exponentially decaying pulse, 445  
 restriction, 442, 447, 448, 450, 451, 453  
 definition of, 445  
 time, definition of, 433
- Spectral:  
 density, 23  
 lines, 64
- Spectrum, 80, 291  
 of sampled signal, 287
- Square, 105  
 integrability criterion, 41, 42, 84, 85, 86,  
 97, 100, 105, 120, 128, 130  
 integrable, 43
- Stage:  
 number, 359  
 -1 vector, 356  
 -2 vector, 357
- n vector, 349
- Step:  
 discontinuity, 148, 153  
 function, 98, 124, 127, 337
- Stochastic, 337
- Strictly band-limited, *see* Band-limited
- Successive differentiation, 145, 154, 155,  
 160, 161, 163, 410
- Sufficient conditions, 38, 84, 97  
 for convergence, 40
- Symmetric range of integration, 25, 30
- Symmetries, 340
- Symmetry property, definition of, 258
- Synthesis, 15, 226, 323  
 equation, 14, 15, 17, 20, 28, 65, 66, 67, 71,  
 80, 134, 146, 191, 297, 338
- T for pulses, 434
- Technology, 338
- Telegraph equation, 20
- Telemetry, 291
- Testing function, 106
- Thomson, 20, 98. *See also* Kelvin
- Time domain, 15, 27, 71, 116, 127, 129, 135,  
 137, 160, 175, 177, 213, 217, 220  
 aliasing, *see* Aliasing  
 analysis, *see* Analysis  
 convolution, 238, 269, 303, 304  
 differentiation, 145, 269  
 theorem, 268  
 multiplication, 239, 241, 270, 286  
 representation, 34  
 sampling, 284, 302  
 theorem, 290
- Time:  
 invariant, 222, 224. *See also* LTI  
 shift, 125, 137, 150, 154, 155, 156  
 shift property, 285  
 definition of, 266
- Trans-Atlantic cable, 20, 98
- Transfer function, 197
- Triangular pulse, 87, 155, 234, 236
- Trigonometric series, 97
- Truth table, 324
- Tukey, 323, 365, 369
- U(t), 123, 124, 148, 149. *See also* Unit step
- Uniform Riemann sum, 374
- Uniform sampling, 374
- Unit circle, 324
- Unit impulse, 109, 114, 115, 149, 214. *See*  
*also* Dirac delta  
 Fourier transform of, 112

- train, 285  
Unit step, 100, 109, 123, 148, 149, 151, 213.  
*See also U(t)*  
Unscrambler, 353, 357
- Vector indices, 351  
Vectors, 9  
Venn, 43, 85
- W*, 349, 358, 448
- definition of, 326  
power of, 334, 359  
Weight of an impulse, 114, 115, 220. *See also* Area under an impulse  
Weighted impulse, 224  
Weights, 285  
White space, 388, 419, 434  
World War II, 291
- Z-curves, 406  
Zero padding, 388, 419, 434



















**NOT**

Macintosh

Disk 1 of 1

**Introduction to  
Fourier Analysis**

by Norman Morrison

© 1994 by John Wiley & Sons, Inc.  
All rights reserved



WILEY  
INTERSCIENCE

ISBN 0-471-01737-X

Morrison

1426  
NUWE BTW NG

R169.00

Comprehensive, user friendly, and  
pedagogically structured . . .

a fast, easy way to learn about the electrical  
engineer's most important mathematical tool

Based on a groundbreaking one-semester course originated by Professor Norman Morrison at the University of Cape Town, this book serves equally well as a course text and a self-study guide for professionals. Offering only relevant mathematics, it covers all the core principles of electrical engineering contained in Fourier analysis, including the time and frequency domains; the representation of waveforms in terms of complex exponentials and sinusoids; complex exponentials and sinusoids as the eigenfunctions of linear systems; convolution; impulse response and the frequency transfer function; magnitude and phase spectra; and modulation and demodulation.

- Covers Fourier analysis exclusively for electrical engineering students and professionals
- Offers a complete FFT system contained on the enclosed disks (one for IBM compatibles, the other for Macintosh)
- Includes dozens of examples drawn from electrical engineering
- Packed with exercises, samples, and end-of-chapter problem sets

**NORMAN MORRISON, PhD**, is an instructor in the Electrical and Electronics Engineering Department at the University of Cape Town in South Africa.

Cover Design: David Levy

**WILEY-INTERSCIENCE**

John Wiley & Sons, Inc.

Professional, Reference and Trade Group

605 Third Avenue, New York, N.Y. 10158-0012

New York • Chichester • Brisbane • Toronto • Singapore

ISBN 0-471-01737-X



9 780471 017370

Includes disks



WILEY-  
INTERSCIENCE

INTRODUCTION TO FOURIER ANALYSIS